Numerical Solution of Static and Dynamic Problems of Functionally Graded Structural Members

A THESIS

SUBMITTED FOR THE AWARD OF THE DEGREE

OF

DOCTOR OF PHILOSOPHY

IN

MATHEMATICS

BY

KARAN KUMAR PRADHAN

(ROLL NO. 511MA102)

UNDER THE SUPERVISION OF

PROF. S. CHAKRAVERTY

Department of Mathematics
National Institute of Technology Rourkela
Rourkela-769 008, Odisha, India

August 2015

Department of Mathematics
National Institute of Technology Rourkela
Rourkela - 769 008, Odisha, India. www.nitrkl.ac.in

Karan Kumar Pradhan

August 11, 2015

Declaration

I hereby declare that the work which is being prepared in this thesis entitled ***Numerical Solution of Static and Dynamic Problems of Functionally Graded Structural Members*** for the award of the degree of ***Doctor of Philosophy*** in Department of Mathematics, National Institute of Technology Rourkela, Rourkela 769008, Odisha, India, is an authentic record of my own research work carried out under the supervision of Prof. (Dr.) S. Chakraverty.

The matter embodied in this thesis has not been submitted by me for the award of any other degree.

KARAN KUMAR PRADHAN
Roll No. 511MA102
Department of Mathematics
National Institute of Technology Rourkela
Rourkela 769008, Odisha, India

Department of Mathematics
National Institute of Technology Rourkela
Rourkela - 769 008, Odisha, India. www.nitrkl.ac.in

Prof. S. Chakraverty

August 11, 2015

Certificate

This is to certify that the thesis entitled ***Numerical Solution of Static and Dynamic Problems of Functionally Graded Structural Members*** is being submitted by **Karan Kumar Pradhan** for the award of the degree of ***Doctor of Philosophy*** in Mathematics, National Institute of Technology Rourkela, Rourkela 769008, Odisha, India, is a record of bonafide research work carried out by him under my supervision and guidance. Mr. Karan Kumar Pradhan has worked for four years on the above problem in Department of Mathematics, National Institute of Technology Rourkela and this has reached the standard for fulfilling the requirements and the regulation relating to the degree. The contents of this thesis, in full or part, have not been submitted to any other university or institution for the award of any other degree or diploma.

Dr. S. Chakraverty
Professor, Department of Mathematics
National Institute of Technology Rourkela
Rourkela 769008, Odisha, India

Dedicated To

My Parents

Acknowledgments

Ninety-nine percent of the failures come from people who have the habit of making excuses.

- George Washington Carver

This thesis is a result of the research that has been carried out at National Institute of Technology Rourkela. During this period, I came across with a great number of people whose contributions and positive criticisms in various ways helped my field of research and they deserve special thanks. It is a true pleasure to convey my gratitude to all of them.

First and foremost, I would like to express my earnest gratitude and indebtedness to my supervisor, Prof. S. Chakraverty for his invaluable advice and guidance from the formative stage of this research and providing me extraordinary experiences throughout the work. The offered flexibility towards work and his profound insights have been true inspirations to my research. It is a great honour for me to have him as my supervisor. I am also thankful to his family members especially his wife Mrs. Shewli Chakraborty and daughters Shreyati and Susprihaa for their love, support and source of inspiration at all the time during my Ph. D. career.

I am grateful to Prof. S. K. Sarangi, Director, National Institute of Technology Rourkela for providing excellent facilities in the Institute for carrying out research. Also I would like to thank the members of my Doctoral Scrutiny Committee and all the faculties and staff members of the Department of Mathematics, National Institute of Technology Rourkela for their continuous advice and useful suggestions to complete this research work.

I am indebted to my lab mates Sukanta, Abhijit, Susmita Didi, Laxmi, Deepti and Nisha for their help and support during my stay in the laboratory and making it an amazing experience in my life. In addition, my sincere obligation and special thanks to Ms. Jaya Chakraborty, Department of Life Science (LEnME), National Institute of Technology Rourkela for her moral support, encouragements and inspirational words in the entire course of research work. The selfless help and encouragements of B. N. Singh, B. Patel and V. K. Verma have always been unfeigned. I cannot resist myself quoting my thanks to the developers of LaTeX compiler for making the thesis writing an experience indeed.

Last but not the least, I would like to acknowledge my deepest sense of gratitude to my parents and all my loved ones. My entire dedication to the work would have not been possible without their blessings, unconditional love, trust, moral support and strength, without whom none of my success is possible.

Karan Kumar Pradhan

Contents

Declaration i

Certificate ii

Dedication iii

Acknowledgement iv

Abstract x

1 Introduction 1

1.1 Literature review . . . 3

1.1.1 Static problems . . . 3

1.1.2 Vibration problems . . . 5

1.1.3 Various beam and plate theories . . . 13

1.1.4 Numerical methods . . . 14

1.2 Gaps . . . 18

1.3 Aims and objectives . . . 19

1.4 Organization of the thesis . . . 19

2 Preliminaries and new theories 23

2.1 Functionally Graded (FG) materials . . . 24

2.2 Existing theories . . . 26

2.2.1 Higher order shear deformation beam theory . . . 26

2.2.2 Classical plate theory . . . 28

2.3 Proposed theories . . . 29

2.3.1 Beam theories . . . 29

2.3.2 Plate theories . . . 31

2.4 Static and vibration problems . . . 33

2.4.1 FG static problem . . . 33
2.4.2 Vibration of FG beam . . . 34
2.4.3 Vibration of FG plate . . . 35

3 Numerical methods **37**
3.1 Rayleigh-Ritz method . . . 38
3.1.1 FG static problem . . . 39
3.1.2 Vibration of FG beam . . . 43
3.1.3 Vibration of FG plate . . . 46
3.2 Differential Quadrature (DQ) method . . . 57
3.2.1 Governing equation for free vibration . . . 57
3.2.2 Generalized Differential Quadrature (GDQ) . . . 58
3.2.3 Discretization of governing equation . . . 62

4 Static analysis of functionally graded plates **64**
4.1 Numerical modeling . . . 65
4.2 Convergence and comparison studies . . . 65
4.3 Results and discussions . . . 69
4.3.1 Effect of aspect ratios . . . 69
4.3.2 Effect of power-law exponents . . . 72
4.3.3 Effect of ratio of Young's moduli of the constituents . . . 74
4.4 Concluding remarks . . . 76

5 Vibration problems of functionally graded beams **78**
5.1 Vibration of uniform FG beam . . . 79
5.1.1 Numerical modeling . . . 79
5.1.2 Convergence and comparison studies . . . 80
5.1.3 Results and discussions . . . 94
5.2 Vibration of non-uniform FG beam . . . 120
5.2.1 Numerical modeling . . . 120
5.2.2 Convergence and comparison studies . . . 120
5.2.3 Results and discussions . . . 122
5.3 Concluding remarks . . . 147

6 Vibration problems of functionally graded rectangular plates 149

6.1 Thin FG rectangular plate . . . 150

6.1.1 Numerical modeling . . . 150

6.1.2 Convergence and comparison studies . . . 151

6.1.3 Results and discussions . . . 155

6.2 Special case of FG rectangular plate . . . 189

6.2.1 Numerical modeling . . . 190

6.2.2 Convergence and comparison studies . . . 191

6.2.3 Results and discussions . . . 195

6.3 Concluding remarks . . . 215

7 Vibration problems of functionally graded elliptic plates 217

7.1 Numerical modeling . . . 218

7.2 Convergence and comparison studies . . . 219

7.3 Results and discussions . . . 221

7.4 Concluding remarks . . . 228

8 Vibration problems of functionally graded triangular plates 230

8.1 Types of FG triangular elements . . . 231

8.2 Numerical modeling . . . 233

8.3 Convergence and comparison studies . . . 236

8.4 Results and discussions . . . 239

8.4.1 Effect of power-law indices (k) . . . 240

8.4.2 Effect of ratio of Young's moduli (E_r) . . . 250

8.4.3 Effect of ratio of mass densities (ρ_r) . . . 256

8.5 Concluding remarks . . . 266

9 Complicating effects 267

9.1 Winkler foundations . . . 268

9.1.1 Numerical modeling . . . 268

9.1.2 Convergence and comparison studies . . . 269

9.1.3 Results and discussions . . . 271

9.2 Winkler and Pasternak foundations . . . 277

9.2.1 Numerical modeling . . . 277

9.2.2 Convergence and comparison studies 280
9.2.3 Results and discussions 282
9.3 Thermal environments 302
9.3.1 Temperature field across the thickness 302
9.3.2 Numerical modeling 304
9.3.3 Results and discussions 306
9.4 Concluding remarks 311

10 Conclusions and future directions **313**
10.1 Conclusions 314
10.2 Future directions 319

References **321**

List of publications **333**

Abstract

The concept of Functionally Graded Materials (FGMs) was first enunciated in 1984 by a group of material scientists in Japan during a space plane project in the form of thermal barrier material which can withstand a huge temperature fluctuation across a very thin cross-section (Loy et al., 1999). Since then, FGMs have taken major attention as heat-shielding advanced structural materials in various engineering applications and in manufacturing industries viz. aerospace, nuclear reactor, automobile, aircrafts, space vehicles, biomedical and steel industries. These materials are generally ceramic-metal composites in which material properties vary continuously in thickness direction from one interface to another in a specific mathematical pattern. The ceramic constituent provides high-temperature resistance due to its low thermal conductivity, whereas the ductile metal constituent prevents fracture caused by stresses due to high temperature gradient in a very short span of time.

In this regard, static and dynamic characteristics of FG structural members are of considerable importance in both research and industrial sectors. On the other hand, these problems are governed by higher-order Partial Differential Equations (PDEs). However it is not always possible to find the analytical solutions for such problems. Accordingly numerical methods may be applied to solve such PDEs. Although there exists various numerical methods to handle these PDEs, but sometimes these are problem dependent and may not handle all sets of boundary conditions along with complicating effects with ease. So it is a challenging task to develop numerical methods which may be general to undertake the investigation.

Present problems have been investigated based on computationally efficient numerical procedures viz. Rayleigh-Ritz and Generalized Differential Quadrature (GDQ). At first, static problem related to thin FG rectangular plates subjected to various sets of possible classical boundary conditions under external mechanical loads is carried out using Rayleigh-Ritz method. Next, this method is also implemented to vibration problems of uniform FG beams based on different existing and newly proposed shear deformation beam theories, whereas GDQ to vibration of Euler-Bernoulli non-uniform FG beam. In addition, free vibration of thin FG plates under various possible classical boundary supports have been studied with different geometries viz. rectangular, elliptic and triangular. Then study on vibration of isotropic thick rectangular plates based on newly proposed shear deformation plate theories has been done. Lastly vibration of FG rectangular plates under different complicating effects is also studied.

The plate vibration problems along with complicating environments have been solved here by means of Rayleigh-Ritz method. In each of these investigations, FG material properties vary gradually in thickness direction either in power-law or exponential law forms. Numerical solution of titled problems are systematically found and corresponding results are reported after the test of convergence and comparison with available results.

Chapter 1

Introduction

Chapter 1

Introduction

The Functionally Graded Materials (FGMs) are well known as thermal barrier materials which can withstand a huge temperature fluctuation across a very thin cross-section. As such, FGMs have taken major attention as heat-shielding advanced structural materials in various engineering applications, designs, architectures and in manufacturing industries. These graded materials are generally ceramic-metal composites in which material properties vary continuously in thickness direction from one interface to another in a specific mathematical pattern. The ceramic constituent provides high-temperature resistance due to its low thermal conductivity, whereas the ductile metal constituent prevents fracture caused by stresses due to high temperature gradient in a very short span of time. As a result, static and dynamic characteristics of FG structural members are of considerable importance in both research and industrial sectors.

It is rightly mentioned by Penny (2004) that “the laws of the universe are written in the language of mathematics. Algebra is sufficient to solve many static problems, but the most important natural phenomena involve change and are described by equations that relate changing quantities. These are generally referred to as differential equations". In the similar fashion, static and dynamic problems associated with structural members are governed by higher-order partial differential equations. However it is not always possible to find the analytical solutions for such problems. Accordingly, the numerical methods may be applied to solve such differential equations. Although there exists various numerical methods to handle these partial differential equations, but sometimes these are problem dependent and may not handle all sets of boundary conditions along with complicating effects with ease. So it is a challenging task to develop numerical methods which may be general to undertake the investigation. As such, we have first surveyed the variety of works done towards the static and dynamic problems of isotropic and functionally graded structural members along with different composites using various analytical and numerical procedures.

1.1 Literature review

In earlier decades, the isotropic structural members along with composites have taken crucial role in different engineering applications, structural design and architectures. In recent years, the thermal withstanding behavior of functionally graded structural members have become significant in these applications. It can easily be noted in (Abrate, 2008) that functionally graded plates behave like homogeneous plates which require no special tools to analyze their mechanics. In this regard, present literature includes the analytical and numerical solutions of static and dynamic problems related to isotropic and functionally graded beams and plates. A brief idea on theoretical formulation associated with mechanics of different structural members may be found in the available resources viz. (Timoshenko and Woinowsky-Krieger, 1959; Wang et al., 2000; Reddy, 2000; Rao, 2004; Bhavikatti, 2005; Chakraverty, 2009) and the literatures provided therein. We start with a brief review on static problems associated with plates. Then literatures related to vibration of functionally graded beams are discussed. Significant studies on plates with different geometries have been reported next, followed by the effect of complicating environments in case of plates. Lastly, a critical survey on proposition of deformation theories and some numerical methods to handle such problems have also been done.

1.1.1 Static problems

In general, static or pure bending analysis provides static deflections, strains and stresses of structural members caused due to the external mechanical loads. On this basis, a number of investigations have been performed for the study of isotropic and functionally graded structural members along with different composites under external mechanical loads and complicated environments. A few of the major contributions related to these investigations based on different analytical and computational procedures have been incorporated in the following paragraph.

In particular, Rayleigh-Ritz method has been used by Chakraverty (1996) for the static deflection of isotropic circular and elliptic plates. Reddy et al. (1999) have studied axisymmetric bending and stretching of functionally graded circular and annular plates using first-order shear deformation plate theory. Werner (1999) has presented a Navier-type three-dimensional exact solution for small deflections in bending of linear elastic isotropic

plates having constant thickness. A closed form solution has been proposed by Cheng and Batra (2000b) for the thermo-mechanical deformations of an isotropic and linear thermoelastic functionally graded elliptic plate with rigidly clamped edge support. The heat conduction and temperature-dependent material properties are introduced in (Huang and Shen, 2001) to study nonlinear dynamic response of functionally graded plates. Nonlinear bending analysis of a simply supported functionally graded rectangular plate subjected to transverse uniform or sinusoidal load under thermal environments has been studied by Shen (2002). Based on classical nonlinear von Karman plate theory, Ma and Wang (2003) have investigated axisymmetric large deflection bending and post-buckling behavior of a functionally graded circular plate under mechanical, thermal and combined thermal-mechanical loadings. A semi-analytical solution is given in (Yang and Shen, 2003a) to present the large deflection and post-buckling responses of functionally graded rectangular plates under transverse and in-plane loads. In another literature, nonlinear bending analysis of shear deformable functionally graded plates subjected to thermo-mechanical loads has been proposed by Yang and Shen (2003b). Third-order shear deformation plate theory has been employed in (Ma and Wang, 2004) to solve axisymmetric bending and buckling of functionally graded circular plates. Kashtalyan (2004) has studied three-dimensional elasticity solution for a functionally graded simply supported plate subjected to transverse loadings. Ferreira et al. (2005) have used third-order shear deformation theory to analyze static deformation of a simply supported FG plate. Free vibration, buckling and static deflections of functionally graded plates have been given by Abrate (2006) under the action of thermal stresses, initial stresses and piezoelectric actuators. An approximate solution for the static analysis of three-dimensional, anisotropic and elastic functionally graded plates has been studied in (Ramirez et al., 2006) using a discrete layer theory in combination with the Ritz method. Zenkour (2006) has presented the static response for a simply supported functionally graded rectangular plate subjected to transverse uniform load. An analytical approach is assumed by Bouazza et al. (2010) to investigate the buckling of functionally graded plates under thermal loads. Neves et al. (2013) have considered Carrera's Unified Formulation (CUF) and collocation method with radial basis functions to find deflections, stresses, free vibration and buckling of functionally graded isotropic and sandwich plates. Thermoelastic bending response of functionally graded sandwich plates has been explained by Tounsi et al. (2013) using a refined trigonometric shear deformation theory. The analyses of dynamic deflection and stresses in FG plates resting on two-parameter elastic

foundations are investigated in (Zenkour and Sobhy, 2013). Zhang (2014) has implemented Ritz method in finding nonlinear bending solutions for FGM rectangular plates with six different boundaries resting on two-parameter elastic foundation. Several other researchers have also presented the bending, buckling and dynamic characteristics of functionally graded plates in various literatures (Nguyen et al., 2008; Brischetto et al., 2008; Saidi et al., 2009; Pradyumna and Bandyopadhyay, 2010; Talha and Singh, 2010; Taj and Chakrabarti, 2013).

1.1.2 Vibration problems

The study on vibration of beams and plates is an extremely important area owing to a wide variety of applications. Since these structural members form integral parts of structures, prior knowledge of their vibration behavior is very essential for an engineer before finalizing the design of a given structure. In particular, beams and plates with different shapes subjected to boundary conditions at the edges are often encountered in several engineering applications such as aeronautical engineering, automobile and telephone industries, machine design, nuclear reactor technology, naval structures and earthquake resistant structures etc. In spite of considering only isotropic cases, recent literature describes the vibration problems concerned with functionally graded beams and plates too. Accordingly, the vibration characteristics may be evaluated with the help of different analytical and computational techniques.

Functionally graded beams

The vibration problems concerned with isotropic structural members and various composites have been studied rigorously in earlier decades. But the research efforts on vibration analysis of functionally graded beams is limited. On the other hand, these problems are to be solved using different shear deformation beam theories (SDBTs) to estimate vibration characteristics of structural beams. A few of the significant investigations associated with vibration of functionally graded beams have been discussed below.

On contrary to FG beams, let us first discuss a few research efforts towards static and dynamic behavior of isotropic beams. A new theory for rectangular beams has been developed by Levinson (1981) which includes warping the cross-sections. Bhat (1986) has revealed the transverse vibration response of rotating uniform cantilever beam with a tip mass by using boundary characteristic orthogonal polynomials in Rayleigh-Ritz method. The finite element equations for a variationally consistent higher order beam theory have been presented by

Heyliger and Reddy (1988) for the static and dynamic behavior of rectangular beams. Reddy (1997) has designed a superconvergent finite element model for static problems of Timoshenko beams.

As such, the free vibration behavior of a simply supported FG beam has been studied by Aydogdu and Taskin (2007) by using Euler-Bernoulli beam theory, parabolic shear deformation theory and exponential shear deformation theory. A new beam theory was considered by Sina et al. (2009) different from traditional first-order shear deformation beam theory to analyze the free vibration of functionally graded beams with an analytical approach. Şimşek (2010b) has examined vibration response of a simply-supported FG beam to a moving mass by using Euler-Bernoulli , Timoshenko and the third-order shear deformation beam theories. Using different higher-order shear deformation beam theories, Şimşek (2010a) has also recently studied the fundamental frequencies of FG beams subjected to different boundary conditions. Mahi et al. (2010) have presented exact solutions to study the free vibration of functionally graded beam based on a unified higher order shear deformation theory, in which material properties are temperature dependent. An improved third order shear deformation theory is introduced in Wattanasakulpong et al. (2011) to study thermal buckling and elastic vibration of functionally graded beams. Alshorbagy et al. (2011) have used finite element method to study the free vibration characteristics of a functionally graded beam. Shahba et al. (2011) have investigated free vibration and stability analysis of axially functionally graded Timoshenko tapered beams using classical and non-classical boundary conditions through finite element approach. Using an analytical method, Thai and Vo (2012) have developed bending and free vibration of functionally graded beams using various higher-order shear deformation beam theories. Free vibration and stability of axially functionally graded tapered Euler-Bernoulli beams are investigated by Shahba and Rajasekaran (2012) using finite element method. Size dependent linear free flexural vibration behavior of FG nanoplates are investigated in Natarajan et al. (2012) using the iso-geometric based finite element method. Şimşek (2012) has found the free longitudinal vibration of axially functionally graded tapered nanorods based on the nonlocal elasticity theory. Free vibration analysis of size-dependent functionally graded nanobeams is studied by Eltaher et al. (2012) using finite element method. Static and buckling behaviors of nonlocal functionally graded Timoshenko nanobeam is investigated in Eltaher et al. (2014) based on finite element method. Vo et al. (2013) have presented static and vibration analysis of FG beams using refined shear deformation theory by using finite

element formulation. Static and free vibration of axially loaded rectangular FG beams is developed in Nguyen et al. (2013) based on the first-order shear deformation beam theory. The plane stress problem of an orthotropic functionally graded beam with arbitrary graded material properties along the thickness direction is investigated recently by the displacement function approach in (Nie et al., 2013). Huang et al. (2013) have investigated the vibration behavior of axially functionally graded Timoshenko beams with non-uniform cross-section by introducing an auxiliary function in the coupled governing equations. Also, the study of dynamic characteristics of functionally graded beams based on different shear deformation theories may have been discussed in (Kahrobaiyan et al., 2012; Lei et al., 2013; Rahmani and Pedram, 2014; Kien, 2014; Komijani et al., 2014; Sharma et al., 2014) and the articles provided therein. In this respect, a few literature concerned with isotropic and functionally graded beams are summarized in Table 1.1.

Table 1.1: Tabular representation of a few literature related to isotropic and FG beams

Structural elements	FG/Isotropic	References
Beam	1. Isotropic 2. FG	1. Bhat (1986); Öz (2000); Levinson (1981); Heyliger and Reddy (1988) 2. Aydogdu and Taskin (2007); Aydogdu (2009); Şimşek and Kocatürk (2009); Şimşek (2010b,a); Alshorbagy et al. (2011); Eltaher et al. (2012); Pradhan and Chakraverty (2013, 2014); Eltaher et al. (2014)

Functionally graded plates

Moreover, the vibration characteristics of isotropic as well as functionally graded plates with specific (or arbitrary) geometrical configurations have also been investigated, but the studies on thin functionally graded plates are scarce. Major findings on numerical solutions of such problems have been added below.

Initially let us first discuss the major investigations performed on numerical solutions of isotropic as well as functionally graded rectangular plates. In this regard, free vibration

frequencies of rectangular plates subject to different possible combinations of classical boundary conditions have been evaluated in (Leissa, 1973; Bhat, 1985; Singh and Chakraverty, 1994a,b) by means of Rayleigh-Ritz method. Roque et al. (2007) have examined free vibration of functionally graded plates based on a refined theory by the multiquadric radial basis function method. Reddy (2000) has presented a general formulation for functionally graded plates using third-order shear deformation plate theory. Free vibration of moderately thick rectangular plates has been investigated by Liu and Liew (1999) using differential quadrature element method. Yang and Shen (2001) have proposed the dynamic response of initially stressed functionally graded rectangular thin plates subject to distributed impulsive lateral loads resting on an elastic foundation. Natural frequencies of square FG plates have been computed by Ferreira et al. (2006) using asymmetric collocation method with multiquadric basis functions. It is clearly mentioned in (Abrate, 2008) that functionally graded plates behave like homogeneous plates using higher-order plate theory. Matsunaga (2008) has estimated the natural frequencies and buckling stresses of functionally graded plates based on a 2-D higher-order shear deformation theory. Exact closed-form solutions of 3-D elasticity theory are presented in (Hosseini-Hashemi et al., 2013) to study both in-plane and out-of-plane free vibrations for functionally graded simply supported rectangular plates.

In particular, a significant number of works on vibration behavior of isotropic elliptic and circular plates may also be found in open literature, whereas detailed analyses on thin functionally graded elliptic and circular plates have not yet been done. A few of major contributions on these studies have been reported here. Accordingly, Mazumdar (1971) has computed fundamental frequencies of elliptic plates subjected to both clamped and simply supported edge supports by the method of constant deflection lines. Leissa and Narita (1980) have analyzed the natural frequencies of simply supported circular plates using classical plate theory with ordinary and modified Bessel functions of the first kind. Galerkin and Bolotin's methods are used by Chen and Hwang (1988) to study dynamic stability of isotropic Mindlin circular plates subjected to periodic radial loads. The spline-finite-strip method with subparametric mapping concept is employed by Cheung and Tham (1988) in static and free vibration analysis of arbitrary shaped plates. Transverse vibration of isotropic elliptic plates subjected to different classical boundary supports can be found in Singh and Chakraverty (1991, 1992a,b). Circular and elliptic plates with variable thickness have been investigated in (Singh and Chakraverty, 1994b) with all three classical boundary conditions. Natural frequencies for

free vibration of nonhomogeneous circular and elliptic plates using two dimensional orthogonal polynomials is studied in (Chakraverty and Petyt, 1997). Liew et al. (1997) used differential quadrature method and linear shear deformation Mindlin theory to analyze axisymmetric free vibration characteristics of moderately thick circular plates. Reddy et al. (1999) have used first-order shear deformation Mindlin plate theory to study axisymmetric bending and stretching of functionally graded solid and annular circular plates. Three-dimensional vibration of circular and annular plates are analyzed in (Liu and Lee, 2000) using finite element method and in (Zhao et al., 2003) applying Chebyshev-Ritz method. Free vibration of solid circular plates has been studied in (Wu and Liu, 2001; Wu et al., 2002) by applying generalized differential quadrature rule. Buckling analysis is presented in (Najafizadeh and Eslami, 2002) for radially loaded functionally graded solid circular plate subject to either clamped or simply supported edge conditions. Ma and Wang (2003) investigated axisymmetric large deflection bending and thermal post-buckling behavior of functionally graded circular plate under mechanical, thermal and combined thermo-mechanical loadings based on classical nonlinear von Karman plate theory. An inverse problem of a functionally graded elliptic plate is developed by Hsieh and Lee (2006) with large deflection and distributed boundary under uniform load. Prakash and Ganpathi (2006) have found free vibration characteristics and thermoelastic stability of functionally graded circular plates using finite element procedure. Chakraverty et al. (2007) have provided vibration behavior of plates by using the effects of non-homogeneity.

It may also be observed that triangular plates have very important applications in structural design and architecture. On this basis, present survey provides the works done in case of isotropic triangular plates and a very few investigations performed in functionally graded triangular plates. As regards, Mirza and Bijlani (1985) have found the natural frequencies and mode shapes of cantilevered triangular plates with variable thickness using the finite element technique. Gorman (1983, 1986, 1989) has proposed a highly accurate analytical solutions (method of superposition) for free vibration of right triangular plates with simply supported edge supports, with combinations of clamped-simply supported boundary supports and different boundary conditions with one edge free respectively. A highly accurate simplified solution has been given by Saliba (1990) to study the free vibration of simply supported right triangular thin plates. Singh and Chakraverty (1992c) have done an exhaustive study on isotropic triangular plates by applying Rayleigh-Ritz method to handle all sets of classical

edge supports. Wanji and Cheung (1998) have found the bending, vibration and buckling of a refined triangular discrete Kirchoff thin plate element (RDKT) in order to improve the results for the original triangular discrete Kirchoff thin plate element (DKT). An approximate method using Green function is developed by Sakiyama and Huang (2000) for free vibration of right triangular plates with variable thickness. Zhong (2000) has applied a triangular differential quadrature method to study free flexural vibration of isosceles triangular Mindlin plates. Reddy's third order plate theory is used by Cheng and Batra (2000a) to study buckling and steady state vibrations of a simply supported FG polygonal plate resting on a Winkler-Pasternak elastic foundation. Non-dimensional influence (Green's) function has been applied by Kang and Lee (2001) in free vibration analysis of arbitrarily shaped plates with clamped edges. Free vibration of cantilevered and completely free isosceles triangular plates has been investigated by Cheung and Zhou (2002) based on exact three-dimensional elasticity theory. Moreover, very few authors have worked especially on FG triangular plates. Belalia and Houmat (2012) have developed a *p*-version finite element method based on a curved triangular *p*-element to analyze nonlinear free vibration of functionally graded sector plates. On this note, a few literature associated with isotropic and FG plates with different geometries (rectangular, elliptic and triangular) are addressed in Table 1.2.

Table 1.2: Tabular representation of a few literature related to isotropic and FG plates with different geometries

Structural elements	FG/Isotropic	References
Rectangular (or square) plate	1. Isotropic 2. FG	1. Leissa (1973); Bhat (1985); Singh and Chakraverty (1994a,b); Liu and Liew (1999) 2. Yang and Shen (2001); Ferreira et al. (2006); Abrate (2008); Hosseini-Hashemi et al. (2013); Chakraverty and Pradhan (2014b,a)
Elliptic (or circular) plate	1. Isotropic 2. FG	1. Mazumdar (1971); Leissa and Narita (1980); Chen and Hwang (1988); Singh and Chakraverty (1991, 1992b,a); Reddy et al. (1999) 2. Najafizadeh and Eslami (2002); Ma and Wang (2003); Hsieh and Lee (2006); Prakash and Ganpathi (2006)
Triangular plate	1. Isotropic 2. FG	1. Gorman (1983, 1986, 1989); Mirza and Bijlani (1985); Saliba (1990); Singh and Chakraverty (1992c); Wanji and Cheung (1998); Cheung and Zhou (2002) 2. Belalia and Houmat (2012)

Complicating effects

As mentioned earlier that the concept of functionally graded materials is derived to withstand a huge temperature fluctuation. In real life applications, the structural members may be under various complicating environments viz. thermal effects, elastic foundations, piezoelectric

effects etc. which play major role in judging vibration characteristics of isotropic as well as functionally graded plates. In this regard, present literature helps to find variety of investigations performed in these domains.

Let us first discuss the studies on the effect of elastic foundation on vibration characteristics of plates. As such, the elastic bending, buckling and vibration of Levy plates resting on various two-parameter elastic foundations is investigated by Lam et al. (2000). Dynamic response of initially stressed functionally graded rectangular thin plates is obtained by Yang and Shen (2001) subjected to partially distributed impulsive lateral loads and without or resting on an elastic foundation. Hosseini-Hashemi and Arsanjani (2005) have presented the exact closed form characteristic equations for the Mindlin plates with two opposite edges simply supported. The exact solutions for free vibration analysis of rectangular Mindlin plates have been obtained by Akhavan et al. (2009) under in-plane loads resting on Pasternak elastic foundation. Free vibration analysis of vertical rectangular Mindlin plates resting on Pasternak elastic foundation is given in Hosseini Hashemi et al. (2010) for different combinations of boundary conditions. Baferani et al. (2011) have presented vibration analysis of functionally graded rectangular plate resting on two parameter elastic foundation based on third order shear deformation theory. Flexural vibration of Lévy-type rectangular plates has been studied by Hosseini-Hashemi et al. (2011) within the framework of third-order shear deformation theory. A refined shear deformation theory is considered by Thai and Choi (2012) for free vibration of functionally graded plates on elastic foundation. Fallah et al. (2013) have studied free vibration analysis of moderately thick FG rectangular plates on elastic foundation.

Next, this paragraph includes different works done on mechanics of structural members in thermal environments. Based on first order shear deformation theory (FSDT), Reddy and Chin (1998) have analyzed the dynamic thermoelastic response of functionally graded cylinders and plates using thermomechanical coupling. Nonlinear bending analysis is presented by Shen (2002) for a simply supported functionally graded plate subjected to a transverse uniform or sinusoidal loads in thermal environments. Yang and Shen (2002) have presented free and forced vibration analyses for initially stressed functionally graded plates in thermal environment. One may also see (Kim, 2005; Kitipornchai et al., 2006; Li et al., 2009a; Malekzadeh and Beni, 2010; Shi and Dong, 2012) and also the literatures therein to get the study associated with the effect of thermal or temperature environment on vibration analysis of functionally graded plates. An analytical model is developed by Bouchafa et al. (2010) for prediction

of thermal residual stresses, arising from the fabrication of exponential functionally graded material systems. Considering the complicating effects, Chakraverty and Pradhan (2014a,b) have investigated free vibration of thin FG rectangular plates in very recent literature.

One of the basic vibration-based harvesting materials, piezoelectric effect is the ability of certain materials to generate an electric charge in response to applied mechanical stress. The piezoelectric materials are useful for vibration control as both an actuator and a sensor and these have paid much attention in various engineering applications. In structural applications, these actuators can be surface bonded or embedded. In this regard, Chen and Ding (2002) have derived three-dimensional theory equations of transversely isotropic piezoelectricity and two independent state equations with variable coefficients for FG piezoelectric rectangular plate. Bian et al. (2006) have found an exact analysis based on state-space formulation to study FG beams integrated with surface piezoelectric actuators and sensors. The plane stress problem of generally anisotropic piezoelectric beams is solved by Huang et al. (2007) with coefficients of elastic compliance, piezoelectric and dielectric impermeability. Moreover, free vibration of statically thermal postbuckled FG material beams with surface bonded piezoelectric layers subject to both temperature rise and voltage is investigated (Li et al., 2009b). Based on the theory of elasticity and piezoelectricity, the state-space based differential quadrature method (SSDQM) is implemented to study free vibration of a functionally graded piezoelectric material (FGPM) under different boundary conditions by Yang and Zhifei (2009). Analytical solution for FG material beams integrated with piezoelectric actuator and sensor has been studied by Alibeigloo (2010) under an applied electric field and thermo-mechanical load. The nonlinear dynamic response and active vibration control of piezoelectric FG plate are analyzed in (Yiqi and Yiming, 2010). A size-dependent FG piezoelectric beam model is developed in (Li et al., 2014) using a variational formulation to find the static bending and free vibration characteristics. On the other hand, one may see a very few works have been done in case of piezoelectric FG plates with different geometries. Harmonic forced vibration of circular FG plate integrated with two uniformly distributed piezoelectric actuator faces has been studied by Jandaghian et al. (2014).

1.1.3 Various beam and plate theories

From the above survey, it may easily be concluded that static and dynamic problems of structural beams and plates are controlled by displacement fields involved in shear deformation

theories. The transverse shear deformation is generally neglected in case of classical beam and plate theory, which results discrepancies in finding mechanics of structural members. Based on this fact, different shear deformation theories have been proposed in various articles. Accordingly, a list of deformation beam and plate theories related to isotropic members are available in (Wang et al., 2000). Further, Reddy (1984a) has given a refined nonlinear theory accounting for the von Karman strains to find exact solutions for simply supported plates. A new higher-order shear deformable laminated composite plate theory is proposed by Aydogdu (2009) using 3-D elasticity bending solutions in an inverse method. Infinitesimal deformations of a homogeneous thick elastic plate have been investigated by Xiao et al. (2007) by using a meshless Petrov-Galerkin (MLPG) method and a higher-order shear and normal deformable plate theory. Moreover, Reddy (2011) has developed a microstructure-dependent nonlinear Euler-Bernoulli and Timoshenko beam theories using the principle of virtual displacements. A general assessment of inverse trigonometric shear deformation theory is developed by Grover et al. (2013) to analyze structural responses of laminated-composite and sandwich plates. A general higher-order shear deformation theory is proposed by Qu et al. (2013) for free and transient vibration analyses of composite laminated beams with arbitrary combinations of classical and non-classical boundary conditions. Thai et al. (2014) have recently introduced an inverse tangent shear deformation theory for the static, free vibration and buckling analysis of laminated composite and sandwich plates. In a similar fashion, a major topic in deriving shear deformation theories can also be found in (Sina et al., 2009; Xiang et al., 2009; Şimşek, 2010a; Thai and Vo, 2012; Şimşek and Reddy, 2013; Qu et al., 2013; Vo et al., 2013) and the literatures mentioned therein.

1.1.4 Numerical methods

It may be seen from the above literature review that various analytical and numerical techniques have been developed and used for the titled problems. Our main aim here is to develop numerical schemes to handle the governing partial differential equations of the said problems. As such the computational methods that have been used by other authors are surveyed below.

In general, a few of the widely used methods may be mentioned as finite difference (FDM), boundary element (BEM), finite element (FEM), differential quadrature (DQM), collocation, Galerkin , Rayleigh-Ritz and meshless Petrov-Galerkin (MLPG) etc. In recent decade, a combination of methods viz. mixed Ritz-DQM, mixed FEM-DQM, mixed FEM-Ritz etc.

have also been implemented in these studies. One may easily find conventional procedure to follow in finite element in open resources (Rao, 2004; Bhavikatti, 2005) and literature given therein. Mirza and Bijlani (1985) have found the natural frequencies and mode shapes of cantilevered triangular plates with variable thickness using the finite element technique. Galerkin and Bolotin's methods are used by Chen and Hwang (1988) to study dynamic stability of isotropic Mindlin circular plates subjected to periodic radial loads. Three-dimensional vibration of circular and annular plates are analyzed in (Liu and Lee, 2000) using finite element method. Natural frequencies of square FG plates have been computed by Ferreira et al. (2006) using asymmetric collocation method with multiquadric basis functions. Neves et al. (2013) have considered Carrera's Unified Formulation (CUF) and collocation method with radial basis functions to find deflections, stresses, free vibration and buckling of functionally graded isotropic and sandwich plates. Alshorbagy et al. (2011) have used finite element method to study the free vibration characteristics of a functionally graded beam. Shahba et al. (2011) have investigated free vibration and stability analysis of axially functionally graded Timoshenko tapered beams using classical and non-classical boundary conditions through finite element approach. Free vibration and stability of axially functionally graded tapered Euler-Bernoulli beams are investigated by Shahba and Rajasekaran (2012) using finite element method. Size dependent linear free flexural vibration behavior of FG nanoplates are investigated in Natarajan et al. (2012) using the iso-geometric based finite element method. Free vibration analysis of size-dependent functionally graded nanobeams is studied by Eltaher et al. (2012) using finite element method. Vo et al. (2013) have presented static and vibration analysis of FG beams using refined shear deformation theory by using finite element formulation. Prakash and Ganpathi (2006) have found free vibration characteristics and thermoelastic stability of functionally graded circular plates using finite element procedure. A mixed Ritz-DQ method has been used in free and forced vibration of functionally graded beams and isotropic rectangular plates in (Khalili et al., 2010; Eftehari and Jafari, 2012, 2013). Moreover these methods generally follow certain systematic algorithms and may not control all combinations of classical boundary conditions with ease.

One of the efficient numerical techniques, so-called Rayleigh-Ritz method has taken a major attention for solving the problems of isotropic structural members. Different investigations performed based on this technique have been discussed here. In this regard, natural frequencies of simply supported elliptic plates are evaluated by Leissa (1967) by means of Rayleigh-Ritz

technique. The procedures followed by this method can easily be found in (Timoshenko and Woinowsky-Krieger, 1959; Kelly, 1999; Rao, 2004; Chakraverty, 2009). The characteristic orthogonal polynomials in Rayleigh-Ritz method were first developed by Bhat (1986) to estimate the transverse vibration response of rotating cantilever beam with a tip mass. In another literature, Bhat (1987) have implemented a set of characteristic orthogonal polynomials to find the natural frequencies and mode shapes of polygonal plates by means of Rayleigh-Ritz method. The natural frequencies of rectangular plates using characteristic orthogonal polynomials have been computed in (Bhat, 1985; Cupial, 1997) using Rayleigh-Ritz method. Kim and Dickinson (1990, 1992) have studied free vibration of isotropic and orthotropic right triangular plates and of general triangular plates respectively by using Rayleigh-Ritz method. Then Singh and Chakraverty (1991, 1992a,b) have developed two-dimensional boundary characteristic orthogonal polynomials and studied transverse vibration of elliptic and circular plates using orthogonal polynomials in Rayleigh-Ritz method satisfying different boundary conditions viz. completely-free, simply-supported and clamped respectively. Axisymmetric vibration of circular and its analogous elliptic plates are examined by Rajalingham and Bhat (1993) using characteristic orthogonal polynomials. Rajalingham et al. (1994) have analyzed vibration of clamped elliptic plates using exact circular plate modes as shape functions in Rayleigh-Ritz method. Transverse vibrations of triangular plates have also been investigated by Singh and Chakraverty (1992c) with various types of boundary conditions at the edges by using boundary characteristics orthogonal polynomials as basis functions in the Rayleigh-Ritz method. The pb-2 Rayleigh-Ritz method is employed by Liew (1993) to study the free flexural vibration of triangular plates with/without curved internal supports. Free vibration analysis of thick cantilevered triangular plates is investigated by Karunasena et al. (1996) using pb-2 Rayleigh-Ritz method based on the Mindlin shear deformation theory. Singh and Saxena (1996) have solved transverse vibration of triangular plates with variable thickness by working out several approximations in Rayleigh-Ritz method. Rayleigh-Ritz method is also employed by Singh and Hassan (1998) to obtain the numerical solution of a triangular plate with arbitrary thickness variation. A fast converging series consisting of a set of static beam functions is developed by Ding (1996) to study vibration characteristics of thin rectangular plates. Ilanko (2009) has commented on the historical bases of Rayleigh and Ritz methods. Carrera et al. (2011) have implemented refined plate theories in finding accurate free vibration analysis of anisotropic simply supported plates. The flapwise and chordwise bending vibration analysis of

rotating pre-twisted Timoshenko beam are examined in (Zhu, 2011) by the use of Rayleigh-Ritz method. Free vibration of the baffled circular plates with radial side cracks and in contact with water on one side is studied by Si et al. (2012) based on Rayleigh-Ritz method.

In spite of using only Rayleigh-Ritz method, another efficient numerical technique viz. Differential Quadrature Method (DQM) is also considered to evaluate vibration characteristics of structural members. As such, present survey also includes the works done by using DQM. Initially, the foundation of DQM has been proposed by Bellman and Casti (1971) and implemented in various classes of partial differential equations by reducing them to ordinary differential equations and then to finite dimensional systems. A precise idea on ways to develop DQM in various forms, numerical solution of different classes of linear and nonlinear partial differential equations, splines and efficiency of this method can be observed in (Bellman et al., 1972, 1975; Naadimuthu et al., 1984). Following the previous approach (Bellman et al., 1972) on DQM, Quan and Chang (1989a,b) have provided new insights in solving distributed system equations by the method of differential quadrature along with results of a series of numerical experiments. The analysis of laminated composite structures has been performed by Bert and Malik (1997) using this method. After a close observation to previous studies (Bellman et al., 1972; Quan and Chang, 1989a,b), Shu and Du (1997) have developed Generalized Differential Quadrature (GDQ) method for implementing clamped and simply supported boundary conditions for the free vibration analysis of beams and plates. In the similar fashion, a few major changes have also been incorporated in DQM in recent decades by combining with other numerical methods. As such, a mixed Ritz-DQ method has been used in free and forced vibration of functionally graded beams and isotropic rectangular plates in (Khalili et al., 2010; Eftehari and Jafari, 2012, 2013). A novel and simple approach is presented by Huang and Li (2010) for free vibration of functionally graded beams with non-uniform cross-section. Hein and Feklistova (2011) have investigated vibrations of non-uniform and functionally graded beams using the Euler-Bernoulli beam theory and Haar matrices. A new approach has been employed by Huang et al. (2013) for investigating the vibration behaviors of axially functionally graded beams with non-uniform cross-section. Rajasekaran (2013) have studied free vibration of axially FG non-uniform beams with different boundary conditions using differential quadrature method.

1.2 Gaps

Above literature review reveals that there are various gaps in the study of static and dynamic problems associated with isotropic as well as functionally graded structural members. In particular, there are very few investigations on static problem of FG plates and vibration of FG beams and plates. Moreover previously used numerical procedures may either be problem dependent or may handle only limited boundary conditions rather than all classical boundary supports. As such, we may point out the following gaps.

- Governing partial differential equations for static and dynamic problems of FG beams and plates with various possible classical boundary conditions are not studied in detail. As such, present study involves the analysis based on two computationally efficient numerical schemes viz. Rayleigh-Ritz and differential quadrature methods may be suitable to handle such problems.

- No exhaustive study on static analysis of thin functionally graded rectangular plates with different classical boundary conditions has been done.

- Vibration of functionally graded beams based on various existing shear deformation beam theories have not yet been studied for all classical boundary conditions. Moreover, existing shear deformation theories may also be modified by means of other mathematical functions which satisfy certain assumptions (Reddy, 1984a; Aydogdu, 2009). Based on these facts, new shear deformation theories may also be proposed to handle above vibration problems.

- Study on vibration of geometrically nonlinear functionally graded beams has not been performed.

- Very few studies on vibration of thin functionally graded plates based on classical plate theory has been carried out. In these problems, different geometrical configurations along with various complicating effects viz. elastic foundation and thermal environment etc. may also be considered.

- Investigation on vibration of thick isotropic rectangular plates based on newly proposed shear deformation plate theories.

1.3 Aims and objectives

In view of the above gaps, following are the aims and objectives of the present investigation.

- Numerical methods viz. Rayleigh-Ritz and generalized differential quadrature are found to be helpful to handle the titled problems, where we may study static and dynamic problems with all classical boundary conditions.
- To analyze static (pure bending) problems concerned with thin functionally graded rectangular plates under the action of external mechanical loads.
- To investigate free vibration of functionally graded beams based on existing shear deformation beam theories and then to propose (new) shear deformation beam theory. Implementation of these theories in vibration of functionally graded beams for the validation.
- To investigate vibration problems of geometrically nonlinear functionally graded beams.
- To estimate vibration characteristics of thin functionally graded plates having different geometrical configurations viz. rectangular, elliptic and triangular. Then to apply the proposed shear deformation theories in finding vibration characteristics of isotropic thick rectangular plates.
- Finally, to study free vibration of thin functionally graded rectangular plates in presence of different complicating effects viz. elastic foundation and thermal environment.

1.4 Organization of the thesis

Present thesis aims to investigate the static and dynamic problems associated with some functionally graded structural members such as beams and plates. These problems are generally governed by various partial differential equations (PDEs) and accordingly we need to develop computationally efficient numerical techniques to handle the titled problems. Typically, the classical boundary conditions considered here are clamped (C), simply supported (S) and free (F). This thesis comprises of ten chapters and short descriptions of each chapter has been stated below.

Chapter 1 introduces previous investigations performed associated with the numerical solutions for static and dynamic problems of FG beams and plates. The gaps are identified as per literature survey and the basic objectives of present investigation have been incorporated.

In Chapter 2, the first part contains the basic assumptions to be considered in case of functionally graded materials. In second part, the shear deformation beam (and plate) theories and their corresponding stress-strain relations have been discussed. We have then proposed a few new shear deformation beam and plate theories by satisfying certain assumptions. Assuming the respective deformation theories, the governing (or equilibrium) equations defining the static analysis of thin functionally graded plate and vibration of functionally graded beams and plates have also been added in the final section of this chapter.

Chapter 3 is based on algorithms concerned with two computationally efficient numerical techniques viz. Rayleigh-Ritz and differential quadrature methods. The Rayleigh-Ritz solution procedure has been discussed to solve the static problem of thin FG rectangular plate and vibration problems of FG beams as well as plates. Next, the numerical algorithms followed by the method of generalized differential quadrature (Shu and Du, 1997) is discussed to investigate vibration of geometrically non-linear FG beam.

Chapter 4 presents static analysis of functionally graded rectangular plates subjected to various sets of possible classical boundary conditions by applying Rayleigh-Ritz method. The material properties of FG rectangular plate are assumed to vary continuously in the thickness direction according to power-law form. Uniformly distributed load (UDL) and hydrostatic pressure are assumed to be the external mechanical loads. Effect of three major parameters viz. aspect ratio (length-to-breadth ratio), power-law index and ratio of Young's moduli of constituents on pure bending parameters have been studied. New results have been incorporated on the basis of convergence and validation with available results in special cases. Computational results on pure bending parameters are diagrammatically demonstrated and the conclusions are drawn.

In Chapter 5, free vibration of functionally graded beams within the framework of existing and newly proposed shear deformation beam theories have been investigated by using Rayleigh-Ritz method. On the other hand, the method of differential quadrature is also applied to study free vibration of geometrically non-linear functionally graded beams. Here also, the power-law variation of material properties of FG beam constituents is considered. The main aim of these problems is to solve the related PDEs to evaluate the natural frequencies. In

each case of shear deformation theories, first five natural frequencies for six possible sets of boundary conditions have been computed after checking the convergence and comparison with existing results. The behavior of free vibration frequencies on the slenderness ratio (length-to-thickness ratio), volume fractions of FG constituents and different shear deformation beam theories are also studied systematically.

In Chapter 6, free vibration of thin functionally graded rectangular (and square) plates subjected to possible combination of classical edge supports has been investigated in detail. The material properties of FG plate constituents are assumed to vary along thickness direction both in power-law and exponential law forms. In both the gradation cases, test of convergence and validation of eigenfrequencies have been performed and six lowest natural frequencies for FG plate with specific boundary supports have been evaluated. This chapter also introduces free vibration of isotropic thick rectangular plates based on newly proposed inverse trigonometric shear deformation plate theories along with some existing plate theories. In case of thick isotropic rectangular plate, first six natural frequencies have been computed for different aspect ratios and thickness-to-length ratios. First six three-dimensional mode shapes for a few combination of edge conditions in FG and thick isotropic plates have also been depicted here.

Chapter 7 includes the solution of vibration of functionally graded elliptic (and circular) plates subjected to all possible classical boundary supports. Effect of aspect ratios (ratio of major and minor axes) and gradation of constituent volume fractions on the six lowest natural frequencies have been investigated. New results for these frequencies have been incorporated after performing a test of convergence. Comparison study is also carried out with existing literature for validation in special cases. Three–dimensional mode shapes for circular and elliptic FG plates with classical boundary conditions at the edges are also demonstrated.

Chapter 8 deals with free vibration of FG triangular plates subjected to various classical boundary conditions at three edges. Different geometries of triangular elements viz. right-angled, equilateral and isosceles are also considered. An exhaustive computation of first six natural frequencies for these triangular plate elements has been carried out after the test of convergence and validation of numerical results in special cases. These evaluations are performed in reference to three major factors viz. power-law index, ratio of Young's moduli and mass densities of FG constituents. Three–dimensional mode shapes for clamped-clamped-clamped and clamped-free-free triangular plates are also plotted corresponding to their first six non–dimensional frequencies.

In Chapter 9, the effect of complicating environments viz. Winkler (or Pasternak) elastic foundations and thermal environments on free vibration of thin FG rectangular plates have been studied. In each case, the numerical formulations of Rayleigh-Ritz method have been discussed too. The FG plate with Winkler (or Pasternak) elastic foundations assumes power-law gradation of material properties, whereas exponential gradation is considered in FG plate under thermal environment. Numerical results for natural frequencies are computed on the basis of the factors involved in these complicating environments viz. foundation modulus in elastic foundation and rise of temperature in thermal environment after the test of convergence and comparison in special cases.

Chapter 10 incorporates the conclusions drawn based on varieties of problems solved on functionally graded beams and plates. Finally future direction of research are also pointed out here.

Chapter 2

Preliminaries and new theories

Chapter 2

Preliminaries and new theories

In this chapter, the basic components to handle the titled problems on functionally graded beams and plates have been incorporated. At first, the concept and variation of material properties in case of these members are mentioned followed by previously proposed shear deformation beam (and plate) theories. Rather than assuming only existing theories, a few new deformation theories have also been proposed based on certain assumptions. Considering the displacement fields of deformation theories, the governing equations related to the static and dynamic problems are also reported.

2.1 Functionally Graded (FG) materials

The functionally graded materials (FGMs) are the special composite materials that have been developed because of their high temperature-resistant properties with a comparatively less thickness. The primary constituents for these materials are metal with ceramic or from a combination of materials. The ceramic constituent provides high-temperature resistance due to its low thermal conductivity. On the other hand, the ductile metal constituent prevents fracture caused by stresses due to high temperature gradient in a very short span of time. In this regard, FGMs have been widely used in most of the industrial applications and structural engineering design viz. aerospace, nuclear, biomedical, electronics and in many other fields. The concept of FGMs was first enunciated in 1984 by a group of material scientists while preparing a space-plane project, in Japan (Loy et al., 1999). The material properties in FGMs vary continuously along thickness direction in a specific mathematical pattern.

The variation of material properties of FG beam (or plate) constituents in power law can be defined as (Aydogdu and Taskin, 2007; Şimşek and Kocatürk, 2009; Sina et al., 2009)

$$\mathcal{P}(z) = (\mathcal{P}_c - \mathcal{P}_m)\left(\frac{z}{h} + \frac{1}{2}\right)^k + \mathcal{P}_m \tag{2.1}$$

and on the other hand, in exponential law as (Aydogdu and Taskin, 2007; Şimşek and Kocatürk, 2009)

$$\mathcal{P}(z) = \mathcal{P}_c e^{-\delta\left(1-\frac{2z}{h}\right)} \tag{2.2}$$

In Eqs. (2.1) and (2.2), $\mathcal{P}_c$ and $\mathcal{P}_m$ denote the values of the material properties of the ceramic and metal constituents of the FG beam (or plate) respectively. In power-law variation, k (power-law exponent) is a non-negative variable parameter. In exponential gradation, $\delta = \frac{1}{2}ln\left(\frac{\mathcal{P}_c}{\mathcal{P}_m}\right)$. According to these gradation behavior, the bottom surface ($z = -h/2$) of FG beam (or plate) is pure metal, whereas the top surface ($z = h/2$) is pure ceramic and for different values of k, one can obtain different volume fractions of material beam (or plate) as mentioned in (Aydogdu and Taskin, 2007). For our present formulations, the material properties viz. Young's modulus (E) and mass density (ρ) are taken to vary along thickness direction and Poisson's ratio (ν) is considered as constant.

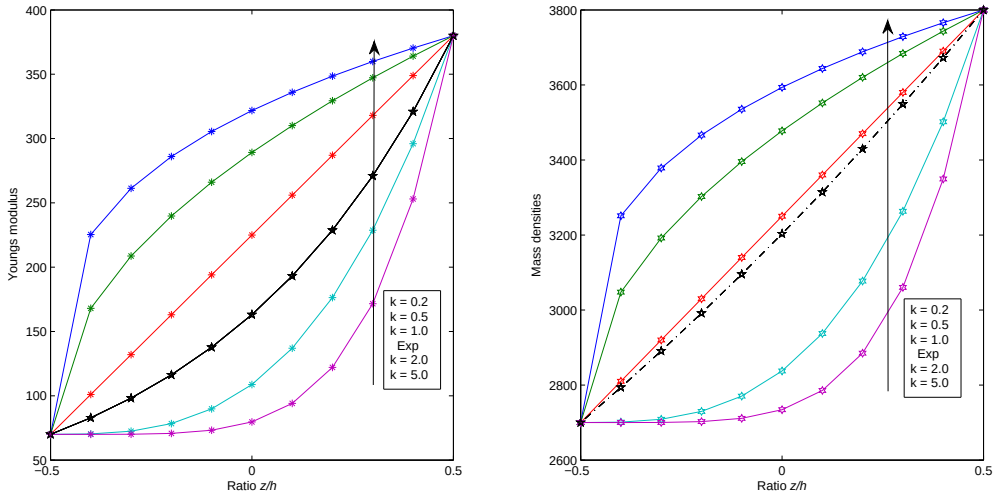

(a) Variation of Young's modulus (b) Variation of mass densities

Figure 2.1: Power-law and exponential variations of (a) Young's modulus and (b) mass densities of the FG beam (or plate)

2.2 Existing theories

2.2.1 Higher order shear deformation beam theory

Let us consider a straight FG beam of length L, width b and thickness h, having rectangular cross-section with cartesian coordinate system O(x, y, z) having the origin at O as shown in Fig. 2.2.

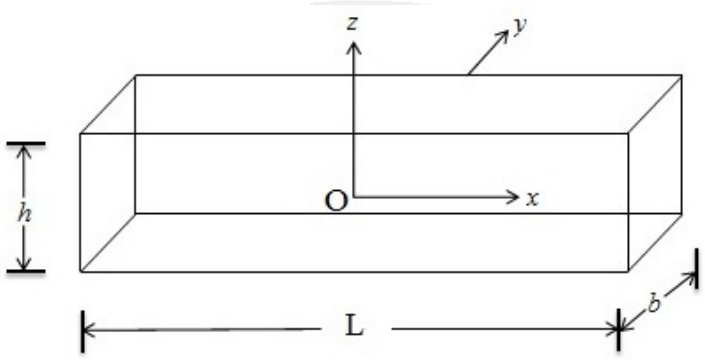

Figure 2.2: A typical functionally graded beam element with cartesian coordinates

The dynamic problems concerned with FG beam are to be handled by the shear deformation beam theories. As such, let the deformation of FG beam be assumed in the $x-z$ plane and the displacement components along x, y and z directions be denoted as u_x, u_y and u_z respectively. Based on the higher order shear deformation beam theory, the axial displacement (u_x) and the transverse displacement (u_z) at any point of the beam are given as below (Aydogdu and Taskin, 2007):

$$\begin{aligned} u_x(x,z) &= u(x,t) - z w_{,x}(x,t) + f(z) v(x,t) \\ u_z(x,z) &= w(x,t) \end{aligned} \tag{2.3}$$

where u and w represent the axial and the transverse displacement of any point on the neutral axis respectively, while v is an unknown function that represents the effect of transverse shear strain on the neutral axis. $f(z)$ represents the shape function determining the distribution of the transverse shear stress and strain through the thickness of the beam and $(\,)_{,x}$ indicates the derivative with respect to x. Different theories can be obtained by choosing their respective shape functions $f(z)$. Present study is concerned with Shear Deformation Beam Theories (SDBTs) viz. Classical Beam Theory (CBT), Timoshenko Beam Theory (TBT), Parabolic Shear Deformation Beam Theory (PSDBT), Exponential Shear Deformation Beam

Theory (ESDBT), Trigonometric Shear Deformation Beam Theory (TSDBT), Hyperbolic Shear Deformation Beam Theory (HSDBT) and a new Shear Deformation Beam Theory (ASDBT), as mentioned in (Şimşek, 2010a). $f(z)$ for these shear deformation beam theories are given below (Şimşek, 2010a):

$$\begin{aligned}
&\text{CBT} : f(z) = 0 \\
&\text{TBT} : f(z) = z \\
&\text{PSDBT} : f(z) = z\left(1 - \frac{4z^2}{3h^2}\right) \\
&\text{ESDBT} : f(z) = ze^{-2(z/h)^2} \\
&\text{HSDBT} : f(z) = h\sinh\left(\frac{z}{h}\right) - z\cosh\left(\frac{1}{2}\right) \\
&\text{TSDBT} : f(z) = \frac{h}{\pi}\sin\left(\frac{\pi z}{h}\right) \\
&\text{ASDBT} : f(z) = z\alpha^{-2(z/h)^2/ln\alpha} \text{ with } \alpha = 3
\end{aligned} \tag{2.4}$$

The following relations represent the kinematic relations as per the above displacement field (Eq. (2.4))

$$\varepsilon_{xx} = u_{,x} - zw_{,xx} + f(z)v_{,x} \tag{2.5}$$

$$\gamma_{xz} = f'(z)v \tag{2.6}$$

where a prime denotes the derivative with respect to z. ε_{xx} and γ_{xz} are the normal and shear strains respectively. By assuming the material constituents of FGM beam to obey the generalized Hooke's law, the state of stresses in the beam can be expressed as

$$\sigma_{xx} = Q_{11}\varepsilon_{xx} \tag{2.7}$$

$$\tau_{xz} = Q_{55}\gamma_{xz} \tag{2.8}$$

where σ_{xx} and τ_{xz} are the normal and the shear stresses respectively and Q_{ij} are the transformed stiffness constants in the beam co-ordinate system, which are defined as

$$Q_{11} = \frac{E(z)}{1-\nu^2}, \quad Q_{55} = \frac{E(z)}{2(1+\nu)}$$

2.2.2 Classical plate theory

The following Fig. 2.3 depicts different geometries of thin FG plates considered in our investigation.

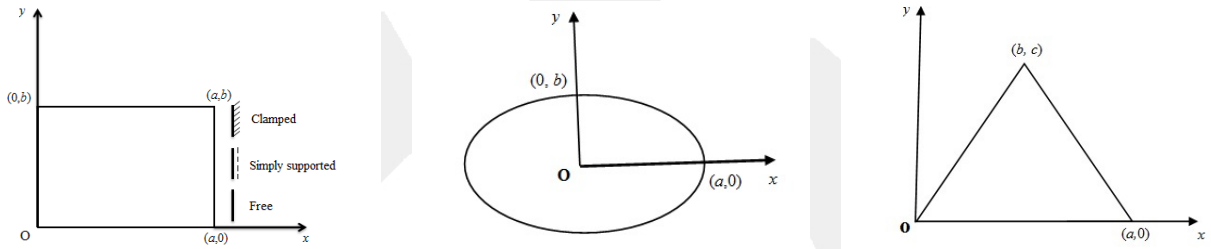

(a) Rectangular (b) Elliptic (c) Triangular

Figure 2.3: Typical functionally graded rectangular, elliptic and triangular plate elements

Classical plate theory (CPT) for the displacement field of FG plate can be expressed as (Wang et al., 2000)

$$\begin{aligned} u_x(x,y,z) &= -z\frac{\partial w}{\partial x} \\ u_y(x,y,z) &= -z\frac{\partial w}{\partial y} \\ u_z(x,y,z) &= w(x,y) \end{aligned} \tag{2.9}$$

where u_x, u_y and u_z are the displacement components along x, y and z coordinate directions respectively and w is the transverse deflection at a point on the mid-plane ($x-y$ plane). The transverse shear deformation has been neglected in case of Kirchoff assumption that is deformation is due to bending and in-plane stretching only. The non-zero linear strains associated with the displacement field can be expressed as

$$\begin{Bmatrix} \epsilon_{xx} \\ \epsilon_{yy} \\ \gamma_{xy} \end{Bmatrix} = \begin{Bmatrix} \frac{\partial u_x}{\partial x} \\ \frac{\partial u_y}{\partial y} \\ \frac{\partial u_x}{\partial y} + \frac{\partial u_y}{\partial x} \end{Bmatrix} = \begin{Bmatrix} -z\frac{\partial^2 w}{\partial x^2} \\ -z\frac{\partial^2 w}{\partial y^2} \\ -2z\frac{\partial^2 w}{\partial x \partial y} \end{Bmatrix} \tag{2.10}$$

where ϵ_{xx} and ϵ_{yy} are the normal strains in x and y directions respectively and γ_{xy} is the shear strain. By assuming the material constituents of FG plate to obey the generalized Hooke's law,

the stress-strain relationships can be expressed in matrix form as

$$\begin{Bmatrix} \sigma_{xx} \\ \sigma_{yy} \\ \tau_{xy} \end{Bmatrix} = \begin{pmatrix} Q_{11} & Q_{12} & 0 \\ Q_{21} & Q_{22} & 0 \\ 0 & 0 & Q_{66} \end{pmatrix} \begin{Bmatrix} \epsilon_{xx} \\ \epsilon_{yy} \\ \gamma_{xy} \end{Bmatrix} \tag{2.11}$$

where σ_{xx}, σ_{yy} are the normal stresses; τ_{xy} is the shear stress and the reduced stiffness components, Q_{ij} $(i, j = 1, 2, 6)$ are given by

$$Q_{11} = Q_{22} = \frac{E(z)}{1-\nu^2}, \quad Q_{12} = Q_{21} = \frac{\nu E(z)}{1-\nu^2}, \quad Q_{66} = \frac{E(z)}{2(1+\nu)}.$$

Here, E and ν are Young's modulus and Poisson's ratio of the material constituents respectively.

2.3 Proposed theories

In this section, we have proposed higher-order deformation beam theories as well as special case of plate theories on the basis of certain assumptions mentioned in previous literature.

2.3.1 Beam theories

Looking into Eqs. (2.3) and (2.4), the displacement field for the FG beam based on a general higher-order shear deformation theory may be decided by the function $f(z)$ and the major criteria to choose the shape functions ($f(z)$) for these models are given as follows (Reddy, 1984a; Aydogdu, 2009):

- Suitable $f(z)$ function should approximately satisfy parabolic shear deformation distribution.
- The boundary conditions should be satisfied on the bottom and top surfaces of the beam.

Accordingly, the authors have proposed two different types of shear deformation theories which involve inverse trigonometric functions and a generalized power-law exponent based function. These theories may be named as Inverse Sine Shear Deformation Beam Theory (ISDBT), Inverse Cosine Shear Deformation Beam Theory (ICDBT), Inverse Tangent Shear

Deformation Beam Theory (ITDBT) and Power-law Exponent based Shear Deformation Beam Theory (PESDBT).

$$\begin{aligned}
&\text{ISDBT}: f(z) = \frac{2z}{\sqrt{3}} - h\arcsin\left(\frac{z}{h}\right)\\
&\text{ICDBT}: f(z) = \frac{2z}{\sqrt{3}} + h\arccos\left(\frac{z}{h}\right)\\
&\text{ITDBT}: f(z) = \frac{4z}{5} - h\arctan\left(\frac{z}{h}\right)\\
&\text{PESDBT}: f(z) = h\left(\frac{z}{h}\right)^{2n+1} - (2n+1)z\left(\frac{1}{2}\right)^{2n}
\end{aligned} \tag{2.12}$$

The derivatives of $f(z)$ in the proposed inverse trigonometric SDBTs yield

$$\frac{\partial f}{\partial z} = \begin{cases} \frac{2}{\sqrt{3}} - \frac{1}{\sqrt{1-\left(\frac{z}{h}\right)^2}}; & \text{for ISDBT and ICDBT} \\ \frac{4}{5} - \frac{1}{1+\left(\frac{z}{h}\right)^2}; & \text{for ITDBT} \end{cases}$$

The transverse shear stress on the bottom and top surfaces of the beam may be found as

$$\tau_{xz}\left(x, \mp\frac{h}{2}\right) = 0 \tag{2.13}$$

On contrary, n is a non-negative integer which will play a key role in PESDBT. It can be viewed that classical or Euler-Bernoulli beam theory is a special case of this model. If we assume $n = 0$, then PESDBT will follow the assumptions of classical beam theory. We can define the limiting value of $f(z)$ associated with PESDBT for very large value of n as

$$\begin{aligned}
\lim_{n\to+\infty} f(z) &= \lim_{n\to+\infty}\left\{h\left(\frac{z}{h}\right)^{2n+1} - (2n+1)z\left(\frac{1}{2}\right)^{2n}\right\}\\
&= \lim_{n\to+\infty} h\left(\frac{z}{h}\right)^{2n+1} - \lim_{n\to+\infty}(2n+1)z\left(\frac{1}{2}\right)^{2n}\\
&= z\left\{\lim_{n\to+\infty}\left(\frac{z}{h}\right)^{2n} - \lim_{n\to+\infty}\left(\frac{2n+1}{2^{2n}}\right)\right\}, \text{ where } -\frac{h}{2} \le z \le +\frac{h}{2}\\
\Rightarrow \lim_{n\to+\infty} f(z) &= 0 \quad \text{(by Squeeze theorem)}
\end{aligned} \tag{2.14}$$

As expressed in Eq. (2.14), it can easily be noticed that limiting value of $f(z)$ approaches to zero for very large value of n. So classical or Euler-Bernoulli beam theory can also be derived from the proposed shear deformation theory by assuming higher values of n. It is also easy

to satisfy the stress free boundary conditions at the top and bottom surfaces of the beam in PESDBT by simply finding the derivative in this case. The constitutive relations in Eqs. (2.7) and (2.8) given for existing beam theories will also be similar to the proposed beam theories except the change in shape functions.

2.3.2 Plate theories

Considering an isotropic thick rectangular plate of length, breadth and uniform thickness as a, b and h respectively. Fig. 2.4 represents the orientation of the plate with its undeformed middle $(x-y)$ surface of the cartesian coordinate system with its origin at O(x,y,z).

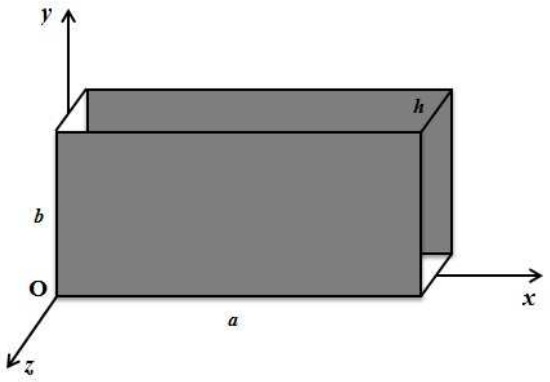

Figure 2.4: A typical isotropic thick rectangular plates with the cartesian coordinates

Let us assume the deformation of the isotropic plate to be in the middle surface $(x-y)$ plane, one can represent the displacement fields of isotropic plate based on generalized higher-order shear deformation plate theory with the similar assumptions (Aydogdu, 2009; Xiang et al., 2009) as follows:

$$\begin{aligned} u_x(x,y,z;t) &= u(x,y;t) - z\frac{\partial w}{\partial x} + f(z)\phi_x(x,y;t) \\ u_y(x,y,z;t) &= v(x,y;t) - z\frac{\partial w}{\partial y} + f(z)\phi_y(x,y;t) \\ u_z(x,y,z;t) &= w(x,y;t) \end{aligned} \tag{2.15}$$

where u, v, w, ϕ_x and ϕ_y are five unknown displacement components of the middle plane of the plate and $f(z)$ denotes the transverse shear function to determine the parabolic distribution of the transverse shear strains and stresses across the thickness. Different researchers have proposed various shear deformation plate theories (SDPTs) by suitably selecting the shape

function, $f(z)$. To the best of our knowledge, the inverse SDPT in present form has not yet been developed.

In view of various recent literatures (Reddy, 1984b,c; Shimpi et al., 2007; Aydogdu, 2009; Thai et al., 2014; Touratier, 1991), we have concluded that the mathematical function deciding the shear deformation theories may take varieties of forms. As such, we have proposed four new shear deformation plate theories which involve inverse trigonometric functions viz. inverse sine, inverse cosine, inverse tangent and inverse cotangent. Accordingly, the proposed SDPTs are defined as Inverse Sine Shear Deformation Plate Theory (ISDPT), Inverse Cosine Shear Deformation Plate Theory (ICDPT), Inverse Tangent Shear Deformation Plate Theory (ITDPT) and Inverse Cotangent Shear Deformation Plate Theory (ICTDPT). The shape functions concerned with these SDPTs are stated below.

$$\begin{aligned}
&\text{ISDPT}: f(z) = \frac{2z}{\sqrt{3}} - h\sin^{-1}\left(\frac{z}{h}\right)\\
&\text{ICDPT}: f(z) = \frac{2z}{\sqrt{3}} + h\cos^{-1}\left(\frac{z}{h}\right)\\
&\text{ITDPT}: f(z) = \frac{4z}{5} - h\tan^{-1}\left(\frac{z}{h}\right)\\
&\text{ICTDPT}: f(z) = \frac{4z}{5} + h\cot^{-1}\left(\frac{z}{h}\right)
\end{aligned} \tag{2.16}$$

Using the displacement field stated in Eq. (2.16), the non-zero strain-displacement relations can be expressed as (Wang et al., 2000; Shimpi and Patel, 2006; Shimpi et al., 2007; Aydogdu, 2009; Xiang et al., 2009)

$$\begin{aligned}
\epsilon_{xx} &= \frac{\partial u_x}{\partial x} = \frac{\partial u}{\partial x} - z\frac{\partial^2 w}{\partial x^2} + f(z)\frac{\partial \phi_x}{\partial x}\\
\epsilon_{yy} &= \frac{\partial u_y}{\partial y} = \frac{\partial v}{\partial y} - z\frac{\partial^2 w}{\partial y^2} + f(z)\frac{\partial \phi_y}{\partial y}\\
\gamma_{xy} &= \frac{\partial u_x}{\partial y} + \frac{\partial u_y}{\partial x} = \left(\frac{\partial u}{\partial y} + \frac{\partial v}{\partial x}\right) - 2z\frac{\partial^2 w}{\partial x \partial y} + f(z)\left(\frac{\partial \phi_x}{\partial y} + \frac{\partial \phi_y}{\partial x}\right)\\
\gamma_{yz} &= \frac{\partial u_y}{\partial z} + \frac{\partial u_z}{\partial y} = \frac{\partial f}{\partial z}\phi_y\\
\gamma_{xz} &= \frac{\partial u_x}{\partial z} + \frac{\partial u_z}{\partial x} = \frac{\partial f}{\partial z}\phi_x
\end{aligned} \tag{2.17}$$

where ϵ_{xx} and ϵ_{yy} are the normal strains in $x-$ and $y-$ directions; γ_{xy}, γ_{yz} and γ_{xz} are the shear strains in $x-y$, $y-z$ and $x-z$ planes respectively. Assuming the material constituents of the plate to obey the generalized Hooke's law, the stress-strain relationships can be written in

matrix form

$$\begin{Bmatrix} \sigma_{xx} \\ \sigma_{yy} \\ \tau_{xy} \\ \tau_{yz} \\ \tau_{xz} \end{Bmatrix} = \begin{pmatrix} Q_{11} & Q_{12} & 0 & 0 & 0 \\ Q_{21} & Q_{22} & 0 & 0 & 0 \\ 0 & 0 & Q_{66} & 0 & 0 \\ 0 & 0 & 0 & Q_{44} & 0 \\ 0 & 0 & 0 & 0 & Q_{55} \end{pmatrix} \begin{Bmatrix} \epsilon_{xx} \\ \epsilon_{yy} \\ \gamma_{xy} \\ \gamma_{yz} \\ \gamma_{xz} \end{Bmatrix} \tag{2.18}$$

Here, σ_{xx}, σ_{yy} are the normal stresses; τ_{xy}, τ_{yz} and τ_{xz} are the shear stresses. The reduced stiffness coefficients, Q_{ij} $(i, j = 1, 2, 4, 5, 6)$ are then given by

$$Q_{11} = Q_{22} = \frac{E}{1-\nu^2}, \quad Q_{12} = Q_{21} = \frac{\nu E}{1-\nu^2} \quad \text{and}$$

$$Q_{44} = Q_{55} = Q_{66} = G = \frac{E}{2(1+\nu)}$$

Moreover, E, G and ν are Young's modulus, shear's modulus and Poisson's ratio of the material constituent respectively.

2.4 Static and vibration problems

Depending on displacement fields of deformed FG beams and plates, the governing equations related to their static and dynamic problems are incorporated in further discussions.

2.4.1 FG static problem

The equation of equilibrium in terms of bending and twisting moments of the isotropic plate under external mechanical load (q) can be represented as

$$\frac{\partial^2 M_x}{\partial x^2} + \frac{\partial^2 M_y}{\partial y^2} - 2\frac{\partial^2 M_{xy}}{\partial x \partial y} = -q \tag{2.19}$$

Here, bending moments are $M_x = -D\left(\frac{\partial^2 w}{\partial x^2} + \nu\frac{\partial^2 w}{\partial y^2}\right)$, $M_y = -D\left(\frac{\partial^2 w}{\partial y^2} + \nu\frac{\partial^2 w}{\partial x^2}\right)$ and twisting moment is $M_{xy} = D(1-\nu)\frac{\partial^2 w}{\partial x \partial y}$, where D is the flexural rigidity of the plate. As regards, there occurs the gradation of volume fractions in thickness direction in case of functionally graded plate. So in the equation of equilibrium, flexural rigidity (D) has been replaced by D_f. Let us

consider the FG rectangular plate be subjected to an external mechanical load q that is either Uniformly Distributed Load (UDL) or hydrostatic pressure. Substituting the expressions of bending and twisting moments in Eq. (2.19), we can obtain the equation of equilibrium in terms of deflections (w) of the plate as

$$\frac{\partial^4 w}{\partial x^4} + 2\frac{\partial^4 w}{\partial x^2 \partial y^2} + \frac{\partial^4 w}{\partial y^4} = \frac{q}{D_f} \tag{2.20}$$

We can also express Eq. (2.20) with the loads considered for pure bending as

$$\text{Uniformly distributed Load} : \frac{\partial^4 w}{\partial x^4} + 2\frac{\partial^4 w}{\partial x^2 \partial y^2} + \frac{\partial^4 w}{\partial y^4} = \frac{q}{D_f} \tag{2.21}$$

$$\text{Hydrostatic pressure} : \frac{\partial^4 w}{\partial x^4} + 2\frac{\partial^4 w}{\partial x^2 \partial y^2} + \frac{\partial^4 w}{\partial y^4} = \frac{qx}{aD_f} \tag{2.22}$$

where D_f is the counterpart of flexural rigidity of isotropic plate in case of functionally graded plate and is given by

$$\begin{aligned}
D_f &= \int_{-h/2}^{h/2} \frac{z^2 E(z)}{1-\nu^2}\,\mathrm{d}z \\
&= \frac{1}{1-\nu^2}\int_{-h/2}^{h/2}\left\{(E_c - E_m)\left(\frac{z}{h}+\frac{1}{2}\right)^k + E_m\right\} z^2\,\mathrm{d}z \\
&= \frac{1}{1-\nu^2}\int_{-h/2}^{h/2}\left\{(E_c - E_m)\left(\frac{z}{h}+\frac{1}{2}\right)^k\right\} z^2\,\mathrm{d}z + \int_{-h/2}^{h/2} E_m z^2\,\mathrm{d}z \\
&= \frac{(E_c - E_m)h^3}{1-\nu^2}\left\{\frac{1}{k+3} - \frac{1}{k+2} + \frac{1}{4(k+1)}\right\} + \frac{E_m h^3}{12(1-\nu^2)} \\
&= D_c\left[12\left(1-\frac{1}{E_{rat}}\right)\left\{\frac{1}{k+3} - \frac{1}{k+2} + \frac{1}{4(k+1)}\right\} + \frac{1}{E_{rat}}\right].
\end{aligned}$$

Here, $D_c = \frac{E_c h^3}{12(1-\nu^2)}$ and $E_{rat} = \frac{E_c}{E_m}$.

2.4.2 Vibration of FG beam

The governing differential equations defining free vibration of functionally graded beam within the framework of general higher-order shear deformation theory can be written as (Aydogdu

and Taskin, 2007)

$$\begin{aligned}
\frac{\partial N_x}{\partial x} &= \rho_0 \ddot{u} + \rho_{01} \ddot{v} - \rho_1 \frac{\partial \ddot{w}}{\partial x} \\
\frac{\partial^2 M_x}{\partial x^2} &= \rho_1 \frac{\partial \ddot{u}}{\partial x} + \rho_{11} \frac{\partial \ddot{v}}{\partial x} + \rho_0 \ddot{w} - \rho_2 \frac{\partial^2 \ddot{w}}{\partial x^2} \\
\frac{\partial M_x^f}{\partial x} - Q_x^f &= \rho_{01} \ddot{u} + \rho_{02} \ddot{v} - \rho_{11} \frac{\partial \ddot{w}}{\partial x}
\end{aligned} \tag{2.23}$$

where $\ddot{(\,)}$ denotes the second time derivatives. Here ρ_i and ρ_{jm} are the inertial coefficients, where $\rho_i = \int_{-h/2}^{h/2} \rho(z) z^i \, \mathrm{d}z, \; i = 0, 1, 2; \; \rho_{jm} = \int_{-h/2}^{h/2} \rho(z) z^j f^m \, \mathrm{d}z, \; j = 0, 1; \; m = 1, 2$ and the force and moment components can be expressed as

$$\begin{aligned}
\left(N_x, M_x, M_x^f\right) &= \int_{-h/2}^{h/2} \sigma_{xx} \left(1, \; z, \; f(z)\right) \mathrm{d}z \\
Q_x^f &= \int_{-h/2}^{h/2} \tau_{xz} f'(z) \, \mathrm{d}z
\end{aligned} \tag{2.24}$$

2.4.3 Vibration of FG plate

Assuming the classical plate theory given in Eq. (2.9), the free vibration problem associated with thin functionally graded plate may be written as

$$\frac{\partial^2 M_x}{\partial x^2} + 2 \frac{\partial^2 M_{xy}}{\partial x \partial y} + \frac{\partial^2 M_y}{\partial y^2} = I_0 \frac{\partial^2 w}{\partial t^2} \tag{2.25}$$

The bending and twisting moments may be found in Eq. (2.19) and $I_0 = \int_{-h/2}^{h/2} \rho(z) \, \mathrm{d}z$ is the inertial coefficient. On the other hand, the equilibrium equations for free vibration of thick isotropic plate (special case of thick FG plate) based on Eq. (2.16) may be presented as

$$\frac{\partial N_{xx}}{\partial x} + \frac{\partial N_{xy}}{\partial y} = I_0 \ddot{u} - I_1 \frac{\partial \ddot{w}}{\partial x} + J_1 \ddot{\phi}_x \tag{2.26a}$$

$$\frac{\partial N_{xy}}{\partial x} + \frac{\partial N_{yy}}{\partial y} = I_0 \ddot{v} - I_1 \frac{\partial \ddot{w}}{\partial y} + J_1 \ddot{\phi}_y \tag{2.26b}$$

$$\frac{\partial^2 M_{xx}}{\partial x^2} + 2 \frac{\partial^2 M_{xy}}{\partial x \partial y} + \frac{\partial^2 M_{yy}}{\partial y^2} = I_1 \left(\frac{\partial \ddot{u}}{\partial x} + \frac{\partial \ddot{v}}{\partial y} \right) - I_2 \bigtriangledown^2 \ddot{w} + J_2 \left(\frac{\partial \ddot{\phi}_x}{\partial x} + \frac{\partial \ddot{\phi}_y}{\partial y} \right) - I_0 \ddot{w} \tag{2.26c}$$

$$\frac{\partial M_{xx}^f}{\partial x} + \frac{\partial M_{xy}^f}{\partial y} + Q_{xz}^f = J_1 \ddot{u} - J_2 \frac{\partial \ddot{w}}{\partial x} + K_2 \ddot{\phi}_x \tag{2.26d}$$

$$\frac{\partial M_{xy}^f}{\partial x} + \frac{\partial M_{yy}^f}{\partial y} + Q_{yz}^f = J_1 \ddot{v} - J_2 \frac{\partial \ddot{w}}{\partial y} + K_2 \ddot{\phi}_y \tag{2.26e}$$

where the force and moment components are

$$\begin{aligned}
\left(N_{xx}, N_{xy}, N_{yy}\right) &= \int_{-h/2}^{h/2} \left(\sigma_{xx}, \tau_{xy}, \sigma_{yy}\right) \mathrm{d}z \\
\left(M_{xx}, M_{xy}, M_{yy}\right) &= \int_{-h/2}^{h/2} z\left(\sigma_{xx}, \tau_{xy}, \sigma_{yy}\right) \mathrm{d}z \\
\left(M_{xx}^f, M_{xy}^f, M_{yy}^f\right) &= \int_{-h/2}^{h/2} f(z)\left(\sigma_{xx}, \tau_{xy}, \sigma_{yy}\right) \mathrm{d}z \\
\left(Q_{xz}^f, Q_{yz}^f\right) &= \int_{-h/2}^{h/2} f'(z)\left(\tau_{xz}, \tau_{yz}\right) \mathrm{d}z.
\end{aligned} \tag{2.27}$$

and the inertial coefficients are

$$\begin{aligned}
(I_0, I_1, I_2) &= \int_{-h/2}^{h/2} \rho\left(1, z, z^2\right) \mathrm{d}z \\
(J_1, J_2, K_2) &= \int_{-h/2}^{h/2} \rho\left(f(z), zf(z), zf^2\right) \mathrm{d}z.
\end{aligned} \tag{2.28}$$

Chapter 3

Numerical methods

Chapter 3

Numerical methods

In general, the numerical methods follow a set of systematic algorithms to solve different physical problems. The present investigation considers two efficient computational methods viz. Rayleigh-Ritz method and generalized differential quadrature. As such, this chapter involves the numerical procedures of Rayleigh-Ritz method in solving the said problems of functionally graded beams and plates followed by that of generalized differential quadrature to investigate free vibration of geometrically non-linear functionally graded beams.

3.1 Rayleigh-Ritz method

The Rayleigh-Ritz method (after Walther Ritz and Lord Rayleigh) was earlier extensively used in the analysis of several isotropic structural members. But the research works on functionally graded structural members by using this method is limited in open literature. As regards, we have successfully implemented this computational procedure in handling static problem of FG plates and vibration problems concerned with FG beams and plates. The summary of the algorithms for this technique has been presented below.

1. To find the expressions for strain and kinetic energies of the FG beam (or plate) for the displacement field of the respective shear deformation beam (or plate) theories.

2. To obtain the maximum strain and kinetic energies by assuming the harmonic type displacements.

3. Consider the amplitudes of displacements as the linear combination of simple algebraic polynomials (generated from Pascal's triangle), which also involves a specific admissible function to satisfy the essential boundary conditions.

4. To equate the maximum strain and kinetic energies to obtain the Rayleigh quotient. Then differentiate the Rayleigh quotient partially with respect to the unknown constant

coefficients involved in linear combination to find the system of equations for pure bending and generalized eigenvalue problem for vibration problems.

3.1.1 FG static problem

Using stress-strain relations of classical plate theory explained in Eq. (2.11), the strain energy (U_c) expressions of thin FG plate may be written as

$$U_c = \frac{1}{2}\int_{\Omega}\left[\int_{-h/2}^{h/2}\left(\sigma_{xx}\epsilon_{xx} + \sigma_{yy}\epsilon_{yy} + \tau_{xy}\gamma_{xy}\right)\mathrm{d}z\right]\mathrm{d}x\mathrm{d}y \tag{3.1}$$

where Ω denotes the midplane (domain) of the FG plate. Using Eqs. (2.10) and (2.11), we can rewrite Eq. (3.1) as follows

$$U_c = \frac{1}{2}\int_{\Omega}\left[D_{11}\left\{\left(\frac{\partial^2 w}{\partial x^2}\right)^2 + \left(\frac{\partial^2 w}{\partial y^2}\right)^2\right\} + 2D_{12}\frac{\partial^2 w}{\partial x^2}\frac{\partial^2 w}{\partial y^2} + 4D_{66}\left(\frac{\partial^2 w}{\partial x \partial y}\right)^2\right]\mathrm{d}x\mathrm{d}y \tag{3.2}$$

The effect of external mechanical load q can also be seen in the expression of potential energy due to vertical deflection w on the horizontal $x-y$ plane. Corresponding potential energy may be expressed as

$$U_{ext} = -\int_{\Omega} wq\,\mathrm{d}x\mathrm{d}y \tag{3.3}$$

Combining Eqs. (3.2) and (3.3), the total potential energy (U) of the system can be given as

$$\begin{aligned} U \;=\; & \frac{1}{2}\int_{\Omega}\left[D_{11}\left\{\left(\frac{\partial^2 w}{\partial x^2}\right)^2 + \left(\frac{\partial^2 w}{\partial y^2}\right)^2\right\} + 2D_{12}\frac{\partial^2 w}{\partial x^2}\frac{\partial^2 w}{\partial y^2}\right. \\ & \left. + 4D_{66}\left(\frac{\partial^2 w}{\partial x \partial y}\right)^2\right]\mathrm{d}x\mathrm{d}y - \int_{\Omega} wq\,\mathrm{d}x\mathrm{d}y \end{aligned} \tag{3.4}$$

where the stiffness coefficients in Eq. (3.4) are

$$(D_{11}, D_{12}, D_{66}) = \int_{-h/2}^{h/2}(Q_{11}, Q_{12}, Q_{66})z^2\,\mathrm{d}z$$

The stiffness coefficient $D_{11} = D_f = \frac{(E_c - E_m)h^3}{1-\nu^2}\left\{\frac{1}{k+3} - \frac{1}{k+2} + \frac{1}{4(k+1)}\right\} + \frac{E_m h^3}{12(1-\nu^2)}$. For constant

Poisson's ratio (ν), one may see that $D_{12} = \nu D_f$ and $D_{66} = \left(\frac{1-\nu}{2}\right) D_f$.

Application of Rayleigh-Ritz method

The deflection function (w) can be represented in the form of a series

$$w(x,y) = \sum_{j=1}^{n} c_j \varphi_j(x,y) \tag{3.5}$$

In Eq. (3.5), $c_j; j = 1,2,\cdots,n$ are unknown constants to be determined and $\varphi_j(x,y) = f\psi_j(x,y); j = 1,2,\cdots,n$ are the admissible functions to represent the deflection surface and at the same time to satisfy the essential boundary conditions. Here, n is the number of polynomials involved in the admissible functions. The function $f = x^p y^q (a-x)^r (b-y)^s$, where the exponents p, q, r and s control various BCs[1] in case of FG rectangular plate. The parameter p takes the values 0, 1 or 2 according as the side $x = 0$ is free (F), simply supported (S) or clamped (C). Similar interpretations can be given to the parameters q, r and s corresponding to the sides $y = 0$, $x = a$ and $y = b$, respectively. The components of ψ_i are taken from Pascal's triangle as given in Table 3.1.

Table 3.1: Ten admissible functions obtained from Pascal's triangle

j	1	2	3	4	5	6	7	8	9	10
ψ_j	1	x	y	x^2	xy	y^2	x^3	x^2y	xy^2	y^3

Substituting the expression of $w(x,y)$ in Eq. (3.4) and minimizing the potential energy of the system as a function of c_j, we get

$$\frac{\partial U}{\partial c_j} = 0; j = 1,2,\cdots,n \tag{3.6}$$

Eq. (3.6) will result to a system of n linear equations with n unknowns $c_1, c_2, \cdots, c_n$. If the functions $\varphi_j; j = 1,2,\cdots,n$ in Eq. (3.5) can represent arbitrary function within the boundary of the plate, this method of computing transverse deflections w brings us to a closer and closer approximation as the number n of the terms of the series increases and by taking n infinitely large we may obtain an exact solution for the concerned problem.

[1]Boundary Conditions

Non-dimensionalization

The non-dimensionalization process involves a change in cartesian co-ordinate system x and y to ξ and η respectively using $\xi = \frac{x}{a}$ $(0 \leq \xi \leq 1)$ and $\eta = \frac{y}{b}$ $(0 \leq \eta \leq 1)$. As such, expressions for admissible functions and strain energy will be modified with the components ξ and η and one may obtain

$$\varphi_j(\xi,\eta) = f\psi_j(\xi,\eta); j = 1,2,\cdots,n$$

with $f = \xi^p \eta^q (1-\xi)^r (1-\eta)^s$ and the total potential energy may be

$$\begin{aligned} U &= \frac{D_f ab}{2b^4} \int_\Omega \left\{ \mu^4 \left(\frac{\partial^2 w}{\partial \xi^2} \right)^2 + 2\nu\mu^2 \frac{\partial^2 w}{\partial \xi^2} \frac{\partial^2 w}{\partial \eta^2} + \left(\frac{\partial^2 w}{\partial \eta^2} \right)^2 \right. \\ &\quad \left. + 2(1-\nu)\mu^2 \left(\frac{\partial^2 w}{\partial \xi \partial \eta} \right)^2 \right\} \mathrm{d}\xi \mathrm{d}\eta - \left\{ ab \int_\Omega wq \, \mathrm{d}\xi \mathrm{d}\eta \right\} \end{aligned} \tag{3.7}$$

where $\mu = \frac{b}{a}$ is the aspect ratio (ratio of the edges) of the FG rectangular plate. As present work considers two types of external loads such as UDL and hydrostatic pressure, Eq. (3.7) needs a little modification in its form. The respective potential energies U' and U'' of the FG plate corresponding to UDL and hydrostatic pressure can be written as

$$\begin{aligned} U' &= \frac{D_f ab}{2b^4} \int_\Omega \left\{ \mu^4 \left(\frac{\partial^2 w}{\partial \xi^2} \right)^2 + 2\nu\mu^2 \frac{\partial^2 w}{\partial \xi^2} \frac{\partial^2 w}{\partial \eta^2} + \left(\frac{\partial^2 w}{\partial \eta^2} \right)^2 \right. \\ &\quad \left. + 2(1-\nu)\mu^2 \left(\frac{\partial^2 w}{\partial \xi \partial \eta} \right)^2 \right\} \mathrm{d}\xi \mathrm{d}\eta - \left\{ qab \int_\Omega w \, \mathrm{d}\xi \mathrm{d}\eta \right\} \end{aligned} \tag{3.8}$$

and

$$\begin{aligned} U'' &= \frac{D_f ab}{2b^4} \int_\Omega \left\{ \mu^4 \left(\frac{\partial^2 w}{\partial \xi^2} \right)^2 + 2\nu\mu^2 \frac{\partial^2 w}{\partial \xi^2} \frac{\partial^2 w}{\partial \eta^2} + \left(\frac{\partial^2 w}{\partial \eta^2} \right)^2 \right. \\ &\quad \left. + 2(1-\nu)\mu^2 \left(\frac{\partial^2 w}{\partial \xi \partial \eta} \right)^2 \right\} \mathrm{d}\xi \mathrm{d}\eta - \left\{ qab \int_\Omega w\xi \, \mathrm{d}\xi \mathrm{d}\eta \right\} \end{aligned} \tag{3.9}$$

According to principle of minimization of potential energy, one may find a system of linear

equations after taking partial differentiation of U' or U'' with respect to c_j's.

$$\sum_{j=1}^{n} a_{ij} c_j = P b_i; i = 1, 2, \cdots, n \tag{3.10}$$

where the matrices are $a_{ij} = \int_{\Omega}\left[\varphi_i^{\xi\xi}\varphi_j^{\xi\xi} + \varphi_i^{\eta\eta}\varphi_j^{\eta\eta} + \nu\left(\varphi_i^{\xi\xi}\varphi_j^{\eta\eta} + \varphi_i^{\xi\xi}\varphi_j^{\eta\eta}\right) + 2(1-\nu)\varphi_i^{\xi\eta}\varphi_j^{\xi\eta}\right] \mathrm{d}\xi\mathrm{d}\eta$,

$b_i = \begin{cases} \int_{\Omega}\varphi_i \,\mathrm{d}\xi\mathrm{d}\eta; & \text{Uniformly distributed load} \\ \int_{\Omega}\varphi_i \xi \,\mathrm{d}\xi\mathrm{d}\eta; & \text{Hydrostatic pressure} \end{cases}$ and $P = \frac{qa^4}{D_f}$ is the non-dimensionalized load.

Pure bending properties

Solving Eq. (3.10), pure bending properties such as maximum deflection, bending moments and normal stresses may be evaluated at the center of the plate. Maximum deflection of the plate at the center ($\xi = 0.5, \eta = 0.5$) may be expressed as

$$w_{max} = \alpha\,|_{\xi=0.5,\eta=0.5}\,\frac{qa^4}{D_c} \tag{3.11}$$

Accordingly, the expressions for other properties can also be obtained using Eq. (3.11). Maximum bending moments may be written as

$$M_x = \beta\,|_{\xi=0.5,\eta=0.5}\,qa^2 \tag{3.12}$$

$$M_y = \beta'\,|_{\xi=0.5,\eta=0.5}\,qa^2 \tag{3.13}$$

and maximum normal stresses, α_{xx} and α_{yy} as

$$\alpha_{xx} = \delta\,|_{\xi=0.5,\eta=0.5}\,\frac{qa^2}{h^2} \tag{3.14}$$

$$\alpha_{yy} = \delta'\,|_{\xi=0.5,\eta=0.5}\,\frac{qa^2}{h^2} \tag{3.15}$$

In the above Eqs. (3.12-3.15), the numerical factors β, β', δ and δ' are of the form

$$\begin{aligned}
\beta &= -\left(\frac{\partial^2\alpha}{\partial\xi^2} + \frac{\nu}{\mu^2}\frac{\partial^2\alpha}{\partial\eta^2}\right), \\
\beta' &= -\left(\nu\frac{\partial^2\alpha}{\partial\xi^2} + \frac{1}{\mu^2}\frac{\partial^2\alpha}{\partial\eta^2}\right), \\
\delta &= 6\beta, \\
\delta' &= 6\beta'.
\end{aligned} \tag{3.16}$$

which are to be computed in subsequent discussion of its corresponding chapter.

3.1.2 Vibration of FG beam

The strain energy S and the kinetic energy T of the beam in cartesian co-ordinates may respectively be written as

$$S = \frac{1}{2}\int_{-L/2}^{L/2}\int_{A}(\sigma_{xx}\varepsilon_{xx} + \tau_{xz}\gamma_{xz})\,\mathrm{d}A\,\mathrm{d}x \tag{3.17}$$

and

$$T = \frac{1}{2}\int_{-L/2}^{L/2}\int_{A}\rho(z)\left[\left(\frac{\partial u_x}{\partial t}\right)^2 + \left(\frac{\partial u_z}{\partial t}\right)^2\right]\mathrm{d}A\,\mathrm{d}x \tag{3.18}$$

where A and ρ are the area of cross-section and the mass density of the rectangular FG beam respectively. Considering the higher order shear deformation beam theory (regardless of the existing or proposed mentioned in Eqs. (2.4) and (2.12)), Eqs. (3.17) and (3.18) become

$$\begin{aligned}
S &= \frac{1}{2}\int_{-L/2}^{L/2}\Big[A_{xx}u_{,x}^2 - 2B_{xx}u_{,x}w_{,xx} + D_{xx}w_{,xx}^2 + 2E_{xx}u_{,x}v_{,x} \\
&\quad -2F_{xx}v_{,x}w_{,xx} + H_{xx}v_{,x}^2 + A_{xz}v^2\Big]\,\mathrm{d}x
\end{aligned} \tag{3.19}$$

and

$$\begin{aligned}
T &= \frac{1}{2}\int_{-L/2}^{L/2}\left[I_A\left\{\left(\frac{\partial u}{\partial t}\right)^2 + \left(\frac{\partial w}{\partial t}\right)^2\right\} - 2I_B\left(\frac{\partial u}{\partial t}\right)\left(\frac{\partial^2 w}{\partial x\partial t}\right) + I_D\left(\frac{\partial^2 w}{\partial x\partial t}\right)^2\right. \\
&\quad \left. +2I_E\left(\frac{\partial u}{\partial t}\right)\left(\frac{\partial v}{\partial t}\right) - 2I_F\left(\frac{\partial v}{\partial t}\right)\left(\frac{\partial^2 w}{\partial x\partial t}\right) + I_H\left(\frac{\partial v}{\partial t}\right)^2\right]\mathrm{d}x
\end{aligned} \tag{3.20}$$

The stiffness coefficients appearing in Eq. (3.19) are defined as

$$\begin{aligned}
(A_{xx}, B_{xx}, D_{xx}) &= \int_A Q_{11}(1, z, z^2)\,\mathrm{d}A \\
(E_{xx}, F_{xx}) &= \int_A f(z) Q_{11}(1, z)\,\mathrm{d}A \\
H_{xx} &= \int_A [f(z)]^2 Q_{11}\,\mathrm{d}A \\
A_{xz} &= \kappa \int_A [f'(z)]^2 Q_{55}\,\mathrm{d}A \quad (\kappa\text{-shear correction factor})
\end{aligned} \tag{3.21}$$

In Eq. (3.21), $\kappa = 5/6$ is introduced in case of TBT, whereas it will be unity for all other SDBTs. As we are neglecting both transverse shear and transverse normal effects in case of CBT, it can be seen that terms associated with $f(z)$ and shear correction factor play no role while evaluating the expression of strain energy. The cross-sectional inertial coefficients in Eq. (3.20) may be written in the following form

$$\begin{aligned}
(I_A, I_B, I_D) &= \int_A \rho(z)(1, z, z^2)\,\mathrm{d}A \\
(I_E, I_F) &= \int_A f(z)\rho(z)(1, z)\,\mathrm{d}A \\
I_H &= \int_A [f(z)]^2 \rho(z)\,\mathrm{d}A
\end{aligned} \tag{3.22}$$

Assuming the displacement components $u(x,t)$, $v(x,t)$ and $w(x,t)$ as the harmonic type, those may be expressed as

$$\begin{aligned}
u(x,t) &= U(x)\sin\omega t \\
v(x,t) &= V(x)\sin\omega t \\
w(x,t) &= W(x)\sin\omega t
\end{aligned} \tag{3.23}$$

where $U(x)$, $V(x)$ and $W(x)$ are the respective amplitudes for these displacement components of free vibration of FG beam and the trigonometric terms indicate the harmonic type displacement with ω as the natural frequency. Substituting Eq. (3.23) into Eqs. (3.19) and (3.20) lead to maximum strain energy (S_{max}) and maximum kinetic energy (T_{max}) as

$$\begin{aligned}
S_{max} = \frac{1}{2}\int_{-L/2}^{L/2} \Bigg[& A_{xx}\left(\frac{\partial U}{\partial x}\right)^2 - 2B_{xx}\left(\frac{\partial U}{\partial x}\right)\left(\frac{\partial^2 W}{\partial x^2}\right) + D_{xx}\left(\frac{\partial^2 W}{\partial x^2}\right)^2 \\
& + 2E_{xx}\left(\frac{\partial U}{\partial x}\right)\left(\frac{\partial V}{\partial x}\right) - 2F_{xx}\left(\frac{\partial V}{\partial x}\right)\left(\frac{\partial^2 W}{\partial x^2}\right) + H_{xx}\left(\frac{\partial V}{\partial x}\right)^2 + A_{xz}V^2 \Bigg]\mathrm{d}x
\end{aligned} \tag{3.24}$$

and

$$T_{max} = \frac{\omega^2}{2}\int_{-L/2}^{L/2}\left[I_A\left(U^2+W^2\right)-2I_B U\frac{\partial W}{\partial x}+I_D\left(\frac{\partial W}{\partial t}\right)^2 +2I_E UV-2I_F V\frac{\partial W}{\partial x}+I_H V^2\right]\mathrm{d}x \tag{3.25}$$

For Rayleigh-Ritz method, the amplitudes of vibration are expressed in terms of algebraic polynomial functions by the following series (Timoshenko and Woinowsky-Krieger, 1959; Kelly, 1999; Rao, 2004; Chakraverty, 2009)

$$U=\sum_{i=1}^{n}c_i\varphi_i,\ \ V=\sum_{j=1}^{n}d_j\psi_j,\ \ W=\sum_{k=1}^{n}e_k f_k$$

where c_i, d_j and e_k are the unknown constant coefficients to be determined and φ_i, ψ_j and f_k are the admissible functions, which must satisfy the essential boundary conditions and can be represented as

$$\varphi_i = f x^{i-1},\quad i=1,2,\cdots,n$$

$$\psi_j = f x^{j-1},\quad j=1,2,\cdots,n$$

$$f_k = f x^{k-1},\quad k=1,2,\cdots,n$$

Here, n is the number of polynomials involved in the admissible functions (Chakraverty, 2009; Bhat, 1986; Singh and Chakraverty, 1992a,b) and $f=\left(x+\frac{L}{2}\right)^p\left(x-\frac{L}{2}\right)^q$ where $p, q = 0, 1$ or 2 are given in Table 3.2, as per the six boundary conditions of rectangular FG beam.

Table 3.2: Admissible function indices for different boundary conditions of rectangular FG beam

BCs	p	q
C-C	2	2
C-S	2	1
C-F	2	0
S-S	1	1
S-F	1	0
F-F	0	0

Accordingly, Rayleigh Quotient (ω^2) can be found by equating S_{max} and T_{max} obtained in Eqs. (3.24) and (3.25). Taking partial derivative of this quotient with respect to the constant

coefficients involved in the admissible functions as follows

$$\frac{\partial \omega^2}{\partial c_i} = 0; \quad i = 1, 2, \cdots, n$$
$$\frac{\partial \omega^2}{\partial d_j} = 0; \quad j = 1, 2, \cdots, n$$
$$\frac{\partial \omega^2}{\partial e_k} = 0; \quad k = 1, 2, \cdots, n$$

results the governing equation for the free vibration of FG beam in the form of generalized eigenvalue problem

$$\Big([K] - \lambda^2 [M]\Big)\{\Delta\} = 0 \tag{3.26}$$

where $[K]$ and $[M]$ are the stiffness and inertia matrices respectively and $\{\Delta\}$ is the column vector of unknown coefficients. The eigenvalue (λ) for the above eigenvalue problem (Eq. (3.26)) is the non-dimensional frequency and its different non-dimensional expressions has been given in its respective chapter.

3.1.3 Vibration of FG plate

In this section, numerical procedures of Rayleigh-Ritz method have been incorporated here to find vibration problems associated with thin functionally graded plates with different geometries followed by that of isotropic thick rectangular plates.

Thin functionally graded plate

Considering the constitutive relations associated with classical plate theory stated in Eq. (2.11), the strain energy **U** and kinetic energy **T** of the plate in cartesian co-ordinates may be written as

$$\mathbf{U} = \frac{1}{2} \int_{\Omega} \left[\int_{-h/2}^{h/2} \Big(\sigma_{xx} \epsilon_{xx} + \sigma_{yy} \epsilon_{yy} + \tau_{xy} \gamma_{xy} \Big) \mathrm{d}z \right] \mathrm{d}x\mathrm{d}y \tag{3.27}$$

and

$$\mathbf{T} = \frac{1}{2} \int_{\Omega} \left[\int_{-h/2}^{h/2} \rho(z) \left(\frac{\partial u_z}{\partial t} \right)^2 \mathrm{d}z \right] \mathrm{d}x\mathrm{d}y \tag{3.28}$$

where Ω denotes the midplane (domain) of the FG plate of any geometry viz. rectangular, elliptic or triangular. Using Eqs. (2.9), (2.10) and (2.11) in Eqs. (3.27) and (3.28) lead to

$$\mathbf{U} = \frac{1}{2}\int_{\Omega}\left[D_{11}\left\{\left(\frac{\partial^2 w}{\partial x^2}\right)^2 + \left(\frac{\partial^2 w}{\partial y^2}\right)^2\right\} + 2D_{12}\frac{\partial^2 w}{\partial x^2}\frac{\partial^2 w}{\partial y^2} + 4D_{66}\left(\frac{\partial^2 w}{\partial x \partial y}\right)^2\right] \mathrm{d}x\mathrm{d}y \tag{3.29}$$

and

$$\mathbf{T} = \frac{1}{2}\int_{\Omega} I_0\left(\frac{\partial w}{\partial t}\right)^2 \mathrm{d}x\mathrm{d}y \tag{3.30}$$

where the stiffness coefficients in Eq. (3.29) are

$$(D_{11}, D_{12}, D_{66}) = \int_{-h/2}^{h/2} (Q_{11}, Q_{12}, Q_{66}) z^2 \, \mathrm{d}z$$

and inertial coefficient, I_0 in Eq. (3.30) is

$$I_0 = \int_{-h/2}^{h/2} \rho(z) \, \mathrm{d}z.$$

The displacement component can be assumed harmonic type as $w(x,y,t) = W(x,y)\cos\omega t$ with $W(x,y)$ as the maximum deflection and ω is the natural frequency of free vibration. Using the above harmonic deflection, Eqs. (3.29) and (3.30) may be transformed into maximum strain ($\mathbf{U}_{max}$) and kinetic energies ($\mathbf{T}_{max}$) respectively as follows

$$\mathbf{U}_{max} = \frac{1}{2}\int_{\Omega}\left[D_{11}\left\{\left(\frac{\partial^2 W}{\partial x^2}\right)^2 + \left(\frac{\partial^2 W}{\partial y^2}\right)^2\right\} + 2D_{12}\frac{\partial^2 W}{\partial x^2}\frac{\partial^2 W}{\partial y^2} + 4D_{66}\left(\frac{\partial^2 W}{\partial x \partial y}\right)^2\right] \mathrm{d}x\mathrm{d}y \tag{3.31}$$

and

$$\mathbf{T}_{max} = \frac{\omega^2}{2}\int_{\Omega} I_0 W^2 \, \mathrm{d}x\mathrm{d}y \tag{3.32}$$

In Rayleigh-Ritz method, one may express the transverse displacement ($W(x,y)$) as the sum

of simple algebraic polynomials involving both x and y (as done before).

$$W(x,y) = \sum_{i=1}^{n} c_i \varphi_i(x,y) \tag{3.33}$$

where c_i are unknown constants to be determined and φ_i are the admissible functions, which satisfy the essential boundary conditions and can be represented as

$$\varphi_i(x,y) = f\psi_i(x,y), \quad i = 0,1,2,\cdots,n \tag{3.34}$$

Here, n is the number of polynomials involved in the admissible functions. The function f in Eq. (3.34) is generally chosen by the geometry of the plate viz. rectangular, elliptic or triangular as given below.

$$\begin{aligned} &\text{Rectangular:} f = x^p y^q (a-x)^r (b-y)^s \\ &\text{Elliptic:} f = \left(1 - \frac{x^2}{a^2} - \frac{y^2}{b^2}\right)^p \\ &\text{Triangular:} f = x^p y^q (1-x-y)^r \end{aligned} \tag{3.35}$$

where the indices p, q, r and s decide the classical boundary conditions at the edges. The parameter p takes the value as 0, 1 or 2 according the edge as free, simply supported or clamped respectively. Similar interpretations can also be given to other parameters. Table 3.1 involves the components of ψ_i generated from Pascal's triangle.

Assuming constant Poisson's ratio (ν), the Rayleigh quotient can be obtained by equating $\mathbf{U}_{max}$ and $\mathbf{T}_{max}$ as

$$\omega^2 = \frac{\int_\Omega D_{11}\left[\left\{\left(\frac{\partial^2 W}{\partial x^2}\right)^2 + \left(\frac{\partial^2 W}{\partial y^2}\right)^2\right\} + 2\nu\frac{\partial^2 W}{\partial x^2}\frac{\partial^2 W}{\partial y^2} + 2(1-\nu)\left(\frac{\partial^2 W}{\partial x \partial y}\right)^2\right] \mathrm{d}x\mathrm{d}y}{\int_\Omega I_0 W^2 \,\mathrm{d}x\mathrm{d}y} \tag{3.36}$$

The stiffness coefficient (D_{11}) and inertial coefficient (I_0) in Eq. (3.36) may be expressed as

$$
\begin{aligned}
D_{11} &= \int_{-h/2}^{h/2} Q_{11} z^2 \, \mathrm{d}z \\
&= \frac{1}{1-\nu^2} \int_{-h/2}^{h/2} E(z) z^2 \, \mathrm{d}z \\
&= \frac{1}{1-\nu^2} \int_{-h/2}^{h/2} \left\{ (E_c - E_m) \left(\frac{z}{h} + \frac{1}{2} \right)^k + E_m \right\} z^2 \, \mathrm{d}z \\
&= \frac{1}{1-\nu^2} \int_{-h/2}^{h/2} \left\{ (E_c - E_m) \left(\frac{z}{h} + \frac{1}{2} \right)^k \right\} z^2 \, \mathrm{d}z + \int_{-h/2}^{h/2} E_m z^2 \, \mathrm{d}z \\
&= \frac{(E_c - E_m) h^3}{1-\nu^2} \left\{ \frac{1}{k+3} - \frac{1}{k+2} + \frac{1}{4(k+1)} \right\} + \frac{E_m h^3}{12(1-\nu^2)},
\end{aligned}
$$

and

$$
\begin{aligned}
I_0 &= \int_{-h/2}^{h/2} \rho(z) \, \mathrm{d}z \\
&= \int_{-h/2}^{h/2} \left\{ (\rho_c - \rho_m) \left(\frac{z}{h} + \frac{1}{2} \right)^k + \rho_m \right\} \mathrm{d}z \\
&= \int_{-h/2}^{h/2} \left\{ (\rho_c - \rho_m) \left(\frac{z}{h} + \frac{1}{2} \right)^k \right\} \mathrm{d}z + \int_{-h/2}^{h/2} \rho_m \, \mathrm{d}z \\
&= \frac{(\rho_c - \rho_m) h}{k+1} + \rho_m h.
\end{aligned}
$$

Now we take partial derivative of ω^2 with respect to unknown constants as

$$
\frac{\partial \omega^2}{\partial c_i} = 0, \quad i = 1, 2, 3, \cdots, n \tag{3.37}
$$

Further manipulation of Eq. (3.37) yields the generalized eigenvalue problem of the form

$$
\left([K]_{n \times n} - \lambda^2 [M]_{n \times n} \right) \{\Delta\} = 0 \tag{3.38}
$$

where $[K]_{n \times n}$ and $[M]_{n \times n}$ are symmetric stiffness and inertia matrices respectively and $\{\Delta\}$ is the column vector of unknown constant coefficients. Solutions of the eigenvalue problem, Eq. (3.38) gives the vibration characteristics viz. non-dimensional frequencies and mode shapes for free vibration of FG plate with different geometric configurations. On the other hand, the numerical modeling for triangular FG plate needs a bit modifications due to the transformation

of geometry from general cartesian co-ordinate system to standard triangle. In the similar fashion, there occurs change in expression of strain energy of deformed FG plate in presence of different complicating environments. So the details about their modeling have been discussed in corresponding chapters.

Thick isotropic rectangular plate

Let us define the strain energy (U) and kinetic energy (T) for the free vibration of thick isotropic plate by considering the constitutive relations given in Eq. (2.18).

$$\mathrm{U} = \frac{1}{2}\int_{\Omega}\left[\int_{-h/2}^{h/2}\left(\sigma_{xx}\epsilon_{xx} + \sigma_{yy}\epsilon_{yy} + \tau_{xy}\gamma_{xy} + \tau_{yz}\gamma_{yz} + \tau_{xz}\gamma_{xz}\right)\mathrm{d}z\right]\mathrm{d}x\mathrm{d}y \tag{3.39}$$

and

$$\mathrm{T} = \frac{1}{2}\int_{\Omega}\left[\int_{-h/2}^{h/2}\rho\left\{\left(\frac{\partial u_x}{\partial t}\right)^2 + \left(\frac{\partial u_y}{\partial t}\right)^2 + \left(\frac{\partial u_z}{\partial t}\right)^2\right\}\mathrm{d}z\right]\mathrm{d}x\mathrm{d}y \tag{3.40}$$

Substituting σ_{ii} $(i = x,\ y)$ and τ_{ij} $(i,\ j = x,\ y,\ z)$ in Eq. (3.39), it becomes

$$\mathrm{U} = \frac{1}{2}\int_{\Omega}\left[\int_{-h/2}^{h/2}\left\{Q_{11}\left(\epsilon_{xx}^2 + \epsilon_{yy}^2\right) + 2Q_{12}\epsilon_{xx}\epsilon_{yy} + Q_{66}\gamma_{xy}^2 + Q_{44}\gamma_{yz}^2 + Q_{55}\gamma_{xz}^2\right\}\mathrm{d}z\right]\mathrm{d}x\mathrm{d}y \tag{3.41}$$

Let us first individually expand the terms involved in Eq. (3.41) as

$$\begin{aligned}\epsilon_{xx}^2 &= \left(\frac{\partial u}{\partial x} - z\frac{\partial^2 w}{\partial x^2} + f(z)\frac{\partial \phi_x}{\partial x}\right)^2 \\ &= \left(\frac{\partial u}{\partial x}\right)^2 - 2z\frac{\partial u}{\partial x}\frac{\partial^2 w}{\partial x^2} + 2f(z)\frac{\partial u}{\partial x}\frac{\partial \phi_x}{\partial x} + z^2\left(\frac{\partial^2 w}{\partial x^2}\right)^2 + f^2\left(\frac{\partial \phi_x}{\partial x}\right)^2 - 2zf(z)\frac{\partial \phi_x}{\partial x}\frac{\partial^2 w}{\partial x^2},\end{aligned} \tag{3.42a}$$

$$\begin{aligned}\epsilon_{yy}^2 &= \left(\frac{\partial v}{\partial y} - z\frac{\partial^2 w}{\partial y^2} + f(z)\frac{\partial \phi_y}{\partial y}\right)^2 \\ &= \left(\frac{\partial v}{\partial y}\right)^2 - 2z\frac{\partial v}{\partial y}\frac{\partial^2 w}{\partial y^2} + 2f(z)\frac{\partial v}{\partial y}\frac{\partial \phi_y}{\partial y} + z^2\left(\frac{\partial^2 w}{\partial y^2}\right)^2 + f^2\left(\frac{\partial \phi_y}{\partial y}\right)^2 - 2zf(z)\frac{\partial \phi_y}{\partial y}\frac{\partial^2 w}{\partial y^2},\end{aligned} \tag{3.42b}$$

$$\epsilon_{xx}\epsilon_{yy} = \left(\frac{\partial u}{\partial x} - z\frac{\partial^2 w}{\partial x^2} + f(z)\frac{\partial \phi_x}{\partial x}\right)\left(\frac{\partial v}{\partial y} - z\frac{\partial^2 w}{\partial y^2} + f(z)\frac{\partial \phi_y}{\partial y}\right)$$
$$= \frac{\partial u}{\partial x}\frac{\partial v}{\partial y} - z\left(\frac{\partial u}{\partial x}\frac{\partial^2 w}{\partial y^2} + \frac{\partial v}{\partial y}\frac{\partial^2 w}{\partial x^2}\right) + f(z)\left(\frac{\partial u}{\partial x}\frac{\partial \phi_y}{\partial y} + \frac{\partial v}{\partial y}\frac{\partial \phi_x}{\partial x}\right) + z^2\frac{\partial^2 w}{\partial x^2}\frac{\partial^2 w}{\partial y^2} \quad (3.42c)$$
$$- zf(z)\left(\frac{\partial \phi_x}{\partial x}\frac{\partial^2 w}{\partial y^2} + \frac{\partial \phi_y}{\partial y}\frac{\partial^2 w}{\partial x^2}\right) + f^2\frac{\partial \phi_x}{\partial x}\frac{\partial \phi_y}{\partial y},$$

$$\gamma_{xy}^2 = \left[\left(\frac{\partial u}{\partial y} + \frac{\partial v}{\partial x}\right) - 2z\frac{\partial^2 w}{\partial x \partial y} + f(z)\left(\frac{\partial \phi_x}{\partial y} + \frac{\partial \phi_y}{\partial x}\right)\right]^2$$
$$= \left(\frac{\partial u}{\partial y} + \frac{\partial v}{\partial x}\right)^2 - 4z\left(\frac{\partial u}{\partial y} + \frac{\partial v}{\partial x}\right)\frac{\partial^2 w}{\partial x \partial y} + 2f(z)\left(\frac{\partial u}{\partial y} + \frac{\partial v}{\partial x}\right)\left(\frac{\partial \phi_x}{\partial y} + \frac{\partial \phi_y}{\partial x}\right) + 4z^2\left(\frac{\partial^2 w}{\partial x \partial y}\right)^2 \quad (3.42d)$$
$$+ f^2\left(\frac{\partial \phi_x}{\partial y} + \frac{\partial \phi_y}{\partial x}\right)^2 - 4zf(z)\left(\frac{\partial \phi_x}{\partial y} + \frac{\partial \phi_y}{\partial x}\right)\frac{\partial^2 w}{\partial x \partial y},$$

$$\gamma_{yz}^2 = \left(\frac{\partial f}{\partial z}\right)^2 \phi_y^2, \quad (3.42e)$$

$$\gamma_{xz}^2 = \left(\frac{\partial f}{\partial z}\right)^2 \phi_x^2. \quad (3.42f)$$

Substituting the expanded terms from Eq. (3.42) in Eq. (3.41), the strain energy (U) takes the form

$$\begin{aligned} \mathrm{U} = \frac{1}{2}\int_\Omega \Bigg[& A_{11}\left\{\left(\frac{\partial u}{\partial x}\right)^2 + \left(\frac{\partial v}{\partial y}\right)^2\right\} - 2B_{11}\left(\frac{\partial u}{\partial x}\frac{\partial^2 w}{\partial x^2} + \frac{\partial v}{\partial y}\frac{\partial^2 w}{\partial y^2}\right) + 2C_{11}\left(\frac{\partial u}{\partial x}\frac{\partial \phi_x}{\partial x} + \frac{\partial v}{\partial y}\frac{\partial \phi_y}{\partial y}\right) \\ & + D_{11}\left\{\left(\frac{\partial^2 w}{\partial x^2}\right)^2 + \left(\frac{\partial^2 w}{\partial y^2}\right)^2\right\} + E_{11}\left\{\left(\frac{\partial \phi_x}{\partial x}\right)^2 + \left(\frac{\partial \phi_y}{\partial y}\right)^2\right\} - 2F_{11}\left(\frac{\partial \phi_x}{\partial x}\frac{\partial^2 w}{\partial x^2} + \frac{\partial \phi_y}{\partial y}\frac{\partial^2 w}{\partial y^2}\right) \\ & + 2A_{12}\frac{\partial u}{\partial x}\frac{\partial v}{\partial y} - 2B_{12}\left(\frac{\partial u}{\partial x}\frac{\partial^2 w}{\partial y^2} + \frac{\partial v}{\partial y}\frac{\partial^2 w}{\partial x^2}\right) + 2C_{12}\left(\frac{\partial u}{\partial x}\frac{\partial \phi_y}{\partial y} + \frac{\partial v}{\partial y}\frac{\partial \phi_x}{\partial x}\right) + 2D_{12}\frac{\partial^2 w}{\partial x^2}\frac{\partial^2 w}{\partial y^2} \\ & + 2E_{12}\frac{\partial \phi_x}{\partial x}\frac{\partial \phi_y}{\partial y} - 2F_{12}\left(\frac{\partial \phi_x}{\partial x}\frac{\partial^2 w}{\partial y^2} + \frac{\partial \phi_y}{\partial y}\frac{\partial^2 w}{\partial x^2}\right) + A_{66}\left(\frac{\partial u}{\partial y} + \frac{\partial v}{\partial x}\right)^2 - 4B_{66}\left(\frac{\partial u}{\partial y} + \frac{\partial v}{\partial x}\right)\frac{\partial^2 w}{\partial x \partial y} \\ & + 2C_{66}\left(\frac{\partial u}{\partial y} + \frac{\partial v}{\partial x}\right)\left(\frac{\partial \phi_x}{\partial y} + \frac{\partial \phi_y}{\partial x}\right) + 4D_{66}\left(\frac{\partial^2 w}{\partial x \partial y}\right)^2 + E_{66}\left(\frac{\partial \phi_x}{\partial y} + \frac{\partial \phi_y}{\partial x}\right)^2 \\ & - 4F_{66}\left(\frac{\partial \phi_x}{\partial y} + \frac{\partial \phi_y}{\partial x}\right)\frac{\partial^2 w}{\partial x \partial y} + H_{44}\phi_y^2 + H_{55}\phi_x^2\Bigg] \mathrm{d}x\mathrm{d}y \end{aligned} \quad (3.43)$$

Then taking time derivative of displacement components leads to the kinetic energy (T) as

$$\begin{aligned}\mathrm{T} \;=\; & \frac{1}{2}\int_{\Omega}\Bigg\{\rho_0\left[\left(\frac{\partial u}{\partial t}\right)^2+\left(\frac{\partial v}{\partial t}\right)^2+\left(\frac{\partial w}{\partial t}\right)^2\right]-2\rho_1\left(\frac{\partial u}{\partial t}\frac{\partial^2 w}{\partial x\partial t}+\frac{\partial v}{\partial t}\frac{\partial^2 w}{\partial y\partial t}\right)\\ & +\rho_2\left[\left(\frac{\partial^2 w}{\partial x\partial t}\right)^2+\left(\frac{\partial^2 w}{\partial y\partial t}\right)^2\right]+2\rho_0^1\left(\frac{\partial u}{\partial t}\frac{\partial \phi_x}{\partial t}+\frac{\partial v}{\partial t}\frac{\partial \phi_y}{\partial t}\right)+\rho_0^2\left[\left(\frac{\partial \phi_x}{\partial t}\right)^2+\left(\frac{\partial \phi_y}{\partial t}\right)^2\right]\\ & -2\rho_1^1\left(\frac{\partial \phi_x}{\partial t}\frac{\partial^2 w}{\partial x\partial t}+\frac{\partial \phi_y}{\partial t}\frac{\partial^2 w}{\partial y\partial t}\right)\Bigg\}\,\mathrm{d}x\mathrm{d}y \qquad (3.44)\end{aligned}$$

The extensional, coupling, bending and transverse shear rigidities (as given in Eq. (3.43)) for the higher-order shear deformation theory can be expressed as,

$$\begin{aligned}(A_{ij},B_{ij},C_{ij}) &= \int_{-h/2}^{h/2} Q_{ij}(1,z,f(z))\,\mathrm{d}z;\ \text{ where }\ i,j=1,\,2,\,6\\ (D_{ij},E_{ij},F_{ij}) &= \int_{-h/2}^{h/2} Q_{ij}(z^2,f^2,zf(z))\,\mathrm{d}z;\ \text{ where }\ i,j=1,\,2,\,6\\ H_{kk} &= \int_{-h/2}^{h/2} Q_{kk}\left(\frac{\partial f}{\partial z}\right)^2\mathrm{d}z;\ \text{ where }\ k=4,\,5\end{aligned}$$

whereas the cross-sectional inertial coefficients in Eq. (3.44) are written as

$$\begin{aligned}\rho_i &= \int_{-h/2}^{h/2}\rho z^i\,\mathrm{d}z;\ \text{ where }\ i,j=0,\,1,\,2\\ \rho_i^j &= \int_{-h/2}^{h/2}\rho z^i f^j\,\mathrm{d}z;\ \text{ where }\ i=0,\,1;\ j=1,\,2.\end{aligned}$$

Let us assume the displacement components $u(x,y,t)$, $v(x,y,t)$, $w(x,y,t)$, $\phi_x(x,y,t)$ and $\phi_y(x,y,t)$ to be the harmonic type and those may be expressed as

$$\begin{aligned}u(x,y,t) &= U(x,y)\exp(i\omega t)\\ v(x,y,t) &= V(x,y)\exp(i\omega t)\\ w(x,y,t) &= W(x,y)\exp(i\omega t)\\ \phi_x(x,y,t) &= \frac{1}{a}\Phi_x(x,y)\exp(i\omega t)\\ \phi_y(x,y,t) &= \frac{1}{b}\Phi_y(x,y)\exp(i\omega t)\end{aligned} \qquad (3.45)$$

In Eq. (3.45), $i=\sqrt{-1}$; $U(x,y)$, $V(x,y)$, $W(x,y)$, $\Phi_x(x,y)$ and $\Phi_y(x,y)$ are the respective amplitudes for these displacement components for free vibration of isotropic plate and the exponential terms indicate the harmonic type variation where ω is the natural frequency. The

mathematical manipulation reveals that the coefficients associated with B_{ij}, C_{ij}, ρ_1 and ρ_0^1 will be zero since $\int_{-h/2}^{h/2} z\,\mathrm{d}z$ and $\int_{-h/2}^{h/2} f(z)\,\mathrm{d}z$ yield the value as zeroes irrespective of the shear deformation theory considered. Substituting the displacement components of Eq. (3.45) in Eqs. (3.43) and (3.44) gives the maximum strain energy (U_{max}) and the maximum kinetic energy (T_{max}) as

$$\begin{aligned}
\mathrm{U}_{max} = \frac{1}{2}\int_{\Omega}\Bigg[& A_{11}\left\{\left(\frac{\partial U}{\partial x}\right)^2+\left(\frac{\partial V}{\partial y}\right)^2\right\}+2A_{12}\frac{\partial U}{\partial x}\frac{\partial V}{\partial y}+A_{66}\left(\frac{\partial U}{\partial y}+\frac{\partial V}{\partial x}\right)^2 \\
& +D_{11}\left\{\left(\frac{\partial^2 W}{\partial x^2}\right)^2+\left(\frac{\partial^2 W}{\partial y^2}\right)^2\right\}+2D_{12}\frac{\partial^2 W}{\partial x^2}\frac{\partial^2 W}{\partial y^2}+4D_{66}\left(\frac{\partial^2 W}{\partial x\partial y}\right)^2 \\
& +\frac{E_{11}}{a^2}\left\{\left(\frac{\partial \Phi_x}{\partial x}\right)^2+\mu^2\left(\frac{\partial \Phi_y}{\partial y}\right)^2\right\}+\frac{2E_{12}}{ab}\frac{\partial \Phi_x}{\partial x}\frac{\partial \Phi_y}{\partial y}+\frac{E_{66}}{a^2}\left(\frac{\partial \Phi_x}{\partial y}+\mu\frac{\partial \Phi_y}{\partial x}\right)^2 \\
& -\frac{2F_{11}}{a}\left(\frac{\partial \Phi_x}{\partial x}\frac{\partial^2 W}{\partial x^2}+\mu\frac{\partial \Phi_y}{\partial y}\frac{\partial^2 W}{\partial y^2}\right)-\frac{2F_{12}}{a}\left(\frac{\partial \Phi_x}{\partial x}\frac{\partial^2 W}{\partial y^2}+\mu\frac{\partial \Phi_y}{\partial y}\frac{\partial^2 W}{\partial x^2}\right) \\
& -\frac{4F_{66}}{a}\left(\frac{\partial \Phi_x}{\partial y}+\mu\frac{\partial \Phi_y}{\partial x}\right)\frac{\partial^2 W}{\partial x\partial y}+\frac{H_{44}}{a^2}\left(\Phi_x^2+\mu^2\Phi_y^2\right)\Bigg]\,\mathrm{d}x\mathrm{d}y
\end{aligned} \tag{3.46}$$

and

$$\begin{aligned}
\mathrm{T}_{max} = \frac{1}{2}\int_{\Omega}\Bigg[& \rho_0\left(U^2+V^2+W^2\right)+\rho_2\left\{\left(\frac{\partial W}{\partial x}\right)^2+\left(\frac{\partial W}{\partial y}\right)^2\right\}+\frac{\rho_0^2}{a^2}\left(\Phi_x^2+\mu^2\Phi_y^2\right) \\
& -\frac{2\rho_1^1}{a}\left(\Phi_x\frac{\partial W}{\partial x}+\mu\Phi_y\frac{\partial W}{\partial y}\right)\Bigg]\,\mathrm{d}x\mathrm{d}y
\end{aligned} \tag{3.47}$$

where $\mu = a/b$ is the aspect ratio of the rectangular plate. Now let us now non-dimensionalize x and y involved in Eqs. (3.46) and (3.47) as

$$X = \frac{x}{a},\ Y = \frac{y}{b},\ \delta = \frac{a}{h}$$

and substituting these variables in Eqs. (3.46) and (3.47), the corresponding expressions can be written as

$$
\begin{aligned}
\mathrm{U}_{max} \;=\; & \frac{Dab}{2a^4}\int_{\Omega}\Bigg[12\delta^2\left\{\left(\frac{\partial U}{\partial X}\right)^2+\mu^2\left(\frac{\partial V}{\partial Y}\right)^2+2\nu\mu\frac{\partial U}{\partial X}\frac{\partial V}{\partial Y}+\frac{1-\nu}{2}\left(\mu\frac{\partial U}{\partial Y}+\frac{\partial V}{\partial X}\right)^2\right\}\\
& +\left\{\left(\frac{\partial^2 W}{\partial X^2}\right)^2+\mu^4\left(\frac{\partial^2 W}{\partial Y^2}\right)^2+2\nu\mu^2\frac{\partial^2 W}{\partial X^2}\frac{\partial^2 W}{\partial Y^2}+2\mu^2(1-\nu)\left(\frac{\partial^2 W}{\partial X\partial Y}\right)^2\right\}\\
& +12C_1\left\{\left(\frac{\partial \Phi_x}{\partial X}\right)^2+\mu^4\left(\frac{\partial \Phi_Y}{\partial Y}\right)^2+2\nu\mu^2\frac{\partial \Phi_X}{\partial X}\frac{\partial \Phi_Y}{\partial Y}+\frac{1-\nu}{2}\mu^2\left(\frac{\partial \Phi_X}{\partial Y}+\frac{\partial \Phi_Y}{\partial X}\right)^2\right\}\\
& -24C_2\left\{\left(\frac{\partial \Phi_X}{\partial X}\frac{\partial^2 W}{\partial X^2}+\mu^4\frac{\partial \Phi_Y}{\partial Y}\frac{\partial^2 W}{\partial Y^2}\right)+\nu\mu^2\left(\frac{\partial \Phi_X}{\partial X}\frac{\partial^2 W}{\partial Y^2}+\frac{\partial \Phi_Y}{\partial Y}\frac{\partial^2 W}{\partial X^2}\right)\right.\\
& \left.+(1-\nu)\mu^2\left(\frac{\partial \Phi_X}{\partial Y}+\frac{\partial \Phi_Y}{\partial X}\right)\frac{\partial^2 W}{\partial X\partial Y}\right\}+6C_3(1-\nu)\delta^2\left(\Phi_X^2+\mu^2\Phi_Y^2\right)\Bigg]\,\mathrm{d}X\mathrm{d}Y \qquad (3.48)
\end{aligned}
$$

and

$$
\begin{aligned}
\mathrm{T}_{max} \;=\; & \frac{\rho hab\omega^2}{2}\int_{\Omega}\Bigg[\left(U^2+V^2+W^2\right)+\frac{1}{12}\left\{\frac{1}{\delta^2}\left(\frac{\partial W}{\partial X}\right)^2+\left(\frac{\mu}{\delta}\right)^2\left(\frac{\partial W}{\partial Y}\right)^2\right\}\\
& +C_1\left\{\frac{1}{\delta^2}\Phi_X^2+\left(\frac{\mu}{\delta}\right)^2\Phi_Y^2\right\}-2C_2\left\{\frac{1}{\delta^2}\Phi_X\frac{\partial W}{\partial X}+\left(\frac{\mu}{\delta}\right)^2\Phi_Y\frac{\partial W}{\partial Y}\right\}\Bigg]\,\mathrm{d}X\mathrm{d}Y \qquad (3.49)
\end{aligned}
$$

Here, $D=\frac{Eh^3}{12(1-\nu^2)}$ is the flexural rigidity of the plate. In Eqs. (3.48) and (3.49), the coefficients C_1, C_2 and C_3 depend on the shear deformation theories and are reported in Table 3.3. In this table, $-\frac{1}{2}\leq\bar{z}\,(=\frac{z}{h})\leq\frac{1}{2}$ is the non-dimensionalized thickness coordinate.

Table 3.3: Shear deformation plate theories and their respective coefficients; C_1, C_2 and C_3

Source	Theory	Coefficients	Expression
Reddy (1984b,c)	PSDPT	C_1	$\int_{-1/2}^{1/2}\left\{\bar{z}\left(1-4\bar{z}^2/3\right)\right\}^2 \mathrm{d}\bar{z}$
		C_2	$\int_{-1/2}^{1/2}\left\{\bar{z}^2\left(1-4\bar{z}^2/3\right)\right\} \mathrm{d}\bar{z}$
		C_3	$\int_{-1/2}^{1/2}\left(1-4\bar{z}^2\right)^2 \mathrm{d}\bar{z}$
Reissner (1975)	2-DPT	C_1	$\int_{-1/2}^{1/2}\left\{\frac{5\bar{z}}{4}\left(1-\frac{4\bar{z}^2}{3}\right)\right\}^2 \mathrm{d}\bar{z}$
		C_2	$\int_{-1/2}^{1/2}\frac{5\bar{z}^2}{4}\left(1-\frac{4\bar{z}^2}{3}\right) \mathrm{d}\bar{z}$
		C_3	$\int_{-1/2}^{1/2}\left(\frac{5}{4}-\frac{15\bar{z}^2}{3}\right)^2 \mathrm{d}\bar{z}$
Touratier (1991)	TSDPT	C_1	$(1/\pi^2)\int_{-1/2}^{1/2}\sin^2(\pi\bar{z})\,\mathrm{d}\bar{z}$
		C_2	$(1/\pi)\int_{-1/2}^{1/2}\bar{z}\sin(\pi\bar{z})\,\mathrm{d}\bar{z}$
		C_3	$\int_{-1/2}^{1/2}\cos^2(\pi\bar{z})\,\mathrm{d}\bar{z}$
Proposed	ISDPT	C_1	$\int_{-1/2}^{1/2}\left(\frac{2\bar{z}}{\sqrt{3}}-\sin^{-1}\bar{z}\right)^2 \mathrm{d}\bar{z}$
		C_2	$\int_{-1/2}^{1/2}\left(\frac{2\bar{z}^2}{\sqrt{3}}-\bar{z}\sin^{-1}\bar{z}\right) \mathrm{d}\bar{z}$
		C_3	$\int_{-1/2}^{1/2}\left(\frac{2}{\sqrt{3}}-\frac{1}{\sqrt{1-\bar{z}^2}}\right)^2 \mathrm{d}\bar{z}$
Proposed	ICDPT	C_1	$\int_{-1/2}^{1/2}\left(\frac{2\bar{z}}{\sqrt{3}}+\cos^{-1}\bar{z}\right)^2 \mathrm{d}\bar{z}$
		C_2	$\int_{-1/2}^{1/2}\left(\frac{2\bar{z}^2}{\sqrt{3}}+\bar{z}\cos^{-1}\bar{z}\right) \mathrm{d}\bar{z}$
		C_3	$\int_{-1/2}^{1/2}\left(\frac{2}{\sqrt{3}}-\frac{1}{\sqrt{1-\bar{z}^2}}\right)^2 \mathrm{d}\bar{z}$
Proposed	ITDPT	C_1	$\int_{-1/2}^{1/2}\left(\frac{4\bar{z}}{5}-\tan^{-1}\bar{z}\right)^2 \mathrm{d}\bar{z}$
		C_2	$\int_{-1/2}^{1/2}\left(\frac{4\bar{z}^2}{5}-\bar{z}\tan^{-1}\bar{z}\right) \mathrm{d}\bar{z}$
		C_3	$\int_{-1/2}^{1/2}\left(\frac{4}{5}-\frac{1}{1+\bar{z}^2}\right)^2 \mathrm{d}\bar{z}$
Proposed	ICTDPT	C_1	$\int_{-1/2}^{1/2}\left(\frac{4\bar{z}}{5}+\cot^{-1}\bar{z}\right)^2 \mathrm{d}\bar{z}$
		C_2	$\int_{-1/2}^{1/2}\left(\frac{4\bar{z}^2}{5}+\bar{z}\cot^{-1}\bar{z}\right) \mathrm{d}\bar{z}$
		C_3	$\int_{-1/2}^{1/2}\left(\frac{4}{5}-\frac{1}{1+\bar{z}^2}\right)^2 \mathrm{d}\bar{z}$

To obtain the generalized eigenvalue problem for the free vibration of isotropic plate, the numerical modeling is based on the use of Rayleigh-Ritz method. According to Rayleigh-Ritz method, again the amplitudes of vibration are expressed in terms of algebraic polynomials by the following series.

$$U=\sum_{i=1}^{n}c_i\varphi_i^u,\;\; V=\sum_{j=1}^{n}d_j\varphi_j^v,\;\; W=\sum_{k=1}^{n}e_k\varphi_k^w,\;\; \Phi_x=\sum_{l=1}^{n}g_l\varphi_l^1,\;\; \Phi_y=\sum_{m=1}^{n}h_m\varphi_m^2$$

where c_i, d_j, e_k, g_l and h_m are the unknown constant coefficients to be determined and φ_i^u, φ_j^v, φ_k^w, φ_l^1 and φ_m^2 are the admissible functions corresponding to the amplitudes; U, V, W, Φ_x and Φ_y respectively. The admissible functions must satisfy the essential boundary conditions

and can be represented as

$$\begin{aligned}
\varphi_i^u(X,Y) &= \mathrm{a}_f\psi_i^u(X,Y), \quad i = 0,1,2,\cdots,n \\
\varphi_j^v(X,Y) &= \mathrm{a}_f\psi_j^v(X,Y), \quad j = 0,1,2,\cdots,n \\
\varphi_k^w(X,Y) &= \mathrm{a}_f\psi_k^w(X,Y), \quad k = 0,1,2,\cdots,n \\
\varphi_l^1(X,Y) &= \mathrm{a}_f\psi_l^1(X,Y), \quad l = 0,1,2,\cdots,n \\
\varphi_m^2(X,Y) &= \mathrm{a}_f\psi_m^2(X,Y), \quad m = 0,1,2,\cdots,n
\end{aligned} \tag{3.50}$$

The function $\mathrm{a}_f = X^pY^q(1-X)^r(1-Y)^s$ with the exponents p, q, r and s, controls various BCs. As mentioned earlier, the parameter p takes the value 0, 1 or 2 according as the side $X = 0$ is free (F), simply supported (S) or clamped (C). Similar interpretations can be given to the parameters q, r and s corresponding to the sides $Y = 0$, $X = 1$ and $Y = 1$, respectively. In present investigation, the flow of different combinations of boundary conditions is demonstrated in Fig. 3.1. For example if we consider the edge support CSCS, then 1 is meant for clamped (C) and accordingly 2, 3 and 4 represent simply supported (S), clamped (C) simply supported (S) edge conditions respectively. Simple algebraic polynomials generated from the Pascal's triangle are again considered here to define the admissible functions mentioned in Eq. (3.50).

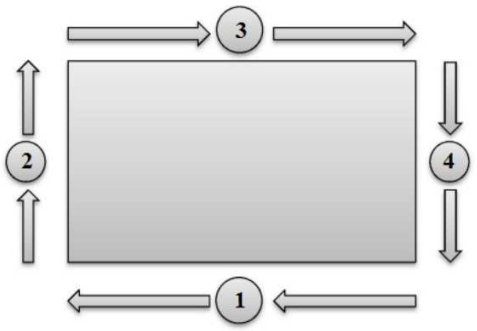

Figure 3.1: The flow of various combinations of boundary supports

Here also, Rayleigh Quotient (ω^2) can be obtained by equating U_{max} and T_{max} given in Eqs. (3.48) and (3.49). Taking the partial derivatives of the Rayleigh Quotient with respect to the

constant coefficients involved in the admissible functions, we have

$$\frac{\partial \omega^2}{\partial c_i} = 0; \;\; i = 1, 2, \cdots, n$$
$$\frac{\partial \omega^2}{\partial d_j} = 0; \;\; j = 1, 2, \cdots, n$$
$$\frac{\partial \omega^2}{\partial e_k} = 0; \;\; k = 1, 2, \cdots, n$$
$$\frac{\partial \omega^2}{\partial g_l} = 0; \;\; l = 1, 2, \cdots, n$$
$$\frac{\partial \omega^2}{\partial h_m} = 0; \;\; m = 1, 2, \cdots, n.$$

This will yield the governing equation for the free vibration of isotropic plate in the form of generalized eigenvalue problem as

$$\left([\mathbf{K}] - \lambda^2 [\mathbf{M}]\right)\{\Delta\} = 0 \tag{3.51}$$

Here, [**K**] and [**M**] are the stiffness and inertia matrices respectively and $\{\Delta\}$ is the column vector of unknown constant coefficients. The eigenvalues (λ) in Eq. (3.51) are the non-dimensional frequencies for the concerned free vibration problem. In this investigation, free vibration eigenfrequencies obtained from this eigenvalue problem are exhaustively studied in further chapters.

3.2 Differential Quadrature (DQ) method

In this section, generalized differential quadrature method as mentioned in (Shu and Du, 1997) is outlined. This method has been implemented to study free vibration of geometrically non-linear functionally graded (FG) beams. The important results based on this study are discussed in Sec. 5.2.

3.2.1 Governing equation for free vibration

In non-uniform functionally graded beam, the material properties of the constituents are assumed to vary along thickness direction in power-law form, as stated in Eq. (2.1). In Euler-Bernoulli beam theory (EBT), the governing equation for free vibration of functionally

graded beam with varying cross-section may be expressed as

$$\frac{\partial^2}{\partial x^2}\left[\left\{\int_A z^2 E(z)\mathrm{d}A\right\}\frac{\partial^2 w}{\partial x^2}\right]+\left\{\int_A \rho(z)\mathrm{d}A\right\}\frac{\partial^2 w}{\partial t^2}=0 \tag{3.52}$$

In Eq. (3.52), $I(x)$ and $A(x)$ are moment of inertia and area of cross-section of the beam, which vary across axial direction (x). The material properties $E(z)$ and $\rho(z)$ are the Young's moduli and mass densities of FG material constituents, which are assumed to vary along thickness direction in power-law form (as stated in Eq. (2.1)). By considering the non-dimensional parameters as $-\frac{1}{2}\leq\xi=x/L\leq\frac{1}{2}$ and $-\frac{1}{2}\leq\bar{z}=z/h\leq\frac{1}{2}$, Eq. (3.52) yields

$$\frac{E_{\text{eff}}}{L^4}\frac{\partial^2}{\partial\xi^2}\left\{I(\xi)\frac{\partial^2 w}{\partial\xi^2}\right\}+\rho_{\text{eff}}A(\xi)\frac{\partial^2 w}{\partial t^2}=0 \tag{3.53}$$

Here, $E_{\text{eff}}=\frac{1}{1-\nu^2}\left\{1+12\,(E_r-1)\left(\frac{1}{k+3}-\frac{1}{k+2}+\frac{1}{4(k+1)}\right)\right\}$; $\rho_{\text{eff}}=\left\{1+\left(\frac{\rho_r-1}{k+1}\right)\right\}$. Let us consider functions $I(\xi)=I_0 f(\xi)$ and $A(\xi)=A_0 g(\xi)$, where $f(\xi)$ and $g(\xi)$ are the factors which claim the functionally graded beam to be geometrically non-linear (or non-uniform). The functions $f(\xi)$ and $g(\xi)$ will take any of the following simple algebraic forms viz. $(1+\alpha\xi)^{m_1}$; $m_1=1,\ 2,\ 3,\ 4$ and $(1+\alpha\xi)^{m_2}$; $m_2=1,\ 2,\ 3,\ 4$. In this regard, $f(\xi)$ and $g(\xi)$ are to be assumed with specific indices m_1 and m_2. Introducing the harmonic type displacement as $w(\xi,t)=W(\xi)\exp(\mathrm{i}\omega t)$, where $W(x)$ is the amplitude and ω is the natural frequency. Next Eq. (3.53) may be transformed to

$$E_{\text{eff}}\left(\bar{I}''W''+2\bar{I}'W'''+\bar{I}W''''\right)-\Omega^2\rho_{\text{eff}}\bar{A}W=0 \tag{3.54}$$

where $\bar{I}=I/I_0$; $\bar{A}=A/A_0$; $(\,)'$ is meant for the partial derivatives with respect to ξ and $\Omega^2=\frac{\omega^2 L^4\rho_m A_0}{E_m I_0}$.

Along with the governing equation, we have also introduced varieties of non-homogeneities in case of functionally graded beam. In non-uniform functionally graded beam, the power-law variations of E_{eff} and ρ_{eff} are to be controlled by the components E_r and ρ_r respectively. Moreover, k also plays major role in evaluating both these material properties.

3.2.2 Generalized Differential Quadrature (GDQ)

In this section, we have discussed various approaches to the differential quadrature method. Bellman et al. (1972) have assumed a sufficiently smooth function $f(x)$ over the interval $[a,b]$,

so that its first derivative $f_x^{(1)}(x)$ at any grid point over $[a,b]$ can be approximated by the following approximation

$$f_x^{(1)}(x_i) \cong \sum_{j=1}^{N} c_{ij}^{(1)} f(x_j), \quad i = 1,2,\cdots,N \tag{3.55}$$

where the coefficient matrix $(c_{ij}^{(1)})$ can be determined in various fashions. $f_x^{(1)}(x_i)$ finds the first order derivative of $f(x)$ with respect to x at x_i. Necessarily, the key procedure in this method is to compute the weighting coefficients $c_{ij}^{(1)}$ using different test functions ($f(x)$ or $g_k(x)$). By demanding Eq. (3.55) to be exact for all polynomials of degree less than or equal to $N-1$. Different approaches towards finding the weighting coefficients are mentioned below:

1. In first approach by Bellman et al. (1972), the test functions $g_k(x) = x^{k-1};\ k = 1,2,\cdots,N$, which gives a set of linear algebraic equations

$$\sum_{j=1}^{N} c_{ij}^{(1)} x_j^k = k x_i^{k-1}, \ \ i = 1,2,\cdots,N; \ \ k = 0,1,\cdots,N-1.$$

   As the matrix is of Vandermonde form, this system of equations has a unique solution. But unfortunately, the concerned matrix becomes ill-conditioned and its inversion is difficult when N is very large.

2. On the other hand, the second approach by Bellman et al. (1972) defines the test function as $g_k(x) = \frac{L_N(x)}{(x-x_k)L_N^{(1)}(x_k)};\ k = 1,2,\cdots,N$, where $L_N(x)$ is the N^{th} order Legendre polynomial and $L_N^{(1)}(x)$ is the first order derivative of $L_N(x)$. In this approach, the necessary condition is that the coordinates of grid points should be the roots of an N^{th} order Legendre polynomial.

3. To overcome such ambiguities of DQM, the generalized differential quadrature (GDQ) approach has been developed by Shu and Du (1997) for the determination of weighting coefficients.

Weighting coefficients of first order derivative (Shu and Du, 1997)

In view of the above, Shu and Du (1997) have taken the benefit of two approaches of (Bellman et al., 1972) and approach of (Quan and Chang, 1989a,b) to derive the test functions in GDQ and

kept no restrictions in deciding the grid points over the domain. For generality, GDQ chooses the base polynomials (or test functions) $g_k(x)$ to be the Lagrange interpolating polynomial

$$g_k(x) = \frac{M(x)}{(x-x_k)M^{(1)}(x_k)} \tag{3.56}$$

where $M(x) = \prod_{j=1}^{N}(x - x_j)$; $M^{(1)}(x) = \prod_{j=1, j\neq k}^{N}(x_k - x_j)$ with $x_1, x_2, \cdots, x_N$ are the coordinates of the grid points and may be chosen arbitrarily. For simplicity, it is considered that

$$M(x) = N(x, x_k)(x - x_k),\ k = 1, 2, \cdots, N$$

with $N(x_i, x_j) = M^{(1)}(x_i)\delta_{ij}$, where δ_{ij} is the Kronecker operator. With these assumptions, Eq. (3.56) converts to

$$g_k(x) = \frac{N(x, x_k)}{M^{(1)}(x_k)} \tag{3.57}$$

By substituting Eq. (3.57) into Eq. (3.55), we obtain

$$c_{ij}^{(1)} = \frac{N^{(1)}(x_i, x_j)}{M^{(1)}(x_j)} \tag{3.58}$$

We can easily find $M^{(1)}(x_j)$ by using its concerned expression. To evaluate $N^{(1)}(x_i, x_j)$, let us differentiate $M(x)$ successively with respect to x and we obtain the following recurrence formulation

$$M^{(m)}(x) = N^{(m)}(x, x_k)(x - x_k) + mN^{(m-1)}(x, x_k),\ k = 1, 2, \cdots, N; m = 1, 2, \cdots, N-1 \tag{3.59}$$

where $M^{(m)}(x)$ and $N^{(m)}(x, x_k)$ are the m^{th} order derivatives of $M(x)$ and $N(x, x_k)$ respectively. The expression of $N^{(1)}(x_i, x_j)$ can be obtained from Eq. (3.59) as $N^{(1)}(x_i, x_j) = \begin{cases} \frac{M^{(1)}(x_i)}{x_i - x_j};\ i \neq j \\ \frac{M^{(2)(x_i)}}{2};\ i = j \end{cases}$.

Substituting this expression in Eq. (3.58), we get

$$c_{ij}^{(1)} = \begin{cases} \frac{M^{(1)}(x_i)}{(x_i - x_j)M^{(1)}(x_j)}; & i \neq j \\ \frac{M^{(2)(x_i)}}{2M^{(1)}(x_i)}; & i = j \end{cases} \tag{3.60}$$

Eq. (3.60) is a simple expression for the computation of $c_{ij}^{(1)}$ without the restriction of choosing grid points x_i. Rather than evaluating $M^{(2)}(x_i)$, it is worth to mention that one set of base polynomials can be derived uniquely by linear combination of another set of base polynomials in a vector space. Moreover, $c_{ij}^{(1)}$ satisfies the relation; $\sum_{j=1}^{N} c_{ij}^{(1)} = 0$ which may be obtained by the base polynomials x^{k-1} when $k = 1$. Here, $c_{ii}^{(1)}$ can easily be determined from $c_{ij}^{(1)}$, $i \neq j$.

Weighting coefficients of second and higher order derivatives (Shu and Du, 1997)

The second and higher order derivatives of the smooth function $f(x)$ may be written with the linear constrained relationships as

$$f_x^{(m)}(x_i) \cong \sum_{j=1}^{N} c_{ij}^{(m)} f(x_j), \quad i = 1, 2, \cdots, N \tag{3.61}$$

Then, the $(m-1)^{\text{th}}$ order derivatives can be expressed as

$$f_x^{(m-1)}(x_i) \cong \sum_{j=1}^{N} c_{ij}^{(m-1)} f(x_j), \quad i = 1, 2, \cdots, N \tag{3.62}$$

Now let us substitute Eq. (3.57) in Eqs. (3.61) and (3.62) and using Eqs. (3.59) and (3.60), a recurrence relation may be written as

$$c_{ij}^{(m)} = \begin{cases} m\left(c_{ij}^{(1)} c_{ii}^{(m-1)} - \frac{c_{ij}^{(m-1)}}{x_i - x_j}\right); & i \neq j \\ \frac{M^{(m+1)}(x_i)}{(m+1)M^{(1)}(x_i)}; & i = j \end{cases} \tag{3.63}$$

$$\text{for } i,\ j = 1, 2, \cdots, N;\ m = 2, 3, \cdots, N-1$$

In $N-$dimensional vector space, the system of equations for $c_{ij}^{(m)}$ derived from Lagrange interpolating polynomials should also be equivalent to that derived from the base polynomials $x^{k-1},\ k = 1, 2, \cdots, N$. As discussed for the weighting coefficients of first order derivatives, the weighting coefficients of higher order derivatives also follow the equation $\sum_{j=1}^{N} c_{ij}^{(m)} = 0$ obtained from the base polynomials x^{k-1} when $k = 1$, i.e. $c_{ii}^{(m)} = \sum_{j=1, i\neq j}^{N} c_{ij}^{(m)}$.

3.2.3 Discretization of governing equation

The non-homogeneous grid points in case of DQM are to be considered as Chebyshev-Gauss-Lobatto points in axial direction (Shu and Du, 1997). The governing equation (Eq. (3.54)) for free vibration of FG beam can be transformed into the following expression by substituting the weighting coefficients of required derivatives,

$$E_{\text{eff}}\left\{\bar{I}^{(2)}(\xi_i)\sum_{j=1}^{N}c_{ij}^{(2)}W(\xi_j)+2\bar{I}^{(1)}(\xi_i)\sum_{j=1}^{N}c_{ij}^{(3)}W(\xi_j)+\bar{I}(\xi_i)\sum_{j=1}^{N}c_{ij}^{(4)}W(\xi_j)\right\}-\Omega^2\rho_{\text{eff}}\bar{A}(\xi_i)W(\xi_i)=0 \tag{3.64}$$

where $i = 1, 2, \cdots, N$; $\bar{I}^{(1)}(\xi_i)$ and $\bar{I}^{(2)}(\xi_i)$ are the values of first and second order derivatives of $I(\xi)$ at ξ. The present study involves combination of two different boundary conditions stated as

1. Clamped (C): $W = 0$ and $W' = 0$.
2. Simply supported (S): $W = 0$ and $W'' = 0$.

The discretized forms of boundary supports can be written in the following form

$$W_1 = 0 \tag{3.65a}$$

$$\sum_{j=1}^{N}c_{ij}^{(n_0)}W(\xi_j)=0 \tag{3.65b}$$

$$W_N = 0 \tag{3.65c}$$

$$\sum_{j=1}^{N}c_{ij}^{(n_1)}W(\xi_j)=0 \tag{3.65d}$$

Here, n_0 and n_1 may be taken either as 1 or 2. n_0 and n_1 solely control the boundary conditions and may produce the following four sets of boundary conditions,

$$\text{C-C} : n_0,\ n_1 = 1$$

$$\text{C-S} : n_0 = 1,\ n_1 = 2$$

$$\text{S-C} : n_0 = 2,\ n_1 = 1$$

$$\text{S-S} : n_0,\ n_1 = 2$$

The boundary supports of $W_{1 \text{ or } N} = 0$ can easily be put into Eq. (3.64), but W_2 and W_{N-1} can be found by solving the concerned expressions (Eqs. (3.65b) and (3.65d)) using the method of elimination or substitution and may be expressed as

$$W_2 = \frac{1}{\mathrm{C}} \sum_{j=3}^{N-2} C_1 W_j; \quad W_{N-1} = \frac{1}{\mathrm{C}} \sum_{j=3}^{N-2} C_N W_j$$

with $\mathrm{C} = c_{1,2}^{(n_0)} c_{N,N-1}^{(n_1)} - c_{1,N-1}^{(n_0)} c_{N,2}^{(n_1)}$; $C_1 = c_{1,N-1}^{(n_0)} c_{N,j}^{(n_1)} - c_{1,j}^{(n_0)} c_{N,N-1}^{(n_1)}$ and $C_N = c_{1,j}^{(n_0)} c_{N,2}^{(n_1)} - c_{1,2}^{(n_0)} c_{N,j}^{(n_1)}$.

Looking into the analysis performed in Shu and Du (1997), we can obtain the generalized eigenvalue problem in discretized form as

$$E_{\text{eff}} \left\{ \bar{I}^{(2)}(\xi_i) \sum_{j=3}^{N-2} C^{(2)} W(\xi_j) + 2\bar{I}^{(1)}(\xi_i) \sum_{j=3}^{N-2} C^{(3)} W(\xi_j) + \bar{I}(\xi_i) \sum_{j=3}^{N-2} C^{(4)} W(\xi_j) \right\} = \Omega^2 \rho_{\text{eff}} \bar{A}(\xi_i) W(\xi_i) \tag{3.66}$$

by implementing four boundary conditions at the edges of the FG beam. Moreover $i = 3, 4, \cdots, N-2$. Accordingly, the coefficient matrices of weighting coefficients in Eq. (3.66) can be given as the following forms:

$$C^{(2)} = c_{i,j}^{(2)} + \left[\frac{C_1 c_{i,2}^{(2)} + C_N c_{i,N-1}^{(2)}}{\mathrm{C}} \right]$$

$$C^{(3)} = c_{i,j}^{(3)} + \left[\frac{C_1 c_{i,2}^{(3)} + C_N c_{i,N-1}^{(3)}}{\mathrm{C}} \right]$$

$$C^{(4)} = c_{i,j}^{(4)} + \left[\frac{C_1 c_{i,2}^{(4)} + C_N c_{i,N-1}^{(4)}}{\mathrm{C}} \right]$$

Consequently, the free vibration frequency (Ω) can be obtained from the generalized eigenvalue problem (Eq. (3.66)).

Chapter 4

Static analysis of functionally graded plates

The contents of this chapter have been published in:

(1) Pradhan, K.K. and Chakraverty, S. (2014). Static analysis of functionally graded thin rectangular plates with various boundary supports. *Archives of Civil and Mechanical Engineering*, 15:721–734 (Elsevier).

Chapter 4

Static analysis of functionally graded plates

This investigation mainly deals with static analysis of FG rectangular plates subjected to various classical boundary conditions within the framework of classical plate theory. Material properties of the FG plate are assumed to vary continuously in the thickness direction according to power-law form. The trial functions denoting the transverse deflection are expressed as linear combination of simple algebraic polynomials. Uniformly Distributed Load (UDL) and hydrostatic pressure are considered to be the external mechanical loads. The Rayleigh-Ritz method is employed in the numerical modelling to obtain the system of linear equations for the pure bending. The objective is to study the effect of aspect ratio and volume fraction of the constituents on numerical factors associated with centroidal (mid-plane) deflection, bending moments and normal stresses. New results for these bending parameters are demonstrated after checking the convergence pattern and verification with the available results in special cases.

4.1 Numerical modeling

The Rayleigh-Ritz procedures for this static problem has already been discussed in Sec. 3.1.1 to obtain the system of linear equations of the form Eq. (3.10) to yield the pure bending properties in detail.

4.2 Convergence and comparison studies

In vew of Eq. (3.10), the pure bending properties viz. mid-plane deflection, bending moments and normal stresses are to be computed based on Eqs. (3.11) to (3.15) after checking test of convergence and validation with available results. In this regard, the convergence of numerical

factors (α,β,$\beta^{'}$,δ and $\delta^{'}$ expressed in Eqs. (3.11) to (3.15)) are demonstrated in Figs. 4.1 and 4.2 with increase in number of polynomials involved in the deflection function (W) in pure bending of the FG rectangular plates. The Poisson's ratio of the ceramic and metal constituents are taken as constant viz. $\nu_c = \nu_m = 0.3$. The convergence test is carried out either under UDL or under hydrostatic pressure for the bending parameters of the simply supported (SSSS) FG plate. Figs. 4.1 (a) and (b) are meant for checking the convergence of the mentioned parameters for the isotropic square plate ($k = 0$, $E_{rat} = 1.0$) under UDL and hydrostatic pressure respectively. Similar convergence tests are also performed in Figs. 4.2 (a) and (b) for FG rectangular plate ($\mu = 2$, $k = 1$ and $E_{rat} = 2.5$) subjected to UDL and hydrostatic pressure respectively. It may also be concluded that increase in number of polynomials plays a crucial role in the convergence of these parameters irrespective of the external load and geometric configurations considered.

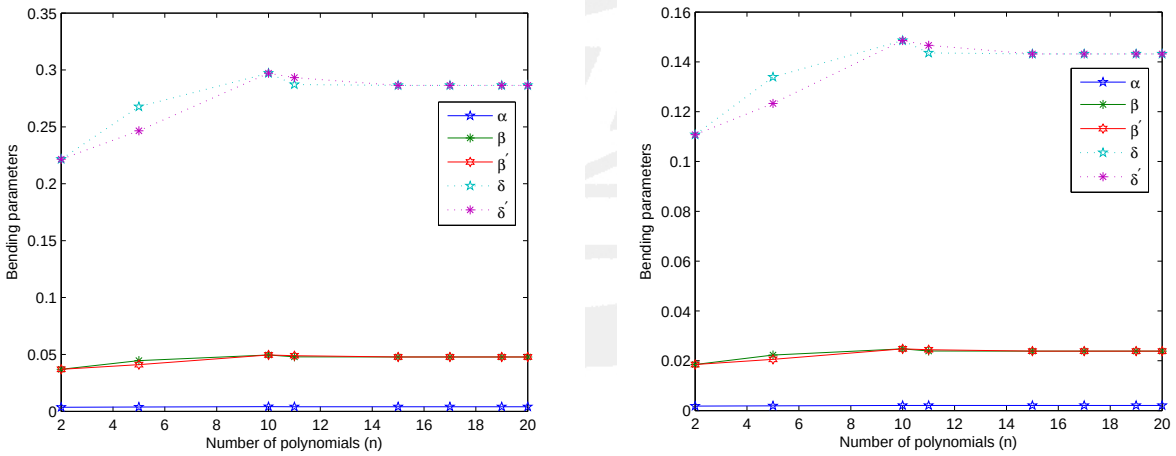

(a) Uniformly distributed load (b) Hydrostatic pressure

Figure 4.1: Convergence of numerical factors α,β,$\beta^{'}$,δ and $\delta^{'}$ of SSSS isotropic square plate ($k = 0$, $E_{rat} = 1.0$) under UDL and hydrostatic pressure

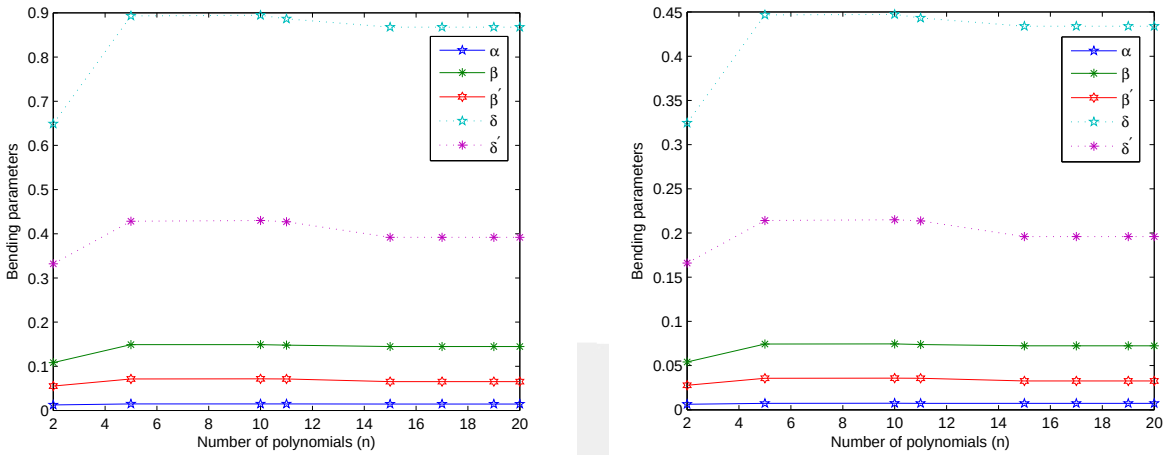

(a) Uniformly distributed load (b) Hydrostatic pressure

Figure 4.2: Convergence of numerical factors α,β,$\beta^{'}$,δ and $\delta^{'}$ of SSSS FG rectangular plate (μ = 2, k = 1 and E_{rat} = 2.5) under UDL and hydrostatic pressure

A few literature positions are available related to finding the pure bending parameters of the FG rectangular plates with arbitrary boundary conditions. The comparison of the numerical factors (α, β and $\beta^{'}$) for the isotropic rectangular plates ($k = 0$ in case of FG plate) with available results are graphically demonstrated in Figs. 4.3 to 4.5. Here, Fig. 4.3 is concerned with the results obtained for the isotropic simply supported rectangular plates for different aspect ratios (μ) under uniformly distributed load and hydrostatic pressure to validate with the exact values stated in (Timoshenko and Woinowsky-Krieger, 1959). On the other hand, comparison of centroidal deflections and bending moments for isotropic rectangular plates with CCCC and CSCS edge supports is performed with (Timoshenko and Woinowsky-Krieger, 1959; Yang and Shen, 2003a) in Fig. 4.4 under uniformly distributed load. On the contrary, centroidal deflections of simply supported isotropic plate under uniformly distributed load are compared in Fig. 4.5 with (Timoshenko and Woinowsky-Krieger, 1959; Werner, 1999; Zenkour, 2006) for different thicknesses, h = 0.01, 0.03 and 0.1. The computations in Fig. 4.5 are based on the formulation provided in (Zenkour, 2006). It can be observed in these figures that the present results are in excellent agreement with the available results, irrespective of the boundary conditions, geometric configuration or external mechanical load considered.

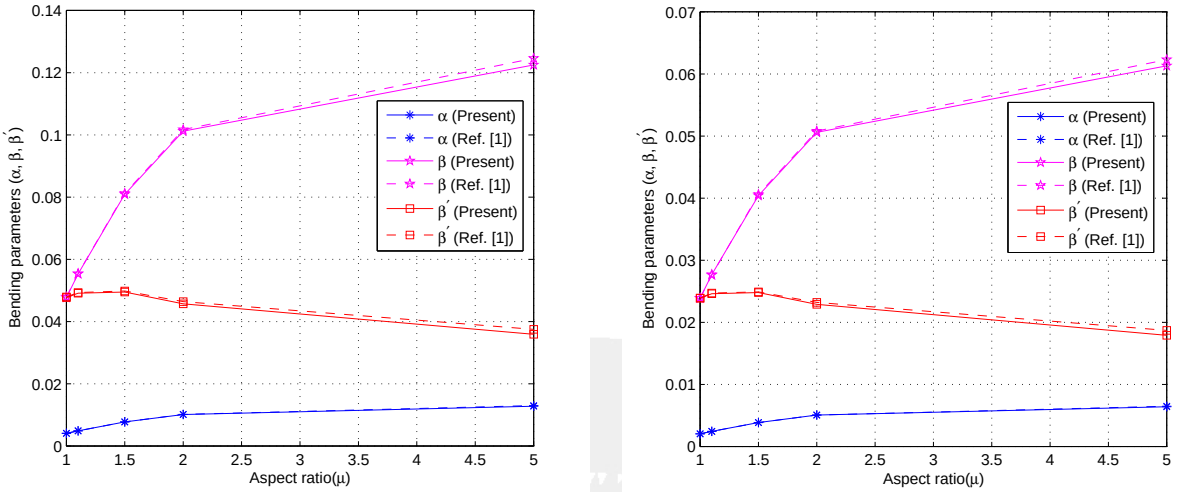

(a) Uniformly distributed load (b) Hydrostatic pressure

Figure 4.3: Comparison of numerical factors (α, β and $\beta^{'}$) of SSSS FG rectangular plates ($k = 0$) under UDL and hydrostatic pressure (Ref. [1] - Timoshenko and Woinowsky-Krieger (1959))

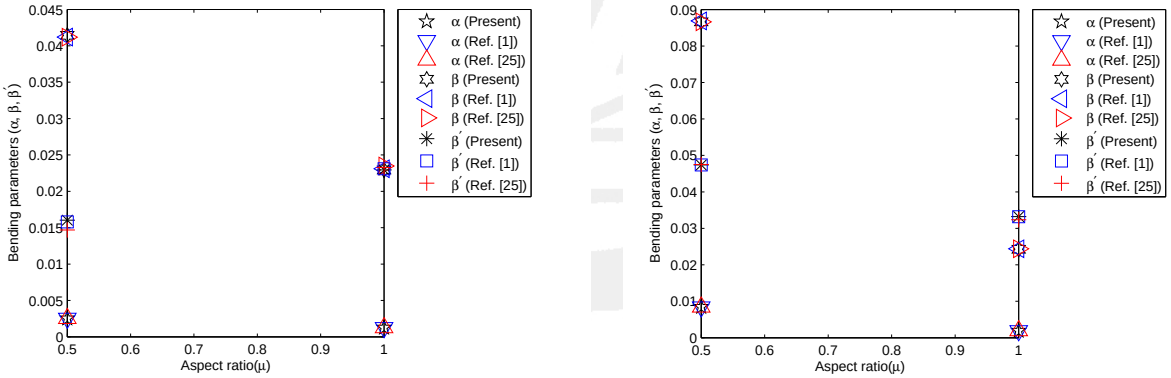

(a) CCCC (b) CSCS

Figure 4.4: Comparison of numerical factors (α, β and $\beta^{'}$) of FG rectangular plates (k = 0) under uniformly distributed load (Ref. [25] - Yang and Shen (2003a))

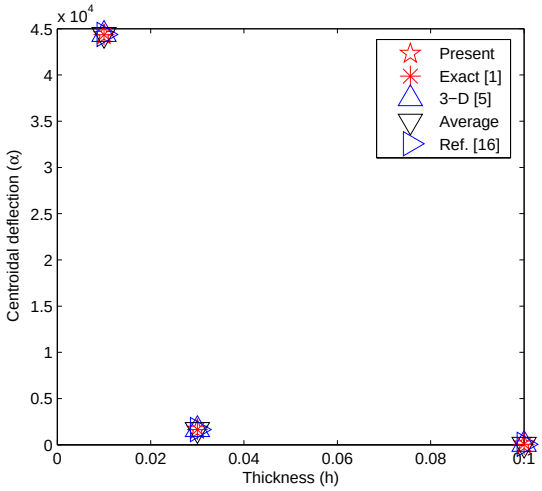

Figure 4.5: Comparison of centroidal deflections of SSSS FG rectangular plates ($k = 0$) under uniformly distributed load (3–D [5] - Werner (1999), Ref. [16] - Zenkour (2006))

4.3 Results and discussions

After excellent validation of the bending parameters, we have computed the new results for maximum deflection, bending moments and normal stresses of the FG rectangular plates subjected to various edge conditions. Here, Poisson's ratio (ν) is assumed to be 0.3. From the numerical formulation, it can be observed that three physical properties that influence these numerical factors are aspect ratio ($\mu = b/a$), power-law exponent (k) and ratio of Young's moduli of the constituents ($E_{rat} = E_c/E_m$).

4.3.1 Effect of aspect ratios

The effect of aspect ratios (μ) on numerical factors related to bending properties subjected to different combinations of boundary conditions are graphically presented in Figs. 4.6 to 4.8. Sets of values of α, β, $\beta^{'}$, δ and $\delta^{'}$ are evaluated with ascending values of μ = 1, 1.5, 2 and 3; power-law index (k) as 1 and E_{rat} = 2.5. As such, Figs. 4.6 (a) and (b) are associated with the effect of μ on the centroidal deflection ($\alpha\,|_{\xi=0.5,\eta=0.5}$) of the FG plate both under UDL and hydrostatic pressure respectively. In a similar fashion, the values of $\beta\,|_{\xi=0.5,\eta=0.5}$ and $\delta\,|_{\xi=0.5,\eta=0.5}$ with increase in μ are shown in Figs. 4.7 (a) and (b) for UDL and in Figs. 4.7 (c) and (d) for hydrostatic pressure respectively. On the other hand, Figs. 4.8 (a) and (b) are concerned with the evaluation of factors $\beta'\,|_{\xi=0.5,\eta=0.5}$ and $\delta'\,|_{\xi=0.5,\eta=0.5}$ under UDL and Figs. 4.8 (c) and (d) under hydrostatic pressure respectively. It can easily be seen in these figures that the values

of α, β and δ are increasing with increase in aspect ratio for any sets of boundary conditions, whereas it is difficult to predict the pattern followed by $\beta^{'}$ and $\delta^{'}$ with ascending values of aspect ratio. It is also worth to mention that aspect ratios play crucial role in evaluating the pure bending properties of the FG rectangular plates.

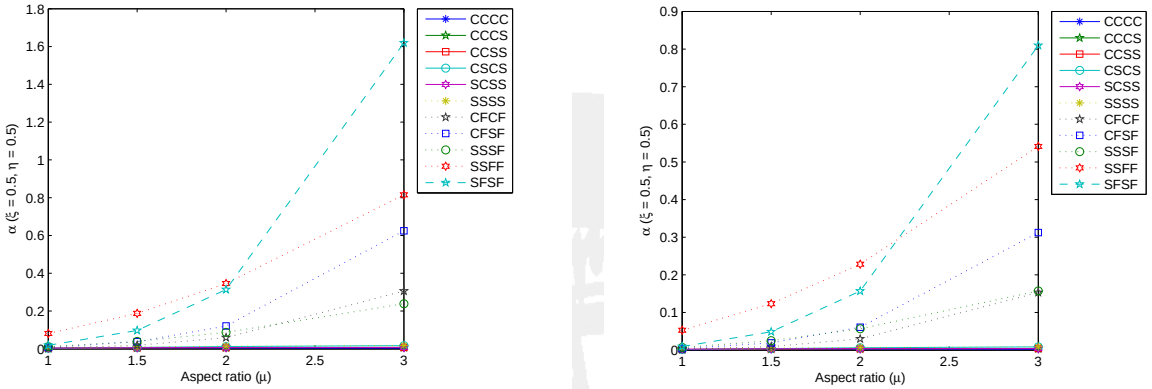

(a) α for UDL (b) α for Hydrostatic pressure

Figure 4.6: Effect of μ on $\alpha\,|_{\xi=0.5,\eta=0.5}$ of FG plates under (a) UDL and (b) Hydrostatic pressure

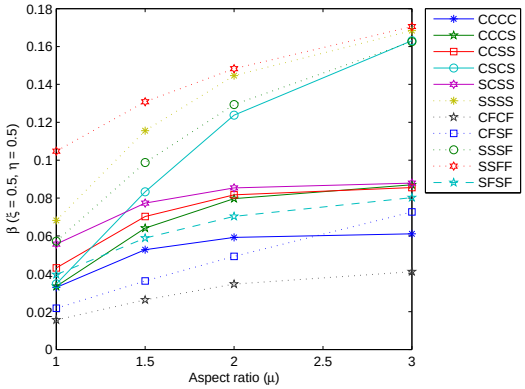

(a) β for UDL

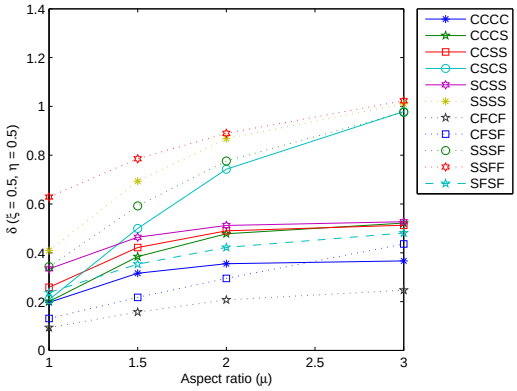

(b) δ for UDL

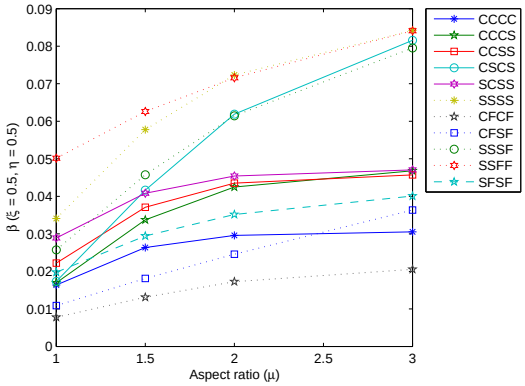

(c) β for Hydrostatic pressure

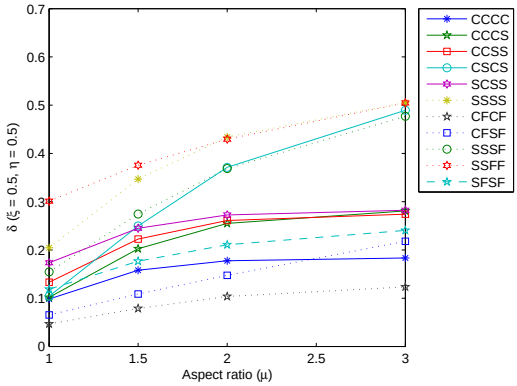

(d) δ for Hydrostatic pressure

Figure 4.7: Effect of μ respectively on (a) $\beta\,|_{\xi=0.5,\eta=0.5}$ and (b) $\delta\,|_{\xi=0.5,\eta=0.5}$ of FG plates under UDL and on (c) $\beta\,|_{\xi=0.5,\eta=0.5}$ and (d) $\delta\,|_{\xi=0.5,\eta=0.5}$ under hydrostatic pressure

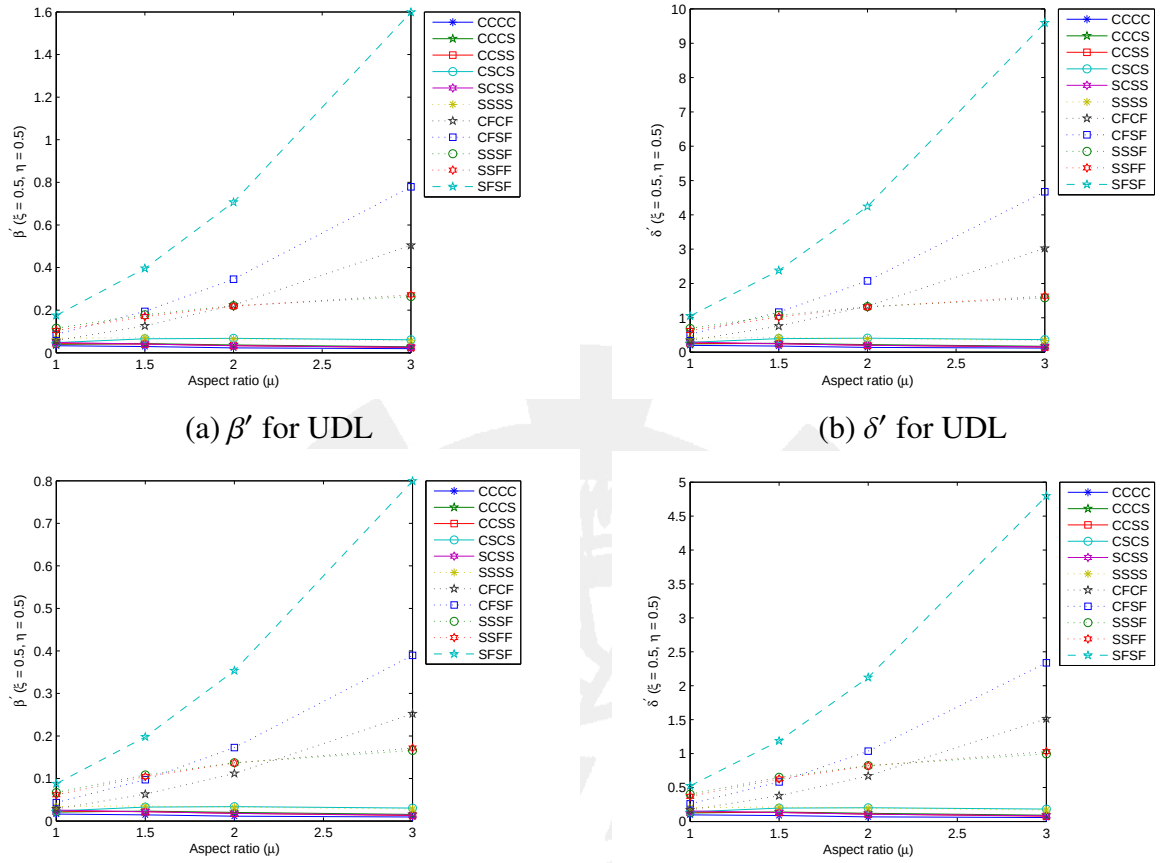

(a) β' for UDL

(b) δ' for UDL

(c) β' for Hydrostatic pressure

(d) δ' for Hydrostatic pressure

Figure 4.8: Effect of μ respectively on (a) $\beta'|_{\xi=0.5,\eta=0.5}$ and (b) $\delta'|_{\xi=0.5,\eta=0.5}$ of FG plates under UDL and on (c) $\beta'|_{\xi=0.5,\eta=0.5}$ and (d) $\delta'|_{\xi=0.5,\eta=0.5}$ under hydrostatic pressure

4.3.2 Effect of power-law exponents

Values for α, β, β', δ and δ' related to pure bending of FG rectangular plates under UDL and hydrostatic pressure are demonstrated in Figs. 4.9 to 4.11 with the increase in power-law exponents ($k = 0,\ 0.5,\ 1,\ 2,\ 10$); keeping $\mu = 2$, $E_{rat} = 2.5$ and $\nu = 0.3$. Here, the effect of k on the maximum deflection ($\alpha|_{\xi=0.5,\eta=0.5}$) under UDL and hydrostatic pressure are shown in Figs. 4.9 (a) and (b) respectively. However, Figs. 4.10 (a) and (b) illustrate the effect of k respectively on $\beta|_{\xi=0.5,\eta=0.5}$ and $\delta|_{\xi=0.5,\eta=0.5}$ of FG plate under UDL, whereas hydrostatic pressure is considered in Figs. 4.10 (c) and (d) to express the behavior of these bending parameters. In a similar manner, Figs. 4.11 (a) and (b) visualize the respective behavior of $\beta'|_{\xi=0.5,\eta=0.5}$ and $\delta'|_{\xi=0.5,\eta=0.5}$ with increase in k for UDL, whereas their response under hydrostatic pressure are illustrated in Figs. 4.11 (c) and (d). It is interesting to note that the pure bending parameters are gradually increasing with increase in power-law exponents (k) involved in gradation behavior of FG plate,

regardless of the edge support and external load assumed.

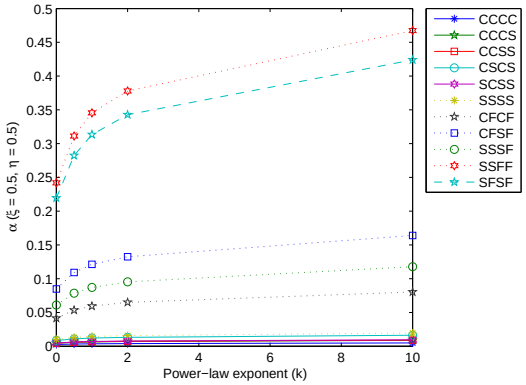

(a) α for UDL

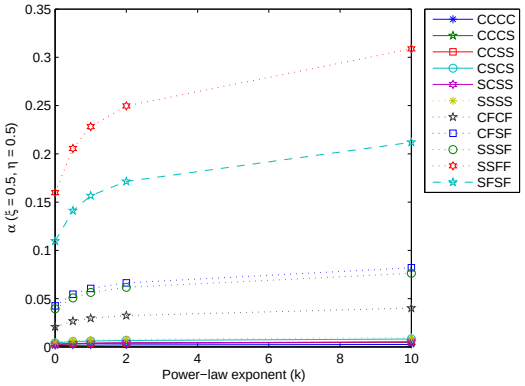

(b) α for Hydrostatic pressure

Figure 4.9: Effect of k on $\alpha\,|_{\xi=0.5,\eta=0.5}$ of FG plates under (a) UDL and (b) Hydrostatic pressure

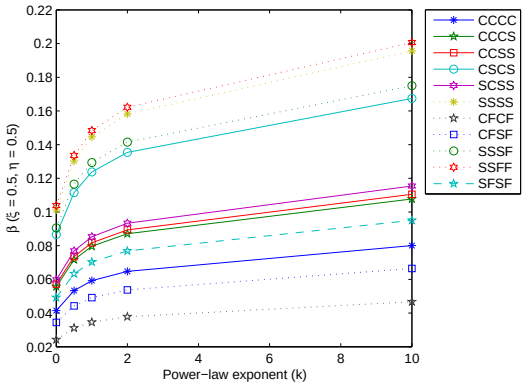

(a) β for UDL

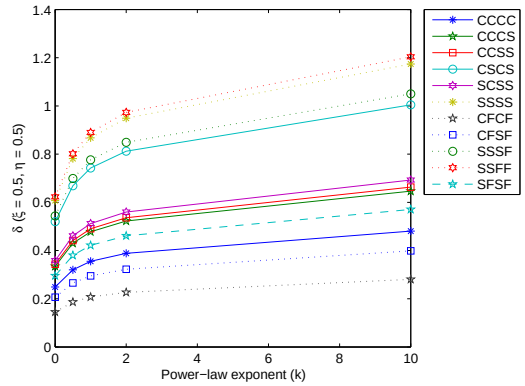

(b) δ for UDL

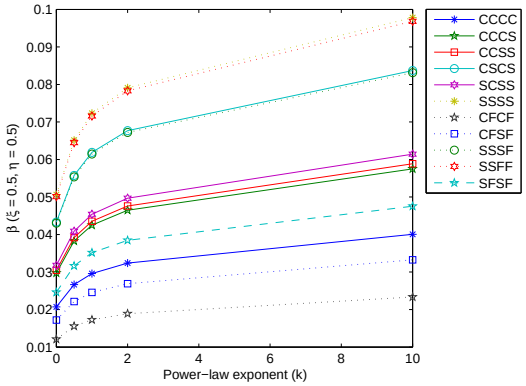

(c) β for Hydrostatic pressure

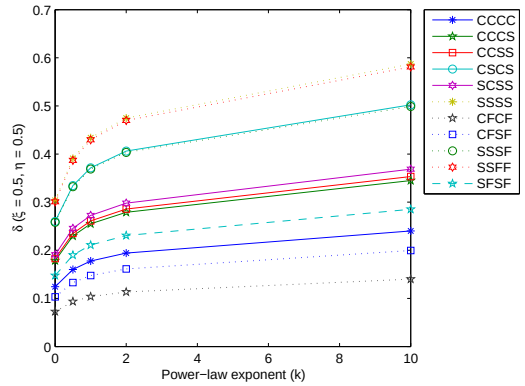

(d) δ for Hydrostatic pressure

Figure 4.10: Effect of k respectively on (a) $\beta\,|_{\xi=0.5,\eta=0.5}$ and (b) $\delta\,|_{\xi=0.5,\eta=0.5}$ of FG plates under UDL and on (c) $\beta\,|_{\xi=0.5,\eta=0.5}$ and (d) $\delta\,|_{\xi=0.5,\eta=0.5}$ under hydrostatic pressure

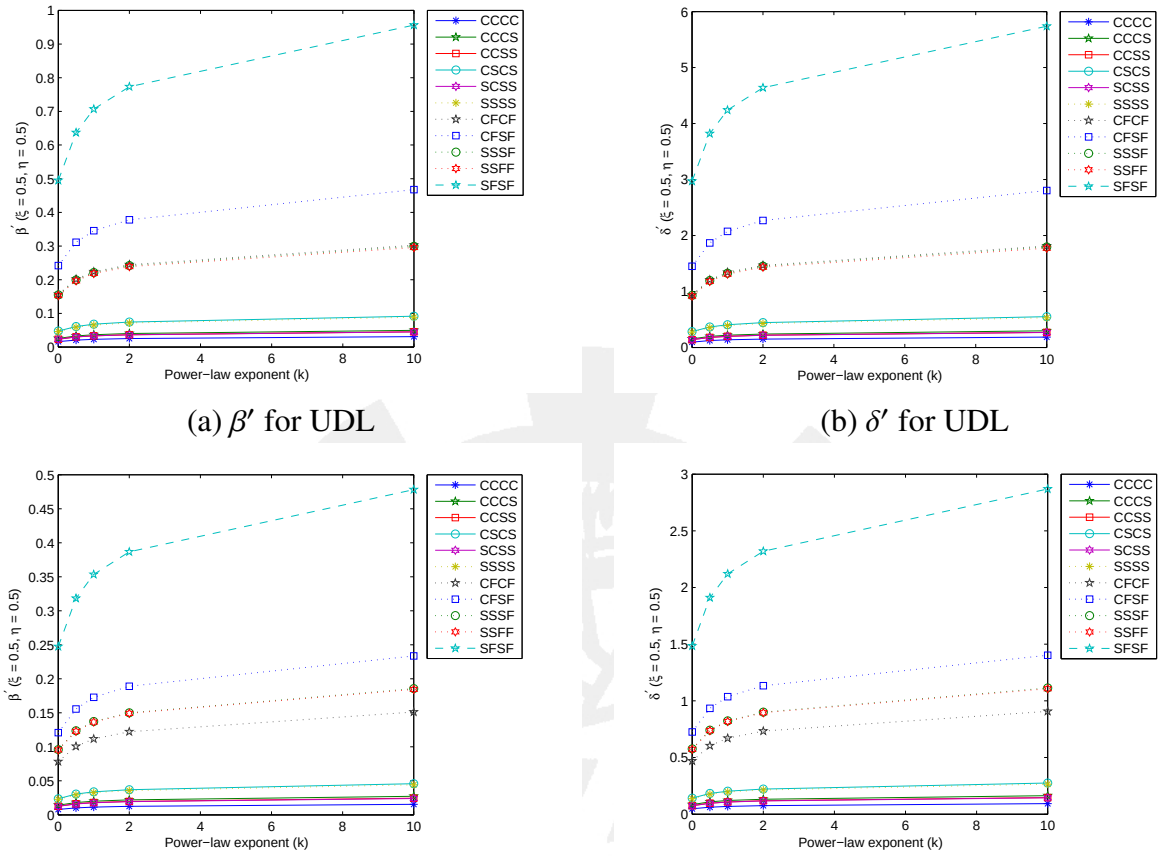

(a) β' for UDL

(b) δ' for UDL

(c) β' for Hydrostatic pressure

(d) δ' for Hydrostatic pressure

Figure 4.11: Effect of k respectively on (a) $\beta'|_{\xi=0.5,\eta=0.5}$ and (b) $\delta'|_{\xi=0.5,\eta=0.5}$ of FG plates under UDL and on (c) $\beta'|_{\xi=0.5,\eta=0.5}$ and (d) $\delta'|_{\xi=0.5,\eta=0.5}$ under hydrostatic pressure

4.3.3 Effect of ratio of Young's moduli of the constituents

The pure bending parameters of FG rectangular plates subjected to various edge conditions with the increase in ratio of Young's moduli of the constituents (E_{rat} = 0.25, 0.5, 1, 2, 4) are graphically illustrated in Figs. 4.12 to 4.14 under UDL and hydrostatic pressure. Other physical parameters involved in these figures are $\mu = 2$, $k = 1$ and $\nu = 0.3$. Consequently, the effect of E_{rat} on $\alpha|_{\xi=0.5,\eta=0.5}$ under UDL and hydrostatic pressure are demonstrated respectively in Figs. 4.12 (a) and (b). Considering the external load as UDL, Figs. 4.13 (a) and (b) represent the values of $\beta|_{\xi=0.5,\eta=0.5}$ and $\delta|_{\xi=0.5,\eta=0.5}$ respectively with increase in E_{rat}, whereas their numerical values are shown in Figs. 4.13 (c) and (d) by assuming hydrostatic pressure. Similarly, the behavior of $\beta'|_{\xi=0.5,\eta=0.5}$ and $\delta'|_{\xi=0.5,\eta=0.5}$ with ascending values of E_{rat} are diagrammatically presented respectively in Figs. 4.14 (a) and (b) under UDL, whereas hydrostatic pressure is assumed in Figs. 4.14 (c) and (d) to visualize the behavior of these bending factors. Irrespective of the edge

support and external mechanical load considered, one may easily notice here the ascending pattern followed by the numerical factors with increase in E_{rat}.

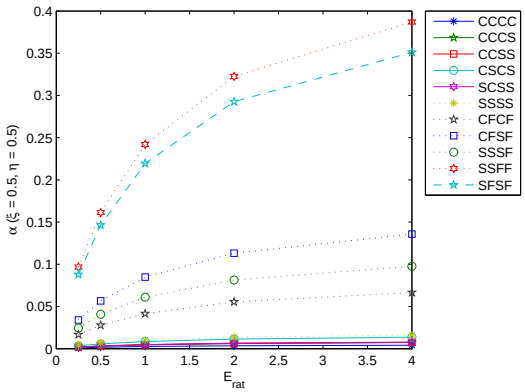

(a) α for UDL

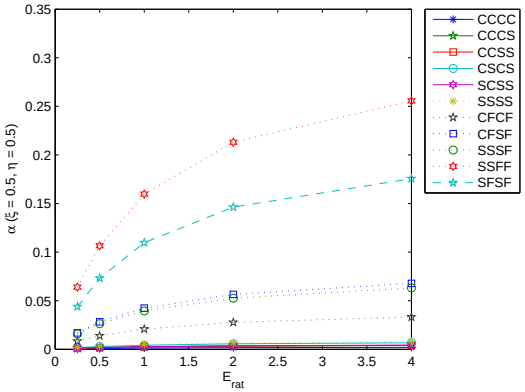

(b) α for Hydrostatic pressure

Figure 4.12: Effect of E_{rat} on $\alpha\,|_{\xi=0.5,\eta=0.5}$ of FG plates under (a) UDL and (b) Hydrostatic pressure

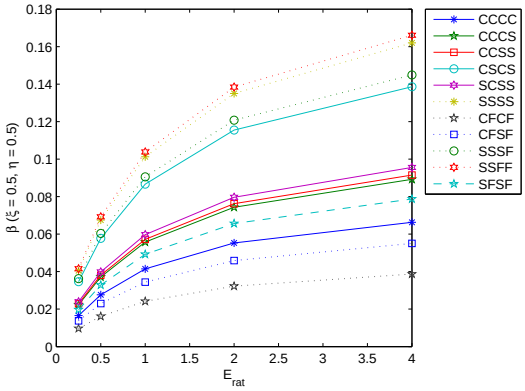

(a) β for UDL

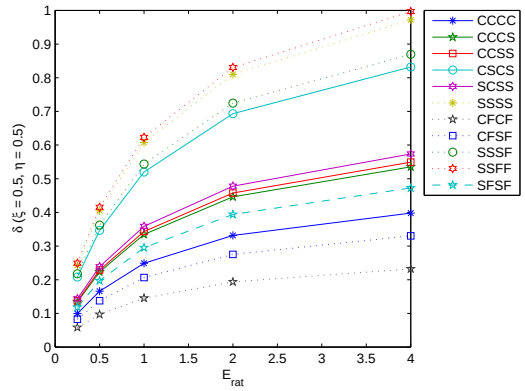

(b) δ for UDL

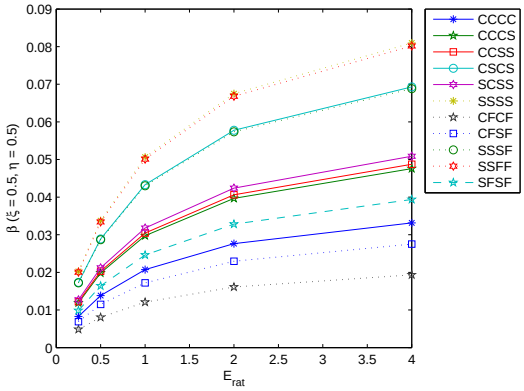

(c) β for Hydrostatic pressure

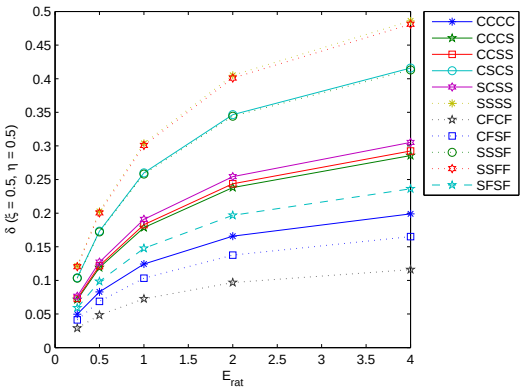

(d) δ for Hydrostatic pressure

Figure 4.13: Effect of E_{rat} respectively on (a) $\beta\,|_{\xi=0.5,\eta=0.5}$ and (b) $\delta\,|_{\xi=0.5,\eta=0.5}$ of FG plates under UDL and on (c) $\beta\,|_{\xi=0.5,\eta=0.5}$ and (d) $\delta\,|_{\xi=0.5,\eta=0.5}$ under hydrostatic pressure

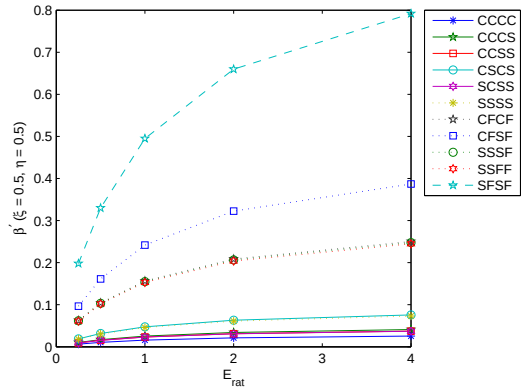

(a) β' for UDL

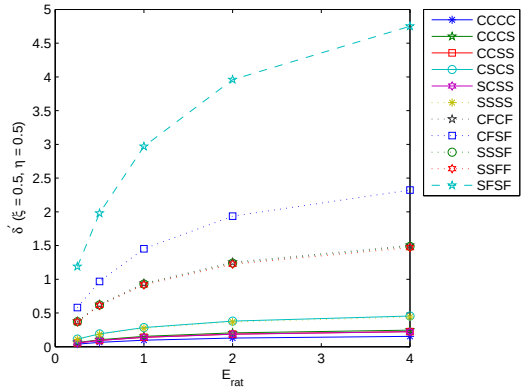

(b) δ' for UDL

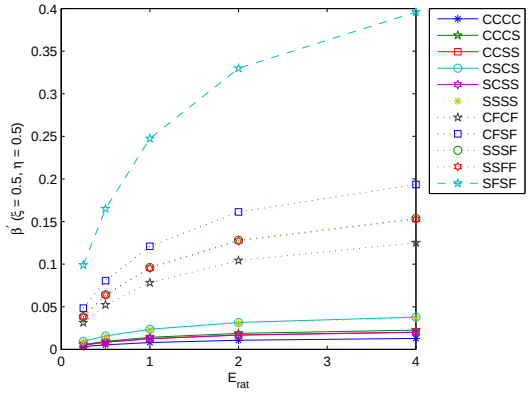

(c) β' for Hydrostatic pressure

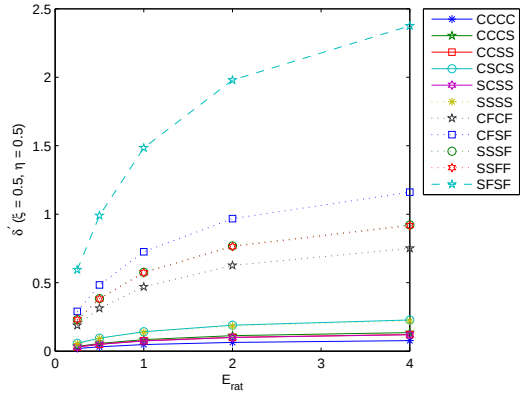

(d) δ' for Hydrostatic pressure

Figure 4.14: Effect of E_{rat} respectively on (a) $\beta'\,|_{\xi=0.5,\eta=0.5}$ and (b) $\delta'\,|_{\xi=0.5,\eta=0.5}$ of FG plates under UDL and on (c) $\beta'\,|_{\xi=0.5,\eta=0.5}$ and (d) $\delta'\,|_{\xi=0.5,\eta=0.5}$ under hydrostatic pressure

4.4 Concluding remarks

Numerical factors associated with pure bending properties viz. centroidal deflection, bending moments and normal stresses of the functionally graded rectangular plates subjected to various arbitrary boundary conditions under UDL and hydrostatic pressure are investigated in the present work. Rayleigh-Ritz method is used in numerical modelling to generate the system of linear equations. It can also be seen that Rayleigh-Ritz method is an efficient computational method, which may handle any sets of boundary conditions easily. In view of the results obtained, one may draw the conclusions as below.

- In Rayleigh-Ritz method, increase in number of polynomials (n) play an important role in the convergence of pure bending parameters of the FG plate.

- Aspect ratios (b/a) and different volume fractions play crucial roles to examine bending

characteristics of FG rectangular plates.

- It is interesting to note here that maximum deflection, bending moment and maximum normal stress with respect to $x-$axis will increase with increase in aspect ratios, whereas it is difficult to predict the pattern followed by maximum bending moment and normal stress with respect to $y-$axis.

- It is also evident that numerical factors associated with bending of FG rectangular plates are gradually increasing with increase in power-law exponents (k) and E_{rat} irrespective of the edge support, geometric configuration and external mechanical loads.

- It can also be conveyed that the bending parameters for FG plates associated with UDL are comparatively greater than those evaluated with the assumption of hydrostatic pressure.

- In addition to the shear deformation effects (neglected in classical plate theory), other deformation plate theories can also be extended easily.

Chapter 5

Vibration problems of functionally graded beams

The contents of this chapter have been published/communicated in:

(1) Pradhan, K.K. and Chakraverty, S. (2013). Free vibration of Euler and Timoshenko functionally graded beams by Rayleigh-Ritz method. *Composites Part B*, 37:175–184 (Elsevier).

(2) Pradhan, K.K. and Chakraverty, S. (2014). Effects of different shear deformation theories on free vibration of functionally graded beams. *International Journal of Mechanical Sciences*, 82:149–160 (Elsevier).

(3) Pradhan, K.K. and Chakraverty, S. (2015). Generalized power-law exponent based shear deformation theory for free vibration of functionally graded beams. *Applied Mathematics and Computation*, 268:1240–1258 (Elsevier).

(4) Pradhan, K.K. and Chakraverty, S. (2015). Natural frequencies of shear deformed functionally graded beams using inverse trigonometric functions. *Journal of the Brazilian Society of Mechanical Sciences and Engineering*, Under review (Springer).

(5) Pradhan, K.K. and Chakraverty, S. (2015). Free vibration of non-uniform functionally graded beams by using differential quadrature method. *Meccanica*, Communicated (Springer).

Chapter 5

Vibration problems of functionally graded beams

In this chapter, free vibration of functionally graded (FG) beams is studied based on various shear deformation beam theories (SDBTs). We have considered here a few previously proposed SDBTs along with newly proposed ones for the displacement fields of deformed FG beam. The material properties in FG beam vary continuously along thickness direction in power-law form. First of all, the numerical procedures of Rayleigh-Ritz method are used to find the generalized eigenvalue problem for free vibration of uniform FG beam. Then the method of generalized differential quadrature (GDQ) is implemented to solve vibration problems related to Euler-Bernoulli non-uniform FG beam. The validation of natural frequencies has been performed after checking the test of convergence to report the new results.

5.1 Vibration of uniform FG beam

As mentioned earlier, the aim of this section is to investigate free vibration of uniform functionally graded beam by means of Rayleigh-Ritz method. As such, new results for natural frequencies are to be computed by finding the generalized eigenvalue problem for the concerned problem.

5.1.1 Numerical modeling

The mathematical modeling for free vibration of FG beam has already been discussed in Sec. 3.1.2 to generate the eigenvalue problem (Eq. (3.26)). The comparison of present results with available literature has been carried out after checking the test of convergence. In this regard, the non-dimensional frequencies of FG beam under different sets of boundary conditions can be obtained based on all the existing and newly proposed SDBTs as mentioned in Eqs. (2.4)

and (2.12).

5.1.2 Convergence and comparison studies

In this section, the convergence of first five non-dimensional frequencies of FG beam subjected to different sets of boundary conditions has been performed. The material properties of FG beam constituents are given below (Sina et al., 2009).

Table 5.1: Material properties of the FG beam constituents (Aluminium and Al_2O_3)

Properties	Unit	Aluminium; $(\,)_m$	Alumina; $(\,)_c$
E	GPa	70	380
ρ	kg/m^3	2700	3800
ν	-	0.23	0.23

The subscripted terms in Table 5.1 that is $(\,)_m$ and $(\,)_c$ are the material properties of the metal and ceramic constituents of FG beam respectively. As mentioned in (Sina et al., 2009), the non-dimensional frequencies will be evaluated as follows

$$\lambda = \frac{\omega L^2}{h}\sqrt{\frac{I_A}{\int_{-h/2}^{h/2} E(z)\mathrm{d}z}},\; I_A = \int_{-h/2}^{h/2}\rho(z)\mathrm{d}z \tag{5.1}$$

In Tables 5.2 and 5.3, the convergence of first five non-dimensional frequencies for C-C FG beam is checked with the increase in the number of polynomials in displacement components using CBT and TBT respectively. In the similar fashion, the convergence pattern of these frequencies of S-S FG beam are reported in Tables 5.4 and 5.5 using CBT and TBT respectively. In these tables, slenderness ratio (L/h) is taken as 5 and power-law index (k) as unity. Moreover first five non-dimensional frequencies of S-S and C-C FG beams based on TBT are incorporated in Tables 5.6 and 5.7 respectively with different slenderness ratios and $k = 0.3$. The fundamental frequencies are also validated with (Sina et al., 2009; Şimşek, 2010a) in Tables 5.6 and 5.7, which are found to be in good agreement. It can be observed that increase in number of polynomials plays a key role in the convergence of non-dimensional frequencies. On contrary, one may also verify the convergence of non-dimensional frequencies of FG beam under any set of edge supports based on other SDBTs.

Table 5.2: Convergence of first five non-dimensional frequencies of C-C FG beam with $L/h = 5$ and $k = 1$ using CBT

n	λ_1	λ_2	λ_3	λ_4	λ_5
2	6.0184	15.2859	18.7637	33.1976	-
5	5.8682	15.0208	16.3766	27.4765	32.7191
8	5.8286	15.0160	16.1670	27.3988	32.1442
11	5.8190	15.0131	16.0119	27.3740	31.9793
14	5.8110	15.0121	15.9643	27.3548	31.8450
15	5.8105	15.0115	15.9404	27.3537	31.8376

Table 5.3: Convergence of first five non-dimensional frequencies of C-C FG beam with $L/h = 5$ and $k = 1$ using TBT

n	λ_1	λ_2	λ_3	λ_4	λ_5
2	5.5977	15.2791	18.6079	32.6268	57.1052
5	5.2016	12.5717	16.1091	21.6487	32.0403
8	5.1219	12.1873	15.9422	21.0416	30.4953
11	5.0748	12.0647	15.8154	20.5341	29.9598
14	5.0590	11.9534	15.7824	20.3872	29.4853
15	5.0515	11.9507	15.7610	20.2969	29.4774

Table 5.4: Convergence of first five non-dimensional frequencies of S-S FG beam with $L/h = 5$ and $k = 1$ using CBT

n	λ_1	λ_2	λ_3	λ_4	λ_5
2	3.1109	11.2824	17.4533	32.4072	-
5	2.7550	9.5117	15.8728	20.4816	31.8019
8	2.7550	9.4798	15.8286	20.1998	31.5139
9	2.7550	9.4798	15.8286	20.1957	31.4957
10	2.7550	9.4798	15.8286	20.1957	31.4957

Table 5.5: Convergence of first five non-dimensional frequencies of S-S FG beam with $L/h = 5$ and $k = 1$ using TBT

n	λ_1	λ_2	λ_3	λ_4	λ_5
2	3.1108	11.0467	17.1864	31.7900	53.0719
5	2.6513	8.6317	15.4036	17.2822	30.5461
8	2.6468	8.6042	15.3925	17.0444	26.4038
9	2.6450	8.6030	15.3920	16.9850	26.4032
10	2.6449	8.5928	15.3890	16.9820	26.2741

Table 5.6: Convergence of first five non-dimensional frequencies of S-S FG beam with $k = 0.3$ using TBT for different L/h

L/h	n	λ_1	λ_2	λ_3	λ_4	λ_5
	3	2.7436	13.5064	31.5140	34.0368	65.0296
	5	2.7396	10.3895	22.4190	31.2411	62.5095
10	8	2.7382	10.3736	22.0642	31.1597	36.7517
	10	2.7378	10.3679	22.0229	31.1592	36.6360
	Sina et al. (2009)	2.695	-	-	-	-
	Şimşek (2010a)	2.701	-	-	-	-
	3	2.7756	13.8995	36.4061	94.2770	194.4858
	5	2.7744	10.9368	24.7787	74.4866	94.9697
30	8	2.7742	10.8982	24.3695	42.8160	70.2439
	10	2.7742	10.8974	24.3570	42.7468	66.2351
	Sina et al. (2009)	2.737	-	-	-	-
	Şimşek (2010a)	2.738	-	-	-	-
	3	2.7793	13.9457	36.7130	314.1700	648.0928
	5	2.7784	11.0100	25.1099	76.5300	141.0338
100	8	2.7784	10.9643	24.6941	43.8368	73.8106
	10	2.7784	10.9642	24.6874	43.7776	68.6585
	Sina et al. (2009)	2.742	-	-	-	-
	Şimşek (2010a)	2.742	-	-	-	-

Table 5.7: Convergence of first five non-dimensional frequencies of C-C FG beam with $k = 0.3$ using TBT for different L/h

L/h	n	λ_1	λ_2	λ_3	λ_4	λ_5
	3	6.0025	16.4281	32.9760	34.2325	66.3549
	8	5.9085	15.3645	28.2359	31.9735	43.4821
10	13	5.8874	15.2536	27.8470	31.6367	42.7630
	17	5.8808	15.2117	27.7302	31.5568	42.4941
	Sina et al. (2009)	5.811	-	-	-	-
	Şimşek (2010a)	5.875	-	-	-	-
	3	6.2168	17.4307	35.6795	98.9047	199.0017
	8	6.1853	16.9236	32.8346	53.6489	79.6691
30	13	6.1807	16.8955	32.7663	53.4353	78.5944
	17	6.1788	16.8877	32.7400	53.3791	78.4686
	Sina et al. (2009)	6.167	-	-	-	-
	Şimşek (2010a)	6.177	-	-	-	-
	3	6.2428	17.5693	35.8678	329.6765	663.3261
	8	6.2201	17.1370	33.5584	55.4290	83.8482
100	13	6.2171	17.1236	33.5370	55.3615	82.5777
	17	6.2159	17.1203	33.5284	55.3477	82.5496
	Sina et al. (2009)	6.212	-	-	-	-
	Şimşek (2010a)	6.214	-	-	-	-

For the shear deformation theories viz. PSDBT, ESDBT, TSDBT, ASDBT, PESDBT and inverse trigonometric SDBTs, the physical properties of FG constituents are taken as (Thai and Vo, 2012; Vo et al., 2013; Şimşek, 2010a): $E_m = 70$ GPa, $\rho_m = 2702$ kg/m^3, $E_c = 380$ GPa, $\rho_c =$

3960 kg/m^3 and $\nu_m = \nu_c = 0.3$ with different slenderness ratios (L/h) and power-law indices (k). For the convergence test in newly proposed PESDBT, the notation for number of polynomials is m and n (power-law index denoting PESDBT) is taken as unity. In Tables 5.8 to 5.15, the non-dimensional frequency may be computed by the following formulation to check the convergence:

$$\lambda = \frac{\omega L^2}{h}\sqrt{\frac{\rho_m}{E_m}} \tag{5.2}$$

It can easily be said that the non-dimensional frequencies gradually converge with increase in number of polynomials regardless of SDBT and other parameters considered.

Table 5.8: Convergence of first five non-dimensional frequencies of FG beam with $L/h = 5$ and $k = 1$ using PSDBT

BCs	n	λ_1	λ_2	λ_3	λ_4	λ_5
C-C	2	8.9371	24.6923	29.9774	52.5714	84.4010
	3	8.5034	22.6687	27.1270	47.6067	55.7833
	4	8.3502	20.0462	26.4320	43.6627	52.8966
	6	8.1878	19.4048	25.9525	33.3363	48.2137
	9	8.0522	19.0412	25.5961	32.2934	47.2373
	10	8.0441	18.8861	25.5918	32.2532	46.5707
S-S	2	5.0230	17.8230	27.7230	51.3506	83.1496
	3	4.2928	17.7191	27.5078	41.1175	56.3212
	4	4.2801	13.9833	24.9005	40.0057	54.5206
	6	4.2723	13.8818	24.8416	27.3943	43.4178
	9	4.2647	13.8502	24.8290	27.3134	42.4286
	10	4.2646	13.8396	24.8259	27.3105	42.2756

Table 5.9: Convergence of first five non-dimensional frequencies of FG beam with $L/h = 10$ and $k = 0.2$ using ESDBT

BCs	n	λ_1	λ_2	λ_3	λ_4	λ_5
C-C	2	11.2275	32.0043	63.7141	121.899	371.647
	3	11.1202	30.3946	60.6124	63.2878	121.963
	4	11.0304	29.0417	59.5323	60.5496	106.869
	6	10.9853	28.6427	52.4646	59.3656	81.3672
	9	10.9440	28.3878	51.9135	58.4866	79.9793
	10	10.9384	28.3186	51.8177	58.4855	79.4583
S-S	2	5.6850	25.1861	58.2237	119.097	370.155
	3	5.0677	25.1472	57.8426	63.2132	119.344
	4	5.0604	19.4014	57.6009	62.6609	115.735
	6	5.0593	19.2880	41.0265	57.5336	69.9765
	9	5.0571	19.2648	40.8079	57.5214	67.8157
	10	5.0570	19.2581	40.8001	57.5210	67.6176

Table 5.10: Convergence of first five non-dimensional frequencies of FG beam with $L/h = 10$ and $k = 0.2$ using TSDBT

BCs	n	λ_1	λ_2	λ_3	λ_4	λ_5
C-C	2	11.2259	32.0039	63.7140	121.899	371.282
	3	11.1183	30.3875	60.6123	63.2851	121.963
	4	11.0282	29.0311	59.5140	60.5495	106.863
	6	10.9829	28.6303	52.4293	59.3655	81.2894
	9	10.9413	28.3740	51.8734	58.4866	79.8969
	10	10.9357	28.3039	51.7773	58.4855	79.3704
S-S	2	5.6850	25.1849	58.2237	119.097	369.788
	3	5.0675	25.1457	57.8426	63.2035	119.344
	4	5.0602	19.3978	57.6007	62.6490	115.735
	6	5.0590	19.2841	41.0060	57.5331	69.9227
	9	5.0568	19.2604	40.7885	57.5209	67.7663
	10	5.0566	19.2535	40.7805	57.5205	67.5647

Table 5.11: Convergence of first five non-dimensional frequencies of FG beam with $L/h = 5$ and $k = 1$ using ASDBT

BCs	n	λ_1	λ_2	λ_3	λ_4	λ_5
C-C	2	8.9422	24.6924	29.9792	52.5777	84.3990
	3	8.5111	22.6854	27.1303	47.6068	55.7929
	4	8.3580	20.0849	26.4339	43.6945	52.9073
	6	8.1971	19.4510	25.9538	33.4480	48.4590
	9	8.0645	19.0940	25.5973	32.4362	47.5044
	10	8.0564	18.9458	25.5929	32.3956	46.8624
S-S	2	5.0230	17.8257	27.7256	51.3565	83.1504
	3	4.2941	17.7224	27.5106	41.1313	56.3470
	4	4.2815	13.9968	24.9067	40.0259	54.5470
	6	4.2741	13.8981	24.8480	27.4683	43.6172
	9	4.2671	13.8695	24.8364	27.3938	42.6105
	10	4.2671	13.8610	24.8339	27.3913	42.4764

Table 5.12: Convergence of first five non-dimensional frequencies of FG beam with $L/h = 5$, $k = 1$ and $n = 1$ using PESDBT

BCs	m	λ_1	λ_2	λ_3	λ_4	λ_5
C-C	2	8.9371	24.6923	29.9774	52.5714	84.4010
	3	8.5034	22.6687	27.1270	47.6067	55.7833
	4	8.3502	20.0462	26.4320	43.6627	52.8966
	6	8.1878	19.4048	25.9525	33.3363	48.2137
	9	8.0522	19.0412	25.5961	32.2934	47.2373
	10	8.0441	18.8861	25.5918	32.2532	46.5707
S-S	2	5.0230	17.8230	27.7230	51.3506	83.1496
	3	4.2928	17.7191	27.5078	41.1175	56.3212
	4	4.2801	13.9833	24.9005	40.0057	54.5206
	6	4.2723	13.8818	24.8416	27.3943	43.4178
	9	4.2647	13.8502	24.8290	27.3134	42.4286
	10	4.2646	13.8396	24.8259	27.3105	42.2756

Table 5.13: Convergence of first five non-dimensional frequencies of FG beam with $L/h = 10$ and $k = 0.2$ using ISDBT

BCs	n	λ_1	λ_2	λ_3	λ_4	λ_5
C-C	2	11.1613	31.9817	63.7125	121.890	340.409
	3	11.0402	30.1140	60.6111	63.1673	121.953
	4	10.9397	28.6225	58.8674	60.5479	106.595
	6	10.8864	28.1665	51.2309	59.3642	78.8402
	9	10.8360	27.8802	50.5719	58.4853	77.4177
	10	10.8303	27.7940	50.4774	58.4844	76.8166
S-S	2	5.6850	25.1287	58.2221	119.089	338.881
	3	5.0579	25.0837	57.8410	62.7869	119.329
	4	5.0497	19.2548	57.5934	62.1758	115.721
	6	5.0482	19.1359	40.3511	57.5157	68.2576
	9	5.0454	19.1083	40.1620	57.4999	66.2398
	10	5.0452	19.0995	40.1538	57.4991	66.0231

Table 5.14: Convergence of first five non-dimensional frequencies of FG beam with $L/h = 10$ and $k = 0.2$ using ICDBT

BCs	n	λ_1	λ_2	λ_3	λ_4	λ_5
C-C	2	11.1613	31.9817	63.7125	121.890	340.408
	3	11.0402	30.1140	60.6111	63.1672	121.953
	4	10.9396	28.6225	58.8674	60.5479	106.595
	6	10.8864	28.1665	51.2310	59.3642	78.8404
	9	10.8360	27.8802	50.5720	58.4853	77.4180
	10	10.8303	27.7941	50.4775	58.4844	76.8169
S-S	2	5.6850	25.1288	58.2222	119.089	338.341
	3	5.0580	25.0839	57.8411	62.7885	119.329
	4	5.0498	19.2560	57.5935	62.1792	115.721
	6	5.0483	19.1376	40.3642	57.5160	68.2950
	9	5.0455	19.1107	40.1749	57.5002	66.2744
	10	5.0454	19.1025	40.1671	57.4995	66.0648

Table 5.15: Convergence of first five non-dimensional frequencies of FG beam with $L/h = 10$ and $k = 0.2$ using ITDBT

BCs	n	λ_1	λ_2	λ_3	λ_4	λ_5
C-C	2	11.1617	31.9818	63.7126	121.891	339.868
	3	11.0406	30.1165	60.6112	63.1676	121.953
	4	10.9402	28.6263	58.8757	60.5480	106.596
	6	10.8871	28.1716	51.2493	59.3643	78.8902
	9	10.8370	27.8867	50.5966	58.4853	77.4755
	10	10.8313	27.8019	50.5024	58.4844	76.8827
S-S	2	5.6850	25.1288	58.2222	119.089	338.341
	3	5.0580	25.0839	57.8411	62.7885	119.329
	4	5.0498	19.2560	57.5935	62.1792	115.721
	6	5.0483	19.1376	40.3642	57.5160	68.2950
	9	5.0455	19.1107	40.1749	57.5002	66.2744
	10	5.0454	19.1025	40.1671	57.4995	66.0648

After looking into the satisfactory test of convergence, one may compare the non-dimensional frequencies of FG beam associated with different edge supports. In Tables 5.16 and 5.17, fundamental frequencies with different slenderness ratios (L/h = 10, 30, 100) and a fixed k are compared with the study of (Sina et al., 2009; Şimşek, 2010a,b) based on all the SDBTs using the expression given in Eq. (5.1). FG constituents own the properties (Sina et al., 2009): E_m = 70 GPa, ρ_m = 2700 kg/m^3, E_c = 380 GPa, ρ_c = 3800 kg/m^3 and $\nu_m = \nu_c$ = 0.23. In Table 5.16, the non-dimensional fundamental frequencies of S-S FG beam with k = 0 within the framework of all the SDBTs have been evaluated and comparisons are performed with the results for CBT and FSDBT^2[1] (TBT) as provided in (Sina et al., 2009) and with those for CBT and TBT as mentioned in (Şimşek, 2010b). In a similar fashion, non-dimensional fundamental frequencies of S-S, C-F and C-C FG beam with k = 0.3 using all the SDBTs are computed in Table 5.17 and comparisons are carried out with the results for FSDBT^2 (TBT) of (Sina et al., 2009), with those obtained using CBT and TBT as given in (Şimşek, 2010b) and with the non-dimensional fundamental frequencies using FSDBT^S[2] (TBT), PSDBT^S[3] (PSDBT) and ASDBT^S[4] (ASDBT) as considered in (Şimşek, 2010a). One may clearly notice here that the fundamental non-dimensional frequencies obtained in the present investigation are approximately close enough to the results provided in these literatures that are used for comparison.

For the verification of present results in Tables 5.18 to 5.20, natural frequencies are computed on the basis of the formulation as stated in Eq. (5.2). In Table 5.18, the properties of the FG constituents are assumed to be E_m = 70 GPa, E_c = 380 GPa and $\nu_m = \nu_c$ = 0.3, as mentioned in (Aydogdu and Taskin, 2007). Considering no gradation of mass density through the thickness of FG constituents (constant density), non-dimensional fundamental frequencies of S-S FG beam are compared with (Aydogdu and Taskin, 2007) in Table 5.18 based on CBT, TBT, PSDBT and ESDBT. Physical properties of FG constituents in Tables 5.19 and 5.20 are taken as (Şimşek, 2010a; Thai and Vo, 2012; Vo et al., 2013): E_m = 70 GPa, ρ_m = 2702 kg/m^3, E_c = 380 GPa, ρ_c = 3960 kg/m^3 and $\nu_m = \nu_c$ = 0.3. Assuming no role of Poisson's ratio (ν) in the expression of Q_{11} (reduced stiffness coefficient), comparison of fundamental frequencies is carried out in Table 5.19 with (Şimşek, 2010a; Thai and Vo, 2012; Vo et al., 2013) subjected to various BCs such as C-C, C-F and S-S, within the framework of CBT and TBT. In a similar way,

[1] FSDBT^2 in (Sina et al., 2009) is same as TBT in present investigation.
[2] FSDBT^S in (Şimşek, 2010a) is same as TBT in the present study.
[3] PSDBT^S in (Şimşek, 2010a) is same as PSDBT in the present study.
[4] ASDBT^S in (Şimşek, 2010a) is same as ASDBT in the present study.

TBT is considered in Table 5.20 for comparison of non-dimensional higher order frequencies for S-S and C-C FG beams with (Thai and Vo, 2012; Vo et al., 2013; Nguyen et al., 2013). A very good agreement of present results can be observed for fundamental and also for higher order natural frequencies of FG beam irrespective of the edge supports. A little discrepancy for third non-dimensional frequencies can be observed in Table 5.20 for S-S FG beam with $L/h = 5$. But it can be viewed that forth frequencies for different power-law exponents (k) are in excellent agreement with that of (Thai and Vo, 2012; Nguyen et al., 2013).

Table 5.16: Comparison of non-dimensional fundamental frequencies of FG beam with $k = 0$

BCs	SDBT	Source	L/h		
			10	30	100
S-S	CBT	Present	2.837	2.847	2.849
		Sina et al. (2009)	2.849	2.849	2.849
		Şimşek (2010b)	2.837	2.847	2.848
	TBT	Present	2.805	2.844	2.848
		Sina et al. (2009)	2.797	2.843	2.848
		Şimşek (2010b)	2.804	2.843	2.848
	PSDBT	Present	2.803	2.844	2.849
	ESDBT	Present	2.804	2.844	2.848
	HSDBT	Present	2.803	2.844	2.849
	TSDBT	Present	2.818	2.846	2.849
	ASDBT	Present	2.804	2.844	2.849

Table 5.17: Comparison of non-dimensional fundamental frequencies of FG beam with $k = 0.3$

BCs	SDBT	Source	L/h		
			10	30	100
S-S	CBT	Present	2.768	2.778	2.779
		Şimşek (2010b)	2.731	2.741	2.743
	TBT	Present	2.738	2.774	2.778
		Sina et al. (2009)	2.695	2.737	2.742
		Şimşek (2010b)	2.701	2.738	2.742
		Şimşek (2010a)	2.701	2.738	2.742
	PSDBT	Present	2.736	2.774	2.778
		Şimşek (2010a)	2.702	2.738	2.742
	ESDBT	Present	2.737	2.774	2.778
	HSDBT	Present	2.737	2.774	2.778
	TSDBT	Present	2.749	2.775	2.779
	ASDBT	Present	2.736	2.774	2.778
		Şimşek (2010a)	2.702	2.738	2.742
C-F	CBT	Present	0.975	0.977	0.977
	TBT	Present	0.971	0.977	0.977
		Sina et al. (2009)	0.969	0.976	0.977
		Şimşek (2010a)	0.970	0.976	0.977
	PSDBT	Present	0.970	0.976	0.977
		Şimşek (2010a)	0.970	0.976	0.977
	ESDBT	Present	0.970	0.977	0.977
	HSDBT	Present	0.970	0.976	0.977
	TSDBT	Present	0.972	0.977	0.977
	ASDBT	Present	0.970	0.976	0.977
		Şimşek (2010a)	0.970	0.976	0.977
C-C	CBT	Present	6.188	6.216	6.220
	TBT	Present	5.881	6.179	6.216
		Sina et al. (2009)	5.811	6.167	6.212
		Şimşek (2010a)	5.875	6.177	6.214
	PSDBT	Present	5.874	6.178	6.215
		Şimşek (2010a)	5.881	6.177	6.214
	ESDBT	Present	5.873	6.177	6.215
	HSDBT	Present	5.871	6.177	6.215
	TSDBT	Present	5.993	6.193	6.215
	ASDBT	Present	5.874	6.178	6.216
		Şimşek (2010a)	5.884	6.177	6.214

Table 5.18: Comparison of non-dimensional fundamental frequencies of S-S FG beam with (Aydogdu and Taskin, 2007) for different slenderness ratios (L/h)

L/h	Theory	Source	$k=0$	$k=0.1$	$k=1$	$k=2$	$k=10$
5	CBT	Present	6.847	6.512	5.176	4.752	3.959
		Aydogdu and Taskin (2007)	6.847	6.499	4.821	4.251	3.737
	TBT	Present	6.569	6.254	4.974	4.549	3.756
		Aydogdu and Taskin (2007)	6.563	6.237	4.652	4.101	3.563
	PSDBT	Present	6.526	6.215	4.942	4.506	3.685
		Aydogdu and Taskin (2007)	6.574	6.248	4.659	4.103	3.548
	ESDBT	Present	6.531	6.220	4.945	4.509	3.688
		Aydogdu and Taskin (2007)	6.584	6.258	4.665	4.109	3.553
20	CBT	Present	6.951	6.612	5.256	4.826	4.021
		Aydogdu and Taskin (2007)	6.951	6.599	4.907	4.334	3.804
	TBT	Present	6.932	6.593	5.242	4.811	4.006
		Aydogdu and Taskin (2007)	6.931	6.580	4.895	4.323	3.791
	PSDBT	Present	6.928	6.589	5.239	4.807	3.999
		Aydogdu and Taskin (2007)	6.932	6.581	4.895	4.323	3.790
	ESDBT	Present	6.928	6.589	5.239	4.808	3.999
		Aydogdu and Taskin (2007)	6.933	6.582	4.896	4.323	3.790

Table 5.19: Comparison of non-dimensional fundamental frequencies of FG beams for different k with various BCs

L/h	Theory	BC	Source	$k=0$	$k=0.2$	$k=0.5$	$k=1$	$k=2$	$k=5$	$k=10$
5	CBT	C-C	Present	12.1826	11.3410	10.3875	9.3993	8.5772	8.1515	7.9041
			Şimşek (2010a)	12.1826	11.3398	10.3718	9.36422	8.52772	8.10955	7.87968
		C-F	Present	1.9385	1.8042	1.6524	1.4954	1.3655	1.2989	1.2593
			Şimşek (2010a)	1.93845	1.8042	1.65057	1.49135	1.35985	1.29416	1.25648
		S-S	Present	5.3953	5.0538	4.7314	4.4488	4.2177	3.9617	3.6977
			Şimşek (2010a)	5.39533	5.02194	4.59360	4.14835	3.77930	3.59487	3.49208
			Thai and Vo (2012)	5.3953	-	4.5936	4.1484	3.7793	3.5949	3.4921
	TBT	C-C	Present	10.0456	9.4267	8.7121	7.9401	7.2281	6.6826	6.3525
			Şimşek (2010a)	10.0344	9.41764	8.70047	7.92529	7.21134	6.66764	6.34062
			Vo et al. (2013)	9.99836	9.38337	-	7.90153	7.19013	6.64465	6.31609
		C-F	Present	1.9021	1.7717	1.6233	1.4688	1.3396	1.2706	1.2301
			Şimşek (2010a)	1.89479	1.76554	1.61737	1.46300	1.33376	1.26445	1.22398
			Vo et al. (2013)	1.89442	1.76477	-	1.46279	1.33357	1.26423	1.22372
		S-S	Present	5.1546	4.8364	4.5313	4.2566	4.0198	3.7464	3.4886
			Şimşek (2010a)	5.15247	4.80657	4.40830	3.99023	3.63438	3.43119	3.31343
			Thai and Vo (2012)	5.1527	-	4.4107	3.9904	3.6264	3.4012	3.2816
			Vo et al. (2013)	5.15260	4.80328	-	3.97108	3.60495	3.40253	3.29625
20	CBT	C-C	Present	12.4142	11.5549	10.5871	9.5907	8.7684	8.3425	8.0797
			Şimşek (2010a)	12.4142	11.5537	10.5713	9.55538	8.71856	8.30064	8.05560
		C-F	Present	1.9525	1.8171	1.6644	1.5070	1.3771	1.3105	1.2699
			Şimşek (2010a)	1.95248	1.81714	1.66265	1.50293	1.37142	1.30574	1.26713
		S-S	Present	5.4777	5.1299	4.8024	4.5161	4.2832	4.0252	3.7568
			Şimşek (2010a)	5.47773	5.09804	4.66458	4.21634	3.84719	3.66283	3.55465
			Thai and Vo (2012)	5.4777	-	4.6641	4.2163	3.8472	3.6628	3.5547
	TBT	C-C	Present	12.2252	11.3850	10.4320	9.4435	8.6203	8.1838	7.9215
			Şimşek (2010a)	12.2235	11.3850	10.4263	9.43135	8.60401	8.16985	7.91275
			Vo et al. (2013)	12.2202	11.3795	-	9.43114	8.60467	8.16977	7.91154
		C-F	Present	1.9501	1.8147	1.6612	1.5025	1.3715	1.3054	1.2661
			Şimşek (2010a)	1.94957	1.81456	1.66044	1.50104	1.36968	1.30375	1.26495
			Vo et al. (2013)	1.94955	1.81408	-	1.50106	1.36970	1.30376	1.26495
		S-S	Present	5.4605	5.1144	4.7881	4.5023	4.2690	4.0095	3.7415
			Şimşek (2010a)	5.46032	5.08265	4.65137	4.20505	3.83676	3.65088	3.54156
			Thai and Vo (2012)	5.4603	-	4.6516	4.2050	3.8361	3.6485	3.5390
			Vo et al. (2013)	5.46033	5.08120	-	4.20387	3.83491	3.64903	3.54045

Table 5.20: Comparison of non-dimensional natural frequencies of FG beams for higher modes with various BCs based on TBT

BC	L/h	Mode	Source	$k=0$	$k=0.2$	$k=0.5$	$k=1$	$k=2$	$k=5$	$k=10$
S-S	5	2	Present	17.8908	16.7317	15.3306	13.7778	12.3619	11.4822	11.1126
			Thai and Vo (2012)	17.8812	-	15.4588	14.0100	12.6405	11.5431	11.0240
			Nguyen et al. (2013)	18.5019	17.3654	16.0161	14.5160	13.0562	11.8698	11.3436
			Present (4^{th} mode)	34.2103	32.1672	29.7504	27.0657	24.4881	22.4290	21.3110
		3	Present	30.2314	28.8311	27.0804	24.9042	22.3517	19.5600	18.0553
			Thai and Vo (2012)	34.2097	-	29.8382	27.0979	24.3152	21.7158	20.5561
			Nguyen et al. (2013)	35.0951	33.11059	30.6771	27.8565	24.8641	22.0568	20.9045
	20	2	Present	21.5755	20.0852	18.3849	16.6146	15.1402	14.3804	13.9476
			Thai and Vo (2012)	21.5732	-	18.3962	16.6344	15.1619	14.3746	13.9263
			Nguyen et al. (2013)	22.5873	21.0309	19.2616	17.4189	15.8723	15.0404	14.5721
		3	Present	47.6037	44.3818	40.7639	37.0394	33.9159	32.0700	30.8925
			Thai and Vo (2012)	47.5930	-	40.6526	36.7679	33.4689	31.5780	30.5369
			Nguyen et al. (2013)	49.7603	46.3777	42.5121	38.4544	34.9818	32.9705	31.8869
C-C	5	2	Present	23.1004	21.7700	20.2077	18.4654	16.7457	15.2301	14.3617
			Vo et al. (2013)	23.87540	22.48400	-	19.04940	17.29240	15.78680	14.90350
		3	Present	30.3513	28.9837	27.3569	25.3859	22.9576	19.9122	18.2304
			Vo et al. (2013)	30.23910	28.88370	-	25.37460	23.01120	19.96340	18.23210
		4	Present	38.6867	36.5446	34.0075	31.1243	28.1712	25.4176	23.8724
			Vo et al. (2013)	38.1841	36.0793	-	30.7500	27.8331	25.0901	23.5501
	20	2	Present	33.0067	30.7650	28.2156	25.5579	23.3181	22.0692	21.3200
			Vo et al. (2013)	33.1335	30.8452	-	25.6223	23.3691	22.1345	21.4015
		3	Present	63.0338	58.8118	53.9936	48.9397	44.6208	42.0801	40.5636
			Vo et al. (2013)	62.9124	58.7017	-	48.8401	44.5197	41.9748	40.4612
		4	Present	100.9961	94.3357	86.7036	78.6406	71.6395	67.2872	64.7111
			Vo et al. (2013)	101.2440	94.6356	-	78.8259	71.5625	66.5576	63.9421

On the other hand, the fundamental non-dimensional frequencies of FG beam based on different SDBTs viz. PSDBT, ESDBT, TSDBT, ASDBT, PESDBT, ISDBT, ICDBT and ITDBT are validated in Tables 5.21 to 5.23 with available results for different L/h and k. C-C edge support is considered in Table 5.21 and in the similar fashion, Tables 5.22 and 5.23 are meant for C-F (cantilever) and S-S edge conditions respectively. The present results are again found to be in excellent agreement with existing ones for the mentioned SDBTs.

Table 5.21: Comparison of fundamental non-dimensional frequencies of C-C FG beam based on different SDBTs with $L/h = 5$ and 20

L/h	Theory	Source	$k = 0$	$k = 0.2$	$k = 0.5$	$k = 1$	$k = 2$	$k = 5$	$k = 10$
5	PSDBT	Present	10.0858	9.4789	8.7614	7.9680	7.1963	6.5120	6.1809
		Şimşek (2010a)	10.0705	9.46641	8.74674	7.95034	7.17674	6.49349	6.16515
	ESDBT	Present	10.1099	9.5001	8.7802	7.9848	7.2082	6.5105	6.1918
		Şimşek (2010a)	10.0944	9.48737	8.76530	7.96695	7.18839	6.49186	6.17594
	TSDBT	Present	10.1099	9.5001	8.7802	7.9848	7.2082	6.5105	6.1918
		Şimşek (2010a)	10.0797	9.47451	8.75394	7.95676	7.18062	6.49028	6.16794
	ASDBT	Present	10.1099	9.5001	8.7802	7.9848	7.2082	6.5105	6.1918
		Şimşek (2010a)	10.0944	9.48737	8.76530	7.96695	7.18839	6.49186	6.17594
	PESDBT	$n = 1$	10.0858	9.4789	8.7614	7.9680	7.1963	6.5120	6.1809
		$n = 5$	10.1767	9.5581	8.8294	8.0314	7.2837	6.6822	6.3258
		$n = 10$	10.2373	9.6093	8.8136	8.0735	7.3335	6.7596	6.4115
	ISDBT	Present	9.7797	9.2030	8.5177	7.7534	6.9967	6.3003	5.9591
	ICDBT	Present	9.7796	9.2031	8.5178	7.7534	6.9967	6.3003	5.9591
	ITDBT	Present	9.7966	9.2179	8.5311	7.7653	7.0030	6.2911	5.9620
20	PSDBT	Present	12.2256	11.3873	10.4344	9.4438	8.6138	8.1587	7.8947
		Şimşek (2010a)	12.2238	11.3873	10.4287	9.43158	8.59751	8.14460	7.88576
	ESDBT	Present	12.2269	11.3884	10.4354	9.4446	8.6141	8.1569	7.8945
		Şimşek (2010a)	12.2251	11.3884	10.4297	9.43242	8.59775	8.14280	7.88558
	TSDBT	Present	12.2269	11.3884	10.4354	9.4446	8.6141	8.1569	7.8945
		Şimşek (2010a)	12.2242	11.3876	10.4290	9.43182	8.59739	8.14346	7.88534
	ASDBT	Present	12.2269	11.3884	10.4354	9.4446	8.6141	8.1569	7.8945
		Şimşek (2010a)	12.2251	11.3884	10.4297	9.43242	8.59775	8.14280	7.88558
	PESDBT	$n = 1$	12.2256	11.3873	10.4344	9.4438	8.6138	8.1587	7.8947
		$n = 5$	12.2396	11.3991	10.4443	9.4529	8.6260	8.1834	7.9178
		$n = 10$	12.2464	11.4047	10.4491	9.4574	8.6314	8.1925	7.9285
	ISDBT	Present	12.1891	11.3554	10.4069	9.4199	8.5909	8.1306	7.8634
	ICDBT	Present	12.1891	11.3554	10.4069	9.4199	8.5909	8.1306	7.8634
	ITDBT	Present	12.1894	11.3556	10.4072	9.4201	8.5903	8.1274	7.8618

Table 5.22: Comparison of fundamental non-dimensional frequencies of cantilever FG beam based on different SDBTs with $L/h = 5$ and 20

L/h	Theory	Source	$k = 0$	$k = 0.2$	$k = 0.5$	$k = 1$	$k = 2$	$k = 5$	$k = 10$
5	PSDBT	Present	1.8955	1.7663	1.6187	1.4645	1.3341	1.2605	1.2192
		Şimşek (2010a)	1.89523	1.76637	1.61817	1.46328	1.33254	1.25916	1.21834
	ESDBT	Present	1.8959	1.7666	1.6190	1.4647	1.3342	1.2602	1.2193
		Şimşek (2010a)	1.89565	1.76673	1.61848	1.46357	1.33268	1.25889	1.21843
	TSDBT	Present	1.8956	1.7664	1.6188	1.4646	1.3341	1.2603	1.2192
		Şimşek (2010a)	1.89536	1.76649	1.61827	1.46339	1.33256	1.25896	1.21831
	ASDBT	Present	1.8955	1.7663	1.6187	1.4645	1.3341	1.2605	1.2192
		Şimşek (2010a)	1.89565	1.76673	1.61848	1.46357	1.33268	1.25889	1.21843
	PESDBT	$n = 1$	1.8955	1.7663	1.6187	1.4645	1.3341	1.2605	1.2192
		$n = 5$	1.8983	1.7687	1.6207	1.4664	1.3366	1.2658	1.2241
		$n = 10$	1.8999	1.7700	1.6218	1.4674	1.3378	1.2678	1.2265
	ISDBT	Present	1.8872	1.7590	1.6125	1.4591	1.3289	1.2543	1.2123
	ICDBT	Present	1.8875	1.7593	1.6130	1.4598	1.3299	1.2551	1.2128
	ITDBT	Present	1.8874	1.7592	1.6126	1.4592	1.3289	1.2537	1.2121
20	PSDBT	Present	1.9496	1.8143	1.6609	1.5021	1.3711	1.3046	1.2653
		Şimşek (2010a)	1.94954	1.81458	1.66049	1.50106	1.36957	1.30332	1.26453
	ESDBT	Present	1.9496	1.8143	1.6609	1.5022	1.3711	1.3046	1.2653
		Şimşek (2010a)	1.94960	1.81464	1.66049	1.50106	1.36957	1.30332	1.26453
	TSDBT	Present	1.9496	1.8143	1.6609	1.5022	1.3711	1.3046	1.2653
		Şimşek (2010a)	1.94960	1.81458	1.66049	1.50106	1.36957	1.30332	1.26453
	ASDBT	Present	1.9496	1.8143	1.6609	1.5022	1.3711	1.3046	1.2653
		Şimşek (2010a)	1.94960	1.81464	1.66049	1.50106	1.36957	1.30332	1.26453
	PESDBT	$n = 1$	1.9496	1.8143	1.6609	1.5021	1.3711	1.3046	1.2653
		$n = 5$	1.9498	1.8145	1.6610	1.5023	1.3713	1.3050	1.2656
		$n = 10$	1.9499	1.8146	1.6611	1.5024	1.3714	1.3052	1.2658
	ISDBT	Present	1.9490	1.8138	1.6604	1.5018	1.3707	1.3042	1.2648
	ICDBT	Present	1.9490	1.8138	1.6606	1.5022	1.3713	1.3047	1.2651
	ITDBT	Present	1.9490	1.8138	1.6604	1.5018	1.3707	1.3041	1.2647

Table 5.23: Comparison of fundamental non-dimensional frequencies of S-S FG beam based on different SDBTs with $L/h = 5$ and 20

L/h	Theory	Source	$k = 0$	$k = 0.2$	$k = 0.5$	$k = 1$	$k = 2$	$k = 5$	$k = 10$
5	PSDBT	Present	5.1629	4.8459	4.5405	4.2632	4.0165	3.7178	3.4617
		Şimşek (2010a)	5.15274	4.80924	4.41108	3.99042	3.62643	3.40120	3.28160
	ESDBT	Present	5.1665	4.8492	4.5435	4.2661	4.0189	3.7179	3.4640
		Şimşek (2010a)	5.15422	4.81053	4.41222	3.99139	3.62671	3.39905	3.28134
		Thai and Vo (2012)	5.1542	-	4.4118	3.9914	3.6267	3.3991	3.2814
	TSDBT	Present	5.1643	4.8472	4.5417	4.2643	4.0174	3.7174	3.4624
		Şimşek (2010a)	5.15422	4.81053	4.41222	3.99139	3.62671	3.39905	3.28134
		Thai and Vo (2012)	5.1531	-	4.4110	3.9907	3.6263	3.3998	3.2811
	ASDBT	Present	5.1665	4.8492	4.5435	4.2661	4.0189	3.7179	3.4640
		Şimşek (2010a)	5.15422	4.81053	4.41222	3.99139	3.62671	3.39905	3.28134
	PESDBT	$n = 1$	5.1629	4.8459	4.5405	4.2632	4.0165	3.7178	3.4617
		$n = 5$	5.1729	4.8546	4.5483	4.2712	4.0299	3.7469	3.4846
		$n = 10$	5.1807	4.8612	4.5542	4.2775	4.0383	3.7603	3.4986
	ISDBT	Present	5.1199	4.8073	4.5050	4.2288	3.9802	3.6766	3.4209
	ICDBT	Present	5.1199	4.8074	4.5050	4.2288	3.9802	3.6766	3.4209
	ITDBT	Present	5.1228	4.8099	4.5074	4.2311	3.9817	3.6752	3.4219
20	PSDBT	Present	5.4606	5.1147	4.7884	4.5024	4.2682	4.0064	3.7386
		Şimşek (2010a)	5.46030	5.08286	4.65159	4.20503	3.83611	3.64850	3.53896
	ESDBT	Present	5.4607	5.1148	4.7885	4.5025	4.2682	4.0062	3.7386
		Şimşek (2010a)	5.46042	5.08292	4.65165	4.20515	3.83617	3.64832	3.53896
		Thai and Vo (2012)	5.4604	-	4.6512	4.2051	3.8361	3.6483	3.5390
	TSDBT	Present	5.4606	5.1147	4.7884	4.5024	4.2682	4.0063	3.7386
		Şimşek (2010a)	5.46036	5.08286	4.65159	4.20509	3.83611	3.64838	3.53896
		Thai and Vo (2012)	5.4603	-	4.6511	4.2051	3.8361	3.6484	3.5389
	ASDBT	Present	5.4607	5.1148	4.7885	4.5025	4.2682	4.0062	3.7386
		Şimşek (2010a)	5.46042	5.08292	4.65165	4.20515	3.83617	3.64832	3.53896
	PESDBT	$n = 1$	5.4606	5.1147	4.7884	4.5024	4.2682	4.0064	3.7386
		$n = 5$	5.4618	5.1157	4.7893	4.5034	4.2697	4.0094	3.7411
		$n = 10$	5.4624	5.1163	4.7898	4.5039	4.2704	4.0105	3.7423
	ISDBT	Present	5.4572	5.1116	4.7856	4.4997	4.2652	4.0029	3.7351
	ICDBT	Present	5.4572	5.1116	4.7856	4.4997	4.2652	4.0029	3.7351
	ITDBT	Present	5.4572	5.1116	4.7856	4.4997	4.2652	4.0026	3.7350

5.1.3 Results and discussions

In view of the above acceptable validation of non-dimensional fundamental and higher order frequencies, first five non-dimensional frequencies of FG beam are reported with different sets of BCs taking all SDBTs. The new results have been evaluated based on previously proposed SDBTs (given in Eq. (2.4)) in Tables 5.24 to 5.29 only for three sets of BCs viz. C-C, S-S and C-F with different slenderness ratios ($L/h = 5$ and 20) and power-law indices ($k = 0$, 0.1, 1, 2, 10). The constituent material properties in these computations are stated in Table 5.1.

To report present results, Poisson's ratio (ν) will play its role in the expression of Q_{11} and it will remain constant through the thickness of the FG beam. Other FG constituents such as Young's modulus and mass densities are assumed to vary along the thickness as per power-law

exponent form. In Tables 5.24 and 5.25, the effect of change of power-law indices on first five non-dimensional frequencies of C-C FG beam are reported with $L/h = 5$ and $L/h = 20$ respectively. In the similar fashion, the effect of variation of power-law exponents on these frequencies are evaluated with S-S edge support in Tables 5.26 and 5.27 and with C-F edge support in Tables 5.28 and 5.29. The number of polynomials (n) involved in displacement components for C-C FG beam is approximately 17, whereas it is 20 for S-S and 25 for C-F FG beam respectively.

One may easily conclude that non-dimensional frequencies are increasing with increase in slenderness ratios (L/h) and are decreasing with increase in power-law exponents (k). It is also interesting to note that the non-dimensional frequencies for $L/h = 5$ using CBT are comparatively greater than those found using other SDBTs, whereas one may experience mere coincidence of frequencies for $L/h = 20$ while comparing the results obtained for different SDBTs of Eq. (2.4). So looking into the new results reported here, one may easily find the non-dimensional frequencies of FG beam taking any slenderness ratio and power-law index subjected to any set of edge supports using the mentioned SDBTs.

Table 5.24: First five non-dimensional frequencies of C-C beam with $L/h = 5$ and different power-law indices (k)

Theory	k	λ_1	λ_2	λ_3	λ_4	λ_5
	0	12.7709	31.8774	33.4380	61.0565	63.7983
	0.1	12.3056	31.1160	32.2394	58.8549	62.3138
CBT	1	9.8372	25.4355	26.9706	46.3706	53.8664
	2	8.9681	22.9435	24.5910	41.6450	49.0744
	10	8.2747	19.1082	21.5967	37.3798	39.9629
	0	10.3768	23.7563	31.8427	39.5711	56.6681
	0.1	10.0436	23.0453	31.0890	38.4343	55.0875
TBT	1	8.2185	19.0273	26.6176	31.9040	45.9129
	2	7.4822	17.2580	24.0597	28.8844	41.5295
	10	6.5540	14.7564	19.1090	24.3983	34.7827
	0	10.4297	24.0206	31.8774	40.2276	57.8710
	0.1	10.1054	23.3343	31.1231	39.1304	56.3429
PSDBT	1	8.2579	19.2216	26.6442	32.3998	46.8435
	2	7.4561	17.2292	24.0602	28.9501	41.7997
	10	6.3743	14.2726	19.1060	23.6151	33.7190
	0	10.4555	24.1328	31.8774	40.5039	58.3709
	0.1	10.1294	23.4389	31.1231	39.3894	56.8116
ESDBT	1	8.2760	19.3027	26.6454	32.6058	47.2228
	2	7.4687	17.2925	24.0592	29.1224	42.1307
	10	6.3860	14.3321	19.1083	23.7740	34.0206
	0	10.4291	24.0175	31.8774	40.2191	57.8553
	0.1	10.1048	23.3312	31.1231	39.1219	56.3270
HSDBT	1	8.2575	19.2193	26.6442	32.3935	46.8314
	2	7.4559	17.2278	24.0603	28.9453	41.7898
	10	6.3743	14.2716	19.1060	23.6112	33.7109
	0	10.4242	23.9551	31.8168	40.1759	57.6631
	0.1	10.0997	23.2695	31.0641	39.0759	56.1312
TSDBT	1	8.2489	19.1684	26.5987	32.3545	46.6708
	2	7.4435	17.1739	24.0199	28.9018	41.6412
	10	6.3640	14.2215	19.0726	23.5775	33.6025
	0	10.4555	24.1328	31.8774	40.5039	58.3709
	0.1	10.1294	23.4389	31.1231	39.3894	56.8116
ASDBT	1	8.2760	19.3027	26.6454	32.6058	47.2228
	2	7.4687	17.2925	24.0592	29.1224	42.1307
	10	6.3860	14.3321	19.1083	23.7740	34.0206

Table 5.25: First five non-dimensional frequencies of C-C beam with $L/h = 20$ and different power-law indices (k)

Theory	k	λ_1	λ_2	λ_3	λ_4	λ_5
	0	13.0137	35.7476	69.7005	114.3730	127.5097
	0.1	12.5379	34.4413	67.1564	110.2026	124.4998
CBT	1	10.0377	27.5608	53.7258	88.0841	106.9229
	2	9.1683	25.1637	49.0277	80.3100	96.9243
	10	8.4590	23.2184	45.2357	74.0505	76.8919
	0	12.7979	34.5081	65.7881	105.2642	127.3707
	0.1	12.3352	33.2767	63.4770	101.6280	124.3629
TBT	1	9.8926	26.7404	51.1299	82.0581	106.7716
	2	9.0322	24.4011	46.6244	74.7656	96.7596
	10	8.2939	22.2877	42.3223	67.4185	76.7162
	0	12.7999	34.5229	65.8427	105.4007	127.5097
	0.1	12.3387	33.2992	63.5541	101.8130	124.4983
PSDBT	1	9.8979	26.7600	51.1847	82.1766	106.8755
	2	9.0312	24.3816	46.5538	74.6002	96.8418
	10	8.2673	22.1381	41.8737	66.4469	76.7877
	0	12.8013	34.5310	65.8688	105.4615	127.5097
	0.1	12.3400	33.3067	63.5781	101.8690	124.4983
ESDBT	1	9.8988	26.7653	51.2021	82.2174	106.8758
	2	9.0314	24.3832	46.5601	74.6163	96.8416
	10	8.2671	22.1372	41.8728	66.4481	76.7882
	0	12.7999	34.5229	65.8426	105.4003	127.5097
	0.1	12.3387	33.2992	63.5539	101.8126	124.4983
HSDBT	1	9.8979	26.7600	51.1846	82.1763	106.8755
	2	9.0312	24.3817	46.5543	74.6012	96.8418
	10	8.2674	22.1385	41.8749	66.4493	76.7877
	0	12.7973	34.4991	65.7713	105.1902	127.2672
	0.1	12.3360	33.2763	63.4855	101.6139	124.2622
TSDBT	1	9.8876	26.7252	51.0991	81.9801	106.6921
	2	9.0175	24.3373	46.4513	74.3729	96.6858
	10	8.2586	22.0995	41.7792	66.2071	76.6510
	0	12.8013	34.5310	65.8688	105.4615	127.5097
	0.1	12.3400	33.3067	63.5781	101.8690	124.4983
ASDBT	1	9.8988	26.7653	51.2021	82.2174	106.8758
	2	9.0314	24.3832	46.5601	74.6163	96.8416
	10	8.2671	22.1372	41.8728	66.4481	76.7882

Table 5.26: First five non-dimensional frequencies of S-S beam $L/h = 5$ and different power-law indices (k)

Theory	k	λ_1	λ_2	λ_3	λ_4	λ_5
	0	5.6558	21.6143	31.6911	45.4414	63.3822
	0.1	5.4593	20.8103	30.9565	43.7893	61.9051
CBT	1	4.6636	16.0568	26.7827	34.2260	53.2876
	2	4.4213	14.2766	24.4096	30.6253	48.3421
	10	3.8763	13.2913	19.6543	28.1193	39.1900
	0	5.3817	18.5438	31.6911	35.2056	53.1934
	0.1	5.2002	17.9252	30.9247	34.1177	51.6402
TBT	1	4.4446	14.3143	25.9506	27.9299	42.8712
	2	4.1959	12.8504	23.2057	25.2823	38.9005
	10	3.6384	11.5197	18.7881	21.9168	32.9732
	0	5.3060	18.4831	31.0642	35.4865	54.0823
	0.1	5.1273	17.8706	30.3157	34.3947	52.5302
PSDBT	1	4.3813	14.2174	25.5089	28.0437	43.4188
	2	4.1278	12.6923	22.8017	25.1730	39.0039
	10	3.5577	11.2350	18.3975	21.3698	32.1831
	0	5.3949	18.6795	31.6911	35.6820	54.2074
	0.1	5.2142	18.0668	30.9259	34.6085	52.6748
ESDBT	1	4.4552	14.3970	25.9777	28.2637	43.6356
	2	4.1948	12.8510	23.1896	25.3619	39.1906
	10	3.6104	11.3330	18.7257	21.4274	32.1755
	0	5.3908	18.6339	31.6911	35.5312	53.8668
	0.1	5.2104	18.0247	30.9255	34.4686	52.3575
HSDBT	1	4.4519	14.3692	25.9679	28.1592	43.3837
	2	4.1921	12.8307	23.1794	25.2751	38.9665
	10	3.6078	11.3103	18.7187	21.3390	31.9603
	0	5.3920	18.6507	31.6911	35.5825	54.0031
	0.1	5.2115	18.0400	30.9257	34.5152	52.4833
TSDBT	1	4.4529	14.3795	25.9715	28.1948	43.4848
	2	4.1927	12.8376	23.1824	25.3039	39.0557
	10	3.6084	11.3174	18.7209	21.3674	32.0435
	0	5.3949	18.6795	31.6911	35.6820	54.2074
	0.1	5.2142	18.0668	30.9259	34.6085	52.6748
ASDBT	1	4.4552	14.3970	25.9777	28.2637	43.6356
	2	4.1948	12.8510	23.1896	25.3619	39.1906
	10	3.6104	11.3330	18.7257	21.4274	32.1755

Table 5.27: First five non-dimensional frequencies of S-S beam with $L/h = 20$ and different power-law indices (k)

Theory	k	λ_1	λ_2	λ_3	λ_4	λ_5
	0	5.7422	22.8985	51.2610	90.4935	126.7643
	0.1	5.5420	22.0597	49.3956	87.1663	123.7531
CBT	1	4.7341	17.5982	39.7292	68.9932	105.2888
	2	4.4900	16.0377	36.3937	62.4870	94.9183
	10	3.9382	14.8299	33.4081	57.8516	76.3703
	0	5.7225	22.5921	49.7814	86.1098	126.7643
	0.1	5.5234	21.7722	48.0054	83.0516	123.7364
TBT	1	4.7184	17.4005	38.7474	66.2688	101.2400
	2	4.4737	15.8563	35.4787	60.0715	92.1499
	10	3.9207	14.6025	32.2938	54.8651	75.8946
	0	5.7227	22.5947	49.7970	86.1498	126.7643
	0.1	5.5237	21.7768	48.0299	83.1175	123.7367
PSDBT	1	4.7186	17.4023	38.7579	66.2939	101.2959
	2	4.4729	15.8473	35.4368	59.9594	91.8916
	10	3.9175	14.5613	32.1025	54.3573	75.8240
	0	5.7228	22.5969	49.8072	86.1805	126.7643
	0.1	5.5238	21.7787	48.0392	83.1456	123.7368
ESDBT	1	4.7187	17.4037	38.7647	66.3132	101.3427
	2	4.4729	15.8477	35.4393	59.9666	91.9121
	10	3.9175	14.5611	32.1019	54.3574	75.8245
	0	5.7227	22.5947	49.7970	86.1496	126.7643
	0.1	5.5237	21.7768	48.0298	83.1173	123.7367
HSDBT	1	4.7186	17.4023	38.7579	66.2938	101.2955
	2	4.4729	15.8473	35.4370	59.9598	91.8925
	10	3.9175	14.5614	32.1029	54.3585	75.8242
	0	5.7225	22.5922	49.7846	86.1171	126.7643
	0.1	5.5235	21.7744	48.0181	83.0864	123.7366
TSDBT	1	4.7184	17.4007	38.7495	66.2739	101.2624
	2	4.4727	15.8453	35.4265	59.9362	91.8476
	10	3.9172	14.5582	32.0867	54.3220	75.8189
	0	5.7228	22.5969	49.8072	86.1805	126.7643
	0.1	5.5238	21.7787	48.0392	83.1456	123.7368
ASDBT	1	4.7187	17.4037	38.7647	66.3132	101.3427
	2	4.4729	15.8477	35.4393	59.9666	91.9121
	10	3.9175	14.5611	32.1019	54.3574	75.8245

Table 5.28: First five non-dimensional frequencies of C-F beam with $L/h = 5$ and different power-law indices (k)

Theory	k	λ_1	λ_2	λ_3	λ_4	λ_5
	0	2.0321	12.1896	15.9398	32.0486	47.8188
	0.1	1.9578	11.7470	15.5652	30.8969	46.6963
CBT	1	1.5664	9.3464	13.4228	24.4870	40.3255
	2	1.4297	8.4787	12.2129	22.1053	36.7305
	10	1.3192	7.8076	9.6956	20.3742	29.1266
	0	1.9827	10.6377	15.9077	25.2861	41.9246
	0.1	1.9115	10.2834	15.5329	24.4931	40.6758
TBT	1	1.5332	8.3236	13.3652	20.0055	33.4633
	2	1.3986	7.5521	12.1359	18.1154	30.2444
	10	1.2817	6.7227	9.6211	15.8025	25.9437
	0	1.9486	10.5856	15.6245	25.4327	42.5695
	0.1	1.8788	10.2376	15.2564	24.6530	41.3403
PSDBT	1	1.5071	8.2692	13.1282	20.0671	33.8649
	2	1.3738	7.4642	11.9190	18.0228	30.2913
	10	1.2547	6.5546	9.4480	15.4059	25.3167
	0	1.9838	10.6886	15.9268	25.5342	42.5491
	0.1	1.9131	10.3501	15.5642	24.8010	41.4340
ESDBT	1	1.5350	8.3688	13.3909	20.2180	34.0074
	2	1.3989	7.5484	12.1549	18.1439	30.3994
	10	1.2764	6.6047	9.6353	15.4431	25.2875
	0	1.9836	10.6852	15.9398	25.5118	42.4810
	0.1	1.9127	10.3367	15.5642	24.7379	41.2697
HSDBT	1	1.5348	8.3590	13.3906	20.1702	33.8804
	2	1.3988	7.5424	12.1549	18.1095	30.2991
	10	1.2763	6.5998	9.6349	15.4114	25.1959
	0	1.9829	10.6460	15.8816	25.3436	42.1192
	0.1	1.9119	10.2995	15.5075	24.5767	40.9193
TSDBT	1	1.5325	8.3267	13.3453	20.0423	33.5970
	2	1.3958	7.5084	12.1148	17.9843	30.0304
	10	1.2743	6.5650	9.6006	15.2868	24.9558
	0	1.9835	10.6739	15.9077	25.4682	42.4061
	0.1	1.9126	10.3256	15.5329	24.6940	41.1909
ASDBT	1	1.5337	8.3480	13.3657	20.1335	33.8121
	2	1.3973	7.5277	12.1327	18.0649	30.2204
	10	1.2753	6.5842	9.6162	15.3660	25.1292

Table 5.29: First five non-dimensional frequencies of C-F beam with $L/h = 20$ and different power-law indices (k)

Theory	k	λ_1	λ_2	λ_3	λ_4	λ_5
	0	2.0468	12.7899	35.6470	63.7593	69.3888
	0.1	1.9719	12.3224	34.3452	62.2520	66.8600
CBT	1	1.5785	9.8618	27.4776	52.9441	53.9887
	2	1.4419	9.0053	25.0796	47.9763	49.2651
	10	1.3304	8.3091	23.1409	38.3908	45.0313
	0	2.0435	12.6516	34.7679	63.6307	66.3961
	0.1	1.5753	9.7654	26.8859	51.3721	53.4646
TBT	1	1.5753	9.7654	26.8859	51.3721	53.4646
	2	1.4384	8.9129	24.5248	46.7401	48.5580
	10	1.3272	8.2010	22.4728	38.3100	42.7970
	0	2.0435	12.6546	34.7893	63.7593	66.4727
	0.1	1.9689	12.1964	33.5456	62.2492	64.1410
PSDBT	1	1.5764	9.7738	26.9179	51.4314	53.5848
	2	1.4397	8.9189	24.5329	46.7072	48.6656
	10	1.3274	8.1880	22.3813	38.3687	42.4996
	0	2.0435	12.6554	34.7947	63.7593	66.4912
	0.1	1.9689	12.1972	33.5506	62.2493	64.1579
ESDBT	1	1.5764	9.7743	26.9214	51.4429	53.5857
	2	1.4397	8.9190	24.5338	46.7105	48.6660
	10	1.3274	8.1878	22.3802	38.3687	42.4972
	0	2.0435	12.6546	34.7893	63.7593	66.4727
	0.1	1.9689	12.1964	33.5456	62.2492	64.1409
HSDBT	1	1.5764	9.7738	26.9179	51.4314	53.5848
	2	1.4397	8.9189	24.5330	46.7076	48.6656
	10	1.3274	8.1880	22.3816	38.3687	42.5006
	0	2.0434	12.6496	34.7538	63.5262	66.3470
	0.1	1.9688	12.1914	33.5114	62.0245	64.0194
TSDBT	1	1.5745	9.7589	26.8624	51.3310	53.3706
	2	1.4371	8.8993	24.4639	46.6040	48.4560
	10	1.3261	8.1751	22.3249	38.2562	42.3271
	0	2.0435	12.6554	34.7947	63.7593	66.4912
	0.1	1.9689	12.1972	33.5506	62.2493	64.1579
ASDBT	1	1.5764	9.7743	26.9214	51.4429	53.5857
	2	1.4397	8.9190	24.5338	46.7105	48.6660
	10	1.3274	8.1878	22.3802	38.3687	42.4972

Analyzing the above Tables 5.24 to 5.29 for first five non-dimensional frequencies of FG beam with different sets of edge supports, one may plot the effects of power-law indices (k) on non-dimensional frequencies for a given slenderness ratio (L/h) within the framework of all SDBTs of Eq. (2.4). But the present study includes the plot of effects of power-law indices on fundamental and fifth non-dimensional frequencies of C-C FG beam respectively in Figs. 5.1 to 5.2 with $L/h = 5$ and 20. It can easily be observed that the non-dimensional frequencies are gradually decreasing with increase in power-law indices and are increasing with increase in slenderness ratios. For $L/h = 5$, the difference among the frequencies at each mode is quite

significant while comparing the results obtained from these mentioned SDBTs, whereas these are found to be negligible for $L/h = 20$ irrespective of the beam theories considered.

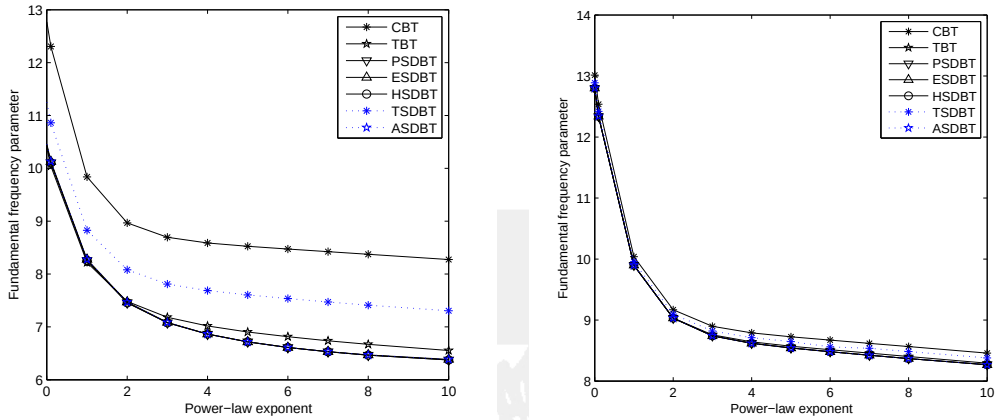

(a) $L/h = 5$ (b) $L/h = 20$

Figure 5.1: Effect of power-law indices on fundamental non-dimensional frequencies of C-C FG beams using all SDBTs

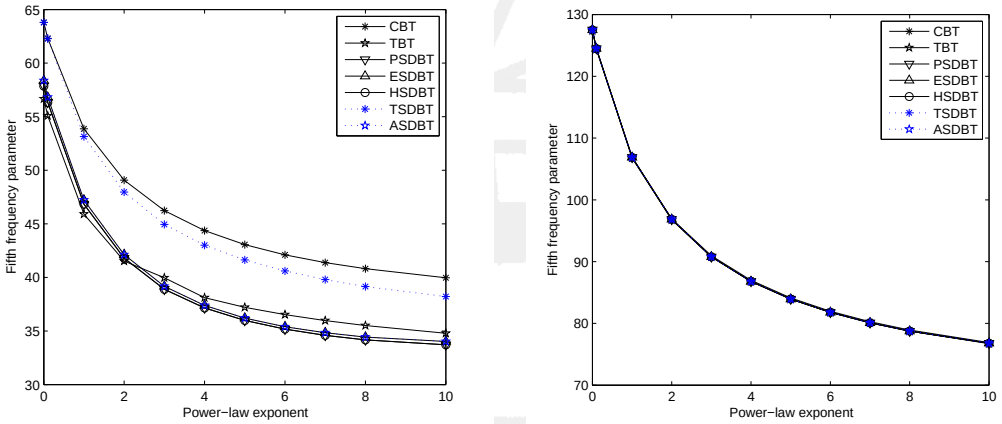

(a) $L/h = 5$ (b) $L/h = 20$

Figure 5.2: Effect of power-law indices on fifth non-dimensional frequencies of C-C FG beams using all SDBTs

Now onwards, newly proposed PESDBT along with four other previously proposed SDBTs viz. CBT, TBT, PSDBT and ASDBT are considered here for the computation of non-dimensional frequencies based on the formulation of Eq. (5.2). Various key factors which influence the free vibration characteristics of FG beam are incorporated in this part as below.

- Effect of slenderness ratios (L/h)
- Effect of power-law exponents (k) associated with variation criterion

- Effect of power-law exponents (n) associated with PESDBT

Effect of slenderness ratios (L/h)

First five non-dimensional frequencies of FG beam based on the given SDBTs subject to different sets of BCs are computed in Tables 5.30 and 5.31 with respect to various slenderness ratios (L/h = 5, 10, 20, 30, 50 and 100). The power-law index (k) considered in variation criterion is taken as unity. Computations related with PESDBT[1] is meant for the PESDBT with $n = 1$ in both these tabulations. Here primary constituents of FG beam own the properties: $E_m = 210$ GPa, $\rho_m = 7800$ kg/m^3, $E_c = 390$ GPa, $\rho_c = 3960$ kg/m^3 and $\nu_m = \nu_c = 0.23$. In Table 5.30, non-dimensional frequencies of C-C and C-S FG beams are incorporated with the above mentioned slenderness ratios, whereas cantilever (C-F) and S-S edge supports are assumed in Table 5.31. Discussion of the benchmark results on the effect of slenderness ratios on free vibration behavior of FG beam are reported as follows.

(1) Non-dimensional frequencies at each mode are increasing with the increase in slenderness ratios irrespective of the SDBTs assumed.

(2) While comparing various SDBTs, the difference among the non-dimensional frequencies is significant for $L/h < 20$. On the contrary, for $L/h \geq 20$, the effect on non-dimensional frequencies is negligible irrespective of the beam theories considered.

(3) While comparing first five frequencies of PSDBT and PESDBT[1], one may observe that results are coinciding for respective sets of BCs.

Table 5.30: Effect of slenderness ratios on frequencies of C-C and C-S FG beams with $k = 1$

BCs	Source	Mode	L/h					
			5	10	20	30	50	100
C-C	CBT	1	8.5673	8.7097	8.7462	8.7530	8.7565	8.7580
		2	21.4275	23.6464	24.0174	24.0873	24.1233	24.1385
		3	22.6259	43.4295	46.8034	47.0943	47.2449	47.3089
		4	39.9727	45.3022	76.7357	77.5664	77.9964	78.1795
		5	44.0661	72.6639	86.8472	115.337	116.316	116.735
	TBT	1	7.1674	8.2570	8.6238	8.6978	8.7365	8.7529
		2	16.5396	21.2710	23.3081	23.7602	24.0032	24.1082
		3	21.6359	38.6665	44.5633	46.0290	46.8468	47.2077
		4	27.7734	43.3570	71.4848	74.9784	77.0101	77.9266
		5	39.8257	58.9882	86.8079	110.107	114.269	116.204
	PSDBT	1	7.1931	8.2599	8.6241	8.6978	8.7365	8.7529
		2	16.6790	21.2927	23.3100	23.7606	24.0033	24.1082
		3	21.6365	38.7345	44.5702	46.0305	46.8471	47.2077
		4	28.1168	43.3571	71.5049	74.9830	77.0107	77.9266
		5	40.5008	59.1568	86.8079	110.118	114.271	116.204
	ASDBT	1	7.2089	8.2636	8.6249	8.6982	8.7366	8.7530
		2	16.7518	21.3142	23.3149	23.7627	24.0040	24.1084
		3	21.6379	38.7961	44.5859	46.0374	46.8495	47.2083
		4	28.2920	43.3576	71.5426	74.9999	77.0168	77.9282
		5	40.8288	59.2917	86.8081	110.152	114.284	116.207
	PESDBT[1]	1	7.1931	8.2599	8.6241	8.6978	8.7365	8.7529
		2	16.6790	21.2927	23.3100	23.7606	24.0033	24.1082
		3	21.6365	38.7345	44.5702	46.0305	46.8471	47.2077
		4	28.1168	43.3571	71.5049	74.9830	77.0107	77.9266
		5	40.5008	59.1568	86.8079	110.118	114.271	116.204
C-S	CBT	1	5.9274	6.0175	6.0405	6.0448	6.0470	6.0479
		2	17.9947	19.1826	19.4719	19.5260	19.5539	19.5656
		3	21.8993	39.0602	40.3794	40.6225	40.7480	40.8012
		4	34.8291	43.3833	68.4385	69.1976	69.5779	69.7385
		5	43.9194	65.0392	86.6256	105.088	105.992	106.369
	TBT	1	5.3243	5.8373	5.9932	6.0236	6.0393	6.0460
		2	14.6605	17.8509	19.0873	19.3501	19.4896	19.5494
		3	21.5849	34.6960	38.9421	39.9459	40.4967	40.7375
		4	26.1370	43.2112	64.7386	67.3871	68.8919	69.5632
		5	38.5800	55.0068	86.5250	101.188	104.475	105.977
	PSDBT	1	5.3367	5.8387	5.9933	6.0236	6.0393	6.046
		2	14.7529	17.8649	19.0886	19.3504	19.4896	19.5494
		3	21.5866	34.7450	38.9472	39.9471	40.4969	40.7375
		4	26.3968	43.2121	64.7545	67.3908	68.8925	69.5632
		5	39.1297	55.1409	86.5253	101.197	104.476	105.977
	ASDBT	1	5.3440	5.8402	5.9936	6.0237	6.0394	6.0460
		2	14.7988	17.8775	19.0913	19.3515	19.4899	19.5495
		3	21.5884	34.7873	38.9576	39.9515	40.4984	40.7379
		4	26.5256	43.2132	64.7820	67.4029	68.8968	69.5642
		5	39.3877	55.2423	86.5260	101.223	104.485	105.979
	PESDBT[1]	1	5.3367	5.8387	5.9933	6.0236	6.0393	6.046
		2	14.7529	17.8649	19.0886	19.3504	19.4896	19.5494
		3	21.5866	34.7450	38.9472	39.9471	40.4969	40.7375
		4	26.3968	43.2121	64.7545	67.3908	68.8925	69.5632
		5	39.1297	55.1409	86.5253	101.197	104.476	105.977

Table 5.31: Effect of slenderness ratios on frequencies of cantilever and S-S FG beams with $k = 1$

BCs	Source	Mode	L/h					
			5	10	20	30	50	100
		1	1.3647	1.3734	1.3756	1.3760	1.3762	1.3763
		2	8.1224	8.4987	8.5933	8.6110	8.6201	8.6239
	CBT	3	10.9145	21.6621	23.9395	24.0564	24.1167	24.1422
		4	21.2570	23.3726	43.3120	46.9819	47.2023	47.2948
		5	32.8266	44.5037	46.6232	65.0265	77.9080	78.1515
		1	1.3367	1.3660	1.3737	1.3751	1.3759	1.3762
		2	7.2376	8.2061	8.5145	8.5753	8.6071	8.6206
	TBT	3	10.8756	21.4503	23.4364	23.8233	24.0310	24.1206
		4	17.3763	21.8945	43.2706	46.1614	46.8955	47.2169
		5	29.0182	39.4609	44.9508	65.0216	77.1096	77.9466
		1	1.3370	1.3660	1.3737	1.3751	1.3759	1.3762
		2	7.2519	8.2076	8.5143	8.5753	8.6071	8.6206
C-F	PSDBT	3	10.8759	21.4557	23.4355	23.8234	24.0310	24.1206
		4	17.4526	21.8999	43.2624	46.1622	46.8956	47.2169
		5	29.2206	39.4995	44.9473	65.0216	77.1099	77.9466
		1	1.3372	1.3661	1.3737	1.3752	1.3759	1.3762
		2	7.2616	8.2099	8.5148	8.5755	8.6072	8.6207
	ASDBT	3	10.8762	21.4625	23.4388	23.8249	24.0316	24.1207
		4	17.4987	21.9069	43.2630	46.1674	46.8974	47.2173
		5	29.3368	39.5420	44.9582	65.0216	77.1149	77.9479
		1	1.3370	1.3660	1.3737	1.3751	1.3759	1.3762
		2	7.2519	8.2076	8.5143	8.5753	8.6071	8.6206
	PESDBT[1]	3	10.8759	21.4557	23.4355	23.8234	24.0310	24.1206
		4	17.4526	21.8999	43.2624	46.1622	46.8956	47.2169
		5	29.2206	39.4995	44.9473	65.0216	77.1099	77.9466
		1	3.8470	3.8945	3.9066	3.9088	3.9100	3.9105
		2	14.3042	15.1609	15.3781	15.4187	15.4395	15.4483
	CBT	3	21.8200	33.4534	34.4621	34.6564	34.7568	34.7994
		4	29.9370	43.0413	60.5991	61.2806	61.6170	61.7581
		5	43.8138	57.9826	86.4342	95.4081	96.1794	96.5086
		1	3.6851	3.8494	3.8950	3.9037	3.9081	3.9100
		2	12.6371	14.5430	15.2049	15.3400	15.4109	15.4411
	TBT	3	21.5362	30.7751	33.6220	34.2648	34.6122	34.7629
		4	24.3635	42.8874	58.1417	60.0869	61.1672	61.6435
		5	37.1989	51.0327	86.3313	92.5903	95.0941	96.2290
		1	3.6904	3.8500	3.8951	3.9037	3.9081	3.9100
		2	12.6934	14.5515	15.2057	15.3401	15.4109	15.4411
S-S	PSDBT	3	21.5385	30.8116	33.6257	34.2656	34.6123	34.7629
		4	24.5556	42.8882	58.1538	60.0897	61.1676	61.6435
		5	37.6354	51.1368	86.3316	92.5975	95.0952	96.2291
		1	3.6929	3.8505	3.8951	3.9037	3.9082	3.9100
		2	12.7183	14.5579	15.2070	15.3407	15.4111	15.4412
	ASDBT	3	21.5406	30.8395	33.6322	34.2683	34.6132	34.7631
		4	24.6425	42.8895	58.1730	60.0979	61.1705	61.6442
		5	37.8297	51.2105	86.3323	92.6169	95.1021	96.2308
		1	3.6904	3.8500	3.8951	3.9037	3.9081	3.9100
		2	12.6934	14.5515	15.2057	15.3401	15.4109	15.4411
	PESDBT[1]	3	21.5385	30.8116	33.6257	34.2656	34.6123	34.7629
		4	24.5556	42.8882	58.1538	60.0897	61.1676	61.6435
		5	37.6354	51.1368	86.3316	92.5975	95.0952	96.2291

The conclusion regarding the effect of slenderness ratios on first five non-dimensional frequencies of FG beam with various edge supports based on PESDBT[1] (Tables 5.30 and 5.31) are diagrammatically represented in Fig. 5.3. The power-law exponent (k) in variation criterion for FG beam is taken as unity. It can easily be seen here that frequencies are increasing with increase in slenderness ratios irrespective of edge conditions assumed. Considering other shear deformation beam theories, similar behavior of non-dimensional frequencies with increase in slenderness ratios may also be depicted.

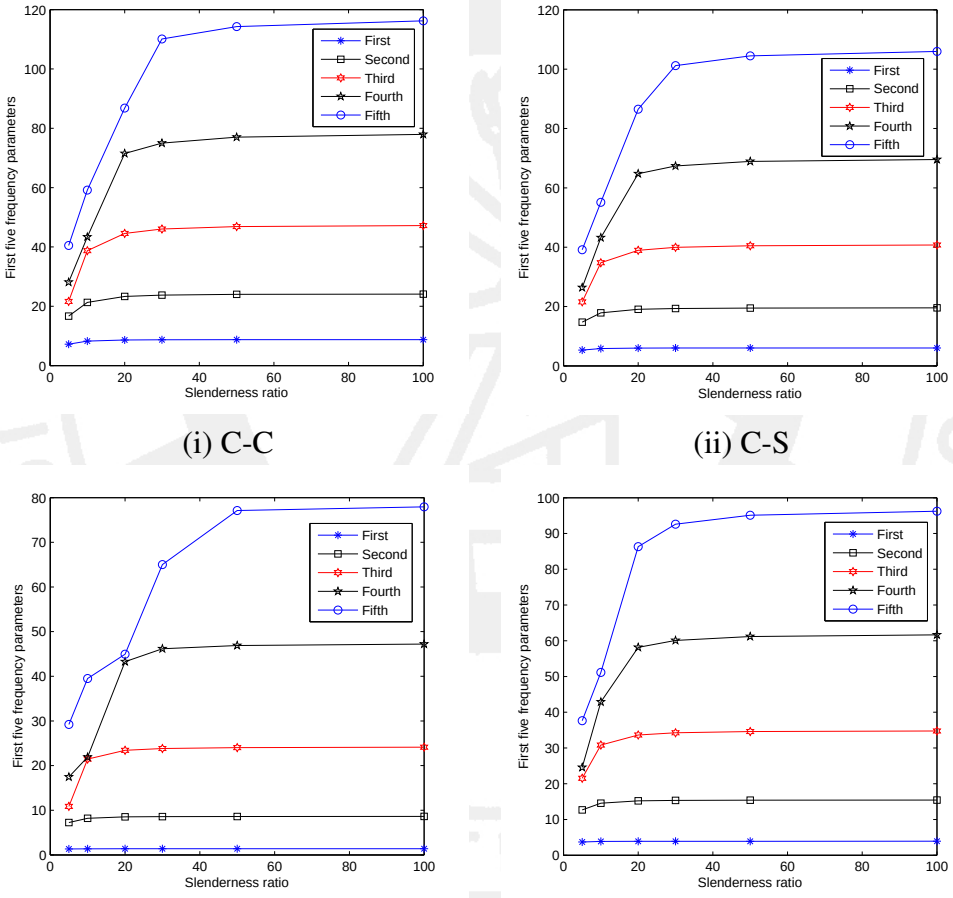

(i) C-C (ii) C-S

(iii) C-F (iv) S-S

Figure 5.3: Effect of L/h on first five non-dimensional frequencies of FG beams subject to various BCs based on PESDBT[1] with $k = 1$

Effect of power-law exponents (k) associated with variation criterion

First five non-dimensional frequencies of functionally graded beams subject to various sets of edge conditions are reported in Tables 5.32 and 5.33 with increase in power-law indices (k = 0, 0.2, 0.5, 1, 2, 5 and 10) and a fixed slenderness ratio ($L/h = 5$). Again the power-law exponent (n) is considered to be unity for PESDBT. In these evaluations, functionally graded beam bears

the material properties of constituents: E_m = 210 GPa, ρ_m = 7800 kg/m^3, E_c = 390 GPa, ρ_c = 3960 kg/m^3 and $\nu_m = \nu_c = 0.23$. Non-dimensional frequencies of C-C and C-S FG beams are incorporated in Table 5.32, whereas cantilever and simply supported edge supports are considered in Table 5.33 respectively. Looking into these tabulations, we may summarize as below:

(1) Irrespective of the shear deformation theory and boundary condition considered, non-dimensional frequencies follow a descending pattern with increase in power-law exponents (k) involved in variation form.

(2) Non-dimensional frequencies concerned with PSDBT are coinciding with PESDBT[1] for different sets of BCs only with a little ambiguity in case of cantilever FG beam. A bit of fluctuations with an absolute error specification of 10^{-5} to 10^{-6} can be observed while comparing results of cantilever FG beam based on PSDBT and PESDBT[1].

Table 5.32: Effect of power-law exponent (k) on frequencies of C-C and C-S FG beams with $L/h = 5$

BCs	Source	Mode	Power-law exponent (k) in variation criterion						
			0	0.2	0.5	1	2	5	10
C-C	CBT	1	12.1067	10.6557	9.4867	8.5673	7.8711	7.2919	6.9681
		2	30.1621	26.7989	23.8770	21.4275	19.3780	17.5363	16.7288
		3	31.6990	27.9261	24.9904	22.6259	20.7382	19.1616	18.2948
		4	57.8812	50.4547	44.5039	39.9727	36.7017	34.1758	32.9302
		5	60.3042	54.0026	48.7285	44.0661	39.8464	35.9080	33.9864
	TBT	1	10.0713	8.9011	7.9442	7.1674	6.5445	6.0045	5.7302
		2	23.2639	20.5743	18.3570	16.5396	15.0623	13.7834	13.1601
		3	30.1621	26.8660	24.0645	21.6359	19.4943	17.5671	16.7406
		4	39.0547	34.5565	30.8377	27.7734	25.2619	23.0782	22.0322
		5	55.9659	49.5413	44.2246	39.8257	36.1943	33.0194	31.5158
	PSDBT	1	10.1083	8.9412	7.9812	7.1931	6.5471	5.9855	5.7226
		2	23.4657	20.7732	18.5379	16.6790	15.1229	13.7711	13.1846
		3	30.1621	26.8682	24.0682	21.6365	19.4901	17.5660	16.7423
		4	39.5482	35.0237	31.2622	28.1168	25.4525	23.1248	22.1490
		5	56.9319	50.4270	45.0277	40.5008	36.6314	33.2252	31.8279
	ASDBT	1	10.1311	8.9607	7.9985	7.2089	6.5605	5.9973	5.7370
		2	23.5715	20.8630	18.6176	16.7518	15.1871	13.8293	13.2510
		3	30.1621	26.8689	24.0696	21.6379	19.4908	17.5669	16.7431
		4	39.8012	35.2375	31.4523	28.2920	25.6101	23.2693	22.3082
		5	57.4047	50.8250	45.3815	40.8288	36.9311	33.5017	32.1258
	PESDBT[1]	1	10.1083	8.9412	7.9812	7.1931	6.5471	5.9855	5.7226
		2	23.4657	20.7732	18.5379	16.6790	15.1229	13.7711	13.1846
		3	30.1621	26.8682	24.0682	21.6365	19.4901	17.5660	16.7423
		4	39.5482	35.0237	31.2622	28.1168	25.4525	23.1248	22.1490
		5	56.9319	50.4270	45.0277	40.5008	36.6314	33.2252	31.8279
C-S	CBT	1	8.3538	7.3560	6.5560	5.9274	5.4475	5.0402	4.8117
		2	25.8027	22.6127	20.0174	17.9947	16.5114	15.3894	14.7984
		3	30.1051	26.8986	24.2326	21.8993	19.7768	17.7373	16.7993
		4	50.2209	43.8690	38.7484	34.8291	32.0322	29.9772	28.8587
		5	60.2101	53.8487	48.5733	43.9194	39.6463	35.5103	33.6110
	TBT	1	7.4787	6.6025	5.8931	5.3243	4.8740	4.4822	4.2757
		2	20.6839	18.2633	16.2743	14.6605	13.3767	12.2875	11.7428
		3	30.1051	26.8147	24.0150	21.5849	19.4449	17.5265	16.7055
		4	36.7997	32.5258	29.0094	26.1370	23.8133	21.8054	20.8224
		5	54.2499	47.9900	42.8273	38.5800	35.1016	32.0684	30.6116
	PSDBT	1	7.4965	6.6217	5.9108	5.3367	4.8754	4.4732	4.2721
		2	20.8194	18.3957	16.3941	14.7529	13.4169	12.2782	11.7588
		3	30.1051	26.8170	24.0192	21.5866	19.4414	17.5253	16.7071
		4	37.1746	32.8783	29.3297	26.3968	23.9551	21.8323	20.9068
		5	55.0385	48.7066	43.4779	39.1297	35.4539	32.2220	30.8603
	ASDBT	1	7.5070	6.6306	5.9188	5.3440	4.8816	4.4786	4.2788
		2	20.8869	18.4526	16.4443	14.7988	13.4575	12.3155	11.8019
		3	30.1051	26.8177	24.0209	21.5884	19.4427	17.5265	16.7081
		4	37.3618	33.0350	29.4688	26.5256	24.0718	21.9402	21.0271
		5	55.4122	49.0178	43.7540	39.3877	35.6918	32.4434	31.1014
	PESDBT[1]	1	7.4965	6.6217	5.9108	5.3367	4.8754	4.4732	4.2721
		2	20.8194	18.3957	16.3941	14.7529	13.4169	12.2782	11.7588
		3	30.1051	26.8170	24.0192	21.5866	19.4414	17.5253	16.7071
		4	37.1746	32.8783	29.3297	26.3968	23.9551	21.8323	20.9068
		5	55.0385	48.7066	43.4779	39.1297	35.4539	32.2220	30.8603

Table 5.33: Effect of power-law exponent (k) on frequencies of cantilever and S-S FG beams with $L/h = 5$

BCs	Source	Mode	Power-law exponent (k) in variation criterion						
			0	0.2	0.5	1	2	5	10
C-F	CBT	1	1.9264	1.6965	1.5111	1.3647	1.2533	1.1602	1.1083
		2	11.5556	10.1460	9.0085	8.1224	7.4661	6.9416	6.6484
		3	15.0556	13.4443	12.0969	10.9145	9.8374	8.8233	8.3784
		4	30.3819	26.6075	23.5840	21.2570	19.5723	18.2607	17.5088
		5	45.1668	40.3577	36.3528	32.8266	29.5878	26.5058	25.1494
	TBT	1	1.8855	1.6614	1.4802	1.3367	1.2266	1.1340	1.0831
		2	10.2346	9.0180	8.0274	7.2376	6.6250	6.1124	5.8437
		3	15.0556	13.4327	12.0684	10.8756	9.7996	8.8024	8.3697
		4	24.5268	21.6327	19.2736	17.3763	15.8768	14.6009	13.9506
		5	40.9427	36.1326	32.2007	29.0182	26.4710	24.2893	23.2063
	PSDBT	1	1.8859	1.6619	1.4807	1.3370	1.2263	1.1330	1.0826
		2	10.2557	9.0418	8.0493	7.2519	6.6233	6.0953	5.8351
		3	15.0556	13.4330	12.0690	10.8759	9.7991	8.8021	8.3699
		4	24.6380	21.7464	19.3776	17.4526	15.8938	14.5612	13.9426
		5	41.2404	36.4188	32.4607	29.2206	26.5503	24.2486	23.2330
	ASDBT	1	1.8863	1.6623	1.4810	1.3372	1.2265	1.1332	1.0828
		2	10.2701	9.0540	8.0602	7.2616	6.6318	6.1029	5.8444
		3	15.0556	13.4331	12.0693	10.8762	9.7993	8.8023	8.3701
		4	24.7064	21.8035	19.4285	17.4987	15.9360	14.5998	13.9870
		5	41.4144	36.5624	32.5880	29.3368	26.6585	24.3492	23.3460
	PESDBT[1]	1	1.8859	1.6619	1.4807	1.3370	1.2263	1.1330	1.0826
		2	10.2557	9.0419	8.0494	7.2517	6.6234	6.0955	5.8350
		3	15.0556	13.4330	12.0690	10.8759	9.7991	8.8022	8.3699
		4	24.6381	21.7471	19.3781	17.4518	15.8944	14.5619	13.9422
		5	41.2405	36.4203	32.4619	29.2188	26.5516	24.2502	23.2322
S-S	CBT	1	5.3617	4.7295	4.2337	3.8470	3.5423	3.2606	3.0992
		2	20.4902	17.9687	15.9129	14.3042	13.1286	12.2425	11.7619
		3	30.0429	26.8307	24.1573	21.8200	19.6905	17.6542	16.7410
		4	43.0781	37.6617	33.2937	29.9370	27.5362	25.7601	24.7741
		5	60.0859	53.7282	48.4595	43.8138	39.5419	35.4031	33.5224
	TBT	1	5.1346	4.5333	4.0587	3.6851	3.3868	3.1111	2.9575
		2	17.9016	15.7771	14.0354	12.6371	11.5531	10.6607	10.2015
		3	30.0429	26.7591	23.9637	21.5362	19.3993	17.4870	16.6694
		4	34.3706	30.3388	27.0363	24.3635	22.2378	20.4233	19.5124
		5	52.3412	46.2647	41.2747	37.1989	33.8916	31.0136	29.6059
	PSDBT	1	5.1421	4.5408	4.0657	3.6904	3.3889	3.1102	2.9581
		2	17.9856	15.8573	14.1074	12.6934	11.5805	10.6599	10.2153
		3	30.0429	26.7614	23.9682	21.5385	19.3965	17.4859	16.6711
		4	34.6496	30.5968	27.2702	24.5556	22.3461	20.4458	19.5786
		5	52.9685	46.8270	41.7859	37.6354	34.1713	31.1266	29.8021
	ASDBT	1	5.1455	4.5437	4.0683	3.6929	3.3911	3.1121	2.9604
		2	18.0231	15.8884	14.1347	12.7183	11.6028	10.6807	10.2396
		3	30.0429	26.7622	23.9699	21.5406	19.3981	17.4873	16.6721
		4	34.7773	30.7022	27.3634	24.6425	22.4258	20.5205	19.6630
		5	53.2513	47.0588	41.9914	37.8297	34.3530	31.2977	29.9909
	PESDBT[1]	1	5.1421	4.5408	4.0657	3.6904	3.3889	3.1102	2.9581
		2	17.9856	15.8573	14.1074	12.6934	11.5805	10.6599	10.2153
		3	30.0429	26.7614	23.9682	21.5385	19.3965	17.4859	16.6711
		4	34.6496	30.5968	27.2702	24.5556	22.3461	20.4458	19.5786
		5	52.9685	46.8270	41.7859	37.6354	34.1713	31.1266	29.8021

As resulted in Tables 5.32 and 5.33, the behavior of first five non-dimensional frequencies of FG beam based on PESDBT[1] with increase in k is plotted in Fig. 5.4 with the slenderness ratio (L/h) as 5. It is evident from this figure that non-dimensional frequencies are showing descending pattern with increase in k regardless of the BCs considered. Similar effect of k on frequencies may also be observed for other shear deformation beam theories.

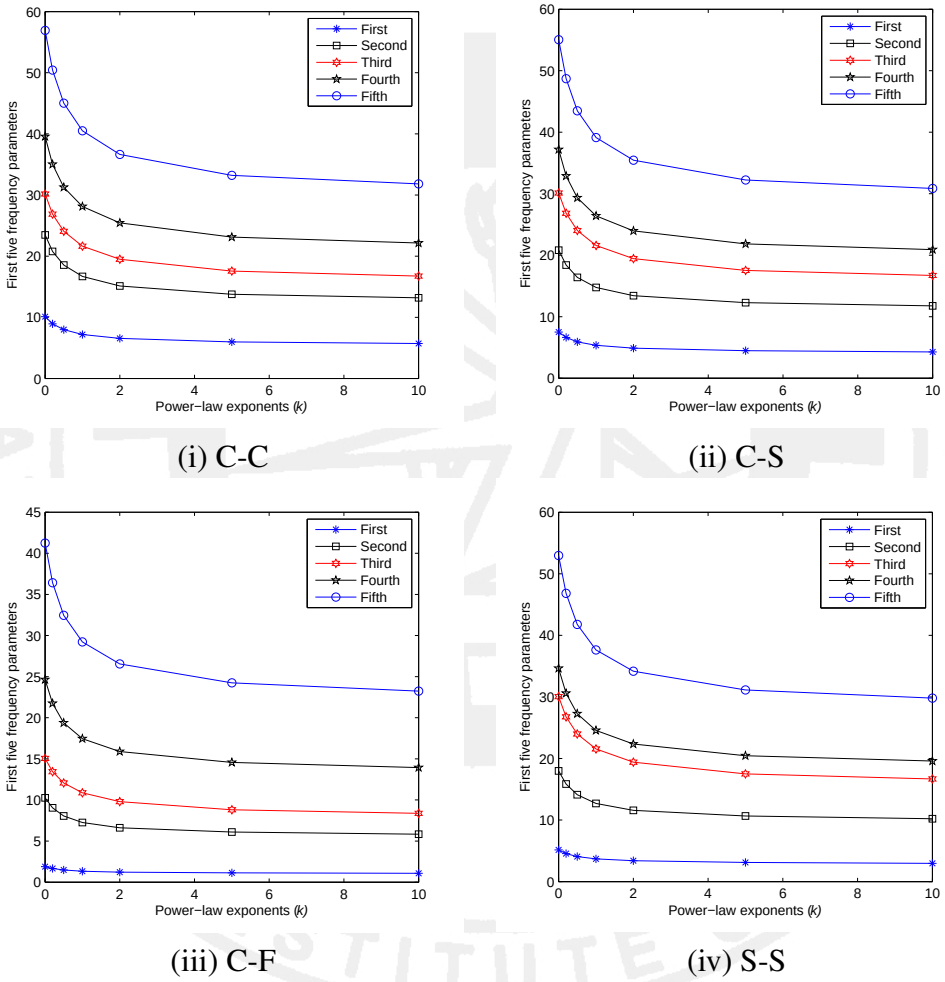

Figure 5.4: Effect of k on first five non-dimensional frequencies of FG beams subject to various BCs based on PESDBT[1] with $L/h = 5$

Effect of power-law exponents (n) associated with PESDBT

Instead of taking all SDBTs assumed in Tables 5.30 to 5.33, only PESDBT is considered in this section to report first five non-dimensional frequencies of FG beam subject to all six sets of classical edge supports. Effect of power-law indices (n) involved in PESDBT on non-dimensional frequencies are incorporated in Tables 5.34 and 5.35. PESDBT is associated with the properties of FG constituents as: E_m = 70 GPa, ρ_m = 2702 kg/m^3, E_c = 380 GPa,

ρ_c = 3960 kg/m^3 and $\nu_m = \nu_c = 0.3$. Here power-law index (k) for variation criteria of physical properties is assumed to be unity. Tables 5.34 and 5.35 are concerned with two different slenderness ratios, $L/h = 5$ and 20 respectively. We may now conclude the following points on the results based on free vibration characteristics of FG beam.

(1) Regardless of slenderness ratio and edge supports implemented, it is evident that non-dimensional frequencies are increasing with increase in the values of n involved in the proposed SDBT.

(2) It can easily be noticed here that frequencies obtained in case of PESDBT with $n = 0$ will follow the behavior of **Euler-Bernoulli FG beam**[5].

(3) Looking into the ascending behavior of free vibration frequencies, one can observe a little fluctuation in non-dimensional frequencies at each mode when we consider very large value of n. It may be evident that frequencies will finally coincide with Euler-Bernoulli beam for very large value of n.

(4) As concluded from the effects of L/h and k, non-dimensional frequencies for PSDBT may also coincide with those using n as unity in the proposed model.

[5]Analysis of functionally graded beam based on classical or Euler-Bernoulli beam theory.

Table 5.34: Effect of power-law exponents (n) on frequencies of functionally graded beams with $L/h = 5$ and $k = 1$

BCs	Mode	Power-law exponent (n) in PESDBT								
		1	3	5	10	30	50	100	200	CBT
C-C	1	7.9680	7.9968	8.0314	8.0735	8.1126	8.1218	8.1290	8.1327	9.3755
	2	18.6207	18.6806	18.7983	18.9487	19.0920	19.1259	19.1525	19.1662	24.2623
	3	25.3862	25.3919	25.3962	25.4012	25.4058	25.4068	25.4076	25.4080	25.6670
	4	31.5143	31.5724	31.8034	32.1079	32.4022	32.4719	32.5269	32.5553	44.2130
	5	45.5201	45.4909	45.8407	46.3218	46.7952	46.9081	46.9971	47.0430	51.2429
C-S	1	5.9349	5.9485	5.9646	5.9842	6.0024	6.0066	6.0100	6.0117	6.5431
	2	16.3317	16.3738	16.4478	16.5423	16.6324	16.6536	16.6702	16.6788	19.5487
	3	24.9772	24.9903	25.0047	25.0221	25.0381	25.0419	25.0448	25.0463	25.6086
	4	29.6084	29.6648	29.8403	30.0710	30.2942	30.3470	30.3886	30.4100	38.2848
	5	43.8186	43.8445	44.1353	44.5299	44.9159	45.0075	45.0795	45.1166	50.9684
C-F	1	1.4645	1.4655	1.4664	1.4674	1.4683	1.4685	1.4686	1.4687	1.4925
	2	8.0125	8.0354	8.0600	8.0887	8.1151	8.1212	8.1262	8.1284	8.9080
	3	12.7328	12.7337	12.7345	12.7354	12.7362	12.7364	12.7365	12.7366	12.7591
	4	19.3830	19.4556	19.5516	19.6662	19.7729	19.7974	19.8178	19.8267	23.3377
	5	32.6162	32.7413	32.9500	33.2040	33.4429	33.4978	33.5441	33.5638	38.3349
S-S	1	4.2632	4.2663	4.2712	4.2775	4.2834	4.2848	4.2858	4.2864	4.4488
	2	13.8327	13.8534	13.8902	13.9379	13.9835	13.9942	14.0027	14.0070	15.3172
	3	24.8238	24.8358	24.8519	24.8722	24.8916	24.8961	24.8997	24.9016	25.5491
	4	27.2748	27.3240	27.4470	27.6093	27.7662	27.8032	27.8323	27.8473	32.6495
	5	42.2306	42.2733	42.5149	42.8446	43.1690	43.2460	43.3065	43.3378	50.8326
S-F	1	5.9733	5.9786	5.9849	5.9928	6.0001	6.0018	6.0031	6.0038	6.1998
	2	12.5037	12.5070	12.5100	12.5135	12.5167	12.5175	12.5180	12.5183	12.6055
	3	17.1015	17.1447	17.1973	17.262	17.3226	17.3367	17.3479	17.3536	19.1106
	4	30.5977	30.7021	30.8467	31.0264	31.1954	31.2349	31.2661	31.2820	35.9094
	5	37.2466	37.2783	37.3066	37.3394	37.3693	37.3763	37.3818	37.3846	38.6742
F-F	1	8.4865	8.4993	8.5095	8.5209	8.5314	8.5338	8.5356	8.5366	8.8114
	2	20.0769	20.1558	20.2223	20.2987	20.368	20.3841	20.3966	20.4031	22.3449
	3	25.3277	25.3353	25.3412	25.3478	25.3537	25.3550	25.3561	25.3566	25.4925
	4	33.9054	34.0842	34.2529	34.4504	34.6309	34.6728	34.7058	34.2275	39.9919
	5	47.3796	47.6262	47.8741	48.1557	48.4017	48.4571	48.5001	48.5221	51.1175

Table 5.35: Effect of power-law exponents (n) on frequencies of functionally graded beams with $L/h = 20$ and $k = 1$

BCs	Mode	Power-law exponent (n) in PESDBT								
		1	3	5	10	30	50	100	200	CBT
C-C	1	9.4438	9.4490	9.4529	9.4574	9.4614	9.4623	9.4630	9.4634	9.5667
	2	25.5599	25.5890	25.6115	25.6369	25.6597	25.6649	25.6691	25.6712	26.2740
	3	48.9471	49.0359	49.1051	49.1837	49.2544	49.2707	49.2835	49.2901	51.2050
	4	78.6623	78.8616	79.0201	79.2007	79.3636	79.4013	79.4308	79.4460	83.9755
	5	101.781	101.782	101.783	101.784	101.785	101.785	101.786	101.786	101.811
C-S	1	6.6254	6.6274	6.6290	6.6308	6.6324	6.6327	6.6330	6.6331	6.6738
	2	20.9569	20.9727	20.9850	20.9989	21.0114	21.0143	21.0166	21.0177	21.3447
	3	42.7407	42.7980	42.8429	42.8939	42.9397	42.9503	42.9586	42.9629	44.1849
	4	71.0299	71.1701	71.2820	71.4095	71.5244	71.5510	71.5718	71.5825	74.7113
	5	100.002	100.049	100.083	100.121	100.153	100.160	100.166	100.169	100.729
C-F	1	1.5021	1.5022	1.5023	1.5024	1.5024	1.5024	1.5024	1.5024	1.5040
	2	9.317	9.3204	9.3230	9.3259	9.3284	9.3290	9.3295	9.3297	9.3964
	3	25.6725	25.6938	25.7099	25.7282	25.7445	25.7483	25.7512	25.7528	26.1802
	4	49.1173	49.1844	49.2354	49.2930	49.3445	49.3562	49.3656	49.3704	50.4900
	5	50.9201	50.9240	50.9272	50.9310	50.9347	50.9356	50.9362	50.9367	51.2900
S-S	1	4.5024	4.5030	4.5034	4.5039	4.5044	4.5045	4.5045	4.5046	4.5161
	2	16.6154	16.6224	16.6279	16.6341	16.6397	16.641	16.6420	16.6425	16.7876
	3	37.0436	37.0773	37.1042	37.1348	37.1623	37.1686	37.1736	37.1762	37.8993
	4	63.4363	63.5279	63.6015	63.6854	63.7609	63.7784	63.7920	63.7991	65.8153
	5	97.0898	97.2979	97.4674	97.6611	97.8359	97.8763	97.9080	97.9243	100.439
S-F	1	6.5489	6.5498	6.5504	6.5512	6.5519	6.5520	6.5522	6.5522	6.5691
	2	20.9383	20.9481	20.9556	20.9641	20.9717	20.9734	20.9748	20.9755	21.1721
	3	42.3909	42.4285	42.4574	42.4900	42.5193	42.5261	42.5314	42.5341	43.2930
	4	50.7788	50.7853	50.7904	50.7962	50.8014	50.8026	50.8004	50.8041	50.9527
	5	71.6894	71.8032	71.8921	71.9929	72.0835	72.1045	72.1209	72.1293	74.5611
F-F	1	9.4849	9.4862	9.4873	9.4884	9.4894	9.4897	9.4898	9.4899	9.5160
	2	25.7549	25.7683	25.7783	25.7895	25.7996	25.8019	25.8037	25.8046	26.0640
	3	49.4271	49.4791	49.5181	49.5619	49.6012	49.6103	49.6174	49.6210	50.6546
	4	79.6003	79.7349	79.8368	79.9519	80.0553	80.0792	80.0979	80.1075	82.8799
	5	101.411	101.414	101.416	101.419	101.421	101.421	101.422	101.422	101.469

The effect of power-law exponent (n) involved in PESDBT on first five non-dimensional frequencies of FG beam in Table 5.34 under various BCs is diagrammatically plotted in Fig. 5.5 with $L/h = 5$ and $k = 1$. It can be observed that frequencies follow an ascending pattern with increase in n irrespective of edge supports considered. It is also evident from Fig. 5.5 that frequencies at respective modes will gradually be constant while taking very large positive values for n. Similar plots may also be depicted for any non-negative values of slenderness ratio and k.

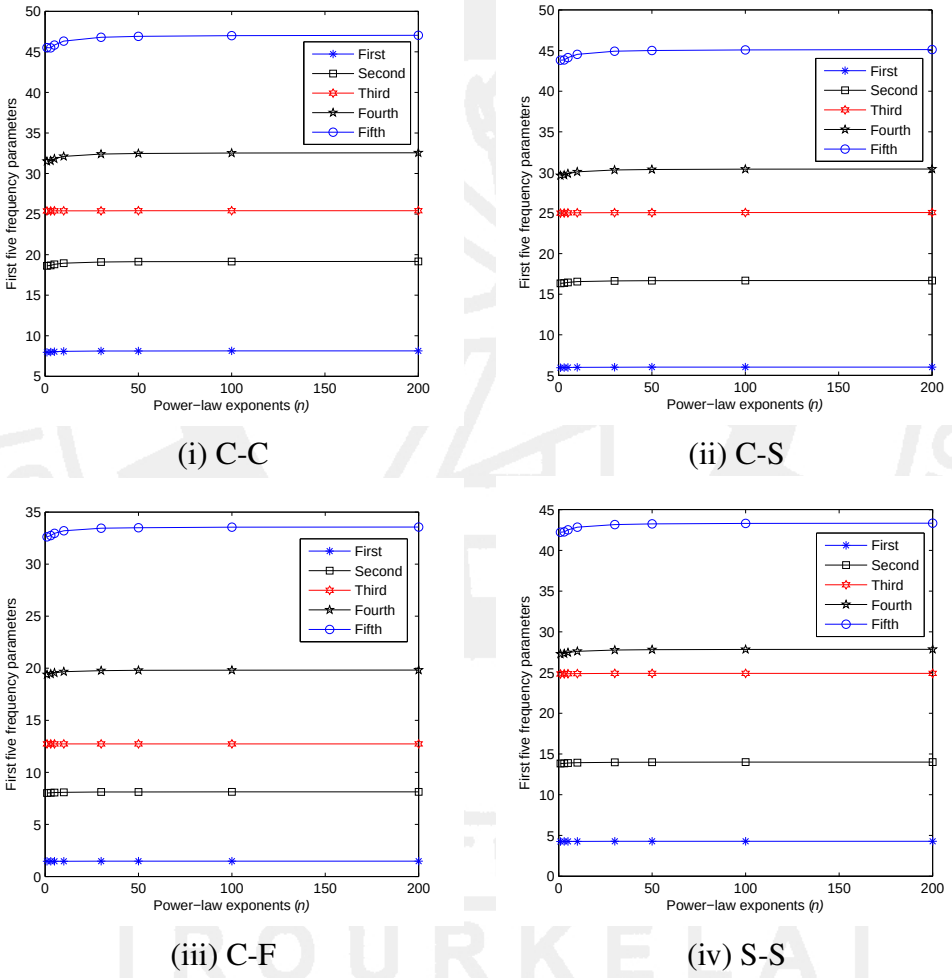

(i) C-C (ii) C-S

(iii) C-F (iv) S-S

Figure 5.5: Effect of n on first five non-dimensional frequencies of FG beams subject to various BCs based on PESDBT with $L/h = 5$ and $k = 1$

In further computations, Eq. (5.2) computes first five non-dimensional frequencies of FG beams subjected to all possible sets of boundary conditions in Tables 5.36 to 5.39 based on the newly proposed inverse trigonometric shear deformation theories stated in Eq. (2.12). Tables 5.36 and 5.38 are meant for C-C, C-S and C-F functionally graded beams, whereas S-S, S-F and F-F boundary supports are considered in Tables 5.37 and 5.39. The first five

non-dimensional frequencies of FG beams in Tables 5.36 and 5.37 are evaluated to check the effect of increase in slenderness ratios (L/h) with a fixed power-law index (k) as unity. In these tables, the physical properties of FG material constituents are: E_m = 70 GPa, ρ_m = 2700 kg/m^3, E_c = 380 GPa, ρ_c = 3800 kg/m^3 and $\nu_m = \nu_c = 0.3$. The effect of increase in power-law indices (k) on the first five natural frequencies are addressed in Tables 5.38 and 5.39 with a fixed slenderness ratio ($L/h = 10$). The FG material properties in these tabulations are assumed as: E_m = 210 GPa, ρ_m = 7800 kg/m^3, E_c = 390 GPa, ρ_c = 3960 kg/m^3 and $\nu_m = \nu_c = 0.23$. Irrespective of the boundary condition and SDBT considered, the non-dimensional frequencies follow ascending behavior with increase in slenderness ratios (L/h) and descending pattern with increase in power-law indices (k). The only exception observed in these computations is that the frequencies associated with ISDBT coincides with those of ICDBT regardless of the slenderness ratio and power-law index assumed. This may be true due to the fact that $\partial f/\partial z$ in case of ISDBT coincides with that of ICDBT. However, the non-dimensional frequencies based on ITDBT are comparatively higher than those computed on the basis of ISDBT and ICDBT.

Table 5.36: Effect of slenderness ratios on non-dimensional frequencies of C-C, C-S and C-F FG beams with $k = 1$ based on ISDBT, ICDBT and ITDBT

BCs	Source	Mode	Slenderness ratio (L/h)					
			5	10	20	30	50	100
C-C	ISDBT	1	9.1096	10.7619	11.3612	11.4851	11.5503	11.5782
		2	20.7196	27.3822	30.5678	31.3070	31.7096	31.8848
		3	30.6296	49.2413	58.1409	60.4866	61.8212	62.4158
		4	34.5693	61.4685	92.7402	98.2205	101.499	103.001
		5	49.4535	74.4612	123.094	143.755	150.385	153.528
	ICDBT	1	9.1096	10.7619	11.3612	11.4851	11.5503	11.5782
		2	20.7195	27.3822	30.5678	31.3070	31.7096	31.8848
		3	30.6296	49.2413	58.1409	60.4866	61.8212	62.4158
		4	34.5693	61.4685	92.7402	98.2205	101.499	103.001
		5	49.4535	74.4612	123.094	143.755	150.385	153.528
	ITDBT	1	9.1271	10.7647	11.3615	11.4852	11.5504	11.5782
		2	20.8088	27.4015	30.5700	31.3076	31.7097	31.8848
		3	30.6298	49.3012	58.1486	60.4886	61.8216	62.4159
		4	34.7909	61.4687	92.7617	98.2262	101.499	103.001
		5	49.8795	74.6035	123.094	143.767	150.388	153.528
C-S	ISDBT	1	6.9213	7.7291	7.9893	8.0410	8.0680	8.0795
		2	18.5534	23.1876	25.1558	25.5897	25.8226	25.9231
		3	29.9524	44.4557	51.0003	52.6248	53.5308	53.9301
		4	33.0413	60.4584	84.1916	88.4281	90.8840	91.9923
		5	48.1514	70.3726	120.148	132.267	137.601	140.066
	ICDBT	1	6.9213	7.7291	7.9893	8.0410	8.0680	8.0795
		2	18.5534	23.1876	25.1558	25.5897	25.8226	25.9231
		3	29.9524	44.4557	51.0003	52.6248	53.5308	53.9301
		4	33.0413	60.4584	84.1916	88.4281	90.8840	91.9923
		5	48.1514	70.3726	120.148	132.267	137.601	140.066
	ITDBT	1	6.9297	7.7303	7.9894	8.0411	8.0680	8.0795
		2	18.6095	23.1990	25.1571	25.5901	25.8226	25.9231
		3	29.9632	44.4958	51.0056	52.6262	53.5311	53.9302
		4	33.2013	60.4628	84.2077	88.4325	90.8848	91.9924
		5	48.4901	70.4778	120.158	132.277	137.602	140.067
C-F	ISDBT	1	1.7587	1.8047	1.8170	1.8193	1.8205	1.8210
		2	9.3347	10.7585	11.2373	11.3338	11.3843	11.4059
		3	15.4141	28.1218	30.8326	31.4397	31.7673	31.9092
		4	22.0998	30.8034	58.6695	60.7920	61.9421	62.4503
		5	36.5446	50.7809	61.6693	92.3564	101.749	103.067
	ICDBT	1	1.7587	1.8047	1.8170	1.8193	1.8205	1.8210
		2	9.3347	10.7585	11.2373	11.3338	11.3843	11.4059
		3	15.4141	28.1218	30.8326	31.4397	31.7673	31.9092
		4	22.0998	30.8034	58.6695	60.7920	61.9421	62.4503
		5	36.5446	50.7809	61.6693	92.3564	101.749	103.067
	ITDBT	1	1.7589	1.8047	1.8170	1.8193	1.8205	1.8210
		2	9.3437	10.7596	11.2374	11.3339	11.3843	11.4059
		3	15.4143	28.1296	30.8335	31.4399	31.7673	31.9092
		4	22.1470	30.8035	58.6728	60.7929	61.9423	62.4504
		5	36.6741	50.8095	61.6694	92.3564	101.749	103.067

Table 5.37: Effect of slenderness ratios on non-dimensional frequencies of S-S, S-F and F-F FG beams with $k = 1$ based on ISDBT, ICDBT and ITDBT

BCs	Source	Mode	Slenderness ratio (L/h)					
			5	10	20	30	50	100
S-S	ISDBT	1	5.0696	5.3558	5.4390	5.4551	5.4634	5.4670
		2	16.0784	18.9400	20.0102	20.2352	20.3543	20.4054
		3	29.7705	39.9669	44.3839	45.4259	45.9972	46.2468
		4	30.8684	58.0741	75.5802	78.8068	80.6145	81.4169
		5	46.8616	67.2874	114.824	121.507	125.531	127.384
	ICDBT	1	5.0696	5.3558	5.4390	5.4551	5.4634	5.4670
		2	16.0784	18.9400	20.0102	20.2352	20.3543	20.4054
		3	29.7705	39.9669	44.3839	45.4259	45.9972	46.2468
		4	30.8684	58.0741	75.5802	78.8068	80.6145	81.4169
		5	46.8616	67.2874	114.824	121.507	125.531	127.384
	ITDBT	1	5.0732	5.3563	5.4391	5.4551	5.4634	5.4670
		2	16.1077	18.9460	20.0109	20.2354	20.3543	20.4054
		3	29.7790	39.9951	44.3878	45.4269	45.9974	46.2468
		4	30.9811	58.0808	75.5915	78.8099	80.6151	81.4170
		5	47.1307	67.3634	114.853	121.515	125.533	127.384
S-F	ISDBT	1	7.1130	7.7272	7.9111	7.9469	7.9655	7.9733
		2	15.0832	23.5260	25.2090	25.5571	25.7415	25.8207
		3	19.8163	30.3355	50.8161	52.6105	53.4510	53.8083
		4	34.6805	46.0694	61.3541	87.3528	90.8523	91.8773
		5	44.5312	71.4752	85.3431	92.8721	136.840	139.903
	ICDBT	1	7.1130	7.7272	7.9111	7.9469	7.9655	7.9733
		2	15.0832	23.5260	25.2090	25.5571	25.7415	25.8207
		3	19.8163	30.3355	50.8161	52.6105	53.4510	53.8083
		4	34.6805	46.0694	61.3541	87.3528	90.8523	91.8773
		5	44.5312	71.4752	85.3431	92.8721	136.840	139.903
	ITDBT	1	7.1165	7.7276	7.9111	7.9469	7.9655	7.9733
		2	15.0840	23.5303	25.2095	25.5572	25.7415	25.8207
		3	19.8444	30.3361	50.8181	52.6112	53.4511	53.8083
		4	34.7739	46.0904	61.3545	87.3541	90.8528	91.8773
		5	44.5439	71.5292	85.3511	92.8729	136.841	139.903
F-F	ISDBT	1	10.1018	11.1292	11.4562	11.5210	11.5548	11.5691
		2	23.2663	28.7404	30.9944	31.4876	31.7517	31.8656
		3	30.5228	51.8380	59.1740	60.9628	61.9578	62.3959
		4	38.5215	61.5377	94.7011	99.1829	101.800	102.983
		5	53.1010	78.6528	122.618	145.321	150.933	153.541
	ICDBT	1	10.1018	11.1292	11.4562	11.5210	11.5548	11.5691
		2	23.2663	28.7404	30.9944	31.4876	31.7517	31.8656
		3	30.5228	51.8380	59.1740	60.9628	61.9578	62.3959
		4	38.5215	61.5377	94.7011	99.1829	101.800	102.983
		5	53.1010	78.6528	122.618	145.321	150.933	153.541
	ITDBT	1	10.1032	11.1293	11.4563	11.5210	11.5548	11.5691
		2	23.2812	28.7428	30.9947	31.4877	31.7517	31.8656
		3	30.5240	51.8507	59.1757	60.9632	61.9580	62.3959
		4	38.5827	61.5383	94.7073	99.1847	101.800	102.983
		5	53.2427	78.6947	122.618	145.325	150.934	153.541

Table 5.38: Effect of power-law exponent (k) on non-dimensional frequencies of C-C, C-S and C-F FG beams with L/h = 10 based on ISDBT, ICDBT and ITDBT

BCs	Source	Mode	Power-law exponent (k) in variation criterion						
			0	0.2	0.5	1	2	5	10
C-C	ISDBT	1	11.5177	10.1639	9.0623	8.1782	7.4829	6.8896	6.5824
		2	29.4150	25.9855	23.1785	20.8999	19.0700	17.4948	16.7215
		3	53.0713	46.9243	41.8690	37.7264	34.3429	31.4113	30.0339
		4	60.3242	53.7543	48.1847	43.3425	39.0453	35.1592	33.4922
		5	80.4524	71.1873	63.5419	57.2267	51.9925	47.4288	45.3609
	ICDBT	1	11.5177	10.1639	9.0623	8.1782	7.4829	6.8896	6.5824
		2	29.4150	25.9855	23.1785	20.8999	19.0700	17.4948	16.7215
		3	53.0713	46.9243	41.8690	37.7264	34.3429	31.4113	30.0339
		4	60.3242	53.7543	48.1847	43.3425	39.0453	35.1592	33.4922
		5	80.4524	71.1873	63.5419	57.2267	51.9925	47.4288	45.3609
	ITDBT	1	11.5201	10.1659	9.0641	8.1799	7.4836	6.8895	6.5838
		2	29.4316	25.9996	23.1914	20.9114	19.0770	17.4985	16.7317
		3	53.1229	46.9676	41.9084	37.7621	34.3677	31.4281	30.0666
		4	60.3242	53.7545	48.1850	43.3426	39.0451	35.1593	33.4925
		5	80.5757	71.2902	63.6350	57.3120	52.0577	47.4792	45.4400
C-S	ISDBT	1	8.1644	7.2015	6.4239	5.8050	5.3214	4.9049	4.6820
		2	24.8428	21.9242	19.5461	19.5461	16.1205	14.8291	14.1725
		3	47.9548	42.3538	37.7638	34.0341	31.0374	28.4704	27.2268
		4	60.2102	753.6396	48.0488	43.1861	38.8962	35.0542	33.4125
		5	75.3835	66.6498	59.4916	53.6290	48.8162	44.6151	42.6508
	ICDBT	1	8.1644	7.2015	6.4239	5.8050	5.3214	4.9049	4.6820
		2	24.8428	21.9242	19.5461	19.5461	16.1205	14.8291	14.1725
		3	47.9548	42.3538	37.7638	34.0341	31.0374	28.4704	27.2268
		4	60.2102	753.6396	48.0488	43.1861	38.8962	35.0542	33.4125
		5	75.3835	66.6498	59.4916	53.6290	48.8162	44.6151	42.6508
	ITDBT	1	8.1654	7.2023	6.4247	5.8057	5.3216	4.9049	4.6826
		2	24.8527	21.9326	19.5538	17.6397	16.1247	14.8313	14.1786
		3	47.9906	42.3837	37.7910	34.0586	31.0542	28.4816	27.2496
		4	60.2102	53.6399	48.0493	43.1865	38.8962	35.0545	33.4129
		5	75.4757	66.7263	59.5609	53.6927	48.8644	44.6517	42.7106
C-F	ISDBT	1	1.9248	1.6960	1.5111	1.3648	1.2527	1.1584	1.1065
		2	11.5085	10.1452	9.0398	8.1594	7.4765	6.8995	6.5929
		3	30.1607	26.5833	23.6606	21.3062	19.3826	17.5646	16.7407
		4	30.1984	26.9445	24.2065	21.8269	19.7663	18.0595	17.2425
		5	54.6645	48.2582	43.0273	38.7916	35.3974	32.4831	31.0598
	ICDBT	1	1.9248	1.6960	1.5111	1.3648	1.2527	1.1584	1.1065
		2	11.5085	10.1452	9.0398	8.1594	7.4765	6.8995	6.5929
		3	30.1607	26.5833	23.6606	21.3062	19.3826	17.5646	16.7407
		4	30.1984	26.9445	24.2065	21.8269	19.7663	18.0595	17.2425
		5	54.6645	48.2582	43.0273	38.7916	35.3974	32.4831	31.0598
	ITDBT	1	1.9248	1.6960	1.5111	1.3648	1.2527	1.1584	1.1065
		2	11.5094	10.1460	9.0406	8.1600	7.4765	6.8989	6.5934
		3	30.1607	26.5879	23.6649	21.3097	19.3832	17.5645	16.7409
		4	30.2050	26.9455	24.2074	21.8280	19.7670	18.0585	17.2464
		5	54.6885	48.2777	43.0455	38.8081	35.4056	32.4849	31.0753

Table 5.39: Effect of power-law exponent (k) on non-dimensional frequencies of S-S, S-F and F-F FG beams with $L/h = 10$ based on ISDBT, ICDBT and ITDBT

BCs	Source	Mode	Power-law exponent (k) in variation criterion						
			0	0.2	0.5	1	2	5	10
S-S	ISDBT	1	5.3525	4.7250	4.2301	3.8414	3.5323	3.2470	3.0870
		2	20.3843	17.9696	16.0060	14.4384	13.2217	12.2005	11.6644
		3	42.7631	37.7345	33.6425	30.3511	27.7418	25.5057	24.3778
		4	60.0859	53.4840	47.7982	42.8510	38.5703	34.8537	33.2877
		5	70.1033	61.9568	55.3687	50.0226	45.6301	41.7304	39.8392
	ICDBT	1	5.3525	4.7250	4.2301	3.8414	3.5323	3.2470	3.0870
		2	20.3843	17.9696	16.0060	14.4384	13.2217	12.2005	11.6644
		3	42.7631	37.7345	33.6425	30.3511	27.7418	25.5057	24.3778
		4	60.0859	53.4840	47.7982	42.8510	38.5703	34.8537	33.2877
		5	70.1033	61.9568	55.3687	50.0226	45.6301	41.7304	39.8392
	ITDBT	1	5.3529	4.7254	4.2304	3.8416	3.5324	3.2471	3.0872
		2	20.3898	17.9742	16.0103	14.4422	13.2242	12.2020	11.6679
		3	42.7874	37.7548	33.6610	30.3679	27.7536	25.5138	24.3934
		4	60.0859	53.4843	47.7988	42.8515	38.5703	34.8537	33.2880
		5	70.1710	62.0127	55.4193	50.0692	45.6657	41.7573	39.8839
S-F	ISDBT	1	8.2860	7.2982	6.4982	5.8647	5.3806	4.9776	4.7580
		2	25.4101	22.3928	19.9437	17.9903	16.4753	15.2055	14.5403
		3	30.0429	26.7730	23.9968	21.5793	19.4384	17.5075	16.6784
		4	49.2468	43.4445	38.7418	34.9661	31.9701	29.3922	28.0876
		5	77.5107	68.3480	60.8198	54.7328	49.9033	45.8659	43.9436
	ICDBT	1	8.2860	7.2982	6.4982	5.8647	5.3806	4.9776	4.7580
		2	25.4101	22.3928	19.9437	17.9903	16.4753	15.2055	14.5403
		3	30.0429	26.7730	23.9968	21.5793	19.4384	17.5075	16.6784
		4	49.2468	43.4445	38.7418	34.9661	31.9701	29.3922	28.0876
		5	77.5107	68.3480	60.8198	54.7328	49.9033	45.8659	43.9436
	ITDBT	1	8.2864	7.2986	6.4985	5.8650	5.3807	4.9776	4.7582
		2	25.4141	22.3962	19.9468	17.9930	16.4764	15.2054	14.5427
		3	30.0429	26.7730	23.9968	21.5794	19.4384	17.5075	16.6785
		4	49.2640	43.4585	38.7548	34.9781	31.9766	29.3944	28.0991
		5	77.5594	68.3865	60.8546	54.7647	49.9238	45.8779	43.9764
F-F	ISDBT	1	11.9077	10.4858	9.3371	8.4295	7.7366	7.1577	6.8407
		2	30.8418	27.1698	24.1988	21.8373	20.0101	18.4716	17.6587
		3	55.9840	49.2471	43.7352	39.3458	35.9385	33.1566	31.8191
		4	60.0859	53.6763	48.3083	43.5935	39.3208	35.2995	33.4878
		5	85.0217	74.9591	66.7432	60.1246	54.8730	50.4243	48.2686
	ICDBT	1	11.9077	10.4858	9.3371	8.4295	7.7366	7.1577	6.8407
		2	30.8418	27.1698	24.1988	21.8373	20.0101	18.4716	17.6587
		3	55.9840	49.2471	43.7352	39.3458	35.9385	33.1566	31.8191
		4	60.0859	53.6763	48.3083	43.5935	39.3208	35.2995	33.4878
		5	85.0217	74.9591	66.7432	60.1246	54.8730	50.4243	48.2686
	ITDBT	1	11.9079	10.4859	9.3373	8.4296	7.7364	7.1573	6.8408
		2	30.8439	27.1715	24.2005	21.8387	20.0095	18.4694	17.6600
		3	55.9950	49.2552	43.7428	39.3525	35.9396	33.1534	31.8261
		4	60.0859	53.6768	48.3092	43.5944	39.3210	35.2995	33.4887
		5	85.0572	74.9859	66.7682	60.1483	54.8849	50.4264	48.2942

5.2 Vibration of non-uniform FG beam

In this section, free vibration of non-uniform functionally graded (FG) beams has been investigated by means of generalized differential quadrature method (GDQM). The displacement field along with governing equation for free vibration are assumed based on classical or Euler-Bernoulli beam theory. The material properties of FG constituents are assumed to vary continuously along thickness direction in a power-law form. Axial gradation of the physical properties viz. moment of inertia and area of cross-section are also considered in this study. The prime objective is to find the effect of volume fractions of constituents and parameters of non-homogeneity on free vibration frequencies of non-uniform FG beam. The new results are evaluated after checking the test of convergence and validation of present results with available literatures.

5.2.1 Numerical modeling

To generate the generalized eigenvalue problem (Eq. (3.66)) for this investigation, the mathematical modeling follows the systematic algorithms of GDQ mentioned in Sec. 3.2. Moreover, the new results for free vibration of non-uniform FG beams are evaluated here after the convergence and comparison studies in subsequent discussions.

5.2.2 Convergence and comparison studies

To the best of our knowledge, the present study on non-uniform FG beam is first of its kind in which FG material properties are graded along thickness direction rather than axially. As such, it is worth considering the convergence and validation of non-dimensional frequencies of non-uniform homogeneous beam (a special case of FG beam with $k = 0$) having $f(\xi) = (1 + \alpha\xi)^3$ and $g(\xi) = (1 + \alpha\xi)$ with various sets of clamped (C) and simply supported (S) edge supports incorporated in Table 5.40. Moreover, the convergence of first six non-dimensional frequencies of non-uniform Al/Al_2O_3 and $SUS304/Si_3N_4$ FG beams (only C-C and C-S edge supports) is checked in Table 5.41 with $\alpha = 0.2$, $k = 1.0$, $f(\xi) = (1 + \alpha\xi)$ and $g(\xi) = (1 + \alpha\xi)^4$. It is interesting to note that there occurs gradual convergence of non-dimensional frequencies with increase in the number of grid points (N) of discretized domain. It can also be noticed that present results are in excellent agreement with the available literature irrespective of the boundary conditions and parameters of non-homogeneity.

Table 5.40: Convergence and comparison of first five non-dimensional frequencies of non-uniform homogeneous beam; $f(\xi) = (1+\alpha\xi)^3$ and $g(\xi) = (1+\alpha\xi)$

BCs	α	N	Mode				
			1	2	3	4	5
C-C	0.0	10	22.3723	61.5963	123.5385	236.0434	255.7144
		11	22.3733	61.6454	120.3128	207.5569	352.0477
		15	22.3733	61.6728	120.9021	199.9365	299.3886
		19	22.3733	61.6728	120.9034	199.8597	298.5597
		20	22.3733	61.6728	120.9034	199.8594	298.5572
		Abrate (1995)	22.3732854	61.672823	120.903392	-	-
		Shu and Du (1997)	22.3733	61.6728	120.9021	199.9365	299.3886
		Leissa and Qatu (2011)	22.373	61.673	120.903	199.859	298.556
	0.1	10	23.4789	64.6432	129.5353	246.1568	271.2178
		11	23.4797	64.6954	126.2718	217.5069	369.9266
		15	23.4796	64.7211	126.8768	209.8080	314.1499
		19	23.4796	64.7211	126.8780	209.7351	313.3110
		20	23.4796	64.7211	126.8780	209.7349	313.3085
		Abrate (1995)	23.479607	64.721068	126.87804	-	-
	0.2	10	24.5633	67.6301	135.2112	254.3041	291.1129
		11	24.5635	67.6864	132.1276	226.7006	388.3326
		15	24.5634	67.7048	132.7230	219.4522	328.5329
		19	24.5634	67.7048	132.7240	219.3962	327.7402
		20	24.5634	67.7048	132.7240	219.3961	327.7379
		Abrate (1995)	24.563418	67.704755	132.72398	-	-
C-S	0.0	10	15.4170	49.9216	109.2703	193.8286	193.8286
		11	15.4182	49.9165	103.7409	195.8272	276.0522
		15	15.4182	49.9648	104.2471	178.4642	273.1126
		19	15.4182	49.9649	104.2477	178.2704	272.0350
		20	15.4182	49.9649	104.2477	178.2697	272.0364
		Abrate (1995)	15.418206	49.964862	104.24770	-	-
		Shu and Du (1997)	15.4182	49.9648	104.2471	178.4642	273.1126
		Leissa and Qatu (2011)	15.418	49.695	104.248	178.270	272.031
	0.1	10	15.9677	52.1157	114.3155	202.3531	202.3531
		11	15.9688	52.1888	108.2875	203.5661	289.2164
		15	15.9687	52.2372	109.1984	187.0720	287.2784
		19	15.9687	52.2372	109.2023	186.8825	285.2908
		20	15.9687	52.2372	109.2024	186.8818	285.2805
		Abrate (1995)	15.9687099	52.237227	109.20235	-	-
	0.2	10	16.5030	54.2636	118.8530	211.5434	211.5434
		11	16.5030	54.4249	112.7453	210.2539	303.3345
		15	16.5029	54.4615	114.0450	195.4562	301.0615
		19	16.5029	54.4615	114.0516	195.3094	298.2576
		20	16.5029	54.4615	114.0516	195.3090	298.2364
		Abrate (1995)	16.502899	54.4614625	114.051623	-	-
S-S	0.0	10	9.8693	39.4174	92.8422	180.1025	180.1025
		11	9.8696	39.4505	88.1271	174.4688	257.9230
		15	9.8696	39.4784	88.8249	158.0619	248.4716
		19	9.8696	39.4784	88.8264	157.9141	246.7488
		20	9.8696	39.4784	88.8264	157.9136	246.7441
		Shu and Du (1997)	9.8696	39.4784	88.8249	158.0619	248.4716
		Leissa and Qatu (2011)	9.8696	39.478	88.826	157.914	246.740

Table 5.41: Convergence of first five non-dimensional frequencies of non-uniform Al/Al_2O_3 and SUS304/Si_3N_4 beam; $\alpha = 0.2$; $k = 1.0$; $f(\xi) = (1 + \alpha\xi)$ and $g(\xi) = (1 + \alpha\xi)^4$

FG constituents	BCs	N	Mode				
			1	2	3	4	5
Al/Al_2O_3	C-C	10	33.1465	91.4050	183.3946	355.2763	355.2763
		11	33.1478	91.4596	178.7275	308.0808	511.5877
		15	33.1477	91.4978	179.4769	296.8670	444.3320
		19	33.1477	91.4978	179.4777	296.7669	443.3858
		20	33.1477	91.4978	179.4777	296.7667	443.3851
	C-S	10	22.1355	73.5863	162.8305	279.9409	279.9409
		11	22.1365	73.4288	154.3197	302.1622	393.6467
		15	22.1368	73.4951	154.1403	264.3596	402.4663
		19	22.1368	73.4952	154.1325	264.0970	403.3578
		20	22.1368	73.4952	154.1325	264.0969	403.3897
SUS304/Si_3N_4	C-C	10	28.5055	78.6069	157.7165	305.5321	305.5321
		11	28.5066	78.6538	153.7029	264.9447	439.9575
		15	28.5065	78.6867	154.3474	255.3010	382.1186
		19	28.5065	78.6867	154.3481	255.2149	381.3049
		20	28.5065	78.6867	154.3481	255.2148	381.3043
	C-S	10	19.0362	63.2831	140.0317	240.7448	240.7448
		11	19.0371	63.1476	132.7126	259.8548	338.5301
		15	19.0373	63.2047	132.5583	227.3452	346.1148
		19	19.0373	63.2047	132.5515	227.1193	346.8814
		20	19.0373	63.2047	132.5515	227.1193	346.9089

5.2.3 Results and discussions

In this part, we have computed new results for non-uniform FG beams with axial gradation behavior of moment of inertia and area of cross-section. The axial gradation criteria are considered with five different combination of $f(\xi)$ and $g(\xi)$. Two different cases of FG beams viz. Al/Al_2O_3 and SUS304/Si_3N_4 have been considered for these evaluations. The material properties of these constituents are tabulated below.

Table 5.42: The material properties of Al/Al_2O_3 and SUS304/Si_3N_4 beam constituents

Properties	Unit	Aluminium (Al)	Al_2O_3	SUS304	Si_3N_4
E	GPa	70	380	208	322
ρ	kg/m^3	2700	3800	8166	2370
ν	-	0.3	0.3	0.3	0.3

In Tables 5.43 to 5.52, first six non-dimensional frequencies of FG beam have been given with different power-law indices (k = 0, 0.1, 0.2, 1.0 and 2.0) and α = -0.2, -0.1, 0, 0.1 and 0.2. The boundary conditions in these evaluations are assumed as combination of clamped (C) and simply supported (S) viz. C-C, C-S and S-S. In terms of FG beam assumed, Tables

5.43 to 5.47 are meant for Al/Al_2O_3, whereas Tables 5.48 to 5.52 are for $SUS304/Si_3N_4$. With reference to the assumptions of non-homogeneity, Tables 5.43 and 5.48 are associated with $f(\xi) = (1+\alpha\xi)$ and $g(\xi) = (1+\alpha\xi)^4$. In the similar fashion, Tables 5.44 and 5.49 are with $f(\xi) = (1+\alpha\xi)^2$ and $g(\xi) = (1+\alpha\xi)^3$; Tables 5.45 and 5.50 are with $f(\xi) = (1+\alpha\xi)^3$ and $g(\xi) = (1+\alpha\xi)^2$; Tables 5.46 and 5.51 are with $f(\xi) = (1+\alpha\xi)^4$ and $g(\xi) = (1+\alpha\xi)$ and Tables 5.47 and 5.52 are with $f(\xi) = (1+\alpha\xi)^4$ and $g(\xi) = (1+\alpha\xi)^4$ respectively. It can easily be noticed here that power-law index (k) and parameter of non-homogeneity (α) have major impact on free vibration of non-uniform FG beam, as the quotient of material properties viz. E_r and ρ_r remain constant for a given FG constituents. Let us first divide these computed results for non-dimensional frequencies into three different cases in terms of non-homogeneities and the following facts may be summarized:

- Case - 1 ($m_1 < m_2$): In Tables 5.43, 5.44, 5.48 and 5.49, the non-dimensional frequencies are decreasing with increase in k and α, irrespective of the boundary conditions considered.

- Case - 2 ($m_1 > m_2$): Looking into Tables 5.45, 5.46, 5.50 and 5.51, the non-dimensional frequencies are increasing with increase in α and follow a descending pattern with increase in k regardless of the boundary supports assumed.

- Case - 3 ($m_1 = m_2$): In this case (Tables 5.47 and 5.52), the eigenfrequencies are gradually decreasing with increase in k. As the natural frequencies take minor changes with increase in values of α in the assumed edge supports, it is difficult to predict their pattern.

Table 5.43: First six non-dimensional frequencies of Al/Al_2O_3 FG beam with different power-law indices (k) and α; $f(\xi) = (1+\alpha\xi)$ and $g(\xi) = (1+\alpha\xi)^4$

BCs	α	k	Ω_1	Ω_2	Ω_3	Ω_4	Ω_5	Ω_6
C-C	-0.2	0.0	53.7727	148.5283	291.4307	481.9464	720.1052	1005.9049
		0.1	51.8509	143.2201	281.0154	464.7223	694.3696	969.9552
		0.2	50.3103	138.9646	272.6656	450.9140	673.7378	941.1350
		1.0	44.7416	123.5830	242.4850	401.0037	599.1638	836.9635
		2.0	42.7690	118.1345	231.7944	383.3243	572.7479	800.0636
	-0.1	0.0	49.7094	137.0887	268.8016	444.3832	663.8678	927.2811
		0.1	47.9328	132.1893	259.1950	428.5016	640.1421	894.1414
		0.2	46.5086	128.2616	251.4936	415.7695	621.1215	867.5738

		1.0	41.3607	114.0647	223.6565	369.7492	552.3714	771.5446
		2.0	39.5372	109.0358	213.7959	353.4478	528.0186	737.5288
	0.0	0.0	46.0619	126.9714	248.9148	411.4687	614.6668	858.5409
		0.1	44.4157	122.4336	240.0189	396.7634	592.6994	827.8578
		0.2	43.0960	118.7958	232.8872	384.9743	575.0885	803.2597
		1.0	38.3258	105.6466	207.1096	342.3627	511.4337	714.3492
		2.0	36.6361	100.9889	197.9786	327.2686	488.8857	682.8551
	0.1	0.0	42.7856	117.9844	231.3340	382.4353	571.3183	798.0064
		0.1	41.2565	113.7678	223.0664	368.7676	550.9001	769.4867
		0.2	40.0306	110.3875	216.4384	357.8104	534.5313	746.6230
		1.0	35.5998	98.1690	192.4815	318.2054	475.3656	663.9815
		2.0	34.0302	93.8409	183.9954	304.1765	454.4077	634.7080
	0.2	0.0	39.8386	109.9667	215.7054	356.6692	532.8825	744.3529
		0.1	38.4148	106.0366	207.9964	343.9223	513.8380	717.7508
		0.2	37.2734	102.8859	201.8162	333.7034	498.5704	696.4242
		1.0	33.1477	91.4978	179.4777	296.7667	443.3851	619.339
		2.0	31.6863	87.4639	171.5650	283.6829	423.8372	592.0338
C-S	-0.2	0.0	38.4739	121.7758	252.7818	431.4130	657.6778	931.8103
		0.1	37.0989	117.4237	243.7477	415.9949	634.1733	898.5087
		0.2	35.9966	113.9347	236.5052	403.6344	615.3301	871.8113
		1.0	32.0123	101.3236	210.3272	358.9573	547.2210	775.3130
		2.0	30.6009	96.8565	201.0543	343.1317	523.0953	741.1312
	-0.1	0.0	34.8763	111.6694	232.3879	397.0007	605.5194	858.0825
		0.1	33.6299	107.6785	224.0827	382.8124	583.8790	827.4158
		0.2	32.6306	104.4790	217.4245	371.4380	566.5302	802.8308
		1.0	29.0189	92.9145	193.3584	330.3246	503.8226	713.9678
		2.0	27.7395	88.8181	184.8337	315.7613	481.6102	682.4905
	0.0	0.0	31.7429	102.8672	214.6242	367.0200	560.0659	793.7850
		0.1	30.6084	99.1909	206.9538	353.9032	540.0499	765.4162
		0.2	29.6989	96.2436	200.8046	343.3877	524.0034	742.6734
		1.0	26.4117	85.5907	178.5781	305.3791	466.0030	660.4691
		2.0	25.2472	81.8172	170.7050	291.9156	445.4580	631.3504
	0.1	0.0	29.0053	95.1465	199.0298	340.6909	520.1372	737.2884
		0.1	27.9687	91.7461	191.9167	328.5150	501.5482	710.9387
		0.2	27.1377	89.0200	186.2143	318.7539	486.6457	689.8146
		1.0	24.1339	79.1667	165.6028	283.4719	432.7803	613.4610
		2.0	23.0699	75.6764	158.3017	270.9743	413.7000	586.4149
	0.2	0.0	26.6051	88.3302	185.2442	317.4050	484.8141	687.3139

		0.1	25.6543	85.1734	178.6238	306.0614	467.4875	662.7502
		0.2	24.8920	82.6426	173.3163	296.9674	453.5970	643.0579
		1.0	22.1368	73.4952	154.1325	264.0969	403.3897	571.8797
		2.0	21.1608	70.2549	147.3371	252.4535	385.6051	546.6668
S-S	-0.2	0.0	23.6839	95.2708	214.3946	381.1330	595.4980	857.5015
		0.1	22.8375	91.8659	206.7324	367.5118	574.2157	826.8556
		0.2	22.1589	89.1363	200.5898	356.5920	557.1541	802.2872
		1.0	19.7062	79.2701	178.3871	317.1218	495.4843	713.4844
		2.0	18.8374	75.7753	170.5224	303.1406	473.6395	682.0284
	-0.1	0.0	21.9207	87.7946	197.5444	351.1869	548.7315	790.2517
		0.1	21.1373	84.6569	190.4844	338.6360	529.1206	762.0091
		0.2	20.5093	82.1415	184.8246	328.5741	513.3988	739.3676
		1.0	18.2391	73.0495	164.3669	292.2052	456.5722	657.5291
		2.0	17.4350	69.8289	157.1203	279.3225	436.4429	628.5401
	0.0	0.0	20.3194	81.2778	182.8750	325.1111	507.9943	731.6110
		0.1	19.5933	78.3730	176.3393	313.4921	489.8393	705.4642
		0.2	19.0111	76.0443	171.0998	304.1773	475.2847	684.5028
		1.0	16.9068	67.6272	152.1612	270.5088	422.6768	608.7372
		2.0	16.1614	64.6457	145.4528	258.5827	404.0420	581.8993
	0.1	0.0	18.8687	75.5535	170.0000	302.2199	472.2214	680.0707
		0.1	18.1944	72.8533	163.9244	291.4190	455.3448	655.7659
		0.2	17.6537	70.6886	159.0537	282.7601	441.8152	636.2811
		1.0	15.6997	62.8643	141.4485	251.4622	392.9120	565.8530
		2.0	15.0075	60.0928	135.2124	240.3758	375.5893	540.9058
	0.2	0.0	17.5557	70.4890	158.6170	281.9789	440.5829	634.4586
		0.1	16.9283	67.9698	152.9482	271.9013	424.8371	611.7839
		0.2	16.4253	65.9502	148.4037	263.8223	412.2139	593.6060
		1.0	14.6072	58.6504	131.9773	234.6206	366.5872	527.9015
		2.0	13.9632	56.0646	126.1587	224.2767	350.4251	504.6274

Table 5.44: First six non-dimensional frequencies of Al/Al_2O_3 FG beam with different power-law indices (k) and α; $f(\xi) = (1+\alpha\xi)^2$ and $g(\xi) = (1+\alpha\xi)^3$

BCs	α	k	Ω_1	Ω_2	Ω_3	Ω_4	Ω_5	Ω_6
C-C	-0.2	0.0	48.4904	133.8060	262.4317	433.9036	648.2542	905.5119

		0.1	46.7575	129.0240	253.0527	418.3965	625.0864	873.1501
		0.2	45.3682	125.1903	245.5338	405.9647	606.5132	847.2062
		1.0	40.3465	111.3333	218.3564	361.0296	539.3801	753.4314
		2.0	38.5677	106.4249	208.7295	345.1126	515.6000	720.2143
	-0.1	0.0	47.2448	130.2627	255.3927	422.1968	630.7087	880.9601
		0.1	45.5563	125.6073	246.2653	407.1081	608.1680	849.4758
		0.2	44.2027	121.8751	238.9481	395.0117	590.0976	824.2353
		1.0	39.3100	108.3851	212.4996	351.2890	524.7814	733.0031
		2.0	37.5769	103.6067	203.1310	335.8014	501.6449	700.6866
	0.0	0.0	46.0619	126.9714	248.9148	411.4687	614.6668	858.5409
		0.1	44.4157	122.4336	240.0189	396.7634	592.6994	827.8578
		0.2	43.0960	118.7958	232.8872	384.9743	575.0885	803.2597
		1.0	38.3258	105.6466	207.1096	342.3627	511.4337	714.3492
		2.0	36.6361	100.9889	197.9786	327.2686	488.8857	682.8551
	0.1	0.0	44.9411	123.9058	242.9249	401.5826	599.9109	837.9402
		0.1	43.3350	119.4776	234.2431	387.2306	578.4709	807.9934
		0.2	42.0474	115.9275	227.2831	375.7248	561.2828	783.9855
		1.0	37.3933	103.0958	202.1258	334.1369	499.1560	697.2084
		2.0	35.7447	98.5506	193.2145	319.4055	477.1493	666.4700
	0.2	0.0	43.8801	121.0423	237.3628	392.4276	586.2667	818.9076
		0.1	42.3119	116.7164	228.8798	378.4028	565.3143	789.6410
		0.2	41.0547	113.2484	222.0791	367.1593	548.5172	766.1784
		1.0	36.5105	100.7133	197.4978	326.5195	487.8034	681.3723
		2.0	34.9008	96.2730	188.7906	312.1240	466.2972	651.3321
C-S	-0.2	0.0	34.6922	109.6820	227.5914	388.3617	592.0101	838.6097
		0.1	33.4524	105.7621	219.4576	374.4822	570.8524	808.6389
		0.2	32.4584	102.6196	212.9368	363.3552	553.8907	784.6118
		1.0	28.8657	91.2609	189.3675	323.1365	492.5822	697.7654
		2.0	27.5931	87.2374	181.0187	308.8901	470.8653	667.0025
	-0.1	0.0	33.1461	106.1040	220.7878	377.1708	575.2660	815.1216
		0.1	31.9615	102.3120	212.8972	363.6913	554.7068	785.9903
		0.2	31.0119	99.2720	206.5714	352.8849	538.2248	762.6362
		1.0	27.5792	88.2839	183.7066	313.8251	478.6503	678.2222
		2.0	26.3633	84.3916	175.6074	299.9892	457.5476	648.3209
	0.0	0.0	31.7429	102.8672	214.6242	367.0200	560.0659	793.7850
		0.1	30.6084	99.1909	206.9538	353.9032	540.0499	765.4162
		0.2	29.6989	96.2436	200.8046	343.3877	524.0034	742.6734
		1.0	26.4117	85.5907	178.5781	305.3791	466.0030	660.4691

		2.0	25.2472	81.8172	170.7050	291.9156	445.4580	631.3504
	0.1	0.0	30.4652	99.9179	208.9970	357.7418	546.1629	774.2588
		0.1	29.3764	96.3470	201.5277	344.9566	526.6437	746.5878
		0.2	28.5035	93.4842	195.5397	334.7069	510.9956	724.4045
		1.0	25.3486	83.1367	173.8960	297.6592	454.4350	644.2223
		2.0	24.2310	79.4714	166.2293	284.5360	434.3999	615.8199
	0.2	0.0	29.2979	97.2138	203.8258	349.2062	533.3651	756.2774
		0.1	28.2509	93.7395	196.5413	336.7260	514.3034	729.2491
		0.2	27.4115	90.9542	190.7015	326.7209	499.0219	707.5809
		1.0	24.3774	80.8867	169.5933	290.5571	443.7866	629.2608
		2.0	23.3026	77.3206	162.1163	277.7471	424.2210	601.5181
S-S	-0.2	0.0	21.3550	85.7859	192.9974	343.0617	535.9978	771.8891
		0.1	20.5918	82.7200	186.0999	330.8012	516.8420	744.3028
		0.2	19.9800	80.2622	180.5703	320.9721	501.4850	722.1873
		1.0	17.7685	71.3782	160.5835	285.4446	445.9771	642.2505
		2.0	16.9851	68.2313	153.5038	272.8600	426.3150	613.9351
	-0.1	0.0	20.8334	83.4137	187.6761	333.6364	521.3055	750.7702
		0.1	20.0889	80.4326	180.9688	321.7127	502.6747	723.9387
		0.2	19.4920	78.0428	175.5917	312.1536	487.7388	702.4283
		1.0	17.3345	69.4044	156.1559	277.6023	433.7524	624.6786
		2.0	16.5702	66.3445	149.2714	265.3634	414.6292	597.1379
	0.0	0.0	20.3194	81.2778	182.8750	325.1111	507.9943	731.6110
		0.1	19.5933	78.3730	176.3393	313.4921	489.8393	705.4642
		0.2	19.0111	76.0443	171.0998	304.1773	475.2847	684.5028
		1.0	16.9068	67.6272	152.1612	270.5088	422.6768	608.7372
		2.0	16.1614	64.6457	145.4528	258.5827	404.0420	581.8993
	0.1	0.0	19.8189	79.3381	178.5069	317.3378	495.8407	714.0985
		0.1	19.1106	76.5026	172.1273	305.9966	478.1200	688.5776
		0.2	18.5428	74.2295	167.0129	296.9045	463.9136	668.1179
		1.0	16.4904	66.0133	148.5267	264.0410	412.5644	594.1658
		2.0	15.7633	63.1029	141.9785	252.4000	394.3753	567.9704
	0.2	0.0	19.3354	77.5630	174.5039	310.2018	484.6710	697.9891
		0.1	18.6443	74.7910	168.2673	299.1156	467.3495	673.0439
		0.2	18.0904	72.5688	163.2676	290.2280	453.4631	653.0457
		1.0	16.0880	64.5364	145.1960	258.1035	403.2706	580.7620
		2.0	15.3787	61.6911	138.7946	246.7243	385.4913	555.1575

Table 5.45: First six non-dimensional frequencies of Al/Al_2O_3 FG beam with different power-law indices (k) and α; $f(\xi) = (1+\alpha\xi)^3$ and $g(\xi) = (1+\alpha\xi)^2$

BCs	α	k	Ω_1	Ω_2	Ω_3	Ω_4	Ω_5	Ω_6
C-C	-0.2	0.0	43.6309	120.2855	235.8204	389.8328	582.3527	813.4092
		0.1	42.0716	115.9866	227.3925	375.9007	561.5401	784.3390
		0.2	40.8215	112.5403	220.6360	364.7315	544.8551	761.0340
		1.0	36.3031	100.0836	196.2144	324.3605	484.5467	676.7973
		2.0	34.7026	95.6711	187.5637	310.0601	463.1841	646.9588
	-0.1	0.0	44.8801	123.7173	242.5383	400.9304	598.9257	836.5552
		0.1	43.2762	119.2958	233.8703	386.6017	577.5209	806.6578
		0.2	41.9903	115.7512	226.9214	375.1146	560.3610	782.6896
		1.0	37.3425	102.9390	201.8041	333.5942	498.3363	696.0560
		2.0	35.6962	98.4007	192.9070	318.8868	476.3657	665.3684
	0.0	0.0	46.0619	126.9714	248.9148	411.4687	614.6668	858.5409
		0.1	44.4157	122.4336	240.0189	396.7634	592.6994	827.8578
		0.2	43.0960	118.7958	232.8872	384.9743	575.0885	803.2597
		1.0	38.3258	105.6466	207.1096	342.3627	511.4337	714.3492
		2.0	36.6361	100.9889	197.9786	327.2686	488.8857	682.8551
	0.1	0.0	47.1861	130.0733	254.9983	421.5270	629.6934	879.5301
		0.1	45.4997	125.4247	245.8850	406.4621	607.1890	848.0969
		0.2	44.1478	121.6979	238.5790	394.3849	589.1476	822.8974
		1.0	39.2612	108.2276	212.1714	350.7316	523.9366	731.8133
		2.0	37.5303	103.4560	202.8172	335.2686	500.8374	699.5493
	0.2	0.0	48.2604	133.0430	260.8268	431.1671	644.0977	899.6512
		0.1	46.5357	128.2882	251.5052	415.7578	621.0785	867.4989
		0.2	45.1530	124.4764	244.0322	403.4044	602.6244	841.7229
		1.0	40.1551	110.6984	217.0210	358.7527	535.9217	748.5551
		2.0	38.3848	105.8180	207.4530	342.9361	512.2940	715.5529
C-S	-0.2	0.0	31.2072	98.5748	204.4782	348.8752	531.7780	753.1119
		0.1	30.0919	95.0519	197.1704	336.4069	512.7730	726.1967
		0.2	29.1978	92.2276	191.3119	326.4112	497.5370	704.6193
		1.0	25.9660	82.0192	170.1361	290.2817	442.4660	626.6270
		2.0	24.8212	78.4031	162.6352	277.4838	422.9587	599.0004
	-0.1	0.0	31.4850	100.7670	209.6675	358.1635	546.2663	773.9414
		0.1	30.3597	97.1657	202.1743	345.3632	526.7435	746.2818

	0.2	29.4577	94.2787	196.1671	335.1014	511.0924	724.1075
	1.0	26.1971	83.8432	174.4539	298.0100	454.5211	643.9582
	2.0	25.0421	80.1468	166.7626	284.8714	434.4822	615.5675
0.0	0.0	31.7429	102.8672	214.6242	367.0200	560.0659	793.7850
	0.1	30.6084	99.1909	206.9538	353.9032	540.0499	765.4162
	0.2	29.6989	96.2436	200.8046	343.3877	524.0034	742.6734
	1.0	26.4117	85.5907	178.5781	305.3791	466.0030	660.4691
	2.0	25.2472	81.8172	170.7050	291.9156	445.4580	631.3504
0.1	0.0	31.9847	104.8869	219.3780	375.5016	573.2686	812.7679
	0.1	30.8417	101.1384	211.5377	362.0817	552.7808	783.7206
	0.2	29.9253	98.1332	205.2523	351.3232	536.3560	760.4340
	1.0	26.6129	87.2712	182.5335	312.4362	476.9883	676.2638
	2.0	25.4396	83.4236	174.4860	298.6616	455.9590	646.4488
0.2	0.0	32.2134	106.8353	223.9528	383.6536	585.9477	830.9889
	0.1	31.0622	103.0172	215.9490	369.9423	565.0067	801.2904
	0.2	30.1392	99.9562	209.5325	358.9502	548.2187	777.4817
	1.0	26.8032	88.8924	186.3400	319.2191	487.5379	691.4245
	2.0	25.6215	84.9733	178.1247	305.1454	466.0435	660.9411
S-S	-0.2	0.0	19.2037	77.0731	173.3642	308.1433	481.4235	693.2917
		0.1	18.5174	74.3186	167.1684	297.1307	464.2181	668.5144
		0.2	17.9672	72.1104	162.2014	288.3020	450.4248	648.6509
		1.0	15.9785	64.1287	144.2478	256.3907	400.5686	576.8536
		2.0	15.2740	61.3014	137.8882	245.0870	382.9084	551.4214
	-0.1	0.0	19.7882	79.2121	178.2155	316.8138	495.0161	712.9080
		0.1	19.0810	76.3811	171.8463	305.4913	477.3248	687.4296
		0.2	18.5140	74.1116	166.7403	296.4142	463.1421	667.0041
		1.0	16.4647	65.9084	148.2843	263.6050	411.8783	593.1753
		2.0	15.7389	63.0027	141.7467	251.9832	393.7194	567.0235
	0.0	0.0	20.3194	81.2778	182.8750	325.1111	507.9943	731.6110
		0.1	19.5933	78.3730	176.3393	313.4921	489.8393	705.4642
		0.2	19.0111	76.0443	171.0998	304.1773	475.2847	684.5028
		1.0	16.9068	67.6272	152.1612	270.5088	422.6768	608.7372
		2.0	16.1614	64.6457	145.4528	258.5827	404.0420	581.8993
	0.1	0.0	20.8068	83.2783	187.3662	333.0835	520.4398	749.5249
		0.1	20.0632	80.3020	180.6700	321.1796	501.8400	722.7379
		0.2	19.4671	77.9160	175.3017	311.6364	486.9289	701.2632
		1.0	17.3123	69.2917	155.8981	277.1422	433.0321	623.6424
		2.0	16.5490	66.2368	149.0249	264.9236	413.9407	596.1474

0.2	0.0	21.2573	85.2199	191.7076	340.7693	532.4175	766.7470
	0.1	20.4976	82.1743	184.8562	328.5907	513.3897	739.3445
	0.2	19.8885	79.7327	179.3636	318.8273	498.1353	717.3764
	1.0	17.6871	70.9073	159.5104	283.5372	442.9982	637.9721
	2.0	16.9073	67.7811	152.4779	271.0367	423.4674	609.8453

Table 5.46: First six non-dimensional frequencies of Al/Al_2O_3 FG beam with different power-law indices (k) and α; $f(\xi) = (1+\alpha\xi)^4$ and $g(\xi) = (1+\alpha\xi)$

BCs	α	k	Ω_1	Ω_2	Ω_3	Ω_4	Ω_5	Ω_6
C-C	-0.2	0.0	39.1715	107.8993	211.4600	349.5038	522.0561	729.1232
		0.1	37.7716	104.0432	203.9027	337.0130	503.3985	703.0654
		0.2	36.6493	100.9517	197.8442	326.9994	488.4411	682.1752
		1.0	32.5927	89.7777	175.9454	290.8047	434.3770	606.6672
		2.0	31.1557	85.8196	168.1883	277.9838	415.2262	579.9206
	-0.1	0.0	42.6127	117.4446	230.2223	380.5569	568.4783	794.0110
		0.1	41.0898	113.2472	221.9944	366.9563	548.1616	765.6341
		0.2	39.8689	109.8823	215.3983	356.0529	531.8741	742.8848
		1.0	35.4559	97.7198	191.5565	316.6425	473.0025	660.6571
		2.0	33.8928	93.4115	183.1112	302.6824	452.1489	631.5301
	0.0	0.0	46.0619	126.9714	248.9148	411.4687	614.6668	858.5409
		0.1	44.4157	122.4336	240.0189	396.7634	592.6994	827.8578
		0.2	43.0960	118.7958	232.8872	384.9743	575.0885	803.2597
		1.0	38.3258	105.6466	207.1096	342.3627	511.4337	714.3492
		2.0	36.6361	100.9889	197.9786	327.2686	488.8857	682.8551
	0.1	0.0	49.5231	136.4943	267.5683	442.2923	660.7014	922.8251
		0.1	47.7533	131.6162	258.0058	426.4854	637.0888	889.8446
		0.2	46.3344	127.7055	250.3396	413.8132	618.1590	863.4047
		1.0	41.2057	113.5702	222.6303	368.0094	549.7368	767.8369
		2.0	39.3891	108.5631	212.8150	351.7847	525.5001	733.9847
	0.2	0.0	52.9994	146.0240	286.2059	473.0674	706.6437	986.9527
		0.1	51.1053	140.8053	275.9773	456.1606	681.3892	951.6803
		0.2	49.5868	136.6215	267.7772	442.6067	661.1431	923.4031
		1.0	44.0982	121.4993	238.1377	393.6158	587.9631	821.1943
		2.0	42.1540	116.1427	227.6387	376.2622	562.0411	784.9896

C-S	-0.2	0.0	28.0053	88.4001	183.3235	312.7463	476.6713	674.9730
		0.1	27.0045	85.2408	176.7718	301.5692	459.6357	650.8504
		0.2	26.2021	82.7081	171.5194	292.6087	445.9785	631.5117
		1.0	23.3019	73.5533	152.5344	260.2207	396.6145	561.6115
		2.0	22.2745	70.3105	145.8095	248.7481	379.1286	536.8513
	-0.1	0.0	29.8911	95.6521	199.0130	339.9545	518.4840	734.5030
		0.1	28.8229	92.2336	191.9005	327.8050	499.9541	708.2528
		0.2	27.9665	89.4930	186.1986	318.0650	485.0990	687.2085
		1.0	24.8709	79.5873	165.5888	282.8593	431.4048	611.1434
		2.0	23.7744	76.0785	158.2884	270.3886	412.3851	584.1994
	0.0	0.0	31.7429	102.8672	214.6242	367.0200	560.0659	793.7850
		0.1	30.6084	99.1909	206.9538	353.9032	540.0499	765.4162
		0.2	29.6989	96.2436	200.8046	343.3877	524.0034	742.6734
		1.0	26.4117	85.5907	178.5781	305.3791	466.0030	660.4691
		2.0	25.2472	81.8172	170.7050	291.9156	445.4580	631.3504
	0.1	0.0	33.5656	110.0591	230.1851	393.9915	601.4865	852.8489
		0.1	32.3661	106.1257	221.9586	379.9108	579.9902	822.3692
		0.2	31.4044	102.9724	215.3636	368.6225	562.7570	797.9342
		1.0	27.9283	91.5747	191.5256	327.8208	500.4670	709.6132
		2.0	26.6970	87.5374	183.0817	313.3679	478.4026	678.3279
	0.2	0.0	35.3635	117.2380	245.7170	420.9058	642.8035	911.7006
		0.1	34.0997	113.0480	236.9354	405.8632	619.8306	879.1176
		0.2	33.0865	109.6891	229.8953	393.8038	601.4136	852.9964
		1.0	29.4242	97.5479	204.4489	350.2148	534.8449	758.5808
		2.0	28.1270	93.2472	195.4352	334.7746	511.2647	725.1366
S-S	-0.2	0.0	17.2228	69.0906	155.3948	276.1951	431.4945	621.3195
		0.1	16.6072	66.6214	149.8412	266.3243	416.0734	599.1144
		0.2	16.1138	64.6419	145.3890	258.4110	403.7106	581.3129
		1.0	14.3302	57.4869	129.2963	229.8083	359.0251	516.9691
		2.0	13.6984	54.9524	123.5959	219.6765	343.1965	494.1771
	-0.1	0.0	18.7840	75.1846	169.1509	300.6976	469.8303	676.6197
		0.1	18.1127	72.4976	163.1057	289.9511	453.0392	652.4382
		0.2	17.5745	70.3435	158.2594	281.3358	439.5780	633.0523
		1.0	15.6293	62.5574	140.7421	250.1956	390.9224	562.9816
		2.0	14.9402	59.7993	134.5371	239.1650	373.6875	538.1610
	0.0	0.0	20.3194	81.2778	182.8750	325.1111	507.9943	731.6110
		0.1	19.5933	78.3730	176.3393	313.4921	489.8393	705.4642
		0.2	19.0111	76.0443	171.0998	304.1773	475.2847	684.5028

	1.0	16.9068	67.6272	152.1612	270.5088	422.6768	608.7372
	2.0	16.1614	64.6457	145.4528	258.5827	404.0420	581.8993
0.1	0.0	21.8331	87.3786	196.5882	349.4757	546.0481	786.3896
	0.1	21.0528	84.2558	189.5624	336.9859	526.5330	758.2851
	0.2	20.4273	81.7523	183.9299	326.9731	510.8882	735.7542
	1.0	18.1663	72.7034	163.5713	290.7814	454.3394	654.3157
	2.0	17.3653	69.4981	156.3598	277.9615	434.3086	625.4684
0.2	0.0	23.3282	93.4932	210.3062	373.8214	584.0429	841.0311
	0.1	22.4945	90.1519	202.7901	360.4615	563.1700	810.9738
	0.2	21.8261	87.4732	196.7646	349.7511	546.4365	786.8774
	1.0	19.4102	77.7910	174.9853	311.0382	485.9530	699.7802
	2.0	18.5545	74.3614	167.2706	297.3252	464.5284	668.9284

Table 5.47: First six non-dimensional frequencies of Al/Al_2O_3 FG beam with different power-law indices (k) and α; $f(\xi) = (1+\alpha\xi)^4$ and $g(\xi) = (1+\alpha\xi)^4$

BCs	α	k	Ω_1	Ω_2	Ω_3	Ω_4	Ω_5	Ω_6
C-C	-0.2	0.0	46.0619	126.9714	248.9148	411.4687	614.6661	858.5430
		0.1	44.4157	122.4336	240.0189	396.7634	592.6988	827.8598
		0.2	43.0960	118.7958	232.8872	384.9743	575.0880	803.2616
		1.0	38.3258	105.6466	207.1096	342.3627	511.4331	714.3510
		2.0	36.6361	100.9889	197.9786	327.2686	488.8852	682.8568
	-0.1	0.0	46.0619	126.9714	248.9148	411.4687	614.6666	858.5414
		0.1	44.4157	122.4336	240.0189	396.7634	592.6993	827.8583
		0.2	43.0960	118.7958	232.8872	384.9743	575.0884	803.2601
		1.0	38.3258	105.6466	207.1096	342.3627	511.4335	714.3496
		2.0	36.6361	100.9889	197.9786	327.2686	488.8856	682.8555
	0.0	0.0	46.0619	126.9714	248.9148	411.4687	614.6668	858.5409
		0.1	44.4157	122.4336	240.0189	396.7634	592.6994	827.8578
		0.2	43.0960	118.7958	232.8872	384.9743	575.0885	803.2597
		1.0	38.3258	105.6466	207.1096	342.3627	511.4337	714.3492
		2.0	36.6361	100.9889	197.9786	327.2686	488.8857	682.8551
	0.1	0.0	46.0619	126.9714	248.9148	411.4687	614.6666	858.5413
		0.1	44.4157	122.4336	240.0189	396.7634	592.6993	827.8582
		0.2	43.0960	118.7958	232.8872	384.9743	575.0884	803.2601
		1.0	38.3258	105.6466	207.1096	342.3627	511.4336	714.3495
		2.0	36.6361	100.9889	197.9786	327.2686	488.8856	682.8554
	0.2	0.0	46.0619	126.9714	248.9148	411.4687	614.6663	858.5423
		0.1	44.4157	122.4336	240.0189	396.7634	592.6990	827.8592
		0.2	43.0960	118.7958	232.8872	384.9743	575.0881	803.2610
		1.0	38.3258	105.6466	207.1096	342.3627	511.4333	714.3504
		2.0	36.6361	100.9889	197.9786	327.2686	488.8853	682.8563
C-S	-0.2	0.0	33.6332	104.7753	216.5816	369.0013	562.0582	795.7333
		0.1	32.4312	101.0308	208.8413	355.8136	541.9710	767.2949
		0.2	31.4676	98.0288	202.6360	345.2414	525.8674	744.4962
		1.0	27.9845	87.1783	180.2068	307.0276	467.6607	662.0901
		2.0	26.7508	83.3348	172.2619	293.4914	447.0426	632.9000
	-0.1	0.0	32.6492	103.7502	215.5188	367.9195	560.9669	794.6575
		0.1	31.4824	100.0423	207.8164	354.7706	540.9187	766.2575
		0.2	30.5470	97.0698	201.6416	344.2293	524.8464	743.4897
		1.0	27.1658	86.3254	179.3225	306.1275	466.7527	661.1950

		2.0	25.9681	82.5195	171.4165	292.6310	446.1746	632.0443
	0.0	0.0	31.7429	102.8672	214.6242	367.0200	560.0659	793.7850
		0.1	30.6084	99.1909	206.9538	353.9032	540.0499	765.4162
		0.2	29.6989	96.2436	200.8046	343.3877	524.0034	742.6734
		1.0	26.4117	85.5907	178.5781	305.3791	466.0030	660.4691
		2.0	25.2472	81.8172	170.7050	291.9156	445.4580	631.3504
	0.1	0.0	30.9049	102.0993	213.8612	366.2606	559.3094	793.0642
		0.1	29.8004	98.4504	206.2181	353.1710	539.3204	764.7212
		0.2	28.9150	95.5252	200.0908	342.6772	523.2956	741.9990
		1.0	25.7145	84.9518	177.9433	304.7473	465.3735	659.8693
		2.0	24.5808	81.2064	170.0982	291.3116	444.8562	630.7771
	0.2	0.0	30.1277	101.4260	213.2032	365.6111	558.6650	792.4583
		0.1	29.0509	97.8011	205.5836	352.5447	538.6990	764.1369
		0.2	28.1877	94.8952	199.4751	342.0695	522.6927	741.4321
		1.0	25.0677	84.3915	177.3958	304.2068	464.8374	659.3651
		2.0	23.9625	80.6709	169.5748	290.7950	444.3437	630.2952
S-S	-0.2	0.0	20.1615	81.4262	183.1096	325.3896	508.2977	731.9418
		0.1	19.4409	78.5161	176.5655	313.7606	490.1318	705.7832
		0.2	18.8633	76.1832	171.3192	304.4378	475.5685	684.8123
		1.0	16.7754	67.7507	152.3564	270.7405	422.9293	609.0124
		2.0	16.0358	64.7637	145.6393	258.8041	404.2832	582.1624
	-0.1	0.0	20.2840	81.3112	182.9276	325.1734	508.0621	731.6850
		0.1	19.5591	78.4052	176.3900	313.5521	489.9046	705.5355
		0.2	18.9779	76.0755	171.1489	304.2355	475.3481	684.5720
		1.0	16.8773	67.6550	152.2049	270.5606	422.7332	608.7987
		2.0	16.1332	64.6722	145.4946	258.6322	404.0958	581.9581
	0.0	0.0	20.3194	81.2778	182.8750	325.1111	507.9943	731.6110
		0.1	19.5933	78.3730	176.3393	313.4921	489.8393	705.4642
		0.2	19.0111	76.0443	171.0998	304.1773	475.2847	684.5028
		1.0	16.9068	67.6272	152.1612	270.5088	422.6768	608.7372
		2.0	16.1614	64.6457	145.4528	258.5827	404.0420	581.8993
	0.1	0.0	20.2904	81.3051	182.9180	325.1621	508.0498	731.6716
		0.1	19.5653	78.3994	176.3808	313.5412	489.8928	705.5226
		0.2	18.9839	76.0699	171.1400	304.2250	475.3366	684.5594
		1.0	16.8827	67.6499	152.1970	270.5512	422.7230	608.7875
		2.0	16.1384	64.6674	145.4870	258.6232	404.0860	581.9474
	0.2	0.0	20.2137	81.3772	183.0319	325.2972	508.1970	731.8321
		0.1	19.4913	78.4689	176.4906	313.6716	490.0347	705.6774

0.2	18.9122	76.1374	171.2465	304.3514	475.4743	684.7096
1.0	16.8188	67.7099	152.2918	270.6637	422.8455	608.9211
2.0	16.0773	64.7248	145.5776	258.7307	404.2031	582.0751

Table 5.48: First six non-dimensional frequencies of SUS304/Si_3N_4 FG beam with different power-law indices (k) and α; $f(\xi) = (1 + \alpha\xi)$ and $g(\xi) = (1 + \alpha\xi)^4$

BCs	α	k	Ω_1	Ω_2	Ω_3	Ω_4	Ω_5	Ω_6
C-C	-0.2	0.0	63.2347	174.6639	342.7120	566.7515	846.8176	1182.9077
		0.1	56.0083	154.7035	303.5472	501.9837	750.0441	1047.7262
		0.2	51.3326	141.7884	278.2063	460.0768	687.4284	960.2592
		1.0	38.4771	106.2795	208.5334	344.8570	515.2716	719.7756
		2.0	34.6014	95.5742	187.5283	310.1203	463.3694	647.2742
	-0.1	0.0	58.4564	161.2113	316.1010	522.5786	780.6844	1090.4490
		0.1	51.7761	142.7883	279.9773	462.8588	691.4686	965.8336
		0.2	47.4537	130.8679	256.6040	424.2181	633.7429	885.2032
		1.0	35.5696	98.0939	192.3411	317.9786	475.0308	663.5164
		2.0	31.9867	88.2131	172.9670	285.9493	427.1820	596.6818
	0.0	0.0	54.1671	149.3138	292.7147	483.8723	722.8258	1009.6129
		0.1	47.9770	132.2504	259.2636	428.5758	640.2220	894.2354
		0.2	43.9717	121.2097	237.6196	392.7972	586.7745	819.5822
		1.0	32.9596	90.8545	178.1110	294.4266	439.8250	614.3292
		2.0	29.6397	81.7029	160.1703	264.7696	395.5224	552.4492
	0.1	0.0	50.3143	138.7454	272.0404	449.7301	671.8496	938.4266
		0.1	44.5644	122.8897	240.9519	398.3354	595.0713	831.1841
		0.2	40.8441	112.6306	220.8365	365.0813	545.3931	761.7946
		1.0	30.6152	84.4238	165.5311	273.6517	408.8070	571.0138
		2.0	27.5314	75.9200	148.8575	246.0874	367.6288	513.4968
	0.2	0.0	46.8488	129.3168	253.6617	419.4301	626.6505	875.3320
		0.1	41.4949	114.5386	224.6735	371.4980	555.0375	775.3000
		0.2	38.0308	104.9766	205.9172	340.4844	508.7015	710.5758
		1.0	28.5065	78.6867	154.3481	255.2148	381.3043	532.6220
		2.0	25.6351	70.7607	138.8009	229.5076	342.8964	478.9722
C-S	-0.2	0.0	45.2440	143.2039	297.2622	507.3260	773.4053	1095.7751
		0.1	40.0735	126.8387	263.2914	449.3493	685.0213	970.5510

		0.2	36.7281	116.2499	241.3111	411.8364	627.8339	889.5268
		1.0	27.5300	87.1367	180.8781	308.6977	470.6016	666.7572
		2.0	24.7570	78.3596	162.6587	277.6033	423.1990	599.5962
	-0.1	0.0	41.0133	131.3191	273.2797	466.8584	712.0689	1009.0739
		0.1	36.3263	116.3121	242.0496	413.5063	630.6944	893.7580
		0.2	33.2937	106.6021	221.8426	378.9857	578.0423	819.1446
		1.0	24.9558	79.9051	166.2852	284.0740	433.2797	614.0013
		2.0	22.4420	71.8564	149.5357	255.4599	389.6364	552.1543
	0.0	0.0	37.3284	120.9681	252.3902	431.6022	658.6172	933.4624
		0.1	33.0626	107.1440	223.5473	382.2792	583.3511	826.7873
		0.2	30.3024	98.1993	204.8850	350.3655	534.6514	757.7648
		1.0	22.7136	73.6067	153.5744	262.6213	400.7554	567.9932
		2.0	20.4257	66.1924	138.1052	236.1680	360.3882	510.7805
	0.1	0.0	34.1092	111.8888	234.0518	400.6401	611.6625	867.0244
		0.1	30.2113	99.1023	207.3046	354.8554	541.7623	767.9417
		0.2	27.6891	90.8289	189.9983	325.2311	496.5345	703.8318
		1.0	20.7548	68.0821	142.4159	243.7815	372.1844	527.5670
		2.0	18.6642	61.2243	128.0706	219.2259	334.6951	474.4263
	0.2	0.0	31.2867	103.8731	217.8404	373.2568	570.1237	808.2562
		0.1	27.7113	92.0026	192.9458	330.6013	504.9706	715.8895
		0.2	25.3978	84.3219	176.8382	303.0019	462.8143	656.1251
		1.0	19.0373	63.2047	132.5515	227.1193	346.9089	491.8077
		2.0	17.1197	56.8382	119.1999	204.2420	311.9655	442.2690
S-S	-0.2	0.0	27.8514	112.0350	252.1203	448.1986	700.2841	1008.3907
		0.1	24.6686	99.2318	223.3082	396.9789	620.2563	893.1528
		0.2	22.6092	90.9476	204.6659	363.8381	568.4756	818.5900
		1.0	16.9470	68.1711	153.4101	272.7199	426.1088	613.5855
		2.0	15.2400	61.3043	137.9575	245.2494	383.1878	551.7804
	-0.1	0.0	25.7780	103.2433	232.3051	412.9831	645.2883	929.3073
		0.1	22.8321	91.4447	205.7575	365.7878	571.5454	823.1070
		0.2	20.9260	83.8107	188.5803	335.2508	523.8313	754.3918
		1.0	15.6854	62.8215	141.3530	251.2919	392.6450	565.4649
		2.0	14.1054	56.4936	127.1148	225.9798	353.0947	508.5069
	0.0	0.0	23.8949	95.5797	215.0544	382.3189	597.3829	860.3480
		0.1	21.1642	84.6570	190.4782	338.6279	529.1146	762.0283
		0.2	19.3974	77.5896	174.5766	310.3583	484.9427	698.4121
		1.0	14.5396	58.1584	130.8563	232.6334	363.4955	523.5046
		2.0	13.0750	52.3002	117.6754	209.2007	326.8814	470.7731

0.1	0.0	22.1889	88.8482	199.9138	355.3997	555.3152	799.7384
	0.1	19.6532	78.6947	177.0679	314.7850	491.8544	708.3451
	0.2	18.0125	72.1251	162.2858	288.5059	450.7930	649.2106
	1.0	13.5015	54.0623	121.6436	216.2536	337.8982	486.6248
	2.0	12.1415	48.6168	109.3907	194.4708	303.8625	437.6082
0.2	0.0	20.6449	82.8925	186.5278	331.5969	518.1096	746.1003
	0.1	18.2856	73.4196	165.2116	293.7024	458.9005	660.8367
	0.2	16.7591	67.2904	151.4193	269.1833	420.5903	605.6683
	1.0	12.5620	50.4384	113.4984	201.7701	315.2593	453.9871
	2.0	11.2967	45.3579	102.0660	181.4462	283.5039	408.2580

Table 5.49: First six non-dimensional frequencies of SUS304/Si_3N_4 FG beam with different power-law indices (k) and α; $f(\xi) = (1+\alpha\xi)^2$ and $g(\xi) = (1+\alpha\xi)^3$

BCs	α	k	Ω_1	Ω_2	Ω_3	Ω_4	Ω_5	Ω_6
C-C	-0.2	0.0	57.0230	157.3510	308.6101	510.2549	762.3234	1064.8491
		0.1	50.5065	139.3691	273.3425	451.9435	675.2058	943.1592
		0.2	46.2900	127.7342	250.5231	414.2140	618.8378	864.4217
		1.0	34.6974	95.7450	187.7831	310.4799	463.8585	647.9394
		2.0	31.2024	86.1008	168.8681	279.2059	417.1351	582.6739
	-0.1	0.0	55.5581	153.1842	300.3326	496.4881	741.6906	1035.9771
		0.1	49.2090	135.6785	266.0109	439.7500	656.9309	917.5867
		0.2	45.1009	124.3517	243.8036	403.0385	602.0886	840.9841
		1.0	33.8060	93.2095	182.7464	302.1031	451.3039	630.3713
		2.0	30.4008	83.8207	164.3387	271.6729	405.8450	566.8754
	0.0	0.0	54.1671	149.3138	292.7147	483.8723	722.8258	1009.6129
		0.1	47.9770	132.2504	259.2636	428.5758	640.2220	894.2354
		0.2	43.9717	121.2097	237.6196	392.7972	586.7745	819.5822
		1.0	32.9596	90.8545	178.1110	294.4266	439.8250	614.3292
		2.0	29.6397	81.7029	160.1703	264.7696	395.5224	552.4492
	0.1	0.0	52.8491	145.7087	285.6709	472.2466	705.4735	985.3873
		0.1	46.8096	129.0573	253.0247	418.2787	624.8527	872.7782
		0.2	42.9018	118.2832	231.9015	383.3597	572.6883	799.9163
		1.0	32.1576	88.6608	173.8250	287.3526	429.2665	599.5884
		2.0	28.9185	79.7302	156.3160	258.4082	386.0274	539.1932

	0.2	0.0	51.6015	142.3413	279.1301	461.4806	689.4284	963.005
		0.1	45.7045	126.0747	247.2314	408.7431	610.6412	852.9543
		0.2	41.8890	115.5496	226.5918	374.6201	559.6632	781.7474
		1.0	31.3985	86.6118	169.8451	280.8017	419.5034	585.9697
		2.0	28.2358	77.8876	152.7369	252.5172	377.2477	526.9462
C-S	-0.2	0.0	40.7968	128.9820	267.6392	456.6993	696.1824	986.1746
		0.1	36.1346	114.2421	237.0537	404.5082	616.6233	873.4755
		0.2	33.1180	104.7048	217.2638	370.7387	565.1460	800.5554
		1.0	24.8240	78.4830	162.8531	277.8924	423.6130	600.0675
		2.0	22.3236	70.5776	146.4493	249.9009	380.9434	539.6240
	-0.1	0.0	38.9786	124.7744	259.6385	443.5392	676.4920	958.5535
		0.1	34.5242	110.5153	229.9672	392.8520	599.1832	849.0109
		0.2	31.6420	101.2892	210.7690	360.0557	549.1617	778.1332
		1.0	23.7177	75.9228	157.9848	269.8847	411.6318	583.2606
		2.0	21.3287	68.2752	142.0713	242.6998	370.1691	524.5100
	0.0	0.0	37.3284	120.9681	252.3902	431.6022	658.6172	933.4624
		0.1	33.0626	107.1440	223.5473	382.2792	583.3511	826.7873
		0.2	30.3024	98.1993	204.8850	350.3655	534.6514	757.7648
		1.0	22.7136	73.6067	153.5744	262.6213	400.7554	567.9932
		2.0	20.4257	66.1924	138.1052	236.1680	360.3882	510.7805
	0.1	0.0	35.8259	117.4998	245.7729	420.6914	642.2677	910.5002
		0.1	31.7318	104.0721	217.6862	372.6152	568.8700	806.4492
		0.2	29.0827	95.3839	199.5131	341.5083	521.3792	739.1246
		1.0	21.7994	71.4963	149.5479	255.9823	390.8070	554.0212
		2.0	19.6036	64.2946	134.4842	230.1977	351.4419	498.2158
	0.2	0.0	34.4533	114.3198	239.6917	410.6538	627.2180	889.3548
		0.1	30.5160	101.2555	212.3000	363.7247	555.5402	787.7202
		0.2	27.9685	92.8024	194.5766	333.3600	509.1622	721.9592
		1.0	20.9642	69.5613	145.8476	249.8746	381.6496	541.1546
		2.0	18.8525	62.5546	131.1567	224.7053	343.2069	486.6453
S-S	-0.2	0.0	25.1127	100.8811	226.9579	403.4282	630.3140	907.7135
		0.1	22.2429	89.3525	201.0214	357.3248	558.2823	803.9809
		0.2	20.3860	81.8931	184.2396	327.4944	511.6754	736.8624
		1.0	15.2806	61.3841	138.0994	245.4780	383.5334	552.3255
		2.0	13.7414	55.2011	124.1889	220.7515	344.9010	496.6910
	-0.1	0.0	24.4994	98.0915	220.7002	392.3443	613.0363	882.8785
		0.1	21.6996	86.8817	195.4788	347.5076	542.9792	781.9841
		0.2	19.8881	79.6286	179.1597	318.4967	497.6498	716.7019

		1.0	14.9074	59.6867	134.2917	238.7337	373.0203	537.2139
		2.0	13.4058	53.6746	120.7648	214.6865	335.4468	483.1015
	0.0	0.0	23.8949	95.5797	215.0544	382.3189	597.3829	860.3480
		0.1	21.1642	84.6570	190.4782	338.6279	529.1146	762.0283
		0.2	19.3974	77.5896	174.5766	310.3583	484.9427	698.4121
		1.0	14.5396	58.1584	130.8563	232.6334	363.4955	523.5046
		2.0	13.0750	52.3002	117.6754	209.2007	326.8814	470.7731
	0.1	0.0	23.3064	93.2987	209.9176	373.1777	583.0907	839.7539
		0.1	20.6429	82.6366	185.9284	330.5314	516.4556	743.7877
		0.2	18.9196	75.7379	170.4066	302.9377	473.3405	681.6943
		1.0	14.1815	56.7704	127.7307	227.0712	354.7990	510.9734
		2.0	12.7530	51.0520	114.8646	204.1988	319.0609	459.5042
	0.2	0.0	22.7377	91.2113	205.2102	364.7861	569.9555	820.8098
		0.1	20.1392	80.7878	181.7590	323.0987	504.8215	727.0085
		0.2	18.4580	74.0434	166.5853	296.1255	462.6777	666.3158
		1.0	13.8354	55.5003	124.8663	221.9650	346.8065	499.4463
		2.0	12.4418	49.9098	112.2888	199.6070	311.8734	449.1382

Table 5.50: First six non-dimensional frequencies of SUS304/Si_3N_4 FG beam with different power-law indices (k) and α; $f(\xi) = (1+\alpha\xi)^3$ and $g(\xi) = (1+\alpha\xi)^2$

BCs	α	k	Ω_1	Ω_2	Ω_3	Ω_4	Ω_5	Ω_6
C-C	-0.2	0.0	51.3084	141.4514	277.3162	458.4292	684.8256	956.5397
		0.1	45.4449	125.2864	245.6248	406.0404	606.5644	847.2273
		0.2	41.6511	114.8272	225.1194	372.1430	555.9268	776.4985
		1.0	31.2201	86.0703	168.7414	278.9450	416.7027	582.0352
		2.0	28.0754	77.4007	151.7444	250.8475	374.7291	523.4081
	-0.1	0.0	52.7774	145.4871	285.2163	471.4796	704.3149	983.7586
		0.1	46.7461	128.8610	252.6221	417.5994	623.8265	871.3356
		0.2	42.8436	118.1033	231.5325	382.7370	571.7478	798.5942
		1.0	32.1140	88.5260	173.5484	286.8859	428.5615	598.5974
		2.0	28.8792	79.6089	156.0672	257.9885	385.3935	538.3020
	0.0	0.0	54.1671	149.3138	292.7147	483.8723	722.8258	1009.6129
		0.1	47.9770	132.2504	259.2636	428.5758	640.2220	894.2354
		0.2	43.9717	121.2097	237.6196	392.7972	586.7745	819.5822

		1.0	32.9596	90.8545	178.1110	294.4266	439.8250	614.3292
		2.0	29.6397	81.7029	160.1703	264.7696	395.5224	552.4492
	0.1	0.0	55.4892	152.9615	299.8687	495.7004	740.4966	1034.2955
		0.1	49.1479	135.4812	265.6000	439.0523	655.8734	916.0973
		0.2	45.0449	124.1709	243.4270	402.3990	601.1193	839.6190
		1.0	33.7640	93.0740	182.4641	301.6238	450.5773	629.3481
		2.0	30.3631	83.6989	164.0849	271.2419	405.1917	565.9553
	0.2	0.0	56.7525	156.4537	306.7229	507.0369	757.4355	1057.9572
		0.1	50.2669	138.5743	271.6709	449.0932	670.8765	937.0549
		0.2	46.0705	127.0058	248.9911	411.6017	614.8699	858.8270
		1.0	34.5328	95.1989	186.6347	308.5218	460.8843	643.7458
		2.0	31.0544	85.6098	167.8354	277.4451	414.4605	578.9027
C-S	-0.2	0.0	36.6986	115.9204	240.4589	410.2646	625.3516	885.6323
		0.1	32.5047	102.6731	212.9795	363.3800	553.8871	784.4231
		0.2	29.7911	94.1017	195.1994	333.0440	507.6471	718.9374
		1.0	22.3304	70.5352	146.3144	249.6378	380.5139	538.8895
		2.0	20.0811	63.4304	131.5765	224.4923	342.1856	484.6084
	-0.1	0.0	37.0252	118.4984	246.5614	421.1873	642.3894	910.1270
		0.1	32.7940	104.9565	218.3846	373.0544	568.9778	806.1186
		0.2	30.0562	96.1944	200.1532	341.9108	521.4780	738.8216
		1.0	22.5291	72.1039	150.0277	256.2840	390.8811	553.7941
		2.0	20.2598	64.8410	134.9157	230.4691	351.5085	498.0116
	0.0	0.0	37.3284	120.9681	252.3902	431.6022	658.6172	933.4624
		0.1	33.0626	107.1440	223.5473	382.2792	583.3511	826.7873
		0.2	30.3024	98.1993	204.8850	350.3655	534.6514	757.7648
		1.0	22.7136	73.6067	153.5744	262.6213	400.7554	567.9932
		2.0	20.4257	66.1924	138.1052	236.1680	360.3882	510.7805
	0.1	0.0	37.6129	123.3432	257.9806	441.5763	674.1431	955.7855
		0.1	33.3145	109.2476	228.4988	391.1134	597.1027	846.5593
		0.2	30.5334	100.1273	209.4231	358.4622	547.2550	775.8863
		1.0	22.8867	75.0518	156.9760	268.6903	410.2026	581.5764
		2.0	20.5814	67.4920	141.1642	241.6258	368.8838	522.9955
	0.2	0.0	37.8818	125.6345	263.3604	451.1627	689.0532	977.2128
		0.1	33.5527	111.2771	233.2638	399.6043	610.3089	865.5379
		0.2	30.7516	101.9874	213.7903	366.2442	559.3587	793.2804
		1.0	23.0503	76.4461	160.2495	274.5235	419.2751	594.6144
		2.0	20.7285	68.7458	144.1079	246.8713	377.0424	534.7202
S-S	-0.2	0.0	22.5829	90.6352	203.8700	362.3653	566.1366	815.285

	0.1	20.0021	80.2775	180.5720	320.9546	501.4391	722.1159
	0.2	18.3323	73.5757	165.4973	294.1604	459.5776	661.8317
	1.0	13.7412	55.1497	124.0508	220.4921	344.4828	496.0852
	2.0	12.3571	49.5946	111.5555	198.2824	309.7838	446.1156
-0.1	0.0	23.2702	93.1505	209.5750	372.5615	582.1209	838.3540
	0.1	20.6109	82.5054	185.6250	329.9855	515.5967	742.5477
	0.2	18.8902	75.6176	170.1285	302.4374	472.5533	680.5578
	1.0	14.1594	56.6802	127.5222	226.6962	354.2089	510.1216
	2.0	12.7332	50.9709	114.6771	203.8616	318.5302	458.7382
0.0	0.0	23.8949	95.5797	215.0544	382.3189	597.3829	860.3480
	0.1	21.1642	84.6570	190.4782	338.6279	529.1146	762.0283
	0.2	19.3974	77.5896	174.5766	310.3583	484.9427	698.4121
	1.0	14.5396	58.1584	130.8563	232.6334	363.4955	523.5046
	2.0	13.0750	52.3002	117.6754	209.2007	326.8814	470.7731
0.1	0.0	24.4680	97.9323	220.3358	391.6941	612.0184	881.4141
	0.1	21.6719	86.7407	195.1561	346.9317	542.0775	780.6870
	0.2	19.8626	79.4993	178.8639	317.9689	496.8234	715.5131
	1.0	14.8883	59.5898	134.0699	238.3380	372.4009	536.3228
	2.0	13.3886	53.5875	120.5654	214.3308	334.8898	482.3002
0.2	0.0	24.9978	100.2156	225.4412	400.7323	626.1037	901.666
	0.1	22.1410	88.7630	199.6780	354.9370	554.5532	798.6251
	0.2	20.2927	81.3529	183.0083	325.3059	508.2576	731.9537
	1.0	15.2106	60.9792	137.1765	243.8376	380.9716	548.6461
	2.0	13.6785	54.8369	123.3590	219.2764	342.5971	493.3822

Table 5.51: First six non-dimensional frequencies of SUS304/Si_3N_4 FG beam with different power-law indices (k) and α; $f(\xi) = (1+\alpha\xi)^4$ and $g(\xi) = (1+\alpha\xi)$

BCs	α	k	Ω_1	Ω_2	Ω_3	Ω_4	Ω_5	Ω_6
C-C	-0.2	0.0	46.0643	126.8857	248.6693	411.0038	613.9191	857.4225
		0.1	40.8001	112.3853	220.2516	364.0347	543.7610	759.4371
		0.2	37.3940	103.0031	201.8644	333.6441	498.3664	696.0372
		1.0	28.0292	77.2074	151.3103	250.0876	373.5575	521.7244
		2.0	25.2059	69.4305	136.0691	224.8968	335.9298	469.1723
	-0.1	0.0	50.1110	138.1105	270.7331	447.5211	668.5098	933.7281

	0.1	44.3844	122.3274	239.7940	396.3788	592.1132	827.0226
	0.2	40.6790	112.1152	219.7753	363.2881	542.6820	757.9805
	1.0	30.4915	84.0375	164.7356	272.3076	406.7748	568.1548
	2.0	27.4202	75.5726	148.1422	244.8787	365.8013	510.9259
0.0	0.0	54.1671	149.3138	292.7147	483.8723	722.8258	1009.6129
	0.1	47.9770	132.2504	259.2636	428.5758	640.2220	894.2354
	0.2	43.9717	121.2097	237.6196	392.7972	586.7745	819.5822
	1.0	32.9596	90.8545	178.1110	294.4266	439.8250	614.3292
	2.0	29.6397	81.7029	160.1703	264.7696	395.5224	552.4492
0.1	0.0	58.2374	160.5124	314.6506	520.1197	776.9609	1085.2089
	0.1	51.5821	142.1692	278.6926	460.6809	688.1706	961.1923
	0.2	47.2759	130.3005	255.4266	422.2221	630.7202	880.9494
	1.0	35.4363	97.6686	191.4586	316.4824	472.7651	660.3279
	2.0	31.8669	87.8306	172.1734	284.6039	425.1446	593.8145
0.2	0.0	62.3254	171.7189	336.5677	556.3100	830.9873	1160.6206
	0.1	55.2029	152.0950	298.1051	492.7355	736.0229	1027.9860
	0.2	50.5944	139.3977	273.2185	451.6006	674.5778	942.1670
	1.0	37.9237	104.4875	204.7947	338.5035	505.6392	706.2144
	2.0	34.1038	93.9627	184.1662	304.4068	454.7072	635.0790
C-S -0.2	0.0	32.9333	103.9553	215.5818	367.7783	560.5481	793.7438
	0.1	29.1697	92.0754	190.9453	325.7490	496.4892	703.0355
	0.2	26.7345	84.3887	175.0047	298.5546	455.0410	644.3442
	1.0	20.0392	63.2547	131.1772	223.7857	341.0823	482.9772
	2.0	18.0207	56.8832	117.9640	201.2443	306.7258	434.3280
-0.1	0.0	35.1509	112.4833	234.0321	399.7742	609.7184	863.7488
	0.1	31.1339	99.6289	207.2871	354.0884	540.0404	765.0405
	0.2	28.5348	91.3116	189.9822	324.5282	494.9564	701.1728
	1.0	21.3886	68.4439	142.4038	243.2546	371.0014	525.5739
	2.0	19.2342	61.5497	128.0598	218.7521	333.6313	472.6340
0.0	0.0	37.3284	120.9681	252.3902	431.6022	658.6172	933.4624
	0.1	33.0626	107.1440	223.5473	382.2792	583.3511	826.7873
	0.2	30.3024	98.1993	204.8850	350.3655	534.6514	757.7648
	1.0	22.7136	73.6067	153.5744	262.6213	400.7554	567.9932
	2.0	20.4257	66.1924	138.1052	236.1680	360.3882	510.7805
0.1	0.0	39.4720	129.4255	270.6894	463.3198	707.3263	1002.9194
	0.1	34.9612	114.6349	239.7553	410.3720	626.4938	888.3067
	0.2	32.0425	105.0649	219.7398	376.1131	574.1924	814.1485
	1.0	24.0179	78.7528	164.7091	281.9208	430.3939	610.2563

		2.0	21.5986	70.8202	148.1183	253.5235	387.0413	548.7866
	0.2	0.0	41.5862	137.8676	288.9543	494.9699	755.9136	1072.1268
		0.1	36.8338	122.1122	255.9329	438.4053	669.5286	949.6053
		0.2	33.7588	111.9180	234.5669	401.8060	613.6345	870.3296
		1.0	25.3044	83.8897	175.8229	301.1793	459.9583	652.3677
		2.0	22.7555	75.4397	158.1126	270.8422	413.6277	586.6562
S-S	-0.2	0.0	20.2533	81.2481	182.7386	324.7955	507.4218	730.6492
		0.1	17.9388	71.9631	161.8554	287.6782	449.4342	647.1514
		0.2	16.4412	65.9555	148.3433	263.6620	411.9142	593.1254
		1.0	12.3237	49.4378	111.1928	197.6315	308.7560	444.5854
		2.0	11.0824	44.4581	99.9926	177.7246	277.6557	399.8033
	-0.1	0.0	22.0893	88.4143	198.9154	353.6095	552.5033	795.6802
		0.1	19.5650	78.3104	176.1835	313.1994	489.3638	704.7507
		0.2	17.9316	71.7729	161.4752	287.0526	448.5104	645.9162
		1.0	13.4409	53.7984	121.0360	215.1643	336.1872	484.1555
		2.0	12.0870	48.3794	108.8443	193.4913	302.3238	435.3876
	0.0	0.0	23.8949	95.5797	215.0544	382.3189	597.3829	860.3480
		0.1	21.1642	84.6570	190.4782	338.6279	529.1146	762.0283
		0.2	19.3974	77.5896	174.5766	310.3583	484.9427	698.4121
		1.0	14.5396	58.1584	130.8563	232.6334	363.4955	523.5046
		2.0	13.0750	52.3002	117.6754	209.2007	326.8814	470.7731
	0.1	0.0	25.6750	102.7541	231.1806	410.9708	642.1327	924.7656
		0.1	22.7408	91.0114	204.7615	364.0054	568.7504	819.0843
		0.2	20.8424	83.4136	187.6675	333.6173	521.2696	750.7050
		1.0	15.6227	62.5238	140.6688	250.0675	390.7249	562.7014
		2.0	14.0491	56.2259	126.4995	224.8787	351.3680	506.0217
	0.2	0.0	27.4331	109.9446	247.3124	439.6004	686.8132	989.0221
		0.1	24.2981	97.3802	219.0498	389.3633	608.3249	875.9976
		0.2	22.2696	89.2507	200.7630	356.8582	557.5403	802.8670
		1.0	16.6925	66.8991	150.4847	267.4880	417.9121	601.8001
		2.0	15.0111	60.1605	135.3267	240.5446	375.8167	541.1821

Table 5.52: First six non-dimensional frequencies of SUS304/Si_3N_4 FG beam with different power-law indices (k) and α; $f(\xi) = (1+\alpha\xi)^4$ and $g(\xi) = (1+\alpha\xi)^4$

BCs	α	k	Ω_1	Ω_2	Ω_3	Ω_4	Ω_5	Ω_6
C-C	-0.2	0.0	54.1671	149.3138	292.7147	483.8723	722.8251	1009.6154
		0.1	47.9770	132.2504	259.2636	428.5758	640.2214	894.2376
		0.2	43.9717	121.2097	237.6196	392.7972	586.7739	819.5842
		1.0	32.9596	90.8545	178.1110	294.4266	439.8246	614.3308
		2.0	29.6397	81.7029	160.1703	264.7696	395.5220	552.4506
	-0.1	0.0	54.1671	149.3138	292.7147	483.8723	722.8256	1009.6135
		0.1	47.9770	132.2504	259.2636	428.5758	640.2219	894.2359
		0.2	43.9717	121.2097	237.6196	392.7972	586.7744	819.5827
		1.0	32.9596	90.8545	178.1110	294.4266	439.8249	614.3296
		2.0	29.6397	81.7029	160.1703	264.7696	395.5223	552.4495
	0.0	0.0	54.1671	149.3138	292.7147	483.8723	722.8258	1009.6129
		0.1	47.9770	132.2504	259.2636	428.5758	640.2220	894.2354
		0.2	43.9717	121.2097	237.6196	392.7972	586.7745	819.5822
		1.0	32.9596	90.8545	178.1110	294.4266	439.8250	614.3292
		2.0	29.6397	81.7029	160.1703	264.7696	395.5224	552.4492
	0.1	0.0	54.1671	149.3138	292.7147	483.8723	722.8257	1009.6134
		0.1	47.9770	132.2504	259.2636	428.5758	640.2219	894.2358
		0.2	43.9717	121.2097	237.6196	392.7972	586.7744	819.5826
		1.0	32.9596	90.8545	178.1110	294.4266	439.8249	614.3295
		2.0	29.6397	81.7029	160.1703	264.7696	395.5223	552.4495
	0.2	0.0	54.1671	149.3138	292.7147	483.8723	722.8253	1009.6146
		0.1	47.9770	132.2504	259.2636	428.5758	640.2216	894.2369
		0.2	43.9717	121.2097	237.6196	392.7972	586.7741	819.5836
		1.0	32.9596	90.8545	178.1110	294.4266	439.8247	614.3303
		2.0	29.6397	81.7029	160.1703	264.7696	395.5222	552.4502
C-S	-0.2	0.0	39.5515	123.2119	254.6921	433.9321	660.9601	935.7535
		0.1	35.0316	109.1314	225.5861	384.3428	585.4262	828.8165
		0.2	32.1070	100.0208	206.7536	352.2568	536.5533	759.6247
		1.0	24.0663	74.9720	154.9750	264.0390	402.1810	569.3873
		2.0	21.6421	67.4202	139.3648	237.4429	361.6702	512.0341
	-0.1	0.0	38.3943	122.0065	253.4422	432.6600	659.6767	934.4883
		0.1	34.0067	108.0637	224.4791	383.2160	584.2895	827.6959
		0.2	31.1677	99.0422	205.7390	351.2241	535.5115	758.5976
		1.0	23.3622	74.2385	154.2145	263.2649	401.4001	568.6174

	2.0	21.0090	66.7606	138.6808	236.7468	360.9679	511.3419
0.0	0.0	37.3284	120.9681	252.3902	431.6022	658.6172	933.4624
	0.1	33.0626	107.1440	223.5473	382.2792	583.3511	826.7873
	0.2	30.3024	98.1993	204.8850	350.3655	534.6514	757.7648
	1.0	22.7136	73.6067	153.5744	262.6213	400.7554	567.9932
	2.0	20.4257	66.1924	138.1052	236.1680	360.3882	510.7805
0.1	0.0	36.3431	120.0651	251.4931	430.7092	657.7275	932.6147
	0.1	32.1898	106.3442	222.7527	381.4882	582.5631	826.0365
	0.2	29.5025	97.4663	204.1567	349.6405	533.9291	757.0767
	1.0	22.1140	73.0572	153.0285	262.0779	400.2140	567.4774
	2.0	19.8865	65.6983	137.6143	235.6794	359.9013	510.3166
0.2	0.0	35.4290	119.2733	250.7192	429.9454	656.9697	931.9022
	0.1	31.3802	105.6428	222.0673	380.8117	581.8919	825.4053
	0.2	28.7605	96.8235	203.5285	349.0205	533.3140	756.4983
	1.0	21.5579	72.5754	152.5576	261.6132	399.7529	567.0438
	2.0	19.3864	65.2650	137.1908	235.2615	359.4867	509.9267
S-S	-0.2	0.0	23.7092	95.7543	215.3302	382.6463	597.7397	860.7370
	0.1	20.9997	84.8116	190.7225	338.9179	529.4306	762.3729
	0.2	19.2466	77.7313	174.8004	310.6241	485.2323	698.7279
	1.0	14.4266	58.2645	131.0241	232.8326	363.7126	523.7412
	2.0	12.9734	52.3957	117.8263	209.3799	327.0766	470.9859
-0.1	0.0	23.8533	95.6190	215.1162	382.3921	597.4626	860.4350
	0.1	21.1273	84.6917	190.5329	338.6927	529.1851	762.1054
	0.2	19.3636	77.6214	174.6267	310.4177	485.0073	698.4827
	1.0	14.5142	58.1822	130.8939	232.6779	363.5440	523.5575
	2.0	13.0522	52.3217	117.7092	209.2408	326.9250	470.8207
0.0	0.0	23.8949	95.5797	215.0544	382.3189	597.3829	860.3480
	0.1	21.1642	84.6570	190.4782	338.6279	529.1146	762.0283
	0.2	19.3974	77.5896	174.5766	310.3583	484.9427	698.4121
	1.0	14.5396	58.1584	130.8563	232.6334	363.4955	523.5046
	2.0	13.0750	52.3002	117.6754	209.2007	326.8814	470.7731
0.1	0.0	23.8608	95.6118	215.1050	382.3788	597.4481	860.4192
	0.1	21.1340	84.6854	190.5230	338.6809	529.1723	762.0914
	0.2	19.3697	77.6157	174.6176	310.4069	484.9956	698.4699
	1.0	14.5188	58.1779	130.8871	232.6698	363.5352	523.5479
	2.0	13.0564	52.3178	117.7031	209.2335	326.9171	470.8120
0.2	0.0	23.7706	95.6966	215.2389	382.5378	597.6212	860.6080
	0.1	21.0541	84.7605	190.6416	338.8217	529.3257	762.2586

0.2	19.2965	77.6845	174.7263	310.5360	485.1361	698.6232
1.0	14.4639	58.2295	130.9686	232.7666	363.6405	523.6627
2.0	13.0070	52.3642	117.7764	209.3205	327.0118	470.9154

In order to view the effect of α and k on vibration of non-uniform FG beam, three different cases have been considered for different values of m_1 and m_2 and demonstrated in Figs. 5.6 to 5.8. Here only results of Al/Al_2O_3 FG beam are considered rather than showing the results of $SUS304/Si_3N_4$ as the effect of these parameters are same irrespective of material compositions and can also be seen in Tables 5.43 to 5.52. Regardless of FG material constituents, similar facts as discussed in Case 1, 2 and 3 can also be depicted in these demonstrations. The descending behavior of natural frequencies with respect to k is independent of the values of m_1 and m_2, whereas their pattern vary significantly with α for different values of m_1 and m_2.

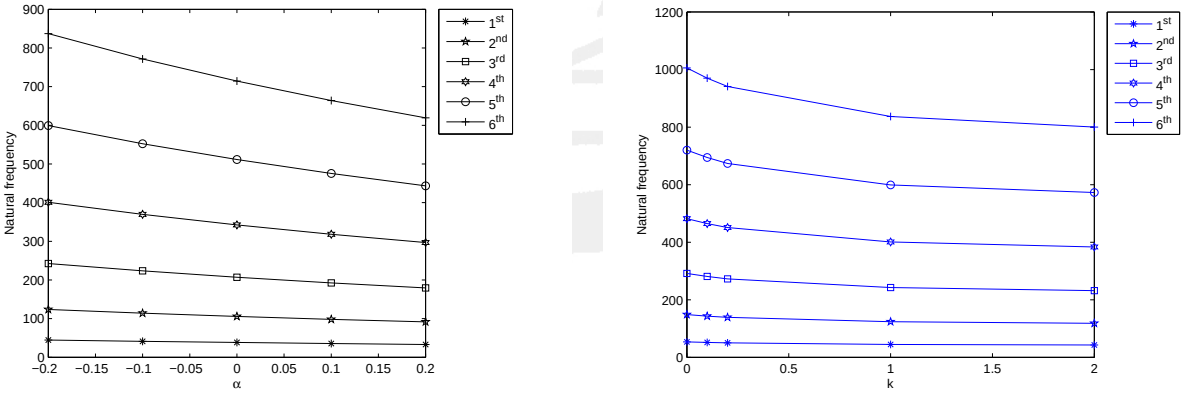

(a) Effect of α (b) Effect of k

Figure 5.6: Effect of α and k on first six frequencies of C-C FG (Al/Al_2O_3) beam with $m_1 = 1$ and $m_2 = 4$

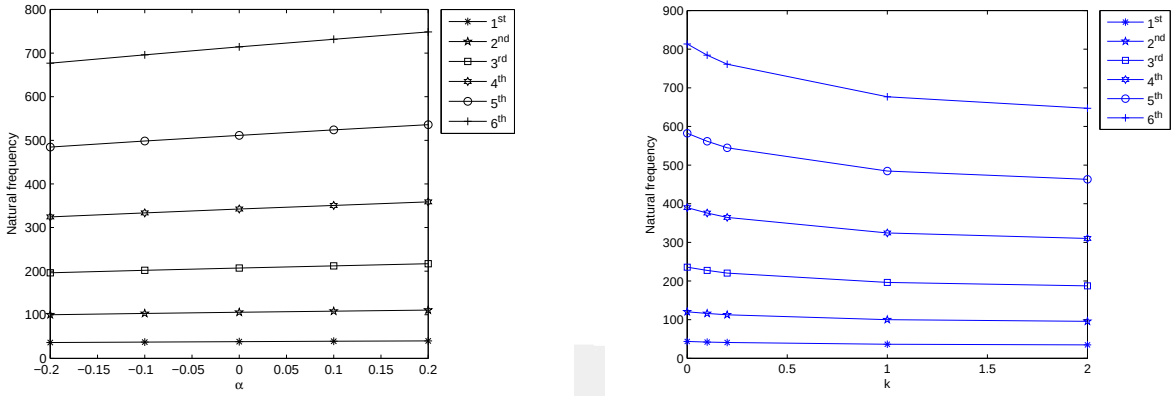

(a) Effect of α (b) Effect of k

Figure 5.7: Effect of α and k on first six frequencies of C-C FG (Al/Al_2O_3) beam with $m_1 = 3$ and $m_2 = 2$

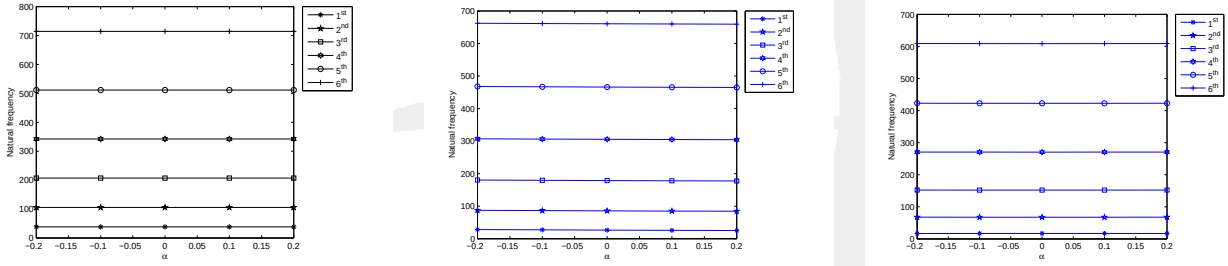

(a) C-C (b) C-S S-S

Figure 5.8: Effect of α on first six frequencies of FG (Al/Al_2O_3) beam with $m_1 = 4$ and $m_2 = 4$

5.3 Concluding remarks

In this investigation, we have studied vibration characteristics of FG beams subjected to various sets of boundary conditions within the framework of different shear deformation beam theories. This study may be the first of its kind to the best of the authors' knowledge about Rayleigh-Ritz method in FG beams to handle any sets of boundary conditions and implementation of GDQ to vibration of non-uniform FG beams (gradation assumed in present form) as well. But one has to keep tract of the convergence pattern to report the corresponding results. By analyzing the above formulations and numerical results, the following conclusions may be drawn.

- In Rayleigh-Ritz method, increase in the number of polynomials (n) is a key factor in deciding the convergence of the non-dimensional frequencies. The proposed PESDBT assumes the number of polynomials as m. The slenderness ratios, power-law variation of

material properties, different material distributions and different SDBTs play crucial role to examine the vibration characteristics of FG beams. The non-dimensional frequencies are increasing with increase in L/h ratios and decreasing with increase in k regardless of the beam theories considered. In case of PESDBT, the eigenfrequencies follow an ascending pattern with the increase in n irrespective of L/h and k assumed. While comparing results based on various SDBTs, the difference among the non-dimensional frequencies at each mode is significant for $L/h < 20$, whereas it becomes gradually negligible for $L/h \geq 20$.

- Furthermore, non-dimensional frequencies associated with PSDBT are coinciding with PESDBT[1] for different sets of BCs. A bit of fluctuations with an absolute error specification of 10^{-5} to 10^{-6} can be observed while analyzing the results for cantilever FG beam based on PSDBT and PESDBT[1]. Again the frequencies computed in PESDBT for $n = 0$ coincides with those for CBT, which may also be true for very large value of n. On the other hand, the results associated with ISDBT coincides with those of ICDBT regardless of the slenderness ratio and power-law exponent assumed. However, the frequencies at each mode based on ITDBT are comparatively higher than those evaluated within the framework of ISDBT and ICDBT.

- In GDQ, power-law index (k), parameter for non-homogeneity (α) and the indices deciding non-homogeneity (m_1, m_2) play crucial role in finding non-dimensional frequencies of Euler-Bernoulli non-uniform FG beam. The behavior of non-dimensional frequencies with reference to these parameters have also been discussed in Sec. 5.2.3. The non-dimensional frequencies follow descending pattern for ascending values of k irrespective of boundary supports and values of m_1 and m_2 considered. On contrary, these will follow descending manner with increase in α while $m_1 < m_2$ and ascending pattern with increase in α while $m_1 > m_2$. But it is difficult to predict the behavior of these frequencies for $m_1 = m_2$.

- Other shear deformation beam theories can also be extended easily in the above analysis.

Chapter 6

Vibration problems of functionally graded rectangular plates

The contents of this chapter have been published in:

(1) Chakraverty, S. and Pradhan, K.K. (2014). Free vibration of functionally graded thin rectangular plates resting on Winkler elastic foundation with general boundary conditions using Rayleigh-Ritz method. *International Journal of Applied Mechanics*, 6(4):145003 (37 pages) (World Scientific).

(2) Chakraverty, S. and Pradhan, K.K. (2014). Free vibration of exponential functionally graded rectangular plates in thermal environment with general boundary conditions. *Aerospace Science and Technology*, 36:132–156 (Elsevier).

(3) Pradhan, K.K. and Chakraverty, S. (2015). Transverse vibration of isotropic thick rectangular plates based on new inverse trigonometric shear deformation theories. *International Journal of Mechanical Sciences*, 94-95:211–231 (Elsevier).

Chapter 6

Vibration problems of functionally graded rectangular plates

This chapter involves free vibration of thin functionally graded rectangular plates subjected to various possible boundary conditions based on classical plate theory. Material properties of the FG plate constituents vary continuously along thickness direction in either power-law or exponential law. Trial functions denoting the displacement components are expressed as linear combination of simple algebraic polynomials, which may handle any combination of boundary conditions easily. The generalized eigenvalue problem can be obtained by means of Rayleigh-Ritz method. The objective is to study the effects of constituent volume fractions, aspect ratios and power-law indices on the natural frequencies. New results for these frequencies have been incorporated after performing a test of convergence and validation with available results in special cases. Accordingly, three-dimensional (3-D) mode shapes are also depicted for six lowest modes of different FG rectangular plates.

6.1 Thin FG rectangular plate

Free vibration of thin functionally graded rectangular plate is to be investigated in this part using Rayleigh-Ritz method. In this regard, we have to compute the natural frequencies by getting the concerned eigenvalue problem along with checking convergence pattern as well as comparison in special cases.

6.1.1 Numerical modeling

In this section, the admissible function for FG rectangular plate is to be assumed in Rayleigh-Ritz method rather than that for other geometries. The numerical formulation for free vibration of FG thin rectangular plates holds the step-by-step Rayleigh-Ritz procedures

mentioned in Sec. 3.1.3 to find the generalized eigenvalue problem of the form Eq. (3.38). The next section mainly deals with numerical results obtained for the above said problem with both the variation patterns of FG material properties. As regards, test of convergence and comparison of natural frequencies with available results in special cases have been carried out to report the new results. Consequently, 3-D mode shapes of FG plates with a few edge supports have also been demonstrated.

6.1.2 Convergence and comparison studies

The convergence of non-dimensional frequencies of FG rectangular plates has been checked with increase in number of polynomials involved in the displacement components. The material properties for this investigation are considered as

Table 6.1: Material properties of the FG plate constituents

Properties	Unit	Aluminium	Al_2O_3	SUS304	Si_3N_4
E	GPa	70	380	208	322
ρ	kg/m^3	2700	3800	8166	2370
ν	-	0.3	0.3	0.3	0.3

The following expression is meant for computing the non-dimensional frequencies as

$$\lambda = \omega a^2 \sqrt{\frac{\rho_c h}{D_c}} \tag{6.1}$$

where D_c(flexural rigidity) = $\frac{E_c h^3}{12(1-\nu^2)}$ of the FG plate due to the deformation effect.

In case of power law gradation, convergence of first seven non-dimensional frequencies of isotropic Al/Al_2O_3 square plate (assuming power-law index as 0 and aspect ratio as unity) with different edge conditions viz. CCCC, CSCS and SSSS, is performed in Table 6.2 with increase in number of polynomials involved in displacement components. Clamped isotropic SUS304/Si_3N_4 rectangular plate with various edge ratio (a/b) viz. 2/5, 2/3, 1.0, 1.5, are considered in Table 6.3 to study the convergence of frequencies. It may be observed in Tables 6.2 and 6.3 that non-dimensional frequencies for isotropic plates converge gradually with increase in number of polynomials.

Table 6.2: Convergence of non-dimensional frequencies for isotropic square Al/Al_2O_3 plate with $k = 0$ in power-law variation

BCs	Sources	λ_1	λ_2	λ_3	λ_4	λ_5	λ_6	λ_7
	10×10	36.0000	73.4329	73.4329	108.5910	137.2938	138.6506	168.8140
	13×13	35.9894	73.4329	73.4329	108.4270	132.1428	137.6999	168.8140
CCCC	16×16	35.9888	73.4172	73.4329	108.2653	131.8982	132.4236	168.8139
	19×19	35.9888	73.4039	73.4152	108.2653	131.8982	132.4236	165.2066
	20×20	35.9888	73.3989	73.4152	108.2653	131.8982	132.4236	165.2066
	10×10	28.9525	54.8846	69.3469	100.8762	135.1902	142.5894	163.3314
	13×13	28.9514	54.8846	69.3469	94.9189	103.7179	135.0244	163.3314
CSCS	16×16	28.9509	54.7571	69.3469	94.7034	103.7178	129.3120	163.2495
	19×19	28.9509	54.7484	69.3439	94.7034	103.7178	129.3120	141.3811
	20×20	28.9509	54.7439	69.3439	94.7034	103.7178	129.3120	141.3811
	10×10	19.7449	49.5132	49.5132	92.5635	139.5994	139.9505	168.7293
	13×13	19.7408	49.5132	49.5132	86.0902	100.1799	139.5995	168.7293
SSSS	16×16	19.7392	49.3736	49.5132	79.4007	100.1729	100.1868	168.6555
	19×19	19.7392	49.3498	49.4909	79.4007	100.1729	100.1868	130.3895
	20×20	19.7392	49.3490	49.4909	79.4007	100.1729	100.1868	130.3895

Table 6.3: Convergence of non-dimensional frequencies for CCCC isotropic rectangular $SUS304/Si_3N_4$ plate with $k = 0$ in power-law variation

a/b	Sources	λ_1	λ_2	λ_3	λ_4	λ_5	λ_6	λ_7
	7×7	23.6482	27.8269	35.8006	63.2107	68.4171	129.0781	223.3135
	9×9	23.6482	27.8171	35.8006	63.1294	68.4171	75.5319	129.0781
2/5	11×11	23.6478	27.8151	35.8006	48.8897	63.1294	68.4171	75.5319
	13×13	23.6467	27.8151	35.7980	48.8897	63.1294	67.4815	75.5319
	14×14	23.6467	27.8151	35.7980	48.8897	63.1294	67.4377	75.5319
	7×7	27.0132	41.8994	66.2992	68.7006	80.3935	131.8556	225.9695
	9×9	27.0132	41.8859	66.1653	68.7006	80.3935	104.1890	131.8556
2/3	11×11	27.0128	41.7228	66.1653	68.7006	80.3935	104.1890	109.3627
	13×13	27.0082	41.7228	66.1653	68.5959	79.8459	104.1890	109.3627
	14×14	27.0082	41.7228	66.1653	68.5959	79.8454	104.1890	109.3627
	7×7	36.0000	73.5504	74.2967	108.5910	137.2938	138.6506	231.5822
	9×9	36.0000	73.4329	74.1843	108.5910	137.2938	138.6506	168.8140
1.0	11×11	35.9995	73.4329	73.4329	108.5910	132.3887	138.0391	168.8140
	13×13	35.9894	73.4329	73.4329	108.4270	132.1428	137.6999	168.8140
	14×14	35.9894	73.4329	73.4329	108.2653	132.1428	137.6999	168.8140
	7×7	60.7797	93.9085	151.4183	154.5763	180.8853	246.0817	296.6751
	9×9	60.7797	93.8763	151.1258	154.5763	180.8853	234.4252	246.0662
1.5	11×11	60.7782	93.8763	148.8718	150.1498	180.8853	234.4252	246.0662
	13×13	60.7678	93.8763	148.8718	149.9028	180.8846	234.4252	246.0662
	14×14	60.7678	93.8763	148.8718	149.9028	179.6522	234.4252	246.0662

On the other hand, the exponential gradation criterion in FG square Al/Al_2O_3 plate with different edge conditions viz. CCCC, CSCS and SSSS are considered in Table 6.4 and clamped FG rectangular $SUS304/Si_3N_4$ plate with various edge ratio (a/b) viz. 2/5, 2/3, 1.0, 1.5, are assumed in Table 6.5 to analyze the convergence of natural frequencies. It may also be observed

in Tables 6.4 and 6.5 that non-dimensional frequencies for isotropic plates converge gradually with increase in number of polynomials in case of exponential variation of material properties. It may also be concluded that number of polynomials involved in displacement components play a major role in the convergence of non-dimensional frequencies irrespective of the edge condition, gradation criteria and configuration of the plate considered.

Table 6.4: Convergence of non-dimensional frequencies for FG Al/Al_2O_3 square plates with exponential gradation

BCs	Sources	λ_1	λ_2	λ_3	λ_4	λ_5	λ_6	λ_7
	7×7	28.3505	57.9220	58.5097	85.5170	108.1209	109.1894	182.3744
	9×9	28.3505	57.8295	58.4213	85.5170	108.1209	109.1894	132.9435
CCCC	11×11	28.3501	57.8295	57.8295	85.5170	104.2581	108.7078	132.9435
	13×13	28.3422	57.8295	57.8295	85.3879	104.0644	108.4407	132.9435
	14×14	28.3422	57.8295	57.8295	85.2605	104.0644	108.4407	132.9435
	7×7	22.8005	43.3085	55.4625	79.4415	106.4643	112.2913	224.8264
	9×9	22.8005	43.2224	55.2722	79.4415	106.4643	112.2913	128.6259
CSCS	11×11	22.7996	43.2224	54.6117	79.4415	81.8807	106.4717	128.6259
	13×13	22.7996	43.2224	54.6117	74.7500	81.6794	106.3337	128.6259
	14×14	22.7996	43.2224	54.6117	74.5803	81.6794	106.3337	128.6259
	7×7	15.5494	39.2356	46.4567	72.8951	109.9366	110.2131	223. 1847
	9×9	15.5494	38.9923	46.2328	72.8951	109.9366	110.2131	132.8768
SSSS	11×11	15.5482	38.9923	38.9923	72.8951	79.0228	110.0754	132.8768
	13×13	15.5462	38.9923	38.9923	67.7973	78.8931	109.9367	132.8768
	14×14	15.5462	38.9923	38.9923	62.5293	78.8931	109.9367	132.8768

Table 6.5: Convergence of non-dimensional frequencies for CCCC FG $SUS304/Si_3N_4$ rectangular plates with exponential gradation

a/b	Sources	λ_1	λ_2	λ_3	λ_4	λ_5	λ_6	λ_7
	7×7	15.1802	17.8626	22.9811	40.5761	43.9182	82.8577	143.3492
	9×9	15.1802	17.8563	22.9811	40.5239	43.9182	48.4853	82.8577
2/5	11×11	15.1800	17.8550	22.9811	31.3832	40.5239	43.9182	48.4853
	13×13	15.1793	17.8550	22.9794	31.3832	40.5239	43.3177	48.4853
	14×14	15.1793	17.8550	22.9794	31.3832	40.5239	43.2896	48.4853
	7×7	17.3403	26.8960	42.5587	44.1002	51.6061	84.6406	145.0541
	9×9	17.3403	26.8874	42.4727	44.1002	51.6061	66.8809	84.6406
2/3	11×11	17.3400	26.7827	42.4727	44.1002	51.6061	66.8809	70.2020
	13×13	17.3371	26.7827	42.4727	44.0330	51.2546	66.8809	70.2020
	14×14	17.3371	26.7827	42.4727	44.0330	51.2543	66.8809	70.2020
	7×7	23.1091	47.2134	47.6925	69.7066	88.1315	89.0025	148.6571
	9×9	23.1091	47.1380	47.6203	69.7066	88.1315	89.0025	108.3649
1.0	11×11	23.1088	47.1380	47.1380	69.7066	84.9829	88.6099	108.3649
	13×13	23.1023	47.1380	47.1380	69.6014	84.8250	88.3922	108.3649
	14×14	23.1023	47.1380	47.1380	69.4976	84.8250	88.3922	108.3649
	7×7	39.0157	60.2816	97.1983	99.2255	116.1137	157.9645	190.4414
	9×9	39.0157	60.2610	97.0106	99.2255	116.1137	150.4820	157.9546
1.5	11×11	39.0147	60.2610	95.5637	96.3840	116.1137	150.4820	157.9546
	13×13	39.0080	60.2610	95.5637	96.2255	116.1133	150.4820	157.9546
	14×14	39.0080	60.2610	95.5637	96.2255	115.3222	150.4820	157.9546

After checking the convergence, a comparison of non-dimensional frequencies with available literature may easily be done. In this regard, the validation is carried out with existing ones for isotropic cases of FG rectangular (or square) plates, which considers $k = 0$ in power-law variation and $\delta = 0$ in exponential gradation. In Table 6.6, comparison of first seven non-dimensional frequencies of FG square Al/Al_2O_3 plate with the available literature is performed. In a similar fashion, FG rectangular $SUS304/Si_3N_4$ plates with different edge ratios are considered in Table 6.7. It is evident from Tables 6.6 and 6.7 that present results for non-dimensional frequencies are in excellent agreement with open literature.

Table 6.6: Comparison of first seven non-dimensional frequencies for isotropic square plates

BCs	Sources	λ_1	λ_2	λ_3	λ_4	λ_5	λ_6	λ_7
CCCC	Present	35.9888	73.3989	73.3989	108.2653	131.8982	132.4236	165.2066
	Leissa (1973)	35.990	73.390	73.390	108.220	131.580	132.200	165.000
	Singh and Chakraverty (1994a)	35.988	73.398	73.398	108.26	131.89	-	-
	Liu and Liew (1999)	35.9375	73.2324	73.2324	107.8890	131.1188	131.7522	-
	Yang and Shen (2001)	35.9879	73.4053	73.4172	108.2728	131.1693	132.0165	-
	Bhat (1985)	35.9855	73.395	73.395	108.22	131.78	132.41	-
	Liew et al. (1993)	35.9875	73.3943	73.3943	108.2172	131.5766	132.2043	-
	Geannakakes (1995)	35.9852	73.3939	73.3939	108.2166	131.5823	132.2070	165.0019
	Cheung and Zhou (1999)	36.004	73.432	73.432	108.27	131.83	-	-
CCCS	Present	31.8278	63.3399	71.0835	100.8305	116.5434	130.6136	153.8345
	Leissa (1973)	31.829	63.347	71.084	100.830	116.400	130.370	-
	Singh and Chakraverty (1994a)	31.827	63.339	71.098	100.83	116.54	-	-
	Yang and Shen (2001)	31.8237	63.3391	71.0829	100.8310	116.2164	130.3377	-
	Liew et al. (1993)	31.8285	63.3322	71.0760	100.7914	116.3557	130.3479	-
CSCS	Present	28.9509	54.7439	69.3271	94.7034	103.7178	129.3120	141.3810
	Leissa (1973)	28.9505	54.7431	69.3270	94.5853	102.2162	129.0955	-
	Singh and Chakraverty (1994a)	28.950	54.873	69.327	94.703	103.71	-	-
	Liu and Liew (1999)	28.9216	54.6658	69.1927	94.3594	101.9944	128.6742	-
	Yang and Shen (2001)	28.9460	54.7410	69.3303	94.6120	102.1651	129.0791	-
	Liew et al. (1993)	28.9515	54.7418	69.3261	94.5834	102.2136	129.0915	-
SSSS	Present	19.7392	49.3490	49.3490	79.4007	100.1729	100.1868	130.3895
	Singh and Chakraverty (1994a)	19.739	49.348	49.348	79.400	100.17	-	-
	Bhat (1985)	19.739	49.348	49.348	78.957	99.304	99.304	-
	Cheung and Zhou (1999)	19.743	49.354	49.354	78.971	98.733	-	-

Table 6.7: Comparison of first seven non-dimensional frequencies for CCCC isotropic rectangular plates

a/b	Sources	λ_1	λ_2	λ_3	λ_4	λ_5	λ_6	λ_7
2/5	Present	23.6442	27.8095	35.4201	46.8183	62.0985	63.0861	67.3955
	Leissa (1973)	23.648	27.817	35.446	46.702	61.554	63.100	-
	Yang and Shen (2001)	23.6530	27.8243	35.4280	46.7023	61.5044	63.1151	67.4557
	Liew et al. (1993)	23.6428	27.8056	35.4158	46.6687	61.5091	63.0758	67.3837
	Geannakakes (1995)	23.6438	27.8070	35.4179	46.6762	62.0651	63.0829	67.3906
2/3	Present	27.0075	41.7073	66.1280	66.6235	79.8454	101.3552	103.2086
	Leissa (1973)	27.010	41.716	66.143	66.552	79.850	100.850	-
	Yang and Shen (2001)	27.0114	41.7184	66.1516	66.5187	79.8664	100.8301	103.1675
	Geannakakes (1995)	27.0050	41.7038	66.1245	66.5225	79.8051	100.8273	103.1261
1.5	Present	60.7626	93.8415	148.7881	149.6842	179.5755	228.0491	232.2193
	Leissa (1973)	60.772	93.860	148.820	149.740	179.660	226.92	-
	Yang and Shen (2001)	60.7527	93.8398	148.7879	149.7063	179.6004	226.9138	232.1345
	Bhat (1985)	60.962	93.835	148.78	149.85	179.57	227.90	-
	Liew et al. (1993)	60.7662	93.8390	148.7798	149.6770	179.5649	226.8228	232.0324

6.1.3 Results and discussions

Power-law gradation

First of all, let us evaluate the natural frequencies of FG rectangular plates with power-law gradation of material properties. Looking into the convergence and comparison of non-dimensional frequencies, new results for free vibration of FG rectangular plates are computed for all 24 possible combinations of BCs with different k and a/b. Consequently, frequencies of clamped FG rectangular plates are reported in Table 6.8. In a similar manner, non-dimensional frequencies of FG plates subject to different sets of BCs are incorporated in Tables 6.9 to 6.31. It may be noticed that non-dimensional frequencies are increasing with increase in aspect ratios for a fixed power-law index irrespective of edge support and geometric configuration considered, whereas one may observe descending pattern of present results with increase in power-law indices for a fixed aspect ratio.

Table 6.8: Effect of aspect ratios on non-dimensional frequencies of CCCC FG rectangular plates with different k

k	a/b	λ_1	λ_2	λ_3	λ_4	λ_5	λ_6
0.0	0.2	22.633	23.440	24.877	27.039	30.818	36.279
	0.5	24.579	31.829	44.819	63.598	63.986	71.119
	1.0	35.989	73.399	73.399	108.27	131.89	132.42
	2.0	98.318	127.32	179.28	254.39	255.95	284.48
0.2	0.2	21.176	21.931	23.275	25.298	28.834	33.943
	0.5	22.997	29.779	41.933	59.503	59.866	66.540
	1.0	33.671	68.673	68.673	101.29	123.41	123.89
	2.0	91.987	119.12	167.73	238.01	239.47	266.16
0.5	0.2	19.879	20.588	21.849	23.748	27.068	31.864
	0.5	21.588	27.956	39.365	55.858	56.199	62.465
	1.0	31.609	64.467	64.467	95.091	115.85	116.31
	2.0	86.354	111.82	157.46	223.43	224.80	249.86
1.0	0.2	18.832	19.503	20.699	22.498	25.642	30.186
	0.5	20.451	26.484	37.292	52.916	53.239	59.175
	1.0	29.945	61.072	61.072	90.082	109.75	110.18
	2.0	81.805	105.93	149.17	211.67	212.96	236.7
2.0	0.2	18.002	18.643	19.786	21.506	24.512	28.855
	0.5	19.549	25.316	35.648	50.583	50.893	56.566
	1.0	28.624	58.379	58.379	86.111	104.91	105.33
	2.0	78.199	101.26	142.59	202.33	203.57	226.26

Table 6.9: Effect of aspect ratios on non-dimensional frequencies of CCCS FG rectangular plates with different k

k	a/b	λ_1	λ_2	λ_3	λ_4	λ_5	λ_6
0.0	0.2	15.771	16.849	18.704	21.458	25.894	35.914
	0.5	18.349	27.056	41.300	52.643	60.693	61.341
	1.0	31.828	63.339	71.084	100.83	116.54	130.61
	2.0	96.574	121.01	167.13	244.24	254.99	280.71
0.2	0.2	14.756	15.765	17.499	20.077	24.227	33.601
	0.5	17.168	25.314	38.640	49.253	56.785	57.392
	1.0	29.778	59.262	66.506	94.338	109.04	122.20
	2.0	90.356	113.22	156.37	228.51	238.58	262.64
0.5	0.2	13.852	14.799	16.428	18.847	22.743	31.543
	0.5	16.116	23.764	36.274	46.236	53.307	53.877
	1.0	27.955	55.632	62.433	88.560	102.36	114.72
	2.0	84.822	106.28	146.79	214.51	223.97	246.55
1.0	0.2	13.122	14.019	15.563	17.854	21.545	29.882
	0.5	15.268	22.512	34.363	43.801	50.499	51.039
	1.0	26.482	52.702	59.145	83.896	96.969	108.68
	2.0	80.355	100.69	139.06	203.22	212.17	233.57
2.0	0.2	12.544	13.402	14.877	17.067	20.595	28.565
	0.5	14.595	21.520	32.848	41.870	48.273	48.789
	1.0	25.315	50.379	56.538	80.197	92.695	103.89
	2.0	76.812	96.247	132.93	194.26	202.82	223.27

Table 6.10: Effect of aspect ratios on non-dimensional frequencies of CCSS FG rectangular plates with different k

k	a/b	λ_1	λ_2	λ_3	λ_4	λ_5	λ_6
0.0	0.2	15.742	16.734	18.454	21.112	26.758	50.335
	0.5	17.769	25.201	38.056	52.357	58.439	59.665
	1.0	27.055	60.546	60.798	92.914	114.95	115.14
	2.0	71.079	100.80	152.23	209.43	233.76	238.66
0.2	0.2	14.728	15.656	17.266	19.753	25.035	47.094
	0.5	16.625	23.578	35.605	48.986	54.676	55.824
	1.0	25.313	56.647	56.883	86.931	107.55	107.72
	2.0	66.502	94.312	142.42	195.94	218.71	223.29
0.5	0.2	13.826	14.698	16.209	18.543	23.502	42.090
	0.5	15.607	22.134	33.425	45.986	51.328	52.405
	1.0	23.763	53.178	53.399	81.607	100.97	101.13
	2.0	62.429	88.536	133.69	183.94	205.31	209.62
1.0	0.2	13.098	13.923	15.355	17.566	22.264	41.881
	0.5	14.785	20.968	31.664	43.564	48.624	49.645
	1.0	22.511	50.377	50.587	77.309	95.647	95.800
	2.0	59.141	83.873	126.66	174.26	194.49	198.58
2.0	0.2	12.520	13.309	14.678	16.792	21.282	40.035
	0.5	14.133	20.044	30.268	41.643	46.481	47.456
	1.0	21.519	48.156	48.357	73.900	91.431	91.577
	2.0	56.533	80.175	121.07	166.57	185.92	189.82

Table 6.11: Effect of aspect ratios on non-dimensional frequencies of CCFF FG rectangular plates with different k

k	a/b	λ_1	λ_2	λ_3	λ_4	λ_5	λ_6
0.0	0.2	3.6132	4.4014	5.9149	8.4583	12.682	22.094
	0.5	4.2898	9.1066	18.402	22.752	28.883	35.057
	1.0	6.9365	23.948	26.603	47.763	62.887	65.783
	2.0	17.159	36.426	73.607	91.006	115.53	140.23
0.2	0.2	3.3806	4.1179	5.5340	7.9137	11.866	20.671
	0.5	4.0136	8.5202	17.217	21.287	27.023	32.799
	1.0	6.4899	22.406	24.890	44.688	58.837	61.547
	2.0	16.054	34.081	68.868	85.147	108.09	131.19
0.5	0.2	3.1735	3.8658	5.1951	7.4290	11.139	19.405
	0.5	3.7678	7.9984	16.163	19.983	25.368	30.791
	1.0	6.0924	21.034	23.366	41.951	55.234	57.778
	2.0	15.071	31.994	64.650	79.932	101.47	123.16
1.0	0.2	3.0064	3.6622	4.9215	7.0377	10.553	18.383
	0.5	3.5694	7.5771	15.311	18.930	24.032	29.169
	1.0	5.7716	19.926	22.135	39.741	52.325	54.735
	2.0	14.277	30.309	61.245	75.722	96.128	116.68
2.0	0.2	2.8738	3.5007	4.7045	6.7275	10.088	17.573
	0.5	3.4119	7.2431	14.636	18.096	22.972	27.883
	1.0	5.5171	19.047	21.159	37.989	50.018	52.322
	2.0	13.648	28.972	58.545	72.383	91.889	111.53

Table 6.12: Effect of aspect ratios on non-dimensional frequencies of CFCF FG rectangular plates with different k

k	a/b	λ_1	λ_2	λ_3	λ_4	λ_5	λ_6
0.0	0.2	0.8771	2.4095	2.8869	4.7523	5.9772	7.9153
	0.5	5.5287	9.0046	15.224	20.709	27.663	30.068
	1.0	22.224	26.478	44.073	61.265	67.649	82.254
	2.0	89.179	93.709	111.01	145.61	245.99	252.95
0.2	0.2	0.8206	2.2543	2.7011	4.4463	5.5924	7.4057
	0.5	5.1727	8.4248	14.244	19.376	25.881	28.132
	1.0	20.793	24.773	41.235	57.321	63.294	76.958
	2.0	83.437	87.676	103.86	136.24	230.15	236.67
0.5	0.2	0.7703	2.1163	2.5356	4.1740	5.2499	6.9521
	0.5	4.8559	7.9088	13.372	18.189	24.296	26.409
	1.0	19.519	23.256	38.709	53.810	59.417	72.244
	2.0	78.327	82.306	97.503	127.89	216.06	222.17
1.0	0.2	0.7298	2.0048	2.4021	3.9542	4.9734	6.5859
	0.5	4.6002	7.4923	12.667	17.231	23.017	25.018
	1.0	18.491	22.031	36.671	50.976	56.288	68.439
	2.0	74.202	77.971	92.367	121.16	204.68	210.47
2.0	0.2	0.6976	1.9164	2.2962	3.7798	4.7541	6.2956
	0.5	4.3973	7.1619	12.109	16.471	22.002	23.915
	1.0	17.676	21.059	35.054	48.729	53.806	65.422
	2.0	70.930	74.533	88.295	115.81	195.66	201.19

Table 6.13: Effect of aspect ratios on non-dimensional frequencies of CFSF FG rectangular plates with different k

k	a/b	λ_1	λ_2	λ_3	λ_4	λ_5	λ_6
0.0	0.2	0.5980	1.9399	2.7417	4.0731	5.6717	7.4502
	0.5	3.7728	7.8280	12.278	18.302	25.844	27.127
	1.0	15.218	20.614	40.211	49.533	56.672	80.300
	2.0	61.254	67.288	88.672	129.82	199.26	206.92
0.2	0.2	0.5595	1.8150	2.5651	3.8109	5.3065	6.9705
	0.5	3.5298	7.3239	11.488	17.123	24.180	25.380
	1.0	14.238	19.286	37.621	46.344	53.023	75.129
	2.0	57.309	62.955	82.962	121.46	186.43	193.59
0.5	0.2	0.5252	1.7039	2.4080	3.5775	4.9815	6.5436
	0.5	3.3136	6.8754	10.784	16.074	22.699	23.826
	1.0	13.366	18.105	35.317	43.506	49.775	70.528
	2.0	53.799	59.099	77.881	114.02	175.01	181.74
1.0	0.2	0.4976	1.6141	2.2812	3.3891	4.7192	6.1989
	0.5	3.1391	6.5133	10.216	15.228	21.504	22.571
	1.0	12.662	17.152	33.457	41.214	47.154	66.814
	2.0	50.966	55.987	73.779	108.02	165.79	172.17
2.0	0.2	0.4756	1.5429	2.1806	3.2396	4.5111	5.9256
	0.5	3.0007	6.2261	9.7656	14.556	20.556	21.576
	1.0	12.104	16.396	31.982	39.397	45.075	63.868
	2.0	48.719	53.518	70.527	103.25	158.48	164.58

Table 6.14: Effect of aspect ratios on non-dimensional frequencies of CFFF FG rectangular plates with different k

k	a/b	λ_1	λ_2	λ_3	λ_4	λ_5	λ_6
0.0	0.2	0.1371	0.8551	1.3620	2.3968	4.1725	5.0445
	0.5	0.8645	3.7049	5.3717	12.104	15.095	23.581
	1.0	3.4865	8.5219	21.325	27.576	31.144	55.497
	2.0	14.019	21.462	41.324	79.533	87.608	100.14
0.2	0.2	0.1283	0.8000	1.2743	2.2425	3.9038	4.7197
	0.5	0.8088	3.4663	5.0258	11.325	14.123	22.062
	1.0	3.2619	7.9732	19.952	25.801	29.138	51.924
	2.0	13.117	20.079	38.663	74.412	81.967	93.697
0.5	0.2	0.1204	0.7510	1.1963	2.1052	3.6647	4.4306
	0.5	0.7593	3.2540	4.7179	10.631	13.258	20.711
	1.0	3.0622	7.4849	18.729	24.221	27.354	48.744
	2.0	12.314	18.850	36.295	69.855	76.947	87.958
1.0	0.2	0.1141	0.7115	1.1333	1.9943	3.4717	4.1972
	0.5	0.7193	3.0827	4.4695	10.071	12.559	19.620
	1.0	2.9009	7.0907	17.743	22.945	25.913	46.177
	2.0	11.665	17.857	34.383	66.176	72.894	83.326
2.0	0.2	0.1091	0.6801	1.0833	1.9064	3.3186	4.0122
	0.5	0.6876	2.9467	4.2724	9.6270	12.006	18.755
	1.0	2.7730	6.7781	16.961	21.933	24.771	44.141
	2.0	11.151	17.070	32.867	63.258	69.680	79.652

Table 6.15: Effect of aspect ratios on non-dimensional frequencies of SCSC FG rectangular plates with different k

k	a/b	λ_1	λ_2	λ_3	λ_4	λ_5	λ_6
0.0	0.2	22.593	23.277	24.521	26.479	35.417	47.242
	0.5	23.816	28.951	39.351	56.145	63.535	69.373
	1.0	28.951	54.744	69.327	94.703	103.72	129.31
	2.0	54.743	94.585	154.97	170.36	207.34	235.68
0.2	0.2	21.138	21.779	22.942	24.775	33.136	44.199
	0.5	22.282	27.087	36.817	52.529	59.444	64.906
	1.0	27.087	51.219	64.863	88.605	97.039	120.99
	2.0	51.218	88.495	144.99	159.39	193.99	220.51
0.5	0.2	19.843	20.445	21.537	23.258	31.107	41.493
	0.5	20.918	25.428	34.562	49.312	55.803	60.931
	1.0	25.428	48.082	60.891	83.179	91.096	113.58
	2.0	48.081	83.075	136.11	149.63	182.11	207.00
1.0	0.2	18.798	19.368	20.403	22.033	29.469	39.308
	0.5	19.816	24.089	32.742	46.715	52.864	57.722
	1.0	24.089	45.549	57.684	78.798	86.298	107.59
	2.0	45.549	78.699	128.94	141.75	172.51	196.10
2.0	0.2	17.969	18.514	19.503	21.061	28.169	37.575
	0.5	18.942	23.027	31.298	44.656	50.533	55.177
	1.0	23.027	43.542	55.140	75.324	82.494	102.85
	2.0	43.541	75.230	123.26	135.50	164.91	187.45

Table 6.16: Effect of aspect ratios on non-dimensional frequencies of SCSS FG rectangular plates with different k

k	a/b	λ_1	λ_2	λ_3	λ_4	λ_5	λ_6
0.0	0.2	15.715	16.628	18.238	21.152	31.139	46.762
	0.5	17.332	23.648	35.345	52.102	54.546	58.684
	1.0	23.646	51.688	58.651	86.245	101.81	113.38
	2.0	51.674	86.139	140.98	169.07	202.34	225.13
0.2	0.2	14.703	15.558	17.063	19.789	29.135	43.751
	0.5	16.216	22.126	33.069	48.747	51.034	54.905
	1.0	22.124	48.359	54.874	80.692	95.251	106.08
	2.0	48.347	80.593	131.90	158.18	189.31	210.63
0.5	0.2	13.803	14.605	16.018	18.578	27.350	41.071
	0.5	15.223	20.771	31.044	45.762	47.908	51.543
	1.0	20.769	45.398	51.513	75.749	89.417	99.579
	2.0	45.386	75.657	123.83	148.49	177.72	197.73
1.0	0.2	13.076	13.835	15.175	17.599	25.909	38.908
	0.5	14.421	19.677	29.409	43.352	45.385	48.828
	1.0	19.675	43.007	48.800	71.760	84.708	94.335
	2.0	42.996	71.673	117.30	140.67	168.36	18.732
2.0	0.2	12.499	13.226	14.506	16.823	24.768	37.193
	0.5	13.785	18.809	28.113	41.440	43.384	46.675
	1.0	18.808	41.111	46.649	68.597	80.973	90.176
	2.0	41.100	68.513	112.13	134.45	160.94	179.06

Table 6.17: Effect of aspect ratios on non-dimensional frequencies of SCSF FG rectangular plates with different k

k	a/b	λ_1	λ_2	λ_3	λ_4	λ_5	λ_6
0.0	0.2	3.8553	4.9006	6.7498	9.7043	22.511	22.581
	0.5	5.7034	12.689	24.944	25.131	33.101	44.223
	1.0	12.687	33.066	41.715	63.260	72.421	92.532
	2.0	41.703	63.018	103.20	159.44	16981	181.89
0.2	0.2	3.6070	4.5851	6.3152	9.0795	21.061	21.127
	0.5	5.3366	11.872	23.338	23.513	30.969	41.376
	1.0	11.870	30.937	39.029	59.187	67.758	86.574
	2.0	39.018	58.960	96.558	149.17	158.87	170.18
0.5	0.2	3.3861	4.3043	5.9284	8.5234	19.771	19.833
	0.5	5.0098	11.145	21.909	22.073	29.073	38.842
	1.0	11.143	29.042	36.639	55.562	63.608	81.272
	2.0	36.628	55.349	90.645	140.04	149.14	159.75
1.0	0.2	3.2078	4.0776	5.6162	8.0745	18.730	18.788
	0.5	4.7459	10.558	20.755	20.911	27.542	36.796
	1.0	10.557	27.513	34.709	52.636	60.258	76.991
	2.0	34.699	52.434	85.870	132.66	141.29	151.34
2.0	0.2	3.0664	3.8978	5.3686	7.7185	17.904	17.960
	0.5	4.5367	10.093	19.839	19.988	26.327	35.174
	1.0	10.091	26.299	33.179	50.315	57.601	73.597
	2.0	33.169	50.122	82.085	126.81	135.06	144.67

Table 6.18: Effect of aspect ratios on non-dimensional frequencies of SSSF FG rectangular plates with different k

k	a/b	λ_1	λ_2	λ_3	λ_4	λ_5	λ_6
0.0	0.2	1.3449	3.0083	5.2662	8.3629	15.989	17.696
	0.5	4.0337	11.687	18.821	24.406	27.859	42.146
	1.0	11.685	27.757	41.220	59.360	62.462	92.071
	2.0	41.199	59.075	95.218	156.59	159.35	179.23
0.2	0.2	1.2583	2.8146	4.9271	7.8245	14.959	16.556
	0.5	3.7739	10.934	17.609	22.834	26.066	39.432
	1.0	10.932	25.970	38.566	55.538	58.439	86.143
	2.0	38.546	55.271	89.087	146.51	149.09	167.69
0.5	0.2	1.1813	2.6422	4.6253	7.3453	14.043	15.542
	0.5	3.5428	10.264	16.531	21.436	24.469	37.017
	1.0	10.263	24.379	36.204	52.137	54.861	80.867
	2.0	36.185	51.886	83.631	137.54	139.96	157.42
1.0	0.2	1.1190	2.5031	4.3817	6.9584	13.304	14.724
	0.5	3.3562	9.7238	15.660	20.307	23.180	35.068
	1.0	9.7222	23.096	34.297	49.391	51.971	76.608
	2.0	34.279	49.153	79.226	130.29	132.59	149.13
2.0	0.2	1.0697	2.3927	4.1886	6.6516	12.717	14.075
	0.5	3.2083	9.2951	14.969	19.412	22.158	33.522
	1.0	9.2935	22.077	32.785	47.213	49.679	73.230
	2.0	32.768	46.986	75.734	124.55	126.74	142.56

Table 6.19: Effect of aspect ratios on non-dimensional frequencies of SFSF FG rectangular plates with different k

k	a/b	λ_1	λ_2	λ_3	λ_4	λ_5	λ_6
0.0	0.2	0.3774	1.5175	2.6044	3.5056	5.3914	6.4419
	0.5	2.3781	6.8806	9.6329	16.254	22.375	26.633
	1.0	9.6317	16.135	37.181	38.972	47.281	72.053
	2.0	38.962	46.751	71.849	114.71	157.09	166.74
0.2	0.2	0.3531	1.4198	2.4367	3.2798	5.0442	6.0271
	0.5	2.2249	6.4375	9.0126	15.208	20.935	24.918
	1.0	9.0115	15.096	34.787	36.463	44.237	67.414
	2.0	36.453	43.741	67.222	107.33	146.97	156.01
0.5	0.2	0.3315	1.3328	2.2875	3.0789	4.7353	5.6580
	0.5	2.0887	6.0433	8.4606	14.276	19.653	23.392
	1.0	8.4596	14.172	32.656	34.229	41.527	63.285
	2.0	34.221	41.062	63.105	100.75	137.97	146.45
1.0	0.2	0.3140	1.2626	2.1670	2.9168	4.4859	5.3600
	0.5	1.9787	5.7249	8.0150	13.524	18.617	22.160
	1.0	8.0141	13.425	30.936	32.427	39.340	59.952
	2.0	32.418	38.899	59.782	95.447	130.70	138.74
2.0	0.2	0.3002	1.2069	2.0715	2.7882	4.2881	5.1237
	0.5	1.8915	5.4726	7.6617	12.928	17.797	21.183
	1.0	7.6608	12.833	29.572	30.997	37.606	57.309
	2.0	30.989	37.184	57.146	91.239	124.94	132.62

Table 6.20: Effect of aspect ratios on non-dimensional frequencies of SSFF FG rectangular plates with different k

k	a/b	λ_1	λ_2	λ_3	λ_4	λ_5	λ_6
0.0	0.2	0.6495	2.0782	3.9007	6.6311	14.759	15.658
	0.5	1.6609	6.3445	14.820	16.336	22.379	29.996
	1.0	3.3671	17.319	19.299	38.408	51.651	54.183
	2.0	6.6438	25.378	59.282	65.346	89.514	119.98
0.2	0.2	0.6076	1.9444	3.6495	6.2041	13.809	14.649
	0.5	1.5540	5.9359	13.866	15.285	20.938	28.064
	1.0	3.1503	16.204	18.057	35.935	48.325	50.694
	2.0	6.2160	23.744	55.465	61.138	83.751	112.26
0.5	0.2	0.5704	1.8253	3.4260	5.8242	12.963	13.752
	0.5	1.4588	5.5724	13.017	14.348	19.655	26.345
	1.0	2.9574	15.212	16951	33.734	45.366	47.589
	2.0	5.8353	22.289	52.068	57.394	78.621	105.38
1.0	0.2	0.5404	1.7292	3.2456	5.5174	12.281	13.028
	0.5	1.3819	5.2789	12.331	13.593	18.620	24.958
	1.0	2.8016	14.410	16.058	31.957	42.976	45.083
	2.0	5.5279	21.116	49.325	54.371	74.480	99.832
2.0	0.2	0.5166	1.6529	3.1025	5.2742	11.739	12.454
	0.5	1.3211	5.0462	11.788	12.993	17.799	23.858
	1.0	2.6781	13.775	15.350	30.548	41.082	43.095
	2.0	5.2843	20.185	47.151	51.974	71.197	95.430

Table 6.21: Effect of aspect ratios on non-dimensional frequencies of SFFF FG rectangular plates with different k

k	a/b	λ_1	λ_2	λ_3	λ_4	λ_5	λ_6
0.0	0.2	0.5897	1.2910	1.9444	3.9586	4.2694	7.0605
	0.5	3.2602	3.7116	10.788	12.319	21.713	23.232
	1.0	6.6445	14.907	25.632	26.297	49.534	51.896
	2.0	13.469	35.311	61.207	70.343	79.623	109.11
0.2	0.2	0.5517	1.2079	1.8192	3.7037	3.9945	6.6059
	0.5	3.0503	3.4726	10.093	11.527	20.315	21.736
	1.0	6.2166	13.947	23.981	24.604	46.344	48.555
	2.0	12.602	33.037	57.266	65.813	74.496	102.08
0.5	0.2	0.5179	1.1339	1.7078	3.4769	3.7499	6.2013
	0.5	2.8635	3.2599	9.4749	10.821	19.071	20.405
	1.0	5.8359	13.093	22.513	23.097	43.506	45.581
	2.0	11.830	31.014	53.759	61.783	69.933	95.829
1.0	0.2	0.4907	1.0742	1.6178	3.2938	3.5524	5.8747
	0.5	2.7127	3.0882	8.9759	10.251	18.066	19.330
	1.0	5.5285	12.403	21.327	21.881	41.215	43.180
	2.0	11.207	29.381	50.928	58.529	66.249	90.782
2.0	0.2	0.4690	1.0268	1.5465	3.1485	3.3958	5.6157
	0.5	2.5931	2.9521	8.5802	9.7989	17.269	18.478
	1.0	5.2848	11.856	20.387	20.916	39.398	41.276
	2.0	10.713	28.085	48.682	55.948	63.329	86.780

Table 6.22: Effect of aspect ratios on non-dimensional frequencies of FFFF FG rectangular plates with different k

k	a/b	λ_1	λ_2	λ_3	λ_4	λ_5	λ_6
0.0	0.2	0.8637	2.4487	2.6067	5.4265	8.5531	11.219
	0.5	5.4209	6.7309	15.078	15.393	22.305	26.454
	1.0	13.714	19.774	24.556	35.597	35.597	63.179
	2.0	21.684	26.924	60.312	61.572	89.219	105.81
0.2	0.2	0.8081	2.2909	2.4388	5.0771	8.0023	10.497
	0.5	5.0719	6.2975	14.107	14.402	20.869	24.750
	1.0	12.831	18.501	22.975	33.305	33.305	59.111
	2.0	20.288	25.190	56.429	57.607	83.475	99.001
0.5	0.2	0.7586	2.1507	2.2895	4.7662	7.5123	9.8544
	0.5	4.7613	5.9118	13.243	13.519	19.591	23.235
	1.0	12.045	17.368	21.568	31.265	31.265	55.490
	2.0	19.045	23.647	52.973	54.079	78.363	92.938
1.0	0.2	0.7186	2.0374	2.1689	4.5152	7.1166	9.3353
	0.5	4.5105	5.6005	12.546	12.808	18.559	22.011
	1.0	11.411	16.453	20.432	29.618	29.618	52.568
	2.0	18.042	22.402	50.183	51.231	74.235	88.043
2.0	0.2	0.6869	1.9476	2.0733	4.3161	6.8028	8.9238
	0.5	4.3116	5.3536	11.993	12.243	17.741	21.040
	1.0	10.908	15.728	19.531	28.313	28.313	50.250
	2.0	17.247	21.414	47.971	48.972	70.963	84.162

Table 6.23: Effect of aspect ratios on non-dimensional frequencies of SFSC FG rectangular plates with different k

k	a/b	λ_1	λ_2	λ_3	λ_4	λ_5	λ_6
0.0	0.2	3.8553	4.9006	6.7498	9.7043	22.511	22.581
	0.5	5.7039	12.689	24.944	25.131	33.101	44.223
	1.0	12.687	33.066	41.715	63260	72.421	92.532
	2.0	41.703	63.018	103.20	159.44	169.81	181.89
0.2	0.2	3.6070	4.5851	6.3152	9.0795	21.061	21.127
	0.5	5.3366	11.872	23.338	23.513	30.969	41.376
	1.0	11.870	30.937	39.029	59.187	67.758	86.574
	2.0	39.018	58.960	96.558	149.17	158.88	170.18
0.5	0.2	3.3861	4.3043	5.9284	8.5234	19.771	19.833
	0.5	5.0098	11.145	21.909	22.073	29.073	38.842
	1.0	11.143	29.042	36.639	55.562	63.608	81.272
	2.0	36.628	55.349	90.645	140.04	149.14	159.75
1.0	0.2	3.2078	4.0776	5.6162	8.0745	18.730	18.788
	0.5	4.7459	10.558	20.755	20.911	27.542	36.796
	1.0	10.557	27.513	34.709	52.636	60.258	76.991
	2.0	34.699	52.434	85.870	132.66	141.29	151.34
2.0	0.2	3.0664	3.8978	5.3686	7.7185	17.904	17.960
	0.5	4.5367	10.093	19.839	19.989	26.327	35.174
	1.0	10.091	26.299	33.179	50.315	57.601	73.597
	2.0	33.169	50.122	82.085	126.81	135.06	144.67

Table 6.24: Effect of aspect ratios on non-dimensional frequencies of SCCC FG rectangular plates with different k

k	a/b	λ_1	λ_2	λ_3	λ_4	λ_5	λ_6
0.0	0.2	22.612	23.355	24.681	26.818	30.092	54.224
	0.5	24.144	30.252	41.782	61.059	63.749	70.179
	1.0	31.828	63.339	71.084	100.83	116.54	130.61
	2.0	73.398	108.23	165.19	210.57	242.77	245.37
0.2	0.2	21.156	21.852	23.091	25.091	28.154	50.733
	0.5	22.589	28.305	39.092	57.127	59.645	65.659
	1.0	29.778	59.262	66.506	94.338	109.04	122.20
	2.0	68.672	101.26	154.56	197.01	227.14	229.57
0.5	0.2	19.860	20.513	21.677	23.555	26.429	47.625
	0.5	21.206	26.571	36.698	53.629	55.992	61.639
	1.0	27.955	55.632	62.433	88.560	102.36	114.72
	2.0	64.467	95.056	145.09	184.95	213.23	215.51
1.0	0.2	18.814	19.433	20.535	22.314	25.038	45.117
	0.5	20.089	25.172	34.765	50.804	53.043	58.392
	1.0	26.482	52.702	59.145	83.896	96.969	108.68
	2.0	61.070	90.049	137.45	175.20	201.99	204.16
2.0	0.2	17.985	18.576	19.630	21.330	23.934	43.128
	0.5	19.203	24.062	33.232	48.564	50.704	55.818
	1.0	25.315	50.379	56.538	80.197	92.695	10.389
	2.0	58.378	86.079	131.39	167.48	193.09	195.16

Table 6.25: Effect of aspect ratios on non-dimensional frequencies of SCCS FG rectangular plates with different k

k	a/b	λ_1	λ_2	λ_3	λ_4	λ_5	λ_6
0.0	0.2	15.742	16.734	18.454	21.112	26.758	50.335
	0.5	17.769	25.201	38.056	52.357	58.439	59.665
	1.0	27.055	60.546	60.798	92.914	114.95	115.14
	2.0	71.079	100.80	152.22	209.43	233.76	238.66
0.2	0.2	14.728	15.656	17.266	19.753	25.035	47.094
	0.5	16.625	23.578	35.605	48.986	54.676	55.824
	1.0	25.313	56.647	56.883	86.931	107.55	107.72
	2.0	66.502	94.312	142.42	195.94	218.71	223.29
0.5	0.2	13.826	14.698	16.209	18.543	23.502	44.209
	0.5	15.607	22.134	33.425	45.986	51.328	52.405
	1.0	23.763	53.178	53.399	81.607	100.97	101.13
	2.0	62.429	88.536	133.69	183.94	205.31	209.62
1.0	0.2	13.098	13.923	15.355	17.567	22.264	41.881
	0.5	14.786	20.968	31.664	43.564	48.624	49.645
	1.0	22.511	50.377	50.587	77.309	95.647	95.800
	2.0	59.141	83.873	126.66	174.26	194.49	198.58
2.0	0.2	12.520	13.309	14.678	16.792	21.282	40.035
	0.5	14.133	20.044	30.268	41.643	46.481	47.456
	1.0	21.519	48.156	48.357	73.900	91.431	91.577
	2.0	56.533	80.175	121.07	166.57	185.92	189.82

Table 6.26: Effect of aspect ratios on non-dimensional frequencies of CFFS FG rectangular plates with different k

k	a/b	λ_1	λ_2	λ_3	λ_4	λ_5	λ_6
0.0	0.2	0.7191	2.2904	4.2444	7.0669	11.058	15.516
	0.5	2.1295	7.7475	16.043	17.787	23.394	34.075
	1.0	5.3600	19.084	24.695	43.296	53.523	63.951
	2.0	16.149	31.488	64.178	90.409	111.86	125.67
0.2	0.2	0.6728	2.1429	3.9711	6.6118	10.346	14.517
	0.5	1.9923	7.2486	15.010	16.642	21.887	31.881
	1.0	5.0149	17.855	23.104	40.509	50.077	59.833
	2.0	15.109	29.461	60.045	84.587	104.65	117.58
0.5	0.2	0.6316	2.0117	3.7279	6.2069	9.7122	13.628
	0.5	1.8703	6.8047	14.091	15.623	20.547	29.929
	1.0	4.7078	16.762	21.689	38.028	47.010	56.168
	2.0	14.184	27.657	56.368	79.407	98.244	110.38
1.0	0.2	0.5983	1.9057	3.5315	5.8799	9.2006	12.909
	0.5	1.7718	6.4463	13.349	14.800	19.465	28.352
	1.0	4.4598	15.879	20.547	36.025	44.534	53.210
	2.0	13.437	26.199	53.399	75.225	93.070	104.57
2.0	0.2	0.5719	1.8217	3.3758	5.6208	8.7949	12.341
	0.5	1.6937	6.1621	12.760	14.148	18.606	27.102
	1.0	4.2632	15.179	19.641	34.437	42.571	50.864
	2.0	12.845	25.045	51.045	71.908	88.967	99.956

Table 6.27: Effect of aspect ratios on non-dimensional frequencies of CFSC FG rectangular plates with different k

k	a/b	λ_1	λ_2	λ_3	λ_4	λ_5	λ_6
0.0	0.2	3.9149	5.1154	7.1327	10.339	15.498	22.546
	0.5	6.5737	14.947	25.359	28.404	34.473	49.088
	1.0	17.555	36.034	51.862	71.219	74.486	106.29
	2.0	63.277	80.610	116.82	179.69	201.17	220.07
0.2	0.2	3.6629	47860	6.6735	9.6736	14.500	21.094
	0.5	6.1504	13.985	23.727	26.575	32.253	45.927
	1.0	16.425	33.714	48.523	66.633	69.689	99.451
	2.0	59.202	75.419	109.30	168.12	188.21	205.90
0.5	0.2	3.4385	4.4929	6.2648	9.0811	13.612	19.802
	0.5	5.7737	13.128	22.274	24.947	30.278	43.115
	1.0	15.419	31.649	45.551	62.552	65.421	93.360
	2.0	55.577	708.01	102.61	157.82	176.69	193.29
1.0	0.2	3.2574	4.2563	5.9348	8.6029	12.895	18.759
	0.5	5.4696	12.437	21.101	23.633	28.683	40.844
	1.0	14.607	29.982	43.152	59.258	61.976	88.443
	2.0	52.649	67.072	97.204	149.51	167.38	183.11
2.0	0.2	3.1138	4.0686	5.6731	8.2236	12.327	17.932
	0.5	5.2285	11.889	20.170	22.591	27.418	39.043
	1.0	13.963	28.660	41.249	56.645	59.243	84.544
	2.0	50.328	64.115	92.918	142.92	160.00	175.04

Table 6.28: Effect of aspect ratios on non-dimensional frequencies of CFSS FG rectangular plates with different k

k	a/b	λ_1	λ_2	λ_3	λ_4	λ_5	λ_6
0.0	0.2	1.4901	3.3241	5.7319	9.1991	14.102	16.035
	0.5	5.1514	14.084	19.338	27.776	29.419	44.967
	1.0	16.811	31.125	51.453	64.735	67.766	104.86
	2.0	62.932	77.417	109.68	170.70	201.09	218.09
0.2	0.2	1.3941	3.1101	5.3628	8.6068	13.194	15.003
	0.5	4.8197	13.177	18.093	25.987	27.525	42.071
	1.0	15.729	29.121	48.140	60.566	63.403	98.107
	2.0	58.879	72.432	102.62	159.71	188.14	204.05
0.5	0.2	1.3088	2.9196	5.0344	8.0797	12.386	14.084
	0.5	4.5245	12.369	16.985	24.396	25.839	39.495
	1.0	14.765	27.337	45.192	56.857	59.519	92.098
	2.0	55.274	67.996	96.332	149.93	176.62	191.55
1.0	0.2	1.2398	2.7658	4.7692	7.6541	11.734	13.342
	0.5	4.2862	11.718	16.090	23.111	24.478	37.415
	1.0	13.988	25.898	42.812	53.862	56.385	87.248
	2.0	52.363	64.415	91.258	142.03	167.31	181.47
2.0	0.2	1.1852	2.6439	4.5589	7.3167	11.216	12.754
	0.5	4.0972	11.202	15.381	22.092	23.399	35.765
	1.0	13.371	24.756	40.924	51.488	53.899	83.401
	2.0	50.054	61.575	87.235	135.77	159.94	173.47

Table 6.29: Effect of aspect ratios on non-dimensional frequencies of SSSS FG rectangular plates with different k

k	a/b	λ_1	λ_2	λ_3	λ_4	λ_5	λ_6
0.0	0.2	10.264	11.449	13.495	16.433	28.514	39.874
	0.5	12.337	19.739	32.421	41.947	49.659	50.916
	1.0	19.739	49.349	49.349	79.401	100.17	100.19
	2.0	49.348	78.958	129.68	167.79	198.63	203.66
0.2	0.2	9.6035	10.712	12.626	15.374	26.678	37.307
	0.5	11.543	18.468	30.333	39.246	46.461	47.637
	1.0	18.468	46.171	46.171	74.288	93.723	93.736
	2.0	46.171	73.874	121.33	156.98	185.84	190.55
0.5	0.2	9.0153	10.056	11.853	14.433	25.044	35.022
	0.5	10.836	17.337	28.476	36.842	43.616	44.719
	1.0	17.337	43.344	43.344	69.738	87.983	87.995
	2.0	43.343	69.349	113.90	147.37	174.46	178.88
1.0	0.2	8.5405	9.5260	11.228	13.673	23.725	33.177
	0.5	10.265	16.424	26.976	34.902	41.319	42.364
	1.0	16.424	41.061	41.061	66.065	83.349	83.360
	2.0	41.060	65.697	107.90	139.61	165.27	169.46
2.0	0.2	8.1639	9.1060	10.733	13.069	22.679	31.715
	0.5	9.8125	15.700	25.787	33.363	39.497	40.497
	1.0	15.699	39.251	39.251	63.153	79.674	79.685
	2.0	39.249	62.800	103.15	133.45	157.99	161.99

Table 6.30: Effect of aspect ratios on non-dimensional frequencies of CCCF FG rectangular plates with different k

k	a/b	λ_1	λ_2	λ_3	λ_4	λ_5	λ_6
0.0	0.2	3.9902	5.3684	7.6058	10.729	16.579	22.576
	0.5	7.7876	17.559	25.856	32.359	36.053	51.535
	1.0	23.961	40.019	63.291	76.759	80.689	117.86
	2.0	90.659	104.17	135.11	192.94	247.72	264.23
0.2	0.2	3.7332	5.0227	7.1161	10.039	15.511	21.123
	0.5	7.2861	16.428	24.191	30.275	33.732	48.216
	1.0	22.418	37.443	59.216	71.816	75.494	110.27
	2.0	84.821	97.465	126.41	180.52	231.77	247.22
0.5	0.2	3.5046	4.7151	6.6802	9.4242	14.561	19.829
	0.5	6.8399	15.422	22.709	28.421	31.666	45.263
	1.0	21.045	35.149	55.589	67.418	70.870	103.52
	2.0	79.627	91.496	118.67	169.46	217.57	232.08
1.0	0.2	3.3200	4.4668	6.3284	8.9278	13.794	18.785
	0.5	6.4796	14.609	21.513	26.924	29.998	42.879
	1.0	19.936	33.298	52.662	63.867	67.138	98.063
	2.0	75.433	86.677	112.42	160.54	206.11	219.85
2.0	0.2	3.1737	4.2699	6.0494	8.5342	13.186	17.957
	0.5	6.1939	13.966	20.565	25.737	28.676	40.989
	1.0	19.057	31.830	50.339	61.051	64.178	93.740
	2.0	72.107	82.856	107.46	153.46	197.03	210.16

Table 6.31: Effect of aspect ratios on non-dimensional frequencies of CSCF FG rectangular plates with different k

k	a/b	λ_1	λ_2	λ_3	λ_4	λ_5	λ_6
0.0	0.2	1.6647	3.6854	6.2933	9.6409	15.569	16.067
	0.5	6.6129	16.819	19.958	31.184	31.795	47.634
	1.0	23.412	35.595	62.961	67.356	77.540	111.42
	2.0	90.418	101.66	128.85	182.05	247.69	262.47
0.2	0.2	1.5575	3.4481	5.8880	9.0202	14.567	15.033
	0.5	6.1871	15.736	18.673	29.176	29.748	44.567
	1.0	21.904	33.303	58.907	63.019	72.548	104.24
	2.0	84.596	95.113	120.55	170.33	23.174	245.57
0.5	0.2	14.621	3.2369	5.5274	8.4678	13.675	14.112
	0.5	5.8082	14.772	17.529	27.389	27.926	41.837
	1.0	20.563	31.264	55.299	59.159	68.104	97.857
	2.0	79.415	89.288	113.17	159.89	217.55	230.53
1.0	0.2	1.3851	3.0665	5.2363	8.0218	12.955	13.369
	0.5	5.5023	13.994	16.606	25.947	26.455	39.634
	1.0	19.479	29.617	52.386	56.043	64.517	92.703
	2.0	75.232	84.585	107.21	151.47	206.09	218.39
2.0	0.2	1.3240	2.9313	5.0055	7.6681	12.383	12.779
	0.5	5.2598	13.377	15.874	24.803	25.289	37.886
	1.0	18.621	28.311	50.077	53.572	61.673	88.616
	2.0	71.915	80.856	102.48	144.79	197.00	208.76

After observing Tables 6.8 to 6.31, one may plot the effect of aspect ratios (a/b) and

power-law indices (k) on non-dimensional frequencies of FG rectangular plates under any combination of BCs. Fig. 6.1 depicts the variation of non-dimensional frequencies for clamped rectangular plates with respect to these parameters. It is evident from Fig. 6.1 that non-dimensional frequencies go on increasing with increase in aspect ratios for a fixed power-law index. It is also interesting to note that frequencies are decreasing with increase in power-law indices for a fixed aspect ratio. Similar behavior may also be observed for other BCs.

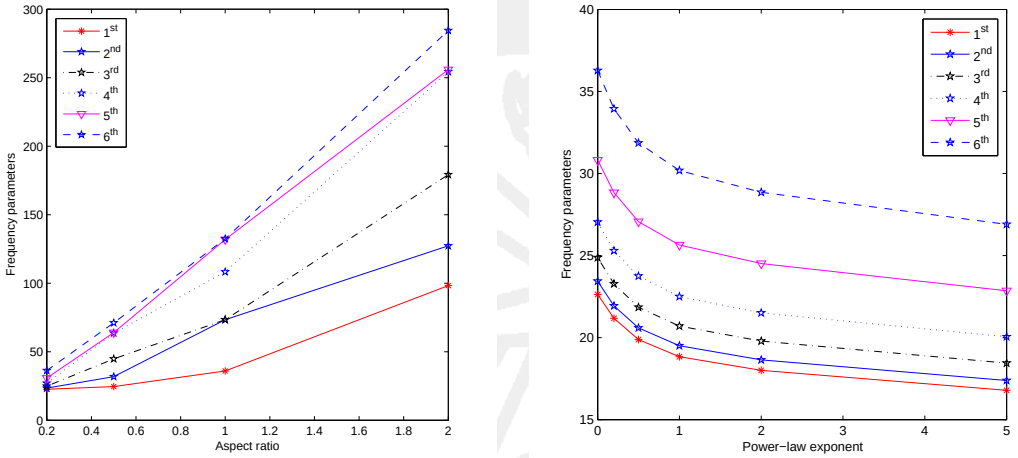

(a) Effect of a/b (b) Effect of k

Figure 6.1: Effect of (a) aspect ratios and (b) power-law indices on non-dimensional frequencies of CCCC FG rectangular plate

First six mode shapes of FG square plates subject to various BCs viz. CCCC, CCCS, CCCF and SSSS, are given in Figs. 6.2 to 6.5 with $k = 0$. With similar BCs, Figs. 6.6 to 6.9 depict first six mode shapes with $k = 0.5$. In a similar way, one may also see the deflected shapes for other sets of BCs.

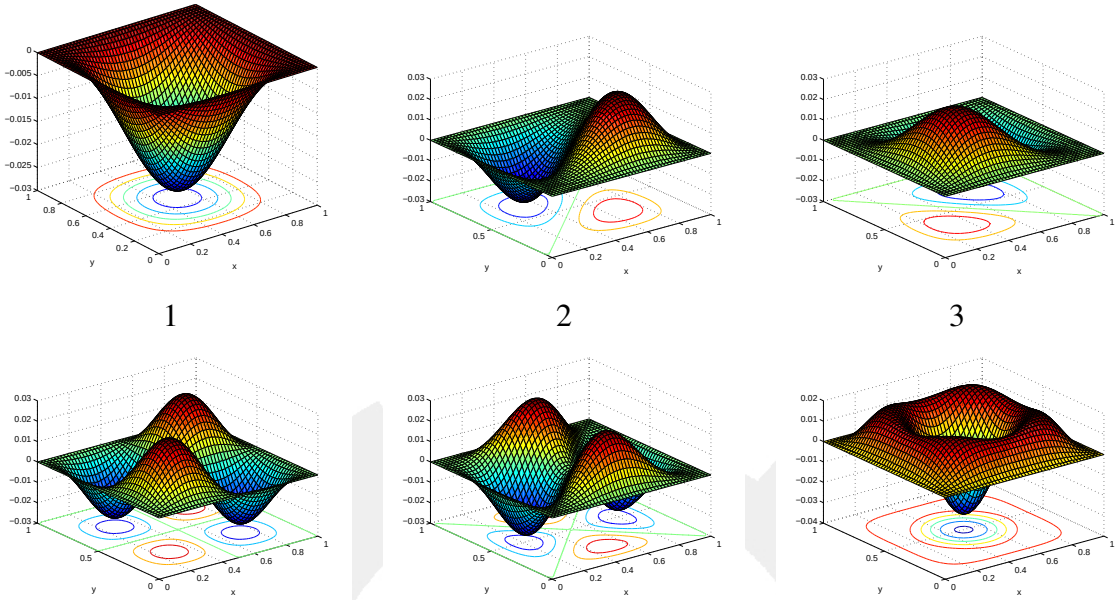

1 2 3

4 5 6

Figure 6.2: First six mode shapes of CCCC FG square plate with $k = 0$

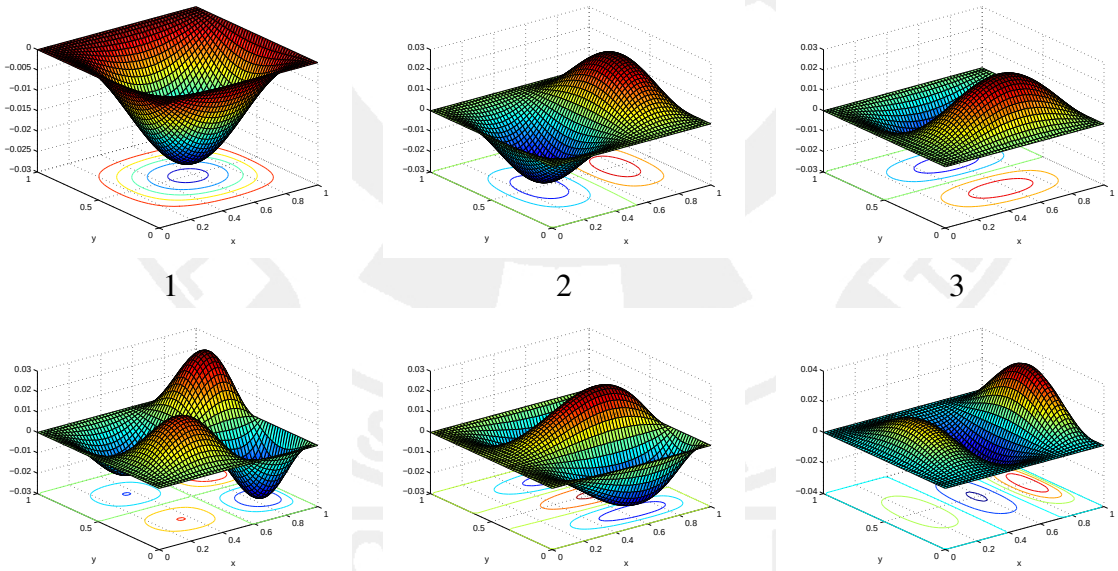

1 2 3

4 5 6

Figure 6.3: First six mode shapes of CCCS FG square plate with $k = 0$

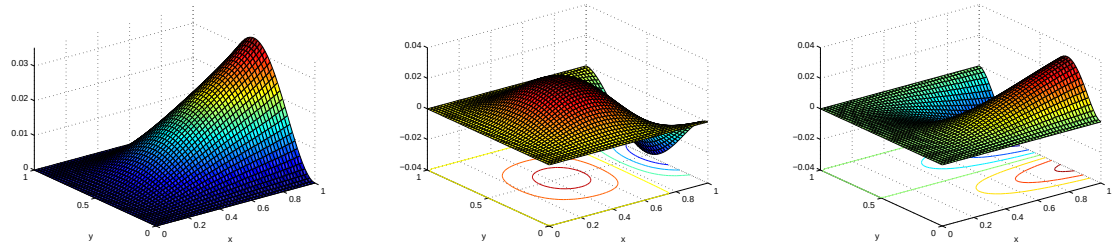

1 2 3

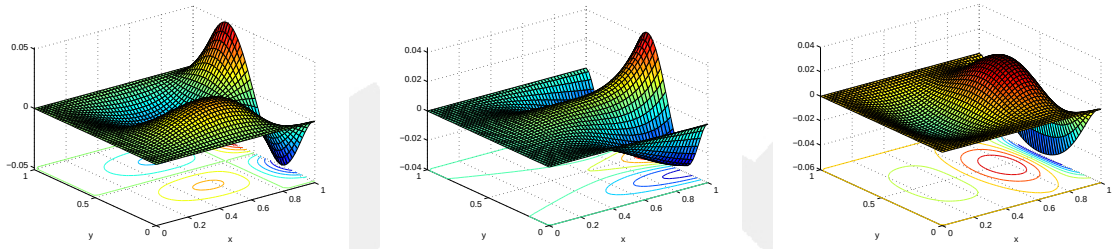

4 5 6

Figure 6.4: First six mode shapes of CCCF FG square plate with $k = 0$

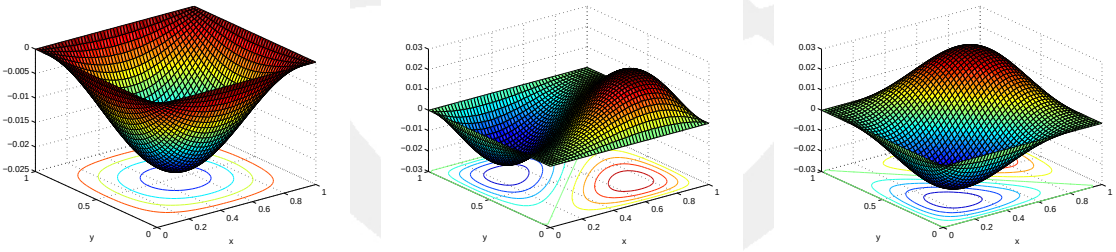

1 2 3

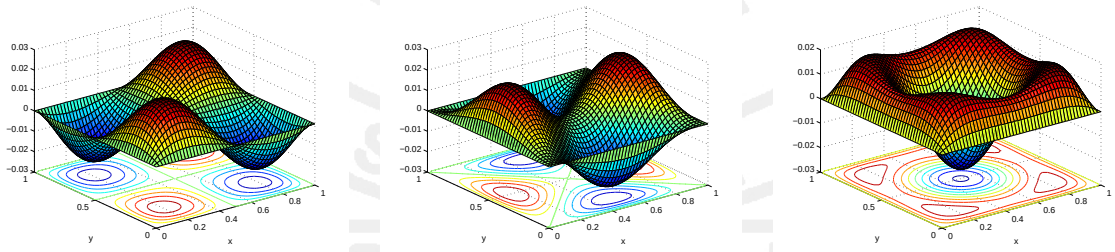

4 5 6

Figure 6.5: First six mode shapes of SSSS FG square plate with $k = 0$

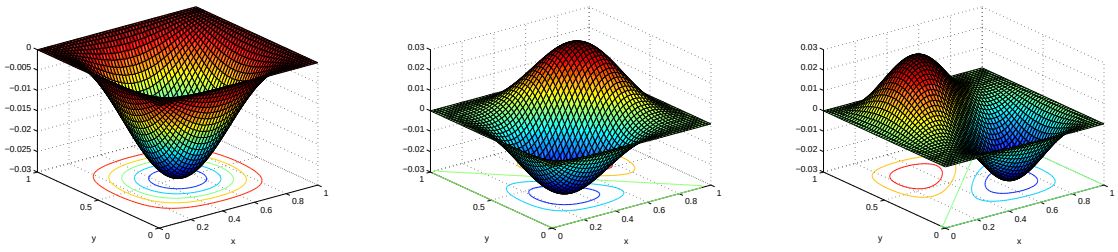

1 2 3

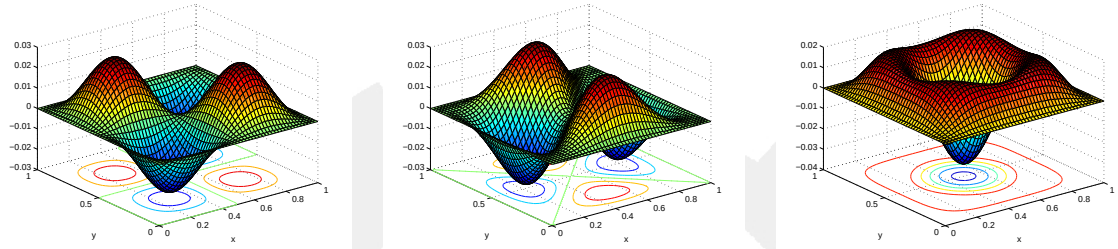

4 5 6

Figure 6.6: First six mode shapes of CCCC FG square plate with $k = 0.5$

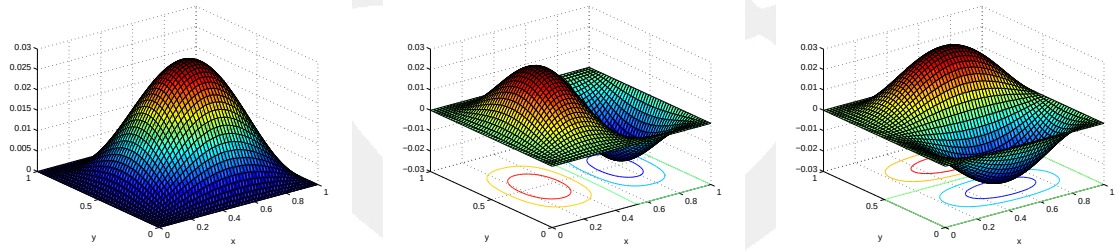

1 2 3

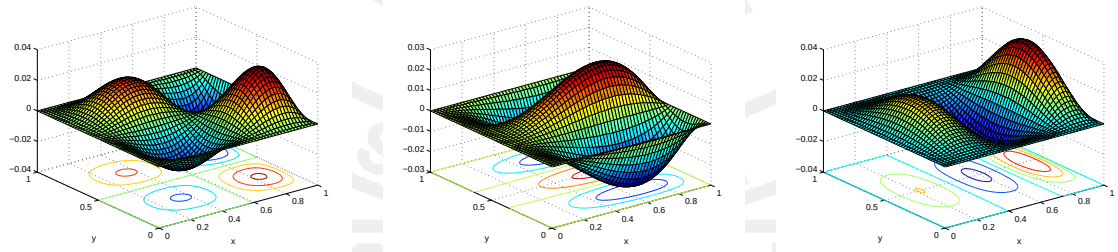

4 5 6

Figure 6.7: First six mode shapes of CCCS FG square plate with $k = 0.5$

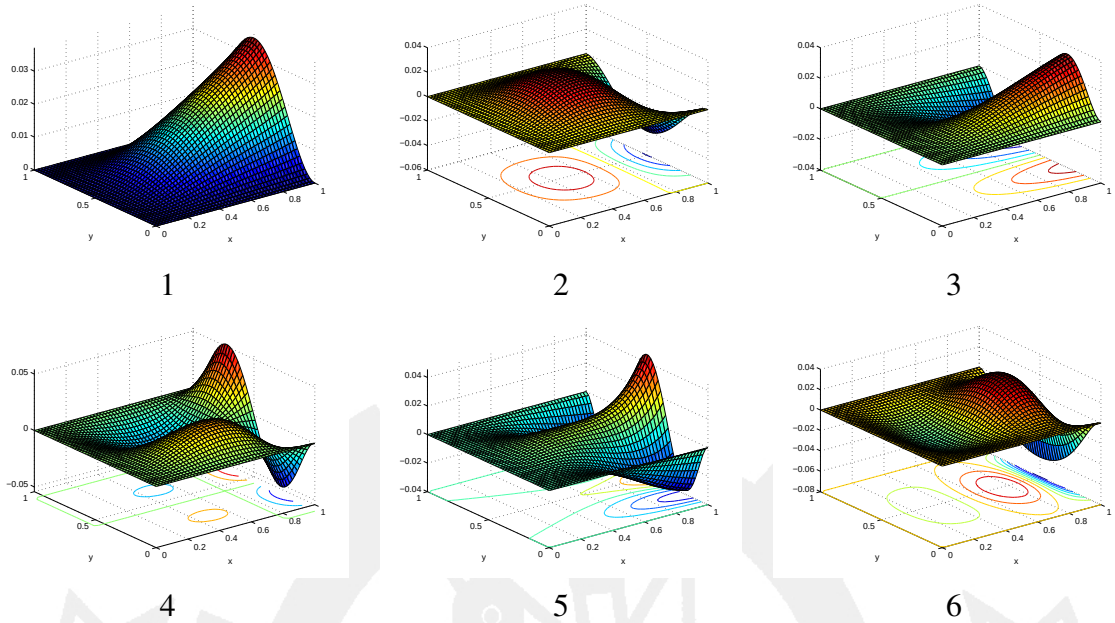

Figure 6.8: First six mode shapes of CCCF FG square plate with $k = 0.5$

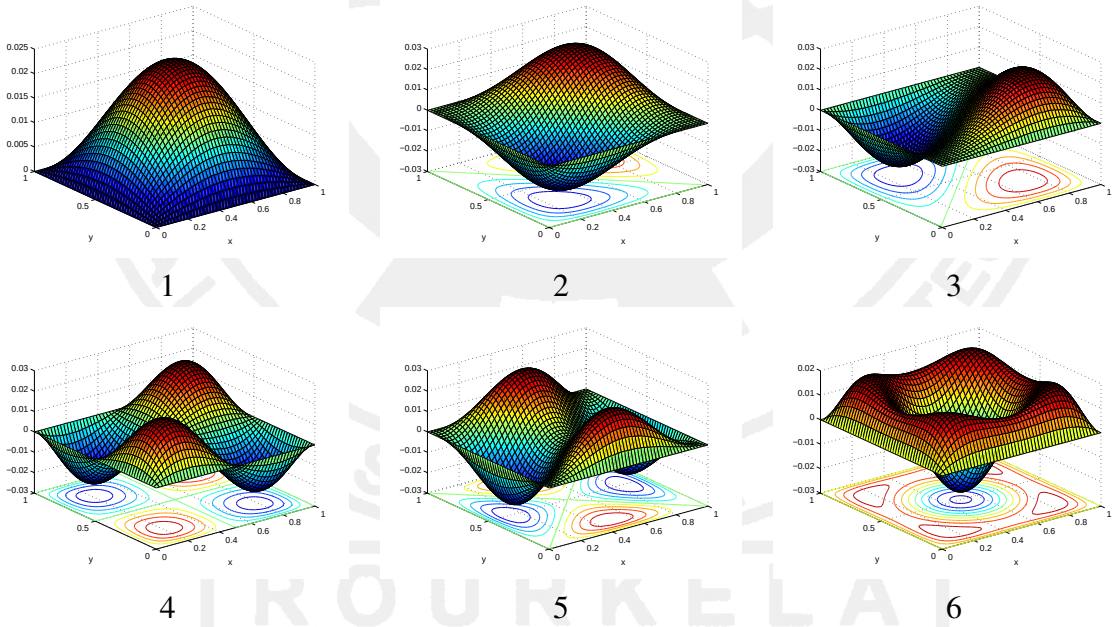

Figure 6.9: First six mode shapes of SSSS FG square plate with $k = 0.5$

Exponential gradation

Now onwards, the natural frequencies of exponential FG plate with 24 possible combinations of boundary conditions have been computed in Table 6.32 with different edge (aspect) ratios viz. $a/b = 0.2, 0.5, 1.0, 2.0, 2.5$. Analyzing results obtained for different edge supports, it may be viewed that the results are increasing with increase in aspect ratios. This fact may be true

because the FG rectangular plate is getting gradually flexible with increase in aspect ratios.

Table 6.32: Effect of aspect ratios on non-dimensional frequencies of exponential FG plate with different combinations of boundary conditions

		Ceramic constituent of Al/Al_2O_3 ($\delta = 0$)						Exponential Al/Al_2O_3 FG plate					
BCs	a/b	λ_1	λ_2	λ_3	λ_4	λ_5	λ_6	λ_1	λ_2	λ_3	λ_4	λ_5	λ_6
CCCC	0.2	17.824	18.459	19.591	21.293	24.269	28.570	15.024	15.559	16.514	17.949	20.458	24.083
	0.5	19.357	25.066	35.296	50.084	50.390	56.008	16.316	21.129	29.752	42.217	42.475	47.210
	1.0	28.342	57.803	57.803	85.261	103.87	104.29	23.890	48.724	48.724	71.868	87.556	87.905
	2.0	77.427	100.26	141.18	200.34	201.56	224.03	65.265	84.515	119.01	168.87	169.90	188.84
	2.5	116.38	136.88	174.46	230.44	310.51	331.93	98.099	115.38	147.06	194.24	261.74	279.79
CCCS	0.2	12.420	13.269	14.729	16.899	20.392	28.283	10.469	11.185	12.416	14.244	17.189	23.840
	0.5	14.450	21.307	32.524	41.457	47.796	48.307	12.181	17.961	27.416	34.945	40.289	40.719
	1.0	25.065	49.881	55.979	79.405	91.779	102.86	21.128	42.046	47.187	66.933	77.364	86.704
	2.0	76.054	95.297	131.62	192.34	200.81	221.07	64.108	80.328	110.94	162.13	169.27	186.34
	2.5	115.37	132.98	166.38	223.12	309.95	310.47	97.247	112.09	140.25	188.07	261.27	261.71
CCSS	0.2	12.397	13.178	14.533	16.626	21.072	39.639	10.449	11.108	12.250	14.015	17.762	33.413
	0.5	13.994	19.846	29.969	41.232	46.022	46.987	11.795	16.729	25.262	34.756	38.793	39.607
	1.0	21.306	47.681	47.879	73.171	90.528	90.673	17.959	40.191	40.359	61.678	76.309	76.431
	2.0	55.975	79.384	119.88	164.93	184.09	187.95	47.183	66.915	101.05	139.02	155.17	158.43
	2.5	82.925	105.13	144.09	206.27	253.32	275.85	69.899	88.618	121.46	173.87	213.53	232.53
CCFF	0.2	2.8455	3.4662	4.6581	6.6611	9.9880	17.390	2.3985	2.9217	3.9264	5.6148	8.4191	14.666
	0.5	3.3783	7.1716	14.492	17.917	22.746	27.608	2.8476	6.0451	12.216	15.103	19.173	23.271
	1.0	5.4626	18.859	20.950	37.614	49.524	51.805	4.6046	15.897	17.659	31.706	41.745	43.668
	2.0	13.513	28.686	57.967	71.669	90.983	110.43	11.391	24.180	48.862	60.412	76.692	93.085
	2.5	19.597	35.148	64.339	109.07	117.08	130.50	16.519	29.627	54.233	91.935	98.686	110.00
CFCF	0.2	0.6907	1.8975	2.2735	3.7425	4.7072	6.2334	0.5822	1.5995	1.9164	3.1547	3.9678	5.2543
	0.5	4.3539	7.0912	11.989	16.309	21.785	23.679	3.6700	5.9774	10.106	13.747	18.363	19.959
	1.0	17.502	20.852	34.708	48.248	53.275	64.776	14.753	17.576	29.256	40.669	44.907	54.602
	2.0	70.230	73.798	87.423	114.67	193.72	199.20	59.199	62.206	73.692	96.659	163.29	167.92
	2.5	109.82	113.39	127.02	153.44	258.69	302.94	92.568	95.578	107.07	129.34	218.07	255.36
CFSF	0.2	0.4710	1.5277	2.1591	3.2077	4.4666	5.8671	0.3970	1.2878	1.8200	2.7038	3.7650	4.9456
	0.5	2.9711	6.1647	9.6692	14.413	20.353	21.363	2.5044	5.1964	8.1504	12.149	17.156	18.007
	1.0	11.984	16.234	31.666	39.008	44.629	63.238	10.102	13.684	26.693	32.881	37.619	53.305
	2.0	48.238	52.989	69.830	102.23	156.92	162.95	40.661	44.667	58.862	86.175	132.27	137.36
	2.5	75.483	80.288	97.580	130.38	242.74	245.64	63.627	67.677	82.253	109.89	204.61	207.05
CFFF	0.2	0.1080	0.6734	1.0726	1.8875	3.2859	3.9726	0.0910	0.5676	0.9041	1.5911	2.7698	3.3486

	0.5	0.6808	2.9177	4.2303	9.5320	11.888	18.570	0.5738	2.4594	3.5658	8.0348	10.021	15.653
	1.0	2.7457	6.7112	16.794	21.717	24.526	43.705	2.3144	5.6570	14.156	18.306	20.674	36.840
	2.0	11.041	16.902	32.543	62.634	68.992	78.866	9.3065	14.247	27.431	52.796	58.156	66.478
	2.5	17.267	23.533	40.323	70.959	107.66	117.13	14.555	19.836	33.989	59.813	90.747	98.732
SCSC	0.2	17.792	18.331	19.311	20.853	27.891	37.204	14.997	15.452	16.278	17.578	23.510	31.360
	0.5	18.755	22.799	30.989	44.215	50.034	54.632	15.809	19.218	26.122	37.269	42.175	46.051
	1.0	22.799	43.112	54.596	74.580	81.679	101.84	19.218	36.340	46.021	62.866	68.849	85.839
	2.0	43.111	74.487	122.04	134.16	163.28	185.60	36.339	62.787	102.87	113.09	137.63	156.45
	2.5	59.727	90.391	137.79	201.39	203.69	232.24	50.345	76.193	116.15	169.76	171.69	195.76
SCSS	0.2	12.376	13.095	14.362	16.657	24.523	36.826	10.432	11.038	12.106	14.041	20.671	31.041
	0.5	13.649	18.623	27.835	41.031	42.956	46.215	11.505	15.698	23.463	34.586	36.209	38.956
	1.0	18.622	40.705	46.188	67.919	80.174	89.286	15.697	34.311	38.933	57.251	67.581	75.261
	2.0	40.694	67.836	111.02	133.14	159.35	177.29	34.302	57.181	93.585	112.23	134.32	149.44
	2.5	57.835	84.600	127.67	193.64	202.97	229.04	48.750	71.312	107.62	163.22	171.09	193.06
SCSF	0.2	3.0361	3.8593	5.3156	7.6423	17.728	17.783	2.5592	3.2531	4.4806	6.4419	14.943	14.989
	0.5	4.4919	9.9930	19.644	19.791	26.067	34.827	3.7863	8.4233	16.559	16.683	21.973	29.356
	1.0	9.9915	26.039	32.851	49.818	57.032	72.870	8.4221	21.949	27.691	41.993	48.074	61.424
	2.0	32.842	49.627	81.274	125.56	133.73	143.24	27.683	41.832	68.508	105.84	112.72	120.74
	2.5	50.152	66.961	98.972	151.77	195.33	213.48	42.275	56.444	83.426	127.93	164.65	179.95
SSSF	0.2	1.0591	2.3691	4.1472	6.5860	12.592	13.936	0.8928	1.9970	3.4958	5.5515	10.614	11.747
	0.5	3.1766	9.2034	14.822	19.220	21.939	33.191	2.6776	7.7578	12.494	16.201	18.494	27.977
	1.0	9.2018	21.859	32.462	46.747	49.189	72.507	7.7564	18.426	27.363	39.404	41.463	61.118
	2.0	32.445	46.522	74.986	123.32	125.49	141.15	27.349	39.215	63.208	103.95	105.78	118.98
	2.5	49.845	64.283	93.376	142.81	195.37	211.54	42.016	54.186	78.709	120.38	164.69	178.31
SFSF	0.2	0.2972	1.1951	2.0510	2.7607	4.2458	5.0731	0.2505	1.0074	1.7289	2.3271	3.5789	4.2763
	0.5	1.8728	5.4185	7.5860	12.800	17.621	20.974	1.5786	4.5674	6.3945	10.789	14.853	17.679
	1.0	7.5851	12.707	29.280	30.691	37.234	56.743	6.3937	10.711	24.681	25.870	31.386	47.830
	2.0	30.683	36.817	56.582	90.338	123.71	131.31	25.864	31.034	47.694	76.149	104.28	110.69
	2.5	48.076	54.351	75.298	110.35	193.62	201.62	40.524	45.814	63.470	93.017	163.21	169.95
SSFF	0.2	0.5115	1.6366	3.0719	5.2221	11.623	12.331	0.4311	1.3795	2.5893	4.4018	9.7975	10.394
	0.5	1.3080	4.9964	11.671	12.865	17.624	23.622	1.1026	4.2116	9.8381	10.844	14.855	19.912
	1.0	2.6516	13.639	15.199	30.247	40.676	42.669	2.2351	11.497	12.811	25.496	34.287	35.967
	2.0	5.2321	19.985	46.685	51.461	70.494	94.488	4.4103	16.846	39.352	43.378	59.421	79.647
	2.5	6.4949	23.286	51.303	77.812	96.479	101.57	5.4747	19.628	43.245	65.589	81.325	85.612
SFFF	0.2	0.4644	1.0167	1.5312	3.1175	3.3623	5.5602	0.3915	0.8570	1.2907	2.6278	2.8341	4.6869
	0.5	2.5675	2.9229	8.4955	9.7022	17.099	18.296	2.1642	2.4638	7.1611	8.1782	14.413	15.422
	1.0	5.2326	11.739	20.185	20.709	39.009	40.869	4.4107	9.8954	17.015	17.457	32.881	34.449
	2.0	10.607	27.808	48.202	55.396	62.704	85.923	8.9411	23.440	40.630	46.695	52.855	72.427

	2.5	13.238	32.406	64.151	75.178	86.535	115.42	11.158	27.316	54.074	63.369	72.943	97.293
FFFF	0.2	0.6802	1.9284	2.0528	4.2735	6.7357	8.8357	0.5733	1.6255	1.7304	3.6022	5.6777	7.4478
	0.5	4.2691	5.3007	11.874	12.122	17.566	20.833	3.5985	4.4681	10.009	10.218	14.806	17.560
	1.0	10.800	15.573	19.338	28.033	28.033	49.754	9.1037	13.127	16.301	23.629	23.629	41.939
	2.0	17.067	21.203	47.497	48.489	70.262	83.331	14.394	17.872	40.036	40.873	59.226	70.242
	2.5	17.076	26.246	48.536	57.468	109.12	122.72	14.386	22.123	40.912	48.441	91.977	103.44
SFSC	0.2	3.0361	3.8593	5.3156	7.6423	17.728	17.783	2.5592	3.2531	4.4806	6.4419	14.943	14.989
	0.5	4.4919	9.9930	19.644	19.791	26.067	34.827	3.7863	8.4233	16.559	16.683	21.973	29.356
	1.0	9.9915	26.039	32.851	49.818	57.032	72.870	8.4221	21.949	27.691	41.993	48.074	61.424
	2.0	32.842	49.627	81.274	125.56	133.73	143.24	27.683	41.832	68.508	105.84	112.72	120.74
	2.5	50.152	66.961	98.972	151.77	195.33	213.48	42.275	56.444	83.426	127.93	164.65	179.95
SCCC	0.2	17.807	18.393	19.436	21.119	23.698	42.702	15.010	15.504	16.383	17.802	19.976	35.995
	0.5	19.013	23.824	32.904	48.085	50.204	55.267	16.027	20.082	27.736	40.532	42.318	46.586
	1.0	25.065	49.881	55.979	79.406	91.779	102.86	21.128	42.046	47.187	66.933	77.364	86.704
	2.0	57.802	85.229	130.09	165.83	191.19	193.23	48.723	71.842	109.66	139.78	161.16	162.88
	2.5	84.302	109.95	153.12	214.99	254.01	278.29	71.060	92.682	129.07	181.22	214.11	234.58
SCCS	0.2	12.397	13.178	14.533	16.626	21.072	39.639	10.449	11.108	12.250	14.015	17.762	33.413
	0.5	13.994	19.846	29.969	41.232	46.022	46.987	11.796	16.729	25.262	34.756	38.793	39.607
	1.0	21.306	47.681	47.879	73.171	90.528	90.673	17.959	40.191	40.359	61.678	76.309	76.431
	2.0	55.975	79.384	119.88	164.93	184.09	187.95	47.183	66.915	101.05	139.02	155.17	158.43
	2.5	82.925	105.13	144.09	206.27	253.32	275.85	69.899	88.618	121.46	173.87	213.53	232.53
CFFS	0.2	0.5663	1.8037	3.3425	5.5653	8.7082	12.219	0.4774	1.5204	2.8175	4.6911	7.3403	10.299
	0.5	1.6770	6.1013	12.634	14.008	18.423	26.835	1.4136	5.1429	10.649	11.808	15.529	22.619
	1.0	4.2211	15.029	19.447	34.097	42.151	50.362	3.5581	12.668	16.393	28.741	35.529	42.452
	2.0	12.718	24.798	50.541	71.198	88.088	98.969	10.720	20.903	42.602	60.015	74.252	83.424
	2.5	18.954	31.535	57.343	102.98	111.54	128.70	15.977	26.582	48.336	86.807	94.023	108.48
CFSC	0.2	3.0831	4.0285	5.6171	8.1424	12.205	17.755	2.5988	3.3957	4.7348	6.8634	10.288	14.966
	0.5	5.1769	11.771	19.971	22.368	27.148	38.658	4.3637	9.9223	16.834	18.855	22.884	32.586
	1.0	13.825	28.377	40.842	56.086	58.659	83.709	11.654	23.920	34.427	47.276	49.445	70.561
	2.0	49.831	63.482	92.001	141.51	158.42	173.31	42.004	53.511	77.550	119.28	133.54	146.09
	2.5	77.008	90.308	118.09	166.24	246.70	251.23	64.912	76.123	99.539	140.13	207.95	211.77
CFSS	0.2	1.1735	2.6178	4.5139	7.2444	11.106	12.628	0.9892	2.2066	3.8049	6.1065	9.3613	10.644
	0.5	4.0568	11.091	15.229	21.874	23.168	35.412	3.4196	9.3490	12.837	18.438	19.529	29.849
	1.0	13.239	24.511	40.520	50.979	53.367	82.578	11.159	20.661	34.156	42.972	44.985	69.607
	2.0	49.559	60.967	86.374	134.43	158.36	171.75	41.775	51.391	72.807	113.31	133.48	144.78
	2.5	76.803	88.233	113.33	161.24	246.83	260.38	64.739	74.374	95.529	135.92	208.06	219.48
SSSS	0.2	8.0834	9.0161	10.628	12.941	22.455	31.402	6.8137	7.6000	8.9582	10.908	18.928	26.469
	0.5	9.7156	15.545	25.532	33.034	39.107	40.097	8.1895	13.103	21.522	27.845	32.964	33.799

	1.0	15.545	38.863	38.863	62.529	78.888	78.899	13.103	32.759	32.759	52.708	66.497	66.506
	2.0	38.862	62.180	102.13	132.13	156.43	160.39	32.758	52.414	86.087	111.38	131.86	135.19
	2.5	56.350	79.669	119.59	177.75	202.09	226.85	47.499	67.155	100.81	149.83	170.35	191.22
CCCF	0.2	3.1423	4.2277	5.9897	8.4500	13.056	17.779	2.6487	3.5636	5.0489	7.1227	11.005	14.987
	0.5	6.1328	13.828	20.362	25.483	28.392	40.584	5.1695	11.656	17.164	21.480	23.933	34.209
	1.0	18.869	31.516	49.843	60.449	63.544	92.815	15.905	26.566	42.014	50.954	53.563	78.236
	2.0	71.395	82.038	106.40	151.94	195.08	208.09	60.181	69.152	89.690	128.08	164.44	175.40
	2.5	110.93	121.09	143.87	186.19	256.03	304.19	93.509	102.07	121.27	156.95	215.82	256.41
CSCF	0.2	1.3110	2.9023	4.9560	7.5924	12.261	12.653	1.1050	2.4464	4.1776	6.3998	10.335	10.666
	0.5	5.2078	13.245	15.717	24.558	25.039	37.512	4.3898	11.165	13.249	20.701	21.106	31.620
	1.0	18.437	28.032	49.582	53.044	61.064	87.741	15.541	23.629	41.794	44.712	51.473	73.959
	2.0	71.205	80.058	101.47	143.37	195.06	206.69	60.021	67.483	85.530	120.85	164.42	174.23
	2.5	110.79	119.51	139.85	179.91	304.26	315.98	93.388	100.73	117.88	151.65	256.47	266.35

First six mode shapes of clamped FG rectangular plate are given in Figs. 6.10 and 6.11 with different aspect ratios viz. a/b = 0.2, 0.5, 1.0 and 2.0. Deflections of 3D mode shapes are depicted in different directions with the variation of a/b. Similarly, 3D mode shapes for other boundary supports can also be presented.

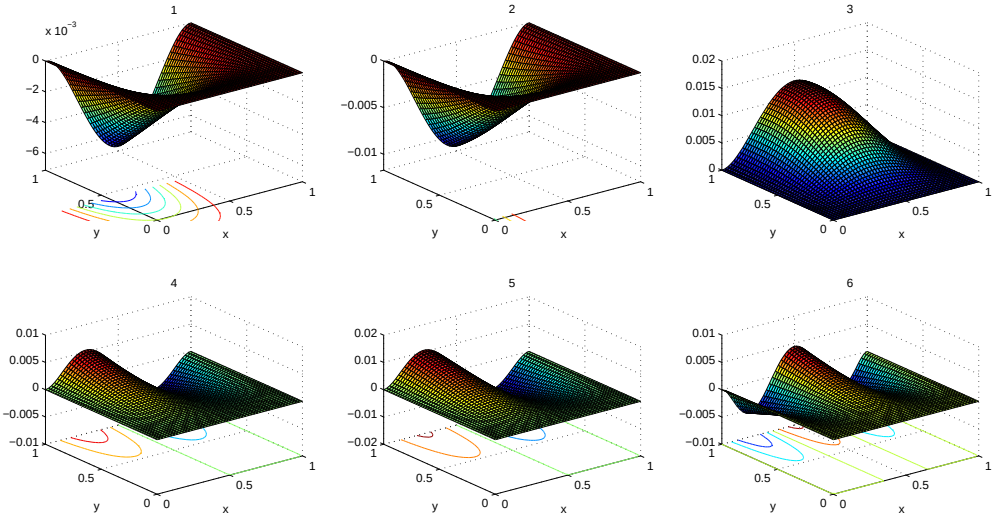

(a) $a/b = 0.2$

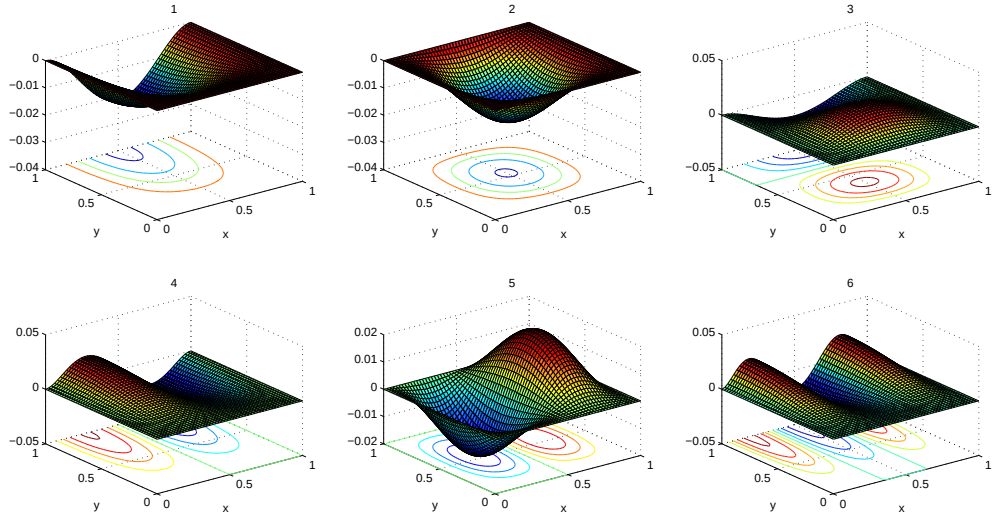

(b) $a/b = 0.5$

Figure 6.10: First six mode shapes of CCCC FG rectangular plate with different $a/b = 0.2, 0.5$

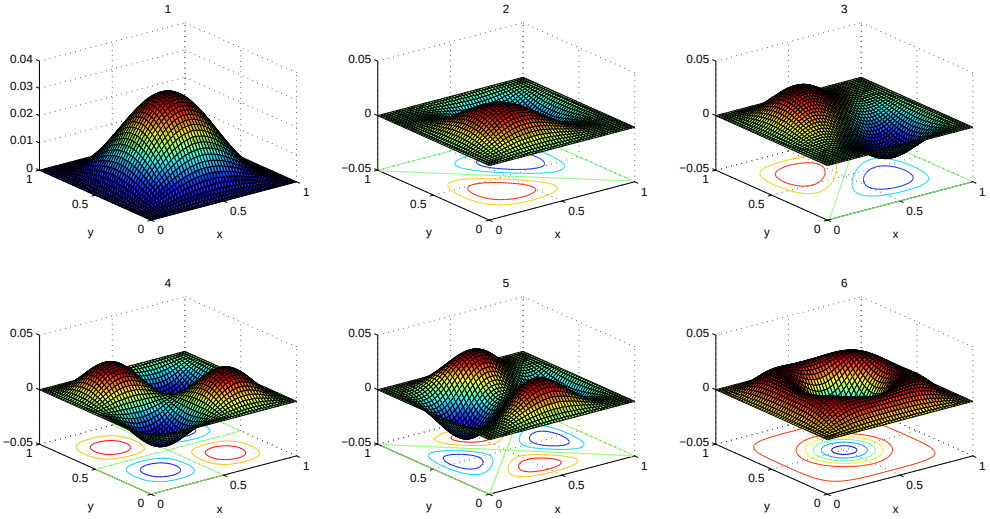

(a) $a/b = 1.0$

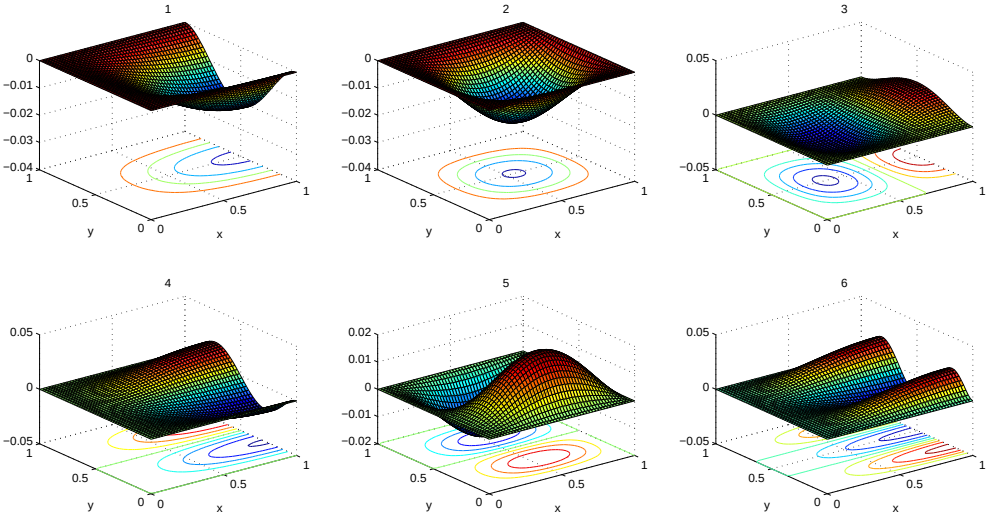

(b) $a/b = 2.0$

Figure 6.11: First six mode shapes of CCCC FG rectangular plate with different $a/b = 1.0, 2.0$

Effect of $E_{rat}\,(= E_c/E_m)$ with constant $\rho_{rat}\,(= \rho_c/\rho_m)$

In Tables 6.33 to 6.38, the effect of E_{rat} on frequencies of exponential FG rectangular plate subject to various edge supports are tabulated with constant $\rho_{rat} = 1$. In Table 6.33, frequencies of FG plate with the variation of E_{rat} viz. $E_{rat} = 0.25$, 0.5, 1.0 and 2.0 are evaluated with a fixed aspect ratio. In a similar fashion, the effect of E_{rat} on the frequencies are also computed in Tables 6.34 to 6.38 with different BCs viz. CCCS, CCSS, CCCF, SSSS, FFFF. It is worth to mention that natural frequencies are decreasing with increase in E_{rat} irrespective of aspect ratio and BC considered. It can be found in the expression of natural frequency that it is inversely

proportional to the Young's modulus of the ceramic constituent of FG rectangular plate and hence this behavior with increase in E_{rat} may in fact be true.

Table 6.33: Effect of E_{rat} on non-dimensional frequencies of CCCC exponential FG rectangular plates

Aspect ratio	E_{rat}	λ_1	λ_2	λ_3	λ_4	λ_5	λ_6
	0.25	34.299	35.522	37.699	40.976	46.704	54.979
	0.5	27.399	28.376	30.116	32.733	37.308	43.919
0.2	1.0	22.633	23.440	24.877	27.039	30.818	36.279
	2.0	19.374	20.065	21.295	23.146	26.381	31.056
	4.0	17.149	17.761	18.849	20.488	23.352	27.489
	0.25	37.249	48.236	67.921	96.379	96.969	107.78
	0.5	29.756	38.532	54.258	76.991	77.462	86.097
0.5	1.0	24.579	31.829	44.819	63.598	63.986	71.119
	2.0	21.041	27.246	38.366	54.441	54.774	60.879
	4.0	18.625	24.118	33.961	48.189	48.484	53.889
	0.25	54.539	111.23	111.23	164.07	199.89	200.68
	0.5	43.568	88.856	88.856	131.07	159.68	160.31
1.0	1.0	35.989	73.399	73.399	108.27	131.89	132.42
	2.0	30.807	62.831	62.831	92.677	112.91	113.36
	4.0	27.269	55.617	55.617	82.036	99.943	100.34
	0.25	148.99	192.94	271.69	385.52	387.88	431.12
	0.5	119.02	154.13	217.03	307.96	309.85	344.39
2.0	1.0	98.318	127.32	179.28	254.39	255.95	284.48
	2.0	84.162	108.99	153.46	217.76	219.09	243.52
	4.0	74.498	96.472	135.84	192.76	193.94	215.56

Table 6.34: Effect of E_{rat} on non-dimensional frequencies of CCCS exponential FG rectangular plates

Aspect ratio	E_{rat}	λ_1	λ_2	λ_3	λ_4	λ_5	λ_6
	0.25	23.901	25.535	28.345	32.519	39.242	54.426
	0.5	19.093	20.398	22.643	25.977	31.347	43.477
0.2	1.0	15.771	16.849	18.704	21.458	25.894	35.914
	2.0	13.500	14.424	16.011	18.369	22.166	30.743
	4.0	11.950	12.767	14.173	16.259	19.621	27.213
	0.25	27.808	41.003	62.588	79.778	91.977	92.960
	0.5	22.214	32.754	49.997	63.729	73.474	74.259
0.5	1.0	18.349	27.056	41.299	52.643	60.693	61.341
	2.0	15.707	23.161	35.353	45.063	51.954	52.509
	4.0	13.904	20.502	31.294	39.889	45.989	46.480
	0.25	48.234	95.989	107.72	152.80	176.62	197.94
	0.5	38.531	76.679	86.053	122.06	141.09	158.12
1.0	1.0	31.828	63.339	71.084	100.83	116.54	130.61
	2.0	27.245	54.220	60.849	86.313	99.763	111.81
	4.0	24.117	47.995	53.862	76.402	88.308	98.969
	0.25	146.35	183.39	253.28	370.13	386.44	425.41
	0.5	116.91	146.49	202.33	295.67	308.69	339.83
2.0	1.0	96.574	121.01	167.13	244.24	254.99	280.71
	2.0	82.669	103.59	143.07	209.07	218.28	240.29
	4.0	73.177	91.693	126.64	185.06	193.22	212.71

Table 6.35: Effect of E_{rat} on non-dimensional frequencies of CCSS exponential FG rectangular plates

Aspect ratio	E_{rat}	λ_1	λ_2	λ_3	λ_4	λ_5	λ_6
	0.25	23.856	25.359	27.967	31.994	40.550	76.281
	0.5	19.057	20.258	22.341	25.558	32.393	60.935
0.2	1.0	15.742	16.734	18.454	21.112	26.758	50.335
	2.0	13.475	14.325	15.797	18.072	22.905	43.088
	4.0	11.928	12.679	13.983	15.997	20.275	38.140
	0.25	26.929	38.191	57.672	79.345	88.562	90.421
	0.5	21.512	30.508	46.070	63.383	70.746	72.231
0.5	1.0	17.769	25.201	38.056	52.357	58.439	59.665
	2.0	15.211	21.572	32.576	44.819	50.025	51.075
	4.0	13.465	19.095	28.836	39.673	44.281	45.210
	0.25	41.001	91.755	92.137	140.81	174.21	174.49
	0.5	32.753	73.296	73.602	112.48	139.16	139.39
1.0	1.0	27.055	60.546	60.798	92.914	114.95	115.14
	2.0	23.159	51.828	52.044	79.536	98.403	98.560
	4.0	20.501	45.877	46.068	70.403	87.104	87.243
	0.25	107.72	152.76	230.69	317.38	354.25	361.68
	0.5	86.047	122.03	184.28	253.53	282.98	288.92
2.0	1.0	71.079	100.80	152.22	209.43	233.76	238.66
	2.0	60.845	86.289	130.31	179.27	200.10	204.29
	4.0	53.858	76.381	115.34	158.69	177.12	180.84

Table 6.36: Effect of E_{rat} on non-dimensional frequencies of CCCF exponential FG rectangular plates

Aspect ratio	E_{rat}	λ_1	λ_2	λ_3	λ_4	λ_5	λ_6
	0.25	6.0469	8.1356	11.526	16.261	25.124	34.214
	0.5	4.8305	6.4989	9.2075	12.989	20.070	27.331
0.2	1.0	3.9902	5.3684	7.6058	10.729	16.579	22.576
	2.0	3.4157	4.5955	6.5107	9.1850	14.192	19.326
	4.0	3.0235	4.0678	5.7631	8.1304	12.562	17.107
	0.25	11.802	26.609	39.183	49.038	54.637	78.099
	0.5	9.4276	21.257	31.301	39.173	43.646	62.387
0.5	1.0	7.7876	17.559	25.856	32.359	36.053	51.535
	2.0	6.6663	15.031	22.133	27.699	30.862	44.115
	4.0	5.9009	13.305	19.592	24.519	27.319	39.049
	0.25	36.311	60.648	95.916	116.32	122.28	178.61
	0.5	29.007	48.447	76.620	92.924	97.682	142.68
1.0	1.0	23.961	40.019	63.291	76.759	80.689	117.86
	2.0	20.511	34.257	54.179	65.707	69.072	100.89
	4.0	18.156	30.324	47.958	58.162	61.141	89.304
	0.25	137.39	157.87	204.76	292.39	375.40	400.43
	0.5	109.75	126.11	163.57	233.57	299.88	319.86
2.0	1.0	90.659	104.17	135.11	192.94	247.72	264.23
	2.0	77.606	89.174	115.66	165.16	212.05	226.19
	4.0	68.695	78.935	102.38	146.19	187.70	200.22

Table 6.37: Effect of E_{rat} on non-dimensional frequencies of SSSS exponential FG rectangular plates

Aspect ratio	E_{rat}	λ_1	λ_2	λ_3	λ_4	λ_5	λ_6
	0.25	15.555	17.350	20.451	24.903	43.211	60.428
	0.5	12.426	13.859	16.337	19.893	34.519	48.271
0.2	1.0	10.264	11.449	13.495	16.433	28.514	39.874
	2.0	8.7865	9.8004	11.552	14.067	24.408	34.133
	4.0	7.7776	8.6751	10.226	12.451	21.606	30.214
	0.25	18.696	29.914	49.133	63.569	75.256	77.160
	0.5	14.935	23.896	39.249	50.781	60.117	61.638
0.5	1.0	12.337	19.739	32.421	41.947	49.659	50.916
	2.0	10.561	16.897	27.753	35.907	42.509	43.585
	4.0	9.3481	14.957	24.566	31.784	37.628	38.580
	0.25	29.914	74.786	74.786	120.33	151.81	151.83
	0.5	23.896	59.742	59.742	96.122	121.27	121.29
1.0	1.0	19.739	49.349	49.349	79.401	100.17	100.19
	2.0	16.897	42.244	42.244	67.969	85.749	85.762
	4.0	14.957	37.393	37.393	60.164	75.904	75.915
	0.25	74.785	119.66	196.53	254.27	301.02	308.64
	0.5	59.740	95.586	156.99	203.12	240.47	246.55
2.0	1.0	49.348	78.958	129.68	167.79	198.63	203.66
	2.0	42.243	67.589	111.01	143.63	170.04	174.34
	4.0	37.392	59.829	98.265	127.14	150.51	154.32

Table 6.38: Effect of E_{rat} on non-dimensional frequencies of FFFF exponential FG rectangular plates

Aspect ratio	E_{rat}	λ_1	λ_2	λ_3	λ_4	λ_5	λ_6
	0.25	1.3089	3.7109	3.9503	8.2237	12.962	17.003
	0.5	1.0456	2.9643	3.1556	6.5693	10.354	13.583
0.2	1.0	0.8637	2.4487	2.6067	5.4265	8.5531	11.219
	2.0	0.7393	2.0961	2.2314	4.6452	7.3216	9.6043
	4.0	0.6544	1.8554	1.9751	4.1118	6.4809	8.5015
	0.25	8.2152	10.201	22.850	23.328	33.802	40.089
	0.5	6.5626	8.1484	18.254	18.635	27.002	32.025
0.5	1.0	5.4209	6.7309	15.078	15.393	22.305	26.454
	2.0	4.6404	5.7618	12.907	13.177	19.094	22.645
	4.0	4.1076	5.1002	11.425	11.664	16.901	20.045
	0.25	20.783	29.967	37.214	53.946	53.946	95.745
	0.5	16.602	23.939	29.728	43.093	43.093	76.484
1.0	1.0	13.714	19.774	24.556	35.597	35.597	63.179
	2.0	11.739	16.927	21.021	30.472	30.472	54.082
	4.0	10.392	14.984	18.607	26.973	26.973	47.872
	0.25	32.861	40.802	91.401	93.310	135.21	160.36
	0.5	26.250	32.594	73.014	74.539	108.01	128.09
2.0	1.0	21.684	26.924	60.312	61.572	89.219	105.81
	2.0	18.562	23.047	51.629	52.707	76.374	90.579
	4.0	16.430	20.401	45.701	46.655	67.605	80.179

Accordingly, first six mode shapes of CCCC FG square plate ($a/b = 1$) with different E_{rat} viz. $E_{rat} = 0.25$, 0.5, 1.0 and 2.0 are demonstrated in Figs. 6.12 and 6.13. It is interesting to note here that respective 3D mode shapes are quite similar, but deflections are occurred in different directions for higher modes.

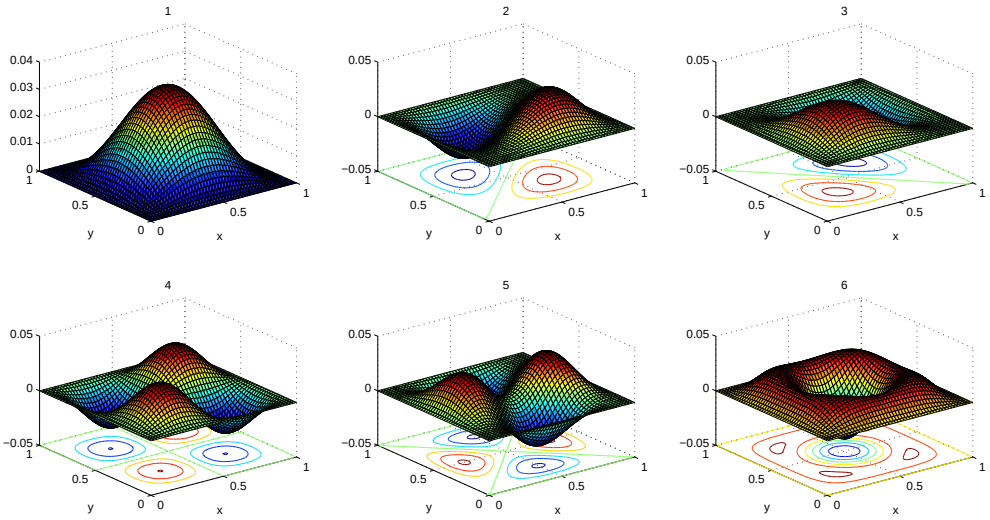

(a) $E_{rat} = 0.25$

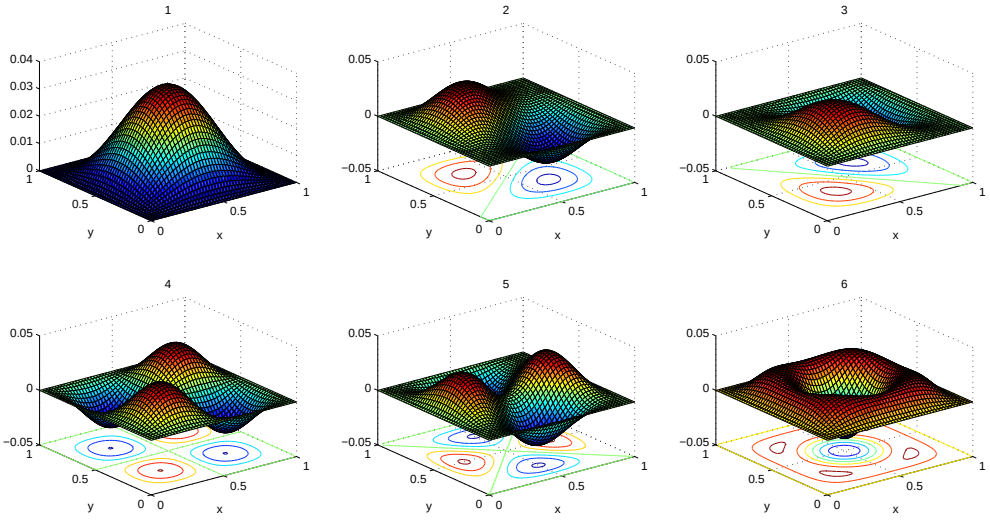

(b) $E_{rat} = 0.5$

Figure 6.12: First six mode shapes of CCCC FG rectangular plate with $a/b = 1.0$ and $E_{rat} = 0.25, 0.5$

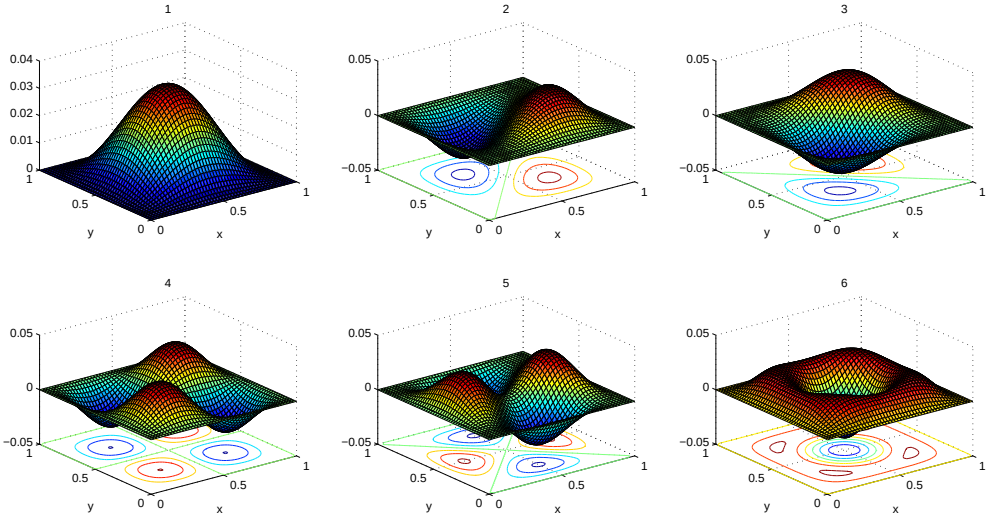

(a) $E_{rat} = 1.0$

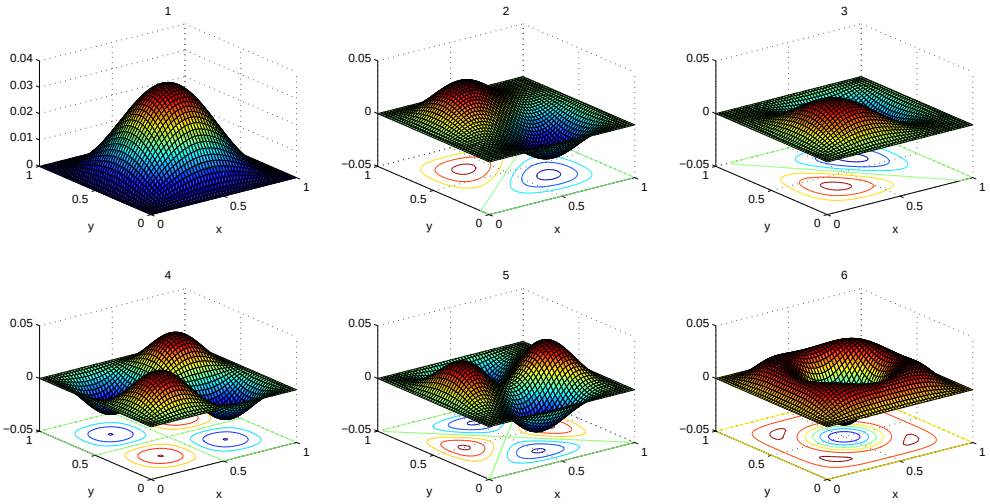

(b) $E_{rat} = 2.0$

Figure 6.13: First six mode shapes of CCCC FG rectangular plate with $a/b = 1.0$ and $E_{rat} = 1.0, 2.0$

Effect of ρ_{rat} with constant E_{rat}

In Tables 6.39 to 6.44, the effect of ρ_{rat} on frequencies of exponential FG rectangular plate satisfying various BCs are estimated with constant $E_{rat} = 1$. In Table 6.39, frequencies of FG plate with the variation of ρ_{rat} viz. $\rho_{rat} = 0.25, 0.5, 1.0$ and 2.0 are evaluated with a fixed aspect ratio. In a similar fashion, effect of ρ_{rat} on these frequencies are incorporated in Tables 6.40 to 6.44 with various edge conditions viz. CCCS, CCSS, CCCF, SSSS, FFFF. One may easily conclude that frequencies are increasing with increase in ρ_{rat} irrespective of the aspect ratio

and BC assumed. The authenticity of this argument can also be observed from the expression of non-dimensional frequency, which is directly proportional to the mass density of the ceramic constituent of FG rectangular plate.

Table 6.39: Effect of ρ_{rat} on non-dimensional frequencies of CCCC exponential FG rectangular plates

Aspect ratio	ρ_{rat}	λ_1	λ_2	λ_3	λ_4	λ_5	λ_6
0.2	0.25	15.385	15.934	16.911	18.380	20.949	24.662
	0.5	18.843	19.515	20.711	22.511	25.658	30.204
	1.0	22.633	23.439	24.877	27.039	30.818	36.279
	2.0	26.648	27.598	29.290	31.836	36.285	42.715
	4.0	30.771	31.868	33.821	36.761	41.899	49.323
0.5	0.25	16.709	21.637	30.467	43.232	43.497	48.346
	0.5	20.464	26.499	37.314	52.948	53.272	59.211
	1.0	24.579	31.829	44.819	63.598	63.986	71.119
	2.0	28.940	37.476	52.770	74.880	75.338	83.737
	4.0	33.417	43.274	60.934	86.464	86.993	96.691
1.0	0.25	24.464	49.895	49.895	73.596	89.662	90.019
	0.5	29.963	61.109	61.109	90.137	109.81	110.25
	1.0	35.989	73.399	73.399	108.27	131.89	132.42
	2.0	42.374	86.421	86.421	127.47	155.29	155.92
	4.0	48.929	99.789	99.789	147.19	179.32	180.04
2.0	0.25	66.834	86.547	121.87	172.93	173.99	193.38
	0.5	81.855	105.99	149.26	211.79	213.09	236.84
	1.0	98.318	127.32	179.28	254.39	255.95	284.48
	2.0	115.76	149.90	211.08	299.52	301.35	334.95
	4.0	133.67	173.09	243.74	345.86	347.97	386.76

Table 6.40: Effect of ρ_{rat} on non-dimensional frequencies of CCCS exponential FG rectangular plates

Aspect ratio	ρ_{rat}	λ_1	λ_2	λ_3	λ_4	λ_5	λ_6
	0.25	10.721	11.454	12.715	14.587	17.602	24.413
	0.5	13.130	14.028	15.572	17.865	21.558	29.900
0.2	1.0	15.771	16.849	18.704	21.458	25.894	35.914
	2.0	18.569	19.839	22.022	25.265	30.488	42.285
	4.0	21.442	22.908	25.429	29.174	35.205	48.827
	0.25	12.474	18.392	28.075	35.785	41.257	41.698
	0.5	15.277	22.526	34.384	43.828	50.529	51.069
0.5	1.0	18.349	27.056	41.299	52.643	60.693	61.341
	2.0	21.605	31.857	48.627	61.982	71.460	72.224
	4.0	24.947	36.785	56.149	71.570	82.515	83.397
	0.25	21.636	43.057	48.321	68.542	79.224	88.788
	0.5	26.498	52.734	59.181	83.947	97.029	108.74
1.0	1.0	31.828	63.339	71.084	100.83	116.54	130.61
	2.0	37.474	74.577	83.694	118.72	137.22	153.79
	4.0	43.272	86.114	96.642	137.08	158.45	177.58
	0.25	65.649	82.259	113.61	166.03	173.34	190.82
	0.5	80.403	100.75	139.14	203.34	212.29	233.71
2.0	1.0	96.574	121.01	167.13	244.24	254.99	280.71
	2.0	113.71	142.48	196.78	287.57	300.24	330.52
	4.0	131.29	164.52	227.22	332.05	346.68	381.65

Table 6.41: Effect of ρ_{rat} on non-dimensional frequencies of CCSS exponential FG rectangular plates

Aspect ratio	ρ_{rat}	λ_1	λ_2	λ_3	λ_4	λ_5	λ_6
	0.25	10.701	11.375	12.545	14.351	18.189	34.217
	0.5	13.106	13.932	15.364	17.577	22.277	41.907
0.2	1.0	15.742	16.734	18.454	21.112	26.758	50.335
	2.0	18.534	19.703	21.728	24.857	31.505	59.265
	4.0	21.402	22.751	25.089	28.703	36.379	68.433
	0.25	12.079	17.131	25.869	35.591	39.726	40.559
	0.5	14.794	20.981	31.683	43.590	48.654	49.675
0.5	1.0	17.769	25.201	38.056	52.357	58.439	59.665
	2.0	20.922	29.672	44.807	61.646	68.807	70.251
	4.0	24.159	34.262	51.739	71.182	79.451	81.118
	0.25	18.392	41.158	41.329	63.161	78.143	78.268
	0.5	22.525	50.408	50.618	77.356	95.705	95.859
1.0	1.0	27.055	60.546	60.798	92.914	114.95	115.14
	2.0	31.855	71.287	71.584	109.39	135.35	135.56
	4.0	36.783	82.315	82.658	126.32	156.29	156.54
	0.25	48.318	68.523	103.48	142.36	158.90	162.24
	0.5	59.177	83.924	126.73	174.36	194.62	198.69
2.0	1.0	71.079	100.80	152.22	209.43	233.76	238.66
	2.0	83.689	118.69	179.23	246.58	275.23	281.00
	4.0	96.635	137.05	206.96	284.73	317.81	324.47

Table 6.42: Effect of ρ_{rat} on non-dimensional frequencies of CCCF exponential FG rectangular plates

Aspect ratio	ρ_{rat}	λ_1	λ_2	λ_3	λ_4	λ_5	λ_6
	0.25	2.7124	3.6493	5.1703	7.2939	11.269	15.347
	0.5	3.3220	4.4695	6.3322	8.9333	13.803	18.796
0.2	1.0	3.9902	5.3684	7.6058	10.729	16.579	22.576
	2.0	4.6981	6.3208	8.9551	12.634	19.519	26.582
	4.0	5.4249	7.2987	10.341	14.588	22.539	30.694
	0.25	5.2938	11.936	17.576	21.997	24.508	35.032
	0.5	6.4836	14.619	21.526	26.940	30.016	42.905
0.5	1.0	7.7876	17.559	25.856	32.359	36.053	51.535
	2.0	9.1691	20.674	30.443	38.099	42.449	60.677
	4.0	10.588	23.872	35.152	43.993	49.016	70.064
	0.25	16.288	27.204	43.024	52.179	54.851	80.117
	0.5	19.948	33.318	52.694	63.906	67.178	98.123
1.0	1.0	23.961	40.019	63.291	76.759	80.689	117.86
	2.0	28.211	47.119	74.519	90.376	95.005	138.77
	4.0	32.576	54.409	86.048	104.36	109.70	160.23
	0.25	61.628	70.814	91.847	131.16	168.39	179.62
	0.5	75.478	86.729	112.49	160.63	206.24	219.99
2.0	1.0	90.659	104.17	135.11	192.94	247.72	264.23
	2.0	106.74	122.65	159.08	227.17	291.66	311.11
	4.0	123.26	141.63	183.69	262.31	336.78	359.24

Table 6.43: Effect of ρ_{rat} on non-dimensional frequencies of SSSS exponential FG rectangular plates

Aspect ratio	ρ_{rat}	λ_1	λ_2	λ_3	λ_4	λ_5	λ_6
	0.25	6.9775	7.7827	9.1736	11.170	19.383	27.106
	0.5	8.5457	9.5318	11.235	13.681	23.739	33.197
0.2	1.0	10.264	11.449	13.495	16.433	28.514	39.874
	2.0	12.085	13.480	15.889	19.348	33.572	46.948
	4.0	13.955	15.565	18.347	22.341	38.766	54.211
	0.25	8.3864	13.418	22.039	28.514	33.757	34.611
	0.5	10.271	16.434	26.992	34.923	41.344	42.389
0.5	1.0	12.337	19.739	32.421	41.947	49.659	50.916
	2.0	14.526	23.241	38.173	49.389	58.469	59.948
	4.0	16.773	26.837	44.078	57.029	67.514	69.223
	0.25	13.418	33.546	33.546	53.975	68.095	68.105
	0.5	16.434	41.086	41.086	66.105	83.399	83.411
1.0	1.0	19.739	49.349	49.349	79.401	100.17	100.19
	2.0	23.241	58.104	58.104	93.487	117.94	117.96
	4.0	26.837	67.093	67.093	107.95	136.19	136.21
	0.25	33.546	53.674	88.156	114.06	135.03	138.45
	0.5	41.085	65.737	107.97	139.69	165.37	169.56
2.0	1.0	49.348	78.958	129.68	167.79	198.63	203.66
	2.0	58.103	92.966	152.69	197.55	233.87	239.79
	4.0	67.091	107.35	176.31	228.12	270.06	276.89

Table 6.44: Effect of ρ_{rat} on non-dimensional frequencies of FFFF exponential FG rectangular plates

Aspect ratio	ρ_{rat}	λ_1	λ_2	λ_3	λ_4	λ_5	λ_6
	0.25	0.5871	1.6645	1.7719	3.6888	5.8142	7.6269
	0.5	0.7191	2.0386	2.1702	4.5179	7.1209	9.3409
0.2	1.0	0.8637	2.4487	2.6067	5.4265	8.5531	11.219
	2.0	1.0169	2.8831	3.0691	6.3893	10.070	13.210
	4.0	1.1742	3.3291	3.5439	7.3777	11.628	15.254
	0.25	3.6850	4.5755	10.249	10.464	15.162	17.983
	0.5	4.5132	5.6039	12.553	12.816	18.570	22.024
0.5	1.0	5.4209	6.7309	15.078	15.393	22.305	26.454
	2.0	6.3827	7.9251	17.753	18.124	26.262	31.147
	4.0	7.3701	9.1511	20.499	20.928	30.325	35.965
	0.25	9.3225	13.442	16.693	24.198	24.198	42.947
	0.5	11.418	16.463	20.444	29.636	29.636	52.599
1.0	1.0	13.714	19.774	24.556	35.597	35.597	63.179
	2.0	16.147	23.283	28.913	41.912	41.912	74.387
	4.0	18.645	26.884	33.385	48.396	48.396	85.895
	0.25	14.740	18.302	40.999	41.855	60.649	71.931
	0.5	18.053	22.415	50.213	51.262	74.280	88.097
2.0	1.0	21.684	26.924	60.312	61.572	89.219	105.81
	2.0	25.531	31.700	71.012	72.496	105.05	124.59
	4.0	29.480	36.604	81.998	83.711	121.29	143.86

Whence first six mode shapes of CCCC FG square plate ($a/b = 1$) are given in Figs. 6.14 and 6.15 with different ρ_{rat} viz. $\rho_{rat} = 0.25$, 0.5, 1.0 and 2.0. In a similar way, 3D mode shapes of exponential FG plate subjected to various BCs with different ρ_{rat} may also be depicted.

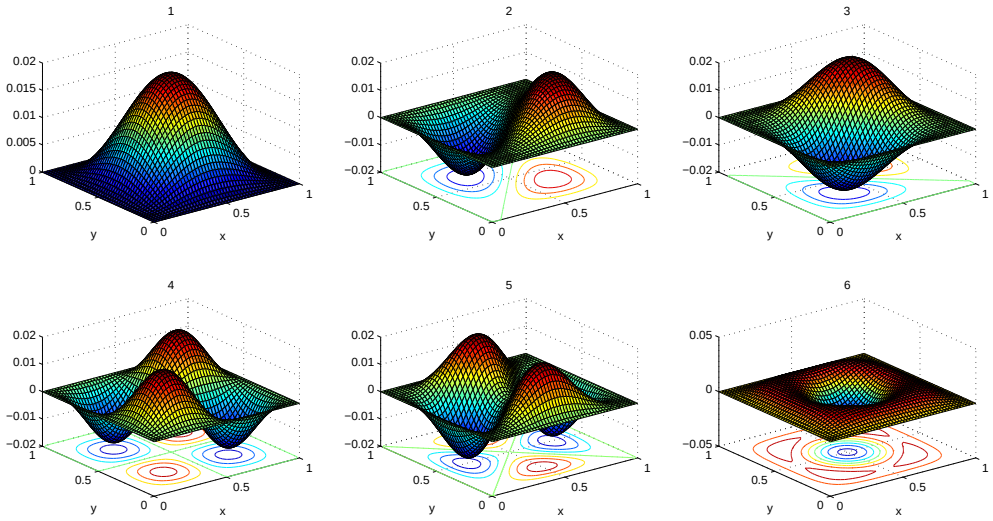

(a) $\rho_{rat} = 0.25$

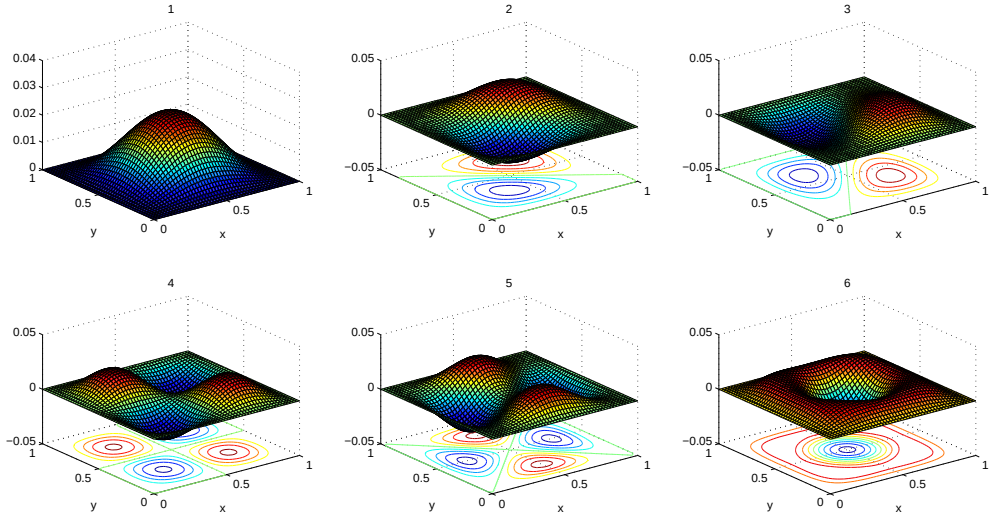

(b) $\rho_{rat} = 0.5$

Figure 6.14: First six mode shapes of CCCC FG rectangular plate with $a/b = 1.0$ and $\rho_{rat} = 0.25, 0.5$

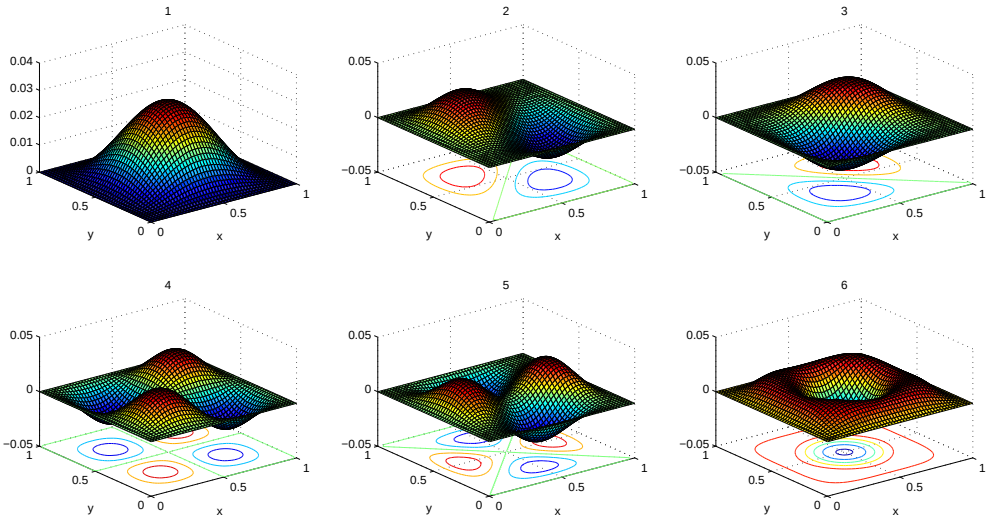

(a) $\rho_{rat} = 1.0$

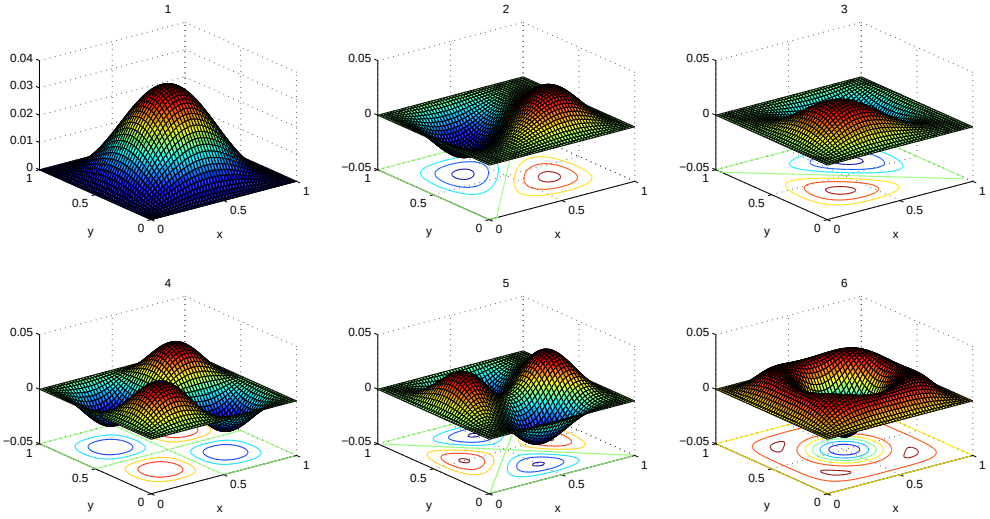

(b) $\rho_{rat} = 2.0$

Figure 6.15: First six mode shapes of CCCC FG rectangular plate with $a/b = 1.0$ and $\rho_{rat} = 1.0, 2.0$

6.2 Special case of FG rectangular plate

This section especially deals with the proposition of four new inverse trigonometric shear deformation theories to study free vibration characteristics of isotropic thick rectangular plates subjected to various boundary conditions. The proposed theories exactly satisfy the transverse shear stress boundary conditions on the bottom and top surfaces of the plate, which were true in earlier shear deformation theories also viz. parabolic shear deformation plate theory (PSDPT;

(Reddy, 1984b,c)), two-dimensional plate theory (2-DPT; (Reissner, 1975)) and trigonometric shear deformation plate theory (TSDPT; (Touratier, 1991)). Inverse sine shear deformation plate theory (ISDPT), inverse cosine shear deformation plate theory (ICDPT), inverse tangent shear deformation plate theory (ITDPT) and inverse cotangent shear deformation plate theory (ICTDPT) as supposed in Eq. (2.16) are four different inverse trigonometric function based proposed theories used in this investigation. There are various methods to handle the said type of problems, but the Rayleigh-Ritz method is found to be efficient because it can very well handle all types of classical boundary conditions. Accordingly, the trial functions denoting the displacement components are expressed as the linear combinations of simple algebraic polynomials. The main objective of this investigation is to study the effects of geometric configurations and deformation theories on the non-dimensional frequencies as these may be important for design engineers.

6.2.1 Numerical modeling

The shape functions of different shear deformation plate theories (both existing and proposed) and their corresponding derivatives have been demonstrated below.

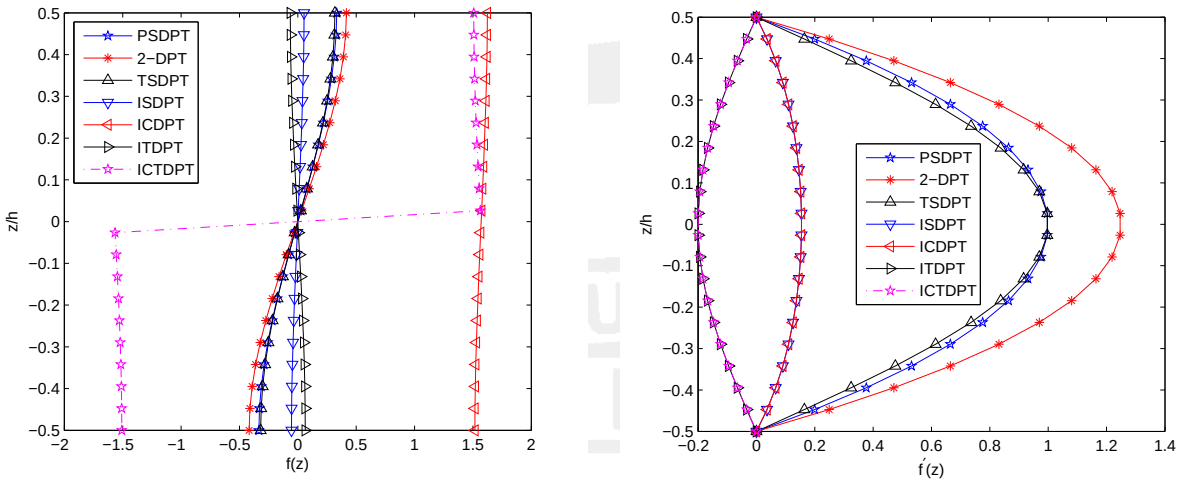

(a)Shape functions (b) Derivatives of shape functions

Figure 6.16: Behavior of shape functions and their derivatives along thickness of the isotropic rectangular plate

The Rayleigh-Ritz formulation for free vibration of thick rectangular plates has already been described in Sec. 3.1.3 to obtain the generalized eigenvalue problem. The new results for non-dimensional frequencies are incorporated after performing a test of convergence and

comparison studies in special cases. 3-D mode shapes are also plotted to demonstrate the deflected shapes of the concerned plate.

6.2.2 Convergence and comparison studies

In this section, the test of convergence of first six non-dimensional frequencies for SCSF rectangular plates subjected to various BCs is carried out in Table 6.45 with increase in number of polynomials (n) involved in deflection function. The non-dimensional frequency is to be computed based on the following formulation (Leissa, 1973):

$$\lambda = \omega a^2 \sqrt{\frac{\rho h}{D}};\ D(\text{flexural rigidity}) = \frac{Eh^3}{12(1-\nu^2)} \tag{6.2}$$

In addition, an inverse tangent shear deformation plate theory (ITSDT) had also been proposed by Thai et al. (2014); given by $f(z) = [h\arctan(2z/h) - z]$ for static, free vibration and buckling for laminated composite and sandwich plates. As mentioned in Table 3.3, the coefficients concerned with ITSDT$^{(\text{Thai et al., 2014})}$ may be expressed as

$$C_1 = \int_{-1/2}^{1/2} (\arctan 2\bar{z} - \bar{z})^2 \, \mathrm{d}\bar{z}, C_2 = \int_{-1/2}^{1/2} \left(\bar{z}\arctan 2\bar{z} - \bar{z}^2\right) \mathrm{d}\bar{z} \text{ and } C_3 = \int_{-1/2}^{1/2} \left(\frac{2}{1+4\bar{z}^2} - 1\right)^2 \mathrm{d}\bar{z}$$

Here, the superscripted notation $(\ )^{(\text{Thai et al., 2014})}$ is meant for the computations considered for (Thai et al., 2014). Rather than taking only the present deformation theories, the convergence test of first six non-dimensional frequencies associated with ITSDT$^{(\text{Thai et al., 2014})}$ has also been performed here in Table 6.45. Comparing the convergence pattern of present ITDPT and ITSDT$^{(\text{Thai et al., 2014})}$. Moreover, it can be seen that convergence of the non-dimensional frequencies is achieved with increase in number of polynomials (n). One can also check the convergence of these frequencies for any combination of edge supports and geometric configurations. As such, the solutions yielded for these SDPTs are validated in further section with available results and an exhaustive analysis among these theories has also been carried out.

Table 6.45: Convergence of first six non-dimensional frequencies of SCSF rectangular plate with $a/b = 2/3$ and $a/h = 20$

Source	n	λ_1	λ_2	λ_3	λ_4	λ_5	λ_6
PSDPT	3	7.9577	25.4771	39.2861	128.1280	193.9805	196.0423
	6	7.4628	24.8609	27.3276	55.8743	60.9294	116.2111
	10	7.4489	20.2492	26.9853	44.1173	60.3256	66.6846
	15	7.4401	20.0617	26.7835	41.1239	42.4020	66.5602
	18	7.4370	20.0432	26.7477	40.9661	42.3639	64.7963
	21	7.4364	19.9661	26.7470	40.3784	41.7627	64.7851
2-DPT	3	7.9532	25.4644	39.1649	128.1280	193.9805	196.0423
	6	7.4571	24.8403	27.2692	55.7276	60.8512	115.0204
	10	7.4421	20.2167	26.9314	43.9945	60.2209	66.3995
	15	7.4314	20.0238	26.7146	40.9954	42.2614	66.2954
	18	7.4276	20.0031	26.6702	40.8178	42.2211	64.4641
	21	7.4269	19.9288	26.6693	40.2284	41.5993	64.4495
TSDPT	3	7.9532	25.4645	39.1657	128.1280	193.9805	196.0423
	6	7.4571	24.8405	27.2696	55.7285	60.8517	115.0294
	10	7.4421	20.2169	26.9317	43.9954	60.2216	66.4018
	15	7.4314	20.0241	26.7151	40.9962	42.2623	66.2974
	18	7.4277	20.0034	26.6707	40.8189	42.2221	64.4665
	21	7.4269	19.9290	26.6699	40.2295	41.6005	64.4519
ISDPT	3	7.9532	25.4645	39.1655	128.1280	193.9805	196.0423
	6	7.4571	24.8404	27.2695	55.7283	60.8516	115.0250
	10	7.4421	20.2168	26.9316	43.9950	60.2214	66.4006
	15	7.4314	20.0240	26.7150	40.9960	42.2620	66.2966
	18	7.4277	20.0033	26.6706	40.8185	42.2217	64.4655
	21	7.4269	19.9289	26.6697	40.2291	41.6000	64.4510
ICDPT	3	7.9721	25.5142	39.6926	128.1280	160.4866	172.4872
	6	7.4811	24.9254	27.5238	56.3674	61.1789	120.5218
	10	7.4709	20.3541	27.1626	44.5386	60.6683	67.6850
	15	7.4690	20.1872	27.0145	41.5566	42.8699	67.4510
	18	7.4689	20.1770	27.0130	41.4762	42.8413	65.9388
	21	7.4689	20.0897	27.0128	40.8954	42.3238	65.9387
ITDPT	3	7.9532	25.4645	39.1657	128.1280	193.9805	196.0423
	6	7.4571	24.8405	27.2696	55.7285	60.8517	115.0292
	10	7.4421	20.2169	26.9317	43.9953	60.2216	66.4017
	15	7.4314	20.0240	26.7151	40.9962	42.2623	66.2974
	18	7.4277	20.0034	26.6707	40.8189	42.2221	64.4664
	21	7.4269	19.9290	26.6699	40.2295	41.6005	64.4519
ITSDT(Thai et al., 2014)	3	7.9681	25.5065	39.5679	128.1280	193.9805	196.0423
	6	7.4761	24.9088	27.4594	56.2156	61.1118	118.8693
	10	7.4646	20.3242	27.1095	44.3939	60.5694	67.2658
	15	7.4599	20.1476	26.9110	41.4172	42.7226	66.8955
	18	7.4579	20.1331	26.9238	41.2188	42.6855	65.5850
	21	7.4575	20.0500	26.9233	40.6382	42.1206	65.5808
ICTDPT	3	7.9718	25.5123	39.6886	128.1280	165.8446	177.4834
	6	7.4806	24.9233	27.5216	56.3621	61.1732	120.5077
	10	7.4705	20.3521	27.1603	44.5347	60.6625	67.6788
	15	7.4685	20.1853	27.0118	41.5527	42.8653	67.4445
	18	7.4684	20.1751	27.0103	41.4720	42.8366	65.9313
	21	7.4684	20.0877	27.0100	40.8911	42.3192	65.9313

After satisfactory convergence of eigenfrequencies, one can easily validate the present results in Tables 6.46 based on all the mentioned SDPTs. In these tabulations, the superscripted notations $(\ )^{P}$, $(\ )^{2\text{-}D}$, $(\ )^{T}$, $(\ )^{I\text{-}1}$, $(\ )^{I\text{-}2}$, $(\ )^{I\text{-}3}$ and $(\ )^{I\text{-}4}$ are meant for the evaluations resulted from PSDPT, 2-DPT, TSDPT, ISDPT, ICDPT, ITDPT and ICTDPT respectively. First six non-dimensional frequencies are evaluated in Table 6.46 with the formulation given in Eq. (6.2) and validated with (Leissa, 1973) and (Hosseini-Hashemi and Arsanjani, 2005). Six different combinations of boundary supports are assumed here viz. SCSC, SCSS, SSSS, SCSF, SSSF and SFSF. The comparison study is performed for very thin square plate ($\mu = 1$) and as such, the length-to-thickness ratio (a/h) is considered to be 100. The number of polynomials taken for computation based on the proposed inverse trigonometric deformation theories is also 36; as was required in (Leissa, 1973). It can also be seen that proposed theories slightly over predict the non-dimensional frequencies than those obtained in (Hosseini-Hashemi and Arsanjani, 2005), in which non-dimensional frequencies are computed based on Mindlin plate theory. In this manner, one can easily see that presently computed non-dimensional frequencies are in excellent agreement with the available literature, especially for thin rectangular plates. If we analyze the results obtained for the SDPTs, Table 6.46 indicates that TSDPT, ISDPT and ITDPT lead to identical results with an absolute error threshold $\geq 10^{-5}$. As such, it is worth to consider any one of the shear deformation theory among these three SDPTs in further section. While comparing the solutions for the new SDPTs, we have found that ICDPT and ICTDPT yield higher results than those for ISDPT (or ITDPT).

Table 6.46: Comparison of first six natural frequencies (λ) of isotropic square plates; $a/h = 100$

BCs	Source	λ_1	λ_2	λ_3	λ_4	λ_5	λ_6
SCSC	Present^{P}	28.9321	54.6935	69.2358	94.4329	102.0874	128.8039
	Present$^{2\text{-}D}$	28.9482	54.7314	69.3110	94.5530	102.2020	129.0392
	Present^{T}	28.9272	54.6822	69.2133	94.3969	102.0531	128.7336
	Present$^{I\text{-}1}$	28.9272	54.6821	69.2133	94.3969	102.0531	128.7335
	Present$^{I\text{-}2}$	28.9434	54.7224	69.2968	94.5338	102.1819	129.0101
	Present$^{I\text{-}3}$	28.9272	54.6821	69.2133	94.3969	102.0531	128.7335
	Present$^{I\text{-}4}$	28.9420	54.7195	69.2917	94.5266	102.1748	128.9984
	(Leissa, 1973)	28.9509	54.7431	69.3270	94.5873	102.2162	129.0955
	(Hosseini-Hashemi and Arsanjani, 2005)	28.9250	54.6743	69.1986	94.3686	102.0112	128.6906
SCSS	Present^{P}	23.6361	51.6334	58.5884	86.0196	100.1532	113.0234
	Present$^{2\text{-}D}$	23.6442	51.6635	58.6335	86.1061	100.2595	113.1805
	Present^{T}	23.6336	51.6244	58.5749	85.9937	100.1214	112.9765
	Present$^{I\text{-}1}$	23.6336	51.6244	58.5749	85.9937	100.1213	112.9764
	Present$^{I\text{-}2}$	23.6416	51.6559	58.6234	86.0904	100.2403	113.1570
	Present$^{I\text{-}3}$	23.6336	51.6244	58.5749	85.9937	100.1214	112.9764
	Present$^{I\text{-}4}$	23.6409	51.6536	58.6200	86.0848	100.2336	113.1482
	(Leissa, 1973)	23.6463	51.6743	58.6464	86.1345	100.2698	113.2281
	(Hosseini-Hashemi and Arsanjani, 2005)	23.6327	51.6210	58.5687	86.9792	100.0830	112.9554
SSSS	Present^{P}	19.7335	49.3125	49.3125	78.8724	98.5774	98.5779
	Present$^{2\text{-}D}$	19.7376	49.3379	49.3379	78.9374	98.6788	98.6788
	Present^{T}	19.7322	49.3048	49.3048	78.8529	98.5471	98.5477
	Present$^{I\text{-}1}$	19.7322	49.3048	49.3048	78.8529	98.5471	98.5476
	Present$^{I\text{-}2}$	19.7363	49.3311	49.3311	78.9243	98.6597	98.6606
	Present$^{I\text{-}3}$	19.7322	49.3048	49.3048	78.8529	98.5471	98.5477
	Present$^{I\text{-}4}$	19.7360	49.3292	49.3292	78.9199	98.6532	98.6542
	(Leissa, 1973)	19.7392	49.3480	49.3480	78.9568	98.6960	98.6980
	(Hosseini-Hashemi and Arsanjani, 2005)	19.7322	49.3045	49.3045	78.8455	98.5222	98.5222
SCSF	Present^{P}	12.6830	33.0385	41.6732	62.9487	72.3018	90.5620
	Present$^{2\text{-}D}$	12.6866	33.0596	41.6946	63.0011	72.3716	90.6516
	Present^{T}	12.6819	33.0322	41.6668	62.9331	72.2810	90.5352
	Present$^{I\text{-}1}$	12.6819	33.0322	41.6668	62.9330	72.2810	90.5352
	Present$^{I\text{-}2}$	12.6858	33.0548	41.6888	62.9903	72.3576	90.6345
	Present$^{I\text{-}3}$	12.6819	33.0322	41.6668	62.9331	72.2810	90.5352
	Present$^{I\text{-}4}$	12.6855	33.0534	41.6874	62.9869	72.3528	90.6287
	(Leissa, 1973)	12.6874	33.0651	41.7019	63.0148	72.3976	90.6114
	(Hosseini-Hashemi and Arsanjani, 2005)	12.6728	32.9925	41.6472	62.8595	72.2171	90.4194
SSSF	Present^{P}	11.6816	27.7403	41.1707	59.0144	61.8010	90.2437
	Present$^{2\text{-}D}$	11.6839	27.7522	41.1902	59.0558	61.8443	90.3314
	Present^{T}	11.6809	27.7367	41.1648	59.0021	61.7880	90.2175
	Present$^{I\text{-}1}$	11.6809	27.7367	41.1648	59.0021	61.7880	90.2174
	Present$^{I\text{-}2}$	11.6834	27.7494	41.1847	59.0466	61.8340	90.3144
	Present$^{I\text{-}3}$	11.6809	27.7367	41.1648	59.0021	61.7881	90.2173
	Present$^{I\text{-}4}$	11.6832	27.7487	41.1833	59.0438	61.8308	90.3087
	(Leissa, 1973)	11.6845	27.7563	41.1967	59.0655	61.8606	90.2941
	(Hosseini-Hashemi and Arsanjani, 2005)	11.6746	27.7042	41.1469	58.9430	61.7308	90.1079
SFSF	Present^{P}	9.6297	16.1284	36.6973	38.9229	46.7269	70.6982
	Present$^{2\text{-}D}$	9.6310	16.1333	36.7181	38.9395	46.7543	70.7559
	Present^{T}	9.6293	16.1269	36.6910	38.9180	46.7186	70.6809
	Present$^{I\text{-}1}$	9.6293	16.1269	36.6910	38.9180	46.7186	70.6809
	Present$^{I\text{-}2}$	9.6306	16.1321	36.7132	38.9344	46.7475	70.7434
	Present$^{I\text{-}3}$	9.6293	16.1269	36.6910	38.9180	46.7186	70.6809
	Present$^{I\text{-}4}$	9.6305	16.1318	36.7119	38.9332	46.7456	70.7393
	(Leissa, 1973)	9.6314	16.1348	36.7256	38.9450	46.7381	70.7401
	(Hosseini-Hashemi and Arsanjani, 2005)	9.6270	16.0971	36.6112	38.9043	46.6393	70.4846

6.2.3 Results and discussions

Results with previously proposed SDPTs

In this section, first six non-dimensional frequencies of isotropic rectangular plates with various combinations of boundary supports are evaluated in Tables 6.47 to 6.54 for different aspect ratios (a/b = 2/3, 1 and 3/2) and thickness-to-length ratios (h/a = 0.01, 0.05, 0.1 and 0.2). The shear deformation theories used in these tabulations are previously proposed SDPTs, assumed in Eq. (2.12). The notations $(\ )^{\mathrm{P}}$, $(\ )^{\text{2-D}}$ and $(\ )^{\mathrm{T}}$ are meant for PSDPT, 2-DPT and TSDPT respectively. On the other hand, $(\ )^{\text{(Hosseini-Hashemi and Arsanjani, 2005)}}$ denote results of (Hosseini-Hashemi and Arsanjani, 2005) for respective h/a. Validation of present results is also performed here with (Hosseini-Hashemi and Arsanjani, 2005) for some specific sets of BCs viz. SSSS, SSCS, CSCS, FSSS, FSFS and FSCS. Looking into the validation with Present$^{\mathrm{T}}$, one can see close approximation of present results and also a few ambiguities at certain higher modes. This may be due to the missing frequencies, which may not be reported in (Hosseini-Hashemi and Arsanjani, 2005). Irrespective of the edge support considered, it can also be observed that eigenfrequencies associated with PSDPT are comparatively higher than those with 2-DPT and TSDPT. But it may be seen that the non-dimensional frequencies of 2-DPT and TSDPT are either identical or fluctuating at certain modes.

Table 6.47: First six non-dimensional frequencies, $\lambda = \omega a^2 \sqrt{\rho h/D}$ of CCCC rectangular plates with different a/b and h/a ratios

Source	a/b	h/a	λ_1	λ_2	λ_3	λ_4	λ_5	λ_6
Present^{P}	2/3	0.01	26.9876	41.6683	66.0366	66.4402	79.6839	100.6392
		0.05	26.5838	40.8415	64.0397	64.5702	76.9488	96.7941
		0.1	25.4651	38.6055	58.9282	59.8259	70.2639	87.4752
		0.2	22.2480	32.6653	45.0393	46.8036	48.0053	49.7122
	1	0.01	35.9552	73.2866	73.2866	107.9975	131.2589	131.8898
		0.05	35.2643	70.8623	70.8623	103.1795	124.3510	125.0616
		0.1	33.4171	64.7966	64.7966	92.1413	109.0529	109.0954
		0.2	28.4746	51.1118	51.1118	54.5477	60.6033	62.1273
	3/2	0.01	60.6732	93.6532	148.3360	149.2584	178.9451	225.9560
		0.05	58.7127	89.6674	138.8906	140.4518	166.2373	208.1185
		0.1	53.8504	80.3135	118.8058	121.7590	135.3479	140.8290
		0.2	42.7972	61.2941	67.6740	84.1523	85.9203	87.0651
Present$^{2\text{-D}}$	2/3	0.01	26.9830	41.6591	66.0143	66.4198	79.6533	100.5982
		0.05	26.4756	40.6313	63.5425	64.1231	76.2971	95.9119
		0.1	25.1048	37.9351	57.4608	58.5144	68.4469	85.0445
		0.2	21.3815	31.2226	44.2801	45.0393	46.0880	48.0053
	1	0.01	35.9472	73.2594	73.2594	107.9428	131.1802	131.8123
		0.05	35.0833	70.2665	70.2665	102.0690	122.7845	123.5118
		0.1	32.8436	63.0939	63.0939	89.2928	105.2130	106.0769
		0.2	27.2157	48.1561	48.1562	54.5477	60.6033	62.1273
	3/2	0.01	60.6497	93.6071	148.2237	149.1560	178.7919	225.7504
		0.05	58.2085	88.7050	136.6933	138.4887	163.4458	204.3489
		0.1	52.4153	77.7944	113.7625	117.1764	134.7905	135.3479
		0.2	40.2753	57.4062	67.6740	78.0016	82.4062	84.1523
Present^{T}	2/3	0.01	26.9830	41.6592	66.0144	66.4199	79.6535	100.5985
		0.05	26.4763	40.6328	63.5463	64.1263	76.3018	95.9185
		0.1	25.1083	37.9417	57.4776	58.5272	68.4667	85.0708
		0.2	21.3969	31.2494	44.3469	45.0393	46.1361	48.0053
	1	0.01	35.9472	73.2596	73.2596	107.9432	131.1808	131.8128
		0.05	35.0846	70.2711	70.2711	102.0780	122.7972	123.5245
		0.1	32.8494	63.1140	63.1140	89.3276	105.2639	106.1267
		0.2	27.2405	48.2324	48.2324	54.5477	60.6033	62.1273
	3/2	0.01	60.6498	93.6074	148.2244	149.1566	178.7928	225.7517
		0.05	58.2126	88.7130	136.7135	138.5053	163.4709	204.3824
		0.1	52.4342	77.8288	113.8506	117.2410	134.8886	135.3479
		0.2	40.3489	57.5260	67.6740	78.2792	82.6111	84.1523

Table 6.48: First six non-dimensional frequencies, $\lambda = \omega a^2 \sqrt{\rho h/D}$ of SSSS rectangular plates with different a/b and h/a ratios

Source	a/b	h/a	λ_1	λ_2	λ_3	λ_4	λ_5	λ_6
Present[P]	2/3	0.01	14.2531	27.4045	43.8365	49.3120	56.9764	78.8659
		0.05	14.1816	27.1433	43.1749	48.4779	55.8722	76.7890
		0.1	13.9681	26.3855	41.3323	46.1898	52.8968	71.4220
		0.2	13.2271	23.9993	36.1100	39.8782	44.4331	45.0085
	1	0.01	19.7334	49.3121	49.3121	78.8648	98.5519	98.5520
		0.05	19.5971	48.4784	48.4784	76.7813	95.3267	95.3294
		0.1	19.1955	46.1860	46.1860	71.4246	87.3535	87.3627
		0.2	17.8625	39.8832	39.8832	53.8069	58.5537	59.8226
	3/2	0.01	32.0610	61.6289	98.5523	110.8509	128.0622	177.1927
		0.05	31.7048	60.3389	95.3303	106.8116	122.7488	167.3376
		0.1	30.6889	56.8910	87.3634	97.0573	110.3149	133.5175
		0.2	27.6110	48.0001	66.7587	69.7405	76.2086	83.0844
Present[2-D]	2/3	0.01	14.2524	27.4021	43.8303	49.3042	56.9660	78.8462
		0.05	14.1657	27.0854	43.0301	48.2964	55.6337	76.3455
		0.1	13.9086	26.1791	40.8453	45.5909	52.1289	70.0770
		0.2	13.0374	23.4278	34.9436	38.4853	43.3138	44.4331
	1	0.01	19.7322	49.3043	49.3043	78.8449	98.5206	98.5208
		0.05	19.5668	48.2966	48.2966	76.3378	94.6471	94.6506
		0.1	19.0849	45.5858	45.5858	70.0856	85.4073	85.4187
		0.2	17.5327	38.5019	38.5019	53.8069	55.9389	59.8226
	3/2	0.01	32.0576	61.6167	98.5212	110.8114	128.0098	177.0934
		0.05	31.6265	60.0601	94.6504	105.9679	121.6525	165.3539
		0.1	30.4163	56.0073	85.4266	94.7138	107.3917	133.5175
		0.2	26.9002	46.1292	66.3340	66.7587	72.2204	80.4346
Present[T]	2/3	0.01	14.2525	27.4022	43.8307	49.3151	56.9716	78.8798
		0.05	14.1667	27.0899	43.0403	48.3257	55.6583	76.4264
		0.05[(Hosseini-Hashemi and Arsanjani, 2005)]	14.1662	27.0866	43.0338	48.3006	55.6341	76.3360
		0.1	13.9092	26.1812	40.8515	45.5971	52.1377	70.0925
		0.1[(Hosseini-Hashemi and Arsanjani, 2005)]	13.9085	26.1803	40.8467	45.5846	52.1001	70.0219
		0.2	13.0416	23.4398	34.9761	38.5137	43.3548	44.4331
		0.2[(Hosseini-Hashemi and Arsanjani, 2005)]	13.0250	23.4005	34.8558	38.3847	43.1236	55.5860
	1	0.01	19.7322	49.3048	49.3048	78.8529	98.5471	98.5477
		0.05	19.5687	48.3100	48.3100	76.3818	94.7362	94.7479
		0.05[(Hosseini-Hashemi and Arsanjani, 2005)]	19.5676	48.3006	48.3006	76.3360	94.6612	94.6612
		0.1	19.0862	45.5936	45.5936	70.1027	85.4344	85.4455
		0.1[(Hosseini-Hashemi and Arsanjani, 2005)]	19.0840	45.5845	45.5845	70.0219	85.3654	85.3654
		0.2	17.5411	38.5419	38.5419	53.8069	56.0129	59.8226
		0.2[(Hosseini-Hashemi and Arsanjani, 2005)]	17.5055	38.3847	38.3847	55.5860	65.7193	65.7193
	3/2	0.01	32.0578	61.6177	98.5234	110.8384	128.0249	177.1752
		0.05	31.6318	60.0816	94.6980	106.0806	121.7630	165.6423
		0.05[(Hosseini-Hashemi and Arsanjani, 2005)]	31.6276	60.0641	94.6612	105.9727	121.6319	165.2949
		0.1	30.4207	56.0208	85.4649	94.7484	107.4418	133.5175
		0.1[(Hosseini-Hashemi and Arsanjani, 2005)]	30.4080	55.9920	85.3654	94.6182	107.1775	-
		0.2	26.9263	46.1945	66.4882	66.7587	72.3573	80.6270
		0.2[(Hosseini-Hashemi and Arsanjani, 2005)]	26.7944	45.8969	65.7193	-	71.6377	79.4758

Table 6.49: First six non-dimensional frequencies, $\lambda = \omega a^2 \sqrt{\rho h/D}$ of SSCS rectangular plates with different a/b and h/a ratios

Source	a/b	h/a	λ_1	λ_2	λ_3	λ_4	λ_5	λ_6
Present[P]	2/3	0.01	15.5742	31.0561	44.5345	55.3424	59.4084	83.5005
		0.05	15.4770	30.6760	43.8407	54.1920	58.1646	81.0905
		0.1	15.1902	29.5949	41.9161	51.1174	54.8521	74.9661
		0.2	14.2263	26.3533	36.5076	43.0890	44.6621	46.2749
	1	0.01	23.6358	51.6323	58.5865	86.0148	100.1191	113.0158
		0.05	23.3899	50.6635	57.2168	83.3373	96.7503	108.3551
		0.1	22.6865	48.0399	53.5974	76.6708	88.4806	97.3755
		0.2	20.5118	41.0450	44.4767	54.0012	60.2784	61.5159
	3/2	0.01	42.4912	68.9211	116.0556	120.7369	147.2674	183.6193
		0.05	41.6547	67.0663	111.4156	115.0915	139.4309	172.8770
		0.1	39.3996	62.3195	100.4902	102.1141	122.2452	133.9752
		0.2	33.3980	51.0466	66.9876	76.8706	77.9664	83.7442
Present[2-D]	2/3	0.01	15.5732	31.0523	44.5279	55.3309	59.3963	83.4768
		0.05	15.4540	30.5864	43.6875	53.9291	57.8908	80.5656
		0.1	15.1062	29.2853	41.4048	50.2849	53.9881	73.4147
		0.2	13.9726	25.5619	35.2991	41.3076	44.4342	46.5221
	1	0.01	23.6332	51.6228	58.5723	85.9876	100.0861	112.9666
		0.05	23.3297	50.4468	56.8953	82.7473	96.0368	107.3261
		0.1	22.4766	47.3425	52.6001	74.9748	86.4589	94.6264
		0.2	19.9551	39.5156	42.4718	54.0012	58.4650	60.2784
	3/2	0.01	42.4821	68.9020	116.0083	120.6752	147.1819	183.5090
		0.05	41.4476	66.6429	110.4306	113.8148	137.7431	170.7030
		0.1	38.7384	61.0683	97.8537	98.8470	118.1428	133.9752
		0.2	31.9884	48.7088	66.9876	72.1287	73.7014	83.7442
Present[T]	2/3	0.01	15.5733	31.0530	44.5290	55.3334	59.3998	83.5525
		0.05	15.4573	30.6030	43.7043	53.9769	57.9361	80.7281
		0.05[(Hosseini-Hashemi and Arsanjani, 2005)]	15.4495	30.5618	43.6749	53.8568	57.8255	80.3834
		0.1	15.1071	29.2883	41.4112	50.2932	53.9979	73.4321
		0.1[(Hosseini-Hashemi and Arsanjani, 2005)]	15.0884	29.1996	41.3592	50.0238	53.7714	72.8944
		0.2	13.9776	25.5771	35.3319	41.3424	44.4779	46.5221
		0.2[(Hosseini-Hashemi and Arsanjani, 2005)]	13.9113	25.3235	35.1279	40.6583	43.9183	-
	1	0.01	23.6336	51.6244	58.5749	85.9937	100.1214	112.9765
		0.05	23.3390	50.4799	56.9532	82.8653	96.1577	107.5137
		0.05[(Hosseini-Hashemi and Arsanjani, 2005)]	23.3165	50.4086	56.8131	82.5585	95.9681	107.0406
		0.1	22.4789	47.3514	52.6124	74.9959	86.4867	94.6629
		0.1[(Hosseini-Hashemi and Arsanjani, 2005)]	22.4260	47.2245	52.3247	74.4019	86.2191	93.7048
		0.2	19.9673	39.5584	42.5265	54.0012	58.5489	60.2784
		0.2[(Hosseini-Hashemi and Arsanjani, 2005)]	19.7988	39.2032	41.7813	57.3380	66.0322	68.6409
	3/2	0.01	42.4834	68.9059	116.0393	120.6858	147.2001	184.2728
		0.05	41.4794	66.7254	110.6344	114.0372	138.1179	171.5393
		0.05[(Hosseini-Hashemi and Arsanjani, 2005)]	41.4044	66.5348	110.2167	113.4983	137.1419	170.3298
		0.1	38.7476	61.0870	97.8923	98.9072	118.2106	133.9752
		0.1[(Hosseini-Hashemi and Arsanjani, 2005)]	38.5769	60.7549	97.2651	97.8687	116.5230	-
		0.2	32.0318	48.7879	66.9876	72.3397	73.8463	83.7442
		0.2[(Hosseini-Hashemi and Arsanjani, 2005)]	31.5267	48.0072	70.0311	72.5296	82.2259	100.9450

Table 6.50: First six non-dimensional frequencies, $\lambda = \omega a^2 \sqrt{\rho h/D}$ of CSCS rectangular plates with different a/b and h/a ratios

Source	a/b	h/a	λ_1	λ_2	λ_3	λ_4	λ_5	λ_6
Present[P]	2/3	0.01	17.3669	35.3208	45.3975	61.9851	62.2498	88.6785
		0.05	17.2250	34.7699	44.6571	60.4103	60.8088	85.8386
		0.1	16.8139	33.2319	42.6135	56.3250	57.0396	78.7335
		0.2	15.4934	28.8552	36.9444	44.8552	46.2750	46.7167
	1	0.01	28.9314	54.6914	69.2318	94.4250	102.0548	128.7904
		0.05	28.4838	53.5073	67.0789	90.8933	98.4655	122.2216
		0.1	27.2492	50.3665	61.6103	82.4561	89.7648	107.5348
		0.2	23.7392	42.3684	48.9746	54.1670	60.5328	62.1419
	3/2	0.01	56.2702	78.8563	122.9108	145.8369	169.5561	188.5756
		0.05	54.5300	76.0229	117.2891	136.6614	158.0942	176.9708
		0.1	50.1367	69.1546	104.5962	117.0437	134.3723	134.7364
		0.2	39.9191	54.4607	67.1861	79.8284	83.1117	84.1030
Present[2-D]	2/3	0.01	17.3655	35.3150	45.3904	61.9683	62.2354	88.6497
		0.05	17.1894	34.6336	44.4915	60.0372	60.4846	85.2049
		0.1	16.6878	32.7756	42.0659	55.1961	56.0462	76.9087
		0.2	15.1396	27.7827	35.6785	44.0587	45.5812	46.7167
	1	0.01	28.9264	54.6793	69.2080	94.3868	102.0188	128.7162
		0.05	28.3675	53.2333	66.5507	90.0917	97.6989	120.7310
		0.1	26.8653	49.5166	60.0702	80.2888	87.6349	103.8316
		0.2	22.8424	40.6345	46.2494	54.1670	60.5328	62.1419
	3/2	0.01	56.2494	78.8245	122.8500	145.7281	169.4198	188.4537
		0.05	54.0793	75.3455	116.0729	134.5234	155.5711	174.6001
		0.1	48.8275	67.3178	101.5312	112.1100	129.1776	134.3723
		0.2	37.6025	51.5053	67.1861	75.2178	77.0174	84.1030
Present[T]	2/3	0.01	17.3657	35.3164	45.3915	61.9727	62.2397	88.6624
		0.05	17.1957	34.6661	44.5160	60.1179	60.5528	85.3998
		0.05[(Hosseini-Hashemi and Arsanjani, 2005)]	17.1780	34.5748	44.4590	59.8841	60.3535	84.8364
		0.1	16.6890	32.7799	42.0727	55.2073	56.0571	76.9290
		0.1[(Hosseini-Hashemi and Arsanjani, 2005)]	16.6455	32.5876	41.9700	54.6728	55.6450	75.9555
		0.2	15.1458	27.8020	35.7122	44.1012	45.6272	46.7167
		0.2[(Hosseini-Hashemi and Arsanjani, 2005)]	15.0147	27.3400	35.4346	42.8936	44.7624	57.9303
	1	0.01	28.9272	54.6822	69.2133	94.3969	102.0531	128.7336
		0.05	28.3872	53.2944	66.6675	90.2853	97.8493	121.0490
		0.05[(Hosseini-Hashemi and Arsanjani, 2005)]	28.3324	53.1373	66.3511	89.7039	97.5475	120.1190
		0.1	26.8693	49.5271	60.0884	80.3153	87.6640	103.8801
		0.1[(Hosseini-Hashemi and Arsanjani, 2005)]	26.7369	49.2606	59.4801	79.1951	87.2072	102.0186
		0.2	22.8606	40.6811	46.3213	54.1670	60.5328	62.1419
		0.2[(Hosseini-Hashemi and Arsanjani, 2005)]	22.5099	40.1384	45.0569	59.1227	66.3706	71.3904
	3/2	0.01	56.2524	78.8331	122.8844	145.7509	169.4531	188.6940
		0.05	54.1512	75.5198	116.3804	134.9666	156.2046	175.3637
		0.05[(Hosseini-Hashemi and Arsanjani, 2005)]	53.9555	75.0706	115.6043	133.7728	154.3074	173.8255
		0.1	48.8450	67.3444	101.5760	112.1969	129.2690	134.3723
		0.1[(Hosseini-Hashemi and Arsanjani, 2005)]	48.4087	66.6351	100.4080	110.1837	126.1069	-
		0.2	37.6734	51.6035	67.1861	75.3739	77.2934	84.1030
		0.2[(Hosseini-Hashemi and Arsanjani, 2005)]	36.6729	50.3588	73.4961	73.7977	84.8230	101.3700

Table 6.51: First six non-dimensional frequencies, $\lambda = \omega a^2 \sqrt{\rho h/D}$ of FSSS rectangular plates with different a/b and h/a ratios

Source	a/b	h/a	λ_1	λ_2	λ_3	λ_4	λ_5	λ_6
Present[P]	2/3	0.01	10.6690	18.2926	33.6764	40.1057	48.3713	57.5396
		0.05	10.6194	18.1365	33.2062	39.5241	47.5206	56.3069
		0.1	10.4820	17.7240	31.9647	37.9185	45.2367	46.9316
		0.2	10.0234	16.4648	23.4658	24.0106	26.5484	28.4303
	1	0.01	11.6810	27.7372	41.1682	59.0035	61.7911	90.1718
		0.05	11.6088	27.3492	40.5277	57.6512	60.2972	87.3592
		0.1	11.4319	26.4258	38.8152	54.2675	56.6024	60.4659
		0.2	10.8712	23.8167	30.2330	31.1640	34.0243	45.7475
	3/2	0.01	13.7030	43.5348	47.7984	81.3382	92.5526	124.2990
		0.05	13.5748	42.7627	46.7307	78.6076	89.5027	118.8469
		0.1	13.3078	40.8203	44.2948	72.4796	82.1617	84.4403
		0.2	12.5164	35.5356	38.0006	41.2770	42.2201	43.1228
Present[2-D]	2/3	0.01	10.6685	18.2909	33.6719	40.1001	48.3631	57.5282
		0.05	10.6083	18.1026	33.1087	39.3968	47.3370	56.0575
		0.1	10.4444	17.6174	31.6604	37.4967	44.6506	46.9316
		0.2	9.9074	16.1752	23.4658	24.0106	26.5484	27.6902
	1	0.01	11.6801	27.7327	41.1618	58.9896	61.7765	90.1441
		0.05	11.5936	27.2728	40.3894	57.3699	60.0119	86.7679
		0.1	11.3850	26.2064	38.3711	53.4395	55.7722	60.4659
		0.2	10.7338	23.2831	30.2330	31.1640	32.9760	34.5283
	3/2	0.01	13.7010	43.5262	47.7853	81.3064	92.5214	124.2464
		0.05	13.5505	42.6024	46.5441	78.0878	88.8719	117.8816
		0.1	13.2399	40.3268	43.7740	71.1031	80.4029	82.5540
		0.2	12.3347	34.4116	36.9137	41.2770	42.2201	43.1228
Present[T]	2/3	0.01	10.6688	18.2921	33.6764	40.1044	48.3742	57.6100
		0.05	10.6127	18.1201	33.1487	39.4206	47.3832	56.1760
		0.05[(Hosseini-Hashemi and Arsanjani, 2005)]	10.0628	18.0794	33.0646	39.3762	47.2942	56.0059
		0.1	10.4449	17.6186	31.6636	37.5022	44.6575	46.9316
		0.1[(Hosseini-Hashemi and Arsanjani, 2005)]	10.4404	17.6033	31.6345	37.4806	44.6033	52.3231
		0.2	9.9103	16.1816	23.4658	24.0106	26.5484	27.7040
		0.2[(Hosseini-Hashemi and Arsanjani, 2005)]	9.8972	16.1546	27.6476	32.2485	37.5758	43.1813
	1	0.01	11.6809	27.7367	41.1648	59.0021	61.7880	90.2175
		0.05	11.6011	27.3108	40.4198	57.4593	60.0895	86.9262
		0.05[(Hosseini-Hashemi and Arsanjani, 2005)]	11.5877	27.2439	40.3718	57.3087	59.9760	86.7166
		0.1	11.3856	26.2093	38.3771	53.4499	55.7821	60.4659
		0.1[(Hosseini-Hashemi and Arsanjani, 2005)]	11.3810	26.1910	38.3610	53.3852	55.7620	78.6490
		0.2	10.7373	23.2965	30.2330	31.1640	33.0061	34.5283
		0.2[(Hosseini-Hashemi and Arsanjani, 2005)]	10.7218	23.2429	32.8922	43.8679	46.6862	61.2416
	3/2	0.01	13.7035	43.5316	47.7974	81.3350	92.5747	124.2745
		0.05	13.5617	42.6409	46.5997	78.2552	89.0388	118.0131
		0.05[(Hosseini-Hashemi and Arsanjani, 2005)]	13.5441	42.5886	46.5188	78.0153	88.8342	117.8897
		0.1	13.2440	40.3590	43.8075	71.1663	80.4702	82.5683
		0.1[(Hosseini-Hashemi and Arsanjani, 2005)]	13.2343	40.3170	43.7524	71.0199	80.3498	-
		0.2	12.3397	34.4448	36.9498	41.2770	42.2201	43.1228
		0.2[(Hosseini-Hashemi and Arsanjani, 2005)]	12.3167	34.3172	36.7879	55.8742	62.3103	77.2283

Table 6.52: First six non-dimensional frequencies, $\lambda = \omega a^2 \sqrt{\rho h/D}$ of FSFS rectangular plates with different a/b and h/a ratios

Source	a/b	h/a	λ_1	λ_2	λ_3	λ_4	λ_5	λ_6
Present[P]	2/3	0.01	9.6967	12.9776	22.9409	39.0820	40.3257	42.6576
		0.05	9.6585	12.8917	22.6631	38.5389	39.6336	41.9736
		0.1	9.5491	12.6580	21.9644	37.0209	37.8044	40.1294
		0.2	9.1731	11.9390	20.0021	32.6446	32.8770	35.0241
	1	0.01	9.6295	16.1262	36.6890	38.9209	46.6971	70.6471
		0.05	9.5886	15.9466	35.9547	38.3670	45.7890	68.5988
		0.1	9.4781	15.5328	34.3018	36.8416	43.5093	63.6343
		0.2	9.1045	14.4007	30.0301	32.4833	37.5297	49.7698
	3/2	0.01	9.5560	21.5945	38.6959	54.7666	65.6791	87.5104
		0.05	9.5132	21.1673	38.1252	53.2993	63.6227	84.8175
		0.1	9.4042	20.3558	36.5991	50.0763	59.1967	78.2042
		0.2	9.0367	18.3062	32.2754	42.2404	48.8428	51.2626
Present[2-D]	2/3	0.01	9.6963	12.9767	22.9380	39.0769	40.3195	42.6510
		0.05	9.6499	12.8721	22.6047	38.4197	39.4957	41.8252
		0.1	9.5189	12.5957	21.7972	36.6195	37.3876	39.6546
		0.2	9.0763	11.7703	19.6004	31.6662	31.9650	33.9234
	1	0.01	9.6291	16.1240	36.6808	38.9157	46.6876	70.6265
		0.05	9.5796	15.9082	35.8207	38.2458	45.5979	68.1824
		0.1	9.4479	15.4322	33.9583	36.4410	42.9451	62.4992
		0.2	9.0089	14.1600	29.3030	31.5147	36.3005	49.7698
	3/2	0.01	9.5555	21.5883	38.6901	54.7481	65.6556	87.4834
		0.05	9.5043	21.0890	38.0021	53.0172	63.3117	84.2546
		0.1	9.3745	20.1787	36.2018	49.3322	58.4245	76.5982
		0.2	8.9431	17.9301	31.3202	40.7738	47.4765	51.2626
Present[T]	2/3	0.01	9.6965	12.9775	22.9421	39.0819	40.3361	42.7019
		0.05	9.6527	12.8878	22.6509	38.4410	39.5860	41.9081
		0.05[(Hosseini-Hashemi and Arsanjani, 2005)]	9.6463	12.8416	22.5355	38.3955	39.3568	41.7615
		0.1	9.5192	12.5964	21.7992	36.6247	37.3918	39.6602
		0.1[(Hosseini-Hashemi and Arsanjani, 2005)]	9.5157	12.5711	21.7490	36.5941	37.3019	39.5886
		0.2	9.0787	11.7743	19.6083	31.6942	31.9813	33.9508
		0.2[(Hosseini-Hashemi and Arsanjani, 2005)]	9.0666	11.7505	19.5561	31.5782	31.9427	33.7882
	1	0.01	9.6293	16.1269	36.6910	38.9180	46.7186	70.6809
		0.05	9.5828	15.9490	35.9151	38.2713	45.7003	68.4461
		0.05[(Hosseini-Hashemi and Arsanjani, 2005)]	9.5771	15.8630	35.7400	38.2240	45.5242	67.9066
		0.1	9.4483	15.4336	33.9626	36.4463	42.9522	62.5135
		0.1[(Hosseini-Hashemi and Arsanjani, 2005)]	9.4458	15.4054	33.9160	36.4246	42.8870	62.3304
		0.2	9.0113	14.1661	29.3182	31.5426	36.3318	49.7698
		0.2[(Hosseini-Hashemi and Arsanjani, 2005)]	8.9997	14.1341	29.2558	31.4338	36.1646	49.8953
	3/2	0.01	9.5559	21.5983	38.6928	54.7810	65.6822	87.6095
		0.05	9.5069	21.1724	38.0331	53.1739	63.4389	84.4587
		0.05[(Hosseini-Hashemi and Arsanjani, 2005)]	9.50330	21.0333	37.9868	52.9372	63.2537	84.2198
		0.1	9.3749	20.1816	36.2072	49.3426	58.4345	76.6209
		0.1[(Hosseini-Hashemi and Arsanjani, 2005)]	9.3729	20.1451	36.1927	49.2667	58.4124	76.5468
		0.2	8.9455	17.9410	31.3479	40.8137	47.5082	51.2626
		0.2[(Hosseini-Hashemi and Arsanjani, 2005)]	8.9345	17.8846	31.2425	40.6053	47.4411	-

Table 6.53: First six non-dimensional frequencies, $\lambda = \omega a^2 \sqrt{\rho h/D}$ of FSCS rectangular plates with different a/b and h/a ratios

Source	a/b	h/a	λ_1	λ_2	λ_3	λ_4	λ_5	λ_6
Present[P]	2/3	0.01	10.9726	20.3254	37.9262	40.2458	49.6911	64.1171
		0.05	10.9149	20.1061	37.2825	39.6514	48.7652	62.4902
		0.1	10.7602	19.5477	35.6133	38.0253	46.3133	47.3914
		0.2	10.2547	17.8984	23.6957	24.0091	25.3478	26.9764
	1	0.01	12.6820	33.0338	41.6709	62.9370	72.2931	90.4848
		0.05	12.5796	32.4173	40.9892	61.2862	70.0727	87.6282
		0.1	12.3400	30.9640	39.2065	57.2805	61.0442	62.1168
		0.2	11.6106	27.0286	30.5221	31.0584	32.0438	34.2757
	3/2	0.01	16.8073	45.2547	60.9121	92.1016	93.6790	141.4078
		0.05	16.5783	44.3391	58.9694	88.2579	90.4795	133.8551
		0.1	16.0992	42.1320	54.5036	79.9432	82.8990	83.2882
		0.2	14.7569	36.3346	41.6441	42.7252	43.1358	44.3408
		0.2	14.7569	36.3346	41.6441	42.7252	43.1358	44.3408
Present[2-D]	2/3	0.01	10.9720	20.3230	37.9195	40.2401	49.6820	64.1010
		0.05	10.9019	20.0572	37.1433	39.5214	48.5640	62.1481
		0.1	10.7175	19.3984	35.1851	37.5990	45.6820	47.3914
		0.2	10.1261	17.5098	23.6957	24.0091	25.3478	26.9764
	1	0.01	12.6806	33.0261	41.6638	62.9190	72.2696	90.4564
		0.05	12.5576	32.2892	40.8428	60.9383	69.6172	87.0291
		0.1	12.2741	30.5913	38.7443	56.2892	61.0442	61.8045
		0.2	11.4293	26.1881	30.5221	31.0584	32.0438	33.2003
	3/2	0.01	16.8034	45.2434	60.8874	92.0532	93.6452	141.3214
		0.05	16.5320	44.1495	58.5821	87.4984	89.8205	132.3734
		0.1	15.9683	41.5678	53.4293	78.0272	81.0861	83.2882
		0.2	14.4398	35.1152	41.6441	42.7252	43.1358	44.3408
Present[T]	2/3	0.01	10.9724	20.3247	37.9234	40.2419	49.6944	64.2053
		0.05	10.9076	20.0817	37.2006	39.5452	48.6243	62.3014
		0.05[(Hosseini-Hashemi and Arsanjani, 2005)]	10.8951	20.0257	37.0603	39.5018	48.4841	61.9924
		0.1	10.7180	19.4001	35.1893	37.6046	45.6893	47.3914
		0.1[(Hosseini-Hashemi and Arsanjani, 2005)]	10.7099	19.3498	35.0192	37.5739	46.5302	-
		0.2	10.1291	17.5174	23.6957	24.0091	25.3478	26.9764
		0.2[(Hosseini-Hashemi and Arsanjani, 2005)]	10.1060	17.3888	29.6707	32.3003	38.0442	45.4110
	1	0.01	12.6819	33.0322	41.6668	62.9331	72.2810	90.5352
		0.05	12.5683	32.3400	40.8757	61.0711	69.7548	87.1938
		0.05[(Hosseini-Hashemi and Arsanjani, 2005)]	12.5482	32.2370	40.8218	60.7824	69.4393	86.9701
		0.1	12.2749	30.5957	38.7505	56.3013	61.0442	62.1168
		0.1[(Hosseini-Hashemi and Arsanjani, 2005)]	12.2606	30.4743	38.7128	55.9736	62.9527	-
		0.2	11.4335	26.2060	30.5221	31.0584	32.0438	33.2307
		0.2[(Hosseini-Hashemi and Arsanjani, 2005)]	11.3931	25.8975	33.0747	45.0445	48.8911	61.3014
	3/2	0.01	16.8078	45.2513	60.9046	92.0920	93.7080	141.6793
		0.05	16.5497	44.1949	58.6816	87.7900	90.0048	133.0920
		0.05[(Hosseini-Hashemi and Arsanjani, 2005)]	16.5179	44.1176	58.4647	87.1780	89.7406	131.7987
		0.1	15.9793	41.6194	53.5497	78.2267	81.1568	83.4623
		0.1[(Hosseini-Hashemi and Arsanjani, 2005)]	15.9404	41.4965	53.0869	77.3057	80.9273	-
		0.2	14.4661	35.2135	41.7312	42.8551	43.9948	45.4152
		0.2[(Hosseini-Hashemi and Arsanjani, 2005)]	14.3646	34.9199	41.2635	58.2641	62.5203	81.1835

Table 6.54: First six non-dimensional frequencies, $\lambda = \omega a^2 \sqrt{\rho h/D}$ of CCCF rectangular plates with different a/b and h/a ratios

Source	a/b	h/a	λ_1	λ_2	λ_3	λ_4	λ_5	λ_6
Present^{P}	2/3	0.01	11.8354	29.2507	29.2889	47.3581	55.4365	67.6376
		0.05	11.7234	28.7342	28.8299	46.1912	54.0622	65.6947
		0.1	11.4477	27.4728	27.6153	43.3800	50.5426	59.0830
		0.2	10.6027	23.9786	24.1401	29.5415	36.3627	39.0140
	1	0.01	23.9171	39.9602	63.1621	76.5939	80.4551	116.4025
		0.05	23.5434	38.9945	61.2276	73.9795	77.4425	110.7705
		0.1	22.5664	36.6779	56.3762	67.8145	70.3985	73.9760
		0.2	19.7699	30.8320	36.9880	44.9771	53.9876	55.1472
	3/2	0.01	51.5489	66.0198	99.5294	139.5627	154.3977	156.0457
		0.05	49.9888	63.5418	94.8775	130.8755	145.1861	145.7036
		0.1	46.0975	57.7546	84.6862	102.5185	112.2945	124.4475
		0.2	36.8862	45.1838	51.2593	64.5123	79.7235	85.2353
Present$^{2\text{-}D}$	2/3	0.01	11.8339	29.2444	29.2835	47.3440	55.4213	67.6178
		0.05	11.6960	28.6227	28.7166	45.9309	53.7344	65.2895
		0.1	11.3606	27.1368	27.2482	42.6369	49.5589	59.0830
		0.2	10.3615	23.2042	23.2551	29.5415	34.8764	39.0140
	1	0.01	23.9124	39.9478	63.1398	76.5650	80.4200	116.3379
		0.05	23.4464	38.7717	60.7519	73.4305	76.7548	109.5898
		0.1	22.2543	36.0472	54.9918	66.3185	68.5616	73.9760
		0.2	19.0157	29.5671	36.9880	42.4653	51.4090	52.1265
	3/2	0.01	51.5295	65.9891	99.4746	139.4584	154.2940	155.9207
		0.05	49.5831	62.9479	93.8770	128.8470	143.3420	143.4002
		0.1	44.9148	56.1732	82.2366	102.5185	107.5898	119.3162
		0.2	34.7217	42.6362	51.2593	60.9130	73.8510	80.4198
Present^{T}	2/3	0.01	11.8338	29.2443	29.2836	47.3444	55.4214	67.6178
		0.05	11.6963	28.6234	28.7177	45.9337	53.7369	65.2949
		0.1	11.3613	27.1401	27.2518	42.6447	49.5685	59.0830
		0.2	10.3647	23.2180	23.2691	29.5415	34.9012	39.0140
	1	0.01	23.9124	39.9476	63.1399	76.5653	80.4204	116.3386
		0.05	23.4471	38.7743	60.7561	73.4340	76.7599	109.6013
		0.1	22.2573	36.0538	55.0079	66.3304	68.5821	73.9760
		0.2	19.0295	29.5929	36.9880	42.5293	51.4657	52.2009
	3/2	0.01	51.5296	65.9889	99.4743	139.4589	154.2930	155.9210
		0.05	49.5862	62.9541	93.8812	128.8654	143.3584	143.4159
		0.1	44.9302	56.1974	82.2718	102.5185	107.6730	119.4005
		0.2	34.7855	42.7147	51.2593	61.0197	74.1159	80.4198

Results with newly proposed SDPTs

It is evident from Table 6.46 that the non-dimensional frequencies of isotropic rectangular plate ($a/h = 100$) subjected to various edge supports based on the proposed deformation plate theories are in excellent agreement with the existing results. We have also found the coincidence of the results associated with trigonometric, inverse sine and cosine related deformation theories. Hence rather than computing eigenfrequencies for all the proposed

SDPTs, we have reported first six non-dimensional frequencies for ICDPT and ICTDPT in Tables 6.55 to 6.63 for nine different combinations of edge conditions viz. CCCS, CCSS, CCFF, CFCF, CFSF, CFFF, CFFS, CFSC and CFSS. Here, the aspect ratios (a/b) are assumed to be 0.5, 2/3, 1, 3/2 and 2, whereas thickness-to-length ratios (h/a) are taken as 0.01, 0.05, 0.1 and 0.2. The number of iterations in these computations is 36. After analyzing the results obtained in Tables 6.47 to 6.63, we may summarize the followings:

- The eigenfrequencies are increasing with increase in aspect ratio and are decreasing with increase in thickness-to-length ratio regardless of the boundary condition assumed. In other words for practical purpose, it is worth to mention that we may not avoid the vibration behavior for lesser thickness-to-length ratio and greater aspect ratio.

- Comparing the non-dimensional frequencies yielded for previously proposed SDPTs, it can easily be noticed that the eigenfrequencies associated with PSDPT are comparatively higher than those with 2-DPT and TSDPT regardless of the edge support assumed. On the other hand, it can be viewed that the solutions obtained for 2-DPT and TSDPT may be either identical or fluctuating with respect to the modes.

- After analyzing the results obtained for newly proposed SDPTs, it may be evident that ICDPT and ICTDPT provide higher frequencies than those obtained for ISDPT (or ITDPT). On the contrary, ICDPT yields higher results than those for ICTDPT, but with very minute absolute errors (at least $\geq 10^{-4}$).

Table 6.55: First six non-dimensional frequencies, $\lambda = \omega a^2 \sqrt{\rho h/D}$ of CCCS rectangular plates with different a/b and h/a ratios

Source	a/b	h/a	λ_1	λ_2	λ_3	λ_4	λ_5	λ_6
ICDPT	0.5	0.01	18.3453	27.0484	41.2386	52.6122	60.5237	74.0634
		0.05	18.3175	26.9860	41.0905	52.3704	60.1979	73.5719
		0.1	18.2364	26.8000	40.6455	51.6464	59.2222	72.1063
		0.2	17.9225	26.0925	38.9984	40.5394	42.2596	43.4125
	2/3	0.01	21.3998	37.9861	55.0689	63.9543	70.3125	95.3074
		0.05	21.3626	37.8660	54.8040	63.6057	69.8765	94.5003
		0.1	21.2532	37.5051	54.0107	62.5602	68.5740	90.3609
		0.2	20.8315	36.1568	45.1804	47.0653	48.4119	49.6408
	1	0.01	31.8179	63.3062	71.0463	100.7392	116.2875	130.2712
		0.05	31.7423	62.9620	70.6463	99.8708	115.0809	128.8692
		0.1	31.5157	61.9313	69.4458	97.3032	109.2526	111.5485
		0.2	30.6547	54.6263	58.2556	60.9561	62.5646	64.2429
	3/2	0.01	58.1627	85.6709	135.5926	147.2942	174.3149	207.5278
		0.05	57.9390	85.0813	133.9946	145.6457	171.8591	203.6882
		0.1	57.2626	83.3223	129.3500	135.5184	140.8320	145.4823
		0.2	54.7708	67.7592	72.4399	77.2327	84.6964	86.6584
	2.0	0.01	96.5261	120.9281	166.8747	235.5665	254.7019	280.2512
		0.05	95.9535	119.8481	164.5737	230.7517	249.8992	274.1832
		0.1	94.2329	116.6560	157.9558	162.1331	169.3244	216.6770
		0.2	81.0666	84.4051	88.1550	106.0116	108.3385	112.0440
ICTDPT	0.5	0.01	18.3447	27.0473	41.2364	52.6092	60.5199	74.0585
		0.05	18.3157	26.9832	41.0860	52.3645	60.1913	73.5638
		0.1	18.2345	26.7971	40.6409	51.6403	59.2156	72.0984
		0.2	17.9206	26.0897	38.9944	40.5394	41.3968	42.3402
	2/3	0.01	21.3990	37.9841	55.0657	63.9499	70.3078	95.3003
		0.05	21.3604	37.8619	54.7979	63.5984	69.8687	94.4899
		0.1	21.2509	37.5009	54.0044	62.5532	68.5664	90.3609
		0.2	20.8293	36.1529	45.1804	47.0653	48.4616	48.4822
	1	0.01	31.8162	63.3021	71.0409	100.7311	116.2782	130.2593
		0.05	31.7389	62.9550	70.6382	99.8596	115.0676	128.8542
		0.1	31.5122	61.9243	69.4379	97.2926	109.2526	111.5354
		0.2	30.6514	54.6263	58.2476	60.9561	62.6204	64.2429
	3/2	0.01	58.1582	85.6642	135.5810	147.2802	174.2982	207.5081
		0.05	57.9323	85.0717	133.9793	145.6288	171.8395	203.6645
		0.1	57.2560	83.3130	129.3355	135.5184	140.8166	145.8566
		0.2	54.7650	67.7592	72.4849	77.2268	84.6964	86.6584
	2.0	0.01	96.5171	120.9172	166.8594	235.5437	254.6752	280.2221
		0.05	95.9423	119.8345	164.5551	230.7255	249.8705	274.1522
		0.1	94.2221	116.6432	157.9386	162.1331	169.6462	216.6770
		0.2	81.0666	84.4445	88.1464	106.0021	108.3385	112.0440

Table 6.56: First six non-dimensional frequencies, $\lambda = \omega a^2 \sqrt{\rho h/D}$ of CCSS rectangular plates with different a/b and h/a ratios

Source	a/b	h/a	λ_1	λ_2	λ_3	λ_4	λ_5	λ_6
ICDPT	0.5	0.01	17.7660	25.1929	37.9640	52.3242	56.0846	59.5658
		0.05	17.7395	25.1363	37.8315	52.0843	55.7920	59.2486
		0.1	17.6620	24.9677	37.4341	51.3660	54.9159	58.2992
		0.2	17.3617	24.3256	35.9606	40.2641	41.1382	42.1146
	2/3	0.01	19.9476	34.0113	54.3441	57.4894	67.7633	90.2164
		0.05	19.9138	33.9074	54.0841	57.1868	67.3491	89.4647
		0.1	19.8139	33.5962	53.3055	56.2807	66.1120	87.2413
		0.2	19.4288	32.4313	44.9067	46.7786	47.9762	49.2411
	1	0.01	27.0482	60.5140	60.7639	92.7890	114.4962	114.6439
		0.05	26.9862	60.1880	60.4391	92.0110	113.3130	113.4628
		0.1	26.8002	59.2122	59.4664	89.7096	108.7412	109.8497
		0.2	26.0926	54.3706	55.7283	55.9940	60.5749	62.0420
	3/2	0.01	44.8769	76.5109	122.2403	129.3122	152.4150	202.8936
		0.05	44.7119	75.9975	120.9500	127.8089	150.3570	199.1659
		0.1	44.2142	74.4660	117.1774	123.4374	134.9106	144.4234
		0.2	42.3749	67.4553	69.1362	72.1609	84.1352	85.7846
	2.0	0.01	71.0478	100.7390	151.7835	209.1680	224.1832	238.0952
		0.05	70.6478	99.8706	149.7365	205.4640	219.6634	233.1968
		0.1	69.4470	97.3024	143.8423	161.2886	168.4585	195.0446
		0.2	65.1816	80.6443	83.9658	88.7004	107.6571	110.9455
ICTDPT	0.5	0.01	17.7655	25.1920	37.9623	52.3212	56.0813	59.5623
		0.05	17.7379	25.1338	37.8276	52.0785	55.7858	59.2421
		0.1	17.6602	24.9651	37.4301	51.3600	54.9097	58.2927
		0.2	17.3600	24.3231	35.9568	40.2641	41.1382	42.1213
	2/3	0.01	19.9470	34.0098	54.3410	57.4861	67.7591	90.2098
		0.05	19.9120	33.9040	54.0781	57.1806	67.3418	89.4544
		0.1	19.8120	33.5927	53.2994	56.2745	66.1048	87.2310
		0.2	19.4270	32.4279	44.9067	46.7786	48.1312	49.2411
	1	0.01	27.0472	60.5104	60.7603	92.7824	114.4871	114.6348
		0.05	26.9837	60.1814	60.4327	92.0011	113.2999	113.4500
		0.1	26.7977	59.2055	59.4600	89.7000	108.7412	109.8368
		0.2	26.0901	54.3706	55.7208	55.9869	60.5749	62.0420
	3/2	0.01	44.8745	76.5059	122.2308	129.3018	152.4024	202.8747
		0.05	44.7076	75.9895	120.9362	127.7948	150.3405	199.1429
		0.1	44.2099	74.4581	117.1636	123.4239	134.9106	144.4096
		0.2	42.3708	67.4553	69.1257	72.2116	84.1352	85.7846
	2.0	0.01	71.0432	100.7318	151.7710	209.1492	224.1623	238.0734
		0.05	70.6409	99.8604	149.7204	205.4401	219.6388	233.1706
		0.1	69.4401	97.2925	143.8273	161.2886	168.7813	195.0177
		0.2	65.1752	80.6443	84.0026	88.6954	107.6571	110.9455

Table 6.57: First six non-dimensional frequencies, $\lambda = \omega a^2 \sqrt{\rho h/D}$ of CCFF rectangular plates with different a/b and h/a ratios

Source	a/b	h/a	λ_1	λ_2	λ_3	λ_4	λ_5	λ_6
ICDPT	0.5	0.01	4.2842	9.1002	18.3623	22.7311	28.8072	33.0046
		0.05	4.2813	9.0890	18.3177	22.6545	28.6975	32.8730
		0.1	4.2743	9.0574	18.1862	22.4268	28.3696	32.4799
		0.2	4.2467	8.9346	17.6853	19.0961	20.9081	22.0961
	2/3	0.01	4.9739	13.2442	23.2845	30.1265	34.1412	52.2647
		0.05	4.9703	13.2195	23.2041	30.0088	34.0003	51.9478
		0.1	4.9613	13.1477	22.9650	29.6572	33.5787	41.9847
		0.2	4.9261	12.8710	20.9923	22.0759	23.8886	25.2928
	1	0.01	6.9284	23.9230	26.5871	47.6607	62.7064	65.5396
		0.05	6.9221	23.8302	26.4987	47.3909	62.1918	65.0272
		0.1	6.9054	23.5534	26.2352	46.5830	49.9352	53.8214
		0.2	6.8402	22.5274	24.9676	26.0955	30.8804	32.7581
	3/2	0.01	11.1906	29.7954	52.3787	67.7684	76.7988	117.5550
		0.05	11.1747	29.6761	51.9830	67.1869	76.1012	115.9809
		0.1	11.1297	29.3185	50.8098	62.8152	64.9909	74.0441
		0.2	10.9550	27.9956	31.4076	31.8239	42.5398	44.1259
	2.0	0.01	17.1347	36.3934	73.4228	90.8812	115.1683	131.9459
		0.05	17.0970	36.2296	72.7448	89.7072	113.4783	129.9197
		0.1	16.9867	35.7385	70.7413	76.3845	76.6019	86.3176
		0.2	16.5647	33.9407	37.6223	38.3009	54.6690	56.0609
ICTDPT	0.5	0.01	4.2842	9.1000	18.3618	22.7303	28.8060	33.0032
		0.05	4.2810	9.0881	18.3157	22.6520	28.6943	32.8692
		0.1	4.2738	9.0564	18.1841	22.4242	28.3663	32.4761
		0.2	4.2462	8.9336	17.6833	19.1895	20.9081	22.0958
	2/3	0.01	4.9739	13.2438	23.2836	30.1252	34.1396	52.2616
		0.05	4.9699	13.2181	23.2016	30.0054	33.9965	51.9419
		0.1	4.9608	13.1461	22.9624	29.6537	33.5748	41.9847
		0.2	4.9255	12.8695	20.9923	21.5626	23.8886	25.2926
	1	0.01	6.9282	23.9220	26.5860	47.6579	62.7025	65.5353
		0.05	6.9214	23.8276	26.4958	47.3854	62.1845	65.0196
		0.1	6.9046	23.5507	26.2322	46.5777	49.9353	54.8270
		0.2	6.8394	22.5250	24.9676	26.2260	30.8804	32.7581
	3/2	0.01	11.1903	29.7940	52.3755	67.7638	76.7932	117.5453
		0.05	11.1735	29.6727	51.9771	67.1790	76.0924	115.9676
		0.1	11.1284	29.3151	50.8040	62.8152	65.4575	74.0358
		0.2	10.9537	27.9926	31.4076	31.9310	42.5398	44.1259
	2.0	0.01	17.1342	36.3913	73.4177	90.8742	115.1589	131.9344
		0.05	17.0952	36.2255	72.7364	89.6968	113.4653	129.9044
		0.1	16.9847	35.7343	70.7333	76.6019	77.0964	86.3081
		0.2	16.5628	33.9371	37.7129	38.3010	54.6691	56.1217

Table 6.58: First six non-dimensional frequencies, $\lambda = \omega a^2 \sqrt{\rho h/D}$ of CFCF rectangular plates with different a/b and h/a ratios

Source	a/b	h/a	λ_1	λ_2	λ_3	λ_4	λ_5	λ_6
ICDPT	0.5	0.01	5.5183	8.9979	15.2070	20.6135	27.3561	29.8983
		0.05	5.5158	8.9836	15.1876	20.5643	27.2123	29.8214
		0.1	5.5103	8.9423	15.1324	19.7967	20.4185	26.7867
		0.2	5.4890	8.7829	9.8984	14.0690	14.9178	19.7210
	2/3	0.01	9.8339	13.6993	27.1143	31.4967	32.8844	52.4856
		0.05	9.8273	13.6745	27.0562	31.3259	32.7777	52.1366
		0.1	9.8102	13.6020	26.8830	30.7075	30.8186	32.4577
		0.2	9.7430	13.3232	15.3538	19.5144	26.2215	29.0046
	1	0.01	22.1953	26.4437	43.6112	61.2043	67.2702	79.7924
		0.05	22.1660	26.3791	43.3516	60.9188	66.8840	78.8614
		0.1	22.0801	26.1854	42.5772	53.7896	60.0591	62.2760
		0.2	21.7461	25.4493	26.8948	30.4362	39.8340	52.2132
	3/2	0.01	50.0646	54.5095	71.2208	105.1732	137.9971	144.1715
		0.05	49.9229	54.2952	70.7021	103.8191	136.5757	142.5332
		0.1	49.4935	53.6469	69.1560	88.7926	94.5915	99.8984
		0.2	44.3963	46.8367	47.8752	51.2540	63.8071	66.7802
	2.0	0.01	89.1115	93.6113	110.0601	142.2732	204.3568	245.5406
		0.05	88.6698	93.0459	109.0412	140.1838	199.2088	241.1108
		0.1	87.3350	91.3451	106.0276	123.3242	127.2529	134.1832
		0.2	61.6621	63.2860	79.8432	80.3632	82.5136	85.3153
ICTDPT	0.5	0.01	5.5182	8.9977	15.2065	20.6127	27.3553	29.8968
		0.05	5.5152	8.9827	15.1859	20.5620	27.2093	29.8179
		0.1	5.5097	8.9413	15.1307	19.7967	20.4161	26.7835
		0.2	5.4883	8.7819	9.8984	14.3096	14.9161	19.7210
	2/3	0.01	9.8336	13.6988	27.1130	31.4955	32.8827	52.4826
		0.05	9.8262	13.6731	27.0531	31.3223	32.7740	52.1306
		0.1	9.8090	13.6005	26.8799	30.7075	30.8150	32.4539
		0.2	9.7419	13.3217	15.3538	19.6886	26.2186	29.0016
	1	0.01	22.1942	26.4423	43.6087	61.1997	67.2651	79.7871
		0.05	22.1634	26.3761	43.3466	60.9118	66.8762	78.8521
		0.1	22.0775	26.1824	42.5722	53.7896	60.0521	63.1472
		0.2	21.7436	25.4465	26.8948	30.5482	39.8299	52.2132
	3/2	0.01	50.0606	54.5053	71.2153	105.1650	137.9839	144.1578
		0.05	49.9169	54.2889	70.6939	103.8072	136.5598	142.5166
		0.1	49.4876	53.6407	69.1482	88.7926	95.1672	99.8876
		0.2	44.3963	46.9095	47.8699	51.2486	63.8010	66.7802
	2.0	0.01	89.1032	93.6028	110.0501	142.2608	204.3374	245.5150
		0.05	88.6592	93.0351	109.0285	140.1682	199.1860	241.0830
		0.1	87.3249	91.3348	106.0158	123.3242	127.6814	134.1694
		0.2	61.6621	63.3399	79.8859	80.3632	82.5050	85.3070

Table 6.59: First six non-dimensional frequencies, $\lambda = \omega a^2 \sqrt{\rho h/D}$ of CFSF rectangular plates with different a/b and h/a ratios

Source	a/b	h/a	λ_1	λ_2	λ_3	λ_4	λ_5	λ_6
ICDPT	0.5	0.01	3.7685	7.8257	12.2680	18.2133	25.7041	32.5970
		0.05	3.7669	7.8135	12.2531	18.1707	25.6405	32.4799
		0.1	3.7634	7.7779	12.2115	18.0454	19.6258	25.4525
		0.2	3.7497	7.6409	9.8129	12.0500	13.8911	17.5690
	2/3	0.01	6.7240	11.4020	21.8922	28.3257	30.2537	45.8435
		0.05	6.7196	11.3817	21.8477	28.2367	30.0901	45.6478
		0.1	6.7087	11.3225	21.7172	27.9713	29.6049	40.7378
		0.2	6.6656	11.0952	15.2225	19.2790	21.2183	26.9791
	1	0.01	15.2037	20.6027	39.7330	49.4632	56.3215	77.4995
		0.05	15.1845	20.5537	39.4985	49.2465	56.0133	76.5926
		0.1	15.1293	20.4078	38.8009	48.5978	53.3356	55.0911
		0.2	14.9146	19.8536	26.6678	30.0930	36.3284	46.2335
	3/2	0.01	34.3490	40.2064	60.0519	97.2576	111.6101	118.6365
		0.05	34.2571	40.0547	59.6236	96.0098	110.5351	117.3655
		0.1	33.9808	39.5984	58.3502	88.0515	92.3986	93.5964
		0.2	32.9370	37.9119	44.0257	46.3337	53.9395	66.5794
	2.0	0.01	61.1985	67.2222	87.6042	124.6660	190.9483	198.6953
		0.05	60.9130	66.8361	86.8190	122.8567	186.1843	195.3466
		0.1	60.0528	65.6777	84.4998	117.6646	122.3002	125.9251
		0.2	56.9334	61.1501	61.5563	62.6231	76.7287	79.5131
ICTDPT	0.5	0.01	3.7685	7.8256	12.2677	18.2127	25.7032	32.5956
		0.05	3.7666	7.8128	12.2519	18.1689	25.6377	32.4763
		0.1	3.7630	7.7771	12.2101	18.0434	19.6258	25.4495
		0.2	3.7493	7.6401	9.8129	12.0486	14.1346	17.5672
	2/3	0.01	6.7239	11.4017	21.8915	28.3245	30.2527	45.8411
		0.05	6.7191	11.3808	21.8454	28.2337	30.0868	45.6426
		0.1	6.7080	11.3214	21.7147	27.9682	29.6014	42.0573
		0.2	6.6649	11.0940	15.2225	19.4552	21.2158	26.9763
	1	0.01	15.2032	20.6020	39.7313	49.4605	56.3182	77.4946
		0.05	15.1830	20.5517	39.4943	49.2410	56.0070	76.5836
		0.1	15.1278	20.4057	38.7966	48.5921	53.3356	55.0848
		0.2	14.9131	19.8515	26.6678	30.2061	36.3248	46.2269
	3/2	0.01	34.3474	40.2044	60.0484	97.2508	111.6017	118.6274
		0.05	34.2537	40.0507	59.6173	95.9989	110.5223	117.3520
		0.1	33.9773	39.5943	58.3440	88.0515	92.3889	94.1778
		0.2	32.9335	37.9080	44.0257	46.4073	53.9344	66.5794
	2.0	0.01	61.1947	67.2180	87.5984	124.6567	190.9315	198.6776
		0.05	60.9068	66.8293	86.8099	122.8434	186.1634	195.3235
		0.1	60.0465	65.6709	84.4911	117.6523	122.3002	126.3581
		0.2	56.9273	61.1501	61.5482	62.6793	76.7192	79.5583

Table 6.60: First six non-dimensional frequencies, $\lambda = \omega a^2 \sqrt{\rho h/D}$ of CFFF rectangular plates with different a/b and h/a ratios

Source	a/b	h/a	λ_1	λ_2	λ_3	λ_4	λ_5	λ_6
ICDPT	0.5	0.01	0.8618	3.7036	5.3662	12.0520	15.0512	23.1905
		0.05	0.8616	3.6984	5.3609	12.0287	15.0191	19.6119
		0.1	0.8612	3.6839	5.3469	9.8060	11.9612	14.9257
		0.2	0.8599	3.6276	4.9030	5.2927	11.7024	13.7539
	2/3	0.01	1.5381	5.1861	9.5520	17.4912	23.7950	27.4095
		0.05	1.5376	5.1786	9.5365	17.4478	23.6756	27.3084
		0.1	1.5365	5.1574	9.4925	15.1985	17.3201	19.3709
		0.2	1.5324	5.0753	7.1132	9.3227	16.8354	18.0439
	1	0.01	3.4771	8.5173	21.3051	27.1935	30.9836	54.3475
		0.05	3.4749	8.5037	21.2284	27.0568	30.8527	53.2294
		0.1	3.4696	8.4643	21.0001	26.6147	30.4612	52.7578
		0.2	3.4494	8.3126	11.8177	13.3074	20.1493	25.2055
	3/2	0.01	7.8525	14.3943	32.5571	49.3227	58.3682	70.8375
		0.05	7.8430	14.3646	32.3733	48.9652	57.8592	70.0649
		0.1	7.8171	14.2777	31.8271	41.6953	43.9757	47.9047
		0.2	7.7163	13.9453	19.7842	21.9879	29.8815	39.7933
	2.0	0.01	13.9892	21.4390	40.7407	76.4084	87.3578	98.7035
		0.05	13.9611	21.3793	40.4925	75.4704	86.2333	97.3874
		0.1	13.8800	21.2022	39.7536	57.4022	61.1384	72.7468
		0.2	13.5690	20.5335	27.9382	30.5692	37.1438	50.9900
ICTDPT	0.5	0.01	0.8618	3.7035	5.3661	12.0517	15.0509	23.1897
		0.05	0.8616	3.6981	5.3604	12.0275	15.0175	19.6119
		0.1	0.8612	3.6835	5.3464	9.8060	11.9598	14.9239
		0.2	0.8599	3.6272	4.9030	5.2921	11.7010	13.9999
	2/3	0.01	1.5381	5.1860	9.5518	17.4907	23.7944	27.4085
		0.05	1.5375	5.1781	9.5356	17.4460	23.6730	27.3053
		0.1	1.5363	5.1568	9.4914	15.1985	17.3181	22.0116
		0.2	1.5322	5.0747	7.5781	9.3217	16.8335	18.2322
	1	0.01	3.4770	8.5171	21.3044	27.1927	30.9822	54.3442
		0.05	3.4746	8.5028	21.2261	27.0538	30.8492	53.2294
		0.1	3.4693	8.4634	20.9977	26.6147	26.6493	28.9958
		0.2	3.4490	8.3116	12.1032	13.3074	20.1471	25.2028
	3/2	0.01	7.8524	14.3937	32.5558	49.3199	58.3645	70.8330
		0.05	7.8422	14.3631	32.3697	48.9596	57.8525	70.0565
		0.1	7.8162	14.2761	31.8234	42.9857	43.9757	47.8992
		0.2	7.7154	13.9437	19.9560	21.9879	29.8783	39.8789
	2.0	0.01	13.9889	21.4381	40.7386	76.4033	87.3512	98.6957
		0.05	13.9596	21.3769	40.4879	75.4615	86.2233	97.3761
		0.1	13.8784	21.1997	39.7490	58.3462	61.1384	72.7385
		0.2	13.5674	20.5312	28.0601	30.5692	37.1399	51.0568

Table 6.61: First six non-dimensional frequencies, $\lambda = \omega a^2 \sqrt{\rho h/D}$ of CFFS rectangular plates with different a/b and h/a ratios

Source	a/b	h/a	λ_1	λ_2	λ_3	λ_4	λ_5	λ_6
ICDPT	0.5	0.01	2.1282	7.7436	16.0335	17.7501	23.2312	32.2863
		0.05	2.1271	7.7346	15.9871	17.7081	23.1538	32.1579
		0.1	2.1245	7.7094	15.8509	17.5852	22.9243	31.7746
		0.2	2.1147	7.6115	15.3393	17.1177	18.9041	20.3434
	2/3	0.01	3.0768	12.0869	17.0575	28.4715	29.8623	47.9191
		0.05	3.0750	12.0646	17.0076	28.3604	29.7519	47.6417
		0.1	3.0707	12.0002	16.8614	28.0291	29.4230	44.4586
		0.2	3.0539	11.7518	16.3132	21.2356	22.7869	24.0146
	1	0.01	5.3554	19.0773	24.6782	43.0850	52.7005	63.7765
		0.05	5.3512	19.0163	24.5925	42.8542	52.3082	63.2675
		0.1	5.3398	18.8358	24.3372	42.1637	51.1450	53.5134
		0.2	5.2956	18.1598	23.3885	25.9345	27.6816	31.0818
	3/2	0.01	9.9356	24.4633	51.4296	57.5191	72.7683	108.8352
		0.05	9.9220	24.3781	51.0334	57.0754	72.1109	107.3580
		0.1	9.8837	24.1243	49.8589	55.7620	64.6242	68.2365
		0.2	9.7351	23.1792	31.6360	34.1182	42.9083	44.4300
	2.0	0.01	16.1302	31.4733	63.3873	90.2912	111.2278	117.2302
		0.05	16.0952	31.3453	62.8488	89.1166	109.5777	115.5524
		0.1	15.9931	30.9625	61.2567	76.0595	81.2271	85.7248
		0.2	15.6023	29.5538	37.4572	40.6136	55.2881	56.0561
ICTDPT	0.5	0.01	2.1281	7.7435	16.0333	17.7496	23.2305	32.2849
		0.05	2.1270	7.7339	15.9857	17.7063	23.1515	32.1542
		0.1	2.1243	7.7086	15.8492	17.5832	22.9218	31.7708
		0.2	2.1145	7.6107	15.3374	17.1157	19.0835	21.1509
	2/3	0.01	3.0768	12.0866	17.0572	28.4704	29.8611	47.9166
		0.05	3.0748	12.0635	17.0061	28.3574	29.7486	47.6364
		0.1	3.0704	11.9989	16.8595	28.0260	29.4196	45.5738
		0.2	3.0535	11.7505	16.3112	21.3956	22.7869	24.0146
	1	0.01	5.3554	19.0769	24.6773	43.0829	52.6981	63.7724
		0.05	5.3507	19.0146	24.5898	42.8495	52.3021	63.2602
		0.1	5.3393	18.8337	24.3344	42.1590	51.1387	54.5247
		0.2	5.2950	18.1577	23.3860	26.0656	27.6816	31.0818
	3/2	0.01	9.9354	24.4624	51.4266	57.5161	72.7634	108.8270
		0.05	9.9211	24.3757	51.0276	57.0688	72.1027	107.3456
		0.1	9.8826	24.1216	49.8532	55.7552	65.4639	68.2365
		0.2	9.7340	23.1766	31.7435	34.1182	42.9083	44.4300
	2.0	0.01	16.1298	31.4718	63.3836	90.2843	111.2191	117.2211
		0.05	16.0936	31.3420	62.8416	89.1063	109.5651	115.5389
		0.1	15.9913	30.9591	61.2496	76.7741	81.2271	85.7154
		0.2	15.6006	29.5506	37.5481	40.6136	55.2881	55.8533

Table 6.62: First six non-dimensional frequencies, $\lambda = \omega a^2 \sqrt{\rho h/D}$ of CFSC isotropic rectangular plates with different a/b and h/a ratios

Source	a/b	h/a	λ_1	λ_2	λ_3	λ_4	λ_5	λ_6
ICDPT	0.5	0.01	6.5710	14.9373	25.3476	28.2909	34.4280	46.7737
		0.05	6.5655	14.9140	25.2583	28.2120	34.2861	46.5620
		0.1	6.5511	14.8471	24.9919	27.9774	33.8615	45.9280
		0.2	6.4945	14.5882	24.0018	27.0931	30.2324	31.2971
	2/3	0.01	9.3208	24.4132	28.0628	43.9458	48.3041	67.0211
		0.05	9.3113	24.3557	27.9596	43.7344	48.0833	66.4764
		0.1	9.2850	24.1854	27.6512	43.1008	47.4221	59.2630
		0.2	9.1821	23.5376	26.5077	29.6315	32.9068	39.0585
	1	0.01	17.5447	36.0186	51.8168	71.0618	74.2918	105.7805
		0.05	17.5166	35.8688	51.5744	70.5658	73.6497	104.7577
		0.1	17.4342	35.4194	50.8482	69.0867	71.7544	74.0798
		0.2	17.1157	33.7673	37.0399	40.0584	48.2160	55.5966
	3/2	0.01	36.4906	54.3818	91.4868	113.8274	132.5790	149.0869
		0.05	36.3815	54.0899	90.5834	112.6989	130.9860	146.6658
		0.1	36.0534	53.2140	87.9266	102.4865	107.2496	109.3876
		0.2	34.8208	50.0698	51.2432	53.2222	79.1781	80.4692
	2.0	0.01	63.2304	80.5597	116.6000	172.8995	200.8001	219.2017
		0.05	62.9168	79.9798	115.2469	169.7986	197.3610	215.0129
		0.1	61.9726	78.2506	111.3004	133.3754	136.1129	161.0648
		0.2	58.5660	66.6877	67.7362	72.2691	97.5077	98.6727
ICTDPT	0.5	0.01	6.5709	14.9369	25.3466	28.2898	34.4264	46.7712
		0.05	6.5650	14.9125	25.2555	28.2089	34.2824	46.5566
		0.1	6.5504	14.8454	24.9891	27.9742	33.8576	45.9225
		0.2	6.4938	14.5866	23.9992	27.0900	30.3451	31.4058
	2/3	0.01	9.3206	24.4123	28.0616	43.9435	48.3014	67.0167
		0.05	9.3105	24.3531	27.9565	43.7296	48.0778	66.4687
		0.1	9.2841	24.1826	27.6481	43.0960	47.4166	59.2630
		0.2	9.1811	23.5349	26.5049	29.6315	33.0103	39.1157
	1	0.01	17.5442	36.0169	51.8139	71.0571	74.2868	105.7723
		0.05	17.5149	35.8649	51.5686	70.5580	73.6413	104.7455
		0.1	17.4325	35.4155	50.8423	69.0790	71.7464	74.0798
		0.2	17.1139	33.7638	37.0399	40.1434	48.2095	55.6585
	3/2	0.01	36.4888	54.3787	91.4801	113.8187	132.5684	149.0738
		0.05	36.3779	54.0843	90.5733	112.6858	130.9712	146.6490
		0.1	36.0497	53.2084	87.9172	102.4865	107.7572	109.3745
		0.2	34.8172	50.0643	51.2432	53.2867	79.1708	80.4692
	2.0	0.01	63.2264	80.5543	116.5911	172.8843	200.7822	219.1819
		0.05	62.9103	79.9715	115.2345	169.7797	197.3377	214.9882
		0.1	61.9661	78.2425	111.2889	133.3754	136.5132	161.0485
		0.2	58.5598	66.6877	67.7854	72.2631	97.5077	98.6615

Table 6.63: First six non-dimensional frequencies, $\lambda = \omega a^2 \sqrt{\rho h/D}$ of CFSS rectangular plates with different a/b and h/a ratios

Source	a/b	h/a	λ_1	λ_2	λ_3	λ_4	λ_5	λ_6
ICDPT	0.5	0.01	5.1488	14.0750	19.3284	27.6887	29.3102	43.9800
		0.05	5.1453	14.0542	19.2693	27.6130	29.2017	43.7659
		0.1	5.1361	13.9947	19.0951	27.3882	28.8785	43.1253
		0.2	5.0996	13.7644	18.4426	26.5402	27.6816	29.9167
	2/3	0.01	8.2128	22.4062	23.7699	39.4166	47.8677	56.0105
		0.05	8.2055	22.3340	23.7154	39.2415	47.6509	55.5878
		0.1	8.1851	22.1202	23.5543	38.7175	47.0016	54.3373
		0.2	8.1051	21.3207	22.9415	29.3412	32.6222	36.8067
	1	0.01	16.8007	31.1126	51.4039	63.9979	67.5288	101.1793
		0.05	16.7752	30.9963	51.1655	63.4816	67.0775	100.0788
		0.1	16.7004	30.6484	50.4515	61.9549	65.7326	73.5675
		0.2	16.4109	29.3611	36.7837	39.8408	47.8621	55.4984
	3/2	0.01	36.0112	50.4455	82.5040	113.5791	130.0038	134.9054
		0.05	35.9056	50.1917	81.7381	112.4564	128.4645	132.8104
		0.1	35.5877	49.4298	79.4819	102.0742	106.9659	109.1618
		0.2	34.3925	46.6831	51.0371	53.0794	71.9796	80.1260
	2.0	0.01	62.8884	77.3669	108.8188	160.0439	200.6466	217.2356
		0.05	62.5790	76.8303	107.6146	157.2836	197.2145	213.1133
		0.1	61.6475	75.2289	104.0957	133.0291	135.9411	149.4872
		0.2	58.2857	66.5146	67.6454	69.6781	92.7506	96.8097
ICTDPT	0.5	0.01	5.1487	14.0747	19.3280	27.6877	29.3091	43.9779
		0.05	5.1450	14.0529	19.2676	27.6101	29.1988	43.7612
		0.1	5.1356	13.9932	19.0931	27.3851	28.8754	43.1206
		0.2	5.0992	13.7629	18.4404	26.5371	27.6786	30.0301
	2/3	0.01	8.2127	22.4056	23.7690	39.4148	47.8651	56.0078
		0.05	8.2048	22.3320	23.7129	39.2374	47.6455	55.5814
		0.1	8.1843	22.1178	23.5517	38.7133	46.9962	54.3307
		0.2	8.1044	21.3183	22.9389	29.3412	32.7263	36.8028
	1	0.01	16.8002	31.1114	51.4010	63.9944	67.5247	101.1721
		0.05	16.7737	30.9933	51.1598	63.4745	67.0703	100.0678
		0.1	16.6988	30.6452	50.4456	61.9479	65.7254	73.5675
		0.2	16.4093	29.3580	36.7837	39.9262	47.8556	55.5605
	3/2	0.01	36.0095	50.4429	82.4988	113.5705	129.9935	134.8948
		0.05	35.9021	50.1868	81.7294	112.4434	128.4501	132.7953
		0.1	35.5841	49.4249	79.4736	102.0742	107.4744	109.1487
		0.2	34.3891	46.6781	51.0371	53.1440	71.9726	80.1260
	2.0	0.01	62.8844	77.3619	108.8112	160.0309	200.6287	217.2161
		0.05	62.5727	76.8227	107.6034	157.2665	197.1913	213.0888
		0.1	61.6412	75.2214	104.0852	133.0291	136.3413	149.4725
		0.2	58.2796	66.5146	67.6920	69.6752	92.7400	96.8097

First six 3-D mode shapes for free vibration of thick isotropic square plates with different boundary conditions viz. CCCC, CFCF and SCSF are demonstrated in Figs. 6.17 to 6.19 for showing the deflected shapes with reference to the eigenfrequencies. As square plate is considered, the aspect ratio (μ) is taken as unity and length-to-thickness ratio (h/a) is assumed to be 0.05. Looking into the numerical modelling and solutions obtained for shear deformation

theories, one can also depict the 3-D mode shapes of isotropic rectangular plates subjected to any combination of boundary supports with specific μ and h/a.

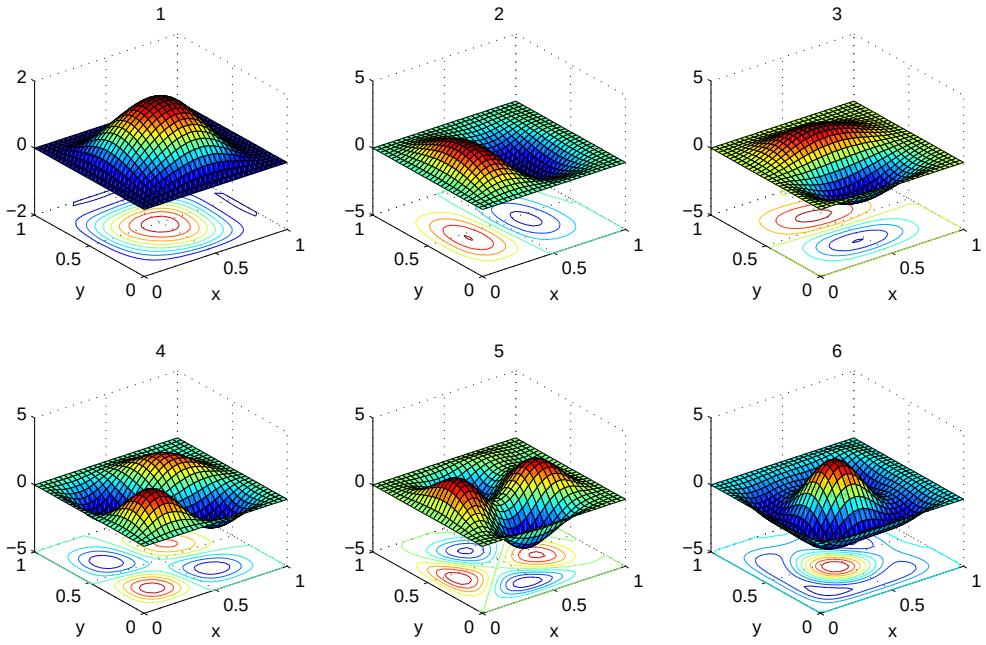

Figure 6.17: First six 3-D mode shapes of CCCC isotropic square plate with $h/a = 0.05$ using PSDPT

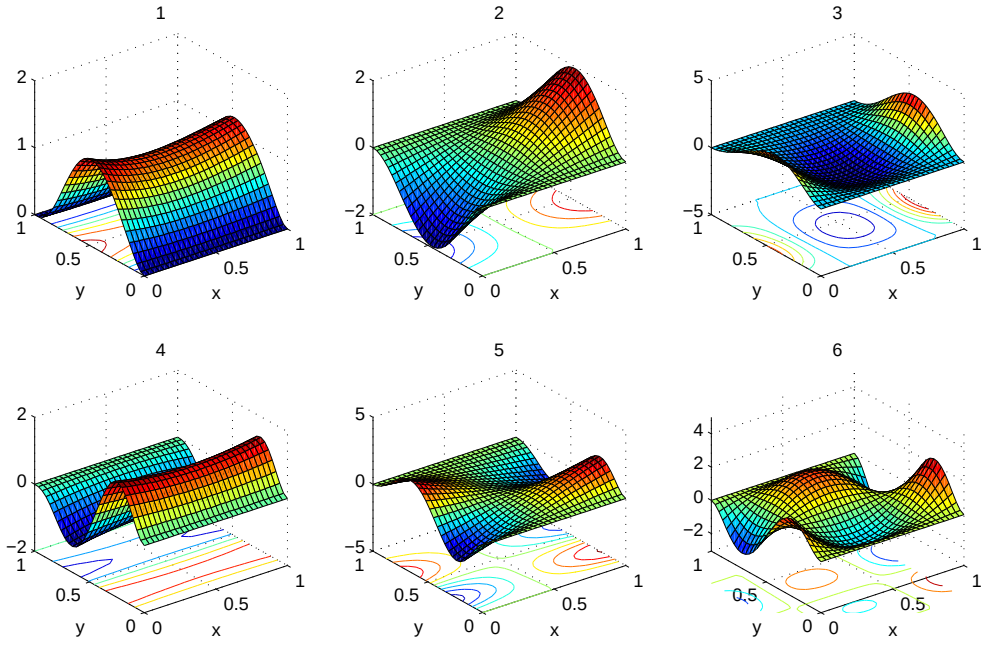

Figure 6.18: First six 3-D mode shapes of CFCF isotropic square plate with $h/a = 0.05$ using PSDPT

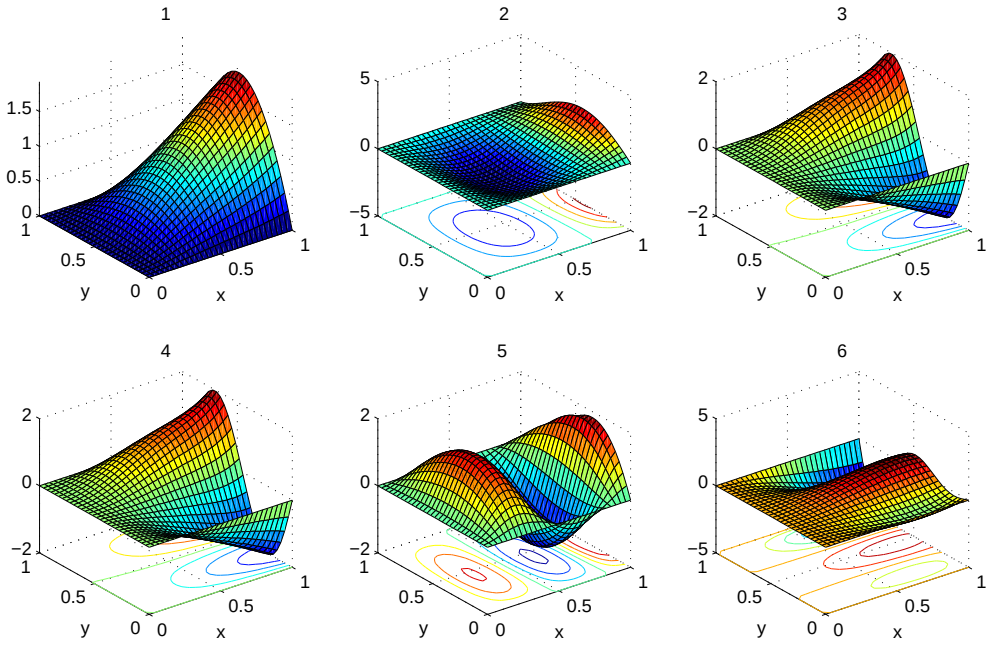

Figure 6.19: First six 3-D mode shapes of SCSF isotropic square plate with $h/a = 0.05$ using PSDPT

6.3 Concluding remarks

The present study involves the evaluation of natural frequencies and mode shapes of thin functionally graded plates with various boundary conditions based on classical plate theory. Both power and exponential gradation of FG material properties have been considered. In addition, vibration problem associated with isotropic thick rectangular plates subjected to different edge conditions has also been investigated. The generalized eigenvalue problem for free vibration can be obtained by means of Rayleigh-Ritz method, which may handle any combination of boundary conditions easily. Looking into the numerical formulation and results, following facts may be concluded.

- The aspect ratios, power-law indices and different material distributions play key factors to examine free vibration characteristics of FG rectangular and square plates.
- In Rayleigh-Ritz method, increase in the number of polynomials (n) play a crucial role in the convergence of non-dimensional frequencies.
- From Tables and Figs., it may be observed that natural frequencies in case of FG plates are increasing with increase in aspect ratios for a fixed power-law index and are

decreasing with increase in power-law exponents for a fixed aspect ratio. This behavior is true irrespective of the edge support, gradation criteria and configuration of the FG plate considered.

- On the other hand in case of exponential gradation, the concerned frequencies are decreasing with increase in E_{rat} and behave reverse with increase in ρ_{rat}. The authenticity of these arguments may be found from the expression of natural frequency.

- In case of isotropic thick plate, aspect ratio (a/b) and thickness-to-length ratio (h/a) are crucial factors that decide the nature of free vibration behavior of thick isotropic plates. Irrespective of the deformation theory and boundary condition assumed, the non-dimensional frequencies are increasing with increase in aspect ratio and are decreasing with increase in thickness-to-length ratio.

- Looking into the non-dimensional frequencies yielded for previously proposed SDPTs, it can easily be noticed that the non-dimensional frequencies associated with PSDPT are comparatively higher than those with 2-DPT and TSDPT regardless of the edge support assumed. On the other hand, it is difficult to compare the solutions obtained for 2-DPT and TSDPT which may fluctuate depending on the modes.

- Comparing the results obtained for the newly proposed SDPTs, it may be evident that ICDPT and ICTDPT provide higher frequencies than those obtained for ISDPT (or ITDPT). On the contrary, ICDPT yields higher results than those for ICTDPT, but with very minute absolute errors (at least $\geq 10^{-4}$). It is also interesting to note that the eigenfrequencies associated with TSDPT, ISDPT and ITDPT are very close to each other and hence present investigation provides solutions for only one of these SDPTs.

- Other shear deformation plate theories can also be extended easily following the above analysis.

Chapter 7

Vibration problems of functionally graded elliptic plates

The contents of this chapter have been published in:

(1) Pradhan, K.K. and Chakraverty, S. (2014). Free vibration of functionally graded thin elliptic plates with various edge supports. *Structural Engineering and Mechanics*, 53 (2):337–354 (Technopress).

Chapter 7

Vibration problems of functionally graded elliptic plates

Free vibration of functionally graded (FG) thin elliptic plates subjected to various classical boundary conditions has been investigated in this chapter by using Rayleigh-Ritz method. The stress-strain relations are considered based on classical plate theory (as discussed in Sec. 2.2.2). The material properties of the FG plate are assumed to vary along thickness direction of the constituents according to power-law form. Trial functions denoting the displacement components are expressed in simple algebraic polynomials, which can handle any classical edge support with ease. The main aim is to study the effect of geometric configurations and gradation of constituent volume fractions on the natural frequencies. New results for frequency parameters are incorporated after performing a test of convergence. A comparison study is carried out with existing literature for verification in special cases. 3-D mode shapes for circular and elliptic FG plates are also presented with various boundary conditions at the edges.

7.1 Numerical modeling

The mathematical modeling for free vibration of functionally graded thin elliptic plates follows the systematic procedures mentioned in Sec. 3.1.3 with power-law variation of material properties as stated in Eq. (2.1). On contrary, the admissible function of FG elliptic plate is also given in the concerned modeling part. Based on the numerical formulation, the natural frequencies for free vibration of FG elliptic plates may now be evaluated after getting the generalized eigenvalue problem of the form Eq. (3.38). 3-D mode shapes are also presented to show the deflected shapes of elliptic plates with respect to a few boundary supports.

7.2 Convergence and comparison studies

In this part, convergence studies for non-dimensional frequencies of isotropic elliptic (or circular) plates (assuming $k = 0$ in case of FG plates) are reported with increase in number of polynomials involved in the displacement component. The material properties of FG constituents are considered in Table 7.1.

Table 7.1: Material properties of the FG elliptic plate constituents

Properties	Unit	Aluminium (Al)	Alumina (Al_2O_3)
E	GPa	70	380
ρ	kg/m^3	2700	3800
ν	-	0.3	0.3

The non-dimensional frequencies of elliptic FG plate may be written as

$$\lambda = \omega a^2 \sqrt{\frac{\rho_c h}{D_c}} \tag{7.1}$$

where D_c(flexural rigidity) = $\frac{E_c h^3}{12(1-\nu^2)}$ of the FG plate due to the deformation effect.

In Tables 7.2 to 7.3, convergence of first six non-dimensional frequencies of isotropic circular and elliptic plates are incorporated. Isotropic circular plate is considered in Table 7.2 and elliptic plate (ratio of semi-major to semi-minor axes; $a/b = 2$) in Table 7.3 respectively with clamped (C) and simply supported (S) edge supports. Rather than taking natural frequencies for combination of symmetric and antisymmetric modes separately, present study computes frequencies for all the modes at a time. This means that earlier authors used deflection function of odd-odd, even-odd, odd-even and even-even polynomials of x and y separately. This investigation considers all the powers of x and y to ease the computation to handle the problem in a single run. So the number of approximations may be seen less in previous works. It is interesting to note here that increase in number of polynomials in displacement component plays a crucial role in the convergence of non-dimensional frequencies irrespective of geometric configuration and edge support of the plate.

Table 7.2: Convergence of non-dimensional frequencies for isotropic circular plate

BCs	Sources	λ_1	λ_2	λ_3	λ_4	λ_5	λ_6
	10×10	10.217	21.275	36.661	43.058	54.650	69.202
	13×13	10.216	21.275	35.609	41.210	54.650	69.202
C	16×16	10.216	21.266	34.941	39.921	52.479	64.682
	19×19	10.216	21.263	34.941	39.921	51.914	62.439
	20×20	10.216	21.261	34.941	39.921	51.209	61.407
	10×10	4.941	13.987	35.665	46.706	59.195	88.161
	13×13	4.938	13.987	30.391	39.456	59.195	88.161
S	16×16	4.935	13.941	25.986	30.503	46.102	59.195
	19×19	4.935	13.915	25.986	30.503	42.362	45.976
	20×20	4.935	13.899	25.986	30.503	40.915	42.362

Table 7.3: Convergence of non-dimensional frequencies for isotropic elliptic plate with $a/b = 2$

BCs	Sources	λ_1	λ_2	λ_3	λ_4	λ_5	λ_6
	10×10	27.395	39.594	61.455	70.023	88.595	95.687
	13×13	27.378	39.594	56.329	70.023	88.595	89.812
C	16×16	27.378	39.503	56.328	70.023	78.029	88.665
	19×19	27.378	39.500	56.328	69.884	78.025	88.665
	20×20	27.378	39.499	56.328	69.884	78.020	88.665
	10×10	13.258	23.910	46.747	55.136	91.258	93.936
	13×13	13.218	23.910	39.388	46.747	76.705	93.936
S	16×16	13.214	23.696	39.366	46.747	62.309	64.636
	19×19	13.214	23.653	39.366	46.341	60.605	64.636
	20×20	13.214	23.645	39.366	46.341	60.497	64.636

After satisfactory test of convergence, we have performed a comparison study for non-dimensional frequencies of elliptic (or circular) plates with the existing literature. As there are not much investigation related to free vibration of elliptic FG plates, it is worth taking isotropic plates to compare the results. First five non-dimensional frequencies of isotropic circular ($a/b = 1.0$) and elliptic plate with different boundary conditions are compared in Table 7.4 assuming Poisson's ratio as $\nu = 0.3$. It may be concluded that frequencies related to present study are in excellent agreement with the previous results.

Table 7.4: Comparison of first five non-dimensional frequencies for isotropic elliptic plate

a/b	BCs	Sources	λ_1	λ_2	λ_3	λ_4	λ_5
1.0	C	Present	10.2158	21.261	34.878	39.773	51.209
	C	Exact	10.216	21.260	34.878	39.773	-
	C	Leissa (1969)	10.2158	21.26	34.88	39.771	51.04
	C	Mazumdar (1971)	10.2151	-	-	-	-
	C	Cheung and Tham (1988)	10.2062	21.27	34.94	40.21	52.05
	C	Singh and Chakraverty (1992a, 1994b)	10.216	21.260	34.878	39.773	-
	C	Rajalingham et al. (1994)	10.2158	21.2604	34.8770	39.7711	51.0300
	C	Chakraverty and Petyt (1997)	10.216	21.260	34.878	39.773	51.030
	C	Wu and Liu (2001); Wu et al. (2002)	10.216	21.260	34.877	39.771	51.030
	C	Prakash and Ganpathi (2006)	10.213	21.259	34.849	-	50.974
	C	Chakraverty et al. (2007)	10.2158	21.2604	34.8770	39.7712	-
	S	Present	4.9351	13.899	25.619	29.737	40.915
	S	Exact	4.935	13.898	25.613	29.720	-
	S	Leissa (1969)	4.9351	13.8982	25.6173	29.7200	39.9573
	S	Leissa and Narita (1980)	4.93515	13.8982	25.6133	29.7200	39.9573
	S	Cheung and Tham (1988)	4.927	13.88	25.54	29.84	40.30
	S	Singh and Chakraverty (1992b, 1994b)	4.9351	13.898	25.613	29.720	-
	S	Chakraverty and Petyt (1997)	4.9351	13.898	25.613	29.720	39.957
	S	Wu and Liu (2001); Wu et al. (2002)	4.935	13.898	25.613	29.720	39.957
	S	Prakash and Ganpathi (2006)	4.935	13.898	25.613	-	39.957
	S	Chakraverty et al. (2007)	4.9351	13.8982	25.6133	29.7201	-
	F	Present	5.3583	9.0035	12.5645	21.2331	22.1935
	F	Exact	5.3583	9.0031	12.439	20.475	-
	F	Leissa (1969)	5.253	9.084	12.23	20.52	21.6
	F	Singh and Chakraverty (1991, 1994b)	5.3583	9.0031	12.439	20.475	-
	F	Chakraverty and Petyt (1997)	5.3583	9.0031	12.439	20.475	21.835
	F	Wu and Liu (2001); Wu et al. (2002)	5.358	9.003	12.439	20.475	21.835
	F	Chakraverty et al. (2007)	5.3583	9.0031	12.4390	20.4746	-
2.0	C	Present	27.377	39.499	55.985	69.863	78.020
	C	Leissa (1969)	27.378	-	-	-	-
	C	Mazumdar (1971)	27.741	-	-	-	-
	C	Singh and Chakraverty (1992a)	27.377	39.497	55.985	69.858	-
	C	Singh and Chakraverty (1994b)	27.377	39.497	55.985	69.858	77.037
	C	Chakraverty et al. (2007)	27.3774	39.4974	55.9758	69.8580	-
	S	Present	13.213	23.645	38.354	46.165	60.497
	S	Singh and Chakraverty (1992b)	13.213	23.641	38.354	46.151	57.625
	S	Singh and Chakraverty (1994b)	13.213	23.641	38.354	46.151	-
	S	Chakraverty et al. (2007)	13.2135	23.6410	38.3259	46.1504	-
	F	Present	6.6706	10.548	17.213	22.353	32.696
	F	Singh and Chakraverty (1994b)	6.6706	10.548	16.923	22.019	-
	F	Chakraverty et al. (2007)	6.6705	10.5476	16.9212	22.0149	-

7.3 Results and discussions

In view of the above verification, the effect of aspect ratios (a/b) on first six non-dimensional frequencies are reported in Tables 7.5 to 7.7 with various boundary conditions and gradation of properties in FG constituents. Clamped edge support is considered in Table 7.5 with different

power-law exponents (k) to evaluate the first six non-dimensional frequencies of elliptic FG plates. In a similar fashion, frequencies are computed for simply supported and completely free edge supports in Tables 7.6 and 7.7 respectively. In case of clamped and simply supported edge supports, it can be observed that frequencies are increasing with increase in aspect ratios and act reverse with increase in power-law indices, whereas frequencies follow peculiar behavior in case of completely free FG elliptic plates that is frequencies are decreasing with increase in k and are showing fluctuations with increase in a/b at higher modes.

Table 7.5: Effect of aspect ratios (a/b) on lowest frequencies of clamped elliptic FG plate

a/b	k	λ_1	λ_2	λ_3	λ_4	λ_5	λ_6
1.0	0.0	10.216	21.261	34.878	39.773	51.209	61.407
	0.1	9.851	20.501	33.631	38.352	49.379	59.213
	1.0	8.500	17.689	29.020	33.093	42.609	51.094
	2.0	8.125	16.909	27.741	31.634	40.730	48.841
1.5	0.0	17.129	28.472	41.487	44.392	57.038	65.369
	0.1	16.517	27.454	40.005	42.806	54.999	63.032
	1.0	14.253	23.690	34.519	36.936	47.458	54.389
	2.0	13.624	22.646	32.998	35.308	45.366	51.992
2.0	0.0	27.377	39.499	55.985	69.863	78.020	88.074
	0.1	26.399	38.087	53.984	67.366	75.232	84.926
	1.0	22.779	32.865	46.582	58.129	64.917	73.282
	2.0	21.775	31.416	44.529	55.566	62.055	70.051
3.0	0.0	56.801	71.626	90.350	116.81	147.34	150.18
	0.1	54.771	69.066	87.121	112.64	142.08	144.81
	1.0	47.261	59.596	75.176	97.195	122.59	124.95
	2.0	45.177	56.969	71.862	92.909	117.19	119.44

Table 7.6: Effect of aspect ratios (a/b) on lowest frequencies of simply supported elliptic FG plate

a/b	k	λ_1	λ_2	λ_3	λ_4	λ_5	λ_6
1.0	0.0	4.935	13.899	25.619	29.736	40.915	51.072
	0.1	4.759	13.402	24.703	28.674	39.453	49.247
	1.0	4.106	11.564	21.316	24.742	34.043	42.495
	2.0	3.925	11.055	20.376	23.651	32.542	40.621
1.5	0.0	8.282	17.835	27.452	31.805	41.409	52.246
	0.1	7.986	17.198	26.471	30.668	39.929	50.379
	1.0	6.891	14.839	22.842	26.463	34.454	43.472
	2.0	6.587	14.186	21.835	25.297	32.935	41.555
2.0	0.0	13.213	23.645	38.354	46.165	60.497	62.848
	0.1	12.741	22.799	36.984	44.515	58.335	60.602
	1.0	10.994	19.673	31.913	38.412	50.337	52.292
	2.0	10.509	18.806	30.506	36.718	48.118	49.987
3.0	0.0	27.081	40.146	57.050	84.282	98.673	116.06
	0.1	26.114	38.711	55.011	81.269	95.146	111.91
	1.0	22.533	33.403	47.469	70.127	82.101	96.569
	2.0	21.539	31.931	45.376	67.035	78.481	92.312

Table 7.7: Effect of aspect ratios (a/b) on lowest frequencies of completely free elliptic FG plate

a/b	k	λ_1	λ_2	λ_3	λ_4	λ_5	λ_6
1.0	0.0	5.358	9.003	12.564	21.233	22.193	37.564
	0.1	5.167	8.682	12.115	20.474	21.400	36.221
	1.0	4.458	7.491	10.454	17.667	18.466	31.255
	2.0	4.262	7.161	9.993	16.888	17.652	29.877
1.5	0.0	6.477	7.986	16.309	16.510	17.767	29.971
	0.1	6.245	7.701	15.726	15.920	17.132	28.899
	1.0	5.389	6.645	13.569	13.737	14.783	24.937
	2.0	5.151	6.352	12.971	13.132	14.131	23.838
2.0	0.0	6.671	10.548	17.212	22.353	27.773	32.696
	0.1	6.432	10.171	16.596	21.554	26.780	31.527
	1.0	5.550	8.776	14.321	18.599	23.108	27.205
	2.0	5.306	8.389	13.689	17.779	22.089	26.005
3.0	0.0	6.757	15.615	17.618	31.415	33.961	51.246
	0.1	6.516	15.057	16.988	30.292	32.748	49.414
	1.0	5.622	12.992	14.659	26.139	28.258	42.639
	2.0	5.374	12.419	14.013	24.986	27.012	40.759

In Tables 7.8 to 7.9, effect of variation of Poisson's ratio (ν) on natural frequencies of elliptic (or circular) FG plates supported by various edge conditions with fixed aspect ratio (a/b) and power-law index (k) are summarized. For both isotropic ($k = 0$) and FG plates, it can be easily seen that frequencies remain constant for different values of ν in case of clamped plates. Assuming simply supported, frequencies are increasing with increase in ν, whereas frequencies are showing fluctuating order while considering free edge condition, keeping both a/b and k fixed. One may conclude that effects of edge supports and Poisson's ratio on free vibration response of FG elliptic plates is also quite similar to that of isotropic elliptic plates.

Table 7.8: Effect of Poisson's ratio (ν) on non-dimensional frequencies of elliptic FG plate with various BCs for $k = 0$

a/b	BC	ν	λ_1	λ_2	λ_3	λ_4	λ_5	λ_6
1.0	C	0.00	10.216	21.260	34.878	39.773	51.209	61.407
		0.25	10.216	21.260	34.878	39.773	51.209	61.407
		0.33	10.216	21.260	34.878	39.773	51.209	61.407
		0.50	10.216	21.260	34.878	39.773	51.209	61.407
	S	0.00	4.4436	13.502	25.249	29.379	40.519	50.644
		0.25	4.8601	13.835	25.559	29.678	40.851	51.002
		0.33	4.9790	13.936	25.654	29.771	40.953	51.114
		0.50	5.2127	14.141	25.849	29.963	41.166	51.347
	F	0.00	6.1531	8.2441	14.148	20.758	24.659	37.779
		0.25	5.5112	8.8902	12.881	21.158	22.701	37.599
		0.33	5.2620	9.0692	12.363	21.277	21.867	37.543
		0.50	4.6404	9.4141	11.021	19.648	21.519	34.641
2.0	C	0.00	27.377	39.499	55.985	69.862	78.019	88.074
		0.25	27.377	39.499	55.985	69.862	78.019	88.074
		0.33	27.377	39.499	55.985	69.862	78.019	88.074
		0.50	27.377	39.499	55.985	69.862	78.019	88.074
	S	0.00	12.646	22.829	37.367	45.803	59.139	62.416
		0.25	13.125	23.519	38.201	46.106	60.283	62.777
		0.33	13.265	23.718	38.444	46.201	60.624	62.889
		0.50	13.546	24.115	38.930	46.399	61.314	63.126
	F	0.00	7.060	12.269	18.235	25.329	27.675	34.809
		0.25	6.778	10.870	17.473	22.938	27.775	33.196
		0.33	6.597	10.346	17.034	21.981	27.768	32.359
		0.50	6.037	9.0676	15.683	19.540	27.710	29.828

Table 7.9: Effect of Poisson's ratio (ν) on non-dimensional frequencies of elliptic FG plate with various BCs for $k = 1$

a/b	BC	ν	λ_1	λ_2	λ_3	λ_4	λ_5	λ_6
1.0	C	0.00	8.5001	17.689	29.019	33.093	42.609	51.094
		0.25	8.5001	17.689	29.019	33.093	42.609	51.094
		0.33	8.5001	17.689	29.019	33.093	42.609	51.094
		0.50	8.5001	17.689	29.019	33.093	42.609	51.094
	S	0.00	3.6973	11.234	21.009	24.445	33.715	42.139
		0.25	4.0439	11.512	21.266	24.694	33.989	42.436
		0.33	4.1428	11.596	21.346	24.771	34.075	42.529
		0.50	4.3372	11.766	21.508	24.931	34.253	42.724
	F	0.00	5.1197	6.8595	11.772	17.272	20.517	31.434
		0.25	4.5856	7.3971	10.718	17.605	18.889	31.284
		0.33	4.3783	7.5461	10.286	17.704	18.194	31.238
		0.50	3.8610	7.8330	9.1701	16.348	17.9045	28.823
2.0	C	0.00	22.779	32.865	46.582	58.129	64.916	73.282
		0.25	22.779	32.865	46.582	58.129	64.916	73.282
		0.33	22.779	32.865	46.582	58.129	64.916	73.282
		0.50	22.779	32.865	46.582	58.129	64.916	73.282
	S	0.00	10.522	18.995	31.092	38.111	49.207	51.933
		0.25	10.921	19.569	31.785	38.362	50.158	52.234
		0.33	11.038	19.735	31.988	38.441	50.442	52.328
		0.50	11.271	20.065	32.392	38.607	51.017	52.524
	F	0.00	5.874	10.208	15.173	21.075	23.027	28.962
		0.25	5.639	9.0445	14.538	19.085	23.111	27.621
		0.33	5.489	8.6086	14.173	18.289	23.105	26.925
		0.50	5.023	7.5447	13.049	16.258	23.056	24.819

Three-dimensional mode shapes of FG circular and elliptic plates are plotted in Figs. 7.1 to 7.3 taking various BCs with $k = 1$. Fig. 7.1 is meant for clamped FG plates. In a similar fashion, Fig. 7.2 is for simply supported and Fig. 7.3 is for completely free FG plates respectively. Looking into the deflected shapes of mode shapes, it is easy to predict the edge support to be clamped, simply supported or free, irrespective of the geometry and power-law exponent used in gradation.

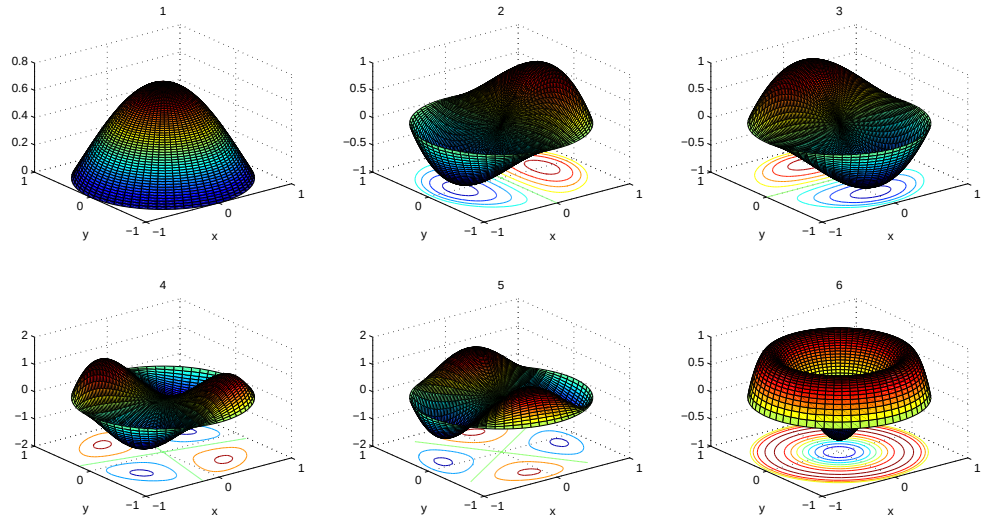

(a) FG circular plate

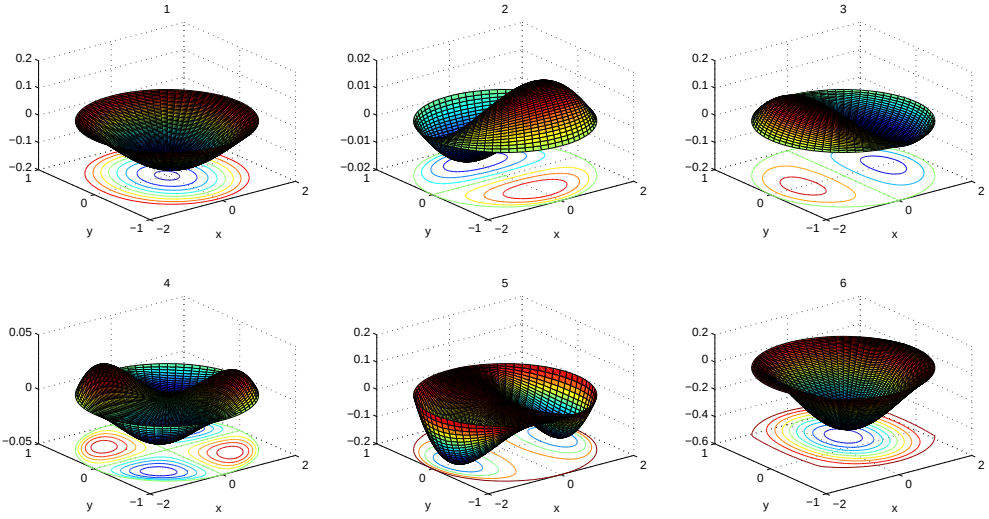

(b) FG elliptic plate

Figure 7.1: Three-dimensional mode shapes of clamped (a) circular and (b) elliptic FG plate with $k = 1$

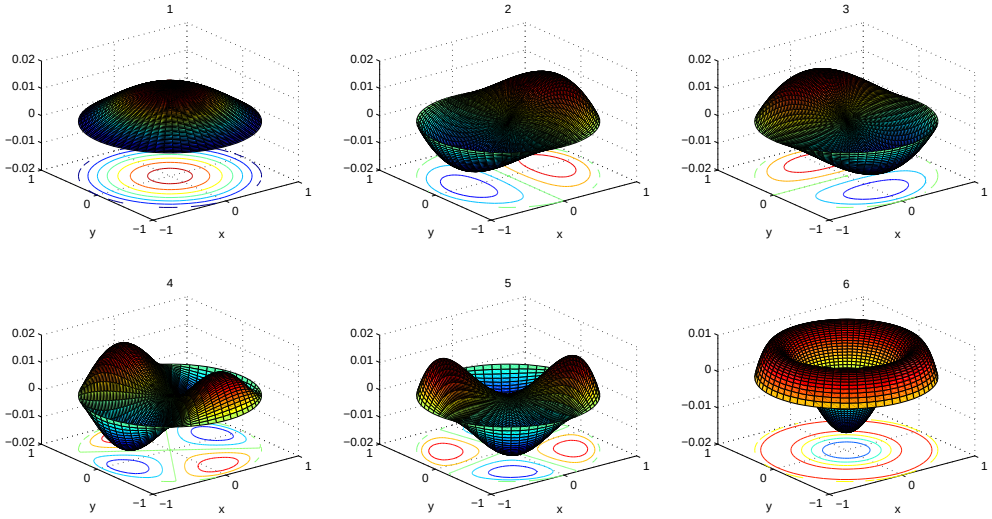

(a) FG circular plate

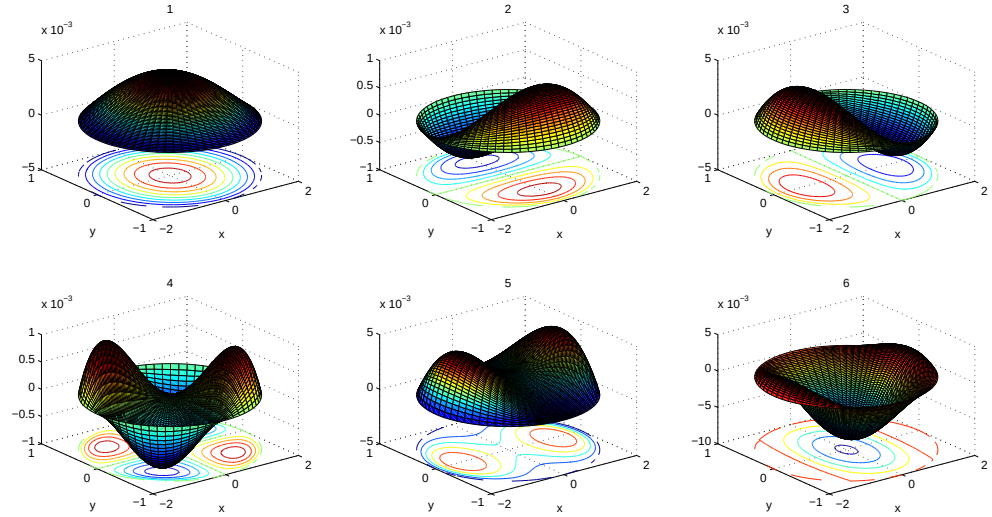

(b) FG elliptic plate

Figure 7.2: 3-D mode shapes of simply-supported (a) circular and (b) elliptic FG plate with $k = 1$

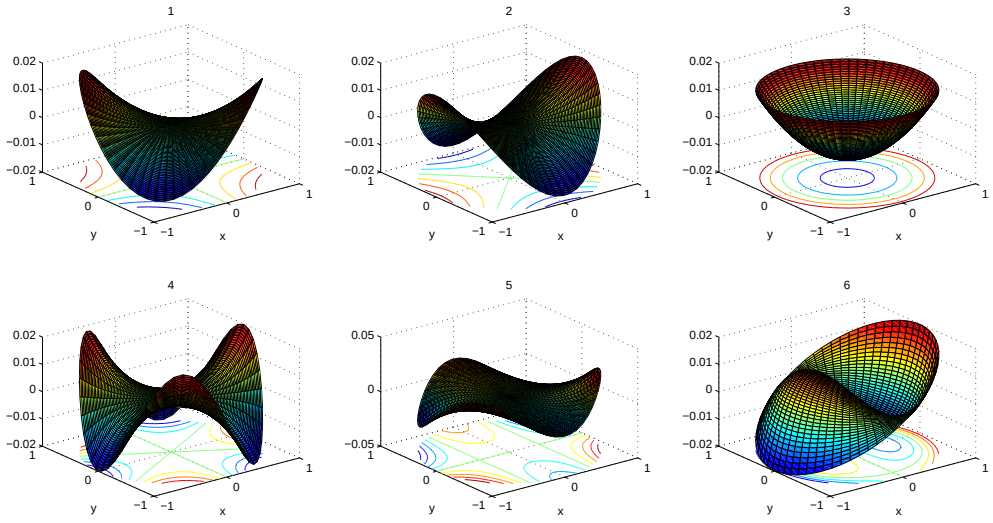

(a) FG circular plate

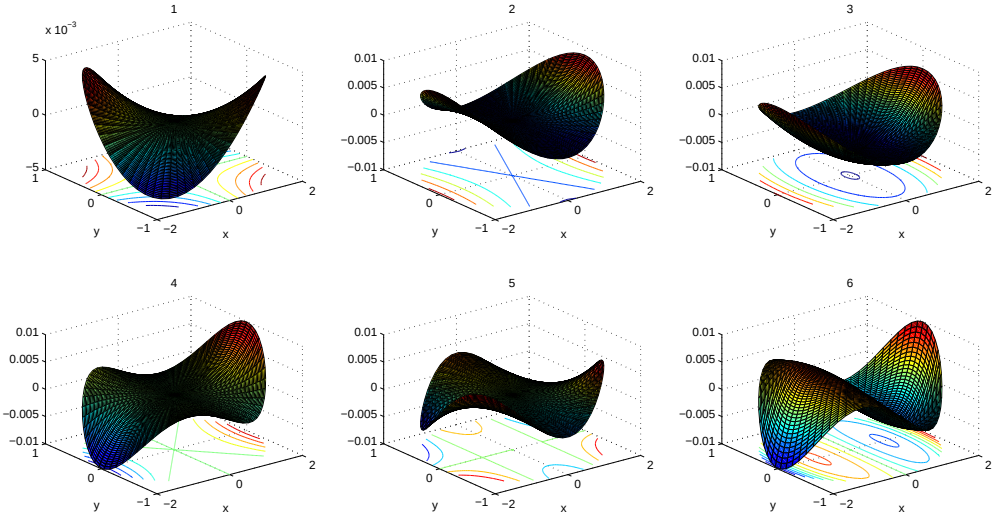

(b) FG elliptic plate

Figure 7.3: 3-D mode shapes of free (a) circular and (b) elliptic FG plate with $k = 1$

7.4 Concluding remarks

The natural frequencies and mode shapes of functionally graded elliptic and circular plates with various boundary conditions based on classical plate theory are evaluated in this investigation. Generalized eigenfrequency equation for free vibration can be obtained by means of Rayleigh-Ritz method. Trial functions denoting displacement component may handle any classical boundary condition very easily. Looking into the numerical formulation and results, one may conclude as follows.

- The aspect ratios (a/b), power-law indices (k) and different material distributions play key factors to study free vibration characteristics of FG elliptic (or circular) plates.

- In Rayleigh-Ritz method, increase in the number of polynomials (n) play a crucial role in the convergence of non-dimensional frequencies.

- From Tables and Figs., it is observed that the frequencies are increasing with increase in aspect ratios for a fixed power-law index and are decreasing with increase in power-law exponents for a fixed aspect ratio. This behavior is true for clamped and simply supported edge supports, whereas there occurs ambiguity with the effect of aspect ratio on frequencies in completely free FG plate.

- Assuming effect of Poisson's ratio (ν), one may see that frequencies are independent of ν for clamped elliptic plates. But frequencies are increasing with increase in ν in case of simply supported and are showing fluctuating behavior while considering free edge condition, keeping both a/b and k fixed.

- Other shear deformation plate theories can also be extended easily following the above analysis.

Chapter 8

Vibration problems of functionally graded triangular plates

The contents of this chapter have been communicated in:

(1) Pradhan, K.K. and Chakraverty, S. (2015). Flexural vibration of functionally graded triangular plates with various boundary conditions. *Aerospace Science and Technology*, Communicated (Elsevier).

Chapter 8

Vibration problems of functionally graded triangular plates

This chapter deals with free vibration of thin functionally graded (FG) thin triangular plates subject to various classical boundary conditions at the three edges. The power-law variation of FG material properties is also considered in this study. The plate displacement components are expressed as the linear combination of simple algebraic polynomials (generated from Pascal's triangle) in the Rayleigh-Ritz method in order to obtain generalized eigenvalue problem. An exhaustive study for free vibration of different types of triangular plate elements has been performed after the test of convergence and validation of numerical results in special cases. 3-D mode shapes for clamped-clamped-clamped (C-C-C) and clamped-free-free (C-F-F) triangular plates are also plotted corresponding to first six non-dimensional frequencies.

8.1 Types of FG triangular elements

In the cartesian coordinate system, a given functionally graded triangle can be completely determined by three numbers a, b and c, as shown in Fig. 8.1. Let us now apply a transformation of coordinates from Cartesian (x,y) to natural coordinate system (ξ,η) to generate a standard triangle as given below (Singh and Chakraverty (1992c)).

$$\xi = \frac{(x - \frac{by}{c})}{a}, \quad \eta = \frac{y}{c}; \quad x = a\xi + b\eta, \quad y = c\eta \tag{8.1}$$

One may notice as truly mentioned in Singh and Chakraverty (1992c) that unlike finite element methods where one element is transformed into another element of similar shape, where we use Eq. (8.1) globally for the whole plate.

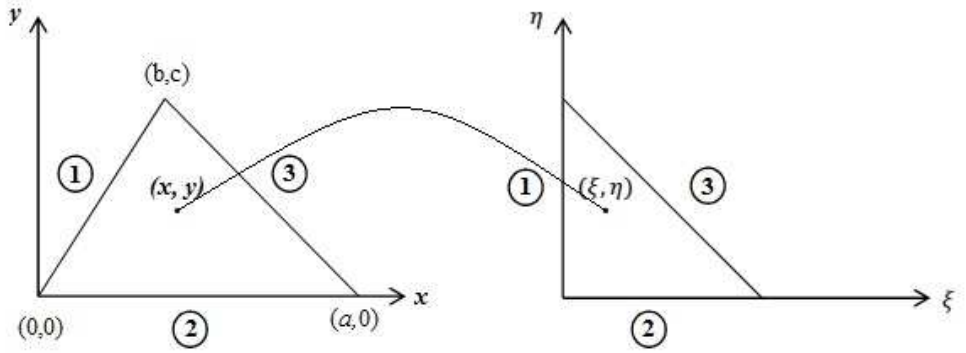

Figure 8.1: Coordinate transformation of given generalized triangle onto the standard triangle (Singh and Chakraverty (1992c))

For present investigation, we have considered four special cases in the same fashion in Singh and Chakraverty (1992c) for FG triangular plates as represented in Fig. 8.2. Four cases as depicted in Figs. 8.2 (a)–(d) have the following features:

- The right–angled triangle is considered in Fig. 8.2 (a) with $\theta = 0$ and different $\mu = 1.0$, 1.5, 2.0, 2.5, 3.0. The lengths of the sides 1, 2 and 3 are μ, 1 and $\sqrt{(1+\mu^2)}$ respectively.
- Fig. 8.2 (b) shows the equilateral triangle with each sides as unity in non–dimensional form. Other geometrical parameters for this triangle are $\theta = 1/\sqrt{3}$ and $\mu = \sqrt{3}/2$.
- A right–angled triangle with angles 30°, 60°and 90°is demonstrated in Fig. 8.2 (c). Sides 1, 2 and 3 have the lengths as $1/\sqrt{3}$, 1 and $2/\sqrt{3}$ respectively. Accordingly, we can find the values of $\theta = 0$ and $\mu = 1/\sqrt{3}$.
- Lastly, Fig. 8.2 (d) represents an isosceles triangle with angles 30°, 30°and 120°. The non–dimensionalized lengths of the sides 1, 2 and 3 are 1, 1 and $\sqrt{3}$ respectively with $\theta = -1/\sqrt{3}$ and $\mu = \sqrt{3}/2$.

In these figures, the boundary conditions may very well be controlled by the assigned edges 1, 2 and 3 respectively.

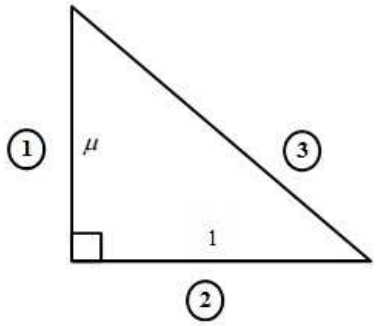

(a) Right–angled triangle with different μ

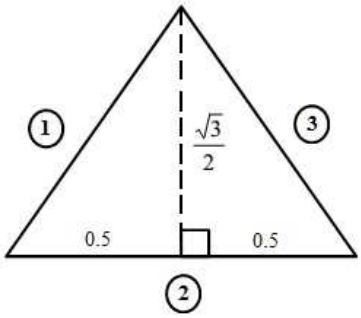

(b) Equilateral triangle

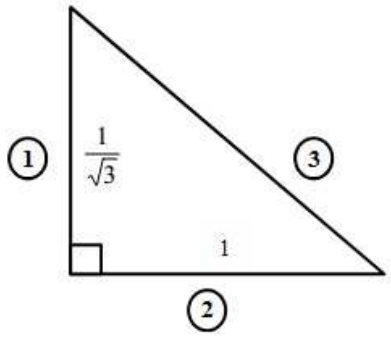

(c) Right–angled triangle with angles 30°, 60°and 90°

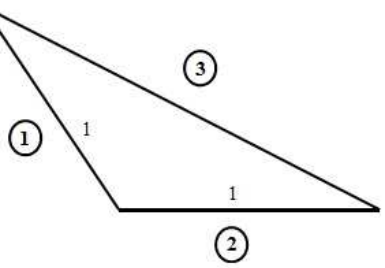

(d) Isosceles triangle with angles 30°, 30°and 120°

Figure 8.2: Four different cases of functionally graded triangular plates

8.2 Numerical modeling

In case of FG triangular plates, there occurs transformation of geometry from general cartesian co-ordinate system to standard triangle. In this regard, the numerical modeling needs a bit of modifications in finding the generalized eigenvalue problem associated with free vibration problem.

Accordingly, we may find the strain energy **U** and kinetic energy **T** of the plate in the form of Eqs. (3.39) and (3.40) respectively. Assuming the coordinate transformation given in Fig. 8.1, the expression for maximum strain and kinetic energies can be written as

$$\mathbf{U}_{max} = \frac{1}{2}\int_{\Omega}\left[D_{11}\left\{\left(\frac{\partial^2 W}{\partial\xi^2}\right)^2 + \left(\frac{\partial^2 W}{\partial\eta^2}\right)^2\right\} + 2D_{12}\frac{\partial^2 W}{\partial\xi^2}\frac{\partial^2 W}{\partial\eta^2} + 4D_{66}\left(\frac{\partial^2 W}{\partial\xi\partial\eta}\right)^2\right]|J(\xi,\eta)|\mathrm{d}\xi\mathrm{d}\eta \quad (8.2)$$

$$\mathbf{T}_{max} = \frac{\omega^2}{2}\int_{\Omega} I_0 W^2 |J(\xi,\eta)|\mathrm{d}\xi\mathrm{d}\eta \quad (8.3)$$

In Eqs. (8.2) and (8.3), $|J(\xi,\eta)|$ represents the Jacobian resulted for the coordinate transformation from (x,y) to (ξ,η) and is given by

$$J(\xi,\eta)=\frac{\partial(x,y)}{\partial(\xi,\eta)}=\begin{pmatrix}\frac{\partial x}{\partial\xi} & \frac{\partial x}{\partial\eta}\\ \frac{\partial y}{\partial\xi} & \frac{\partial y}{\partial\eta}\end{pmatrix}=\begin{pmatrix}a & b\\ 0 & c\end{pmatrix}=ac.$$

Application of Rayleigh-Ritz method

The amplitude $W(\xi,\eta)$ may be expressed as the sum of series of simple algebraic polynomials involving both ξ and η as follows

$$W(\xi,\eta)=\sum_{i=1}^{n}c_i\varphi_i(\xi,\eta)$$

where c_i are unknown constants to be determined and φ_i are the admissible functions, which satisfy the essential boundary conditions and are represented as

$$\varphi_i(\xi,\eta)=f\psi_i(\xi,\eta),\quad i=0,1,2,\cdots,n$$

Here, n is the number of polynomials involved in the admissible functions. The function $f=\xi^p\eta^q(1-\xi-\eta)^r$ with the exponents p, q and r, which control various boundary conditions (BCs). The parameter $p=0$, 1 or 2 according as the side $\xi=0$ is free (F), simply supported (S) or clamped (C). Similar interpretations can be given to the parameters q and r corresponding to the sides $\eta=0$ and $\xi+\eta=1$ respectively. The components of ψ_i may be generated from Pascal's triangle as given in Table 8.1.

Table 8.1: Ten algebraic polynomials obtained from Pascal's triangle

i	1	2	3	4	5	6	7	8	9	10
ψ_i	1	ξ	η	ξ^2	$\xi\eta$	η^2	ξ^3	$\xi^2\eta$	$\xi\eta^2$	η^3

Assuming constant Poisson's ratio (ν), the Rayleigh quotient is obtained by equating $\mathbf{U}_{max}$ and $\mathbf{T}_{max}$ as

$$\omega^2=\frac{\int_\Omega D_{11}\left[\left\{\left(\frac{\partial^2W}{\partial\xi^2}\right)^2+\left(\frac{\partial^2W}{\partial\eta^2}\right)^2\right\}+2\nu\frac{\partial^2W}{\partial\xi^2}\frac{\partial^2W}{\partial\eta^2}+2(1-\nu)\left(\frac{\partial^2W}{\partial\xi\partial\eta}\right)^2\right]\mathrm{d}\xi\mathrm{d}\eta}{\int_\Omega I_0W^2\,\mathrm{d}\xi\mathrm{d}\eta}\qquad(8.4)$$

Next we take the partial derivatives(s) of ω^2 with respect to unknown constants as follows

$$\frac{\partial \omega^2}{\partial c_i} = 0, \quad i = 1, 2, 3, \cdots, n \tag{8.5}$$

Further manipulation of Eq. (8.5) yields the generalized eigenvalue problem of the form

$$\sum_{j=1}^{n} (a_{ij} - \lambda^2 b_{ij}) c_j = 0, \quad i = 1, 2, 3, \cdots, n \tag{8.6}$$

where

$$\begin{aligned} a_{ij} \;=\; & \left[12\left(1-\frac{1}{E_r}\right)\left\{\frac{1}{k+3}-\frac{1}{k+2}+\frac{1}{4(k+1)}\right\}+\frac{1}{E_r}\right]\int_{\Omega}\left[A_1\varphi_i^{\xi\xi}\varphi_j^{\xi\xi}+A_2\varphi_i^{\eta\eta}\varphi_j^{\eta\eta}\right. \\ & +A_3\varphi_i^{\xi\eta}\varphi_j^{\xi\eta}+A_4\left(\varphi_i^{\xi\xi}\varphi_j^{\xi\eta}+\varphi_i^{\xi\eta}\varphi_j^{\xi\xi}\right)+A_5\left(\varphi_i^{\xi\eta}\varphi_j^{\eta\eta}+\varphi_i^{\eta\eta}\varphi_j^{\xi\eta}\right) \\ & \left.+A_6\left(\varphi_i^{\xi\xi}\varphi_j^{\eta\eta}+\varphi_i^{\eta\eta}\varphi_j^{\xi\xi}\right)\right]\mathrm{d}\xi\mathrm{d}\eta, \end{aligned}$$

$$b_{ij} = \left\{\frac{(1-1/\rho_r)}{k+1}+\frac{1}{\rho_r}\right\}\int_{\Omega}\varphi_i\varphi_j\,\mathrm{d}\xi\mathrm{d}\eta, \;\; \lambda^2 = \omega^2 a^4 \rho_c h/D_c$$

with $E_r = E_c/E_m$ and $\rho_r = \rho_c/\rho_m$ are the ratios of Young's moduli and mass densities of FG constituents respectively and $D_c = E_c h^3/12(1-\nu^2)$ is meant for the flexural rigidity of the ceramic constituent of the plate. In the expression of a_{ij}, the superscripted notations stand for partial differentiation and $A_1, A_2, \cdots, A_6$ are defined as

$$\begin{aligned} & A_1 = \left(1+\theta^2\right)^2, \quad A_2 = \frac{1}{\mu^4}, \quad A_3 = \frac{2\left(1-\nu+2\theta^2\right)}{\mu^2}, \\ & A_4 = \frac{-2\theta\left(1+\theta^2\right)}{\mu}, \quad A_5 = \frac{-2\theta}{\mu^3}, \quad A_6 = \frac{\nu+\theta^2}{\mu^2}; \\ & \text{with } \theta = \frac{b}{c}, \quad \mu = \frac{c}{a}. \end{aligned}$$

In the eigenvalue problem (Eq. (8.6)), λ and $c_j = [c_1, c_2, c_3, \cdots, c_n]^T$ refer to the non-dimensional frequency (or frequency parameter) and the column vector of unknown constants respectively. Consequently, we have computed free vibration characteristics for different types of FG triangular plates along with 3-D mode shapes in subsequent discussions.

8.3 Convergence and comparison studies

The physical parameters that mainly influence the free vibration of FG plates are power-law indices (k), E_r and ρ_r. Along with these parameters, two geometric parameters viz. θ and μ also play crucial roles in these computations. As a result, this section involves the convergence of non-dimensional frequencies for one of the FG triangular plates (Fig. 8.2 (a)) and the verification with the available results in special cases.

The convergence of six lowest non-dimensional frequencies of C-C-C FG triangular plate (Fig. 8.2 (a)) is shown in Table 8.2 for different values of power-law index (k), E_r and ρ_r. The respective values of θ and μ are assumed as 0 and 1. It is evident from this table that there occurs convergence of non-dimensional frequencies with the increase in number of polynomials involved in displacement component, irrespective of the other parameters and edge condition. It can also be noticed here that FG triangular plates yield same results for $k = 0$ and for combined effects of $E_r = 1.0$ and $\rho_r = 1.0$. Hence, isotropic plate results can be obtained from FG plate either by assuming k as 0 or for simultaneous effects of E_r and ρ_r as unity.

Table 8.2: Convergence of first six non-dimensional frequencies of C-C-C FG triangular plates with various parameters; $\theta = 0$ and $\mu = 1$

Parameter(s)	Value	n	λ_1	λ_2	λ_3	λ_4	λ_5	λ_6
k ($E_r = 2.0$, $\rho_r = 1.0$)	0	5	94.4970	179.7568	222.8206	305.4952	421.2256	-
		8	94.2693	164.0299	209.9348	291.1884	334.5662	442.9953
		10	94.1526	159.8475	202.0756	290.8454	328.9007	371.6805
		13	93.8589	159.6815	196.7425	255.4264	310.7635	363.8529
		15	93.8094	159.5177	196.4910	248.4158	299.3326	354.9414
	0.1	5	91.7145	174.4639	216.2597	296.4999	408.8226	-
		8	91.4936	159.2000	203.7533	282.6144	324.7150	429.9514
		10	91.3803	155.1408	196.1256	282.2815	319.2162	360.7364
		13	91.0953	154.9797	190.9494	247.9054	301.6131	353.1393
		15	91.0472	154.8207	190.7053	241.1012	290.5188	344.4903
	2.0	5	79.0618	150.3953	186.4251	255.5956	352.4226	-
		8	78.8714	137.2372	175.6441	243.6257	279.9182	370.6365
		10	78.7737	133.7380	169.0686	243.3387	275.1780	310.9702
		13	78.5280	133.5991	164.6066	213.7051	260.0034	304.4212
		15	78.4866	133.4621	164.3961	207.8396	250.4396	296.9653
E_r ($k = 1.0$, $\rho_r = 1.0$)	1.0	5	94.4970	179.7568	222.8206	305.4952	421.2256	-
		8	94.2693	164.0299	209.9348	291.1884	334.5662	442.9953
		10	94.1526	159.8475	202.0756	290.8454	328.9007	371.6805
		13	93.8589	159.6815	196.7425	255.4264	310.7635	363.8529
		15	93.8094	159.5177	196.4910	248.4158	299.3326	354.9414
	2.0	5	81.8368	155.6740	192.9683	264.5666	364.7920	-
		8	81.6396	142.0540	181.8089	252.1766	289.7428	383.6452
		10	81.5385	138.4320	175.0026	251.8795	284.8363	321.8848
		13	81.2842	138.2882	170.3840	221.2057	269.1291	315.1059
		15	81.2413	138.1464	170.1662	215.1344	259.2296	307.3883
	2.5	5	79.0618	150.3953	186.4251	255.5956	352.4226	-
		8	78.8714	137.2372	175.6441	243.6257	279.9182	370.6365
		10	78.7737	133.7380	169.0686	243.3387	275.1780	310.9702
		13	78.5280	133.5991	164.6066	213.7051	260.0034	304.4212
		15	78.4866	133.4621	164.3961	207.8396	250.4396	296.9653
ρ_r ($k = 1.0$, $E_r = 1.0$)	1.0	5	94.4970	179.7568	222.8206	305.4952	421.2256	-
		8	94.2693	164.0299	209.9348	291.1884	334.5662	442.9953
		10	94.1526	159.8475	202.0756	290.8454	328.9007	371.6805
		13	93.8589	159.6815	196.7425	255.4264	310.7635	363.8529
		15	93.8094	159.5177	196.4910	248.4158	299.3326	354.9414
	2.0	5	109.1157	207.5653	257.2911	352.7554	486.3894	-
		8	108.8528	189.4054	242.4119	336.2354	386.3238	511.5269
		10	108.7180	184.5760	233.3369	335.8393	379.7818	429.1797
		13	108.3790	184.3843	227.1786	294.9410	358.8388	420.1412
		15	108.3217	184.1952	226.8882	286.8458	345.6395	409.8511
	2.5	5	112.9455	214.8505	266.3215	365.1366	503.4608	-
		8	112.6734	196.0532	250.9201	348.0367	399.8831	529.4807
		10	112.5338	191.0543	241.5266	347.6267	393.1115	444.2432
		13	112.1829	190.8559	235.1522	305.2929	371.4334	434.8874
		15	112.1237	190.6601	234.8516	296.9136	357.7708	424.2362

In view of the convergence of non-dimensional frequencies, Tables 8.3 to 8.5 are meant for the comparison of present results with the available results in specil cases ($k = 0$; functionally graded plate behaves as isotropic). As no literature is available based on the vibration analysis

of FG triangular plates, we have carried out the validation with the results of isotropic plates. The fundamental non-dimensional frequencies of isotropic right-angled triangular plate is considered in Table 8.3 with different values of μ =1.0, 1.5, 2.0, 2.5 and 3.0. In a similar fashion, first five non-dimensional frequencies of the right-angled and equilateral triangular plates mentioned respectively in Figs. 8.2 (b) and (c) are assumed in Table 8.4. On the other hand, Table 8.5 considers the isosceles triangular plate with angles 30°, 30°and 120°for the comparison of first six non-dimensional frequencies. In these tabulations, it can easily be seen that present results are in excellent agreement with the existing literature.

Table 8.3: Comparison of fundamental non-dimensional frequencies of isotropic right-angled triangular plates with different μ

Sides	Source	$\mu = c/a$				
1-2-3		1.0	1.5	2.0	2.5	3.0
C-C-C	Present	93.8002	65.4639	53.4671	46.9018	42.7799
	Kim and Dickinson (1990)	93.79	65.46	53.45	46.89	42.76
	Singh and Chakraverty (1992c)	93.80	65.46	53.46	46.91	42.81
	Singh and Saxena (1996)	93.791	-	53.448	-	-
F-S-C	Present	31.7854	19.3552	14.4568	11.9106	10.3690
	Kim and Dickinson (1990)	31.78	19.35	14.46	11.91	10.36
	Singh and Chakraverty (1992c)	31.78	19.35	14.46	11.93	10.39
	Singh and Saxena (1996)	31.784	-	14.455	-	-
F-C-F	Present	6.1730	2.8786	1.6581	1.0753	0.7528
	Kim and Dickinson (1990)	6.168	2.876	1.656	1.074	0.7514
	Singh and Chakraverty (1992c)	6.173	2.878	1.658	1.075	0.7528
	Singh and Saxena (1996)	6.1693	-	1.6569	-	-

Table 8.4: Comparison of first five non-dimensional frequencies of isotropic triangular plates mentioned in Figs. 8.2 (b) and (c)

Sides 1-2-3	Plate mentioned in	Source	λ_1	λ_2	λ_3	λ_4	λ_5
C-C-C	Fig. 8.2 (b)	Present	99.0221	189.0510	189.0510	296.8529	316.8320
		Singh and Chakraverty (1992c)	99.022	189.05	189.22	296.85	316.83
		Singh and Saxena (1996)	99.020	189.02	189.22	-	-
	Fig. 8.2 (c)	Present	176.5822	280.9494	380.8706	416.4873	558.4695
		Singh and Chakraverty (1992c)	176.58	280.95	380.92	416.53	558.48
		Singh and Saxena (1996)	176.58	279.80	380.06	-	-
C-C-S	Fig. 8.2 (b)	Present	81.6027	165.1243	165.3528	268.1460	286.8021
		Singh and Chakraverty (1992c)	81.604	165.12	165.52	271.30	286.95
		Singh and Saxena (1996)	81.601	165.00	165.33	-	-
	Fig. 8.2 (c)	Present	137.0544	231.2049	323.9988	362.3161	493.2550
		Singh and Chakraverty (1992c)	137.05	231.20	324.00	362.31	493.97
		Singh and Saxena (1996)	137.02	230.52	321.25	-	-
F-F-S	Fig. 8.2 (b)	Present	22.6596	26.6623	70.6584	74.2863	91.5426
		Singh and Chakraverty (1992c)	22.666	26.717	71.033	74.867	91.959
		Singh and Saxena (1996)	22.646	26.661	69.488	-	-
	Fig. 8.2 (c)	Present	31.8430	68.7922	88.4578	150.3555	167.7079
		Singh and Chakraverty (1992c)	31.843	68.904	88.635	150.70	167.90
		Singh and Saxena (1996)	31.836	68.252	86.485	-	-
F-C-F	Fig. 8.2 (b)	Present	8.9216	35.1313	38.5031	90.5857	93.5195
		Bhat (1987)	8.9221	35.132	38.505	90.590	93.525
		Singh and Chakraverty (1992c)	8.9219	35.155	38.503	91.624	96.725
		Singh and Saxena (1996)	8.9208	35.105	38.487	-	-
	Fig. 8.2 (c)	Present	16.9606	49.7370	87.6047	108.4652	180.4222
		Singh and Chakraverty (1992c)	16.960	49.737	87.604	108.46	180.78
		Singh and Saxena (1996)	16.948	49.712	87.338	-	-

Table 8.5: Comparison of first six non-dimensional frequencies of isotropic isosceles triangular plates with angles 30°, 30°and 120°

Sides 1-2-3	Source	λ_1	λ_2	λ_3	λ_4	λ_5	λ_6
F-C-F	Present	5.7167	21.5246	37.4540	56.0597	74.6846	120.6420
	Mirza and Bijlani (1985)	5.7667	21.100	35.950	54.143	67.425	102.56
	Bhat (1987)	5.7170	21.525	37.455	56.061	74.625	120.65
	Singh and Chakraverty (1992c)	5.7167	21.524	37.456	56.141	74.769	121.16

8.4 Results and discussions

In view of the above test of convergence and comparison studies, we have now evaluated the first six non-dimensional frequencies of FG triangular plates included in Figs. 8.2 (a)-(d) for different combination of boundary conditions. As such, we have incorporated the effect of three major physical parameters viz. k, E_r and ρ_r in three subsections, as discussed in Sec. 8.3.

8.4.1 Effect of power-law indices (k)

The variation of first six non-dimensional frequencies of the right-angled FG triangular element (Fig. 8.2 (a)) with increase in k are computed in Tables 8.6 to 8.11 subjected to six different boundary supports viz. C-C-C, C-C-S, S-S-S, C-C-F, C-S-F and C-F-F and also for different values of μ = 1.0, 1.5, 2.0, 2.5 and 3.0. Similar results for the FG triangular plates of Figs. 8.2 (b) to 8.2 (d) are reported in Tables 8.12 to 8.14 respectively. Ten different combination of edge supports viz. C-C-C, C-C-S, C-C-F, S-S-S, S-C-S, S-C-F, S-F-S, F-F-F, F-C-F and F-F-S are considered in Tables 8.12 to 8.14. The physical and geometric parameters concerned with these plates have been taken the same as stated in Sec. 8.1. The ratio of Young's moduli (E_r) and the ratio of mass densities (ρ_r) of the FG material constituents are assumed to be 2.0 and 1.0 respectively along with the power-law indices k = 0.1, 0.2, 1.0, 2.0 and 5.0. In these tabulations, it may be noted that the non-dimensional frequencies are decreasing with increase in k irrespective of the boundary support and geometry considered. Other than this, the descending behavior with increase in μ can also be indicated in Tables 8.6 to 8.11. After analyzing the present results, one may also find the similar effect of power-law exponents (k) on the frequencies of FG triangular plates for other boundary conditions.

Table 8.6: Effect of k on first six non–dimensional frequencies of C–C–C FG right–angled triangle (Fig. 8.2 (a)) for $\theta = 0$, $E_r = 2.0$ and $\rho_r = 1.0$

μ	k	λ_1	λ_2	λ_3	λ_4	λ_5	λ_6
1.0	0.1	91.0472	154.8207	190.7053	241.1012	290.5188	344.4903
	0.2	88.8830	151.1406	186.1722	235.3702	283.6130	336.3016
	1.0	81.2413	138.1464	170.1662	215.1344	259.2296	307.3883
	2.0	78.4866	133.4621	164.3961	207.8396	250.4396	296.9653
	5.0	75.2148	127.8987	157.5433	199.1757	240.0000	284.5863
1.5	0.1	63.5941	103.6130	137.4716	164.7291	207.8836	247.8950
	0.2	62.0825	101.1501	134.2039	160.8134	202.9421	242.0024
	1.0	56.7450	92.4538	122.6658	146.9876	185.4943	221.1964
	2.0	54.8208	89.3189	118.5064	142.0035	179.2045	213.6961
	5.0	52.5356	85.5956	113.5665	136.0841	171.7344	204.7881
2.0	0.1	51.8958	81.3229	116.2544	127.2009	167.5871	184.1184
	0.2	50.6622	79.3899	113.4910	124.1773	163.6035	179.7419
	1.0	46.3065	72.5644	103.7337	113.5012	149.5378	164.2887
	2.0	44.7364	70.1038	100.2163	109.6526	144.4673	158.7180
	5.0	42.8715	67.1816	96.0388	105.0817	138.4451	152.1018
2.5	0.1	45.5936	69.5275	98.9260	106.8867	148.7133	160.8342
	0.2	44.5098	67.8748	96.5745	104.3459	145.1783	157.0111
	1.0	40.6831	62.0393	88.2716	95.3749	132.6967	143.5122
	2.0	39.3036	59.9357	85.2785	92.1409	128.1972	138.6459
	5.0	37.6652	57.4372	81.7236	88.3000	122.8533	132.8665
3.0	0.1	41.6979	61.2381	85.8599	99.1123	139.5690	151.6590
	0.2	40.7067	59.7824	83.8190	96.7564	136.2514	148.0540
	1.0	37.2070	54.6427	76.6127	88.4378	124.5372	135.3252
	2.0	35.9453	52.7898	74.0149	85.4391	120.3144	130.7365
	5.0	34.4470	50.5893	70.9296	81.8775	115.2991	125.2868

Table 8.7: Effect of k on first six non–dimensional frequencies of C–C–S FG right–angled triangle (Fig. 8.2 (a)) for $\theta = 0$, $E_r = 2.0$ and $\rho_r = 1.0$

μ	k	λ_1	λ_2	λ_3	λ_4	λ_5	λ_6
1.0	0.1	71.2630	129.1405	163.5442	216.1318	268.2843	314.6799
	0.2	69.5691	126.0708	159.6567	210.9943	261.9071	307.1998
	1.0	63.5879	115.2320	145.9303	192.8542	239.3898	280.7885
	2.0	61.4318	111.3246	140.9821	186.3149	231.2725	271.2675
	5.0	58.8710	106.6841	135.1052	178.5483	221.6319	259.9597
1.5	0.1	49.5298	86.3298	117.5549	146.0365	186.6522	228.8853
	0.2	48.3524	84.2777	114.7606	142.5651	182.2154	223.4446
	1.0	44.1954	77.0320	104.8941	130.3082	166.5496	204.2341
	2.0	42.6968	74.4199	101.3373	125.8897	160.9022	197.3089
	5.0	40.9170	71.3177	97.1131	120.6420	154.1950	189.0841
2.0	0.1	40.1110	67.3078	98.9876	107.7777	154.1249	183.8509
	0.2	39.1575	65.7079	96.6347	105.2157	150.4613	179.4807
	1.0	35.7910	60.0587	88.3266	96.1699	137.5255	164.0500
	2.0	34.5774	58.0222	85.3316	92.9089	132.8622	158.4874
	5.0	33.1360	55.6035	81.7745	89.0360	127.3239	151.8808
2.5	0.1	34.9769	56.4548	84.9497	91.4952	139.2663	167.6156
	0.2	34.1455	55.1128	82.9304	89.3204	135.9559	163.6313
	1.0	31.2098	50.3746	75.8006	81.6411	124.2672	149.5632
	2.0	30.1516	48.6664	73.2303	78.8728	120.0535	144.4918
	5.0	28.8947	46.6378	70.1777	75.5850	115.0491	138.4686
3.0	0.1	31.7412	49.0864	75.6319	85.3760	131.7924	160.4156
	0.2	30.9867	47.9196	73.8341	83.3466	128.6596	156.6025
	1.0	28.3226	43.7997	67.4863	76.1809	117.5982	143.1387
	2.0	27.3623	42.3145	65.1980	73.5977	113.6106	138.2851
	5.0	26.2217	40.5507	62.4802	70.5298	108.8748	132.5207

Table 8.8: Effect of k on first six non–dimensional frequencies of S–S–S FG right–angled triangle (Fig. 8.2 (a)) for $\theta = 0$, $E_r = 2.0$ and $\rho_r = 1.0$

μ	k	λ_1	λ_2	λ_3	λ_4	λ_5	λ_6
1.0	0.1	47.9233	99.3824	128.9791	176.4169	232.3638	278.5150
	0.2	46.7842	97.0200	125.9132	172.2234	226.8404	271.8945
	1.0	42.7619	88.6788	115.0879	157.4166	207.3380	248.5186
	2.0	41.3120	85.6718	111.1855	152.0789	200.3075	240.0918
	5.0	39.5899	82.1006	106.5507	145.7395	191.9577	230.0835
1.5	0.1	33.3722	65.1384	93.2169	125.9122	169.3949	197.5589
	0.2	32.5789	63.5900	91.0011	122.9192	165.3684	192.8628
	1.0	29.7780	58.1229	83.1773	112.3513	151.1509	176.2816
	2.0	28.7682	56.1521	80.3569	108.5417	146.0257	170.3042
	5.0	27.5690	53.8113	77.0073	104.0171	139.9386	163.2051
2.0	0.1	27.0194	49.9471	79.9467	104.5365	139.2573	167.1121
	0.2	26.3771	48.7598	78.0464	102.0516	135.9471	163.1398
	1.0	24.1094	44.5678	71.3364	93.2778	124.2591	149.1140
	2.0	23.2919	43.0565	68.9175	90.1149	120.0457	144.0578
	5.0	22.3209	41.2617	66.0447	86.3585	115.0416	138.0527
2.5	0.1	23.4781	42.6898	72.4929	87.0437	119.2492	145.1404
	0.2	22.9200	41.6751	70.7697	84.9746	116.4146	141.6903
	1.0	20.9495	38.0921	64.6854	77.6690	106.4059	129.5086
	2.0	20.2391	36.8005	62.4920	75.0354	102.7979	125.1172
	5.0	19.3955	35.2664	59.8870	71.9075	98.5127	119.9017
3.0	0.1	21.2926	38.4803	67.1948	71.3749	107.6519	128.4438
	0.2	20.7864	37.5656	65.5975	69.6783	105.0930	125.3906
	1.0	18.9993	34.3359	59.9578	63.6877	96.0577	114.6103
	2.0	18.3551	33.1717	57.9248	61.5282	92.8005	110.7240
	5.0	17.5900	31.7889	55.5102	58.9634	88.9321	106.1085

Table 8.9: Effect of k on first six non–dimensional frequencies of C–C–F FG right–angled triangle (Fig. 8.2 (a)) for $\theta = 0$, $E_r = 2.0$ and $\rho_r = 1.0$

μ	k	λ_1	λ_2	λ_3	λ_4	λ_5	λ_6
1.0	0.1	28.2419	61.9956	87.7987	114.9823	166.0811	207.7691
	0.2	27.5706	60.5219	85.7117	112.2492	162.1333	202.8303
	1.0	25.2003	55.3186	78.3427	102.5986	148.1940	185.3921
	2.0	24.3458	53.4428	75.6863	99.1197	143.1690	179.1058
	5.0	23.3309	51.2151	72.5313	94.9879	137.2010	171.6398
1.5	0.1	19.2022	40.4770	62.9945	75.6968	115.1200	137.8951
	0.2	18.7458	39.5149	61.4971	73.8974	112.3836	134.6173
	1.0	17.1341	36.1176	56.2099	67.5441	102.7215	123.0437
	2.0	16.5531	34.8929	54.3039	65.2538	99.2384	118.8715
	5.0	15.8631	33.4384	52.0403	62.5337	95.1016	113.9163
2.0	0.1	14.9956	29.7532	52.2692	57.3964	87.6623	96.9940
	0.2	14.6392	29.0460	51.0267	56.0320	85.5785	94.6884
	1.0	13.3806	26.5488	46.6398	51.2147	78.2210	86.5477
	2.0	12.9269	25.6485	45.0583	49.4781	75.5686	83.6130
	5.0	12.3880	24.5794	43.1800	47.4156	72.4186	80.1276
2.5	0.1	12.5795	23.9678	42.3090	48.7249	72.5474	83.1392
	0.2	12.2805	23.3981	41.3033	47.5667	70.8229	81.1630
	1.0	11.2247	21.3864	37.7523	43.4772	64.7340	74.1851
	2.0	10.8441	20.6613	36.4722	42.0029	62.5390	71.6696
	5.0	10.3921	19.8000	34.9518	40.2520	59.9320	68.6820
3.0	0.1	11.0219	20.4341	34.0282	44.5809	66.1853	76.3127
	0.2	10.7599	19.9483	33.2194	43.5212	64.6120	74.4987
	1.0	9.8348	18.2333	30.3633	39.7795	59.0571	68.0938
	2.0	9.5014	17.6150	29.3338	38.4306	57.0545	65.7848
	5.0	9.1053	16.8808	28.1110	36.8286	54.6762	63.0426

Table 8.10: Effect of k on first six non–dimensional frequencies of C–S–F FG right–angled triangle (Fig. 8.2 (a)) for $\theta = 0$, $E_r = 2.0$ and $\rho_r = 1.0$

μ	k	λ_1	λ_2	λ_3	λ_4	λ_5	λ_6
1.0	0.1	17.4411	46.7136	73.4769	97.7727	150.6387	194.8939
	0.2	17.0266	45.6032	71.7303	95.4486	147.0580	190.2612
	1.0	15.5627	41.6825	65.5633	87.2425	134.4148	173.9036
	2.0	15.0350	40.2691	63.3402	84.2842	129.8570	168.0069
	5.0	14.4083	38.5905	60.6999	80.7708	124.4439	161.0035
1.5	0.1	13.3522	33.3703	52.8577	67.2324	107.6886	137.9586
	0.2	13.0349	32.5771	51.6013	65.6343	105.1288	134.6793
	1.0	11.9142	29.7763	47.1649	59.9914	96.0904	123.1003
	2.0	11.5102	28.7666	45.5656	57.9572	92.8322	118.9262
	5.0	11.0304	27.5675	43.6662	55.5412	88.9624	113.9688
2.0	0.1	11.1886	25.5073	44.5847	52.2049	89.3005	115.0949
	0.2	10.9226	24.9010	43.5249	50.9640	87.1778	112.3591
	1.0	9.9835	22.7601	39.7829	46.5824	79.6828	102.6991
	2.0	9.6450	21.9884	38.4339	45.0029	76.9809	99.2167
	5.0	9.2430	21.0718	36.8318	43.1269	73.7719	95.0809
2.5	0.1	9.8524	20.6162	39.8671	45.4740	76.3031	93.2331
	0.2	9.6182	20.1262	38.9195	44.3930	74.4893	91.0170
	1.0	8.7913	18.3958	35.5734	40.5764	68.0852	83.1918
	2.0	8.4932	17.7721	34.3672	39.2005	65.7765	80.3710
	5.0	8.1391	17.0312	32.9346	37.5664	63.0346	77.0207
3.0	0.1	8.9312	17.6209	36.4697	41.7231	65.9988	73.2754
	0.2	8.7189	17.2020	35.6028	40.7314	64.4299	71.5336
	1.0	7.9693	15.7231	32.5419	37.2295	58.8906	65.3836
	2.0	7.6990	15.1899	31.4384	35.9671	56.8938	63.1665
	5.0	7.3781	14.5567	30.1279	34.4678	54.5221	60.5334

Table 8.11: Effect of k on first six non–dimensional frequencies of C–F–F FG right–angled triangle (Fig. 8.2 (a)) for $\theta = 0$, $E_r = 2.0$ and $\rho_r = 1.0$

μ	k	λ_1	λ_2	λ_3	λ_4	λ_5	λ_6
1.0	0.1	5.9987	22.8112	31.8762	58.0127	80.5269	112.6798
	0.2	5.8561	22.2690	31.1185	56.6337	78.6127	110.0014
	1.0	5.3527	20.3544	28.4431	51.7646	71.8540	100.5441
	2.0	5.1712	19.6642	27.4786	50.0094	69.4176	97.1348
	5.0	4.9556	18.8445	26.3332	47.9247	66.5239	93.0858
1.5	0.1	5.6303	17.9534	29.0088	41.0118	69.1853	85.0815
	0.2	5.4965	17.5266	28.3192	40.0370	67.5408	83.0591
	1.0	5.0239	16.0198	25.8845	36.5948	61.7340	75.9182
	2.0	4.8536	15.4766	25.0068	35.3540	59.6407	73.3439
	5.0	4.6512	14.8314	23.9644	33.8802	57.1546	70.2866
2.0	0.1	5.3557	14.9572	27.8093	31.4758	61.5841	77.7571
	0.2	5.2284	14.6017	27.1482	30.7276	60.1202	75.9088
	1.0	4.7789	13.3463	24.8142	28.0858	54.9514	69.3826
	2.0	4.6169	12.8938	23.9728	27.1335	53.0881	67.0300
	5.0	4.4244	12.3563	22.9735	26.0024	50.8751	64.2358
2.5	0.1	5.1512	12.9362	26.7216	27.1358	56.0674	71.4806
	0.2	5.0287	12.6287	26.0864	26.4908	54.7346	69.7815
	1.0	4.5964	11.5429	23.8437	24.2133	50.0288	63.7821
	2.0	4.4405	11.1515	23.0352	23.3922	48.3325	61.6193
	5.0	4.2554	10.6867	22.0749	22.4171	46.3177	59.0507
3.0	0.1	4.9914	11.5374	24.1492	26.5355	51.7979	56.1124
	0.2	4.8727	11.2631	23.5752	25.9048	50.5667	54.7785
	1.0	4.4538	10.2948	21.5483	23.6776	46.2193	50.0690
	2.0	4.3028	9.9457	20.8176	22.8748	44.6520	48.3712
	5.0	4.1234	9.5311	19.9499	21.9212	42.7907	46.3549

Table 8.12: Effect of k on first six non-dimensional frequencies of equilateral FG triangular plates (Fig. 8.2 (b)) with $\theta = 1/\sqrt{3}$ and $\mu = \sqrt{3}/2$

k	BCs	λ_1	λ_2	λ_3	λ_4	λ_5	λ_6
0.1	C-C-C	96.1142	183.7803	183.7803	293.5942	310.8578	310.8578
	C-C-S	79.2065	160.7861	161.0844	265.9415	287.1341	291.1617
	C-C-F	38.8604	93.1608	99.0763	171.5459	198.5175	200.1511
	S-S-S	51.0889	120.9208	120.9208	212.9728	236.0465	236.0465
	S-C-S	64.2459	139.6457	140.1539	246.0838	261.1685	265.6640
	S-C-F	25.7909	73.3945	82.4641	148.2524	177.4789	180.2259
	S-F-S	15.6200	56.4846	66.7480	121.1134	151.6160	153.6938
	F-F-F	34.2342	35.5200	35.5200	108.6637	108.6637	115.2961
	F-C-F	8.6622	34.3530	37.4139	92.8219	96.3350	112.0160
	F-F-S	22.0114	26.0639	70.0937	73.3966	90.1712	185.3062
0.2	C-C-C	93.8295	179.4117	179.4117	286.6154	303.4686	303.4686
	C-C-S	77.3238	156.9641	157.2553	259.6200	280.3089	284.2406
	C-C-F	37.9366	90.9463	96.7212	167.4682	193.7986	195.3935
	S-S-S	49.8745	118.0464	118.0464	207.9103	230.4355	230.4355
	S-C-S	62.7188	136.3262	136.8223	240.2343	254.9605	259.3490
	S-C-F	25.1778	71.6498	80.5039	144.7283	173.2602	175.9419
	S-F-S	15.2487	55.1419	65.1614	118.2345	148.0120	150.0405
	F-F-F	33.4205	34.6757	34.6757	106.0807	106.0807	112.5554
	F-C-F	8.4563	33.5364	36.5246	90.6155	94.0451	109.3533
	F-F-S	21.4882	25.4444	68.4276	71.6519	88.0278	180.9014
1.0	C-C-C	85.7626	163.9869	163.9869	261.9738	277.3781	277.3781
	C-C-S	70.6759	143.4692	143.7354	237.2993	256.2095	259.8033
	C-C-F	34.6751	83.1273	88.4057	153.0702	177.1369	178.5946
	S-S-S	45.5866	107.8975	107.8975	190.0354	210.6240	210.6240
	S-C-S	57.3266	124.6057	125.0591	219.5804	233.0404	237.0517
	S-C-F	23.0132	65.4898	73.5826	132.2854	158.3643	160.8154
	S-F-S	13.9377	50.4011	59.5592	108.0694	135.2868	137.1409
	F-F-F	30.5472	31.6945	31.6945	96.9605	96.9605	102.8786
	F-C-F	7.7293	30.6531	33.3844	82.8249	85.9596	99.9518
	F-F-S	19.6407	23.2568	62.5446	65.4917	80.4597	165.3485
2.0	C-C-C	82.8545	158.4264	158.4264	253.0908	267.9727	267.9727
	C-C-S	68.2794	138.6044	138.8616	229.2529	247.5219	250.9938
	C-C-F	33.4993	80.3086	85.4080	147.8799	171.1305	172.5388
	S-S-S	44.0408	104.2389	104.2389	183.5916	203.4821	203.4821
	S-C-S	55.3827	120.3805	120.8186	212.1348	225.1384	229.0137
	S-C-F	22.2328	63.2692	71.0875	127.7999	152.9944	155.3624
	S-F-S	13.4651	48.6921	57.5396	104.4049	130.6994	132.4907
	F-F-F	29.5114	30.6198	30.6198	93.6728	93.6728	99.3901
	F-C-F	7.4672	29.6137	32.2524	80.0164	83.0449	96.5626
	F-F-S	18.9748	22.4682	60.4238	63.2710	77.7314	159.7418
5.0	C-C-C	79.4007	151.8224	151.8224	242.5406	256.8022	256.8022
	C-C-S	65.4332	132.8267	133.0732	219.6965	237.2039	240.5311
	C-C-F	32.1029	76.9609	81.8477	141.7155	163.9969	165.3465
	S-S-S	42.2050	99.8936	99.8936	175.9386	194.9999	194.9999
	S-C-S	53.0741	115.3625	115.7823	203.2919	215.7535	219.4672
	S-C-F	21.3061	60.6318	68.1242	122.4725	146.6168	148.8861
	S-F-S	12.9038	46.6624	55.1411	100.0528	125.2512	126.9678
	F-F-F	28.2812	29.3434	29.3434	89.7680	89.7680	95.2470
	F-C-F	7.1559	28.3793	30.9080	76.6809	79.5831	92.5373
	F-F-S	18.1838	21.5316	57.9050	60.6335	74.4912	153.0830

Table 8.13: Effect of k on first six non-dimensional frequencies of FG right-angled triangular plates (Fig. 8.2 (c)) with angles 30°, 60°and 90°

k	BCs	λ_1	λ_2	λ_3	λ_4	λ_5	λ_6
0.1	C-C-C	171.4750	273.4001	378.0292	436.6760	557.5210	638.2764
	C-C-S	133.0728	227.5203	322.4896	376.8116	504.7479	608.4365
	C-C-F	50.7597	103.8812	172.2018	197.2515	303.4861	338.8338
	S-S-S	89.7121	169.7380	257.5380	344.1051	462.1235	540.3853
	S-C-S	116.0340	206.8043	296.1916	365.4608	507.7390	596.6455
	S-C-F	36.6036	87.7666	144.9766	176.0460	294.0350	376.8694
	S-F-S	22.3134	64.3916	126.2444	139.7782	279.1071	346.0023
	F-F-F	24.8248	52.9835	78.6936	98.3006	139.4496	225.1636
	F-C-F	16.4769	49.2063	85.1041	107.1639	196.0819	242.0130
	F-F-S	31.1018	67.2067	86.4201	165.3371	217.8876	234.3610
0.2	C-C-C	167.3990	266.9013	369.0433	426.2960	544.2685	623.1044
	C-C-S	129.9096	222.1121	314.8239	367.8546	492.7498	593.9737
	C-C-F	49.5532	101.4119	168.1085	192.5628	296.2721	330.7796
	S-S-S	87.5796	165.7033	251.4162	335.9256	451.1386	527.5401
	S-C-S	113.2758	201.8885	289.1510	356.7737	495.6699	582.4630
	S-C-F	35.7335	85.6803	141.5304	171.8613	287.0457	367.9110
	S-F-S	21.7830	62.8609	123.2435	136.4556	272.4726	337.7777
	F-F-F	24.2347	51.7241	76.8231	95.9639	136.1349	219.8114
	F-C-F	16.0853	48.0367	83.0812	104.6166	191.4209	236.2602
	F-F-S	30.3625	65.6092	84.3659	161.4070	212.7083	228.7901
1.0	C-C-C	153.0070	243.9546	337.3150	389.6455	497.4754	569.5334
	C-C-S	118.7408	203.0162	287.7571	336.2286	450.3860	542.9073
	C-C-F	45.2929	92.6931	153.6555	176.0073	270.8003	302.3411
	S-S-S	80.0500	151.4571	229.8009	307.0447	412.3523	482.1852
	S-C-S	103.5370	184.5313	264.2914	326.1003	453.0550	532.3862
	S-C-F	32.6613	78.3140	129.3624	157.0856	262.3671	336.2801
	S-F-S	19.9102	57.4565	112.6477	124.7239	249.0470	308.7375
	F-F-F	22.1511	47.2771	70.2183	87.7135	124.4308	200.9133
	F-C-F	14.7024	43.9067	75.9383	95.6222	174.9637	215.9479
	F-F-S	27.7521	59.9685	77.1126	147.5301	194.4209	209.1200
2.0	C-C-C	147.8188	235.6826	325.8773	376.4334	480.6069	550.2216
	C-C-S	114.7145	196.1323	277.9998	324.8277	435.1142	524.4983
	C-C-F	43.7571	89.5500	148.4453	170.0392	261.6180	292.0892
	S-S-S	77.3356	146.3214	222.0088	296.6333	398.3702	465.8352
	S-C-S	100.0263	178.2742	255.3298	315.0428	437.6927	514.3339
	S-C-F	31.5538	75.6585	124.9760	151.7591	253.4707	324.8775
	S-F-S	19.2351	55.5083	108.8280	120.4948	240.6022	298.2687
	F-F-F	21.4000	45.6740	67.8373	84.7393	120.2115	194.1007
	F-C-F	14.2038	42.4179	73.3634	92.3799	169.0310	208.6255
	F-F-S	26.8111	57.9351	74.4978	142.5277	187.8284	202.0292
5.0	C-C-C	141.6570	225.8581	312.2930	360.7417	460.5727	527.2855
	C-C-S	109.9326	187.9565	266.4113	311.2872	416.9764	502.6345
	C-C-F	41.9331	85.8171	142.2573	162.9511	250.7124	279.9135
	S-S-S	74.1119	140.2220	212.7543	284.2681	381.7641	446.4168
	S-C-S	95.8566	170.8428	244.6863	301.9102	419.4475	492.8938
	S-C-F	30.2385	72.5047	119.7664	145.4330	242.9048	311.3349
	S-F-S	18.4333	53.1944	104.2915	115.4719	230.5727	285.8354
	F-F-F	20.5080	43.7701	65.0095	81.2069	115.2005	186.0096
	F-C-F	13.6117	40.6497	70.3052	88.5290	161.9849	199.9289
	F-F-S	25.6934	55.5200	71.3924	136.5864	179.9987	193.6075

Table 8.14: Effect of k on first six non-dimensional frequencies of isosceles FG triangular plates (Fig. 8.2 (d)) with angles 30°, 30°and 120°

k	BCs	λ_1	λ_2	λ_3	λ_4	λ_5	λ_6
0.1	C-C-C	137.6361	213.6173	296.0524	354.9282	453.3632	616.0397
	C-C-S	104.1299	172.6731	261.8057	313.4529	425.4168	547.3025
	C-C-F	33.8016	68.5302	111.8262	154.5037	243.4675	320.7225
	S-S-S	71.6489	135.0420	214.8276	256.3671	386.7775	508.6849
	S-C-S	86.6240	152.3939	239.0463	288.2326	401.4156	526.6853
	S-C-F	18.6026	47.2619	81.2986	131.6930	209.0212	253.5735
	S-F-S	23.9881	59.8452	106.6091	150.9550	208.1678	317.1308
	F-F-F	13.3306	27.4809	49.3394	54.9804	99.5320	138.8216
	F-C-F	5.5679	21.1764	37.5645	55.5857	92.0183	138.1714
	F-F-S	22.1655	43.6699	88.7802	93.6692	170.7119	202.5393
0.2	C-C-C	134.3645	208.5395	289.0151	346.4914	442.5866	601.3962
	C-C-S	101.6547	168.5686	255.5825	306.0020	415.3045	534.2929
	C-C-F	32.9981	66.9012	109.1680	150.8311	237.6802	313.0988
	S-S-S	69.9458	131.8320	209.7210	250.2731	377.5837	496.5933
	S-C-S	84.5649	148.7714	233.3641	281.3812	391.8738	514.1658
	S-C-F	18.1604	46.1385	79.3661	128.5626	204.0527	247.5460
	S-F-S	23.4179	58.4227	104.0750	147.3667	203.2196	309.5924
	F-F-F	13.0137	26.8277	48.1665	53.6735	97.1661	135.5217
	F-C-F	5.4355	20.6731	36.6716	54.2644	89.8310	134.8870
	F-F-S	21.6386	42.6319	86.6699	91.4427	166.6540	197.7249
1.0	C-C-C	122.8126	190.6105	264.1672	316.7021	404.5355	549.6916
	C-C-S	92.9150	154.0760	233.6090	279.6937	379.5990	488.3574
	C-C-F	30.1611	61.1494	99.7824	137.8635	217.2458	286.1804
	S-S-S	63.9323	120.4979	191.6904	228.7561	345.1212	453.8990
	S-C-S	77.2945	135.9809	213.3008	257.1897	358.1827	469.9607
	S-C-F	16.5990	42.1717	72.5427	117.5095	186.5094	226.2634
	S-F-S	21.4046	53.3998	95.1272	134.6970	185.7480	282.9755
	F-F-F	11.8949	24.5212	44.0255	49.0590	88.8123	123.8704
	F-C-F	4.9682	18.8957	33.5188	49.5990	82.1078	123.2902
	F-F-S	19.7783	38.9666	79.2185	83.5810	152.3261	180.7256
2.0	C-C-C	118.6482	184.1472	255.2098	305.9633	390.8184	531.0526
	C-C-S	89.7644	148.8516	225.6877	270.2098	366.7275	471.7981
	C-C-F	29.1384	59.0760	96.3989	133.1888	209.8794	276.4765
	S-S-S	61.7644	116.4120	185.1906	220.9994	333.4188	438.5081
	S-C-S	74.6735	131.3701	206.0681	248.4689	346.0374	454.0252
	S-C-F	16.0362	40.7418	70.0829	113.5250	180.1852	218.5912
	S-F-S	20.6788	51.5892	91.9016	130.1296	179.4496	273.3803
	F-F-F	11.4916	23.6897	42.5326	47.3955	85.8008	119.6701
	F-C-F	4.7997	18.2550	32.3822	47.9172	79.3237	119.1096
	F-F-S	19.1076	37.6454	76.5323	80.7469	147.1610	174.5975
5.0	C-C-C	113.7024	176.4710	244.5713	293.2091	374.5271	508.9156
	C-C-S	86.0226	142.6467	216.2799	258.9460	351.4404	452.1311
	C-C-F	27.9237	56.6134	92.3805	127.6368	201.1305	264.9516
	S-S-S	59.1898	111.5593	177.4709	211.7870	319.5202	420.2288
	S-C-S	71.5608	125.8939	197.4781	238.1114	331.6127	435.0991
	S-C-F	15.3677	39.0434	67.1615	108.7927	172.6742	209.4792
	S-F-S	19.8168	49.4386	88.0707	124.7051	171.9692	261.9844
	F-F-F	11.0125	22.7022	40.7597	45.4198	82.2242	114.6817
	F-C-F	4.5997	17.4940	31.0324	45.9198	76.0171	114.1445
	F-F-S	18.3111	36.0761	73.3421	77.3809	141.0265	167.3194

8.4.2 Effect of ratio of Young's moduli (E_r)

In this part, the effect of ratio of Young's moduli (E_r) on the first six non-dimensional frequencies has been performed in Tables 8.15 to 8.23. Especially, the common parameters in these computations are $k = 1.0$ and $\rho_r = 1.0$. Here, increasing values of the ratio of Young's moduli (E_r) are considered to be 1.0, 1.5, 2.0, 2.5 and 3.0. Unlike Tables 8.6 to 8.11, FG right-angled triangular plates (Fig. 8.2 (a)) subjected to same combination of boundary conditions and μ are also considered in Tables 8.15 to 8.20. On the other hand, Tables 8.21 to 8.23 involves the similar edge conditions as stated in Tables 8.12 to 8.14. Moreover, Tables 8.21 to 8.23 are meant for the eigenfrequencies of FG triangular elements mentioned in Figs. 8.2 (b) to 8.2 (d) respectively. It can be noticed here that the non-dimensional frequencies are showing descending behavior with ascending values of E_r. This proposition is true because of the fact that the Young's modulus (E_c) is inversely proportional to λ, as observed in the concerned expression.

Table 8.15: Effect of E_r on first six non-dimensional frequencies of C-C-C FG right-angled triangle (Fig. 8.2 (a)) for $\theta = 0$, $k = 1.0$ and $\rho_r = 1.0$

μ	E_r	λ_1	λ_2	λ_3	λ_4	λ_5	λ_6
1.0	1.0	93.8094	159.5177	196.4910	248.4158	299.3326	354.9414
	2.0	81.2413	138.1464	170.1662	215.1344	259.2296	307.3883
	2.5	78.4866	133.4621	164.3961	207.8396	250.4396	296.9653
	3.0	76.5950	130.2457	160.4342	202.8306	244.4040	289.8085
1.5	1.0	65.5234	106.7565	141.6423	169.7267	214.1904	255.4156
	2.0	56.7450	92.4538	122.6658	146.9876	185.4943	221.1964
	2.5	54.8208	89.3189	118.5064	142.0035	179.2045	213.6961
	3.0	53.4997	87.1663	115.6504	138.5812	174.8857	208.5460
2.0	1.0	53.4702	83.7901	119.7814	131.0599	172.6714	189.7042
	2.0	46.3065	72.5644	103.7337	113.5012	149.5378	164.2887
	2.5	44.7364	70.1038	100.2163	109.6526	144.4673	158.7180
	3.0	43.6582	68.4144	97.8011	107.0100	140.9856	154.8929
2.5	1.0	46.9768	71.6368	101.9272	110.1294	153.2250	165.7136
	2.0	40.6831	62.0393	88.2716	95.3749	132.6967	143.5122
	2.5	39.3036	59.9357	85.2785	92.1409	128.1972	138.6459
	3.0	38.3564	58.4912	83.2232	89.9203	125.1077	135.3046
3.0	1.0	42.9629	63.0959	88.4648	102.1192	143.8032	156.2600
	2.0	37.2070	54.6427	76.6127	88.4378	124.5372	135.3252
	2.5	35.9453	52.7898	74.0149	85.4391	120.3144	130.7365
	3.0	35.0791	51.5176	72.2312	83.3800	117.4148	127.5858

Table 8.16: Effect of E_r on first six non-dimensional frequencies of C-C-S FG right-angled triangle (Fig. 8.2 (a)) for $\theta = 0$, $k = 1.0$ and $\rho_r = 1.0$

μ	E_r	λ_1	λ_2	λ_3	λ_4	λ_5	λ_6
1.0	1.0	73.4250	133.0584	168.5058	222.6888	276.4235	324.2267
	2.0	63.5879	115.2320	145.9303	192.8542	239.3898	280.7885
	2.5	61.4318	111.3246	140.9821	186.3149	231.2725	271.2675
	3.0	59.9513	108.6417	137.5844	181.8247	225.6989	264.7300
1.5	1.0	51.0324	88.9488	121.1213	150.4670	192.3149	235.8292
	2.0	44.1954	77.0320	104.8941	130.3082	166.5496	204.2341
	2.5	42.6968	74.4199	101.3373	125.8897	160.9022	197.3089
	3.0	41.6678	72.6264	98.8951	122.8558	157.0245	192.5538
2.0	1.0	41.3279	69.3498	101.9907	111.0474	158.8008	189.4286
	2.0	35.7910	60.0587	88.3266	96.1699	137.5255	164.0500
	2.5	34.5774	58.0222	85.3316	92.9089	132.8622	158.4874
	3.0	33.7441	56.6239	83.2751	90.6698	129.6603	154.6678
2.5	1.0	36.0380	58.1675	87.5269	94.2710	143.4914	172.7007
	2.0	31.2098	50.3746	75.8006	81.6411	124.2672	149.5632
	2.5	30.1516	48.6664	73.2303	78.8728	120.0535	144.4918
	3.0	29.4249	47.4936	71.4655	76.9720	117.1603	141.0095
3.0	1.0	32.7042	50.5756	77.9265	87.9661	135.7907	165.2824
	2.0	28.3226	43.7997	67.4863	76.1809	117.5982	143.1387
	2.5	27.3623	42.3145	65.1980	73.5977	113.6106	138.2851
	3.0	26.7028	41.2948	63.6267	71.8240	110.8726	134.9525

Table 8.17: Effect of E_r on first six non-dimensional frequencies of S-S-S FG right-angled triangle (Fig. 8.2 (a)) for $\theta = 0$, $k = 1.0$ and $\rho_r = 1.0$

μ	E_r	λ_1	λ_2	λ_3	λ_4	λ_5	λ_6
1.0	1.0	49.3772	102.3974	132.8920	181.7691	239.4133	286.9646
	2.0	42.7619	88.6788	115.0879	157.4166	207.3380	248.5186
	2.5	41.3120	85.6718	111.1855	152.0789	200.3075	240.0918
	3.0	40.3164	83.6072	108.5059	148.4138	195.4801	234.3056
1.5	1.0	34.3846	67.1145	96.0449	129.7321	174.5341	203.5525
	2.0	29.7780	58.1229	83.1773	112.3513	151.1509	176.2816
	2.5	28.7682	56.1521	80.3569	108.5417	146.0257	170.3042
	3.0	28.0749	54.7988	78.4204	105.9258	142.5065	166.1999
2.0	1.0	27.8391	51.4624	82.3722	107.7080	143.4821	172.1820
	2.0	24.1094	44.5678	71.3364	93.2778	124.2591	149.1140
	2.5	23.2919	43.0565	68.9175	90.1149	120.0457	144.0578
	3.0	22.7305	42.0189	67.2566	87.9432	117.1526	140.5860
2.5	1.0	24.1904	43.9850	74.6922	89.6844	122.8670	149.5437
	2.0	20.9495	38.0921	64.6854	77.6690	106.4059	129.5086
	2.5	20.2391	36.8005	62.4920	75.0354	102.7979	125.1172
	3.0	19.7514	35.9136	60.9859	73.2270	100.3205	122.1019
3.0	1.0	21.9385	39.6477	69.2333	73.5403	110.9179	132.3405
	2.0	18.9993	34.3359	59.9578	63.6877	96.0577	114.6103
	2.5	18.3551	33.1717	57.9248	61.5282	92.8005	110.7240
	3.0	17.9127	32.3722	56.5288	60.0454	90.5640	108.0556

Table 8.18: Effect of E_r on first six non-dimensional frequencies of C-C-F FG right-angled triangle (Fig. 8.2 (a)) for $\theta = 0$, $k = 1.0$ and $\rho_r = 1.0$

μ	E_r	λ_1	λ_2	λ_3	λ_4	λ_5	λ_6
1.0	1.0	29.0988	63.8764	90.4624	118.4707	171.1197	214.0724
	2.0	25.2003	55.3186	78.3427	102.5986	148.1940	185.3921
	2.5	24.3458	53.4428	75.6863	99.1197	143.1690	179.1058
	3.0	23.7590	52.1549	73.8622	96.7309	139.7187	174.7894
1.5	1.0	19.7848	41.7050	64.9056	77.9933	118.6126	142.0786
	2.0	17.1341	36.1176	56.2099	67.5441	102.7215	123.0437
	2.5	16.5531	34.8929	54.3039	65.2538	99.2384	118.8715
	3.0	16.1542	34.0520	52.9952	63.6812	96.8468	116.0067
2.0	1.0	15.4506	30.6559	53.8549	59.1377	90.3218	99.9366
	2.0	13.3806	26.5488	46.6398	51.2147	78.2210	86.5477
	2.5	12.9269	25.6485	45.0583	49.4781	75.5686	83.6130
	3.0	12.6153	25.0304	43.9724	48.2857	73.7474	81.5979
2.5	1.0	12.9612	24.6949	43.5926	50.2031	74.7484	85.6615
	2.0	11.2247	21.3864	37.7523	43.4772	64.7340	74.1851
	2.5	10.8441	20.6613	36.4722	42.0029	62.5390	71.6696
	3.0	10.5828	20.1633	35.5932	40.9907	61.0318	69.9423
3.0	1.0	11.3563	21.0540	35.0606	45.9334	68.1932	78.6279
	2.0	9.8348	18.2333	30.3633	39.7795	59.0571	68.0938
	2.5	9.5014	17.6150	29.3338	38.4306	57.0545	65.7848
	3.0	9.2724	17.1905	28.6268	37.5044	55.6795	64.1994

Table 8.19: Effect of E_r on first six non-dimensional frequencies of C-S-F FG right-angled triangle (Fig. 8.2 (a)) for $\theta = 0$, $k = 1.0$ and $\rho_r = 1.0$

μ	E_r	λ_1	λ_2	λ_3	λ_4	λ_5	λ_6
1.0	1.0	17.9703	48.1308	75.7060	100.7389	155.2088	200.8066
	2.0	15.5627	41.6825	65.5633	87.2425	134.4148	173.9036
	2.5	15.0350	40.2691	63.3402	84.2842	129.8570	168.0069
	3.0	14.6727	39.2986	61.8137	82.2530	126.7274	163.9579
1.5	1.0	13.7573	34.3827	54.4613	69.2721	110.9556	142.1440
	2.0	11.9142	29.7763	47.1649	59.9914	96.0904	123.1003
	2.5	11.5102	28.7666	45.5656	57.9572	92.8322	118.9262
	3.0	11.2328	28.0733	44.4675	56.5604	90.5949	116.0601
2.0	1.0	11.5280	26.2811	45.9373	53.7887	92.0098	118.5867
	2.0	9.9835	22.7601	39.7829	46.5824	79.6828	102.6991
	2.5	9.6450	21.9884	38.4339	45.0029	76.9809	99.2167
	3.0	9.4126	21.4584	37.5077	43.9183	75.1256	96.8256
2.5	1.0	10.1513	21.2417	41.0766	46.8536	78.6180	96.0617
	2.0	8.7913	18.3958	35.5734	40.5764	68.0852	83.1918
	2.5	8.4932	17.7721	34.3672	39.2005	65.7765	80.3710
	3.0	8.2885	17.3438	33.5389	38.2558	64.1913	78.4340
3.0	1.0	9.2021	18.1554	37.5761	42.9889	68.0010	75.4984
	2.0	7.9693	15.7231	32.5419	37.2295	58.8906	65.3836
	2.5	7.6990	15.1899	31.4384	35.9671	56.8938	63.1665
	3.0	7.5135	14.8239	30.6808	35.1003	55.5226	61.6442

Table 8.20: Effect of E_r on first six non-dimensional frequencies of C-F-F FG right-angled triangle (Fig. 8.2 (a)) for $\theta = 0$, $k = 1.0$ and $\rho_r = 1.0$

μ	E_r	λ_1	λ_2	λ_3	λ_4	λ_5	λ_6
1.0	1.0	6.1807	23.5033	32.8433	59.7726	82.9699	116.0983
	2.0	5.3527	20.3544	28.4431	51.7646	71.8540	100.5441
	2.5	5.1712	19.6642	27.4786	50.0094	69.4176	97.1348
	3.0	5.0465	19.1903	26.8164	48.8042	67.7446	94.7939
1.5	1.0	5.8011	18.4980	29.8889	42.2561	71.2843	87.6627
	2.0	5.0239	16.0198	25.8845	36.5948	61.7340	75.9182
	2.5	4.8536	15.4766	25.0068	35.3540	59.6407	73.3439
	3.0	4.7366	15.1036	24.4041	34.5019	58.2034	71.5763
2.0	1.0	5.5182	15.4110	28.6530	32.4307	63.4524	80.1162
	2.0	4.7789	13.3463	24.8142	28.0858	54.9514	69.3826
	2.5	4.6169	12.8938	23.9728	27.1335	53.0881	67.0300
	3.0	4.5056	12.5830	23.3950	26.4796	51.8087	65.4146
2.5	1.0	5.3074	13.3286	27.5323	27.9591	57.7683	73.6492
	2.0	4.5964	11.5429	23.8437	24.2133	50.0288	63.7821
	2.5	4.4405	11.1515	23.0352	23.3922	48.3325	61.6193
	3.0	4.3335	10.8828	22.4800	22.8285	47.1676	60.1343
3.0	1.0	5.1428	11.8874	24.8818	27.3406	53.3694	57.8147
	2.0	4.4538	10.2948	21.5483	23.6776	46.2193	50.0690
	2.5	4.3028	9.9457	20.8176	22.8748	44.6520	48.3712
	3.0	4.1991	9.7060	20.3159	22.3235	43.5759	47.2055

Table 8.21: Effect of E_r on first six non-dimensional frequencies of equilateral FG triangular plates (Fig. 8.2 (b)) with $\theta = 1/\sqrt{3}$ and $\mu = \sqrt{3}/2$

E_r	BCs	λ_1	λ_2	λ_3	λ_4	λ_5	λ_6
1.0	C-C-C	99.0301	189.3558	189.3558	302.5013	320.2886	320.2886
	C-C-S	81.6095	165.6640	165.9714	274.0097	295.8453	299.9950
	C-C-F	40.0393	95.9871	102.0821	176.7503	204.5401	206.2233
	S-S-S	52.6389	124.5893	124.5893	219.4339	243.2077	243.2077
	S-C-S	66.1950	143.8823	144.4059	253.5495	269.0919	273.7237
	S-C-F	26.5733	75.6211	84.9659	152.7500	182.8633	185.693
	S-F-S	16.0939	58.1982	68.7730	124.7878	156.2157	158.3566
	F-F-F	35.2728	36.5976	36.5976	111.9604	111.9604	118.7939
	F-C-F	8.9250	35.3952	38.5490	95.6379	99.2576	115.4143
	F-F-S	22.6792	26.8547	72.2202	75.6233	92.9068	190.9280
2.0	C-C-C	85.7626	163.9869	163.9869	261.9738	277.3781	277.3781
	C-C-S	70.6759	143.4692	143.7354	237.2993	256.2095	259.8033
	C-C-F	34.6751	83.1273	88.4057	153.0702	177.1369	178.5946
	S-S-S	45.5866	107.8975	107.8975	190.0354	210.6240	210.6240
	S-C-S	57.3266	124.6057	125.0591	219.5804	233.0404	237.0517
	S-C-F	23.0132	65.4898	73.5826	132.2854	158.3643	160.8154
	S-F-S	13.9377	50.4011	59.5592	108.0694	135.2868	137.1409
	F-F-F	30.5472	31.6945	31.6945	96.9605	96.9605	102.8786
	F-C-F	7.7293	30.6531	33.3844	82.8249	85.9596	99.9518
	F-F-S	19.6407	23.2568	62.5446	65.4917	80.4597	165.3485
2.5	C-C-C	82.8545	158.4264	158.4264	253.0908	267.9727	267.9727
	C-C-S	68.2794	138.6044	138.8616	229.2529	247.5219	250.9938
	C-C-F	33.4993	80.3086	85.4080	147.8799	171.1305	172.5388
	S-S-S	44.0408	104.2389	104.2389	183.5916	203.4821	203.4821
	S-C-S	55.3827	120.3805	120.8186	212.1348	225.1384	229.0137
	S-C-F	22.2328	63.2692	71.0875	127.7999	152.9944	155.3624
	S-F-S	13.4651	48.6921	57.5396	104.4049	130.6994	132.4907
	F-F-F	29.5114	30.6198	30.6198	93.6728	93.6728	99.3901
	F-C-F	7.4672	29.6137	32.2524	80.0164	83.0449	96.5626
	F-F-S	18.9748	22.4682	60.4238	63.2710	77.7314	159.7418
3.0	C-C-C	80.8577	154.6084	154.6084	246.9913	261.5146	261.5146
	C-C-S	66.6339	135.2641	135.5151	223.7280	241.5566	244.9449
	C-C-F	32.6920	78.3731	83.3497	144.3160	167.0063	168.3806
	S-S-S	42.9794	101.7267	101.7267	179.1671	198.5782	198.5782
	S-C-S	54.0480	117.4794	117.9069	207.0223	219.7126	223.4945
	S-C-F	21.6970	61.7444	69.3743	124.7199	149.3073	151.6182
	S-F-S	13.1406	47.5186	56.1529	101.8888	127.5496	129.2976
	F-F-F	28.8001	29.8818	29.8818	91.4153	91.4153	96.9948
	F-C-F	7.2872	28.9000	31.4751	78.0880	81.0435	94.2354
	F-F-S	18.5175	21.9267	58.9676	61.7462	75.8581	155.8921

Table 8.22: Effect of E_r on first six non-dimensional frequencies of FG right-angled triangular plates (Fig. 8.2 (c)) with angles 30°, 60°and 90°

E_r	BCs	λ_1	λ_2	λ_3	λ_4	λ_5	λ_6
1.0	C-C-C	176.6773	281.6946	389.4979	449.9239	574.4351	657.6405
	C-C-S	137.1100	234.4229	332.2733	388.2433	520.0610	626.8953
	C-C-F	52.2997	107.0327	177.4260	203.2358	312.6933	349.1134
	S-S-S	92.4337	174.8875	265.3512	354.5446	476.1434	556.7795
	S-C-S	119.5542	213.0784	305.1774	376.5482	523.1429	614.7466
	S-C-F	37.7140	90.4292	149.3749	181.3869	302.9555	388.3029
	S-F-S	22.9903	66.3451	130.0744	144.0188	287.5747	356.4993
	F-F-F	25.5779	54.5909	81.0811	101.2828	143.6803	231.9947
	F-C-F	16.9768	50.6991	87.6860	110.4150	202.0306	249.3552
	F-F-S	32.0453	69.2456	89.0420	170.3531	224.4979	241.4710
2.0	C-C-C	153.0070	243.9546	337.3150	389.6455	497.4754	569.5334
	C-C-S	118.7408	203.0162	287.7571	336.2286	450.3860	542.9073
	C-C-F	45.2929	92.6931	153.6555	176.0073	270.8003	302.3411
	S-S-S	80.0500	151.4571	229.8009	307.0447	412.3523	482.1852
	S-C-S	103.5370	184.5313	264.2914	326.1003	453.0550	532.3862
	S-C-F	32.6613	78.3140	129.3624	157.0856	262.3671	336.2801
	S-F-S	19.9102	57.4565	112.6477	124.7239	249.0470	308.7375
	F-F-F	22.1511	47.2771	70.2183	87.7135	124.4308	200.9133
	F-C-F	14.7024	43.9067	75.9383	95.6222	174.9637	215.9479
	F-F-S	27.7521	59.9685	77.1126	147.5301	194.4209	209.1200
2.5	C-C-C	147.8188	235.6826	325.8773	376.4334	480.6069	550.2216
	C-C-S	114.7145	196.1323	277.9998	324.8277	435.1142	524.4983
	C-C-F	43.7571	89.5500	148.4453	170.0392	261.6180	292.0892
	S-S-S	77.3356	146.3214	222.0088	296.6333	398.3702	465.8352
	S-C-S	100.0263	178.2742	255.3298	315.0428	437.6927	514.3339
	S-C-F	31.5538	75.6585	124.9760	151.7591	253.4707	324.8775
	S-F-S	19.2351	55.5083	108.8280	120.4948	240.6022	298.2687
	F-F-F	21.4000	45.6740	67.8373	84.7393	120.2115	194.1007
	F-C-F	14.2038	42.4179	73.3634	92.3799	169.0310	208.6255
	F-F-S	26.8111	57.9351	74.4978	142.5277	187.8284	202.0292
3.0	C-C-C	144.2564	230.0026	318.0237	367.3613	469.0243	536.9613
	C-C-S	111.9499	191.4055	271.3000	316.9994	424.6280	511.8579
	C-C-F	42.7025	87.3919	144.8677	165.9413	255.3130	285.0499
	S-S-S	75.4718	142.7951	216.6584	289.4845	388.7695	454.6086
	S-C-S	97.6156	173.9778	249.1763	307.4503	427.1444	501.9385
	S-C-F	30.7934	73.8352	121.9641	148.1018	247.3621	317.0480
	S-F-S	18.7715	54.1705	106.2053	117.5909	234.8037	291.0805
	F-F-F	20.8843	44.5733	66.2024	82.6971	117.3144	189.4229
	F-C-F	13.8615	41.3957	71.5953	90.1535	164.9573	203.5977
	F-F-S	26.1649	56.5388	72.7025	139.0928	183.3018	197.1603

Table 8.23: Effect of E_r on first six non-dimensional frequencies of isosceles FG triangular plates (Fig. 8.2 (d)) with angles 30°, 30°and 120°

E_r	BCs	λ_1	λ_2	λ_3	λ_4	λ_5	λ_6
1.0	C-C-C	141.8117	220.0980	305.0341	365.6960	467.1174	634.7292
	C-C-S	107.2890	177.9117	269.7484	322.9624	438.3232	563.9066
	C-C-F	34.8270	70.6093	115.2188	159.1910	250.8538	330.4526
	S-S-S	73.8226	139.1389	221.3450	264.1448	398.5116	524.1175
	S-C-S	89.2520	157.0172	246.2985	296.9771	413.5938	542.6639
	S-C-F	19.1669	48.6957	83.7651	135.6883	215.3625	261.2665
	S-F-S	24.7159	61.6608	109.8434	155.5346	214.4833	326.7519
	F-F-F	13.7350	28.3146	50.8362	56.6484	102.5516	143.0332
	F-C-F	5.7368	21.8189	38.7042	57.2720	94.8100	142.3632
	F-F-S	22.8380	44.9948	91.4736	96.5110	175.8910	208.6840
2.0	C-C-C	122.8126	190.6105	264.1672	316.7021	404.5355	549.6916
	C-C-S	92.9150	154.0760	233.6090	279.6937	379.5990	488.3574
	C-C-F	30.1611	61.1494	99.7824	137.8635	217.2458	286.1804
	S-S-S	63.9323	120.4979	191.6904	228.7561	345.1212	453.8990
	S-C-S	77.2945	135.9809	213.3008	257.1897	358.1827	469.9607
	S-C-F	16.5990	42.1717	72.5427	117.5095	186.5094	226.2634
	S-F-S	21.4046	53.3998	95.1272	134.6970	185.7480	282.9755
	F-F-F	11.8949	24.5212	44.0255	49.0590	88.8123	123.8704
	F-C-F	4.9682	18.8957	33.5188	49.5990	82.1078	123.2902
	F-F-S	19.7783	38.9666	79.2185	83.5810	152.3261	180.7256
2.5	C-C-C	118.6482	184.1472	255.2098	305.9633	390.8184	531.0526
	C-C-S	89.7644	148.8516	225.6877	270.2098	366.7275	471.7981
	C-C-F	29.1384	59.0760	96.3989	133.1888	209.8794	276.4765
	S-S-S	61.7644	116.4120	185.1906	220.9994	333.4188	438.5081
	S-C-S	74.6735	131.3701	206.0681	248.4689	346.0374	454.0252
	S-C-F	16.0362	40.7418	70.0829	113.5250	180.1852	218.5912
	S-F-S	20.6788	51.5892	91.9016	130.1296	179.4496	273.3803
	F-F-F	11.4916	23.6897	42.5326	47.3955	85.8008	119.6701
	F-C-F	4.7997	18.2550	32.3822	47.9172	79.3237	119.1096
	F-F-S	19.1076	37.6454	76.5323	80.7469	147.1610	174.5975
3.0	C-C-C	115.7888	179.7093	249.0593	298.5896	381.3997	518.2542
	C-C-S	87.6011	145.2643	220.2487	263.6977	357.8894	460.4278
	C-C-F	28.4362	57.6522	94.0757	129.9789	204.8213	269.8135
	S-S-S	60.2759	113.6065	180.7275	215.6733	325.3834	427.9401
	S-C-S	72.8739	128.2040	201.1019	242.4808	337.6979	443.0832
	S-C-F	15.6497	39.7599	68.3939	110.7890	175.8428	213.3232
	S-F-S	20.1804	50.3459	89.6868	126.9935	175.1248	266.7918
	F-F-F	11.2146	23.1188	41.5076	46.2533	83.7330	116.7861
	F-C-F	4.6841	17.8151	31.6018	46.7624	77.4120	116.2391
	F-F-S	18.6471	36.7381	74.6879	78.8009	143.6144	170.3897

8.4.3 Effect of ratio of mass densities (ρ_r)

In this section, Tables 8.24 to 8.32 show the effect of ascending values of the ratio of mass densities (ρ_r = 1.0, 1.5, 2.0, 2.5, 3.0) on free vibration frequencies (λ) of FG triangular plates. The triangular plate in Fig. 8.2 (a) is assumed in Tables 8.24 to 8.29 along with the same set of values for μ and boundary supports, as supposed in Tables 8.6 to 8.11. Similarly, the

non-dimensional frequencies of the plates stated in Fig. 8.2 (b) to 8.2 (d) are reported in Tables 8.30 to 8.32 respectively. The similar boundary conditions are assumed in Tables 8.30 to 8.32, as mentioned in Tables 8.12 to 8.14. The common numerical factors in these computations are $k = 1.0$ and $E_r = 1.0$. It is also interesting to note here that frequencies are increasing with increase in ρ_r. It may be true because of the fact that λ is directly proportional to ρ_c, as observed in its usual expression. One can also interpret the eigenfrequencies of the FG plate with other sets of BCs after looking into the present results.

Rather than the effects of k, E_r and ρ_r in Tables 8.6 to 8.32, there is also another parameter viz. μ which has major impact on the non-dimensional frequencies of FG triangular plates. As such, it is important to observe the descending pattern of frequencies with the ascending values of μ for triangular plate of Fig. 8.2 (a).

Table 8.24: Effect of ρ_r on first six non-dimensional frequencies of C-C-C FG right-angled triangle (Fig. 8.2 (a)) for $\theta = 0$, $k = 1.0$ and $E_r = 1.0$

μ	ρ_r	λ_1	λ_2	λ_3	λ_4	λ_5	λ_6
1.0	1.0	93.8094	159.5177	196.4910	248.4158	299.3326	354.9414
	2.0	108.3217	184.1952	226.8882	286.8458	345.6395	409.8511
	2.5	112.1237	190.6601	234.8516	296.9136	357.7708	424.2362
	3.0	114.8926	195.3685	240.6513	304.2460	366.6060	434.7127
1.5	1.0	65.5234	106.7565	141.6423	169.7267	214.1904	255.4156
	2.0	75.6600	123.2717	163.5544	195.9835	247.3257	294.9286
	2.5	78.3155	127.5984	169.2949	202.8622	256.0065	305.2801
	3.0	80.2495	130.7494	173.4756	207.8719	262.3286	312.8190
2.0	1.0	53.4702	83.7901	119.7814	131.0599	172.6714	189.7042
	2.0	61.7421	96.7525	138.3116	151.3350	199.3838	219.0516
	2.5	63.9091	100.1484	143.1661	156.6466	206.3818	226.7399
	3.0	65.4873	102.6215	146.7016	160.5150	211.4784	232.3393
2.5	1.0	46.9768	71.6368	101.9272	110.1294	153.2250	165.7136
	2.0	54.2441	82.7191	117.6954	127.1665	176.9290	191.3496
	2.5	56.1480	85.6224	121.8264	131.6298	183.1389	198.0656
	3.0	57.5346	87.7368	124.8349	134.8804	187.6615	202.9569
3.0	1.0	42.9629	63.0959	88.4648	102.1192	143.8032	156.2600
	2.0	49.6093	72.8569	102.1503	117.9171	166.0497	180.4336
	2.5	51.3505	75.4140	105.7356	122.0558	171.8777	186.7665
	3.0	52.6186	77.2764	108.3468	125.0700	176.1223	191.3787

Table 8.25: Effect of ρ_r on first six non-dimensional frequencies of C-C-S FG right-angled triangle (Fig. 8.2 (a)) for $\theta = 0$, $k = 1.0$ and $E_r = 1.0$

μ	ρ_r	λ_1	λ_2	λ_3	λ_4	λ_5	λ_6
1.0	1.0	73.4250	133.0584	168.5058	222.6888	276.4235	324.2267
	2.0	84.7839	153.6426	194.5738	257.1389	319.1864	374.3847
	2.5	87.7597	159.0352	201.4030	266.1641	330.3893	387.5250
	3.0	89.9269	162.9626	206.3767	272.7370	338.5483	397.0949
1.5	1.0	51.0324	88.9488	121.1213	150.4670	192.3149	235.8292
	2.0	58.9272	102.7093	139.8588	173.7443	222.0661	272.3122
	2.5	60.9954	106.3142	144.7676	179.8424	229.8603	281.8699
	3.0	62.5017	108.9396	148.3427	184.2836	235.5367	288.8307
2.0	1.0	41.3279	69.3498	101.9907	111.0474	158.8008	189.4286
	2.0	47.7213	80.0782	117.7688	128.2265	183.3673	218.7333
	2.5	49.3963	82.8888	121.9022	132.7271	189.8032	226.4105
	3.0	50.6161	84.9358	124.9126	136.0048	194.4904	232.0017
2.5	1.0	36.0380	58.1675	87.5269	94.2710	143.4914	172.7007
	2.0	41.6131	67.1661	101.0674	108.8548	165.6896	199.4176
	2.5	43.0737	69.5235	104.6147	112.6754	171.5051	206.4168
	3.0	44.1374	71.2404	107.1982	115.4580	175.7404	211.5143
3.0	1.0	32.7042	50.5756	77.9265	87.9661	135.7907	165.2824
	2.0	37.7635	58.3996	89.9817	101.5745	156.7976	190.8516
	2.5	39.0890	60.4494	93.1399	105.1396	162.3009	197.5502
	3.0	40.0543	61.9422	95.4400	107.7361	166.3090	202.4287

Table 8.26: Effect of ρ_r on first six non-dimensional frequencies of S-S-S FG right-angled triangle (Fig. 8.2 (a)) for $\theta = 0$, $k = 1.0$ and $E_r = 1.0$

μ	ρ_r	λ_1	λ_2	λ_3	λ_4	λ_5	λ_6
1.0	1.0	49.3772	102.3974	132.8920	181.7691	239.4133	286.9646
	2.0	57.0159	118.2384	153.4505	209.8888	276.4506	331.3581
	2.5	59.0171	122.3883	158.8364	217.2556	286.1536	342.9883
	3.0	60.4745	125.4107	162.7588	222.6207	293.2202	351.4584
1.5	1.0	34.3846	67.1145	96.0449	129.7321	174.5341	203.5525
	2.0	39.7039	77.4972	110.9031	149.8018	201.5346	235.0421
	2.5	41.0975	80.2172	114.7956	155.0596	208.6081	243.2917
	3.0	42.1124	82.1982	117.6305	158.8888	213.7597	249.2998
2.0	1.0	27.8391	51.4624	82.3722	107.7080	143.4821	172.1820
	2.0	32.1458	59.4237	95.1152	124.3704	165.6788	198.8186
	2.5	33.2741	61.5093	98.4536	128.7356	171.4939	205.7968
	3.0	34.0958	63.0283	100.8849	131.9148	175.7290	210.8790
2.5	1.0	24.1904	43.9850	74.6922	89.6844	122.8670	149.5437
	2.0	27.9326	50.7895	86.2471	103.5586	141.8746	172.6782
	2.5	28.9130	52.5721	89.2743	107.1934	146.8541	178.7389
	3.0	29.6270	53.8704	91.4789	109.8405	150.4807	183.1528
3.0	1.0	21.9385	39.6477	69.2333	73.5403	110.9179	132.3405
	2.0	25.3324	45.7813	79.9438	84.9170	128.0769	152.8137
	2.5	26.2216	47.3881	82.7497	87.8974	132.5722	158.1772
	3.0	26.8691	48.5584	84.7932	90.0681	135.8461	162.0834

Table 8.27: Effect of ρ_r on first six non-dimensional frequencies of C-C-F FG right-angled triangle (Fig. 8.2 (a)) for $\theta = 0$, $k = 1.0$ and $E_r = 1.0$

μ	ρ_r	λ_1	λ_2	λ_3	λ_4	λ_5	λ_6
1.0	1.0	29.0988	63.8764	90.4624	118.4707	171.1197	214.0724
	2.0	33.6003	73.7581	104.4570	136.7982	197.5921	247.1895
	2.5	34.7797	76.3469	108.1232	141.5995	204.5272	255.8654
	3.0	35.6386	78.2323	110.7934	145.0964	209.5780	262.1841
1.5	1.0	19.7848	41.7050	64.9056	77.9933	118.6126	142.0786
	2.0	22.8455	48.1568	74.9465	90.0589	136.9620	164.0582
	2.5	23.6474	49.8470	77.5770	93.2198	141.7691	169.8164
	3.0	24.2313	51.0780	79.4928	95.5218	145.2701	174.0100
2.0	1.0	15.4506	30.6559	53.8549	59.1377	90.3218	99.9366
	2.0	17.8408	35.3983	62.1863	68.2863	104.2946	115.3969
	2.5	18.4670	36.6408	64.3690	70.6830	107.9552	119.4471
	3.0	18.9230	37.5456	65.9586	72.4286	110.6212	122.3969
2.5	1.0	12.9612	24.6949	43.5926	50.2031	74.7484	85.6615
	2.0	14.9663	28.5152	50.3364	57.9696	86.3120	98.9134
	2.5	15.4916	29.5161	52.1031	60.0042	89.3414	102.3851
	3.0	15.8741	30.2450	53.3898	61.4860	91.5477	104.9135
3.0	1.0	11.3563	21.0540	35.0606	45.9334	68.1932	78.6279
	2.0	13.1131	24.3111	40.4845	53.0393	78.7428	90.7917
	2.5	13.5734	25.1643	41.9054	54.9009	81.5065	93.9783
	3.0	13.9086	25.7858	42.9403	56.2567	83.5193	96.2991

Table 8.28: Effect of ρ_r on first six non-dimensional frequencies of C-S-F FG right-angled triangle (Fig. 8.2 (a)) for $\theta = 0$, $k = 1.0$ and $E_r = 1.0$

μ	ρ_r	λ_1	λ_2	λ_3	λ_4	λ_5	λ_6
1.0	1.0	17.9703	48.1308	75.7060	100.7389	155.2088	200.8066
	2.0	20.7503	55.5767	87.4178	116.3233	179.2197	231.8715
	2.5	21.4786	57.5273	90.4860	120.4060	185.5100	240.0098
	3.0	22.0090	58.9480	92.7206	123.3795	190.0912	245.9369
1.5	1.0	13.7573	34.3827	54.4613	69.2721	110.9556	142.1440
	2.0	15.8856	39.7017	62.8865	79.9885	128.1205	164.1338
	2.5	16.4432	41.0952	65.0937	82.7960	132.6174	169.8946
	3.0	16.8492	42.1100	66.7012	84.8407	135.8924	174.0902
2.0	1.0	11.5280	26.2811	45.9373	53.7887	92.0098	118.5867
	2.0	13.3114	30.3468	53.0438	62.1099	106.2437	136.9321
	2.5	13.7786	31.4119	54.9056	64.2898	109.9727	141.7382
	3.0	14.1189	32.1877	56.2615	65.8775	112.6885	145.2384
2.5	1.0	10.1513	21.2417	41.0766	46.8536	78.6180	96.0617
	2.0	11.7217	24.5278	47.4312	54.1018	90.7802	110.9225
	2.5	12.1331	25.3887	49.0959	56.0007	93.9665	114.8157
	3.0	12.4327	26.0157	50.3084	57.3837	96.2870	117.6510
3.0	1.0	9.2021	18.1554	37.5761	42.9889	68.0010	75.4984
	2.0	10.6257	20.9641	43.3891	49.6393	78.5208	87.1781
	2.5	10.9986	21.6999	44.9120	51.3816	81.2768	90.2379
	3.0	11.2702	22.2358	46.0211	52.6505	83.2839	92.4663

Table 8.29: Effect of ρ_r on first six non-dimensional frequencies of C-F-F FG right-angled triangle (Fig. 8.2 (a)) for $\theta = 0$, $k = 1.0$ and $E_r = 1.0$

μ	ρ_r	λ_1	λ_2	λ_3	λ_4	λ_5	λ_6
1.0	1.0	6.1807	23.5033	32.8433	59.7726	82.9699	116.0983
	2.0	7.1369	27.1392	37.9241	69.0195	95.8054	134.0588
	2.5	7.3874	28.0918	39.2552	71.4420	99.1680	138.7640
	3.0	7.5698	28.7855	40.2246	73.2062	101.6170	142.1908
1.5	1.0	5.8011	18.4980	29.8889	42.2561	71.2843	87.6627
	2.0	6.6986	21.3597	34.5127	48.7931	82.3120	101.2242
	2.5	6.9337	22.1094	35.7240	50.5057	85.2010	104.7770
	3.0	7.1049	22.6554	36.6062	51.7529	87.3050	107.3645
2.0	1.0	5.5182	15.4110	28.6530	32.4307	63.4524	80.1162
	2.0	6.3719	17.7951	33.0856	37.4477	73.2685	92.5102
	2.5	6.5955	18.4197	34.2468	38.7621	75.8401	95.7571
	3.0	6.7584	18.8745	35.0926	39.7193	77.7130	98.1218
2.5	1.0	5.3074	13.3286	27.5323	27.9591	57.7683	73.6492
	2.0	6.1285	15.3906	31.7915	32.2843	66.7051	85.0428
	2.5	6.3436	15.9307	32.9074	33.4175	69.0464	88.0276
	3.0	6.5002	16.3242	33.7200	34.2427	70.7515	90.2015
3.0	1.0	5.1428	11.8874	24.8818	27.3406	53.3694	57.8147
	2.0	5.9384	13.7264	28.7311	31.5702	61.6257	66.7587
	2.5	6.1468	14.2082	29.7395	32.6783	63.7886	69.1018
	3.0	6.2986	14.5590	30.4739	33.4852	65.3639	70.8083

Table 8.30: Effect of ρ_r on first six non-dimensional frequencies of equilateral FG triangular plates (Fig. 8.2 (b)) with $\theta = 1/\sqrt{3}$ and $\mu = \sqrt{3}/2$

ρ_r	BCs	λ_1	λ_2	λ_3	λ_4	λ_5	λ_6
1.0	C-C-C	99.0301	189.3558	189.3558	302.5013	320.2886	320.2886
	C-C-S	81.6095	165.6640	165.9714	274.0097	295.8453	299.9950
	C-C-F	40.0393	95.9871	102.0821	176.7503	204.5401	206.2233
	S-S-S	52.6389	124.5893	124.5893	219.4339	243.2077	243.2077
	S-C-S	66.1950	143.8823	144.4059	253.5495	269.0919	273.7237
	S-C-F	26.5733	75.6211	84.9659	152.7500	182.8633	185.6936
	S-F-S	16.0939	58.1982	68.7730	124.7878	156.2157	158.3566
	F-F-F	35.2728	36.5976	36.5976	111.9604	111.9604	118.7939
	F-C-F	8.9250	35.3952	38.5490	95.6379	99.2576	115.4143
	F-F-S	22.6792	26.8547	72.2202	75.6233	92.9068	190.9280
2.0	C-C-C	114.3501	218.6493	218.6493	349.2984	369.8374	369.8374
	C-C-S	94.2345	191.2923	191.6472	316.3991	341.6127	346.4044
	C-C-F	46.2334	110.8364	117.8742	204.0936	236.1826	238.1262
	S-S-S	60.7821	143.8633	143.8633	253.3805	280.8320	280.8320
	S-C-S	76.4354	166.1409	166.7455	292.7738	310.7206	316.0689
	S-C-F	30.6842	87.3197	98.1101	176.3806	211.1523	214.4205
	S-F-S	18.5837	67.2015	79.4122	144.0925	180.3824	182.8545
	F-F-F	40.7295	42.2593	42.2593	129.2807	129.2807	137.1714
	F-C-F	10.3057	40.8708	44.5126	110.4331	114.6128	133.2690
	F-F-S	26.1876	31.0091	83.3927	87.3223	107.2796	220.4647
2.5	C-C-C	118.3636	226.3235	226.3235	361.5582	382.8181	382.8181
	C-C-S	97.5420	198.0064	198.3737	327.5042	353.6027	358.5626
	C-C-F	47.8561	114.7265	122.0114	211.2570	244.4722	246.4840
	S-S-S	62.9155	148.9127	148.9127	262.2737	290.6888	290.6888
	S-C-S	79.1182	171.9722	172.5980	303.0497	321.6263	327.1624
	S-C-F	31.7612	90.3845	101.5536	182.5712	218.5634	221.9463
	S-F-S	19.2359	69.5602	82.1995	149.1499	186.7135	189.2724
	F-F-F	42.1591	43.7425	43.7425	133.8182	133.8182	141.9859
	F-C-F	10.6674	42.3053	46.0749	114.3092	118.6355	137.9465
	F-F-S	27.1068	32.0974	86.3197	90.3871	111.0449	228.2026
3.0	C-C-C	121.2866	231.9126	231.9126	370.4869	392.2718	392.2718
	C-C-S	99.9508	202.8961	203.2726	335.5919	362.3350	367.4173
	C-C-F	49.0380	117.5597	125.0245	216.4740	250.5094	252.5710
	S-S-S	64.4692	152.5901	152.5901	268.7506	297.8673	297.8673
	S-C-S	81.0720	176.2191	176.8603	310.5335	329.5689	335.2417
	S-C-F	32.5455	92.6166	104.0615	187.0798	223.9609	227.4273
	S-F-S	19.7109	71.2780	84.2294	152.8332	191.3244	193.9465
	F-F-F	43.2002	44.8227	44.8227	137.1229	137.1229	145.4923
	F-C-F	10.9308	43.3500	47.2127	117.1320	121.5652	141.3531
	F-F-S	27.7762	32.8901	88.4514	92.6193	113.7872	233.8381

Table 8.31: Effect of ρ_r on first six non-dimensional frequencies of FG right-angled triangular plates (Fig. 8.2 (c)) with angles 30°, 60°and 90°

ρ_r	BCs	λ_1	λ_2	λ_3	λ_4	λ_5	λ_6
1.0	C-C-C	176.6773	281.6946	389.4979	449.9239	574.4351	657.6405
	C-C-S	137.1100	234.4229	332.2733	388.2433	520.0610	626.8953
	C-C-F	52.2997	107.0327	177.4260	203.2358	312.6933	349.1134
	S-S-S	92.4337	174.8875	265.3512	354.5446	476.1434	556.7795
	S-C-S	119.5542	213.0784	305.1774	376.5482	523.1429	614.7466
	S-C-F	37.7140	90.4292	149.3749	181.3869	302.9555	388.3029
	S-F-S	22.9903	66.3451	130.0744	144.0188	287.5747	356.4993
	F-F-F	25.5779	54.5909	81.0811	101.2828	143.6803	231.9947
	F-C-F	16.9768	50.6991	87.6860	110.4150	202.0306	249.3552
	F-F-S	32.0453	69.2456	89.0420	170.3531	224.4979	241.4710
2.0	C-C-C	204.0093	325.2729	449.7534	519.5274	663.3006	759.3779
	C-C-S	158.3210	270.6882	383.6761	448.3048	600.5147	723.8764
	C-C-F	60.3905	123.5907	204.8739	234.6765	361.0671	403.1214
	S-S-S	106.7333	201.9427	306.4012	409.3929	549.8031	642.9136
	S-C-S	138.0493	246.0417	352.3886	434.8004	604.0734	709.8482
	S-C-F	43.5484	104.4187	172.4833	209.4475	349.8228	448.3735
	S-F-S	26.5470	76.6087	150.1970	166.2986	332.0626	411.6500
	F-F-F	29.5348	63.0362	93.6243	116.9514	165.9077	267.8844
	F-C-F	19.6031	58.5423	101.2511	127.4963	233.2849	287.9306
	F-F-S	37.0028	79.9580	102.8168	196.7069	259.2278	278.8267
2.5	C-C-C	211.1697	336.6894	465.5390	537.7619	686.5813	786.0308
	C-C-S	163.8778	280.1889	397.1425	464.0395	621.5917	749.2832
	C-C-F	62.5101	127.9286	212.0647	242.9132	373.7399	417.2703
	S-S-S	110.4795	209.0306	317.1554	423.7619	569.1003	665.4788
	S-C-S	142.8947	254.6774	364.7568	450.0612	625.2753	734.7627
	S-C-F	45.0769	108.0836	178.5371	216.7988	362.1010	464.1107
	S-F-S	27.4787	79.2975	155.4686	172.1354	343.7175	426.0982
	F-F-F	30.5715	65.2486	96.9104	121.0561	171.7308	277.2867
	F-C-F	20.2912	60.5971	104.8048	131.9712	241.4728	298.0365
	F-F-S	38.3015	82.7644	106.4255	203.6109	268.3263	288.6131
3.0	C-C-C	216.3846	345.0040	477.0355	551.0420	703.5365	805.4419
	C-C-S	167.9248	287.1082	406.9500	475.4990	636.9420	767.7868
	C-C-F	64.0538	131.0878	217.3016	248.9120	382.9695	427.5749
	S-S-S	113.2078	214.1926	324.9876	434.2267	583.1542	681.9129
	S-C-S	146.4234	260.9667	373.7645	461.1755	640.7166	752.9077
	S-C-F	46.1901	110.7527	182.9461	222.1526	371.0432	475.5719
	S-F-S	28.1573	81.2558	159.3080	176.3863	352.2056	436.6207
	F-F-F	31.3264	66.8600	99.3036	124.0456	175.9717	284.1343
	F-C-F	20.7923	62.0935	107.3930	135.2303	247.4360	305.3965
	F-F-S	39.2474	84.8082	109.0537	208.6391	274.9526	295.7404

Table 8.32: Effect of ρ_r on first six non-dimensional frequencies of isosceles FG triangular plates (Fig. 8.2 (d)) with angles 30°, 30°and 120°

ρ_r	BCs	λ_1	λ_2	λ_3	λ_4	λ_5	λ_6
1.0	C-C-C	141.8117	220.0980	305.0341	365.6960	467.1174	634.7292
	C-C-S	107.2890	177.9117	269.7484	322.9624	438.3232	563.9066
	C-C-F	34.8270	70.6093	115.2188	159.1910	250.8538	330.4526
	S-S-S	73.8226	139.1389	221.3450	264.1448	398.5116	524.1175
	S-C-S	89.2520	157.0172	246.2985	296.9771	413.5938	542.6639
	S-C-F	19.1669	48.6957	83.7651	135.6883	215.3625	261.2665
	S-F-S	24.7159	61.6608	109.8434	155.5346	214.4833	326.7519
	F-F-F	13.7350	28.3146	50.8362	56.6484	102.5516	143.0332
	F-C-F	5.7368	21.8189	38.7042	57.2720	94.8100	142.3632
	F-F-S	22.8380	44.9948	91.4736	96.5110	175.8910	208.6840
2.0	C-C-C	163.7501	254.1473	352.2230	422.2694	539.3807	732.9222
	C-C-S	123.8866	205.4347	311.4786	372.9249	506.1320	651.1432
	C-C-F	40.2148	81.5326	133.0432	183.8180	289.6611	381.5738
	S-S-S	85.2430	160.6638	255.5872	305.0081	460.1616	605.1987
	S-C-S	103.0593	181.3079	284.4010	342.9196	477.5769	626.6143
	S-C-F	22.1321	56.2290	96.7236	156.6794	248.6792	301.6845
	S-F-S	28.5394	71.1998	126.8363	179.5959	247.6639	377.3006
	F-F-F	15.8599	32.6949	58.7006	65.4120	118.4164	165.1605
	F-C-F	6.6243	25.1943	44.6917	66.1320	109.4771	164.3869
	F-F-S	26.3710	51.9555	105.6247	111.4413	203.1014	240.9675
2.5	C-C-C	169.4975	263.0674	364.5854	437.0904	558.3120	758.6465
	C-C-S	128.2349	212.6451	322.4110	386.0140	523.8964	673.9973
	C-C-F	41.6263	84.3942	137.7128	190.2697	299.8277	394.9665
	S-S-S	88.2349	166.3028	264.5579	315.7134	476.3125	626.4402
	S-C-S	106.6765	187.6715	294.3830	354.9555	494.3391	648.6074
	S-C-F	22.9089	58.2025	100.1184	162.1785	257.4075	312.2732
	S-F-S	29.5411	73.6988	131.2880	185.8995	256.3565	390.5432
	F-F-F	16.4165	33.8424	60.7609	67.7078	122.5726	170.9573
	F-C-F	6.8568	26.0786	46.2603	68.4532	113.3196	170.1566
	F-F-S	27.2966	53.7791	109.3319	115.3527	210.2299	249.4250
3.0	C-C-C	173.6832	269.5639	373.5889	447.8844	572.0996	777.3814
	C-C-S	131.4016	217.8964	330.3730	395.5466	536.8340	690.6417
	C-C-F	42.6542	86.4784	141.1136	194.9684	307.2319	404.7202
	S-S-S	90.4139	170.4097	271.0912	323.5099	488.0751	641.9102
	S-C-S	109.3109	192.3061	301.6528	363.7212	506.5468	664.6248
	S-C-F	23.4746	59.6398	102.5909	166.1836	263.7642	319.9848
	S-F-S	30.2706	75.5188	134.5302	190.4903	262.6873	400.1877
	F-F-F	16.8219	34.6782	62.2614	69.3799	125.5995	175.1791
	F-C-F	7.0261	26.7226	47.4027	70.1436	116.1180	174.3586
	F-F-S	27.9707	55.1072	112.0319	118.2013	215.4216	255.5846

The new results for triangular plates may be used to demonstrate the three-dimensional (or 3-D) mode shapes corresponding to the non-dimensional frequencies. As such, Figs. 8.3 to 8.6 represent the 3-D mode shapes of triangular plates corresponding to the first six smallest eigenvalues. 3-D mode shapes of the isotropic equilateral triangular plate ($k = 0$ in case of FG plate) is considered here in Figs. 8.3 and 8.4 with the edge supports C-C-C and C-F-F respectively. On the other hand, Figs. 8.5 and 8.6 are meant for the first six mode shapes

of equilateral FG plate with $k = 1$, $E_r = 2.0$ and $\rho_r = 1.0$ subjected to C-C-C and C-F-F edge conditions respectively. Similarly, one may easily plot the mode shapes for other configurations of the FG triangular plates using different sets of BCs.

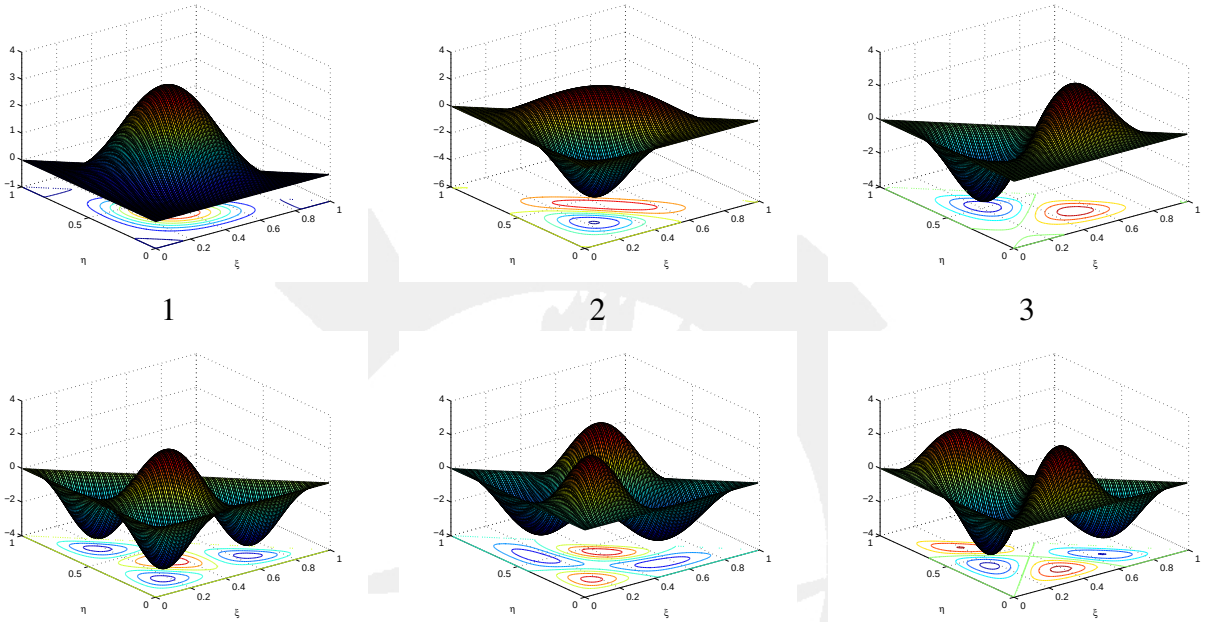

1 2 3

4 5 6

Figure 8.3: First six 3-D mode shapes of C-C-C equilateral triangular plate with $k = 0$

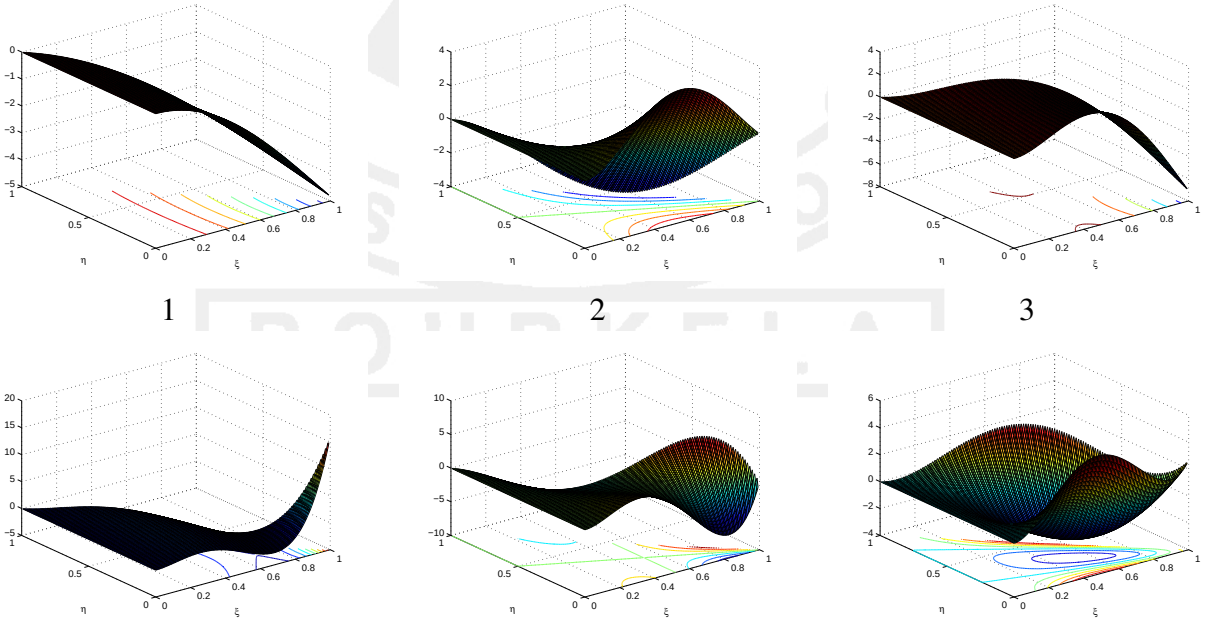

1 2 3

4 5 6

Figure 8.4: First six 3-D mode shapes of C-F-F equilateral triangular plate with $k = 0$

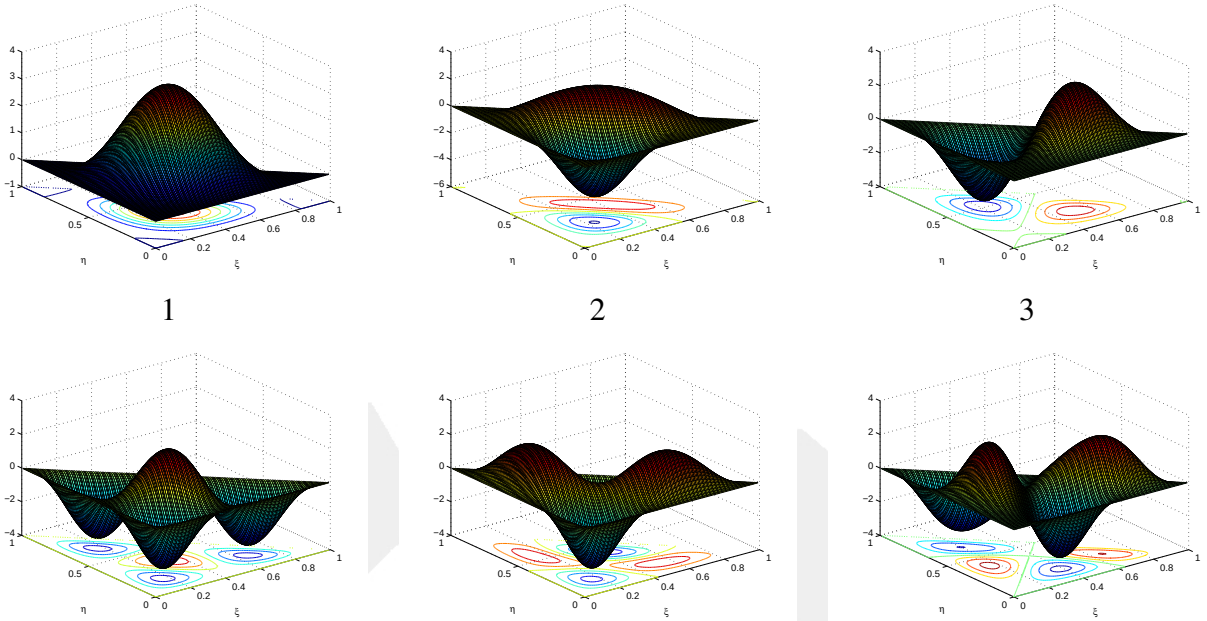

1 2 3

4 5 6

Figure 8.5: First six 3-D mode shapes of C-C-C FG equilateral triangular plate with $k = 1$, $E_r = 2.0$ and $\rho_r = 1.0$

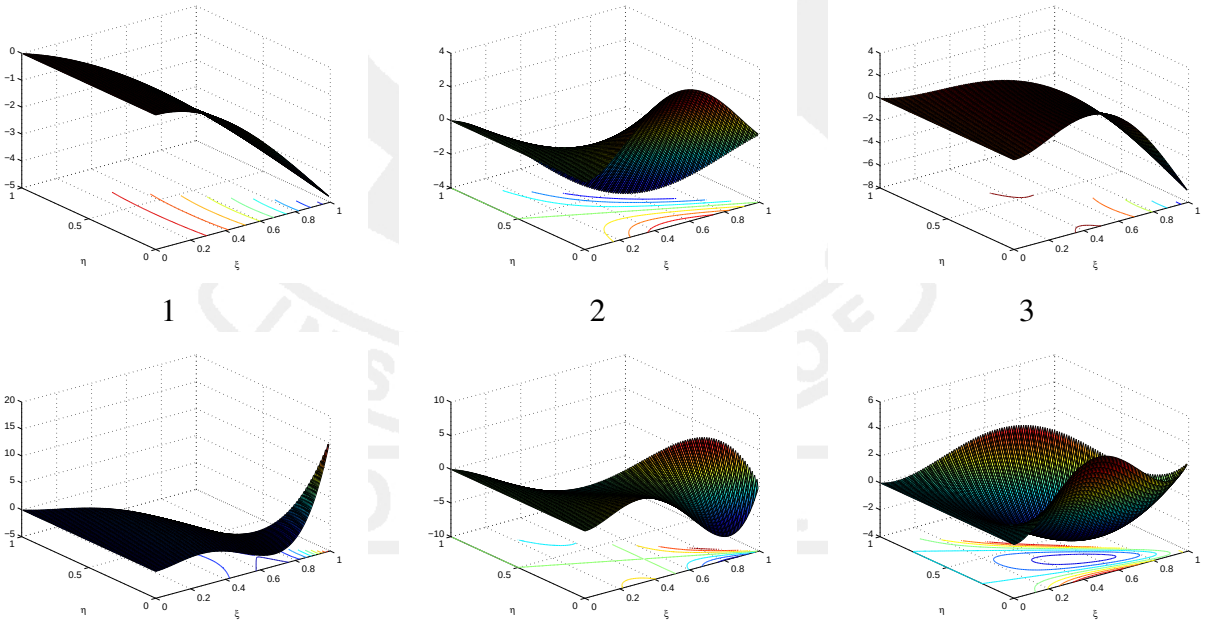

1 2 3

4 5 6

Figure 8.6: First six 3-D mode shapes of C-F-F FG equilateral triangular plate with $k = 1$, $E_r = 2.0$ and $\rho_r = 1.0$

8.5 Concluding remarks

In present study, free vibration of FG triangular plates subjected to various combinations of boundary conditions has been investigated. Free vibration eigenfrequencies along with 3-D mode shapes have been incorporated with reference to different volume fractions of the FG plate. It may be worth mentioning that the Rayleigh-Ritz method is one of the computationally efficient technique, which may handle any combinations of boundary conditions very easily. We hope that the present results may serve as benchmark for other researchers in future investigations. From the above numerical results and discussions, one may summarize the following facts for the free vibration of FG triangular plates.

- The present method assumes the simple algebraic polynomials as the admissible functions for computing the frequencies and mode shapes of a triangular plate with any set of boundary conditions. The geometric configuration and boundary conditions can be controlled by five parameters viz. p, q, r, μ and θ.

- The method can easily be extended to other geometries by a suitable selection of the admissible function. Also, suitable modifications can be made to include variable thickness and other complicating effects.

- Increase in the number of polynomials (n) play an important role in the convergence of non-dimensional frequencies. Moreover, different volume fractions developed from the parameters viz. k, E_r and ρ_r also have major roles in the variation of frequencies. Each of the eigenfrequencies follow descending pattern due to increase in k and E_r, whereas we get just reverse pattern (ascending behavior) with increase in ρ_r. Rather than these parameters, the factor μ also play a crucial role in evaluating vibration characteristics of the FG triangular plates (Fig. 8.2 (a)). It may be viewed (in this case) that frequencies are decreasing with increase in μ.

- The functionally graded plate behaves as isotropic either for $k = 0$ or for the combined values of $E_r = 1.0$ and $\rho_r = 1.0$.

- In addition to the shear deformation effects (neglected in classical plate theory), the analysis may also be extended for other deformation plate theories.

Chapter 9

Complicating effects

The contents of this chapter have been published/communicated in:

(1) Chakraverty, S. and Pradhan, K.K. (2014). Free vibration of functionally graded thin rectangular plates resting on Winkler elastic foundation with general boundary conditions using Rayleigh-Ritz method. *International Journal of Applied Mechanics*, 6(4):145003 (37 pages) (World Scientific).

(2) Chakraverty, S. and Pradhan, K.K. (2014). Free vibration of exponential functionally graded rectangular plates in thermal environment with general boundary conditions. *Aerospace Science and Technology*, 36:132–156 (Elsevier).

(3) Pradhan, K.K. and Chakraverty, S. (2015). Free vibration of FG Levy plate resting on elastic foundations. *Engineering and Computational Mechanics*, Under review (Proceedings of the ICE).

Chapter 9

Complicating effects

This chapter reflects the effect of different complicating effects viz. Winkler (or Pasternak) elastic foundations and thermal environments on vibration characteristics of functionally graded rectangular plates. The presence of complicating environments mainly manipulates the expression of strain energy as given in Sec. 3.1.3 with a specific term. The basic assumptions mentioned in case of Rayleigh-Ritz method are also considered in these problems. It can further be seen in subsequent sections that the factors associated with these complicating environments play major roles in finding free vibration of rectangular FG plates.

9.1 Winkler foundations

This investigation deals with free vibration of FG rectangular plates resting on a uniform Winkler elastic foundations and subjected to various combination of classical boundary conditions. The FG material properties are assumed to vary along thickness direction in power-law form. As such, there occurs change in the expression of maximum strain energy as mentioned in Eq. (3.31). The main objective is to find the effects of power-law indices and Winkler foundation modulus on the free vibration eigenfrequencies. The new results for eigenfrequencies are incorporated based on the test of convergence and validation of present results with existing ones.

9.1.1 Numerical modeling

Let us first express the strain energy of FG rectangular plate due to Winkler elastic foundation as below.

$$\mathbf{U}_f = \frac{1}{2}\int_{\Omega} k(x,y)w^2 \,\mathrm{d}x\mathrm{d}y \tag{9.1}$$

where $k(x,y)$ is the Winkler elastic foundation modulus. While assuming the harmonic behavior of the displacement component ($w(x,y)$), Eq. (9.1) yields the maximum strain energy $(\mathbf{U}_f)_{max}$ of the FG plate with the effect of elastic foundation as

$$(\mathbf{U}_f)_{max} = \frac{1}{2}\int_{\Omega} k(x,y)W^2 \,\mathrm{d}x\mathrm{d}y \tag{9.2}$$

The maximum strain energy associated with free vibration of thin FG rectangular plate (in the absence of elastic foundation) has already been expressed in Eq. (3.31). Accordingly, the effective maximum strain energy of the FG plate can be transformed into $\mathbf{U}_{eff} = \mathbf{U}_{max} + (\mathbf{U}_f)_{max}$; where $\mathbf{U}_{max} = \frac{1}{2}\int_{\Omega}\left[D_{11}\left\{\left(\frac{\partial^2 W}{\partial x^2}\right)^2 + \left(\frac{\partial^2 W}{\partial y^2}\right)^2\right\} + 2D_{12}\frac{\partial^2 W}{\partial x^2}\frac{\partial^2 W}{\partial y^2} + 4D_{66}\left(\frac{\partial^2 W}{\partial x \partial y}\right)^2\right]\mathrm{d}x\mathrm{d}y$. In case of FG plates resting on elastic foundation, the Rayleigh-Ritz method can be used by equating $\mathbf{U}_{eff}$ and maximum kinetic energy ($\mathbf{T}_{max}$). In general, Rayleigh quotient $\left(\omega^2\right)$ can be found by equating $\mathbf{U}_{eff}$ and $\mathbf{T}_{max}$.

$$\omega^2 = \frac{\mathbf{U}_{eff}}{\int_{\Omega} I_0 W^2 \,\mathrm{d}x\mathrm{d}y} \tag{9.3}$$

Substituting the Rayleigh quotient involved in Eq. (9.3) into Eq. (3.37), the generalized eigenvalue problem for free vibration of rectangular FG plate laying on elastic foundation can be given as

$$\left([K + K_f]_{n\times n} - \lambda^2[M]_{n\times n}\right)\{\Delta\} = 0 \tag{9.4}$$

Here, $[K_f]_{n\times n}$ in Eq. (9.4) denotes the stiffness matrices due to elastic foundation. In the absence of elastic foundation, the generalized eigenvalue problem takes the form of Eq. (3.38).

9.1.2 Convergence and comparison studies

First of all, the test of convergence of non-dimensional frequencies with increase in number of polynomials is carried out. A convergence of first six non-dimensional frequencies of isotropic square plate ($k = 0$) subjected to SSSS and SCSC edge supports is performed in Table 9.1 with three different elastic moduli; $k_w = 0$, 10^2 and 10^3. The present analysis concerned with the functionally graded material, which is out of the scope of (Lam et al., 2000). Hence, fundamental and sixth mode non-dimensional frequencies have been verified in Table 9.1 with (Lam et al., 2000) rather than checking only the convergence. It is evident that present

results are in excellent agreement with the existing results. With the similar assumptions for edge conditions (SSSS and SCSC) and elastic moduli (k_w = 0, 10^2 and 10^3) in case of functionally graded rectangular plates, the convergence of first six non-dimensional frequencies are performed in Table 9.2 with the power-law index (k) and aspect ratio (a/b) as 1.0 and 2.0 respectively. It can easily be observed in Tables 9.1 and 9.2 that frequencies at each mode are gradually converging with the increase in number of polynomials (n) even if in the presence of Winkler foundation.

Table 9.1: Convergence of first six non-dimensional frequencies of isotropic square plate ($k = 0$) with different elastic moduli (k_w)

BCs	k_w	Source	λ_1	λ_2	λ_3	λ_4	λ_5	λ_6
SSSS	0	7×7	19.7449	49.8221	58.9915	92.5635	139.599	139.951
		10×10	19.7449	49.5132	49.5132	92.5635	139.599	139.951
		14×14	19.7408	49.5132	49.5132	79.4007	100.179	139.599
		21×21	19.7392	49.3490	49.3490	79.4007	100.173	100.187
		28×28	19.7392	49.3490	49.3490	78.9633	98.7193	98.7194
		Lam et al. (2000)	19.74	-	-	-	-	98.69
	10^2	7×7	22.1328	50.8158	59.8331	93.1021	139.957	140.307
		10×10	22.1328	50.5129	50.5129	93.1021	139.957	140.307
		14×14	22.1292	50.5129	50.5129	80.0280	100.678	139.957
		21×21	22.1277	50.3520	50.3520	80.0280	100.671	100.685
		28×28	22.1277	50.3520	50.3520	79.5940	99.2245	99.2246
		Lam et al. (2000)	22.13	-	-	-	-	99.20
	10^3	7×7	37.2808	59.0105	66.9328	97.8162	143.136	143.479
		10×10	37.2808	58.7499	58.7499	97.8162	143.136	143.479
		14×14	37.2787	58.7499	58.7499	85.4662	105.052	143.136
		21×21	37.2778	58.6116	58.6116	85.4662	105.046	105.059
		28×28	37.2778	58.6116	58.6116	85.0600	103.661	103.661
		Lam et al. (2000)	37.28	-	-	-	-	103.64
SCSC	0	7×7	28.9525	63.4980	69.5923	100.876	135.190	142.589
		10×10	28.9525	54.8846	69.3469	100.876	135.190	142.589
		14×14	28.9520	54.8846	69.3469	94.7034	129.312	142.254
		21×21	28.9509	54.7439	69.3271	94.7034	103.718	129.312
		28×28	28.9509	54.7439	69.3271	94.5862	102.245	129.098
		Lam et al. (2000)	28.95	-	-	-	-	129.09
	10^2	7×7	30.6308	64.2806	70.3071	101.371	135.559	142.939
		10×10	30.6308	55.7881	70.0642	101.371	135.559	142.939
		14×14	30.6303	55.7881	70.0642	95.2299	129.698	142.605
		21×21	30.6293	55.6498	70.0446	95.2299	104.199	129.698
		28×28	30.6293	55.6498	70.0446	95.1134	102.732	129.484
		Lam et al. (2000)	30.63	-	-	-	-	129.48
	10^3	7×7	42.8748	70.9366	76.4401	105.717	138.839	146.054
		10×10	42.8748	63.3428	76.2167	105.717	138.839	146.054
		14×14	42.8744	63.3428	76.2167	99.8436	133.123	145.726
		21×21	42.8737	63.2210	76.1987	99.8436	108.432	133.123
		28×28	42.8737	63.2210	76.1987	99.7324	107.023	132.914
		Lam et al. (2000)	42.87	-	-	-	-	132.91

Table 9.2: Convergence of first six non-dimensional frequencies of functionally graded rectangular plate ($a/b = 2$, $k = 1$) with different elastic moduli (k_w)

BCs	k_w	Source	λ_1	λ_2	λ_3	λ_4	λ_5	λ_6
SSSS	0	7×7	49.3650	81.5687	165.723	209.285	238.646	306.833
		10×10	49.3650	79.1231	165.723	168.476	238.646	303.298
		14×14	49.3576	79.1231	129.684	168.476	198.635	303.298
		21×21	49.3480	78.9579	129.684	167.787	198.635	203.662
		28×28	49.3480	78.9579	128.327	167.787	197.410	203.662
	10^2	7×7	50.3677	82.1794	166.024	209.523	238.856	306.996
		10×10	50.3677	79.7525	166.024	168.772	238.856	303.463
		14×14	50.3605	79.7525	130.069	168.772	198.887	303.463
		21×21	50.3511	79.5886	130.069	168.085	198.887	203.908
		28×28	50.3510	79.5886	128.716	168.085	197.663	203.908
	10^3	7×7	58.6251	87.4840	168.713	211.660	240.732	308.458
		10×10	58.6251	85.2083	168.713	171.418	240.732	304.942
		14×14	58.6189	85.2083	133.484	171.418	201.136	304.942
		21×21	58.6108	85.0550	133.484	170.741	201.136	206.103
		28×28	58.6108	85.0550	132.166	170.741	199.927	206.103
SCSC	0	7×7	54.7588	96.7358	160.333	211.792	243.031	253.303
		10×10	54.7588	94.6101	160.333	171.204	243.031	253.303
		14×14	54.7518	94.6101	154.968	171.204	207.337	253.303
		21×21	54.7431	94.5854	154.968	170.362	207.337	235.684
		28×28	54.7431	94.5854	154.777	170.362	206.708	235.684
	10^2	7×7	55.6644	97.2513	160.644	212.028	243.237	253.499
		10×10	55.6644	95.1372	160.644	171.496	243.237	253.499
		14×14	55.6576	95.1372	155.291	171.496	207.578	253.499
		21×21	55.6490	95.1125	155.291	170.655	207.578	235.896
		28×28	55.6489	95.1125	155.099	170.655	206.949	235.896
	10^3	7×7	63.2339	101.773	163.421	214.140	245.079	255.269
		10×10	63.2339	99.7551	163.421	174.099	245.079	255.269
		14×14	63.2279	99.7551	158.162	174.099	209.735	255.269
		21×21	63.2203	99.7316	158.162	173.272	209.735	237.796
		28×28	63.2203	99.7316	157.975	173.272	209.113	237.796

9.1.3 Results and discussions

The new results for eigenfrequencies of FG plate with Winkler foundation are incorporated with different aspect ratios (a/b), power-law indices (k) and various foundation parameters (k_w). In Tables 9.3 to 9.5, first six non-dimensional frequencies of FG square plates subjected to various combinations of boundary supports are evaluated with the increase in power-law indices (k = 0, 0.2, 0.5, 2.0, 5.0), whereas Tables 9.6 to 9.8 address the effect of increase in aspect ratios (a/b = 0.2, 0.5, 1.0, 2.0) on first six non-dimensional frequencies of rectangular FG plates with $k = 1$. Here, k_w is considered to be 10^2 in Tables 9.3 and 9.6, 5×10^2 in Tables 9.4 and 9.7 and 10^3 in Tables 9.5 and 9.8 respectively. Analyzing the results obtained in these tabulations, we may summarize as follows for the effect of k, a/b along with k_w.

- Non-dimensional frequencies are showing a descending pattern with increase in power-law indices (k) irrespective of the foundation index and boundary condition assumed, whereas act reverse with increase in aspect ratios (a/b).

- It is evident that non-dimensional frequencies are increasing with increase in foundation parameters (k_w) regardless of the aspect ratio and power-law index considered.

- Irrespective of k and k_w assumed, it can also be observed that second non-dimensional frequencies for CCCC and SSSS square FG plates are coinciding with the respective third mode frequencies. But no coincidence can be observed for natural frequencies of rectangular FG plates ($a/b \neq 1$). This proposition may be true because of the identical edge supports at all edges of the FG square plate.

Table 9.3: First six non-dimensional frequencies of square FG Al/Al_2O_3 plates with different power-law indices (k) and $k_w = 10^2$

k	Mode	CCCC	SCSC	SSSC	SCSF	SSSS	CCCF	SSSF	SFSF
0	1	37.3498	30.6293	25.6739	16.1545	22.1277	25.9529	15.3795	13.8839
	2	74.0770	55.6498	52.6341	34.5442	50.3520	41.2496	29.5029	18.9828
	3	74.0770	70.0446	59.4929	42.8889	50.3520	64.0676	42.3981	38.0640
	4	108.686	95.1134	86.7364	63.8334	79.5940	77.3910	59.9401	40.2345
	5	131.962	102.732	100.934	73.1060	99.2245	81.2345	62.6785	47.8216
	6	131.962	129.484	113.735	91.3156	99.2246	117.162	91.0134	72.7439
0.2	1	35.0331	28.7294	24.0814	15.1525	20.7552	24.3431	14.4255	13.0227
	2	69.4821	52.1979	49.3693	32.4015	47.2287	38.6909	27.6729	17.8053
	3	69.4821	65.6998	55.8026	40.2286	47.2287	60.0936	39.7682	35.7030
	4	101.944	89.2136	81.3562	59.8739	74.6569	72.5905	56.2221	37.7388
	5	123.777	96.3600	94.6728	68.5713	93.0697	76.1956	58.7906	44.8552
	6	124.377	121.453	106.679	85.6514	93.0698	109.895	85.3679	68.2317
0.5	1	32.9799	27.0456	22.6700	14.2644	19.5388	22.9164	13.5801	12.2595
	2	65.4099	49.1387	46.4759	30.5025	44.4607	36.4233	26.0510	16.7618
	3	65.4099	61.8493	52.5321	37.8709	44.4607	56.5716	37.4374	33.6105
	4	95.9694	83.9850	76.5881	56.3648	70.2814	68.3361	52.9270	35.5270
	5	116.522	90.7126	89.1242	64.5525	87.6151	71.7299	55.3450	42.2264
	6	117.087	114.335	100.428	80.6316	87.6151	103.454	80.3647	64.2328
2.0	1	30.0655	24.6556	20.6667	13.0039	17.8121	20.8913	12.3800	11.1761
	2	59.6297	44.7964	42.3689	27.8070	40.5318	33.2046	23.7490	15.2806
	3	59.6297	56.3837	47.8899	34.5243	40.5318	51.5725	34.1291	30.6404
	4	87.4887	76.5634	69.8201	51.3840	64.0708	62.2974	48.2499	32.3875
	5	106.225	82.6965	81.2485	58.8481	79.8727	65.3913	50.4542	38.4949
	6	106.741	104.231	91.5530	73.5063	79.8727	94.3118	73.2630	58.5566
5.0	1	28.1456	23.0812	19.3470	12.1735	16.6747	19.5573	11.5895	10.4625
	2	55.8220	41.9358	39.6633	26.0314	37.9436	31.0843	22.2324	14.3048
	3	55.8220	52.7833	44.8318	32.3197	37.9436	48.2792	31.9498	28.6838
	4	81.9020	71.6743	65.3616	48.1028	59.9794	58.3193	45.1689	30.3194
	5	99.4422	77.4157	76.0602	55.0903	74.7723	61.2156	47.2324	36.0367
	6	99.9245	97.5751	85.7067	68.8124	74.7723	88.2893	68.5847	54.8174

Table 9.4: First six non-dimensional frequencies of square FG Al/Al_2O_3 plates with different power-law indices (k) and $k_w = 5 \times 10^2$

k	Mode	CCCC	SCSC	SSSC	SCSF	SSSS	CCCF	SSSF	SFSF
0	1	42.3676	36.5808	32.5446	25.7093	29.8268	32.7651	25.2295	24.3467
	2	76.7294	59.1346	56.3059	39.9162	54.1786	45.8424	35.6430	27.5744
	3	76.7294	72.8440	62.7646	47.3229	54.1786	67.1168	46.8785	42.9985
	4	110.511	97.1934	89.0123	66.8932	82.0683	79.9335	63.1887	44.9312
	5	133.469	104.661	102.896	75.7924	101.220	83.6603	65.7920	51.8353
	6	134.102	131.019	115.479	93.4802	101.220	118.857	93.1850	75.4432
0.2	1	39.7395	34.3117	30.5259	24.1146	27.9766	30.7328	23.6646	22.8365
	2	71.9700	55.4665	52.8133	37.4402	50.8180	42.9989	33.4321	25.8640
	3	71.9700	68.3255	58.8714	44.3875	50.8180	62.9536	43.9707	40.3313
	4	103.656	91.1646	83.4910	62.7439	76.9777	74.9753	59.2692	42.1442
	5	125.190	98.1691	96.5135	71.0911	94.9415	78.4709	61.7110	48.6200
	6	125.784	122.893	108.317	87.6817	94.9415	111.484	87.4048	70.7636
0.5	1	37.4105	32.3008	28.7368	22.7013	26.3370	28.9316	22.2776	21.4981
	2	67.7520	52.2157	49.7180	35.2459	47.8396	40.4788	31.4727	24.3481
	3	67.7520	64.3211	55.4211	41.7861	47.8396	59.2640	41.3937	37.9676
	4	97.5807	85.8216	78.5978	59.0666	72.4662	70.5812	55.7956	39.6742
	5	117.853	92.4156	90.8570	66.9246	89.3772	73.8719	58.0943	45.7705
	6	118.412	115.690	101.969	82.5428	89.3772	104.950	82.2822	66.6163
2.0	1	34.1046	29.4464	26.1974	20.6952	24.0096	26.3749	20.3090	19.5984
	2	61.7648	47.6015	45.3245	32.1313	43.6121	36.9017	28.6915	22.1965
	3	61.7648	58.6372	50.5236	38.0935	43.6121	54.0269	37.7358	34.6125
	4	88.9577	78.2377	71.6522	53.8470	66.0625	64.3440	50.8650	36.1682
	5	107.438	84.2490	82.8281	61.0106	81.4791	67.3440	52.9606	41.7259
	6	107.948	105.467	92.9577	75.2487	81.4791	95.6760	75.0111	60.7295
5.0	1	31.9268	27.5660	24.5245	19.3737	22.4765	24.6907	19.0121	18.3469
	2	57.8207	44.5619	42.4302	30.0795	40.8272	34.5453	26.8594	20.7791
	3	57.8207	54.8928	47.2974	35.6610	40.8272	50.5770	35.3261	32.4022
	4	83.2772	73.2417	67.0768	50.4085	61.8440	60.2352	47.6169	33.8587
	5	100.578	78.8692	77.5390	57.1147	76.2761	63.0436	49.5787	39.0614
	6	101.055	98.7322	87.0218	70.4435	76.2761	89.5665	70.2211	56.8515

Table 9.5: First six non-dimensional frequencies of square FG Al/Al_2O_3 plates with different power-law indices (k) and $k_w = 10^3$

k	Mode	CCCC	SCSC	SSSC	SCSF	SSSS	CCCF	SSSF	SFSF
0	1	47.9063	42.8737	39.4861	34.0730	37.2778	39.6681	33.7124	33.0570
	2	79.9212	63.2210	60.5834	45.7526	58.6116	51.0052	42.0764	35.5014
	3	79.9212	76.1987	66.6288	52.3399	58.6116	70.7436	51.9384	48.4652
	4	112.750	99.7324	91.7780	70.5316	85.0600	83.0022	67.0285	50.1878
	5	135.329	107.023	105.298	79.0221	103.661	86.5970	69.4880	56.4526
	6	135.953	132.914	117.625	96.1173	103.661	120.942	95.8303	78.6872
0.2	1	44.9347	40.2143	37.0368	31.9595	34.9655	37.2075	31.6213	31.0065
	2	74.9638	59.2995	56.8255	42.9146	54.9760	47.8414	39.4664	33.2992
	3	74.9638	71.4722	62.4959	49.0933	54.9760	66.3555	48.7167	45.4589
	4	105.756	93.5461	86.0851	66.1566	79.7838	77.8537	62.8708	47.0747
	5	126.935	100.385	98.7661	74.1204	97.2306	81.2255	65.1778	52.9509
	6	127.520	124.669	110.329	90.1553	97.2306	113.439	89.8860	73.8063
0.5	1	42.3012	37.8574	34.8661	30.0864	32.9163	35.0268	29.7680	29.1893
	2	70.5703	55.8241	53.4951	40.3995	51.7540	45.0375	37.1534	31.3477
	3	70.5703	67.2834	58.8332	46.2160	51.7540	62.4665	45.8615	42.7947
	4	99.5582	88.0636	81.0398	62.2793	75.1079	73.2908	59.1860	44.3157
	5	119.495	94.5013	92.9777	69.7764	91.5321	76.4650	61.3578	49.8476
	6	120.047	117.363	103.863	84.8715	91.5321	106.791	84.6180	69.4807
2.0	1	38.5631	34.5120	31.7851	27.4277	30.0075	31.9316	27.1375	26.6099
	2	64.3342	50.8910	48.7678	36.8295	47.1806	41.0576	33.8702	28.5775
	3	64.3342	61.3376	53.6342	42.1320	47.1806	56.9464	41.8088	39.0130
	4	90.7604	80.2816	73.8785	56.7758	68.4707	66.8142	53.9559	40.3996
	5	108.936	86.1503	84.7614	63.6104	83.4436	69.7079	55.9357	45.4427
	6	109.438	106.992	94.6843	77.3715	83.4436	97.3544	77.1404	63.3408
5.0	1	36.1006	32.3082	29.7554	25.6763	28.0913	29.8925	25.4046	24.9106
	2	60.2260	47.6413	45.6537	34.4777	44.1678	38.4358	31.7074	26.7527
	3	60.2260	57.4208	50.2093	39.4416	44.1678	53.3100	39.1390	36.5217
	4	84.9648	75.1551	69.1608	53.1503	64.0984	62.5477	50.5104	37.8198
	5	101.979	80.6491	79.3488	59.5484	78.1151	65.2566	52.3639	42.5408
	6	102.449	100.159	88.6381	72.4308	78.1152	91.1377	72.2145	59.2961

Table 9.6: First six non-dimensional frequencies of rectangular FG Al/Al_2O_3 plates with different aspect ratios (a/b) ($k = 1$, $k_w = 10^2$)

a/b	Mode	CCCC	SCSC	SSSC	SCSF	SSSS	CCCF	SSSF	SFSF
0.2	1	20.7627	20.7321	15.6302	8.9932	12.0249	9.0343	8.4668	8.3972
	2	21.3841	21.2588	16.2815	9.3446	12.7557	9.5239	8.7627	8.4873
	3	22.4924	22.2052	17.4385	10.1028	14.0462	10.5343	9.4642	8.6711
	4	24.1907	23.7516	19.2779	11.5935	16.1414	12.2821	10.9219	8.8727
	5	26.5785	26.0659	22.6105	14.2881	19.1048	14.9679	13.4316	9.5285
	6	31.5777	40.5201	37.8399	20.6689	34.4954	20.7133	15.8245	9.9816
0.5	1	22.2658	21.6744	16.7906	9.6603	13.3260	10.6336	9.0482	8.6252
	2	27.9957	25.7017	21.5436	13.5559	18.5680	16.9547	12.9055	10.1856
	3	38.4955	33.8600	30.6109	22.3779	28.1980	23.2617	17.8839	11.6512
	4	54.0218	47.8536	44.5146	22.5503	36.1849	28.3325	21.8417	15.9304
	5	54.3441	53.9696	45.3946	28.9923	42.2543	31.3795	24.7636	20.1590
	6	60.2336	58.7763	49.9323	37.4941	43.5406	43.8483	35.9169	23.6677
1.0	1	31.3411	25.7017	21.5435	13.5556	18.5679	21.7777	12.9053	11.6503
	2	62.1596	46.6969	44.1664	28.9868	42.2514	34.6134	24.7565	15.9289
	3	62.1596	58.7759	49.9217	35.9890	42.2514	53.7605	35.5771	31.9404
	4	91.2006	79.8117	72.7824	53.5640	66.7891	64.9405	50.2970	33.7616
	5	110.732	86.2050	84.6956	61.3448	83.2615	68.1656	52.5948	40.1281
	6	111.269	108.653	95.4373	76.6249	83.2615	98.3131	76.3713	61.0410
2.0	1	82.9221	46.6962	44.1655	35.9850	42.2506	76.5099	35.5731	33.7399
	2	107.163	79.8110	72.7629	53.5395	66.7845	87.8121	50.2696	40.1172
	3	150.514	130.148	118.536	86.9926	108.008	113.675	79.7449	59.9563
	4	213.629	143.201	142.039	134.001	141.045	157.191	127.755	96.6233
	5	214.933	173.656	169.578	136.714	165.863	208.012	133.838	132.082
	6	238.733	197.945	181.497	151.810	171.103	221.539	149.855	138.802

Table 9.7: First six non-dimensional frequencies of rectangular FG Al/Al_2O_3 plates with different aspect ratios (a/b) ($k = 1$, $k_w = 5 \times 10^2$)

a/b	Mode	CCCC	SCSC	SSSC	SCSF	SSSS	CCCF	SSSF	SFSF
0.2	1	26.6972	26.6734	22.9337	19.0402	20.6458	19.0596	18.7972	18.7660
	2	27.1833	27.0848	23.3824	19.2086	21.0798	19.2965	18.9324	18.8065
	3	28.0635	27.8338	24.2023	19.5887	21.8848	19.8147	19.2671	18.8902
	4	29.4422	29.0824	25.5595	20.3975	23.2851	20.7966	20.0235	18.9836
	5	31.4336	31.0013	28.1582	22.0409	25.4292	22.4875	21.4956	19.2987
	6	35.7604	43.8580	41.3945	26.6243	38.3612	26.6588	23.0665	19.5265
0.5	1	27.8822	27.4122	23.7397	19.3642	21.4297	19.8676	19.0662	18.8691
	2	32.6406	30.6958	27.3089	21.5734	25.0284	23.8561	21.1708	19.6315
	3	41.9947	37.7908	34.9095	27.9718	32.8143	28.6837	24.5251	20.4304
	4	56.5685	50.7111	47.5731	28.1099	39.8873	32.9299	27.5447	23.1393
	5	56.8765	56.5187	48.3975	33.4993	45.4651	35.5854	29.9147	26.2304
	6	62.5279	61.1253	52.6772	41.0786	46.6629	46.9502	39.6443	29.0140
1.0	1	35.5515	30.6957	27.3088	21.5732	25.0283	27.4939	21.1706	20.4299
	2	64.3853	49.6211	47.2475	33.4945	45.4624	38.4674	29.9088	23.1383
	3	64.3853	61.1250	52.6672	39.7097	45.4624	56.3191	39.3368	36.0810
	4	92.7319	81.5571	74.6922	56.1316	68.8653	67.0739	53.0230	37.7027
	5	111.997	87.8234	86.3423	63.5991	84.9360	70.2012	55.2075	43.4962
	6	112.528	109.942	96.9016	78.4412	84.9360	99.7352	78.1935	63.3060
2.0	1	84.6034	49.6204	47.2466	39.7061	45.4617	78.3289	39.3331	37.6833
	2	108.469	81.5564	74.6732	56.1082	68.8609	89.4015	52.9970	43.4861
	3	151.446	131.225	119.718	88.5966	109.305	114.908	81.4917	62.2608
	4	214.287	144.184	143.028	135.047	142.039	158.084	128.852	98.0699
	5	215.588	174.465	170.407	137.740	166.710	208.688	134.886	133.144
	6	239.322	198.655	182.271	152.735	171.924	222.173	150.792	139.813

Table 9.8: First six non-dimensional frequencies of rectangular FG Al/Al_2O_3 plates with different aspect ratios (a/b) ($k = 1$, $k_w = 10^3$)

a/b	Mode	CCCC	SCSC	SSSC	SCSF	SSSS	CCCF	SSSF	SFSF
0.2	1	32.6313	32.6118	29.6313	26.7318	27.8982	26.7457	26.5593	26.5372
	2	33.0302	32.9492	29.9800	26.8521	28.2209	26.9150	26.6551	26.5659
	3	33.7583	33.5676	30.6238	27.1253	28.8272	27.2889	26.8939	26.6252
	4	34.9128	34.6100	31.7073	27.7150	29.9042	28.0101	27.4409	26.6915
	5	36.6078	36.2374	33.8371	28.9458	31.6023	29.2874	28.5328	26.9166
	6	40.3840	47.7031	45.4485	32.5717	42.7042	32.5999	29.7343	27.0803
0.5	1	33.6077	33.2189	30.2595	26.9636	28.4832	27.3274	26.7504	26.6103
	2	37.6493	35.9763	33.1337	28.5915	31.2807	30.3509	28.2889	27.1562
	3	45.9959	42.1925	39.6325	33.6821	37.8000	34.2756	30.8795	27.7392
	4	59.5992	54.0711	51.1396	33.7968	44.0801	37.9004	33.3282	29.7908
	5	59.8915	59.5519	51.9074	38.3962	49.1848	40.2292	35.3122	32.2505
	6	65.2825	63.9403	55.9192	45.1610	50.2941	50.5607	43.8604	34.5525
1.0	1	40.1992	35.9762	33.1336	28.5914	31.2806	33.2863	28.2888	27.7388
	2	67.0636	53.0501	50.8369	38.3920	49.1823	42.7995	35.3072	29.7900
	3	67.0636	63.9400	55.9097	43.9195	49.1823	59.3625	43.5826	40.6682
	4	94.6111	83.6876	77.0129	59.1846	71.3757	69.6490	56.2450	42.1137
	5	113.558	89.8054	88.3575	66.3091	86.9838	72.6654	58.3089	47.3706
	6	114.081	111.531	98.7015	80.6541	86.9838	101.485	80.4133	66.0282
2.0	1	86.6591	53.0495	50.8360	43.9162	49.1816	80.5449	43.5793	42.0963
	2	110.080	83.6869	76.9945	59.1624	71.3715	91.3492	56.2205	47.3614
	3	152.604	132.559	121.179	90.5617	110.904	116.429	83.6239	65.0267
	4	215.107	145.396	144.253	136.345	143.273	159.194	130.211	99.8487
	5	216.403	175.471	171.437	139.013	167.763	209.530	136.185	134.459
	6	240.056	199.539	183.234	153.883	172.945	222.964	151.955	141.067

9.2 Winkler and Pasternak foundations

In this section, free vibration of thin FG Lévy plates resting on Winkler and Pasternak elastic foundations has been investigated. A simple power-law form mentioned in Eq. (2.1) is also assumed here to judge the variation of material properties of the FG constituents along thickness direction. The prime objective is to find the effect of different physical and geometrical parameters along with elastic foundations on free vibration characteristics of FG Lévy plates. Here also, new results of eigenfrequencies and their corresponding 3-D mode shapes are incorporated here after performing the test of convergence and validation of present results with the available literature in special cases.

9.2.1 Numerical modeling

The expressions of strain and kinetic energies of FG Lévy plate in presence of Winkler and Pasternak elastic foundations can be written as below

$$\mathbf{U} = \frac{1}{2}\int_{\Omega}\left[D_{11}\left\{\left(\frac{\partial^2 w}{\partial x^2}\right)^2+\left(\frac{\partial^2 w}{\partial y^2}\right)^2\right\}+2D_{12}\frac{\partial^2 w}{\partial x^2}\frac{\partial^2 w}{\partial y^2}+4D_{66}\left(\frac{\partial^2 w}{\partial x\partial y}\right)^2+ k_w w^2+k_p\left\{\left(\frac{\partial w}{\partial x}\right)^2+\left(\frac{\partial w}{\partial y}\right)^2\right\}\right]\mathrm{d}x\mathrm{d}y \tag{9.5}$$

$$\mathbf{T} = \frac{1}{2}\int_{\Omega} I_0\left(\frac{\partial w}{\partial t}\right)^2 \mathrm{d}x\mathrm{d}y \tag{9.6}$$

where k_w and k_p represent the Winkler and Pasternak foundation moduli respectively; the stiffness coefficients ($D_{ij};\ i,j=1,2,6$) are

$$(D_{11},D_{12},D_{66}) = \int_{-h/2}^{h/2}(Q_{11},Q_{12},Q_{66})z^2\,\mathrm{d}z$$

and inertial coefficient, $I_0 = \int_{-h/2}^{h/2}\rho(z)\,\mathrm{d}z$.

Assuming harmonic type displacement as $w(x,y,t) = W(x,y)\cos\omega t$; where $W(x,y)$ and ω are respective maximum deflection and natural frequency of free vibration. Accordingly, Eqs. (9.5) and (9.6) may be transformed into maximum strain energy ($\mathbf{U}_{max}$) and kinetic energy ($\mathbf{T}_{max}$) respectively as follows

$$\mathbf{U}_{max} = \frac{1}{2}\int_{\Omega}\left[D_{11}\left\{\left(\frac{\partial^2 W}{\partial x^2}\right)^2+\left(\frac{\partial^2 W}{\partial y^2}\right)^2\right\}+2D_{12}\frac{\partial^2 W}{\partial x^2}\frac{\partial^2 W}{\partial y^2}+4D_{66}\left(\frac{\partial^2 W}{\partial x\partial y}\right)^2+ k_w W^2+k_p\left\{\left(\frac{\partial W}{\partial x}\right)^2+\left(\frac{\partial W}{\partial y}\right)^2\right\}\right]\mathrm{d}x\mathrm{d}y$$

$$\mathbf{T}_{max} = \frac{\omega^2}{2}\int_{\Omega} I_0 W^2\,\mathrm{d}x\mathrm{d}y$$

Let us now consider the cartesian coordinates x and y as the non-dimensionalized parameters ($\xi = x/a$) and ($\eta = y/b$) respectively in natural coordinate system. Consequently, the expressions for maximum strain and kinetic energies can be written as

$$\mathbf{U}_{max} = \frac{D_c ab}{2}\int_{\Omega}\left[\overline{D}_{11}\left\{\left(\frac{\partial^2 W}{\partial\xi^2}\right)^2+\mu^4\left(\frac{\partial^2 W}{\partial\eta^2}\right)^2\right\}+2\overline{D}_{12}\mu^2\frac{\partial^2 W}{\partial\xi^2}\frac{\partial^2 W}{\partial\eta^2}+4\overline{D}_{66}\mu^2\left(\frac{\partial^2 W}{\partial\xi\partial\eta}\right)^2+ K_w W^2+K_p\left\{\left(\frac{\partial W}{\partial\xi}\right)^2+\mu^2\left(\frac{\partial W}{\partial\eta}\right)^2\right\}\right]\mathrm{d}\xi\mathrm{d}\eta \tag{9.7}$$

$$\mathbf{T}_{max} = \frac{\rho_c h\omega^2 ab}{2}\int_{\Omega} I_0 W^2\,\mathrm{d}\xi\mathrm{d}\eta \tag{9.8}$$

where the flexural rigidity $D_c = \frac{\rho_c h^3}{12(1-\nu^2)}$ and other components in Eqs. (9.7) and (9.8) are $\overline{D}_{11} = \frac{D_{11}}{D_c}$, $\overline{D}_{12} = \frac{D_{12}}{D_c}$, $\overline{D}_{66} = \frac{D_{66}}{D_c}$, $\mu = \frac{a}{b}$, $K_w = \frac{k_w a^4}{D_c}$ and $K_p = \frac{k_p a^2}{D_c}$.

The amplitude $W(\xi,\eta)$ may be expressed as the sum of series of simple algebraic polynomials involving both ξ and η as follows

$$W(\xi,\eta) = \sum_{i=1}^{n} c_i\varphi_i(\xi,\eta)$$

where c_i are unknown constants to be determined and $\varphi_i(\xi,\eta) = f\psi_i(\xi,\eta)$, $i = 1,2,\cdots,n$ are the admissible functions. Here, n is the number of polynomials involved in the admissible functions. The function $f = \xi^p\eta^q(1-\xi)^r(1-\eta)^s$ with the exponents p, q, r and s, controls various boundary conditions (BCs). The parameter $p = 0$, 1 or 2 according as the side $\xi = 0$ is free (F), simply supported (S) or clamped (C). Similar interpretations can be given to the parameters q, r and s corresponding to the sides $\eta = 0$, $\xi = 1$ and $\eta = 1$, respectively. The components of ψ_i will be generated from Pascal's triangle as given in Table 3.1.

Assuming constant Poisson's ratio (ν), the Rayleigh quotient (ω^2) can be obtained by equating $\mathbf{U}_{max}$ and $\mathbf{T}_{max}$ and differentiating this quotient partially with respect to unknown constants as follows

$$\frac{\partial\omega^2}{\partial c_i} = 0, \quad i = 1,2,\cdots,n \tag{9.9}$$

Further manipulation of Eq. (9.9) yields the generalized eigenvalue problem of the form

$$\sum_{j=1}^{n}(a_{ij}-\lambda^2 b_{ij})c_j = 0, \quad i = 1,2,\cdots,n \tag{9.10}$$

where

$$a_{ij} = \int_{\Omega}\left\{\left(\varphi_i^{\xi\xi}\varphi_j^{\xi\xi}+\mu^4\varphi_i^{\eta\eta}\varphi_j^{\eta\eta}\right)+2\nu\mu^2\left(\varphi_i^{\xi\xi}\varphi_j^{\eta\eta}+\varphi_i^{\eta\eta}\varphi_j^{\xi\xi}\right)+2(1-\nu)\mu^2\varphi_i^{\xi\eta}\varphi_j^{\xi\eta}\right.$$
$$\left.+K_w\varphi_i\varphi_j+K_p\left(\varphi_i^{\xi}\varphi_j^{\xi}+\mu^2\varphi_i^{\eta}\varphi_j^{\eta}\right)\right\}\mathrm{d}\xi\mathrm{d}\eta,$$

$$b_{ij}=\left\{\frac{(1-1/\rho_r)}{k+1}+\frac{1}{\rho_r}\right\}\int_{\Omega}\varphi_i\varphi_j\,\mathrm{d}\xi\mathrm{d}\eta,\quad \lambda^2=\frac{\omega^2a^4\rho_ch}{D_c}$$

with $=\left[12\left(1-\frac{1}{E_r}\right)\left\{\frac{1}{k+3}-\frac{1}{k+2}+\frac{1}{4(k+1)}\right\}+\frac{1}{E_r}\right]$, $E_r=E_c/E_m$ and $\rho_r=\rho_c/\rho_m$ are the ratios of Young's moduli and mass densities of FG constituents respectively and $D_c=E_ch^3/12(1-\nu^2)$ is meant for the flexural rigidity of the ceramic constituent of the plate. In the eigenvalue problem (Eq. (9.10)), λ and $c_j=[c_1,c_2,c_3,\cdots,c_n]^T$ refer to the non-dimensional frequency and the column vector of unknown constants respectively.

9.2.2 Convergence and comparison studies

We have considered six different BCs for the FG Lévy plates viz. SSSS, SCSS, SSSF, SCSC, SCSF and SFSF. Here, the flow of BCs is demonstrated in Fig. 9.1. For example, if we consider the edge support SCSF, then 1 is meant for simply supported (S) and accordingly 2, 3 and 4 represent clamped (C), simply supported (S), completely free (F) edge conditions respectively. In Fig. 9.1 for Lévy plates, 1 and 3 are always kept to be simply supported and other edges 2 and 4 vary as per different BCs.

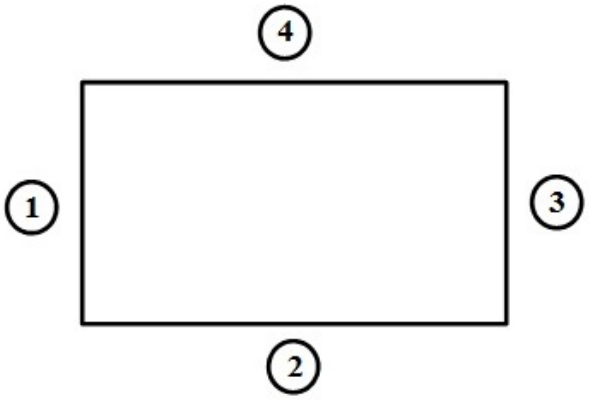

Figure 9.1: The flow of various combinations of boundary supports in FG Lévy plate

The convergence and comparison of first six non-dimensional frequencies of isotropic Lévy plates ($k=0$ in case of FG plates) has been performed in Table 9.9 with or without

two-parameter elastic foundations. The convergence of non-dimensional frequencies may be achieved by increasing the number of polynomials (n) in the displacement component and validation is carried out with (Leissa, 1973; Lam et al., 2000). From the validation, it may be noticed that present results are in excellent agreement with the available literature, irrespective of the elastic foundations and boundary support considered.

Table 9.9: Convergence and validation of first six non-dimensional frequencies of square isotropic Lévy plates with and without elastic foundations

Sides (1234)	K_w	K_p	Source	n	λ_1	λ_2	λ_3	λ_4	λ_5	λ_6
SSSS	0	0	Present	6	19.7449	58.9915	58.9915	92.5635	139.5994	139.9505
				10	19.7449	49.5132	49.5132	92.5635	139.5994	139.9505
				15	19.7392	49.5132	49.5132	79.4007	100.1729	100.1868
				21	19.7392	49.3490	49.3490	79.4007	100.1729	100.1868
				28	19.7392	49.3490	49.3490	78.9633	98.7193	98.7194
			Leissa (1973)		19.7392	49.3480	49.3480	78.9568	98.6960	98.6980
			Lam et al. (2000)		19.74	-	-	-	-	98.69
	100	100	Present	6	49.6374	93.7017	93.7017	130.6446	175.4651	175.8185
				10	49.6374	86.5505	86.5505	130.6446	175.4651	175.8185
				15	49.6342	86.5505	86.5505	119.6471	141.6475	141.6547
				21	49.6342	86.4300	86.4300	119.6471	141.6475	141.6547
				28	49.6342	86.4300	86.4300	119.2940	140.4129	140.4129
			Lam et al. (2000)		49.63	-	-	-	-	140.39
SCSS	0	0	Present	6	23.6839	59.3808	60.8613	112.9597	143.7141	188.3806
				10	23.6484	52.4178	59.0289	92.4408	117.2825	141.0695
				15	23.6465	51.8317	58.6604	87.4429	103.5119	115.9702
				21	23.6463	51.6878	58.6505	86.2451	101.8059	113.3767
				28	23.6463	51.6754	58.6464	86.1580	100.4370	113.2943
			Leissa (1973)		23.6463	51.6743	58.6464	86.1345	100.2698	113.2281
			Lam et al. (2000)		23.65	-	-	-	-	113.23
	100	100	Present	6	52.3986	93.9500	95.4994	150.0129	179.9075	222.0115
				10	52.3095	88.9811	93.7799	130.4488	154.9408	176.9928
				15	52.2900	88.3913	93.6491	126.3429	144.7836	154.5166
				21	52.2868	88.2490	93.6308	125.2959	143.1058	152.6885
				28	52.2864	88.2303	93.6250	125.2078	141.8965	152.6275
			Lam et al. (2000)		52.29	-	-	-	-	152.57
SSSF	0	0	Present	6	11.7425	29.7563	51.9222	69.7889	81.2621	133.4299
				10	11.6932	28.1215	41.5901	68.6699	76.9290	118.6152
				15	11.6851	27.8133	41.4342	60.0336	63.5644	92.3070
				21	11.6846	27.7575	41.2203	59.3603	62.4616	92.0709
				28	11.6845	27.7565	41.2019	59.1001	61.8756	90.4624
			Leissa (1973)		11.6845	27.7563	41.1967	59.0655	61.8606	90.2941
			Lam et al. (2000)		11.68	-	-	-	-	90.29
	100	100	Present	6	38.5174	67.2652	85.2154	111.2268	135.6676	168.5720
				10	38.4856	65.7311	77.8585	107.3175	122.1629	168.4878
				15	38.4767	65.0341	77.7426	100.5745	111.4925	133.6523
				21	38.4746	64.9238	77.6025	99.6789	108.4398	133.4568
				28	38.4742	64.9204	77.5879	99.4255	107.6855	132.1688
			Lam et al. (2000)		38.47	-	-	-	-	132.05

9.2.3 Results and discussions

One may see the generalized eigenvalue problem (Eq. (9.10)), the results related to free vibration characteristics of FG Lévy plates may be influenced by four different parameters viz. aspect ratio (μ), power-law index (k), ratio of Young's moduli (E_r) and ratio of mass densities (ρ_r). An exhaustive study of their effect on non-dimensional frequencies is carried out in the next sections. The number of polynomials involved in displacement component is taken up to 28 (as stated in (Leissa, 1973)) and four different cases of elastic foundations are also considered below.

(i) Case 1: $K_w = 0$ and $K_s = 0$;

(ii) Case 2: $K_w = 100$ and $K_s = 0$;

(iii) Case 3: $K_w = 0$ and $K_s = 100$;

(iv) Case 4: $K_w = 100$ and $K_s = 100$.

Effect of aspect ratio (μ)

The effect of aspect ratios (μ) on first six eigenfrequencies of FG Lévy plates may be observed in Tables 9.10 to 9.13 with above cases of elastic foundations along with different combination of boundary supports. In Tables 9.10 to 9.13, the ascending values of μ are 0.1, 0.2, 0.5, 1.0 and 2.0 and the power-law index (k) is assumed to be unity. We have considered here FG Al/Al_2O_3 plate and hence E_r and ρ_r are also taken accordingly, which will remain same for Tables 9.14 to 9.17. The important results in Tables 9.10 to 9.13 are summarized as below:

- $\mu = 1$ provides the eigenfrequencies of square FG plate and the remaining values of μ are for rectangular ones.
- Irrespective of the elastic foundations and edge support, it can easily be noticed that the non-dimensional frequencies follow the ascending behavior with increase in μ except only for a bit of fluctuations on fundamental frequencies in case of SFSF.
- It is also evident to say that the two-parameter elastic foundations (Case 4. effect of both Winkler and Pasternak foundations) yield higher values for the non-dimensional frequencies than other three cases. The least values for the frequencies are obtained for the FG plate without elastic foundation (Case 1).

Table 9.10: Effect of μ on first six non-dimensional frequencies of functionally graded Lévy plates; $K_w = 0$, $K_s = 0$, $k = 1$

BCs	μ	λ_1	λ_2	λ_3	λ_4	λ_5	λ_6
SSSS	0.1	8.2941	8.5406	8.9518	9.6184	10.4612	14.5537
	0.2	8.5405	9.5260	11.1694	13.6727	17.0187	33.1773
	0.5	10.2650	16.4242	26.6937	34.9018	41.0638	42.3643
	1.0	16.4240	41.0608	41.0608	65.7015	82.1395	82.1395
	2.0	41.0600	65.6969	106.7748	139.6073	164.2550	169.4571
SCSS	0.1	8.2984	8.5572	8.9876	9.5946	10.6647	12.1939
	0.2	8.5717	9.6444	11.4175	13.8934	17.8138	23.1721
	0.5	10.7489	17.9171	29.3106	35.1491	41.9858	44.9437
	1.0	19.6749	42.9966	48.7968	71.6878	83.5686	94.2665
	2.0	57.6836	78.7001	116.7609	173.3926	176.9454	195.2297
SSSF	0.1	8.2109	8.3773	8.7046	9.2544	10.2004	13.0633
	0.2	8.2420	8.8839	10.1516	12.1819	15.5865	27.2149
	0.5	8.5695	12.2867	19.6585	31.6011	33.1123	37.0897
	1.0	9.7221	23.0948	34.2820	49.1742	51.4836	75.2693
	2.0	13.4249	38.8897	62.6398	79.9821	92.4091	138.5145
SCSC	0.1	8.3022	8.5737	9.0214	9.6588	10.4828	12.4449
	0.2	8.6072	9.7772	11.6861	14.3366	17.7185	24.5630
	0.5	11.3872	19.6749	32.1956	35.4375	42.9978	49.0252
	1.0	24.0886	45.5497	57.6836	78.7005	85.0726	107.4157
	2.0	79.2632	96.3545	130.1092	186.8605	211.4559	230.7359
SCSF	0.1	8.2073	8.3858	8.7229	9.2483	10.4075	11.7653
	0.2	8.2458	8.9473	10.3151	12.3524	15.8423	20.7346
	0.5	8.6745	13.1081	21.4643	33.1526	33.8266	37.5752
	1.0	10.5565	27.5118	34.7022	52.4568	60.2561	75.5222
	2.0	18.9836	42.2273	82.2810	83.0180	110.0703	144.9403
SFSF	0.1	8.1935	8.2673	8.5023	9.0049	9.6974	12.8216
	0.2	8.1651	8.4425	9.3581	11.1318	13.6167	24.1242
	0.5	8.1011	9.7248	14.7165	23.8618	32.6761	34.3452
	1.0	8.0138	13.4254	30.5587	32.4266	38.9103	59.9520
	2.0	7.9148	22.8999	32.0601	53.7084	72.7003	87.7749

Table 9.11: Effect of μ on first six non-dimensional frequencies of functionally graded Lévy plate; $K_w = 100$, $K_s = 0$, $k = 1$

BCs	μ	λ_1	λ_2	λ_3	λ_4	λ_5	λ_6
SSSS	0.1	13.6278	13.7791	14.0377	14.4719	15.0453	18.1310
	0.2	13.7791	14.4107	15.5460	17.4317	20.1633	34.8949
	0.5	14.9095	19.6641	28.8006	36.5385	42.4636	43.7225
	1.0	19.6640	42.4607	42.4607	66.5853	82.8481	82.8482
	2.0	42.4600	66.5808	107.3209	140.0255	164.6106	169.8018
SCSS	0.1	13.6303	13.7894	14.0606	14.4561	15.1875	16.2977
	0.2	13.7985	14.4892	15.7252	17.6054	20.8388	25.5709
	0.5	15.2467	20.9271	31.2416	36.7748	43.3558	46.2261
	1.0	22.4505	44.3354	49.9805	72.4987	84.2653	94.8847
	2.0	58.6883	79.4394	117.2605	173.7294	177.2755	195.5289
SSSF	0.1	13.5772	13.6785	13.8814	14.2326	14.8651	16.9580
	0.2	13.5961	13.9945	14.8317	16.2887	18.9700	29.2844
	0.5	13.7971	16.3672	22.4361	33.3999	34.8332	38.6338
	1.0	14.5411	25.5008	35.9469	50.3490	52.6069	76.0420
	2.0	17.2381	40.3650	63.5663	80.7097	93.0396	138.9359
SCSC	0.1	13.6327	13.7997	14.0822	14.4988	15.0603	16.4863
	0.2	13.8205	14.5780	15.9213	17.9572	20.7574	26.8377
	0.5	15.7033	22.4505	33.9629	37.0505	44.3366	50.2035
	1.0	26.4042	46.8156	58.6884	79.4399	85.7571	107.9586
	2.0	79.9974	96.9594	130.5577	187.1731	211.7322	230.9892
SCSF	0.1	13.5751	13.6838	13.8929	14.2286	15.0080	15.9795
	0.2	13.5984	14.0349	14.9441	16.4166	19.1807	23.3847
	0.5	13.8626	16.9925	24.0341	34.8715	35.5129	39.1001
	1.0	15.1117	29.5605	36.3478	53.5597	61.2187	76.2924
	2.0	21.8472	43.5898	82.9885	83.7192	110.6002	145.3431
SFSF	0.1	13.5668	13.6114	13.7554	14.0717	14.5246	16.7725
	0.2	13.5496	13.7186	14.3002	15.5190	17.3878	26.4368
	0.5	13.5111	14.5429	18.2619	26.1975	34.4188	36.0072
	1.0	13.4590	17.2384	32.4154	34.1820	40.3848	60.9193
	2.0	13.4003	25.3245	33.8345	54.7861	73.5000	88.4384

Table 9.12: Effect of μ on first six non-dimensional frequencies of functionally graded Lévy plate; $K_w = 0$, $K_s = 100$, $k = 1$

BCs	μ	λ_1	λ_2	λ_3	λ_4	λ_5	λ_6
SSSS	0.1	35.1328	35.6803	36.5786	37.8866	39.5476	45.2362
	0.2	35.6803	37.8070	41.1607	45.7414	51.3987	71.0557
	0.5	39.3427	50.7713	66.8070	78.2470	86.3498	87.4718
	1.0	50.7712	86.3478	86.3478	116.3991	135.2312	135.2312
	2.0	86.3473	116.3958	162.4913	197.7575	223.7408	228.3980
SCSS	0.1	35.1382	35.7013	36.6242	37.8908	39.6978	41.9155
	0.2	35.7068	37.9072	41.3721	45.9035	51.8321	58.9640
	0.5	39.6641	51.8029	68.6912	78.4417	87.0805	89.2395
	1.0	52.9117	87.7742	92.0272	121.0661	136.4214	144.8406
	2.0	98.4973	126.3626	170.6411	226.2614	234.9829	250.3040
SSSF	0.1	34.9945	35.3613	36.0875	37.2107	39.0190	43.3038
	0.2	35.1312	36.5756	39.3390	43.3657	49.7031	64.0780
	0.5	36.0779	44.3190	58.1615	76.1261	76.5798	81.6040
	1.0	39.3039	66.3039	78.1248	98.6982	107.1168	128.0310
	2.0	50.4358	85.8271	128.8996	134.4314	156.6912	201.4463
SCSC	0.1	35.1413	35.7193	36.6508	37.9612	39.5691	42.0653
	0.2	35.7285	38.0023	41.5395	46.2400	51.7812	59.5769
	0.5	40.0155	52.9203	70.6625	78.6446	87.7875	92.2285
	1.0	55.4720	89.4729	98.4977	126.3643	137.5274	155.3614
	2.0	114.2046	139.4251	181.0151	243.2219	259.2071	281.1895
SCSF	0.1	34.9958	35.3768	36.1243	37.2331	38.9625	41.5248
	0.2	35.1379	36.6436	39.5053	43.5265	48.9661	58.1707
	0.5	36.1647	44.9787	59.6039	76.1796	78.1140	82.0454
	1.0	39.9676	70.0250	78.4995	101.4933	114.2805	128.3487
	2.0	54.9188	88.7469	136.5755	146.5920	172.6097	203.6114
SFSF	0.1	34.9485	35.1323	35.6796	36.6830	38.0944	46.8325
	0.2	34.9474	35.6776	37.8003	41.4416	46.4805	72.0597
	0.5	34.9429	39.3115	50.6117	68.1610	75.4416	78.1582
	1.0	34.9359	50.4453	75.3911	84.2015	85.8584	116.1225
	2.0	34.9230	75.2935	82.2905	112.3440	125.4598	160.0090

Table 9.13: Effect of μ on first six non-dimensional frequencies of functionally graded Lévy plate; $K_w = 100$, $K_s = 100$, $k = 1$

BCs	μ	λ_1	λ_2	λ_3	λ_4	λ_5	λ_6
SSSS	0.1	36.7592	37.2828	38.1434	39.3995	40.9993	46.5106
	0.2	37.2828	39.3229	42.5574	47.0021	52.5238	71.8737
	0.5	40.8016	51.9100	67.6764	78.9906	87.0242	88.1376
	1.0	51.9099	87.0222	87.0222	116.9003	135.6629	135.6629
	2.0	87.0217	116.8970	162.8507	198.0529	224.0019	228.6538
SCSS	0.1	36.7643	37.3029	38.1871	39.4035	41.1441	43.2878
	0.2	37.3082	39.4193	42.7618	47.1599	52.9480	59.9473
	0.5	41.1116	52.9194	69.5371	79.1835	87.7493	89.8922
	1.0	54.0053	88.4378	92.6603	121.5480	136.8493	145.2436
	2.0	99.0890	126.8244	170.9834	226.5196	235.2316	250.5374
SSSF	0.1	36.6270	36.9776	37.6727	38.7499	40.4896	44.6334
	0.2	36.7576	38.1405	40.7980	44.6935	50.8657	64.9840
	0.5	37.6635	45.6191	59.1581	76.8902	77.3395	82.3173
	1.0	40.7642	67.1798	78.8695	99.2887	107.6612	128.4868
	2.0	51.5819	86.5055	129.3523	134.8655	157.0638	201.7363
SCSC	0.1	36.7673	37.3201	38.2126	39.4712	41.0200	43.4329
	0.2	37.3289	39.5107	42.9238	47.4875	52.8982	60.5503
	0.5	41.4507	54.0137	71.4851	79.3845	88.4510	92.8602
	1.0	56.5161	90.1240	99.0895	126.8261	137.9518	155.7373
	2.0	114.7153	139.8438	181.3378	243.4621	259.4326	281.3973
SCSF	0.1	36.6283	36.9924	37.7080	38.7715	40.4351	42.9096
	0.2	36.7640	38.2057	40.9584	44.8495	50.1458	59.1672
	0.5	37.7466	46.2602	60.5768	76.9432	78.8589	82.7548
	1.0	41.4045	70.8549	79.2407	102.0677	114.7909	128.8034
	2.0	55.9732	89.4033	137.0029	146.9903	172.9481	203.8983
SFSF	0.1	36.5830	36.7587	37.2821	38.2436	39.5993	48.0646
	0.2	36.5820	37.2802	39.3165	42.8290	47.7217	72.8665
	0.5	36.5778	40.7716	51.7539	69.0134	76.2126	78.9026
	1.0	36.5711	51.5912	76.1626	84.8929	86.5366	116.6249
	2.0	36.5587	76.0659	82.9979	112.8632	125.9249	160.3740

Effect of power-law index (k)

The variation of first six non-dimensional frequencies of rectangular FG Al/Al_2O_3 plate with increasing values of power-law index (k = 0.1, 0.2, 0.5, 1.0, 2.0 and 5.0) is reported in Tables 9.14 to 9.17 subject to various edge supports. Looking into these computations, we may draw the following conclusions.

- Case 1: The non-dimensional frequencies follow descending pattern with the ascending values of k in the absence of elastic foundation.
- Case 2: In the presence of Winkler foundation, the eigenfrequencies are decreasing with the increasing values of k except SFSF FG plate. In SFSF FG plate, we may get fluctuations in the fundamental frequencies with ascending value of k.

- Cases 3 and 4: With the effect of both foundations, first six lowest frequencies of only SCSC FG Lévy plate follow descending behavior with increase in k, whereas these frequencies fluctuate randomly at different modes for remaining five combinations of boundary supports.

Table 9.14: Effect of k on first six non-dimensional frequencies of functionally graded Lévy plate; $K_w = 0$, $K_s = 0$, $\mu = 2.0$

BCs	k	λ_1	λ_2	λ_3	λ_4	λ_5	λ_6
SSSS	0.0	49.3480	78.9579	128.3273	167.7871	197.4100	203.6621
	0.1	47.5844	76.1360	123.7410	161.7906	190.3548	196.3835
	0.2	46.1705	73.8738	120.0643	156.9834	184.6988	190.5484
	0.5	43.3429	69.3495	112.7111	147.3691	173.3872	178.8785
	1.0	41.0600	65.6969	106.7748	139.6073	164.2550	169.4571
	2.0	39.2498	62.8005	102.0673	133.4523	157.0134	161.9861
	5.0	36.5961	58.5545	95.1665	124.4296	146.3977	151.0342
SCSS	0.0	69.3270	94.5857	140.3291	208.3919	212.6619	234.6369
	0.1	66.8494	91.2053	135.3139	200.9443	205.0617	226.2512
	0.2	64.8631	88.4954	131.2934	194.9736	198.9687	219.5286
	0.5	60.8906	83.0756	123.2525	183.0327	186.7831	206.0839
	1.0	57.6836	78.7001	116.7609	173.3926	176.9454	195.2297
	2.0	55.1404	75.2304	111.6132	165.7481	169.1443	186.6224
	5.0	51.4124	70.1440	104.0670	154.5418	157.7084	174.0048
SSSF	0.0	16.1348	46.7396	75.2837	96.1266	111.0619	166.4737
	0.1	15.5581	45.0692	72.5932	92.6911	107.0927	160.5241
	0.2	15.0959	43.7300	70.4362	89.9370	103.9106	155.7545
	0.5	14.1713	41.0518	66.1224	84.4289	97.5468	146.2155
	1.0	13.4249	38.8897	62.6398	79.9821	92.4091	138.5145
	2.0	12.8331	37.1751	59.8782	76.4559	88.3350	132.4077
	5.0	11.9654	34.6617	55.8298	71.2867	82.3626	123.4555
SCSC	0.0	95.2625	115.8037	156.3718	224.5784	254.1383	277.3101
	0.1	91.8580	111.6651	150.7833	216.5523	245.0558	267.3994
	0.2	89.1286	108.3472	146.3030	210.1179	237.7744	259.4542
	0.5	83.6700	101.7116	137.3429	197.2495	223.2122	243.5642
	1.0	79.2632	96.3545	130.1092	186.8605	211.4559	230.7359
	2.0	75.7687	92.1065	124.3730	178.6223	202.1332	220.5633
	5.0	70.6459	85.8791	115.9641	166.5455	188.4669	205.6509
SCSF	0.0	22.8155	50.7509	98.8895	99.7752	132.2880	174.1965
	0.1	22.0001	48.9371	95.3553	96.2094	127.5602	167.9710
	0.2	21.3464	47.4831	92.5220	93.3507	123.7701	162.9801
	0.5	20.0390	44.5750	86.8556	87.6336	116.1899	152.9986
	1.0	18.9836	42.2273	82.2810	83.0180	110.0703	144.9403
	2.0	18.1467	40.3656	78.6535	79.3579	105.2175	138.5502
	5.0	16.9198	37.6365	73.3357	73.9925	98.1038	129.1828
SFSF	0.0	9.5125	27.5223	38.5314	64.5495	87.3748	105.4923
	0.1	9.1725	26.5386	37.1544	62.2426	84.2522	101.7222
	0.2	8.9000	25.7501	36.0504	60.3931	81.7488	98.6997
	0.5	8.3549	24.1731	33.8425	56.6944	76.7422	92.6550
	1.0	7.9148	22.8999	32.0601	53.7084	72.7003	87.7749
	2.0	7.5659	21.8903	30.6466	51.3405	69.4951	83.9051
	5.0	7.0544	20.4103	28.5746	47.8694	64.7965	78.2323

Table 9.15: Effect of k on first six non-dimensional frequencies of functionally graded Lévy plate; $K_w = 100$, $K_s = 0$, $\mu = 2.0$

BCs	k	λ_1	λ_2	λ_3	λ_4	λ_5	λ_6
SSSS	0.0	50.3510	79.5886	128.7163	168.0849	197.6631	203.9075
	0.1	48.6516	76.8075	124.1553	162.1077	190.6244	196.6448
	0.2	47.2947	74.5815	120.5011	157.3176	184.9830	190.8239
	0.5	44.6014	70.1429	113.2011	147.7442	173.7060	179.1876
	1.0	42.4600	66.5808	107.3209	140.0255	164.6106	169.8018
	2.0	40.7978	63.7794	102.6725	133.9158	157.4075	162.3682
	5.0	38.3545	59.6693	95.8564	124.9581	146.8471	151.4699
SCSS	0.0	70.0445	95.1129	140.6850	208.6317	212.8969	234.8499
	0.1	67.6132	91.7666	135.6929	201.1997	205.3119	226.4781
	0.2	65.6680	89.0870	131.6929	195.2429	199.2325	219.7678
	0.5	61.7928	83.7391	123.7007	183.3348	187.0791	206.3523
	1.0	58.6883	79.4394	117.2605	173.7294	177.2755	195.5289
	2.0	56.2528	76.0494	112.1669	166.1214	169.5102	186.9541
	5.0	52.6785	71.0772	104.6982	154.9676	158.1257	174.3831
SSSF	0.0	18.9824	47.7974	75.9449	96.6453	111.5112	166.7737
	0.1	18.5677	46.1945	73.2971	93.2435	107.5711	160.8437
	0.2	18.2470	44.9153	71.1781	90.5192	104.4150	156.0914
	0.5	17.6495	42.3784	66.9541	85.0819	98.1124	146.5935
	1.0	17.2381	40.3650	63.5663	80.7097	93.0396	138.9359
	2.0	16.9883	38.8060	60.9041	77.2620	89.0336	132.8748
	5.0	16.5820	36.5133	56.9979	72.2051	83.1588	123.9882
SCSC	0.0	95.7859	116.2347	156.6912	224.8009	254.3350	277.4903
	0.1	92.4153	112.1240	151.1234	216.7893	245.2652	267.5914
	0.2	89.7161	108.8310	146.6617	210.3677	237.9953	259.6566
	0.5	84.3288	102.2542	137.7452	197.5298	223.4600	243.7913
	1.0	79.9974	96.9594	130.5577	187.1731	211.7322	230.9892
	2.0	76.5820	92.7767	124.8701	178.9688	202.4395	220.8440
	5.0	71.5726	86.6430	116.5309	166.9407	188.8163	205.9711
SCSF	0.0	24.9107	51.7267	99.3938	100.2751	132.6655	174.4833
	0.1	24.2220	49.9755	95.8923	96.7416	127.9622	168.2764
	0.2	23.6799	48.5769	93.0881	93.9118	124.1938	163.3021
	0.5	22.6328	45.7997	87.4905	88.2628	116.6652	153.3599
	1.0	21.8472	43.5898	82.9885	83.7192	110.6002	145.3431
	2.0	21.2888	41.8724	79.4373	80.1348	105.8048	138.9966
	5.0	20.4468	39.3484	74.2288	74.8778	98.7732	129.6919
SFSF	0.0	13.8017	29.2827	39.8079	65.3195	87.9452	105.9652
	0.1	13.6688	28.4078	38.5117	63.0622	84.8595	102.2257
	0.2	13.5749	27.7153	37.4793	61.2568	82.3889	99.2305
	0.5	13.4344	26.3632	35.4401	57.6623	77.4600	93.2503
	1.0	13.4003	25.3245	33.8345	54.7861	73.5000	88.4384
	2.0	13.4594	24.5581	32.6057	52.5334	70.3809	84.6403
	5.0	13.4743	23.4173	30.7945	49.2267	65.8056	79.0701

Table 9.16: Effect of k on first six non-dimensional frequencies of functionally graded Lévy plate; $K_w = 0$, $K_s = 100$, $\mu = 2.0$

BCs	k	λ_1	λ_2	λ_3	λ_4	λ_5	λ_6
SSSS	0.0	85.8489	118.8699	171.1696	211.9691	242.3022	248.0679
	0.1	85.6297	117.9228	168.7892	208.3461	237.7144	243.2437
	0.2	85.5375	117.2744	167.0240	205.6032	234.2092	239.5492
	0.5	85.6763	116.3971	164.0282	200.7185	227.8396	232.8018
	1.0	86.3473	116.3958	162.4913	197.7575	223.7408	228.3980
	2.0	87.4952	117.1653	162.2257	196.4692	221.6150	226.0303
	5.0	88.5604	117.6203	161.1430	193.8951	217.8246	221.8982
SCSS	0.0	101.4516	131.6475	181.5286	248.0430	256.2871	275.8023
	0.1	100.4857	130.0973	178.6782	242.8202	251.1163	269.7513
	0.2	99.8003	128.9680	176.5367	238.7928	247.1438	265.0702
	0.5	98.7658	127.1346	172.7887	231.3288	239.8394	256.3366
	1.0	98.4973	126.3626	170.6411	226.2614	234.9829	250.3040
	2.0	98.9015	126.5184	169.8865	223.2750	232.2528	246.6168
	5.0	98.9471	126.1281	168.1235	218.3189	227.6097	240.6269
SSSF	0.0	47.9790	84.9364	129.4577	138.7482	161.8780	215.6343
	0.1	48.3180	84.8068	128.9072	137.3613	160.2552	212.2227
	0.2	48.6327	84.7839	128.5743	136.3734	159.0903	209.6513
	0.5	49.4430	85.0546	128.3358	134.8653	157.2778	204.5658
	1.0	50.4358	85.8271	128.8996	134.4314	156.6912	201.4463
	2.0	51.6086	87.0530	130.1887	134.9396	157.1841	200.0365
	5.0	52.8471	88.2111	131.1729	134.9724	157.0511	197.2775
SCSC	0.0	122.0333	148.7463	194.9879	266.7988	289.5932	314.7085
	0.1	120.0267	146.3376	191.4857	261.1501	282.5636	306.9744
	0.2	118.5097	144.5212	188.8211	256.7931	277.0815	300.9378
	0.5	115.8172	141.3144	184.0225	248.7142	266.6846	289.4700
	1.0	114.2046	139.4251	181.0151	243.2219	259.2071	281.1895
	2.0	113.5313	138.6821	179.5647	239.9760	254.2645	275.6764
	5.0	112.1092	137.0636	176.8407	234.6105	246.5411	267.0991
SCSF	0.0	53.5455	88.5609	141.3757	151.1314	181.4436	218.8095
	0.1	53.6543	88.2819	139.8862	149.7278	179.0440	214.9737
	0.2	53.7845	88.1391	138.8161	148.7142	177.2572	212.0611
	0.5	54.2256	88.1696	137.1431	147.1207	174.2024	206.8394
	1.0	54.9188	88.7469	136.5755	146.5920	172.6097	203.6114
	2.0	55.8521	89.8166	136.9770	147.0113	172.2992	202.1171
	5.0	56.7508	90.7526	136.8566	146.7416	171.0121	199.2334
SFSF	0.0	32.8799	73.8986	78.7658	112.1846	128.7988	166.6219
	0.1	33.1855	73.9114	79.2369	111.8194	127.6431	164.6832
	0.2	33.4605	73.9932	79.6785	111.6280	126.8342	163.2700
	0.5	34.1371	74.4382	80.8350	111.6409	125.6606	160.9747
	1.0	34.9230	75.2935	82.2905	112.3440	125.4598	160.0090
	2.0	35.8198	76.5224	84.0428	113.6687	126.1135	160.2074
	5.0	36.7843	77.7333	85.8309	114.8076	126.3762	159.7007

Table 9.17: Effect of k on first six non-dimensional frequencies of functionally graded Lévy plate; $K_w = 100$, $K_s = 100$, $\mu = 2.0$

BCs	k	λ_1	λ_2	λ_3	λ_4	λ_5	λ_6
SSSS	0.0	86.4293	119.2898	171.4615	212.2049	242.5085	248.2694
	0.1	86.2273	118.3575	169.0931	208.5924	237.9303	243.4547
	0.2	86.1495	117.7215	167.3382	205.8586	234.4334	239.7684
	0.5	86.3198	116.8716	164.3653	200.9940	228.0824	233.0394
	1.0	87.0217	116.8970	162.8507	198.0529	224.0019	228.6538
	2.0	88.2005	117.6929	162.6072	196.7843	221.8944	226.3042
	5.0	89.3014	118.1792	161.5514	194.2346	218.1269	222.1950
SCSS	0.0	101.9432	132.0267	181.8038	248.2445	256.4821	275.9835
	0.1	100.9955	130.4915	178.9653	243.0316	251.3207	269.9416
	0.2	100.3253	129.3747	176.8340	239.0127	247.3563	265.2683
	0.5	99.3245	127.5691	173.1087	231.5679	240.0700	256.5524
	1.0	99.0890	126.8244	170.9834	226.5196	235.2316	250.5374
	2.0	99.5260	127.0071	170.2508	223.5523	232.5195	246.8679
	5.0	99.6108	126.6495	168.5149	218.6206	227.8990	240.9006
SSSF	0.0	49.0100	85.5230	129.8433	139.1081	162.1865	215.8660
	0.1	49.3693	85.4102	129.3050	137.7347	160.5753	212.4645
	0.2	49.7012	85.4013	128.9822	136.7581	159.4202	209.9017
	0.5	50.5498	85.7028	128.7663	135.2750	157.6293	204.8361
	1.0	51.5819	86.5055	129.3523	134.8655	157.0638	201.7363
	2.0	52.7954	87.7618	130.6637	135.3979	157.5778	200.3460
	5.0	54.0796	88.9550	131.6743	135.4597	157.4701	197.6112
SCSC	0.0	122.4424	149.0820	195.2442	266.9862	289.7658	314.8674
	0.1	120.4538	146.6881	191.7537	261.3467	282.7453	307.1416
	0.2	118.9522	144.8842	189.0991	256.9976	277.2711	301.1123
	0.5	116.2940	141.7055	184.3229	248.9366	266.8920	289.6611
	1.0	114.7153	139.8438	181.3378	243.4621	259.4326	281.3973
	2.0	114.0757	139.1281	179.9094	240.2340	254.5081	275.9010
	5.0	112.6955	137.5436	177.2129	234.8912	246.8082	267.3457
SCSF	0.0	54.4713	89.1237	141.7289	151.4618	181.7190	219.0379
	0.1	54.6030	88.8617	140.2528	150.0704	179.3305	215.2125
	0.2	54.7526	88.7331	139.1940	149.0670	177.5534	212.3087
	0.5	55.2367	88.7951	137.5461	147.4964	174.5197	207.1068
	1.0	55.9732	89.4033	137.0029	146.9903	172.9481	203.8983
	2.0	56.9506	90.5038	137.4286	147.4322	172.6584	202.4234
	5.0	57.9003	91.4759	137.3372	147.1900	171.3970	199.5638
SFSF	0.0	34.3670	74.5722	79.3981	112.6294	129.1865	166.9217
	0.1	34.6985	74.6029	79.8824	112.2777	128.0448	164.9947
	0.2	34.9953	74.6998	80.3351	112.0976	127.2477	163.5915
	0.5	35.7215	75.1779	81.5168	112.1355	126.1002	161.3181
	1.0	36.5587	76.0659	82.9979	112.8632	125.9249	160.3740
	2.0	37.5096	77.3278	84.7768	114.2125	126.6039	160.5936
	5.0	38.5341	78.5764	86.5952	115.3802	126.8966	160.1128

Effect of ratio of Young's moduli (E_r)

In this section, the effect of increase in E_r on first six lowest eigenfrequencies of FG plates subjected to different edge supports are evaluated in Tables 9.18 to 9.21. Ascending values of the ratios of Young's moduli (E_r) are taken as 0.1, 0.2, 0.5, 1.0, 2.0 and 5.0. The common

numerical factors assumed in these computations are: $k = 1$, $\mu = 2.0$ and $\rho_r = 1.5$. In these tabulations, it is evident that the eigenfrequencies are also decreasing with increase in E_r regardless of the elastic foundation and edge support assumed. This statement can be validated by looking into the expression of λ which is inversely proportional to E_c.

Table 9.18: Effect of E_r on first six non-dimensional frequencies of functionally graded Lévy plate; $K_w = 0$, $K_s = 0$, $k = 1$, $\mu = 2.0$ and $\rho_r = 1.5$

BCs	E_r	λ_1	λ_2	λ_3	λ_4	λ_5	λ_6
SSSS	0.1	126.7774	202.8464	329.6788	431.0529	507.1554	523.2174
	0.2	93.6313	149.8120	243.4839	318.3537	374.5591	386.4217
	0.5	66.2073	105.9331	172.1691	225.1100	264.8533	273.2414
	1.0	54.0580	86.4940	140.5755	183.8016	216.2518	223.1007
	2.0	46.8156	74.9060	121.7420	159.1768	187.2795	193.2108
	5.0	41.8732	66.9980	108.8893	142.3721	167.5079	172.8130
SCSS	0.1	178.1043	242.9951	360.5120	535.3685	546.3384	602.7930
	0.2	131.5388	179.4638	266.2558	395.3959	403.4976	445.1921
	0.5	93.0119	126.9000	188.2713	279.5871	285.3159	314.7984
	1.0	75.9439	103.6134	153.7229	228.2819	232.9595	257.0318
	2.0	65.7694	89.7319	133.1279	197.6979	201.7488	222.5961
	5.0	58.8259	80.2586	119.0732	176.8264	180.4496	199.0960
SSSF	0.1	41.4510	120.0761	193.4073	246.9536	285.3232	427.6786
	0.2	30.6136	88.6821	142.8408	182.3873	210.7251	315.8616
	0.5	21.6471	62.7077	101.0037	128.9673	149.0052	223.3479
	1.0	17.6748	51.2006	82.4691	105.3014	121.6622	182.3628
	2.0	15.3068	44.3410	71.4204	91.1937	105.3626	157.9308
	5.0	13.6908	39.6598	63.8803	81.5661	94.2391	141.2576
SCSC	0.1	244.7338	297.5052	401.7264	576.9524	652.8932	712.4225
	0.2	180.7479	219.7221	296.6946	426.1076	482.1936	526.1589
	0.5	127.8081	155.3670	209.7948	301.3035	340.9623	372.0505
	1.0	104.3548	126.8566	171.2967	246.0133	278.3946	303.7780
	2.0	90.3739	109.8611	148.3473	213.0538	241.0968	263.0795
	5.0	80.8329	98.2627	132.6859	190.5611	215.6435	235.3054
SCSF	0.1	58.6140	130.3815	254.0517	256.3271	339.8541	447.5190
	0.2	43.2893	96.2931	187.6296	189.3101	250.9989	330.5147
	0.5	30.6102	68.0895	132.6742	133.8625	177.4830	233.7092
	1.0	24.9931	55.5948	108.3280	109.2982	144.9143	190.8228
	2.0	21.6446	48.1465	93.8148	94.6551	125.4995	165.2573
	5.0	19.3596	43.0636	83.9105	84.6621	112.2501	147.8107
SFSF	0.1	58.6140	130.3815	254.0517	256.3271	339.8541	447.5190
	0.2	43.2893	96.2931	187.6296	189.3101	250.9989	330.5147
	0.5	30.6102	68.0895	132.6742	133.8625	177.4830	233.7092
	1.0	24.9931	55.5948	108.3280	109.2982	144.9143	190.8228
	2.0	21.6446	48.1465	93.8148	94.6551	125.4995	165.2573
	5.0	19.3596	43.0636	83.9105	84.6621	112.2501	147.8107

Table 9.19: Effect of E_r on first six non-dimensional frequencies of functionally graded Lévy plate; $K_w = 100$, $K_s = 0$, $k = 1$, $\mu = 2.0$ and $\rho_r = 1.5$

BCs	E_r	λ_1	λ_2	λ_3	λ_4	λ_5	λ_6
SSSS	0.1	127.2498	203.1420	329.8607	431.1921	507.2737	523.3321
	0.2	94.2699	150.2120	243.7302	318.5421	374.7193	386.5769
	0.5	67.1074	106.4980	172.5173	225.3764	265.0797	273.4609
	1.0	55.1568	87.1849	141.0017	184.1277	216.5291	223.3694
	2.0	48.0802	75.7028	122.2338	159.5533	187.5997	193.5211
	5.0	43.2824	67.8876	109.4389	142.7929	167.8657	173.1599
SCSS	0.1	178.4409	243.2419	360.6784	535.4806	546.4482	602.8925
	0.2	131.9941	179.7978	266.4810	395.5476	403.6463	445.3269
	0.5	93.6548	127.3720	188.5897	279.8016	285.5261	314.9889
	1.0	76.7299	104.1909	154.1127	228.5446	233.2169	257.2651
	2.0	66.6754	90.3981	133.5778	198.0012	202.0460	222.8654
	5.0	59.8372	81.0028	119.5760	177.1654	180.7818	199.3971
SSSF	0.1	42.8741	120.5748	193.7173	247.1964	285.5334	427.8189
	0.2	32.5145	89.3561	143.2602	182.7160	211.0097	316.0515
	0.5	24.2610	63.6573	101.5960	129.4317	149.4073	223.6163
	1.0	20.7942	52.3594	83.1935	105.8696	122.1544	182.6915
	2.0	18.8228	45.6742	72.2556	91.8492	105.9305	158.3102
	5.0	17.5339	41.1449	64.8128	82.2984	94.8737	141.6817
SCSC	0.1	244.9788	297.7068	401.8757	577.0563	652.9851	712.5067
	0.2	181.0795	219.9950	296.8967	426.2483	482.3180	526.2729
	0.5	128.2767	155.7527	210.0806	301.5026	341.1383	372.2118
	1.0	104.9282	127.3287	171.6466	246.2571	278.6100	303.9754
	2.0	91.0354	110.4059	148.7512	213.3352	241.3455	263.3074
	5.0	81.5718	98.8715	133.1373	190.8757	215.9216	235.5603
SCSF	0.1	59.6288	130.8408	254.2878	256.5611	340.0306	447.6531
	0.2	44.6538	96.9142	187.9492	189.6268	251.2378	330.6962
	0.5	32.5113	68.9651	133.1257	134.3099	177.8208	233.9658
	1.0	27.2884	56.6638	108.8805	109.8458	145.3277	191.1369
	2.0	24.2588	49.3770	94.4522	95.2868	125.9766	165.6200
	5.0	22.2439	44.4350	84.6226	85.3678	112.7834	148.2160
SFSF	0.1	26.7808	71.5495	99.5933	166.1920	224.7372	271.2360
	0.2	21.1129	53.3564	73.9244	122.9629	166.1436	200.4571
	0.5	16.8189	38.5156	52.8432	87.2923	117.7364	141.9561
	1.0	15.1190	32.0776	43.6074	71.5539	96.3392	116.0791
	2.0	14.1929	28.3148	38.1602	62.2091	83.6118	100.6765
	5.0	13.6070	25.7950	34.4814	55.8567	74.9449	90.1810

Table 9.20: Effect of E_r on first six non-dimensional frequencies of functionally graded Lévy plate; $K_w = 0$, $K_s = 100$, $k = 1$, $\mu = 2.0$ and $\rho_r = 1.5$

BCs	E_r	λ_1	λ_2	λ_3	λ_4	λ_5	λ_6
SSSS	0.1	148.3046	224.9923	352.2577	453.8069	529.9946	545.7410
	0.2	121.1965	178.6575	273.2797	348.5443	404.9471	416.4102
	0.5	101.5144	143.8634	212.2253	266.0989	306.3248	314.2202
	1.0	94.0427	130.2154	187.5069	232.2006	265.4288	271.7448
	2.0	90.0748	122.8241	173.8346	213.2401	242.4072	247.7895
	5.0	87.6078	118.1676	165.0886	201.0072	227.4786	232.2316
SCSS	0.1	195.8818	262.9715	381.9812	555.3139	568.3775	623.3883
	0.2	154.7164	205.6821	294.6645	422.0020	432.8674	472.6970
	0.5	123.5256	161.8095	226.6480	316.0729	325.5175	352.6027
	1.0	111.1346	144.2126	198.8546	271.7175	280.7484	302.1262
	2.0	104.3448	134.5281	183.3728	246.5493	255.4322	273.4016
	5.0	100.0188	128.3486	173.4123	230.1171	238.9537	254.6044
SSSF	0.1	65.2474	143.2746	226.4470	270.3026	313.7477	453.5410
	0.2	58.7112	118.1245	184.7873	212.9012	247.6833	350.0076
	0.5	54.2235	99.9458	153.9574	169.3122	197.4346	269.2877
	1.0	52.5583	93.0431	141.8138	151.9911	177.3284	236.2155
	2.0	51.6753	89.3661	135.1222	142.5219	166.2347	217.3742
	5.0	51.1246	87.0718	130.8186	136.5127	159.1249	204.7653
SCSC	0.1	258.7179	314.6684	421.5475	598.1576	670.4406	730.8851
	0.2	199.2441	242.4356	323.0150	454.4025	505.6825	550.8858
	0.5	152.7695	186.0532	245.5806	340.1298	373.3945	406.2282
	1.0	133.6808	162.9434	213.5986	292.2635	317.2334	344.7459
	2.0	122.9905	150.0321	195.6408	265.1012	285.0051	309.4343
	5.0	116.0740	141.7006	184.0142	247.3701	263.7620	286.1445
SCSF	0.1	80.7628	153.2430	277.3079	286.3158	366.8961	470.5321
	0.2	69.8605	125.3532	218.0289	227.9098	286.3263	361.0374
	0.5	61.8571	104.9130	172.8815	183.5186	224.1118	275.1201
	1.0	58.6562	97.0137	154.8693	165.5561	198.7615	239.6938
	2.0	56.8652	92.7463	144.9891	155.4657	184.5732	219.8247
	5.0	55.7004	90.0521	138.7004	148.8699	175.3683	206.9722
SFSF	0.1	42.3159	108.6547	120.7989	194.4692	247.3163	312.9922
	0.2	38.9570	97.2947	100.6592	158.9574	195.5870	253.8024
	0.5	36.7798	86.3155	89.3660	132.9477	156.5195	204.6414
	1.0	36.0181	80.9519	86.2836	122.8921	141.0921	182.5251
	2.0	35.6288	78.1232	84.5595	117.4475	132.6958	170.3267
	5.0	35.3921	76.3712	83.4284	113.9987	127.3857	162.5233

Table 9.21: Effect of E_r on first six non-dimensional frequencies of functionally graded Lévy plate; $K_w = 100$, $K_s = 100$, $k = 1$, $\mu = 2.0$ and $\rho_r = 1.5$

BCs	E_r	λ_1	λ_2	λ_3	λ_4	λ_5	λ_6
SSSS	0.1	148.7087	225.2588	352.4280	453.9391	530.1078	545.8510
	0.2	121.6905	178.9930	273.4992	348.7164	405.0952	416.5543
	0.5	102.1037	144.2798	212.5079	266.3243	306.5206	314.4111
	1.0	94.6786	130.6754	187.8267	232.4588	265.6548	271.9655
	2.0	90.7385	123.3116	174.1794	213.5213	242.6546	248.0315
	5.0	88.2900	118.6742	165.4517	201.3055	227.7422	232.4898
SCSS	0.1	196.1879	263.1995	382.1383	555.4219	568.4830	623.4845
	0.2	155.1037	205.9736	294.8680	422.1441	433.0060	472.8239
	0.5	124.0104	162.1799	226.9125	316.2627	325.7018	352.7728
	1.0	111.6732	144.6280	199.1561	271.9382	280.9621	302.3248
	2.0	104.9183	134.9734	183.6997	246.7925	255.6670	273.6209
	5.0	100.6169	128.8152	173.7579	230.3777	239.2047	254.8399
SSSF	0.1	66.1606	143.6928	226.7119	270.5245	313.9389	453.6732
	0.2	59.7244	118.6314	185.1117	213.1828	247.9254	350.1790
	0.5	55.3189	100.5444	154.3466	169.6662	197.7382	269.5104
	1.0	53.6878	93.6858	142.2362	152.3853	177.6664	236.4694
	2.0	52.8237	90.0350	135.5655	142.9423	166.5952	217.6501
	5.0	52.2850	87.7582	131.2764	136.9515	159.5016	205.0581
SCSC	0.1	258.9497	314.8591	421.6898	598.2579	670.5301	730.9672
	0.2	199.5450	242.6829	323.2007	454.5346	505.8012	550.9948
	0.5	153.1617	186.3754	245.8248	340.3062	373.5551	406.3759
	1.0	134.1289	163.3112	213.8793	292.4687	317.4225	344.9199
	2.0	123.4774	150.4315	195.9472	265.3274	285.2155	309.6282
	5.0	116.5898	142.1234	184.3400	247.6126	263.9894	286.3541
SCSF	0.1	81.5024	153.6340	277.5241	286.5253	367.0596	470.6596
	0.2	70.7141	125.8310	218.3040	228.1729	286.5358	361.2035
	0.5	62.8196	105.4833	173.2282	183.8452	224.3794	275.3381
	1.0	59.6703	97.6302	155.2563	165.9181	199.0632	239.9440
	2.0	57.9107	93.3909	145.4023	155.8512	184.8980	220.0975
	5.0	56.7674	90.7160	139.1323	149.2724	175.7101	207.2619
SFSF	0.1	43.7108	109.2055	121.2945	194.7775	247.5588	313.1839
	0.2	40.4679	97.9095	101.2535	159.3344	195.8936	254.0387
	0.5	38.3764	87.0079	90.0349	133.3982	156.9023	204.9344
	1.0	37.6471	81.6897	86.9762	123.3794	141.5167	182.8535
	2.0	37.2748	78.8875	85.2661	117.9573	133.1472	170.6786
	5.0	37.0486	77.1528	84.1445	114.5238	127.8558	162.8920

Effect of ratio of mass densities (ρ_r)

The expression of λ conveys that the non-dimensional frequency is directly proportional to ρ_r. As such, first six non-dimensional frequencies of FG Lévy plate with different values of ρ_r are incorporated in Tables 9.22 to 9.25. Increasing values of ρ_r are 0.1, 0.2, 0.5, 1.0 and 2.0 in these computations. Other major components supposed in these tabulations are: $k = 1$, $\mu = 2.0$ and $E_r = 3.0$. Irrespective of elastic foundation and edge condition, it can easily be noted that the non-dimensional frequencies are following ascending behavior with increasing values of ρ_r.

Table 9.22: Effect of ρ_r on first six non-dimensional frequencies of functionally graded Lévy plate; $K_w = 0$, $K_s = 0$, $k = 1$, $\mu = 2.0$ and $E_r = 3.0$

BCs	ρ_r	λ_1	λ_2	λ_3	λ_4	λ_5	λ_6
SSSS	0.1	17.1808	27.4896	44.6778	58.4160	68.7293	70.9060
	0.2	23.2629	37.2211	60.4941	79.0956	93.0600	96.0072
	0.5	32.8987	52.6386	85.5515	111.8581	131.6067	135.7747
	1.0	40.2925	64.4688	104.7788	136.9976	161.1846	166.2894
	2.0	46.5258	74.4422	120.9881	158.1912	186.1199	192.0145
	5.0	52.0174	83.2289	135.2688	176.8632	208.0884	214.6787
SCSS	0.1	24.1366	32.9305	48.8563	72.5528	74.0394	81.6901
	0.2	32.6811	44.5881	66.1518	98.2369	100.2498	110.6089
	0.5	46.2180	63.0571	93.5527	138.9279	141.7746	156.4246
	1.0	56.6053	77.2289	114.5782	170.1513	173.6377	191.5802
	2.0	65.3621	89.1763	132.3036	196.4738	200.4996	221.2177
	5.0	73.0771	99.7021	147.9199	219.6644	224.1653	247.3290
SSSF	0.1	5.6174	16.2726	26.2104	33.4670	38.6668	57.9587
	0.2	7.6060	22.0332	35.4891	45.3145	52.3551	78.4764
	0.5	10.7565	31.1597	50.1891	64.0844	74.0413	110.9824
	1.0	13.1740	38.1627	61.4689	78.4870	90.6817	135.9252
	2.0	15.2120	44.0665	70.9781	90.6290	104.7102	156.9529
	5.0	17.0075	49.2678	79.3560	101.3263	117.0695	175.4787
SCSC	0.1	33.1661	40.3177	54.4417	78.1882	88.4796	96.5470
	0.2	44.9072	54.5904	73.7144	105.8673	119.8020	130.7252
	0.5	63.5083	77.2025	104.2479	149.7189	169.4255	184.8734
	1.0	77.7815	94.5534	127.6770	183.3675	207.5031	226.4227
	2.0	89.8144	109.1808	147.4287	211.7345	239.6039	261.4505
	5.0	100.4155	122.0679	164.8303	236.7264	267.8853	292.3105
SCSF	0.1	7.9433	17.6692	34.4289	34.7373	46.0568	60.6475
	0.2	10.7553	23.9242	46.6170	47.0345	62.3612	82.1170
	0.5	15.2103	33.8339	65.9263	66.5168	88.1920	116.1310
	1.0	18.6287	41.4379	80.7429	81.4661	108.0127	142.2309
	2.0	21.5106	47.8484	93.2339	94.0689	124.7224	164.2341
	5.0	24.0496	53.4962	104.2387	105.1723	139.4438	183.6193
SFSF	0.1	3.3118	9.5820	13.4149	22.4732	30.4200	36.7277
	0.2	4.4842	12.9741	18.1639	30.4289	41.1889	49.7296
	0.5	6.3416	18.3482	25.6876	43.0330	58.2499	70.3282
	1.0	7.7669	22.4718	31.4608	52.7044	71.3413	86.1341
	2.0	8.9684	25.9482	36.3278	60.8578	82.3778	99.4591
	5.0	10.0270	29.0110	40.6157	68.0411	92.1012	111.1987

Table 9.23: Effect of ρ_r on first six non-dimensional frequencies of functionally graded Lévy plate; $K_w = 100$, $K_s = 0$, $k = 1$, $\mu = 2.0$ and $E_r = 3.0$

BCs	ρ_r	λ_1	λ_2	λ_3	λ_4	λ_5	λ_6
SSSS	0.1	17.7020	27.8183	44.8808	58.5714	68.8615	71.0341
	0.2	23.9686	37.6662	60.7689	79.3060	93.2389	96.1807
	0.5	33.8968	53.2681	85.9403	112.1557	131.8597	136.0200
	1.0	41.5149	65.2398	105.2549	137.3621	161.4945	166.5898
	2.0	47.9372	75.3324	121.5379	158.6121	186.4778	192.3614
	5.0	53.5955	84.2242	135.8835	177.3337	208.4885	215.0665
SCSS	0.1	24.5103	33.2054	49.0421	72.6779	74.1621	81.8013
	0.2	33.1871	44.9604	66.4033	98.4064	100.4159	110.7595
	0.5	46.9337	63.5836	93.9084	139.1677	142.0095	156.6375
	1.0	57.4818	77.8736	115.0138	170.4449	173.9254	191.8410
	2.0	66.3743	89.9207	132.8065	196.8128	200.8318	221.5189
	5.0	74.2087	100.5344	148.4822	220.0434	224.5368	247.6657
SSSF	0.1	7.0525	16.8220	26.5550	33.7375	38.9012	58.1153
	0.2	9.5491	22.7771	35.9556	45.6808	52.6725	78.6885
	0.5	13.5044	32.2117	50.8489	64.6024	74.4901	111.2824
	1.0	16.5395	39.4511	62.2770	79.1215	91.2314	136.2925
	2.0	19.0981	45.5542	71.9113	91.3616	105.3449	157.3771
	5.0	21.3524	50.9312	80.3992	102.1454	117.7792	175.9529
SCSC	0.1	33.4391	40.5425	54.6084	78.3043	88.5823	96.6411
	0.2	45.2768	54.8949	73.9401	106.0246	119.9410	130.8527
	0.5	64.0311	77.6331	104.5671	149.9414	169.6222	185.0536
	1.0	78.4217	95.0807	128.0680	183.6400	207.7439	226.6435
	2.0	90.5536	109.7897	147.8802	212.0492	239.8820	261.7053
	5.0	101.2420	122.7486	165.3351	237.0782	268.1962	292.5955
SCSF	0.1	9.0154	18.1764	34.6920	34.9980	46.2537	60.7972
	0.2	12.2070	24.6110	46.9731	47.3875	62.6279	82.3197
	0.5	17.2633	34.8052	66.4300	67.0160	88.5692	116.4177
	1.0	21.1431	42.6275	81.3598	82.0776	108.4747	142.5820
	2.0	24.4139	49.2220	93.9462	94.7750	125.2557	164.6395
	5.0	27.2956	55.0319	105.0351	105.9617	140.0402	184.0726
SFSF	0.1	5.3991	10.4879	14.0763	22.8742	30.7174	36.9744
	0.2	7.3104	14.2007	19.0594	30.9718	41.5916	50.0636
	0.5	10.3384	20.0829	26.9540	43.8007	58.8194	70.8006
	1.0	12.6619	24.5964	33.0118	53.6447	72.0387	86.7127
	2.0	14.6207	28.4015	38.1188	61.9436	83.1831	100.1272
	5.0	16.3465	31.7538	42.6181	69.2550	93.0016	111.9456

Table 9.24: Effect of ρ_r on first six non-dimensional frequencies of functionally graded Lévy plate; $K_w = 0$, $K_s = 100$, $k = 1$, $\mu = 2.0$ and $E_r = 3.0$

BCs	ρ_r	λ_1	λ_2	λ_3	λ_4	λ_5	λ_6
SSSS	0.1	34.5314	46.8109	65.7955	80.3931	91.1743	93.1362
	0.2	46.7557	63.3823	89.0875	108.8527	123.4506	126.1071
	0.5	66.1225	89.6361	125.9887	153.9410	174.5855	178.3423
	1.0	80.9833	109.7813	154.3040	188.5384	213.8227	218.4239
	2.0	93.5114	126.7645	178.1750	217.7054	246.9012	252.2141
	5.0	104.5489	141.7270	199.2057	243.4021	276.0439	281.9840
SCSS	0.1	39.6910	51.0436	69.2511	92.4711	95.9166	102.4217
	0.2	53.7419	69.1134	93.7664	125.2064	129.8717	138.6796
	0.5	76.0025	97.7411	132.6057	177.0686	183.6663	196.1226
	1.0	93.0837	119.7079	162.4081	216.8639	224.9443	240.2001
	2.0	107.4837	138.2267	187.5328	250.4129	259.7434	277.3592
	5.0	120.1705	154.5422	209.6680	279.9701	290.4019	310.0970
SSSF	0.1	19.9963	34.2930	51.6779	54.1901	63.1881	81.9230
	0.2	27.0752	46.4330	69.9722	73.3738	85.5570	110.9243
	0.5	38.2901	65.6661	98.9557	103.7662	120.9959	156.8706
	1.0	46.8956	80.4243	121.1955	127.0871	148.1891	192.1265
	2.0	54.1503	92.8659	139.9445	146.7476	171.1141	221.8485
	5.0	60.5419	103.8273	156.4627	164.0688	191.3114	248.0342
SCSC	0.1	46.3991	56.6222	73.6738	99.4156	106.4248	115.4996
	0.2	62.8247	76.6669	99.7548	134.6094	144.0998	156.3872
	0.5	88.8476	108.4233	141.0746	190.3665	203.7879	221.1648
	1.0	108.8156	132.7909	172.7804	233.1504	249.5882	270.8705
	2.0	125.6494	153.3337	199.5096	269.2188	288.1997	312.7743
	5.0	140.4803	171.4323	223.0585	300.9958	322.2170	349.6923
SCSF	0.1	21.8867	35.5243	55.0915	59.1123	69.8838	82.8255
	0.2	29.6348	48.1001	74.5942	80.0385	94.6231	112.1462
	0.5	41.9099	68.0238	105.4922	113.1915	133.8173	158.5987
	1.0	51.3289	83.3118	129.2010	138.6307	163.8921	194.2429
	2.0	59.2695	96.2002	149.1885	160.0769	189.2463	224.2924
	5.0	66.2653	107.5551	166.7978	178.9714	211.5838	250.7665
SFSF	0.1	13.8174	30.0327	32.6745	44.9782	50.5142	64.6319
	0.2	18.7089	40.6644	44.2414	60.9007	68.3966	87.5120
	0.5	26.4583	57.5082	62.5668	86.1266	96.7274	123.7607
	1.0	32.4047	70.4328	76.6284	105.4831	118.4663	151.5753
	2.0	37.4178	81.3288	88.4828	121.8014	136.7931	175.0240
	5.0	41.8343	90.9284	98.9268	136.1781	152.9394	195.6828

Table 9.25: Effect of ρ_r on first six non-dimensional frequencies of functionally graded Lévy plate; $K_w = 100$, $K_s = 100$, $k = 1$, $\mu = 2.0$ and $E_r = 3.0$

BCs	ρ_r	λ_1	λ_2	λ_3	λ_4	λ_5	λ_6
SSSS	0.1	34.7936	47.0047	65.9335	80.5061	91.2739	93.2338
	0.2	47.1108	63.6447	89.2744	109.0057	123.5855	126.2392
	0.5	66.6248	90.0072	126.2530	154.1574	174.7763	178.5291
	1.0	81.5983	110.2358	154.6277	188.8035	214.0564	218.6526
	2.0	94.2216	127.2893	178.5487	218.0115	247.1710	252.4783
	5.0	105.3430	142.3138	199.6236	243.7442	276.3456	282.2794
SCSS	0.1	39.9194	51.2214	69.3822	92.5693	96.0113	102.5104
	0.2	54.0511	69.3541	93.9440	125.3395	129.9999	138.7997
	0.5	76.4398	98.0815	132.8568	177.2568	183.8477	196.2925
	1.0	93.6193	120.1248	162.7157	217.0943	225.1665	240.4082
	2.0	108.1022	138.7082	187.8879	250.6790	259.9999	277.5995
	5.0	120.8620	155.0805	210.0651	280.2676	290.6887	310.3656
SSSF	0.1	20.4459	34.5571	51.8535	54.3576	63.3318	82.0339
	0.2	27.6839	46.7905	70.2100	73.6006	85.7516	111.0744
	0.5	39.1509	66.1718	99.2920	104.0869	121.2711	157.0829
	1.0	47.9499	81.0436	121.6073	127.4800	148.5262	192.3865
	2.0	55.3678	93.5811	140.4201	147.2012	171.5032	222.1488
	5.0	61.9031	104.6268	156.9944	164.5759	191.7465	248.3699
SCSC	0.1	46.5946	56.7826	73.7971	99.5071	106.5102	115.5782
	0.2	63.0894	76.8840	99.9217	134.7332	144.2154	156.4937
	0.5	89.2220	108.7303	141.3107	190.5415	203.9514	221.3155
	1.0	109.2741	133.1669	173.0695	233.3647	249.7885	271.0550
	2.0	126.1789	153.7679	199.8434	269.4664	288.4309	312.9874
	5.0	141.0723	171.9178	223.4318	301.2726	322.4755	349.9305
SCSF	0.1	22.2982	35.7793	55.2563	59.2659	70.0138	82.9351
	0.2	30.1919	48.4454	74.8173	80.2464	94.7991	112.2947
	0.5	42.6978	68.5121	105.8077	113.4856	134.0662	158.8087
	1.0	52.2939	83.9098	129.5874	138.9909	164.1969	194.5001
	2.0	60.3839	96.8907	149.6347	160.4928	189.5982	224.5894
	5.0	67.5112	108.3271	167.2967	179.4365	211.9773	251.0986
SFSF	0.1	14.4604	30.3338	32.9515	45.1798	50.6939	64.7724
	0.2	19.5795	41.0722	44.6166	61.1738	68.6398	87.7023
	0.5	27.6895	58.0849	63.0973	86.5128	97.0714	124.0297
	1.0	33.9126	71.1392	77.2781	105.9561	118.8876	151.9048
	2.0	39.1589	82.1444	89.2331	122.3475	137.2796	175.4045
	5.0	43.7810	91.8403	99.7656	136.7887	153.4833	196.1082

Three-dimensional (3-D) mode shapes corresponding to first six eigenfrequencies have been depicted in Figs. 9.2 to 9.7 by considering FG Al/Al_2O_3 Lévy square plate with the parameters: $k = 1$, $K_w = 100$ and $K_s = 100$. All the six combination of boundary supports are also taken here. One may also depict the mode shapes of FG Lévy plates for different sets of parameters.

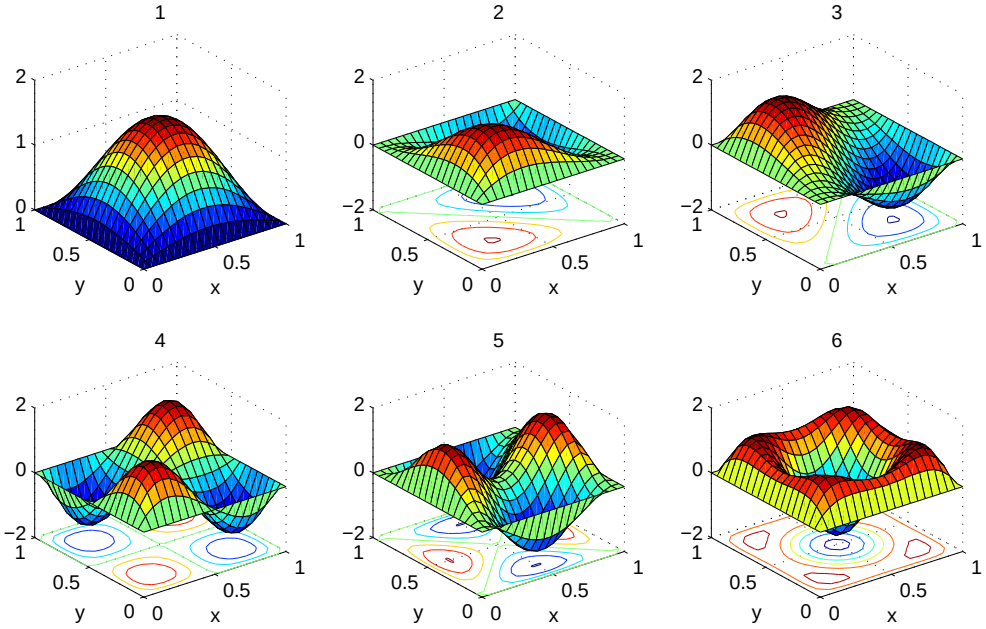

Figure 9.2: First six 3-D mode shapes of SSSS Al/Al_2O_3 Lévy square plate with $k = 1$, $K_w = 100$ and $K_s = 100$

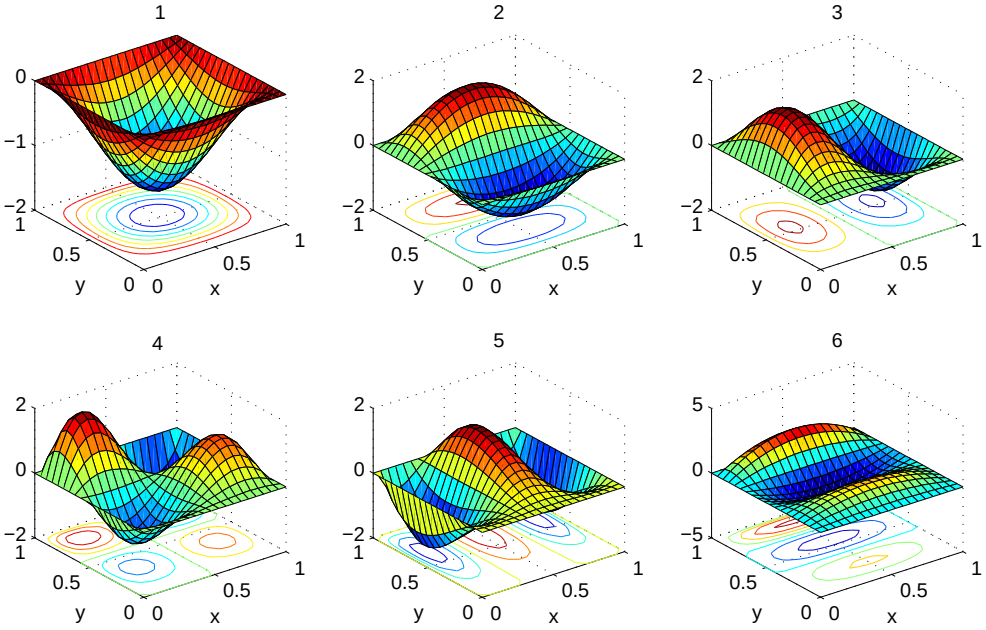

Figure 9.3: First six 3-D mode shapes of SCSS Al/Al_2O_3 Lévy square plate with $k = 1$, $K_w = 100$ and $K_s = 100$

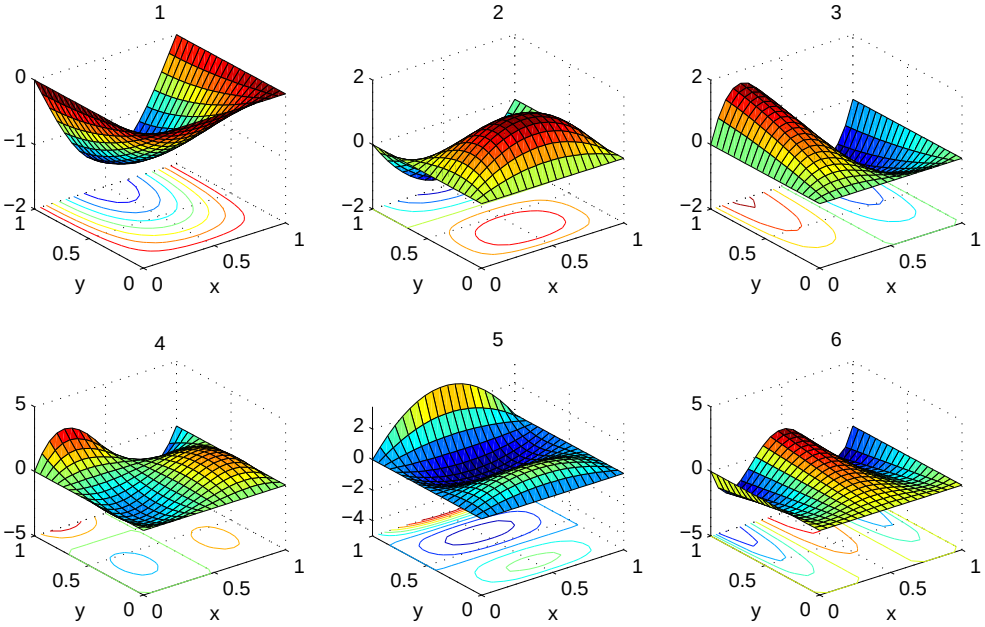

Figure 9.4: First six 3-D mode shapes of SSSF Al/Al_2O_3 Lévy square plate with $k = 1$, $K_w = 100$ and $K_s = 100$

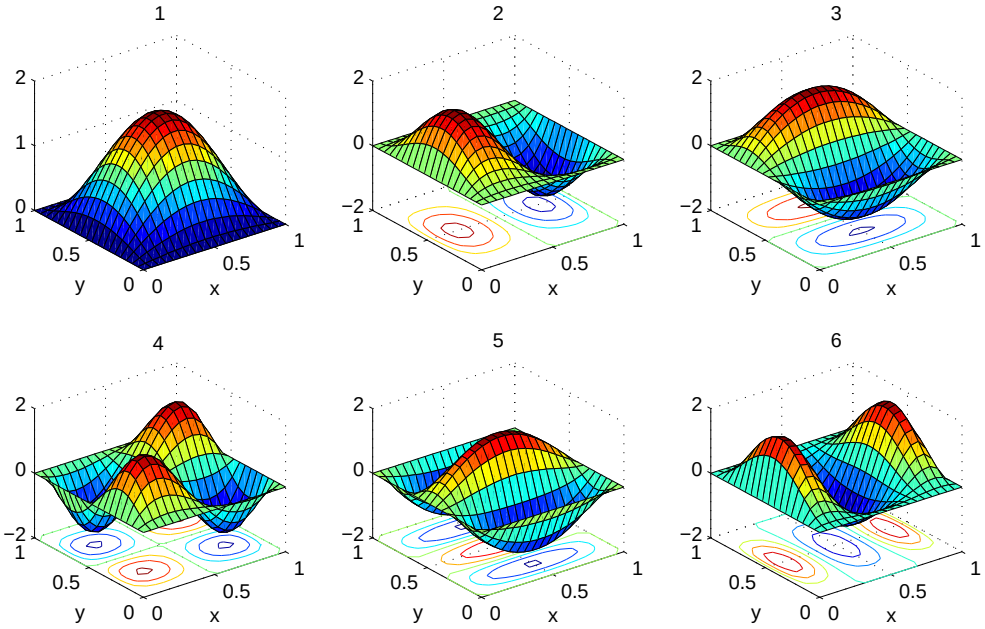

Figure 9.5: First six 3-D mode shapes of SCSC Al/Al_2O_3 Lévy square plate with $k = 1$, $K_w = 100$ and $K_s = 100$

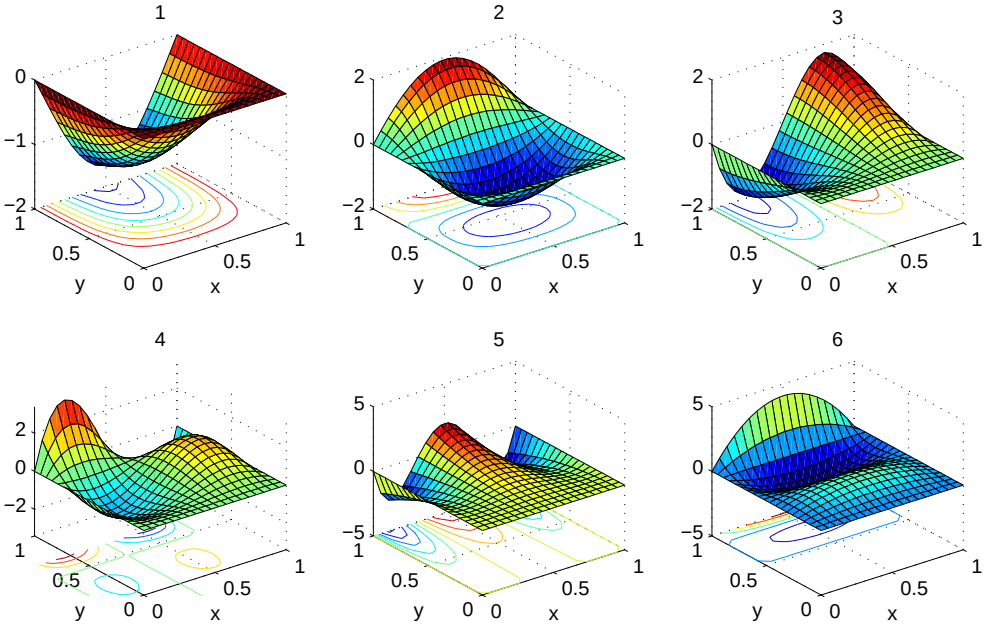

Figure 9.6: First six 3-D mode shapes of SCSF Al/Al_2O_3 Lévy square plate with $k = 1$, $K_w = 100$ and $K_s = 100$

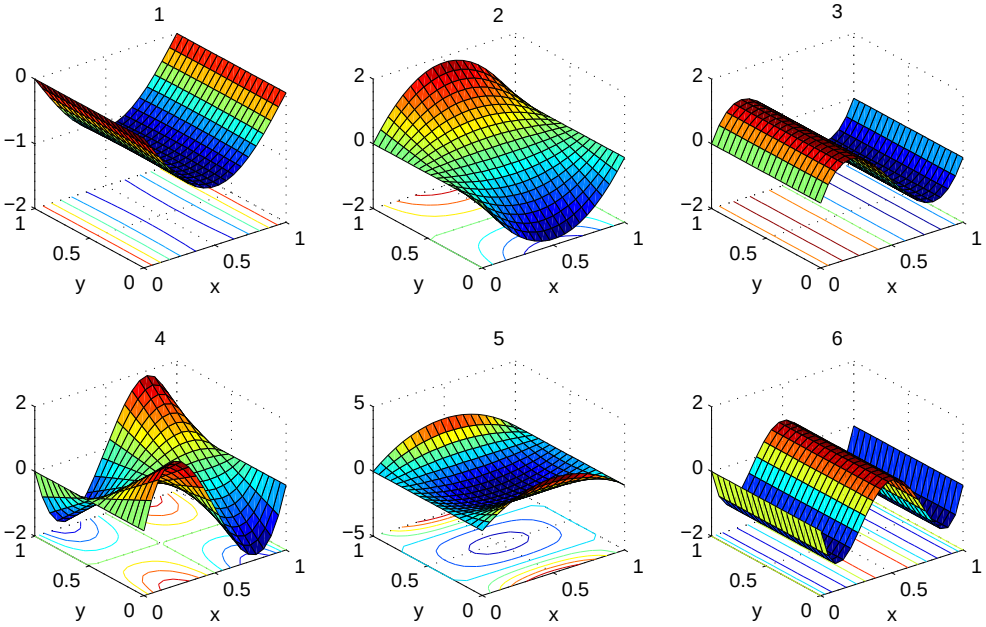

Figure 9.7: First six 3-D mode shapes of SFSF Al/Al_2O_3 Lévy square plate with $k = 1$, $K_w = 100$ and $K_s = 100$

9.3 Thermal environments

This investigation involves the exponential variation of temperature dependent material properties (as stated in Eq. (2.2)) to evaluate the effect of thermal environment on free vibration of FG plate. In addition, the material properties of FG constituents also follow the exponential gradation form to vary along thickness direction. Accordingly, new results for exponential FG plate under the consideration of thermal conditions are incorporated after checking the convergence of frequencies and comparison studies in special cases. The effect of temperature gradients on free vibration eigenfrequencies has also been investigated.

9.3.1 Temperature field across the thickness

The main objective of this investigation is to study the free vibration of functionally graded plates (exponential gradation behavior is supposed for the volume fractions) in thermal environment. As such, let us first discuss the two different cases of temperature rise and its impact on mechanical properties. The temperature variation is assumed to occur in thickness direction only and one-dimensional temperature is considered to be constant in the plane of the plate. As mentioned in (Li et al., 2009a; Shi and Dong, 2012), two cases of temperature gradation is assumed across the thickness.

Uniform temperature rise

The temperature field across the thickness in case of uniform temperature rise can be expressed as,

$$T = T_0 + \Delta T \tag{9.11}$$

Here, T_0 and ΔT denote the respective initial uniform temperature of the plate and temperature change in Eq. (9.11).

Linear temperature rise

Let us assume that T_c and T_m are the temperatures at the top and bottom face of the FG plate. The temperature variation is now a linear function involving the thickness coordinate (z). As

such, the temperature field under linear temperature rise can be written as,

$$T(z) = T_m + \Delta T\left(\frac{z}{h} + \frac{1}{2}\right) \tag{9.12}$$

In Eq. (9.12), $\Delta T = T_c - T_m$ is the temperature gradient and T_m = 300 K represents the initial temperature. The material properties that is Young's modulus (E), Poisson's ratio (ν) and thermal expansion coefficient (α) are nonlinear functions of temperature as stated in (Reddy and Chin, 1998; Shen, 2002; Yang and Shen, 2002; Kim, 2005; Kitipornchai et al., 2006; Li et al., 2009a; Malekzadeh and Beni, 2010; Shi and Dong, 2012),

$$\mathcal{P}(T) = \mathcal{P}_0^T\left(\mathcal{P}_{-1}^T T^{-1} + 1 + \mathcal{P}_1^T T + \mathcal{P}_2^T T^2 + \mathcal{P}_3^T T^3\right) \tag{9.13}$$

where $T = T_0 + \Delta T(z)$ denotes the environmental temperature and T_0 is the free stress or room temperature; $\mathcal{P}_{-1}^T, \mathcal{P}_0^T, \mathcal{P}_1^T, \mathcal{P}_2^T$ and $\mathcal{P}_3^T$ are the constant coefficients in the cubic expression of the respective temperature-dependent material property.

Table 9.26: Temperature-dependent coefficients of Young's modulus (E), Poisson's ratio (ν), thermal expansion coefficient (α) and mass density (ρ) of Si_3N_4 and SUS304 (Kim, 2005)

Properties (Unit)	Material	$\mathcal{P}_{-1}^T$	$\mathcal{P}_0^T$	$\mathcal{P}_1^T$	$\mathcal{P}_2^T$	$\mathcal{P}_3^T$	$\mathcal{P}$ (at T = 300 K)
E (GPa)	SUS304	0	201.04	3.079×10^{-4}	-6.534×10^{-7}	0	207.7877
	Si_3N_4	0	348.43	-3.070×10^{-4}	2.160×10^{-7}	-8.946×10^{-11}	322.2715
ν (no unit)	SUS304	0	0.3262	-2.002×10^{-4}	3.797×10^{-7}	0	0.3178
	Si_3N_4	0	0.2400	0	0	0	0.2400
α (1/K)	SUS304	0	12.330×10^{-6}	8.086×10^{-6}	0	0	1.5321×10^{-5}
	Si_3N_4	0	5.8723×10^{-6}	9.095×10^{-6}	0	0	7.4746×10^{-6}
ρ (kg/m^3)	SUS304	0	8166	0	0	0	8166
	Si_3N_4	0	2370	0	0	0	2370

It can easily be noticed in (Reddy and Chin, 1998; Shen, 2002; Yang and Shen, 2002; Kim, 2005; Kitipornchai et al., 2006; Li et al., 2009a; Malekzadeh and Beni, 2010; Shi and Dong, 2012) that the effect of thermal environment in functionally graded plates assumes the power-law variation of material properties only. Present study may be the first where we assume the corresponding exponential gradation of material properties in thermal environment as

$$\begin{aligned}
E(z,T) &= E_c(T)e^{-\delta\left(1-\frac{2z}{h}\right)}; \delta = \frac{1}{2}ln\left(\frac{E_c(T)}{E_m(T)}\right)\\
\alpha(z,T) &= \alpha_c(T)e^{-\delta\left(1-\frac{2z}{h}\right)}; \delta = \frac{1}{2}ln\left(\frac{\alpha_c(T)}{\alpha_m(T)}\right)\\
\nu(z,T) &= \nu_c(T)e^{-\delta\left(1-\frac{2z}{h}\right)}; \delta = \frac{1}{2}ln\left(\frac{\nu_c(T)}{\nu_m(T)}\right)
\end{aligned} \tag{9.14}$$

One can observe in Table 9.26 that only mass density (ρ) includes non-zero value only in the coefficient viz. $\mathcal{P}_0^T$ (free stress state). Hence mass density will vary exponentially without involving the effect of temperature in its expression.

9.3.2 Numerical modeling

State under temperature gradient

Initially let us assume the free stress temperature be $T_0 = 300$ K. Now, the plate is acted upon by a thermal gradient, ΔT (either uniform or linear temperature rise) (Kim, 2005). As a result, constitutive relations can be written as

$$d_{ij} = \frac{\partial u_x}{\partial i}\frac{\partial u_x}{\partial j} + \frac{\partial u_y}{\partial i}\frac{\partial u_y}{\partial j} + \frac{\partial u_z}{\partial i}\frac{\partial u_z}{\partial j} \quad (i, j = x, y) \tag{9.15}$$

In Eq. (9.15), d_{ij} are the components of strains due to temperature gradation. Consequently, corresponding thermal stresses can be defined in matrix form as (Kim, 2005; Kitipornchai et al., 2006)

$$\begin{Bmatrix} \sigma_{xx}^T \\ \sigma_{yy}^T \\ \tau_{xy}^T \end{Bmatrix} = -\begin{pmatrix} Q_{11} & Q_{12} & 0 \\ Q_{21} & Q_{22} & 0 \\ 0 & 0 & Q_{66} \end{pmatrix}\begin{pmatrix} 1 & 0 \\ 0 & 1 \\ 0 & 0 \end{pmatrix}\begin{Bmatrix} \alpha(z,T) \\ \alpha(z,T) \end{Bmatrix}\Delta T(z) \tag{9.16}$$

In Table 9.26, the coefficients for Poisson's ratio in cubic expansion vary with a certain temperature. So, the reduced stiffness coefficients in Eq. (9.16) will be

$$Q_{11} = Q_{22} = \frac{E(z,T)}{1-\nu^2(z,T)},\ Q_{12} = Q_{21} = \frac{\nu(z,T)E(z,T)}{1-\nu^2(z,T)},\ Q_{66} = \frac{E(z,T)}{2[1+\nu(z,T)]}.$$

Energy expressions in thermal environment

Let $\mathbf{U}_T$ be the strain energy from the thermal stresses (as stated in Eq. (9.16)) due to temperature rise. Then $\mathbf{U}_T$ can be given as

$$\mathbf{U}_T = \frac{1}{2}\int_V \left(\sigma_{xx}^T d_{xx} + \sigma_{yy}^T d_{yy} + \tau_{xy}^T d_{xy}\right) \mathrm{d}V \tag{9.17}$$

where

$$\sigma_{xx}^{T} = -(Q_{11} + Q_{12})\,\alpha(z,T)\Delta T(z),$$
$$\sigma_{yy}^{T} = -(Q_{12} + Q_{22})\,\alpha(z,T)\Delta T(z),$$
$$\tau_{xy}^{T} = 0$$

and

$$d_{xx} = z^2\left\{\left(\frac{\partial^2 w}{\partial x^2}\right)^2 + \left(\frac{\partial^2 w}{\partial x \partial y}\right)^2\right\} + \left(\frac{\partial w}{\partial x}\right)^2$$
$$d_{yy} = z^2\left\{\left(\frac{\partial^2 w}{\partial x \partial y}\right)^2 + \left(\frac{\partial^2 w}{\partial y^2}\right)^2\right\} + \left(\frac{\partial w}{\partial y}\right)^2$$
$$d_{xy} = z^2\left(\frac{\partial^2 w}{\partial x^2} + \frac{\partial^2 w}{\partial y^2}\right)\frac{\partial^2 w}{\partial x \partial y} + \frac{\partial w}{\partial x}\frac{\partial w}{\partial y}$$

Substituting these terms in Eq. (9.17), leads to

$$\begin{aligned}\mathbf{U}_T \;=\; & -\frac{1}{2}\int_{\Omega}\Bigg[\left(D_{11}^{T} + D_{12}^{T}\right)\left\{\left(\frac{\partial^2 w}{\partial x^2}\right)^2 + 2\left(\frac{\partial^2 w}{\partial x \partial y}\right)^2 + \left(\frac{\partial^2 w}{\partial y^2}\right)^2\right\} \\ & + \left(A_{11}^{T} + A_{12}^{T}\right)\left\{\left(\frac{\partial w}{\partial x}\right)^2 + \left(\frac{\partial w}{\partial y}\right)^2\right\}\Bigg]\,\mathrm{d}x\,\mathrm{d}y \end{aligned} \tag{9.18}$$

Here, thermal stiffness coefficients in Eq. (9.18) are defined as

$$(D_{11}^{T}, D_{12}^{T}) = \int_{-h/2}^{h/2} (Q_{11}, Q_{12})\, z^2 \alpha \Delta T\, \mathrm{d}z$$
$$(A_{11}^{T}, A_{12}^{T}) = \int_{-h/2}^{h/2} (Q_{11}, Q_{12})\, \alpha \Delta T\, \mathrm{d}z$$

Using harmonic type deflection; $w(x,y,t) = W(x,y)\cos\omega t$, Eq. (9.18) yields maximum thermal strain energy, $(\mathbf{U}_T)_{max}$ as

$$\begin{aligned}(\mathbf{U}_T)_{max} \;=\; & -\frac{1}{2}\int_{\Omega}\Bigg[\left(D_{11}^{T} + D_{12}^{T}\right)\left\{\left(\frac{\partial^2 W}{\partial x^2}\right)^2 + 2\left(\frac{\partial^2 W}{\partial x \partial y}\right)^2 + \left(\frac{\partial^2 W}{\partial y^2}\right)^2\right\} \\ & + \left(A_{11}^{T} + A_{12}^{T}\right)\left\{\left(\frac{\partial W}{\partial x}\right)^2 + \left(\frac{\partial W}{\partial y}\right)^2\right\}\Bigg]\,\mathrm{d}x\,\mathrm{d}y \end{aligned} \tag{9.19}$$

Due to temperature rise or thermal environment, the effective strain energy ($\mathbf{U}_{eff}$) will be obtained using expressions involved in Eq. (3.31) and (9.19) as $\mathbf{U}_{eff} = \mathbf{U}_{max} + (\mathbf{U}_T)_{max}$;

where $\mathbf{U}_{max} = \frac{1}{2}\int_{\Omega}\left[D_{11}\left\{\left(\frac{\partial^2 W}{\partial x^2}\right)^2 + \left(\frac{\partial^2 W}{\partial y^2}\right)^2\right\} + 2D_{12}\frac{\partial^2 W}{\partial x^2}\frac{\partial^2 W}{\partial y^2} + 4D_{66}\left(\frac{\partial^2 W}{\partial x \partial y}\right)^2\right] \mathrm{d}x\mathrm{d}y$. In case of functionally graded plates under thermal environment, Rayleigh-Ritz method is being used by equating $\mathbf{U}_{eff}$ and maximum kinetic energy ($\mathbf{T}_{max}$) to get the Rayleigh quotient (ω^2). Differentiate this quotient with respect to the unknown constants (c_i; $i = 1, 2, 3, \cdots, n$) and generalized eigenvalue problem for exponential FG plate under thermal environment of the form Eq. (3.38) can easily be obtained.

9.3.3 Results and discussions

The target of this work is to study the free vibration of exponential FG plate in thermal environments. To validate our results in thermal condition, we could not find any paper related to exponential FG plate with thermal environments. But one can have papers concerned with FG plate having power-law variation of temperature dependent material properties. So, we compute results for power-law based FG plate in thermal environments and as such, a convergence study is performed in Table 9.27 for first eight natural frequencies of CCCC FG plate with power-law variation of material properties. The convergence of free vibration frequencies of clamped exponential FG plate under uniform and linear temperature environments is tabulated in Table 9.28. The material properties under initial stress free temperature ($T = 300$ K) are considered (as stated in Table 9.26). The power-law exponents (k) are taken as 2.0 and 10.0 in both uniform and linear temperature conditions; other physical parameters are $a = 0.2$ m, $h/b = 0.1$ and temperature gradient (ΔT) = 300 K. First eight non-dimensional frequencies are evaluated with two different aspect ratios, $a/b = 0.5$ and 1.0. Frequencies associated with uniform rise of temperature condition for power-law based FG plate are validated with (Yang and Shen, 2002; Li et al., 2009a).

In validation, one may observe mere discrepancies of our results. This is due to the fact that transverse shear deformation effects are ignored in classical plate theory, based on which the present investigation is performed. The Diff. % used in the table is the percentage differences of the computed results (CPT) and the results taken from the available literature. It can be viewed that the Diff. % is significant for $a/b = 0.5$, whereas this is insignificant for $a/b = 1$ except at higher modes. Regardless of the thermal condition and variation form assumed, one may say that the number of polynomials (n) involved in deflection function (W) plays a key role for the convergence of frequencies at each mode. It can also easily be noticed that frequencies associated with linear temperature rise is higher than that for uniform rise of temperature.

Table 9.27: Convergence and comparison of first eight natural frequencies of CCCC FG (SUS304/Si_3N_4) plates with different thermal conditions (a = 0.2 m, h/b = 0.1, T = 300 K, ΔT = 300 K)

a/b (Thermal state)	k	Source	λ_1	λ_2	λ_3	λ_4	λ_5	λ_6	λ_7	λ_8
0.5 (Uniform rise)	2.0	8×8	9.9116	12.8535	18.4206	25.8682	29.0255	52.4124	55.0152	90.4206
		10×10	9.9116	12.8418	18.4206	25.8243	27.2368	29.0255	33.8882	52.4124
		13×13	9.9106	12.8418	18.4095	25.8243	27.2368	28.7053	33.8882	49.8405
		15×15	9.9101	12.8418	18.0820	25.8243	27.2368	28.6941	33.8882	40.0102
		Yang and Shen (2002)	9.2196	11.6913	15.2957	20.4667	21.2323	21.4468	22.4853	25.4461
		Diff. %	7.5057	9.8407	18.2162	23.5387	28.2800	33.7919	50.7127	57.2351
		Li et al. (2009a)	9.2111	11.5890	15.5999	19.9043	20.0234	20.7922	21.9073	25.0100
		Diff. %	7.6049	10.8103	15.9109	29.7423	36.0249	38.0042	54.6891	59.9768
	10.0	8×8	9.9029	12.8433	18.4066	25.8473	29.0036	52.3713	54.9737	90.3504
		10×10	9.9029	12.8316	18.4066	25.8034	27.2164	29.0036	33.8643	52.3713
		13×13	9.9020	12.8316	18.3955	25.8034	27.2164	28.6837	33.8643	49.8012
		15×15	9.9016	12.8316	18.0683	25.8034	27.2164	28.6725	33.8643	39.9803
		Yang and Shen (2002)	7.9839	10.1219	13.3088	17.6295	18.3727	18.9066	19.3778	21.9914
		Li et al. (2009a)	7.8170	9.8332	13.2410	16.8733	16.9943	17.6538	18.5960	21.2369
1.0 (Uniform rise)	2.0	8×8	3.6322	7.4211	7.4848	10.9601	13.8504	13.9879	17.0379	23.3609
		10×10	3.6322	7.4092	7.4092	10.9601	13.8504	13.9879	17.0374	17.0374
		13×13	3.6312	7.4092	7.4092	10.9437	13.3312	13.8915	17.0374	17.0374
		15×15	3.6311	7.4092	7.4092	10.9276	13.3066	13.3596	17.0374	17.0374
		Yang and Shen (2002)	3.6636	7.2544	7.2544	10.3924	11.7054	12.3175	14.4520	-
		Diff. %	-0.8871	2.1339	2.1339	5.1499	14.1319	8.4603	17.8896	-
		Li et al. (2009a)	3.7202	7.3010	7.3010	10.3348	12.2256	12.3563	14.8112	14.8112
		Diff. %	-2.3950	1.4819	1.4819	5.7359	8.8421	8.1197	15.0305	15.0305
	10.0	8×8	3.6297	7.4159	7.4795	10.9530	13.8403	13.9777	17.0267	23.3436
		10×10	3.6297	7.4039	7.4039	10.9530	13.8403	13.9777	17.0261	17.0261
		13×13	3.6286	7.4039	7.4039	10.9367	13.3216	13.8813	17.0261	17.0261
		15×15	3.6285	7.4039	7.4039	10.9205	13.2969	13.3499	17.0261	17.0261
		Yang and Shen (2002)	3.1835	6.3001	6.3001	9.0171	10.2372	10.6781	12.6015	12.9948
		Li et al. (2009a)	3.1398	6.1857	6.1857	8.7653	10.3727	10.4866	12.5971	12.5971

Table 9.28: Convergence of first eight natural frequencies of CCCC exponential FG ($SUS304/Si_3N_4$) plates with different thermal conditions (a = 0.2 m, h/b = 0.1, T = 300 K, ΔT = 300 K)

a/b (Thermal state)	Source	λ_1	λ_2	λ_3	λ_4	λ_5	λ_6	λ_7	λ_8
0.5 (Uniform rise)	8×8	9.9168	12.8597	18.4289	25.8804	29.0383	52.4360	55.0390	90.4605
	10×10	9.9168	12.8480	18.4289	25.8365	27.2488	29.0383	33.9022	52.4360
	13×13	9.9158	12.8480	18.4178	25.8365	27.2488	28.7179	33.9022	49.8631
	15×15	9.9153	12.8480	18.0903	25.8365	27.2488	28.7068	33.9022	40.0276
0.5 (Linear rise)	8×8	9.9296	12.8750	18.4499	25.9118	29.0712	52.4979	55.1015	90.5662
	10×10	9.9296	12.8633	18.4499	25.8679	27.2794	29.0712	33.9382	52.4979
	13×13	9.9286	12.8633	18.4388	25.8679	27.2794	28.7505	33.9382	49.9223
	15×15	9.9282	12.8633	18.1108	25.8679	27.2794	28.7393	33.9382	40.0727
1.0 (Uniform rise)	8×8	3.6337	7.4241	7.4878	10.9642	13.8561	13.9936	17.0442	23.3707
	10×10	3.6337	7.4121	7.4121	10.9642	13.8561	13.9936	17.0437	17.0437
	13×13	3.6326	7.4121	7.4121	10.9477	13.3367	13.8972	17.0437	17.0437
	15×15	3.6326	7.4121	7.4121	10.9316	13.3120	13.3651	17.0437	17.0437
1.0 (Linear rise)	8×8	3.6376	7.4319	7.4958	10.9749	13.8714	14.0088	17.0612	23.3968
	10×10	3.6376	7.4199	7.4199	10.9749	13.8714	14.0088	17.0607	17.0607
	13×13	3.6365	7.4199	7.4199	10.9584	13.3513	13.9125	17.0607	17.0607
	15×15	3.6364	7.4199	7.4199	10.9422	13.3265	13.3796	17.0607	17.0607

Now onwards, effect of aspect ratios on first eight non-dimensional frequencies of exponential functionally graded ($SUS304/Si_3N_4$) plate under two different thermal environments are incorporated in Tables 9.29 to 9.32. Here also, the material properties of FG constituents are taken as mentioned in Table 9.26. Only clamped and simply supported edge supports are considered here. Tables 9.29 and 9.30 are meant for CCCC FG plate subjected to uniform and linear temperature rise respectively, whereas similar assumptions are considered in Tables 9.31 and 9.32 for FG plate with SSSS edge support. Initial free stress or room temperature (T) is taken as 300 K and temperature gradient (ΔT) are assumed to be 0, 300 and 500 for each aspect ratio (a/b). Physical parameters involved in these computations are: a/b = 0.5 and 1.0, h/b (thickness-to-breadth ratio) = 0.1, 0.2 and 0.25. Looking into the results evaluated in these tables, we may summarize the following related to thermal effects.

- Irrespective of the edge support and thermal state considered, frequency parameters are increasing with increase in thickness-to-breadth (h/b) ratio and are decreasing with increase in the temperature gradient (ΔT).

- For the exponential FG plate with a certain edge condition and $\Delta T = 0$, non-dimensional frequencies coincide for the respective aspect ratio and thickness-to-breadth ratio assumed. For non-zero temperature gradients, natural frequencies at each mode

associated with linear temperature rise are comparatively higher than that of uniform case.

- It can also be noticed that the second non-dimensional frequency is coinciding with the third for FG square plate irrespective of the thermal condition and h/b considered. But no coincidence can be observed for natural frequencies of rectangular FG plates. This proposition may be true because of the fact that either clamped or simply supported boundary condition is assumed at all the edges of the exponential FG plate.

Table 9.29: First eight non-dimensional frequencies of CCCC exponential FG (SUS304/Si_3N_4) plate subjected to uniform temperature rise (a = 0.2 m, T = 300 K)

a/b	h/b	ΔT	λ_1	λ_2	λ_3	λ_4	λ_5	λ_6	λ_7	λ_8
0.5	0.1	0	9.7888	12.6982	17.9305	25.7085	27.1141	28.5726	33.7716	39.9238
		300	9.6126	12.4895	17.6933	25.4651	26.8669	28.3191	33.5096	39.6563
		500	9.4931	12.3483	17.5334	25.3015	26.7009	28.1489	33.3338	39.4769
	0.2	0	9.9043	12.8350	18.0822	25.8507	27.2603	28.7210	33.9221	40.0661
		300	9.8465	12.7664	17.9997	25.7515	27.1613	28.6179	33.8122	39.9423
		500	9.8078	12.7205	17.9444	25.6851	27.0951	28.5491	33.7387	39.8596
	0.25	0	9.9180	12.8514	18.1004	25.8677	27.2778	28.7388	33.9401	40.0832
		300	9.8742	12.7992	18.0361	25.7856	27.1964	28.6536	33.8483	39.9765
		500	9.8448	12.7643	17.9931	25.7308	27.1419	28.5967	33.7869	39.9053
1.0	0.1	0	3.4699	7.2307	7.2307	10.7436	13.1288	13.1854	16.8703	16.8703
		300	3.2831	7.0144	7.0144	10.5126	12.8889	12.9493	16.6329	16.6329
		500	3.1518	6.8662	6.8662	10.3556	12.7265	12.7895	16.4728	16.4728
	0.2	0	3.5981	7.3781	7.3781	10.8995	13.2863	13.3403	17.0236	17.0236
		300	3.5491	7.3153	7.3153	10.8289	13.2081	13.2628	16.9424	16.9424
		500	3.5161	7.2732	7.2732	10.7816	13.1557	13.2109	16.8881	16.8881
	0.25	0	3.6132	7.3956	7.3956	10.9180	13.3051	13.3588	17.0419	17.0419
		300	3.5796	7.3505	7.3505	10.8662	13.2458	13.2999	16.9792	16.9792
		500	3.5570	7.3204	7.3204	10.8316	13.2062	13.2606	16.9373	16.9373

Table 9.30: First eight non-dimensional frequencies of CCCC exponential FG (SUS304/Si_3N_4) plate subjected to linear temperature rise (a = 0.2 m, T = 300 K)

a/b	h/b	ΔT	λ_1	λ_2	λ_3	λ_4	λ_5	λ_6	λ_7	λ_8
0.5	0.1	0	9.7888	12.6982	17.9305	25.7085	27.1141	28.5726	33.7716	39.9238
		300	9.7073	12.6016	17.8208	25.5962	27.0000	28.4557	33.6508	39.8008
		500	9.6525	12.5368	17.7472	25.5211	26.9237	28.3775	33.5701	39.7186
	0.2	0	9.9043	12.8350	18.0822	25.8507	27.2603	28.7210	33.9221	40.0661
		300	9.8778	12.8036	18.0445	25.8056	27.2153	28.6742	33.8722	40.0102
		500	9.8601	12.7825	18.0192	25.7756	27.1853	28.6429	33.8389	39.9729
	0.25	0	9.9180	12.8514	18.1004	25.8677	27.2778	28.7388	33.9401	40.0832
		300	9.8980	12.8276	18.0711	25.8306	27.2411	28.7003	33.8987	40.0353
		500	9.8847	12.8117	18.0516	25.8059	27.2165	28.6747	33.8711	40.0033
1.0	0.1	0	3.4699	7.2307	7.2307	10.7436	13.1288	13.1854	16.8703	16.8703
		300	3.3841	7.1307	7.1307	10.6367	13.0178	13.0761	16.7604	16.7604
		500	3.3255	7.0633	7.0633	10.5648	12.9433	13.0028	16.6868	16.6868
	0.2	0	3.5981	7.3781	7.3781	10.8995	13.2863	13.3403	17.0236	17.0236
		300	3.5755	7.3492	7.3492	10.8670	13.2504	13.3048	16.9865	16.9865
		500	3.5603	7.3298	7.3298	10.8453	13.2265	13.2810	16.9616	16.9616
	0.25	0	3.6132	7.3956	7.3956	10.9180	13.3051	13.3588	17.0419	17.0419
		300	3.5977	7.3749	7.3749	10.8943	13.2781	13.3319	17.0134	17.0134
		500	3.5873	7.3611	7.3611	10.8785	13.2600	13.3140	16.9943	16.9943

Table 9.31: First eight non-dimensional frequencies of SSSS exponential FG (SUS304/Si_3N_4) plate subjected to uniform temperature rise (a = 0.2 m, T = 300 K)

a/b	h/b	ΔT	λ_1	λ_2	λ_3	λ_4	λ_5	λ_6	λ_7	λ_8
0.5	0.1	0	4.7368	7.7528	12.8694	16.7878	19.8426	30.4575	30.8328	37.2910
		300	4.4581	7.4795	12.5934	16.5006	19.5552	30.1819	30.5772	36.9665
		500	4.2622	7.2916	12.4059	16.3064	19.3612	29.9969	30.4057	36.7485
	0.2	0	4.9289	7.9423	13.0567	16.9751	20.0293	30.6239	30.9792	37.4761
		300	4.8569	7.8671	12.9730	16.8795	19.9323	30.5169	30.8718	37.3389
		500	4.8083	7.8166	12.9169	16.8154	19.8673	30.4455	30.8000	37.2472
	0.25	0	4.9515	7.9648	13.0789	16.9974	20.0516	30.6439	30.9967	37.4983
		300	4.9026	7.9124	13.0178	16.9244	19.9771	30.5569	30.9069	37.3834
		500	4.8697	7.8772	12.9769	16.8755	19.9272	30.4989	30.8470	37.3066
1.0	0.1	0	1.7312	4.7541	4.7541	7.7815	9.8815	9.8830	16.8528	16.8528
		300	1.4121	4.4761	4.4761	7.5088	9.6060	9.6075	16.6062	16.6062
		500	1.1513	4.2808	4.2808	7.3213	9.4178	9.4194	16.4398	16.4398
	0.2	0	1.9339	4.9458	4.9458	7.9706	10.0689	10.0704	17.0129	17.0129
		300	1.8655	4.8739	4.8739	7.8954	9.9876	9.9891	16.9297	16.9297
		500	1.8185	4.8253	4.8253	7.8449	9.9330	9.9345	16.8740	16.8740
	0.25	0	1.9568	4.9683	4.9683	7.9929	10.0912	10.0926	17.0321	17.0321
		300	1.9127	4.9194	4.9194	7.9406	10.0324	10.0339	16.9681	16.9681
		500	1.8827	4.8866	4.8866	7.9054	9.9931	9.9945	16.9254	16.9254

Table 9.32: First eight non-dimensional frequencies of SSSS exponential FG ($SUS304/Si_3N_4$) plate subjected to linear temperature rise ($a = 0.2$ m, $T = 300$ K)

a/b	h/b	ΔT	λ_1	λ_2	λ_3	λ_4	λ_5	λ_6	λ_7	λ_8
0.5	0.1	0	4.7368	7.7528	12.8694	16.7878	19.8426	30.4575	30.8328	37.2910
		300	4.6087	7.6265	12.7416	16.6549	19.7096	30.3302	30.7149	37.1415
		500	4.5214	7.5412	12.6557	16.5658	19.6204	30.2451	30.6362	37.0415
	0.2	0	4.9289	7.9423	13.0567	16.9751	20.0293	30.6239	30.9792	37.4761
		300	4.8956	7.9076	13.0181	16.9313	19.9849	30.5753	30.9305	37.4139
		500	4.8732	7.8843	12.9924	16.9020	19.9552	30.5428	30.8979	37.3724
	0.25	0	4.9515	7.9648	13.0789	16.9974	20.0516	30.6439	30.9967	37.4983
		300	4.9289	7.9406	13.0509	16.9641	20.0177	30.6045	30.9563	37.4465
		500	4.9138	7.9245	13.0322	16.9419	19.9950	30.5783	30.9293	37.4119
1.0	0.1	0	1.7312	4.7541	4.7541	7.7815	9.8815	9.8830	16.8528	16.8528
		300	1.5900	4.6264	4.6264	7.6555	9.7541	9.7556	16.7387	16.7387
		500	1.4885	4.5392	4.5392	7.5703	9.6682	9.6697	16.6621	16.6621
	0.2	0	1.9339	4.9458	4.9458	7.9706	10.0689	10.0704	17.0129	17.0129
		300	1.9023	4.9125	4.9125	7.9358	10.0315	10.0329	16.9749	16.9749
		500	1.8809	4.8902	4.8902	7.9126	10.0064	10.0078	16.9494	16.9494
	0.25	0	1.9568	4.9683	4.9683	7.9929	10.0912	10.0926	17.0321	17.0321
		300	1.9364	4.9457	4.9457	7.9688	10.0642	10.0657	17.0029	17.0029
		500	1.9226	4.9306	4.9306	7.9527	10.0462	10.0476	16.9835	16.9835

9.4 Concluding remarks

The present investigation is dealt with free vibration of FG plates under various complicating environments. The vibration of FG rectangular plates with power-law variation based material properties is to be handled under Winkler and Pasternak elastic foundations, whereas thermal environment is assumed to study the vibration characteristics of exponential FG plate. The generalized eigenvalue problem in each case can be found by using Rayleigh-Ritz method, which is one of the computationally efficient procedure to handle such problems. Effect of elastic foundation moduli and temperature gradients on free vibration characteristics of the plates may be summarized as follows.

- Considering the effect of Winkler elastic foundation, it may be observed that the non-dimensional frequencies are increasing with increase in aspect ratios for a fixed power-law index and are decreasing with increase in power-law exponents for a fixed aspect ratio. This behavior is in fact true irrespective of the edge support, gradation criteria and configuration of the FG plate (or in the presence of Winkler elastic foundation) considered.

- A very interesting result may be seen for the effect of ascending values of power-law index (k) on free vibration characteristics of FG plates, which mainly depends on the presence of elastic foundations. Without elastic foundation, the eigenfrequencies follow descending behavior. They are also decreasing while considering the Winkler elastic foundation except for SFSF FG plate, where fundamental frequencies follow fluctuating behavior with increase in k. Moreover in presence of either Pasternak or Winkler-Pasternak foundations, the frequencies may also decrease for SCSC Lévy plate whereas the behavior for other five combinations of edge conditions may not be straightforward.

- On the other hand in presence of Winkler and Pasternak foundations, the non-dimensional frequencies are gradually decreasing with increase in values of E_r and are increasing with ascending values of ρ_r, which can be noticed from the concerned expression of λ.

- While looking into the results obtained for the exponential FG plate with thermal environments, it is worth to mention that frequency parameters are increasing with increase in thickness-to-breadth (h/b) ratio and are decreasing with increase in the temperature gradient (ΔT) regardless of the edge condition and thermal state considered.

- Consequently, other complicating effects can also taken into consideration to check the vibration characteristics of functionally graded plates with different geometries.

Chapter 10

Conclusions and future directions

Chapter 10

Conclusions and future directions

10.1 Conclusions

Based on the varieties of problems solved in case of functionally graded structural members, the conclusions are drawn along with the directions for future work. The present investigation provides the numerical solutions of static analysis of functionally graded rectangular plates, vibration problems of functionally graded beams and plates (with different geometries) and vibration of rectangular plates with complicating environments. In addition, new shear deformation beam (and plate) theories are proposed based on certain assumptions and those are used in vibration problems of functionally graded beams and thick isotropic rectangular plates. The main objective of this study has been to implement computationally efficient numerical techniques to the said problems.

In the following paragraphs, important conclusions have been drawn with reference to various proposed methods and the application problems mentioned in previous chapters.

- First of all, the basic tools to handle the titled problems are incorporated in Chapters 1, 2 and 3. In particular, the origin and history of functionally graded structural members along with governing equations associated with static and dynamic problems of these members are included in Chapters 1 and 2 respectively. Furthermore, the systematic algorithms of numerical schemes viz. Rayleigh-Ritz and generalized differential quadrature have been exhaustively discussed to solve these problems in Chapter 3. It may be noted that material properties in FG beams and plates generally vary spatially along thickness direction in the forms of power-law or exponential law. Also only essential boundary conditions need to be satisfied in Rayleigh-Ritz method rather than considering the natural ones, based on which the admissible functions of displacements are defined. The trial functions denoting the deflection components may be expressed as linear combination of simple algebraic polynomials. On the other hand, generalized differential

quadrature solves the physical problems by discretizing the governing equations after satisfying the natural boundary conditions. The computational efficiency of these methods have been discussed while solving the said problems in other chapters.

- The static analysis of thin functionally graded rectangular plates subjected to various classical boundary conditions has been studied in Chapter 4 using Rayleigh-Ritz method. The analysis has been done based on displacement field of classical plate theory. Material properties of FG plate constituents are assumed to vary spatially in thickness direction according to power-law form. Uniformly Distributed Load (UDL) and hydrostatic pressure are considered to be the external mechanical loads. The effect of aspect ratio (breadth-to-length ratio) and volume fraction of the constituents on numerical factors associated with mid-plane deflection, bending moments and normal stresses are studied. We have certainly found that increase in number of polynomials (n) play an important role in the convergence of pure bending parameters. The maximum deflection, bending moment and maximum normal stress with respect to $x-$axis are increasing with increase in aspect ratios, whereas it is difficult to predict the pattern followed by maximum bending moment and normal stress with respect to $y-$axis. The mentioned parameters are increasing with increase in power-law exponents and the ratio of Young's moduli of constituents. Moreover the numerical factors under UDL are comparatively higher than those evaluated under hydrostatic pressure.

- Free vibration problem concerned with functionally graded beams subjected to various sets of classical edge supports has been incorporated in Chapter 5. Two different types of FG beams are considered here. First, the vibration problem of uniform FG beam is analyzed based on Rayleigh-Ritz method, whereas that of non-uniform FG beam by generalized differential quadrature. In both these problems, material properties of FG beam constituents vary gradually along thickness direction with respect to power-law form. The deformed uniform FG beam considers its displacement fields on the basis of different existing and newly proposed shear deformation beam theories (SDBTs). In each case of shear deformation theories, first five natural frequencies for different sets of boundary conditions have been computed after checking the convergence and comparison with existing results.

  In Rayleigh-Ritz method, the slenderness ratios, power-law variation of material

properties, different material distributions and different SDBTs play vital roles in finding the vibration characteristics. Increase in the number of polynomials is a key component in deciding the convergence of the non-dimensional frequencies. The frequencies are increasing with increase in slenderness (length-to-thickness) ratios and are decreasing with increase in power-law indices irrespective of the SDBT and edge support assumed. Rather than these concerns, the results associated with different newly proposed SDBTs can also be analyzed in various ways. In case of PESDBT, these frequencies follow an ascending pattern with increase in power-law index determining deformation theory. While comparing various SDBTs, the difference among the non-dimensional frequencies at each mode is significant for $L/h < 20$. For $L/h \geq 20$, the effect of power-law indices on non-dimensional frequencies is negligible irrespective of the beam theories considered. In addition, the eigenfrequencies associated with PSDBT are coinciding with PESDBT[1] for different sets of BCs. A bit of fluctuations with an absolute error specification of 10^{-5} to 10^{-6} can be observed while analyzing the results for cantilever FG beam based on PSDBT and PESDBT[1]. On contrary, the frequencies computed in PESDBT for $n = 0$ and for very large value of n coincides with those for CBT. The results associated with ISDBT coincides with those of ICDBT regardless of the slenderness ratio and power-law index assumed. However, the frequencies at each mode based on ITDBT are comparatively higher than those evaluated within the framework of ISDBT and ICDBT.

In generalized differential quadrature, the governing equation for free vibration has been considered for Euler-Bernoulli FG beam. It has been seen that the power-law index (k), parameter for non-homogeneity (α) and the indices deciding non-homogeneity (m_1, m_2) play crucial roles in evaluating the natural frequencies. The behavior of these frequencies with reference to these parameters have also been discussed in Sec. 5.2.3. The computed results follow descending behavior for ascending values of k irrespective of boundary supports and assumed values of m_1 and m_2. On contrary, these will follow descending manner with increase in α while $m_1 < m_2$ and ascending pattern with increase in α while $m_1 > m_2$. But it is difficult to predict the behavior of these frequencies for $m_1 = m_2$.

- Free vibration problems concerned with thin functionally graded plates with different geometries have been studied in Chapters 6, 7 and 8 by means of Rayleigh-Ritz method. In each problem, displacement field is assumed based on classical plate theory and the plate is subjected to various classical boundary supports. Chapter 6 is

meant for FG rectangular plates and also for isotropic thick rectangular plates (special case of FG plate handled via inverse trigonometric shear deformation theories). In the similar fashion, Chapters 7 and 8 are meant for FG elliptic and triangular plates respectively. The trial functions denoting displacement component may be expressed as linear combination of simple algebraic polynomials (generated from Pascal's triangle). Six lowest natural frequencies with respect to various physical and geometric parameters have been evaluated in these problems along with three-dimensional mode shapes for a few boundary conditions. Regardless of plate geometries considered, it may be noted that increase in the number of polynomials play a crucial role in the convergence of non-dimensional frequencies in Rayleigh-Ritz method.

In FG rectangular plates of Chapter 6, both power-law and exponential law gradation of FG material properties are considered. In case of power-law gradation, it is evident that natural frequencies are increasing with increase in aspect (length-to-breadth) ratios for a fixed power-law index and are decreasing with increase in power-law indices for a fixed aspect ratio. On the other hand in case of exponential gradation, the concerned frequencies are decreasing with increase in ratio of Young's moduli and behave reverse with increase in ratio of mass densities. In case of isotropic thick plate also, these frequencies are increasing with increase in aspect ratio and are decreasing with increase in thickness-to-length ratio.

In Chapter 7 for FG elliptic plates, only power-law variation form of material properties is assumed. It can be viewed that the frequencies are increasing with increase in aspect (semi major-to-semi minor axes) ratios for a fixed power-law index and are decreasing with increase in power-law exponents for a fixed aspect ratio. Assuming effect of Poisson's ratio (ν), one may see that frequencies are independent of ν for clamped elliptic plates. But frequencies are increasing with increase in ν in case of simply supported and are showing fluctuating behavior while considering free edge condition, keeping both aspect ratio and power-law index fixed.

Finally power-law gradation for material properties of FG triangular plates is given in Chapter 8. The eigenfrequencies follow descending pattern due to increase in power-law exponent and ratio of Young's moduli, whereas we may get just reverse pattern (ascending behavior) with increase in ratio of mass densities. Rather than the effect of these parameters, the frequencies are decreasing with increase in μ (height) in case of FG

right-angled triangular plates.

- The effect of complicating environments viz. Winkler (or Pasternak) elastic foundations and thermal environments on free vibration of thin FG rectangular plates have been studied in Chapter 9. The vibration of FG rectangular plates with power-law variation based material properties is handled under Winkler and Pasternak elastic foundations, whereas thermal environment is assumed to study the vibration characteristics of exponential FG plate. These analyses have also been done using Rayleigh-Ritz method and similar interpretations for trail functions are also assumed as considered in earlier chapters.

  Considering the effect of Winkler elastic foundation, it may be observed that the non-dimensional frequencies are increasing with increase in aspect (length-to-breadth) ratios for a fixed power-law index (k) and are decreasing with increase in power-law exponents for a fixed aspect ratio. Without elastic foundation, the eigenfrequencies follow similar behavior with increase in k. They are also decreasing while considering the Winkler elastic foundation except for SFSF FG plate, where fundamental frequencies follow fluctuating behavior with increase in k. Moreover in presence of either Pasternak or Winkler-Pasternak foundations, the frequencies may also decrease for SCSC Lévy plate, whereas the behavior for other five combinations of edge conditions may not be straightforward. On the other hand, the results are gradually decreasing with increase in values of ratio of Young's moduli (E_r) and are increasing with ascending values of ratio of mass densities (ρ_r) in presence of both Winkler and Pasternak foundations. While looking into the results obtained for the exponential FG plate with thermal environments, it is worth to mention that frequencies are increasing with increase in thickness-to-breadth (h/b) ratio and are decreasing with increase in the temperature gradient (ΔT) regardless of the edge condition and thermal state (uniform or linear rise) considered.

The above conclusions convey that the developed methods viz. Rayleigh-Ritz and generalized differential quadrature are computationally efficient to solve the titled problems. The newly proposed shear deformation theories are helpful in understanding vibration problems of functionally graded beams and plates. But there are few limitations on these analyses which may open a new vista for future research. Accordingly, the future directions have been

discussed in the following section.

10.2 Future directions

Although exhaustive investigations have been performed related to the titled problems, but we may not claim that proposed methods are most general and computationally efficient for solving any types of static and dynamic problems. As such, there may still be some gaps which may be extended for doing future research in the following ways.

- In general, this work presents only linear problems. The non-linearities in different aspects can be applied to handle non-linear problems. The Rayleigh-Ritz method is computationally efficient only to solve linear problems. We may implement DQM or other numerical methods to solve non-linear problems.
- In recent decades, mechanical behavior of micro- and nano-functionally graded structural members has taken crucial attention in engineering applications. Their mechanical behavior can be found in various potential applications viz. biomedical devices, aerospace, textiles, civil engineering, bionics engineering, energy, electronic engineering, and micro-electro-mechanical systems (MEMS) etc. As such, the mechanics of such members are important to investigate.
- Most important scope of structural analysis and design is also to study their instabilities and failures due to external stimulus, loads and environmental hazards. It is worth to study these structural instabilities in engineering design by using various computational techniques.
- We may apply different peculiar substrates on functionally graded members to enhance their utilities in various real life application problems. Accordingly, the related mathematical models may be interesting to investigate.
- On the other hand, we may also apply combination of methods to handle these studies in a more efficient manner which are called mixed numerical methods viz. mixed-Ritz, mixed-differential quadrature and mixed-finite element method etc.
- In addition to the shear deformation effects (neglected in classical plate theory), other deformation plate theories can also be extended easily. New shear deformation theories

may be proposed for various structural members.

- Anisotropic properties may be considered in case of FG structural members to find their mechanical behavior.
- The effect of add-on vibration may be dictated in the titled problems.
- We may find the conglomeration of different materials under single FG members. In addition, we may also apply the principles of Electro Discharge Machining (EDM) or Electro Chemical Machining (ECM) to FG beam (or plate).
- A few significant facets viz. removal of stress concentration and fracture propagation may also be applied to the FG materials.
- The present study may also be extended to annular plates and plates with holes subjected to non-classical boundary conditions under different complicating effects.

References

Abrate, S. (1995). Vibration of non–uniform rods and beams. *Journal of Sound and Vibration*, 185(4):703–716.

Abrate, S. (2006). Free vibration, buckling, and static deflections of functionally graded plates. *Composite Science and Technology*, 66:2383–2394.

Abrate, S. (2008). Functionally graded plates behave like homogeneous plates. *Composites Part B*, 39:151–158.

Akhavan, H., Hashemi, S. H., Taher, H. R. D., Alibeigloo, A., and Vahabi, S. (2009). Exact solutions for rectangular Mindlin plates under in-plane loads resting on Pasternak elastic foundation. Part II: Frequency analysis. *Computational Materials Science*, 44:951–961.

Alibeigloo, A. (2010). Thermoelasticity analysis of functionally graded beam with integrated surface piezoelectric layer. *Composite Structures*, 92:1535–1543.

Alshorbagy, A. E., Eltaher, M. A., and Mahmoud, F. F. (2011). Free vibration characteristics of a functionally graded beam by finite element method. *Applied Mathematical Modelling*, 35:412–425.

Aydogdu, M. (2009). A new shear deformation theory for laminated composite plates. *Composite Structures*, 89:94–101.

Aydogdu, M. and Taskin, V. (2007). Free vibration analysis of functionally graded beams with simply-supporterd edges. *Materials and Design*, 28:1651–1656.

Baferani, A. H., Saidi, A. R., and Ehteshami, H. (2011). Accurate solution for free vibration analysis of functionally graded thick rectangular plates resting on elastic foundation. *Composite Structures*, 93:1842–1853.

Belalia, S. A. and Houmat, A. (2012). Nonlinear free vibration of functionally graded shear deformable sector plates by a curved triangular *p*–element. *European Journal of Mechanics - A/Solids*, 35:1–9.

Bellman, R. and Casti, J. (1971). Differential quadrature and long term integration. *Journal of Mathematical Analysis and Applications*, 34:235–238.

Bellman, R., Kashef, B., Lee, E. S., and Vasudevan, R. (1975). Differential quadrature and splines. *Computers and Mathematics with Applications*, 1:371–376.

Bellman, R., Kashef, B. G., and Casti, J. (1972). Differential quadrature: A technique for the rapid solution of nonlinear partial differential equations. *Journal of Computational Physics*, 10:40–52.

Bert, C. W. and Malik, M. (1997). Differential quadrature: a powerful new technique for analysis of composite structures. *Composite structures*, 39(3–4):179–189.

Bhat, R. B. (1985). Natural frequencies of rectangular plates using characteristic orthogonal polynomials in Rayleigh–Ritz method. *Journal of Sound and Vibration*, 102:493–499.

Bhat, R. B. (1986). Transverse vibrations of a rotating uniform cantilever beam with tip mass as predicted by using beam characteristic orthogonal polynomials in the Rayleigh–Ritz method. *Journal of Sound and Vibration*, 105:199–210.

Bhat, R. B. (1987). Flexural vibration of polygonal plates using characteristic orthogonal polynomials in two variables. *Journal of Sound and Vibration*, 114(1):65–71.

Bhavikatti, S. S. (2005). *Finite Element Analysis*. New Age International Publishers, New Delhi.

Bian, Z. G., Lim, C. W., and Chen, W. Q. (2006). On functionally graded beams with integrated surface piezoelectric layers. *Composite Structures*, 72:339–351.

Bouazza, M., Tounsi, A., Adda-Bedia, E. A., and Megueni, A. (2010). Thermoelastic stability analysis of functionally graded plates: An analytical approach. *Computational Materials Science*, 49:865–870.

Bouchafa, A., Benzair, A., Tounsi, A., Draiche, K., Mechab, I., and Bedia, E. (2010). Analytical modelling thermal residual stresses in exponential functionally graded material system. *Materials and Design*, 31:560–563.

Brischetto, S., Leetsch, R., Carrera, E., Wallmersperger, T., and Kröplin, B. (2008). Thermo–mechanical bending of functionally graded plates. *Journal of Thermal Stresses*, 31:286–308.

Carrera, E., Fazzolari, F. A., and Demasi, L. (2011). Vibration analysis of anisotropic simply–supported plates by using variable kinetic and Rayleigh–Ritz method. *Journal of Vibration and Acoustics*, 133:1–16.

Chakraverty, S. (1996). Efficient method for finding deflection of circular and elliptic plates. *IE(I) Journal-CV*, 77:01–11.

Chakraverty, S. (2009). *Vibration of plates*. CRC Press, Taylor and Francis Group, FL.

Chakraverty, S., Jindal, R., and Agarwal, V. (2007). Effect of non–homogeneity on natural frequencies of vibration of plates. *Meccanica*, 42:585–599.

Chakraverty, S. and Petyt, M. (1997). Natural frequencies for free vibration of nonhomogeneous elliptic and circular plates using two dimensional orthogonal polynomials. *Applied Mathematical Modelling*, 21:399–417.

Chakraverty, S. and Pradhan, K. K. (2014a). Free vibration of exponential functionally graded rectangular plates in thermal environment with general boundary conditions. *Aerospace Science and Technology*, 36:132–156.

Chakraverty, S. and Pradhan, K. K. (2014b). FREE VIBRATION OF FUNCTIONALLY GRADED THIN RECTANGULAR PLATES RESTING ON WINKLER ELASTIC FOUNDATION WITH GENERAL BOUNDARY CONDITIONS USING RAYLEIGHŰRITZ METHOD. *International Journal of Applied Mechanics*, 06:1450043.

Chen, L. W. and Hwang, J. R. (1988). Axisymmetric dynamic stability of transversely isotropic Mindlin circular plates. *Journal of Sound and Vibration*, 121:307–315.

Chen, W. Q. and Ding, H. J. (2002). On free vibration of functionally graded piezoelectric rectangular plate. *Acta Mechanica*, 153:207–216.

Cheng, Z. Q. and Batra, R. C. (2000a). Exact correspondece between eigenvalues of membranes and functionally graded simply supported polygonal plates. *Journal of Sound and Vibration*, 229(4):879–895.

Cheng, Z. Q. and Batra, R. C. (2000b). Three-dimensional thermoelastic deformations of a functionally graded elliptic plate. *Composites: Part B*, 31:97–106.

Cheung, Y. K. and Tham, L. G. (1988). Free vibration and static analysis of general plate by spline finite strip. *Computational Mechanics*, 3:187–197.

Cheung, Y. K. and Zhou, D. (1999). The free vibrations of tapered rectangular plates using a new set of beam functions with the Rayleigh–Ritz method. 223(5):703–722.

Cheung, Y. K. and Zhou, D. (2002). Three–dimensional vibration analysis of clamped and completely free isosceles triangular plates. *International Journal of Solids and Structures*, 39:673–687.

Şimşek, M. (2010a). Fundamental frequency analysis of functionally graded beams by using different higher-order beam theories. *Nuclear Engineering and Design*, 240:697–705.

Şimşek, M. (2010b). Vibration analysis of a functionally graded beam under a moving mass by using different beam theories. *Composite Stuctures*, 92:904–917.

Şimşek, M. (2012). Nonlocal effects in the free longitudinal vibration of axially functionally graded tapered nanorods. *Computational Materials Science*, 61:257–265.

Şimşek, M. and Kocatürk, T. (2009). Free and forced vibration of a functionally graded beam subjected to a concentrated moving harmonic load. *Composite Structures*, 90:465–473.

Şimşek, M. and Reddy, J. N. (2013). Bending and vibration of functionally graded microbeams using a new higher order theory and the modified couple stress theory. *International Journal of Engineering Science*, 64:37–53.

Cupial, P. (1997). Calculation of the natural frequencies of composite plates by the Rayleigh–Ritz method with orthogonal polynomials. *Journal of Sound and Vibration*, 201(3):385–387.

Ding, Z. (1996). Natural frequencies of rectangular plates using a set of static beam functions in Rayleigh–Ritz method. *Journal of Sound and Vibration*, 189(1):81–87.

Eftehari, S. A. and Jafari, A. A. (2012). A mixed method for free and forced vibration of rectangular plates. *Applied Mathematical Modeling*, 36:2814–2831.

Eftehari, S. A. and Jafari, A. A. (2013). Modified mixed Ritz–DQ formulation for free vibration of thick rectangular and skew plates with general boundary conditions. *Applied Mathematical Modeling*, 37:7398–7426.

Eltaher, M. A., Emam, S. A., , and Mahmoud, F. F. (2012). Free vibration analysis of functionally graded size–dependent nanobeams. *Applied Mathematics and Computation*, 218:7406–7420.

Eltaher, M. A., Khairy, A., Sadoun, A. M., and Omar, F. A. (2014). Static and buckling analysis of functionally graded Timoshenko nanobeams. *Applied Mathematics and Computation*, 229:283–295.

Fallah, A., Aghdam, M. M., and Kargarnovin, M. H. (2013). Free vibration analysis of moderately thick functionally graded plates on elastic foundation using the extended Kantorovich method. *Archives of Applied Mechanics*, 83:177–191.

Ferreira, A. J. M., Batra, R. C., Roque, C. M. C., Qian, L. F., and Jorge, R. M. N. (2006). Natural frequencies of functionally graded plates by a meshless method. *Composite Structures*, 75:593–600.

Ferreira, A. J. M., Batra, R. C., Roque, C. M. C., Qian, L. F., and Martins, P. A. L. S. (2005). Static analysis of functionally graded plates using third–order shear deformation theory and a meshless method. *Composite Structures*, 69(4):449–457.

Geannakakes, G. N. (1995). Natural frequencies of arbitrarily shaped plates using the Rayleigh–Ritz method together with natural co-ordinate regions and normalized characteristic polynomials. *Journal of Sound and Vibration*, 182(3):441–478.

Gorman, D. J. (1983). A highly accurate analytical solution for free vibraion analysis of simply supported right triangular plates. *Journal of Sound and Vibration*, 89(1):107–118.

Gorman, D. J. (1986). Free vibration analysis of right triangular plates with combinations of clamped–simply supported boundary conditions. *Journal of Sound and Vibration*, 106(3):419–431.

Gorman, D. J. (1989). Accurate free vibration analysis of right triangular plate with one free edge. *Journal of Sound and Vibration*, 131(1):115–125.

Grover, N., Singh, B. N., and Maiti, D. K. (2013). A general assessment of a new inverse trigonometric shear deformation theory for laminated composite and sandwich plates using finite element method. *Journal of Aerospace Engineering*, 0(0):1–14.

Hein, H. and Feklistova, L. (2011). Free vibrations of non–uniform and axially functionally graded beams using haar wavelets. *Engineering structures*, 33:3696–3701.

Heyliger, P. and Reddy, J. (1988). A higher order beam finite element for bending and vibration problems. *Journal of Sound and Vibration*, 126(2):309–326.

Hosseini-Hashemi, S. and Arsanjani, M. (2005). Exact characteristic equations for some classical boundary conditions of vibrating moderately thick rectangular plates. *International Journal of Solids and Structures*, 42:819–853.

Hosseini-Hashemi, S., Fadaee, M., and Taher, H. R. D. (2011). Exact solutions for free flexural vibration of Lévy–type rectangular thick plates via third order shear deformation plate theory. *Applied Mathematical Modelling*, 35:708–727.

Hosseini Hashemi, S., Karimi, M., and Rokni Damavandi Taher, H. (2010). Vibration analysis of rectangular Mindlin plates on elastic foundations and vertically in contact with stationary fluid by the Ritz method. *Ocean Engineering*, 37:174–185.

Hosseini-Hashemi, S., Salehipour, H., Atashipour, S., and Sbrulati, R. (2013). On the exact in–plane and out–of–plane free vibration analysis of thick functionally graded plates: Explicit 3–D elasticity solutions. *Composites: Part B*, 46:108–115.

Hsieh, J. J. and Lee, L. T. (2006). An inverse problem for a functionally graded elliptic plate with large deflection and slightly disturbed boundary. *International Journal of Solids and Structures*, 43:5981–5993.

Huang, D. J., Ding, H. J., and Chen, W. Q. (2007). Piezoelasticity solutions for functionally graded piezoelectric beams. *Smart Materials and Structures*, 16:687–695.

Huang, X. L. and Shen, H. S. (2001). Nonlinear vibration and dynamic response of functionally graded plates in thermal environments. *International Journal of Solids and Structures*, 41:2403–2427.

Huang, Y. and Li, X. F. (2010). A new approach for free vibration of axially functionally graded beams with non–uniform cross–section. *Journal of Sound and Vibration*, 329:2291–2303.

Huang, Y., Yang, L. E., and Luo, Q. Z. (2013). Free vibration of axially functionally graded Timoshenko beams with non-uniform cross-section. *Composites: Part B*, 42:1493–1498.

Ilanko, S. (2009). Comments on the historical bases of the rayleigh and ritz methods. *Journal of Sound and Vibration*, 319:731–733.

Jandaghian, A. A., Jafari, A. A., and Rahmani, O. (2014). Vibrational response of functionally graded circular plate integrated with piezoelectric layers: An exact solution. *Engineering Solid Mechanics*, 2:119–130.

Kahrobaiyan, M. H., Rahaeifard, M., Tajalli, S. A., and Ahmadian, M. T. (2012). A strain gradient functionally graded Euler–Bernoulli beam formulation. *International Journal of Engineering Science*, 52:65–76.

Kang, S. W. and Lee, J. M. (2001). Free vibration analysis of arbitrarily shaped plates with clamped edges using wave–type functions. *Journal of Sound and Vibration*, 242(1):9–26.

Karunasena, W., Kitipornchai, S., and Al-Bermani, F. G. A. (1996). Free vibration of cantilevered arbitrary triangular Mindlin plates. *International Journal of Mechanical Sciences*, 38(4):431–442.

Kashtalyan, M. (2004). Three–dimensional elasticity solution for bending of functionally graded rectangular plates. *European Journal of Mechanics A/Solids*, 23:853–864.

Kelly, S. G. (1999). *Fundamentals of Mechanical Vibrations*. McGraw–Hill series in mechanical engineering, Singapore, Second edition.

Khalili, S. M. R., Jafari, A. A., and Eftehari, S. A. (2010). A mixed Ritz–DQ method for forced vibration of functionally graded beams carrying moving loads. *Composite Structures*, 92:2497–2511.

Kien, N. D. (2014). Large displacement behavior of tapered cantilever Euler–Bernoulli beams made of functionally graded material. *Applied Mathematics and Computation*, 237:340–355.

Kim, C. S. and Dickinson, S. M. (1990). The free flexural vibration of right triangular isotropic and orthotropic plates. *Journal of Sound and Vibration*, 141(2):291–311.

Kim, C. S. and Dickinson, S. M. (1992). The free flexural vibration of isotropic and orthotropic general triangular shaped plates. *Journal of Sound and Vibration*, 152(3):383–403.

Kim, Y. W. (2005). Temperature dependent vibration analysis of functionally graded rectangular plates. *Journal of Sound and Vibraiton*, 284:531–549.

Kitipornchai, S., Yang, J., and Liew, K. M. (2006). Random vibration of the functionally graded laminates in thermal environments. *Computer Methods in Applied Mechanics and Engineering*, 195:1075–1095.

Komijani, M., Reddy, J. N., and Eslami, E. R. (2014). Nonlinear analysis of microstructure–dependent functionally graded piezoelectric material actuators. *Journal of the Mechanics and Physics of Solids*, 63:214–227.

Lam, K. Y., Wang, C. M., and He, X. Q. (2000). Canonical exact solutions for Levy–plates on two–parameter foundation using Green's functions. *Engineering Structures*, 22:364–378.

Lei, J., He, Y., Zhang, B., Gan, Z., and Zeng, P. (2013). Bending and vibration of functionally graded sinusoidal microbeams based on the strain gradient elasticity theory. *International Journal of Engineering Science*, 72:36–52.

Leissa, A. W. (1967). Vibration of a simply–supported elliptic plate. *Journal of Sound and Vibration*, 6:145–148.

Leissa, A. W. (1969). *Vibration of plates*. Scientific and Technical Information Divison, NASA, Washington, DC.

Leissa, A. W. (1973). The free vibration of rectangular plates. *Journal of Sound and Vibration*, 31(3):257–293.

Leissa, A. W. and Narita, Y. (1980). Natural frequencies of simply supported circular plates. *Journal of Sound and Vibration*, 70:221–229.

Leissa, A. W. and Qatu, M. S. (2011). *Vibration of continuous systems*. McGraw–Hill.

Levinson, M. (1981). A new rectangular beam theory. *Journal of Sound and Vibration*, 74(1):81–87.

Li, Q., Iu, V. P., and Kou, K. P. (2009a). Three-dimensional vibration analysis of functionally graded material plates in thermal environment. *Journal of Sound and Vibration*, 324:733–750.

Li, S., Su, H., and Cheng, C. (2009b). Free vibration of functionally graded material beams with surface-bonded piezoelectric layers in thermal environment. *Applied Mathematics and Mechanics*, 30(8):969–982.

Li, Y. S., Feng, W. J., and Cai, Z. Y. (2014). Bending and free vibration of functionally graded piezoelectric beam based on modified strain gradient theory. *Composite Structures*, 115:41–50.

Liew, K. M. (1993). On the use of pb–2 Rayleigh–Ritz method for free flexural vibration of triangular plates with curved internal supports. *Journal of Sound and Vibration*, 165(2):329–340.

Liew, K. M., Han, J. B., and Xiao, Z. M. (1997). Vibration analysis of circular mindlin plates using the differential quadrature method. *Journal of Sound and Vibration*, 205:617–630.

Liew, K. M., Xiang, Y., and Kitipornchai, S. (1993). Transverse vibration of thick rectangular plates–I. compressive sets of boundary conditions. *Computers and Structures*, 49(1):1–29.

Liu, C. F. and Lee, Y. T. (2000). Finite element analysis of three–dimensional vibrations of thick circular and annular plates. *Journal of Sound and Vibration*, 233:63–80.

Liu, F. L. and Liew, K. M. (1999). Analysis of vibrating thick rectangular plates with mixed boundary constraints using differential quadrature element method. *Journal of Sound and Vibration*, 225(5):915–934.

Loy, C. T., Lam, K. Y., and Reddy, J. N. (1999). Vibration of functionally graded cylindrical shells. *International Journal of Mechanical Sciences*, 41:309–324.

Ma, L. S. and Wang, T. J. (2003). Nonlinear bending and post–buckling of functionally graded circular plate under mechanical and thermal loadings. *International Journal of Solids and Sturcutres*, 40:3311–3330.

Ma, L. S. and Wang, T. J. (2004). Relationships between axisymmetric bending and buckling solutions of FGM circular plates based on third–order plate theory and classical plate theory. *International Journal of Solids and Structures*, 41:85–101.

Mahi, A., Adda Bedia, E. A., Tounsi, A., and Mechab, I. (2010). An analytical method for temperature-dependent free vibration analysis of functionally graded beams with general boundary conditions. *Composite Structures*, 92:1877–1887.

Malekzadeh, P. and Beni, A. A. (2010). Free vibration of functionally graded arbitrary straight-sided quadrilateral plates in thermal environment. *Composite Structures*, 92:2758–2767.

Matsunaga, H. (2008). Free vibration and stability of functionally graded plates according to a 2–D higher-order deformation theory. *Composite Structures*, 82:499–512.

Mazumdar, J. (1971). Transverse vibration of elastic plates by the method of constant deflection lines. *Journal of Sound and Vibration*, 18:147–155.

Mirza, S. and Bijlani, M. (1985). Vibration of triangular plates of variable thickness. *Computers and Structures*, 21:1129–1135.

Naadimuthu, G., Bellman, R., Wang, K. M., and Lee, E. S. (1984). Differential quadrature and partial differential equations: some numerical results. *Journal of Mathematical Analysis and Applications*, 98:220–235.

Najafizadeh, M. M. and Eslami, M. R. (2002). Buckling analysis of circular plates of functionally graded materials under radial compression. *International Journal of Mechanical Sciences*, 44:2479–2493.

Natarajan, S., Chakraborty, S., Thangavel, M., Bordas, S., and Rabczuk, T. (2012). Size–dependent free flxural vibration behavior of functionally graded nanoplates. *Computational Materials Science*, 65:74–80.

Neves, A. M. A., Ferreira, A. J. M., Carrera, E., Cinefra, M., Roque, C. M. C., Jorge, R. M. N., and Soares, C. M. M. (2013). Static, free vibration and buckling analysis of isotropic and sandwich functionally graded plates using a quasi–3D higher–order shear deformation theory and a meshless technique. *Composites: Part B*, 44:657–674.

Nguyen, T. K., Sab, K., and Bonnet, G. (2008). First–order shear deformation plate models for functionally graded materials. *Composite Structures*, 83:25–36.

Nguyen, T. K., Vo, T. P., and Thai, H. T. (2013). Static and free vibration analysis of axially loaded functionally graded beams based on the first–order shear deformation theory. *Composites: Part B*, 55:147–157.

Nie, G. J., Zhong, Z., and Chen, S. (2013). Analytical solution for a functionally graded beam with arbitrary graded material properties. *Composites: Part B*, 44:274–282.

Öz, H. R. (2000). Calculation of the natural frequencies of a beam-mass system using finite element method. *Mathematical and Computational Applications*, 5:67–75.

Penny, E. (2004). *Differential equations and boundary value problems*. Pearson Education (Singapore) Pte. Ltd., Singapore, Third edition.

Pradhan, K. K. and Chakraverty, S. (2013). Free vibration of Euler and Timoshenko functionally graded beams beams by Rayleigh–Ritz method. *Composites: Part B*, 54:175–184.

Pradhan, K. K. and Chakraverty, S. (2014). Effects of different shear deformation theories on free vibration of functionally graded beams. *International Journal of Mechanical Sciences*, 82:149–160.

Pradyumna, S. and Bandyopadhyay, J. N. (2010). Dynamic instability of functionally graded shells using higher–order theory. *Journal of Engineering Mechanics*, 136(5):551–561.

Prakash, T. and Ganpathi, M. (2006). Axisymmetric flexural vibration and thermoelastic stability of FGM circular plates using finite element method. *Composites: Part B*, 37:642–649.

Qu, Y., Long, X., Li, H., and Meng, G. (2013). A variation formulation for dynamic analysis of composite laminated beams based on a general higher–order shear deformation theory. *Composite Structures*, 102:175–192.

Quan, J. R. and Chang, C. T. (1989a). New insights in solving distributed system equations by the quadrature method–I. Analysis. *Computers and Chemical Engineering*, 13(7):779–788.

Quan, J. R. and Chang, C. T. (1989b). New insights in solving distributed system equations by the quadrature method–II. Numerical experiments. *Computers and Chemical Engineering*, 13(9):1017–1024.

Rahmani, O. and Pedram, O. (2014). Analysis and modeling the size effect on vibration of functionally graded nanobeams based on nonlocal Timoshenko beam theory. *International Journal of Engineering Science*, 77:55–70.

Rajalingham, C. and Bhat, R. B. (1993). Axisymmetric vibration of circular plates and its analogous elliptic plates using characteristic orthogonal polynomials. *Journal of Sound and Vibration*, 161:109–118.

Rajalingham, C., Bhat, R. B., and Xistris, G. D. (1994). Vibration of clamped elliptic plates using exact circular plate modes as shape functions in Rayleigh–Ritz method. *International Journal of Mechanical Sciences*, 36:231–246.

Rajasekaran, S. (2013). Buckling and vibration of axially functionally graded nonuniform beams using differential transformation based dynamic stiffness approach. *Meccanica*, 48:1053–1070.

Ramirez, F., Heyliger, P. R., and Pan, E. (2006). Static analysis of functionally graded elastic anisotropic plates using a discrete layer approach. *Composites: Part B*, 37:10–20.

Rao, S. S. (2004). *The Finite Element Method in Engineering*. Elsevier Science and Technology Books, Miami.

Reddy, J. (1997). On the dynamic behaviour of the Timoshenko beam finite elements. *Sadhana*, 24:175–198.

Reddy, J. N. (1984a). A refined nonlinear theory of plates with transverse shear deformation. *International Journal of Solids and Structures*, 20(9/10):881–896.

Reddy, J. N. (1984b). A refined nonlinear theory of plates with transverse shear deformation. *International Journal of Solids and Structures*, 20:881–896.

Reddy, J. N. (1984c). A simple higher–order theory for laminated composite plates. *Journal of Applied Mechanics*, 51:745–752.

Reddy, J. N. (2000). Analysis of functionally graded plates. *International Journal of Numerical Methods in Engineering*, 47:663–684.

Reddy, J. N. (2011). Microstructure–dependent couple stress theories of functionally graded beams. *Journal of the Mechanics and Physics of Solids*, 59:2382–2399.

Reddy, J. N. and Chin, C. D. (1998). Thermomechanical analysis of functionally graded cylinders and plates. *Journal of Thermal Stresses*, 21:593–626.

Reddy, J. N., Wang, C. M., and Kitipornchai, S. (1999). Axisymmetric bending of functionally graded circular and annular plates. *European Journal of Mechanics A/Solids*, 18:185–199.

Reissner, E. (1975). On transverse bending of plates including the effects of transverse shear deformation. *International Journal of Solids and Structures*, 25:495–502.

Roque, C. M. C., Ferreira, A. J. M., and Jorge, R. M. N. (2007). A radial basis function approach for the free vibration analysis of functionally graded plates using a refined theory. *Journal of Sound and Vibration*, 300:1048–1070.

Saidi, A. R., Rasouli, A., and Sahraee, S. (2009). Axisymmetric bending and buckling analysis of thick functionally graded circular plates using unconstrained third–order shear deformation plate theory. *Composite Strctures*, 89:110–119.

Sakiyama, T. and Huang, M. (2000). Free–vibration analysis of right triangular plates with variable thickness. *Journal of Sound and Vibration*, 234(5):841–858.

Saliba, H. T. (1990). Transverse free vibration of simply supported right triangular thin plates: a highly accurate simplified solution. *Journal of Sound and Vibration*, 139(2):289–297.

Shahba, A., Attarnejad, R., Marvi, M. T., and Hajilar, S. (2011). Free vibration and stability analysis of axially functionally graded tapered timoshenko beams with classical and non-classical boundary conditions. *Composites: Part B*, 42:801–808.

Shahba, A. and Rajasekaran, S. (2012). Free vibration and stability of tapered Euler–Bernoulli beams made of axially functionally graded materials. *Applied Mathematical Modelling*, 36:3094–3111.

Sharma, D. K., Sharma, J. N., Dhaliwal, S. S., and Wali, V. (2014). Vibration analysis of axisymmetric functionally graded viscothermoelastic spheres. *Acta Mechanica Sinica*, 30(1):100–111.

Shen, H. S. (2002). Nonlinear bending response of functionally graded plates subjected to trnsverse loads and in thermal environments. *International Journal of Mechanical Sciences*, 44:561–584.

Shi, P. and Dong, C. Y. (2012). Vibration analysis of functionally graded annular plates with mixed boundary conditions in thermal environment. *Journal of Sound and Vibration*, 331:3649–3662.

Shimpi, R. P. and Patel, H. G. (2006). Free vibrations of plates using two variable refined plate theory. *Journal of Sound and Vibration*, 296:979–999.

Shimpi, R. P., Patel, H. G., and Arya, H. (2007). New first–order shear deformation plate theories. *Journal of Applied Mechanics*, 74:523–533.

Shu, C. and Du, H. (1997). Implementation of clamped and simply supported boundary conditions in the gdq free vibration analysis. *Interational Journal of Solids and Structures*, 34(7):819–835.

Si, X. H., Lu, W. X., and Chu, F. L. (2012). Modal analysis of circular plates with radial side cracks and in contact with water on one side based on the Rayleigh–Ritz method. *Journal of Sound and Vibration*, 331:231–251.

Sina, S. A., Navazi, H. M., and Haddadpour, H. (2009). An analytical method for free vibration analysis of functionally graded beams. *Materials and Design*, 30:741–747.

Singh, B. and Chakraverty, S. (1991). Transverse vibration of completely-free elliptic and circular plates using orthogonal polynomials in the Rayleigh-Ritz Method. *International Journal of Mechanical Sciences*, 33:741–751.

Singh, B. and Chakraverty, S. (1992a). On the use of orthogonal polynomials in Rayleigh-Ritz method for the study of transverse vibration of elliptic plates. *Computers and Structures*, 43:439–443.

Singh, B. and Chakraverty, S. (1992b). Transverse vibration of simply-supported elliptic and circular plates using boundary characteristic orthogonal polynomials in two dimensions. *Journal of Sound and Vibration*, 152:149–155.

Singh, B. and Chakraverty, S. (1992c). Transverse vibration of triangular plates using characteristic orthogonal polynomials in two variables. *International Journal of Mechanical Sciences*, 34(12):947–955.

Singh, B. and Chakraverty, S. (1994a). Flexural vibration of skew plates using boundary characteristic orthogonal polynomials in two variables. *Journal of Sound and Vibration*, 173(2):157–178.

Singh, B. and Chakraverty, S. (1994b). Use of characteristic orthogonal polynomials in two dimensions for transverse vibration of elliptic and circular plates with variable thickness. *Journal of Sound and Vibration*, 173:289–299.

Singh, B. and Hassan, S. M. (1998). Transverse vibration of triangular plate with arbitrary thickness variation and various boundary conditions. *Journal of Sound and Vibration*, 214(1):29–55.

Singh, B. and Saxena, V. (1996). Transverse vibration of triangular plates with variable thickness. *Journal of Sound and Vibration*, 194(4):471–496.

Taj, G. and Chakrabarti, A. (2013). Static and dynamic analysis of functionally graded skew plates. *Journal of Engineering Mechanics*, 139(7):848–857.

Talha, M. and Singh, B. N. (2010). Static response and free vibration analysis of FGM plates using higher order shear deformation theory. *Appied Mathematical Modelling*, 34:3991–4011.

Thai, C. H., Ferreira, A. J. M., Bordas, S. P. A., Rabczuk, T., and Nguyen-Xuan, H. (2014). Isogeometric analysis of laminated composite and sandwich plates using a new inverse trigonometric shear deformation theory. *European Journal of Mechanics A/Solids*, 43:89–108.

Thai, H.-T. and Choi, D.-H. (2012). A refined shear deformation theory for free vibration of functionally graded plates on elastic foundation. *Composites Part B: Engineering*, 43:2335–2347.

Thai, H. T. and Vo, T. P. (2012). Bending and free vibration of functionally graded beams using various higher–order shear deformation beam theories. *International Journal of Mechanical Sciences*, 62:57–66.

Timoshenko, S. and Woinowsky-Krieger, S. (1959). *Theory of plates and shells*. McGraw–Hill, Singapore, Second edition.

Tounsi, A., Houari, M. S. A., Benyoucef, S., and Bedia, E. A. A. (2013). A refined trigonometric shear deformation theory for thermoelastic bending of functionally graded sandwich paltes. *Aerospace Science and Technology*, 24:209–220.

Touratier, M. (1991). An efficient standard plate theory. *International Journal of Engineering Science*, 29(8):901–916.

Vo, T. P., Thai, H. T., Nguyen, T. K., and Inam, F. (2013). Static and vibration analysis of functionally graded beams using refined shear deformation theory. *Meccanica, Springer Netherlands*, pages 1–14.

Wang, C. M., Reddy, J. N., and Lee, K. H. (2000). *Shear Deformation of Beams and Plates: Relationship with Classical Solutions*. Elsevier Science Ltd, Oxford.

Wanji, C. and Cheung, Y. K. (1998). Refined triangular discrete Kirchoff plate element for thin plate bending, vibration and buckling analysis. *International Journal for Numerical Methods in Engineering*, 41:1507–1525.

Wattanasakulpong, N., Prusty, B. G., and Kelly, D. W. (2011). Thermal buckling and elastic vibration of third–order shear deformable functionally graded beams. *International Journal of Mechanical Sciences*, 53:734–743.

Werner, H. (1999). A three–dimensional solution for rectangular plate bending free of transversal normal stresses. *Communications in Numerical Methods in Engineering*, 15:295–302.

Wu, T. Y. and Liu, G. R. (2001). Free vibration analysis of circular plates with variable thickness by the generalized differential quadrature rule. *International Journal of Solids and Structures*, 38:7967–7980.

Wu, T. Y., Wang, Y. Y., and Liu, G. R. (2002). Free vibration analysis of circular plates using generalized differential quadrature rule. *Computer methods in Applied Mechanics and Engineering*, 191:5365–5380.

Xiang, S., Wang, K., Ai, Y., Sha, Y., and Shi, H. (2009). Analysis of isotropic, sandwich and laminated plates by a meshless method and various shear deformation theories. *Composite Structures*, 91:31–37.

Xiao, J. R., Batra, R. C., Gilhooley, D. F., Gillespie Jr., J. W., and McCarthy, M. A. (2007). Analysis of thick plates by using a higher–order shear and normal deformable plate theory and mlpg method with radial basis functions. *Computer Methods in Applied Mechanics and Engineering*, 197:979–987.

Yang, J. and Shen, H. S. (2001). Dynamic response of initially stressed functionally graded rectangular thin plates. *Composite Structures*, 54:497–508.

Yang, J. and Shen, H. S. (2002). Vibration characteristics and transient response of shear–deformable functionally graded plates in thermal environments. *Journal of Sound and Vibration*, 255(3):579–602.

Yang, J. and Shen, H. S. (2003a). Nonlinear analysis of functionally graded plates under transverse and in–plane loads. *International Journal of Non–Linear Mechanics*, 38:467–482.

Yang, J. and Shen, H. S. (2003b). Nonlinear bending analysis of shear deformable functionally graded plates subjected to thermo–mechanical loads under various boundary conditions. *Composites: Part B*, 34:103–115.

Yang, L. and Zhifei, S. (2009). Free vibration of functionally graded piezoelectric beam via state-space based differential quadrature. *Composite Structures*, 87:257–264.

Yiqi, M. and Yiming, F. (2010). Nonlinear dynamic response and active vibration control for piezoelectric functionally graded plate. *Journal of Sound and Vibration*, 329:2015–2028.

Zenkour, A. M. (2006). Generalized shear deformation theory for bending analysis of functionally graded plates. *Applied Mathematical Modelling*, 30:67–84.

Zenkour, A. M. and Sobhy, M. (2013). Dynamic bending response of thermoelastic functionally graded plates resting on elastic foundations. *Aerospace Science and Technology*, 29:7–17.

Zhang, D. G. (2014). Nonlinear bending analysis of FGM rectangular plates with various supported boundaries resting on two-paramter elastic foundations. *Archives of Applied Mechanics*, 84:1–20.

Zhao, D., Au, F. T. K., Cheung, Y. K., and Lo, S. H. (2003). Three–dimensional vibration analysis of circular and annular plates via the Chebyshev–Ritz method. *International Journal of Solids and Structures*, 40:3089–3105.

Zhong, H. Z. (2000). Free vibration analysis of isosceles triangular Mindlin plates by the triangular differential quadrature method. *Journal of Sound and Vibration*, 237(4):697–708.

Zhu, T. L. (2011). The vibrations of pre–twisted rotating Timoshenko beams by the Rayleigh–Ritz method. *Computational Mechanics*, 47:395–408.

List of publications

Journals (Published/Accepted)

1. Pradhan, K.K. and Chakraverty, S. (2015). Free vibration of FG Levy plate resting on elastic foundations. **Engineering and Computational Mechanics**, 1500014 (26 pages) (Proceedings of ICE).

2. Pradhan, K.K. and Chakraverty, S. (2015). Generalized power-law exponent based shear deformation theory for free vibration of functionally graded beams. **Applied Mathematics and Computation**, 268:1240–1258 (Elsevier).

3. Pradhan, K.K. and Chakraverty, S. (2015). Transverse vibration of isotropic thick rectangular plates based on new inverse trigonometric shear deformation theories. **International Journal of Mechanical Sciences**, 94-95:211–231 (Elsevier).

4. Pradhan, K.K. and Chakraverty, S. (2014). Free vibration of functionally graded thin elliptic plates with various edge supports. **Structural Engineering and Mechanics**, 53 (2):337–354 (Technopress).

5. Pradhan, K.K. and Chakraverty, S. (2014). Static analysis of functionally graded thin rectangular plates with various boundary supports. **Archives of Civil and Mechanical Engineering**, 15:721–734 (Elsevier).

6. Chakraverty, S. and Pradhan, K.K. (2014). Free vibration of functionally graded thin rectangular plates resting on Winkler elastic foundation with general boundary conditions using Rayleigh-Ritz method. **International Journal of Applied Mechanics**, 6(4):145003 (37 pages) (World Scientific).

7. Chakraverty, S. and Pradhan, K.K. (2014). Free vibration of exponential functionally graded rectangular plates in thermal environment with general boundary conditions. **Aerospace Science and Technology**, 36:132–156 (Elsevier).

8. Pradhan, K.K. and Chakraverty, S. (2014). Effects of different shear deformation theories on free vibration of functionally graded beams. **International Journal of Mechanical Sciences**, 82:149–160 (Elsevier).

9. Pradhan, K.K. and Chakraverty, S. (2013). Free vibration of Euler and Timoshenko functionally graded beams by Rayleigh-Ritz method. **Composites Part B**, 37:175–184 (Elsevier).

Journals (Communicated/Under review)

1. Pradhan, K.K. and Chakraverty, S. (2015). Natural frequencies of shear deformed functionally graded beams using inverse trigonometric functions. **Journal of the Brazilian Society of Mechanical Sciences and Engineering**, Under review (Springer).

2. Pradhan, K.K. and Chakraverty, S. (2015). Flexural vibration of functionally graded triangular plates with various boundary conditions. **Aerospace Science and Technology**, Communicated (Elsevier).

3. Pradhan, K.K. and Chakraverty, S. (2015). Free vibration of non-uniform functionally graded beams by using differential quadrature method. **Meccanica**, Communicated (Springer).

Conferences

1. Pradhan, K.K. and Chakraverty, S. (2013). Free vibration of functionally graded beams with variable thickness. **Third International conference of Gwalior Academy of Mathematical Sciences (GAMS) on Mathematical, Computational & Integrative Sciences, NIT BHOPAL**.